frontiers | Research Topics

Stem cell-derived retinal and brain organoid culture for disease modeling

Edited by
Lin Cheng, Carla Mellough, Kin-Sang Cho and Maeve Ann Caldwell

Published in
Frontiers in Cellular Neuroscience

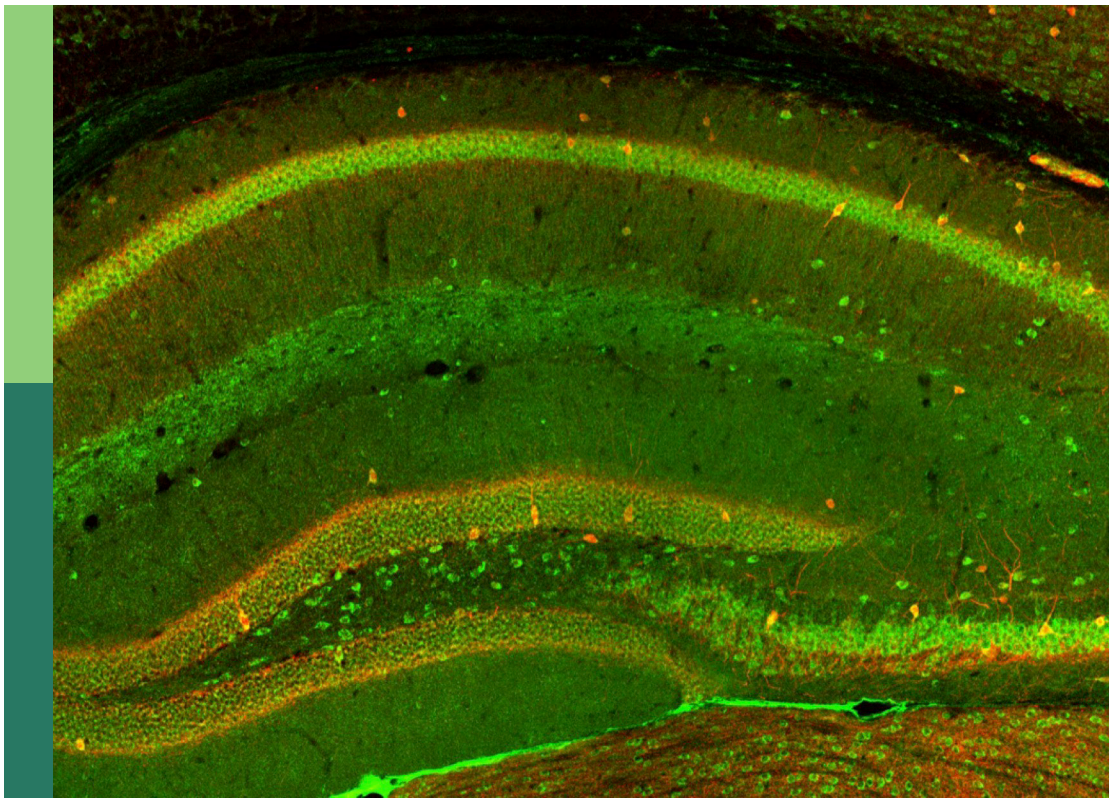

ISSN 1664-8714
ISBN 978-2-8325-4922-3
DOI 10.3389/978-2-8325-4922-3

About Frontiers

Frontiers is more than just an open access publisher of scholarly articles: it is a pioneering approach to the world of academia, radically improving the way scholarly research is managed. The grand vision of Frontiers is a world where all people have an equal opportunity to seek, share and generate knowledge. Frontiers provides immediate and permanent online open access to all its publications, but this alone is not enough to realize our grand goals.

Frontiers journal series

The Frontiers journal series is a multi-tier and interdisciplinary set of open-access, online journals, promising a paradigm shift from the current review, selection and dissemination processes in academic publishing. All Frontiers journals are driven by researchers for researchers; therefore, they constitute a service to the scholarly community. At the same time, the *Frontiers journal series* operates on a revolutionary invention, the tiered publishing system, initially addressing specific communities of scholars, and gradually climbing up to broader public understanding, thus serving the interests of the lay society, too.

Dedication to quality

Each Frontiers article is a landmark of the highest quality, thanks to genuinely collaborative interactions between authors and review editors, who include some of the world's best academicians. Research must be certified by peers before entering a stream of knowledge that may eventually reach the public - and shape society; therefore, Frontiers only applies the most rigorous and unbiased reviews. Frontiers revolutionizes research publishing by freely delivering the most outstanding research, evaluated with no bias from both the academic and social point of view. By applying the most advanced information technologies, Frontiers is catapulting scholarly publishing into a new generation.

What are Frontiers Research Topics?

Frontiers Research Topics are very popular trademarks of the *Frontiers journals series*: they are collections of at least ten articles, all centered on a particular subject. With their unique mix of varied contributions from Original Research to Review Articles, Frontiers Research Topics unify the most influential researchers, the latest key findings and historical advances in a hot research area.

Find out more on how to host your own Frontiers Research Topic or contribute to one as an author by contacting the Frontiers editorial office: frontiersin.org/about/contact

Stem cell-derived retinal and brain organoid culture for disease modeling

Topic editors

Lin Cheng — The University of Iowa, United States

Carla Mellough — Lions Eye Institute, Australia

Kin-Sang Cho — Schepens Eye Research Institute, Harvard Medical School, United States

Maeve Ann Caldwell — Trinity College Dublin, Ireland

Citation

Cheng, L., Mellough, C., Cho, K.-S., Caldwell, M. A., eds. (2024). *Stem cell-derived retinal and brain organoid culture for disease modeling*. Lausanne: Frontiers Media SA. doi: 10.3389/978-2-8325-4922-3

Table of contents

frontiers | Frontiers in Cellular Neuroscience

TYPE Editorial
PUBLISHED 13 March 2024
DOI 10.3389/fncel.2024.1367482

OPEN ACCESS

EDITED AND REVIEWED BY
Dirk M. Hermann,
University of Duisburg-Essen, Germany

*CORRESPONDENCE
Lin Cheng
✉ kjade.cheng@gmail.com
Maeve Ann Caldwell
✉ maeve.caldwell@tcd.ie
Kin-Sang Cho
✉ kinsang_cho@meei.harvard.edu
Carla B. Mellough
✉ carlamellough@lei.org.au

RECEIVED 08 January 2024
ACCEPTED 15 January 2024
PUBLISHED 13 March 2024

CITATION
Cheng L, Caldwell MA, Cho K-S and Mellough CB (2024) Editorial: Stem cell-derived retinal and brain organoid culture for disease modeling.
Front. Cell. Neurosci. 18:1367482.
doi: 10.3389/fncel.2024.1367482

Editorial: Stem cell-derived retinal and brain organoid culture for disease modeling

Lin Cheng[1,2]*, Maeve Ann Caldwell[3]*, Kin-Sang Cho[4]* and Carla B. Mellough[5]*

[1]Department of Ophthalmology and Visual Sciences, University of Iowa Carver College of Medicine, Iowa City, IA, United States, [2]Center for the Prevention and Treatment of Visual Loss, Veterans Affairs Medical Center, Iowa City, IA, United States, [3]Discipline of Physiology, Trinity College Institute for Neuroscience, Trinity College Dublin, Dublin, Ireland, [4]Schepens Eye Research Institute of Massachusetts Eye and Ear, Harvard Medical School, Boston, MA, United States, [5]Centre for Ophthalmology and Visual Sciences (incorporating Lions Eye Institute), The University of Western Australia, Nedlands, WA, Australia

KEYWORDS

retinal organoids (ROs), brain organoids (BOs), stem cells, central nervous system (CNS) diseases, neurodegenerative disorders

Editorial on the Research Topic
Stem cell-derived retinal and brain organoid culture for disease modeling

CNS organoids are an emerging research tool in stem cell biology to recapitulate retinal and brain development and can be used for studying disease mechanisms, regenerative medicine, precision medicine, and cell treatment. Retinal organoids (ROs) consist of neural retina and retinal pigment epithelium (RPE). Brain organoids (BOs) consist of multiple neural lineage cells and contain fluid-filled ventricle-like structures surrounded by a ventricular/subventricular (VZ/SVZ) zone-like layer of neural stem cells (NSCs). The BO culture protocol could be further refined to culture-specific brain regions such as the cerebral cortex, forebrain, midbrain, hindbrain, brainstem, choroid plexus, cerebellum, thalamus, spinal cord, etc., in organoids. This editorial article frames the aim of this Research Topic as gathering promising, recent, and novel research trends on modeling central nervous system (CNS) diseases using the retinal and brain organoids.

There are two main approaches to establishing ROs (Cheng and Kuehn, 2023) and many approaches for generating different regions of BOs (Mayhew and Singhania, 2023). The modification and improvement of these methods are continuously ongoing. One advantage of ROs and BOs is that we can control the specificity of cell populations and maturity by timing the culture system.

For the 3-dimensional (3D) organoids, quantifying and analyzing multidimensional data for the complex *in vitro* models (organoids, organ-on-chip) is difficult. Kegeles et al.'s paper introduced a deep learning-based computer algorithm to recognize and predict RO differentiation based on bright-field imaging. This paper leverages a machine-learning tool (convolutional neural networks, CNNs) to analyze images. Image acquisition and analysis are universal, robust, and non-invasive and can generate quantitative, decision-making data to assess retinal differentiation without chemical probes or reporter gene expression.

The patient-derived organoids can be grown to model developmental diseases. Eintracht et al. and Vielle et al. reviewed the use of human induced pluripotent stem cells (hiPSC)-derived ROs to model developmental eye disorders such as microphthalmia caused by a VSX2 variant. Eintracht et al. also reviewed the spatiotemporal gene expression patterns and interactions between the embryonic germ layers during vertebrate eye development. Vielle et al. reviewed the limitations of the ROs to model eye developmental disorders, such as RPE not juxtaposed to the apical side of the neural retina, no optic nerve (retinal ganglion cells dying as ROs mature), no macula formation, lack of microglia, no yolk sac derivatives that invade the optic cup during the period of retinogenesis *in vivo*, and absence blood vessels. ROs are neuroectodermal derivatives and will not have mesodermal original cells or tissues.

ROs can be an effective platform for identifying molecular therapeutic targets and for future clinical applications. Singh and Nasonkin pointed out that the implicit limitation of ROs is the absence of a uniform layer of RPE and the direct exposure of most photoreceptors in the developing organoids to neural medium. Li et al. reviewed the methods to augment RO production, reduction of RO heterogeneity, and transplantation of RO-derived retinal ganglion cells and photoreceptors. Garita-Hernandez et al. generated a hiPSC line with enhanced gene expression in cone cells using a 1.7-kb L-opsin promoter. They fused the red-shifted opsin Jaws with a fluorescent reporter gene driven by an L-opsin promoter, enabling enriched cell sorting of the cone cells. This study underscores the importance of promoter activity in restricting, improving, and controlling the kinetics of transgene expression during the maturation of ROs. Ning et al. explored an approach to selecting and expanding the Müller glial cells (MGCs) from hiPSC-derived ROs. ROs older than 120 days are an optimal source for enriching MGCs with high purity and expansion ability. MGCs could be passaged at least 10 times serially, yielding large numbers of cells in a relatively short period of time.

Speaking of BOs, cortical organoids can be used to model Alzheimer's disease (AD) in Down syndrome (DS). Zhao and Haddad found DS patient iPSC-derived cortical organoids have much higher amyloid beta (Aß) immunoreactivity, a significantly higher number of amyloid plaques, an increased Tau phosphorylation (pTau S396) and insoluble Tau/total Tau in DS organoids than control organoids. They found the signature of AD is present in DS much earlier than predicted, even in early fetal brain development.

Parkinson's disease (PD) is a progressive neurodegenerative disease, being the second most common after AD (Parkinson's Foundation, 2023). Midbrain dopaminergic (DA) neurons are selectively lost in PD. The presynaptic neuronal protein alpha-synuclein (α-syn), which tends to accumulate and aggregate in PD brains as Lewy bodies, is the key driver of PD. Therefore, preventing the propagation of α-syn could slow PD progression. However, multiple cell types, such as astrocytes, microglia, and oligodendrocytes, are involved in α-syn deposition. Koh et al. proposed midbrain organoids are a promising platform for investigating α-syn accumulation, aggregation, and transmission in PD due to (1) dopaminergic neurons in organoids are far more mature than those in 2D; (2) genetically resembling the prenatal midbrain; (3) midbrain organoids contained spatially organized groups of dopaminergic neurons with other neuronal, astroglial, and oligodendrocyte cells also being differentiated, which could permit the study of how these cell types interplay with each other; and (4) they contain both mature and aged neurons, which is more clinically relevant. The authors also proposed to co-culture PD iPSC-derived neurons with healthy neurons, either in 2D or as organoids, to study α-syn propagation.

Since Lancaster et al. (2013) reported the first method of human cerebral organoids containing ventricles and neural layers of the cerebral cortex, a great effort has been put into human BO development and disease modeling. However, neural circuit formation with BOs has rarely been investigated. A paper published in this Research Topic raises the challenges in modeling human neural circuit formation using the BOs. Matsui et al. used fused organoids to study the neural circuit, such as glutamatergic excitatory neuron-rich cerebral organoids fused with GABAergic interneuron-rich subpallium organoids to model neuronal migration between distant components. Human cerebral organoids fused with thalamic organoids are also used to model the thalamocortical circuit involved in transmitting sensory and motor information in the human brain. They pointed out that the current organoids possess multiple randomly positioned neural tube-like structures and, therefore, lack a fixed structural axis. As such, organoids don't have gradients of molecules that are required for proper neuronal migration, axonal guidance, and synapse formation that leads to circuit formation. The authors also stressed that the myeloid cells (such as microglia, vascular endothelial cells, and pericytes) in BOs might help study vasculature-mediated neural circuit formation.

To overcome organoid-to-organoid variability and batch-to-batch variation, Eigenhuis et al. developed a simplified protocol for the robust and reproducible generation of cortical organoids from hiPSC. The cortical organoids contain apical radial glial and intermediate progenitors, deep and upper layer neurons, and astrocytes. Unlike the "self-patterned" generation of cortical organoids, the authors used exogenous patterning factors to guide or direct region-specific identities in organoids.

In summary, ROs and BOs are promising and powerful research tools in CNS disease modeling. However, there are still challenges and limitations of ROs and BOs in the application that need to be tackled. Integrating with other technologies, such as organ-on-chip, omics, live imaging, machine learning, artificial intelligence, and asssembloids (different organoids co-cultured together), will broaden the utilization of ROs and BOs and provide unprecedented insight into CNS diseases.

Author contributions

LC: Writing—original draft. MC: Writing—review & editing. K-SC: Writing—review & editing. CM: Writing—review & editing.

Funding

The author(s) declare that no financial support was received for the research, authorship, and/or publication of this article.

Conflict of interest

The authors declare that the research was conducted in the absence of any commercial or financial relationships that could be construed as a potential conflict of interest.

The author(s) declared that they were an editorial board member of Frontiers, at the time of submission. This had no impact on the peer review process and the final decision.

Publisher's note

References

Cheng, L., and Kuehn, M. H. (2023). Human retinal organoids in therapeutic discovery: a review of applications. *Handb. Exp. Pharmacol.* 281, 157–187. doi: 10.1007/164_2023_691

Lancaster, M. A., Renner, M., Martin, C. A., Wenzel, D., Bicknell, L. S., Hurles, M. E., et al. (2013). Cerebral organoids model human brain development and microcephaly. *Nature* 501, 373–379. doi: 10.1038/nature12517

Mayhew, C. N., and Singhania, R. (2023). A review of protocols for brain organoids and applications for disease modeling. *STAR Protoc.* 4:101860. doi: 10.1016/j.xpro.2022.101860

Parkinson's Foundation (2023). Available online at: https://www.parkinson.org/understanding-parkinsons/statistics (accessed December 20, 2023).

frontiers in Cellular Neuroscience

MINI REVIEW
published: 09 November 2018
doi: 10.3389/fncel.2018.00413

Patient-Derived Induced Pluripotent Stem Cells and Organoids for Modeling Alpha Synuclein Propagation in Parkinson's Disease

Yong Hui Koh[1,2], *Li Yi Tan*[1] *and Shi-Yan Ng*[1,2,3,4]*

[1] *Institute of Molecular and Cell Biology, Singapore, Singapore,* [2] *Department of Physiology, Yong Loo Lin School of Medicine, National University of Singapore, Singapore, Singapore,* [3] *National Neuroscience Institute, Singapore, Singapore,* [4] *The Third Affliated Hospital of Guangzhou Medical University, Guangzhou, China*

Parkinson's disease (PD) is an age-associated, progressive neurodegenerative disorder characterized by motor impairment and in some cases cognitive decline. Central to the disease pathogenesis of PD is a small, presynaptic neuronal protein known as alpha synuclein (a-syn), which tends to accumulate and aggregate in PD brains as Lewy bodies or Lewy neurites. Numerous *in vitro* and *in vivo* studies confirm that a-syn aggregates can be propagated from diseased to healthy cells, and it has been suggested that preventing the spread of pathogenic a-syn species can slow PD progression. In this review, we summarize the works of recent literature elucidating mechanisms of a-syn propagation, and discussed the advantages in using patient-derived induced pluripotent stem cells (iPSCs) and/or induced neurons to study a-syn transmission.

Keywords: iPSCs, alpha synuclein (α-synuclein), lewy body disease, organoids, disease modeling

OPEN ACCESS

Edited by:
Alessandro Tozzi,
University of Perugia, Italy

Reviewed by:
Daniela Merlo,
Istituto Superiore di Sanità (ISS), Italy
Daniella Rylander Ottosson,
Lund University, Sweden

***Correspondence:**
Shi-Yan Ng
syng@imcb.a-star.edu.sg

Received: *11 June 2018*
Accepted: *23 October 2018*
Published: *09 November 2018*

Citation:
Koh YH, Tan LY and Ng S-Y (2018) Patient-Derived Induced Pluripotent Stem Cells and Organoids for Modeling Alpha Synuclein Propagation in Parkinson's Disease. Front. Cell. Neurosci. 12:413. doi: 10.3389/fncel.2018.00413

INTRODUCTION

Parkinson's disease (PD) is a progressive and chronic neurological disorder and the second most prevalent neurodegenerative disease after Alzheimer's disease, affecting an estimated seven to ten million people worldwide. Dopaminergic (DA) neurons in the substantia nigra par compacta (SNpc) are selectively lost in PD, leading to a constellation of motor deficits that include bradykinesia (slowed movements), tremors and muscle rigidity. In some patients, symptoms of dementia are also present. Approximately 15% of people with PD have a family history of the disease (termed familial PD) while the others are sporadic cases. Mutations in several genes are each associated with the occurrence of PD, including alpha synuclein (SNCA), leucine-rich repeat kinase 2 (LRRK2), and other autosomal recessive mutations in genes such as Parkin (PARK2), PTEN-induced putative kinase 1 (PINK1) and Protein/nucleic acid deglycase DJ-1 (PARK7), and has been extensively reviewed in Klein and Westenberger (2012). Although the exact cause for sporadic PD is yet to be identified, the largest risk factors for PD are genetics, advanced age and exposure to environmental toxins such as paraquat (Ascherio and Schwarzschild, 2016).

One of the pathological hallmarks of PD is the formation of intracellular inclusions termed Lewy bodies, which are caused by aggregates of a-syn protein. Multiple *in vivo* studies—both human and mouse—have confirmed that a-syn aggregates can be transferred from affected neurons to healthy neural cells (Kordower et al., 2008; Li et al., 2008; Pan-Montojo et al., 2012; Recasens et al., 2014). It is becoming increasingly appreciated that misfolded a-syn can transmit to anatomically connected areas (Braak et al., 2003), and this could explain why a substantial proportion of PD

patients also suffer from cognitive impairment, depression and psychosis. Several mechanisms of a-syn transmission have been proposed, including receptor-mediated endocytosis, direct cell-to-cell transfer through tunneling nanotubes or through a trans-synaptic pathway (Pan-Montojo et al., 2010; Luk et al., 2012b; Holmes et al., 2013; Abounit et al., 2016; Mao et al., 2016; Rostami et al., 2017). Although the mechanism of spread remains slightly controversial, it is well accepted that limiting the spread of a-syn aggregates can slow the progression of PD, and potentially prevent other PD-associated decline in cognitive functions.

In recent years, scientific advances in the field of induced pluripotent stem cells (iPSCs), direct reprogramming into induced neurons and the formation of neural organoids have enabled the modeling of PD using patient-derived cells, and opened up possibilities for the discovery of prognostic and therapeutic agents. Over the years, differentiation protocols have dramatically evolved to give rise to specific midbrain DA neuron populations that are lost in PD. From co-culture with mouse PA6 or MS5 stromal cells (Kawasaki et al., 2000; Perrier et al., 2004) that gave rise to low DA neuron yield, midbrain DA differentiation has now become more reproducible and efficient with chemically defined protocols (Kriks et al., 2011; Kirkeby et al., 2012; Doi et al., 2014; Paik et al., 2018). Disease modeling efforts by multiple groups worldwide has now uncovered that midbrain DA neurons derived from PD patients exhibit mitochondrial dysfunction and a-syn aggregation (Devi et al., 2008; Byers et al., 2011; Cooper et al., 2012; Imaizumi et al., 2012; Ryan et al., 2013; Flierl et al., 2014; Shaltouki et al., 2015; Chung et al., 2016; Kouroupi et al., 2017). iPSC-derived midbrain DA neurons are also useful for potential cell replacement therapies, an undertaking that is initiated by the GForce-PD group, a global team of scientists and clinicians that are committed to accelerate the translation of stem cell-based therapies to the clinic for Parkinson's disease human trials (Barker et al., 2015). While cell replacement therapy can correct the motor deficits in PD patients, it is unlikely to rectify the non-motor symptoms such as dementia, depression, delusions or hallucinations, which are common in advanced-staged PD patients. Therefore, slowing down PD progression remains an attractive therapeutic option. The focus of this mini-review will be to highlight the complexity of a-syn propagation and how iPSC-derived cell types and organoids can address some of this complexity.

ALPHA SYNUCLEIN PROPAGATION AS THE CENTRAL MECHANISM IN THE DEVELOPMENT OF PD

Lewy bodies and lewy neurites are the histological hallmark of PD. The main protein constituent of Lewy bodies and Lewy neurites is a-syn, a 140-amino acid presynaptic nerve terminal protein that comprises an amphipathic N-terminal alpha-helical domain, a hydrophobic center of non-amyloid beta component and a hydrophilic C-terminal domain. Under the native physiological state, a-syn does not have a defined structure and exists in an amorphic state. Although the exact functions of a-syn is still unknown, knockout studies have revealed roles of a-syn in synaptic vesicle release and trafficking, fatty acid binding, and the regulation of enzymes and transporters that are essential for neuronal survival (Sharon et al., 2001; Kanaan and Manfredsson, 2012; Stefanis, 2012). In the pathological state, a-syn becomes misfolded and therefore prone to aggregation. First, it forms soluble oligomers and then further aggregate into insoluble fibrils. These insoluble fibrils are made up of β-sheets consisting of two or more polypeptide chains connected by hydrogen bonds. Although the exact pathogenic form of a-syn is still debatable, recent studies suggest that soluble oligomers could be more toxic than insoluble fibrils (Karpinar et al., 2009; Winner et al., 2011); presumably because soluble oligomers can be transmitted more readily than insoluble fibrils. The misfolding, aggregation and accumulation of a-syn has serious neurotoxic implications (Stefanis et al., 2001; Tanaka et al., 2001; Snyder et al., 2003; Cuervo et al., 2004; Xilouri et al., 2009; Kamp et al., 2010; Nakamura et al., 2011), and is extensively reviewed in Lashuel et al. (2012). A-syn is also thought to be the pathogenic agent that underlies the progression of PD when toxic a-syn species transmit from diseased to healthy cells.

Braak and colleagues first suggested a prion-like mechanism in PD progression (Braak et al., 2003). They proposed that Lewy pathology spread through a stereotyped pattern of six stages, beginning from the peripheral nervous system of the gut and olfactory bulb and gradually progresses into the central nervous system. Within the brain, it spreads from the brainstem to the multiple cortical regions of the brain in a caudal-to-rostral fashion. Following on, in 2008, the serendipitous discoveries from two separate studies uncovered the presence of Lewy bodies in grafted neurons of PD patients whom have received transplantation a decade or two ago (Kordower et al., 2008; Li et al., 2008). Such observation further supports the prion-like spreading of a-syn in PD. Subsequently, many groups have attempted to recapitulate the prion-like capacity of a-syn in *in vivo* and *in vitro* models. The first few studies demonstrated the host-to-graft transfer of a-syn by transplanting neural stem cells or naïve rodent neurons into the brains of transgenic mice expressing human a-syn (Desplats et al., 2009; Hansen et al., 2011; Kordower et al., 2011; Angot et al., 2012). It was shown that human a-syn was taken up by the grafted cells and can act as a seeding template or a nucleation process to form aggregates with the intracellular mouse a-syn. In a unique mouse model that incorporates both preformed fibrils (PFFs) and a-syn overexpression, it was also shown that PFFs were necessary for the transmission of a-syn as simply overexpression of a-syn was not sufficient to result in the propagation phenomenon (Thakur et al., 2017). Other studies went even further to prove the prion-like capacity of a-syn when pathogenic a-syn were detected in neurons distant from the site of injection (Luk et al., 2012a,b; Mougenot et al., 2012; Rey et al., 2013; Sacino et al., 2013; Recasens et al., 2014; Peelaerts et al., 2015; Shimozawa et al., 2017).

The molecular mechanisms of a-syn propagation are slowly becoming unraveled. Detection of extracellular a-syn confirmed that cells secrete a-syn either as a naked entity or packaged

into exosomes and exocytosed (Emmanouilidou et al., 2010; Danzer et al., 2012). Soluble oligomeric and monomeric a-syn were readily detected in cell culture media, in a calcium-dependent manner (Emmanouilidou et al., 2010), suggesting that dysregulation in neuronal activity can impact a-syn exocytosis and propagation. In humans, monomeric and oligomeric a-syn are also detected in human blood plasma and cerebrospinal fluid (Borghi et al., 2000; El-Agnaf et al., 2006; Lee et al., 2006; Tokuda et al., 2006), with increased levels of oligomeric a-syn in PD patients (El-Agnaf et al., 2006). It is also shown that elevated a-syn burden, caused by increased a-syn production (through overexpression or duplication and triplication mutations), or reduced clearance through lysosomal or proteosomal systems, would increase a-syn exocytosis (Alvarez-Erviti et al., 2011; Lee et al., 2013; Fernandes et al., 2016). Extracellular a-syn can interact with different surface proteins on the cells that facilitate its uptake via receptor-mediated endocytosis. Heparan sulfate proteoglycan interact with a-syn fibrils and induce uptake via macropinocytosis (Holmes et al., 2013). By means of a proteomics screen, Mao et al. (2016) has identified a few surface proteins that interact well with preformed fibrils (PFFs) of a-syn (Mao et al., 2016). Lymphocyte-activation gene 3 (LAG3) was one receptor found to have the strongest interaction specifically to a-syn PFFs but not monomers. LAG3, a transmembrane protein, facilitates the uptake of a-syn PFFs in neighboring neurons, astrocytes and microglial via endocytosis. Through genetic knockdown and antibody-blocking intervention, uptake of a-syn was reduced, which led to decreased neuronal toxicity and inter-neuronal propagation *in vitro* and *in vivo* (Mao et al., 2016).

One major caveat of the abovementioned studies is the assumption that fibrillar forms of a-syn are present extracellularly. Indeed, a-syn has been detected in human cerebrospinal fluid (CSF) exosomal vesicles (Alvarez-Erviti et al., 2011; Danzer et al., 2012; Stuendl et al., 2016), but these are mainly soluble a-syn monomers or oligomers. It is not clear whether fibrillar forms of a-syn are present extracellularly.

VARIOUS NEURAL CELL TYPES CONTRIBUTE TO ALPHA SYNUCLEIN PATHOLOGY

Alpha synuclein deposits are also found in astrocytes at advanced disease stages (Braak et al., 2007) and in oligodendrocytes as glial cytoplasmic inclusions (Ubhi et al., 2011). This means that pathogenic a-syn can also be transferred from neurons to other cell types such as astrocytes and oligodendrocytes. Astrocytes have been observed to take up extracellular a-syn *in vitro* (Lee et al., 2010; Fellner et al., 2013; Rannikko et al., 2015; Lindström et al., 2017). Glial cytoplasmic inclusions develop despite the lack of a-syn mRNA in oligodendrocytes (Miller et al., 2005), suggesting that a-syn is not produced by the oligodendrocytes but rather internalized from the external microenvironment. Studies have shown that monomeric and oligomeric forms in a-syn are internalized by oligodendrocytes *in vitro* (Kisos et al., 2012; Konno et al., 2012) and *in vivo* (Reyes et al., 2014) with suggestions of dynamin-mediated mechanisms involved in the uptake. Overall, the role of astrocytes and oligodendrocytes in pathogenic a-syn propagation or PD disease progression remain largely unknown. Studies by Abounit et al. (2016) proposed a model for propagation of pathogenic a-syn species by interneuronal transfer of fibrillar a-syn-laden lysosomes. a-syn PFFs within specialized cellular structures known as tunneling nanotubes (TNTs) were detected and these can seed soluble a-syn aggregation in the cytosol of recipient cells (Abounit et al., 2016). Apart from interneuronal TNTs, inter-astrocytic TNTs also spread a-syn aggregates. Using human embryonic stem cell-derived astrocytes, Rostami et al. (2017) demonstrated that failure of diseased astrocytes to degrade a-syn PFFs led them to unload their burden to surrounding astrocytes through TNTs (Rostami et al., 2017).

It is postulated that astrocytes and microglia play key roles in clearance of toxic a-syn species from the extracellular environment, and consistent with this notion, astrocytes are capable of extensive uptake of a-syn oligomers, which they then attempt to degrade via the lysosomal pathway (Lindström et al., 2017). Incomplete degradation caused by a-syn overburden can result in cellular damage in recipient astrocytes, including lysosomal defects and mitochondrial damage. Internalization of a-syn has also been shown to cause astrocyte activation and neuroinflammation (Yu et al., 2018), which impacts neuronal survival. Microglia are the primary immune cells of the central nervous system, and are known to be activated by aggregated a-syn (Zhang et al., 2005). In particular, microglial phagocytosis of a-syn was thought to be a mechanism that promotes a-syn clearance. It has been reported by several studies that toll-like receptor 4 (TLR4) is required for a-syn dependent activation of microglia, and TLR4 ablation led to impaired microglia phagocytosis and suppressed cytokine release, enhancing neurodegeneration in those mice (Stefanova et al., 2011; Fellner et al., 2013).

Taken together, these are key evidence supporting the notion that propagation of a-syn is a key driver underlying PD pathogenesis and progression; and that interaction between multiple cell types regulate this process. Therefore, cellular systems using neuroblastoma cell lines (such as mouse Neuro-2a and human SH-SY5Y) or neural stem cell lines do not recapitulate the complexity of a-syn propagation. Animal models are also valuable tools for studying a-syn propagation. To this end, wild-type mice with a single inoculation of a-syn fibrils or pathological a-syn purified from postportem PD brains showed a-syn propagation to anatomically connected brain regions (Luk et al., 2012b; Blesa and Przedborski, 2014; Masuda-Suzukake et al., 2014; Recasens et al., 2014) that is reviewed in Blesa and Przedborski (2014). Though important, the conservation of a-syn transmission between mouse and human has to be established, and that eventual drug screening approaches would be more feasible and have a high throughput if performed in cultured human cells. Therefore, we propose that human induced pluripotent stem cell (iPSC)-derived neurons and neural organoids are ideal cellular platforms for studying a-syn pathology.

INDUCED PLURIPOTENT STEM CELLS AND MIDBRAIN DIFFERENTIATION

Induced pluripotent stem cells or iPSCs revolutionize the way human diseases are modeled *in vitro*. iPSCs are typically skin or blood cells genetically reprogrammed to revert back to an embryonic stem cell (ESC)-like state by ectopic expression of ESC transcription factors OCT4, SOX2, c-MYC and KLF4 (Takahashi and Yamanaka, 2006). Several methods of reprogramming iPSCs have now been described (Takahashi and Yamanaka, 2006; Carey et al., 2009; Sommer et al., 2009; Somers et al., 2010) and are also summarized in **Table 1** and reviewed in Malik and Rao (2013) and Seki and Fukuda (2015). Importantly, these iPSCs behave like ESCs with the capacity to self-renew and retain its pluripotency. iPSCs also retain the genetic mutations from their donors, making these attractive cellular models for modeling human diseases. Thus far, human iPSCs has become a promising tool to address the ethical issues of handling embryonic material, clinical applications for personalized treatments, and research applications as model systems to investigate human diseases in the fields of neuro-developmental and degenerative diseases (Ardhanareeswaran et al., 2017).

For meaningful disease modeling, one of the greatest hurdles is to be able to produce large amounts of the cell type of interest with high efficiency and reproducibility. One of the earliest methods of deriving DA neurons from ESCs was to co-culture with stromal feeder cells MS5 or PA6 (Kawasaki et al., 2000; Perrier et al., 2004). This stromal co-culture method, however, was chemically undefined, resulting in a heterogeneous population of neurons with overall low DA neuron yield, and the physical co-culture of human iPSCs with mouse stromal cells made it undesirable for downstream analyses or applications. The labs of Lorenz Studer and Malin Parmar have made significant progress in a chemically defined protocol for efficient differentiation of midbrain DA neurons. These methods made use of the knowledge on developmental patterning to efficiently differentiate iPSCs into midbrain-regionalized floorplate progenitor cells (Fasano et al., 2010; Kirkeby and Parmar, 2012) using chemical inhibitors of SMAD signaling (achieved by LDN-193189 and SB431542), early high-dose Sonic Hedgehog (SHH) pathway agonists (such as Purmorphamine or recombinant SHH) and partial glycogen synthase kinase (GSK) inhibitors/Wnt activation (by CHIR99021) (Cooper et al., 2010; Devine et al., 2011; Kriks et al., 2011; Kirkeby et al., 2012). This revised strategy produces midbrain DA neurons that expresses the specific forehead box protein A2 (FOXA2) and LIM Homeobox Transcription Factor 1 Alpha (LMX1A) markers and demonstrates efficient dopamine release *in vitro* (Kirkeby et al., 2012) and *in vivo* after transplantation (Kriks et al., 2011).

However, even with a chemically-defined approach, a heterogeneous mix of both substantia nigra pars compacta (SNpc or A9-subtype) and ventral tegmental area (VTA or A10-subtype) DA neurons are produced, and it remains a challenge to derive only A9 DA neurons—the neuronal subtype that is lost in PD. Previous work from the laboratories of Ole Isacson and Thomas Perlmann showed that the transcription factor Orthodenticle Homeobox 2 (Otx2) is a marker, and controls the specification of mouse A10 VTA DA neurons, while Sox6 defines the A9 SNpc DA neurons (Panman et al., 2014). SOX6 is also shown to localize to neuromelanin and Tyrosine hydroxylase (TH)-positive neurons in the human SNpc (Panman et al., 2014). A recent article that made use of single cell RNA profiling confirmed that Sox6 and Otx2 mark SNpc and VTA neurons respectively, while also adding a panel of genes specific to SNpc vs. VTA that they found from single cell RNA-seq (Poulin et al., 2014). This genetic information would be helpful in subsequent efforts to direct A9 DA neuron-specific differentiation. One possibility is to overexpress SOX6, or knockdown OTX2 expression in iPSC-derived floorplate cells as they differentiate into neurons. It has previously been shown in mice that ablation of Otx2 results in severely diminished VTA DA neuron differentiation (Di Giovannantonio et al., 2013) but it remains to be determined if overexpression of SOX6 and/or knockdown of OTX2 will drive the SNpc DA neuron transcriptional program in human iPSC-derived cultures.

BRAIN ORGANOIDS AND DISEASE MODELING

More recently, the ability to generate three-dimensional (3D) neural organoids has challenged the way we think about conventional cellular differentiation and disease modeling approaches. The two-dimensional approach to differentiate cells forces cells into a monolayer that is uniformly exposed to extracellular signals but does not represent their *in vivo* context, and does not fully maintain the complex cell-cell and cell-matrix interactions, resulting in the tendency to lose important physiological function. A landmark paper by Lancaster et al. (2013) showed that neural organoids mimick the cytoarchitecture of the developing cortex. The development of a protocol for brain-like organoids focused on two aims: the induction and differentiation of neural tissue and achieving a 3-D spatial organization that captures the development of specific brain regions. Firstly, iPSCs can be stimulated to form germ layers within iPSC aggregates known as embryoid bodies (EBs) (Evans, 2011). Specific media compositions are used to induce the formation of neural rosettes (Zhang et al., 2001) (polarized organization of epithelial cells) within the EBs. The subsequent change to differentiation medium (usually Neurobasal medium and B27 supplement for neuronal survival and differentiation with specific morphogens) facilitates the development of an organized neuroepithelium that would form various brain structures. Due to the absence of a basement membrane for the EBs to establish proper apical-basal polarity to form the neuroepithelium, an external structural support is required to ensure proper orientation of the neuroepithelium. For most organoid protocols, hydrogels (usually matrigel) are used to encapsulate the EBs to promote the accurate growth and formation of brain-like structures. When EBs are encapsulated within stagnant matrigel droplets, the diffusion of nutrients and oxygen is very poor causing death to the cells at the center of the organoids. Hence, after establishing the proper growth and

TABLE 1 | Gene delivery methods used for iPSC generation.

Methods	Types	Subtypes	Advantages	Disadvantages
Viral	Integrating	Lentiviral (Somers et al., 2010)	• Ability to infect non-dividing and proliferating cells i.e., somatic cells	• Incorporation of vector sequence into host genome • Solution: single cassette reprogramming vector • & cre/loxp mediated transgene excision e.g., STEMCCA
	Non-integrating	Adenovirus (Zhou and Freed, 2009)	• Does not integrate into host genome	• Very low reprogramming efficiency compared to lentiviral delivery
		Sendai virus (RNA virus) (Fusaki et al., 2009; Ban et al., 2011)	• Does not enter nucleus and gets diluted out of cells • Can produce large amounts of protein	• Difficult to remove replicating virus
Nonviral	mRNA transfection (Warren et al., 2010)		• No integration into host genome • Higher efficiency than original retroviral system • Commercially available	• Labor intensive • Technically complex
	miRNA transfection (Miyoshi et al., 2011; Subramanyam et al., 2011)		• Absence of breaks in existing genes • Avoids reactivation of transgenes	• No established reprogramming protocol available
	Transposons i.e., Piggybac (Kaji et al., 2009; Woltjen et al., 2009; Yusa et al., 2009)		• Highly active in mammalian cells • Vector can be removed from the host genome by expressing transposase	• Low reprogramming efficiency
	Episomal plasmids (Yu et al., 2009; Chen et al., 2011)		• No integration into host genome • More stable expression compared to standard plasmids	• Requires changes to cell culture methods
	Recombinant proteins (Kim et al., 2009; Zhou et al., 2009)		• Absence of breaks in existing genes • Avoids reactivation of transgenes	• Lower reprogramming efficiency compared to retroviral systems • Challenging to generate and purify
	Small molecules (Hou et al., 2013)		• Nonimmunogenic • Easy to handle	• No established protocol for human somatic cells

differentiation within the matrigel droplet, the organoids have to be cultured in a spinning bioreactor to increase diffusion efficiency that promotes tissue survival. Neural organoids can capture the key features of the human brain such as ventricle-like spaces, distinct proliferative layers of cells, and the choroid plexus (Marton and Paşca, 2016); offering a great potential to be used as models of neurodevelopmental and neurodegenerative conditions. Furthermore, protocols have already been established for various brain regions such as cerebral (Lancaster and Knoblich, 2014; Muguruma et al., 2015), forebrain (Qian et al., 2016), and midbrain (Jo et al., 2016) organoids.

Although mostly used to model neurodevelopmental diseases, neural organoids can also be extremely useful for modeling a degenerative disorder such as PD. Since organoids mimick the brain's microenvironment, it has been postulated that culturing of neurons in such a 3D microenvironment would promote their maturation. Jo et al. (2016) reported the generation of a midbrain organoid with A9 neurons that produces neuromelanin (a dark pigment expressed in the SNpc of humans). So far, none of the 2D differentiation protocols have given rise *in vitro* to neuromelanin-producing DA neurons. Of significance, the accumulation of neuromelanin in DA neurons increases with age, suggesting that DA neurons in organoids are far more mature than those in 2D. Comparisons of gene expression between DA neurons cultured in 2D vs. 3D organoids also suggest that neurons in organoids are more mature, expressing dopamine transporter (DAT or SLC1A3) (Jo et al., 2016; Monzel et al., 2017), and genetically resembling the prenatal midbrain (Jo et al., 2016). Recently, Monzel et al. (2017) managed to derive midbrain-specific organoids that contained spatially-organized groups of dopaminergic neurons with other neuronal, astroglial, and oligodendrocyte differentiation. Functionally, they detected the presence of synaptic connections and electrophysiological activity. Since PD is an age-onset neurodegenerative disorder, it is critical to model cellular and molecular aspects of the disease with mature and aged neurons rather than neurons of an embryonic resemblance. Moreover, the heterogeneity of cell types within midbrain organoids would be useful to study the interplay and contributions of other cell types to the a-synuclein pathology of PD. As such, midbrain organoids are a very promising platform for investigating late phenotypes associated with PD–a unique feature that 2D culture models cannot offer.

DIRECT REPROGRAMMING OF FIBROBLASTS INTO INDUCED DOPAMINERGIC NEURONS (IDANS)

Apart from differentiation of iPSCs toward DA neurons that mimic neural developmental processes, overexpression of key transcription factors in patient-derived fibroblasts can be directly transdifferentiated into neurons, including midbrain DA neurons

(Xu et al., 2017). Wernig and colleagues have reported viral-based transdifferentiation of mouse and human fibroblasts into induced neurons (iNs) by overexpressing up to four neuronal transcription factors, namely, achaetescute homolog 1 (ASCL1), BRN2 (also known as POU3F2), myelin transcription factor 1-like protein (MYT1L) and neuronal differentiation 1 (NEUROD1) (Vierbuchen et al., 2010; Pang et al., 2011). These iNs obtained were morphologically and electrophysiologically similar to bona fide neurons, and resembled excitatory neurons of the cerebral cortex (Heinrich et al., 2014). Building onto this knowledge of direct reprogramming, it has also been shown that midbrain DA neurons can be directly converted from fibroblasts. To do so, several groups have reported direct reprogramming of DA neurons using a cocktail of transcription factors specific to the midbrain lineage (**Table 2**). The factors that were used for induced DA neurons (iDANs) are extensively reviewed in Jang and Jung (2017). Overall, regardless of the combination of transcription factors used, the efficiency of iDAN conversion from fibroblasts is typically below 20%, even though iDANs demonstrated spontaneous and rebound action potentials which are characteristics of midbrain DA neurons *in vivo*. This low efficiency of conversion is potentially a limiting factor for disease modeling studies especially when large numbers of cells are required for high throughput screening. Recently, this hurdle has been overcome by a reprogramming strategy that involves ASCL1, LMX1A, and NURR1 in combination with p53-small hairpin RNA (shRNA) and miR-124, as well as small molecule and trophic factor supplements that maintain the identity and survival of midbrain DA neurons (Jiang et al., 2015). This transdifferentiation approach resulted in more than 50% TH^+ iDANs, and it was concluded from this study that G1 arrest was crucial for efficient transdifferentiation, and that addition of patterning small molecules such as SB431542, CHIR99021, Purmorphamine (SHH pathway agonist), Dorsomorphin and trophic factors significantly enhanced reprogramming efficiency.

Another method for generating DA neurons from patient fibroblasts is to derive expandable dopaminergic precursors known as floorplate progenitor cells. This has been achieved in mouse fibroblasts by ectopic expression of Brn2, Sox2, and FoxA2 (Tian et al., 2015), resulting in acquisition of floorplate identity which include expression of Otx2, Corin and Lmx1a expression. Induced floorplate progenitors generated with this method were shown to differentiate primarily into TH^+ midbrain DA neurons (with more than 90% efficiency), even without addition of Shh and Fgf8. Although this has not been demonstrated for human cells, we expect similar results based on previous iN studies where

TABLE 2 | List of different strategies used to derive induced dopaminergic neurons. Adapted and revised from Jang and Jung (2017).

No.	Type of transdifferentiated cells	Transcription factors	miRNA	Small molecules	TH+ differentiation efficiency	Characterization tests	References
1	Human induced dopaminergic neurons (iDAN)	Ascl1, Brn2, Myt1l, Lmx1a and FoxA2	N/A	N/A	∼10%	Expression of dopaminergic neuron markers and electrophysiological profile of functional dopaminergic neurons	Pfisterer et al., 2011
2	Mouse and human iDAN	Ascl1, Lmx1a and Nurr1	N/A	N/A	∼15%-20%	Expression of dopaminergic neuron markers, electrophysiological profile of functional dopaminergic neurons and dopamine release	Caiazzo et al., 2011
3	Mouse iDAN	Ascl1, Lmx1b and Nurr1	N/A	N/A	∼18%	Expression of dopaminergic neuron markers, electrophysiological profile of functional dopaminergic neurons and dopamine release	Addis et al., 2011
4	Mouse iDAN	Ascl1, Pitx3, Lmx1a, Nurr1, FoxA2 and EN1	N/A	Sonic hedgehog (Shh) and fibroblast growth factor 8 (FGF8)	∼7%	Expression of dopaminergic neuron markers, electrophysiological profile of functional dopaminergic neurons, dopamine release and relief PD-like symptoms in PD mice	Kim et al., 2011
5	Human iDAN	Ascl1, Ngn2, Sox2, Nurr1 and Pitx3	N/A	N/A	∼40%	Expression of dopaminergic neuron markers, dopamine uptake and release, electrophysiological profile of functional dopaminergic neurons and relief PD-like symptoms in PD mice	Liu et al., 2012
6	Human iDAN	Ascl1, Lmx1a and Nurr1	miR124	p53 suppressor, G1 cell cycle arrest and Tet1 agonist	∼60%	Expression of dopaminergic neuron markers, DA uptake and release, electrophysiological profile of functional dopaminergic neurons	Jiang et al., 2015
7	Mouse induced neural progenitor cells (iNPCs) with midbrain identity	Foxa2, Brn2 and Sox2	N/A	N/A	∼90%	Expression of dopaminergic neuron proliferative progenitor cell markers, capable of deriving functional dopaminergic neurons and to rescue MPTP-lesioned mice	Tian et al., 2015

the same reprogramming factors worked similarly in mouse and human cells. If so, this could be an ideal method for disease modeling because large numbers of DA neurons can be derived from these self-renewing induced floorplate progenitors.

Although transdifferentiation technologies may not be compatible with neural organoid formation, because directed reprogramming forces fibroblasts to take on a specific cell fate rather than allow for a "self-organizing" approach that is important for organoid formation, there are distinct advantages in using iNs for disease modeling. Two recent studies (Mertens et al., 2015; Huh et al., 2016) found that iNs from aged fibroblasts retained the aging cellular and molecular characteristics while iPSCs made from the same patient fibroblasts were epigenetically reprogrammed to erase the aging signatures and subsequent neurons differentiated from these iPSCs did not acquire aging characteristics. Since PD is an age-onset neurodegenerative disease, iNs that retain aged signatures could be an especially relevant cellular model to understand the role of aging in neuronal decline. It is unclear, however, if induced floorplate progenitors retain aged cellular signatures that also make them suitable models for studying aged-associated neuronal decline.

IPSC-DERIVED MIDBRAIN CULTURES AS AN *IN VITRO* MODEL OF A-SYN TRANSMISSION

Despite numerous *in vivo* and *in vitro* studies that were discussed in the previous sections demonstrating transmission and propagation of a-syn in PD pathology, there is still a lack of a robust and reproducible *in vitro* model that could allow us to accurately study its role in PD pathogenesis. As such, it makes it even more difficult to screen for potential therapeutic compounds that could halt PD progression.

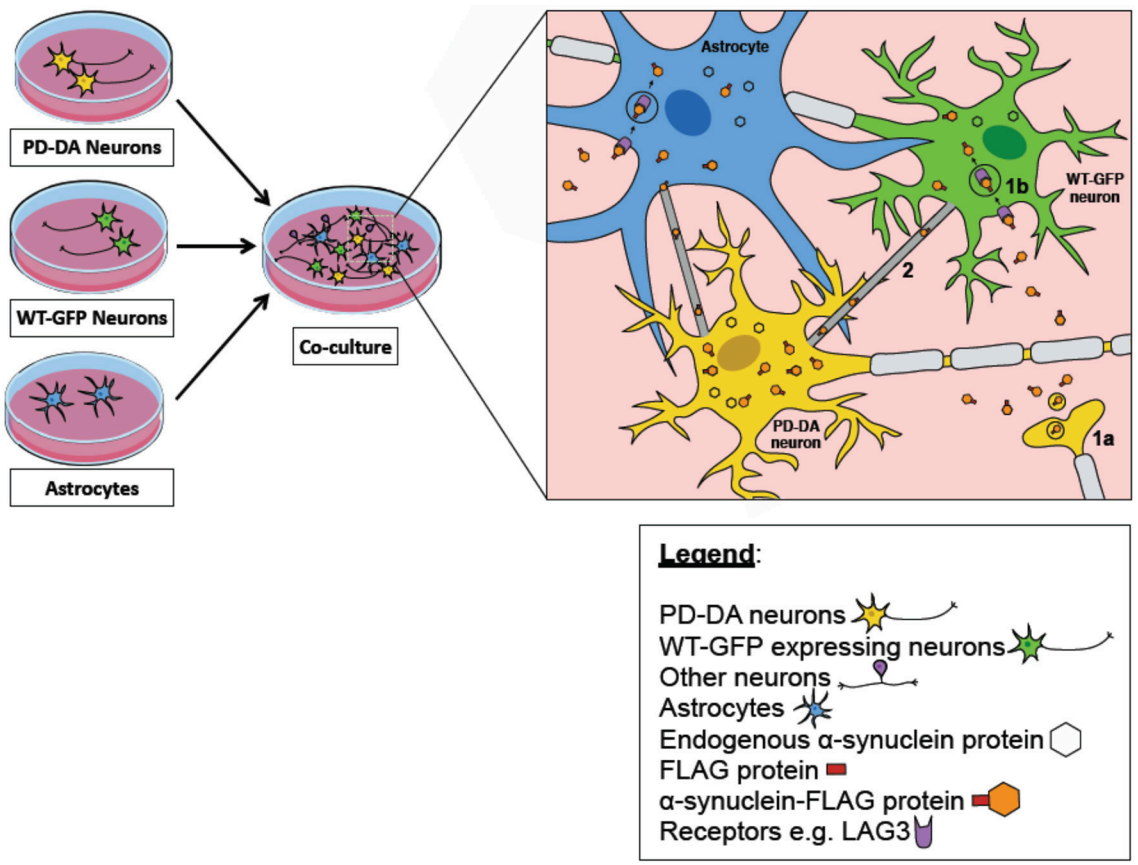

FIGURE 1 | iPSC-derived midbrain cultures as an *in vitro* model of alpha synuclein transmission. A co-culture model of PD-DA neurons (cells in yellow), WT-GFP neurons (cells in green), and astrocytes (in blue) can be used to track the transfer of pathogenic alpha-synuclein (orange hexagon) between diseased and healthy neurons/astrocytes. PD-DA neurons are derived from the iPSCs of PD patients with their alpha synuclein tagged with a FLAG protein (red rectangle). WT-GFP neurons are derived from the iPSCs of healthy subjects and are constitutively expressing GFP as a reporter–the successful transmission of alpha-synuclein between diseased and healthy neurons can be defined as GFP-expressing cells co-expressing the FLAG signal. Several mechanisms have been postulated to be involved in the propagation of diseased alpha-synuclein to healthy neurons/astrocytes. One mechanism describes that pathogenic alpha synuclein secreted by PD-DA neurons (1a) could interact with various surface proteins on healthy neurons/astrocytes to induce uptake through receptor-mediated endocytosis (1b), for example LAG3 receptor. Furthermore, there are also specialized structures known as tunneling nanotubes (TNTs) between neuron-neuron and neuron-astrocytes that are involved in the spread of alpha synuclein (2).

One obvious advantage of patient-derived iPSCs is that the iPSCs can be differentiated into disease-relevant DA neurons, and phenotypes observed in these *in vitro* neurons are well correlated with clinical observations (Torrent et al., 2015). Apart from being an endless source of midbrain DA neurons, using patient-derived cells (with their specific mutations) removes the need to rely on an artificial overexpression system that is not representative of PD pathology. Recent advances in the CRISPR/Cas9 technology has greatly availed genome-editing strategies to stem cell labs to create isogenic pairs of iPSCs. These typically take the form of "corrected iPSCs" where the disease-causing mutation is corrected to become wild-type, or "mutation-introduced iPSCs," where wild-type iPSCs have their genomic DNA altered into a known disease-causing mutation (Soldner et al., 2011; Hockemeyer and Jaenisch, 2016; Bassett, 2017). The rationale for generating isogenic pairs of iPSCs is to minimize genetic variation that is inherent between different individuals and/or cell lines, and is crucial in disease modeling studies to identify disease-related molecular and cellular events.

Importantly, a-syn aggregation has been observed in DA neurons derived from PD iPSCs. By differentiating a-syn A53T iPSCs into midbrain DA neurons, Kouroupi et al. (2017) detected the presence of the pathological form of a-syn that is phosphorylated on serine 129 in the dendrites of PD neurons, reminiscent of Lewy neurites in PD patients (Kouroupi et al., 2017). Protein aggregates, as revealed by Thioflavin S staining, also showed high concentrations of a-syn and such inclusion bodies were observed in the cell bodies as well as along neurites. iPSCs derived from patients with PINK1 and Parkin mutations also differentiate into midbrain DA neurons that showed a time-dependent increased a-syn accumulation (Chung et al., 2016). It was also demonstrated that mutant PINK1 and Parkin DA neurons had significantly more insoluble a-syn protein, indicative of aggregated a-syn. These studies have proven that important cellular features of PD are recapitulated in iPSC-derived neurons, similar to what has been observed for other neurodegenerative diseases.

Critically, what has not been elucidated in these iPSC studies is the transmission and propagation of endogenous a-syn aggregates. While important discoveries pertaining to mechanistic spread of a-syn have been made using exogenously-added PFFs, this approach over-simplifies the physiological conditions in which a-syn isoforms exist. Therefore, it remains to be determined if LAG3 or heparan sulfate proteoglycan reduction can protect neurons against a-syn propagation. It would also be important to establish that TNTs transport endogenously-formed a-syn aggregates from host to recipient cells in iNs or iPSC-derived cultures. We propose that these endogenous propagation studies can be performed by co-culturing PD iPSC-derived neural cultures with healthy neural cultures, either in 2D or as organoids (**Figure 1**). One possible method to track a-syn transfer from diseased to healthy cells, a-syn from PD patients has to be tagged with a small reporter protein such as Y-FAST (Plamont et al., 2016), while healthy cells should express a different reporter such as constitutive expression of CFP. Successful transmission events would then be defined as CFP-expressing cells co-stained with Y-FAST. It also remains to be discovered whether monomeric, oligomeric or fibrillar forms of a-syn are transmitted from host to recipient cells.

An advantage of organoid models vs. conventional 2D cultures is that the cytoarchitecture of cells in organoids closely resemble that of a brain—which may enhance neuronal maturation and/or function that promotes aggregate transmission. Since PD is an age-onset neurodegenerative disease, it is also likely that the maturation status of neurons is critical for a-syn transmission. Neurons grown in 3D cultures are also known to be more mature (Jo et al., 2016), and accumulate aggregates (Choi et al., 2014). The heterogeneity of neural cells in organoids is also an ideal system for studying selective neuronal vulnerability in PD. In particular, there are key questions left unanswered: Are specific neural types (astrocytes, DA neurons or other neuronal subtypes) more susceptible to a-syn transmission? What is the molecular signature of neurons with a-syn aggregates? Will attenuating key molecular events downstream of a-syn transmission protect neurons from cell death? Single-cell RNA-seq data of organoid-derived neural cells are expected to give us insights to some of these questions.

CONCLUDING REMARKS

Alpha synuclein accumulation, aggregation and transmission are key events in the pathology of PD, and strategies to prevent any of these events are thought to be able to slow down disease progression. Patient-derived iPSCs, coupled with the use of genome-editing tools, have become powerful tools in disease modeling, but its utility in modeling a-syn propagation has not been explored. In this review, we present a point-of-view that iNs and iPSC-derived neurons can be a physiologically relevant, all-in-one model that provides the opportunity to study a-syn accumulation, aggregation and transmission concurrently.

AUTHOR CONTRIBUTIONS

All three authors wrote the manuscript. LYT designed the graphics. S-YN edited the manuscript.

ACKNOWLEDGMENTS

We thank Winanto for assistance with graphics. YHK is a recipient of the NUS Research Scholarship (YLL School of Medicine/Physiology). This work is funded by the Institute of Molecular and Cell Biology (Biomedical Science Institutes) and the National Medical Research Council (Grant ID: NMRC/OFYIRG/0011/2016).

REFERENCES

Abounit, S., Bousset, L., Loria, F., Zhu, S., de Chaumont, F., Pieri, L., et al. (2016). Tunneling nanotubes spread fibrillar alpha-synuclein by intercellular trafficking of lysosomes. *EMBO J.* 35, 2120–2138. doi: 10.15252/embj.201593411

Addis, R. C., Hsu, F. C., Wright, R. L., Dichter, M. A., Coulter, D. A., and Gearhart, J. D. (2011). Efficient conversion of astrocytes to functional midbrain dopaminergic neurons using a single polycistronic vector. *PLoS ONE* 6:e28719. doi: 10.1371/journal.pone.0028719

Alvarez-Erviti, L., Seow, Y., Schapira, A. H., Gardiner, C., Sargent, I. L., Wood, M. J., et al. (2011). Lysosomal dysfunction increases exosome-mediated alpha-synuclein release and transmission. *Neurobiol Dis.* 42, 360–367. doi: 10.1016/j.nbd.2011.01.029

Angot, E., Steiner, J. A., Lema Tomé, C. M., Ekström, P., Mattsson, B., Björklund, A., et al. (2012). Alpha-synuclein cell-to-cell transfer and seeding in grafted dopaminergic neurons *in vivo*. *PLoS ONE* 7:e39465. doi: 10.1371/journal.pone.0039465

Ardhanareeswaran, K., Mariani, J., Coppola, G., Abyzov, A., and Vaccarino, F. M. (2017). Human induced pluripotent stem cells for modelling neurodevelopmental disorders. *Nat. Rev. Neurol.* 13, 265–278. doi: 10.1038/nrneurol.2017.45

Ascherio, A., and Schwarzschild, M. A. (2016). The epidemiology of Parkinson's disease: risk factors and prevention. *Lancet Neurol.* 15, 1257–1272. doi: 10.1016/S1474-4422(16)30230-7

Ban, H., Nishishita, N., Fusaki, N., Tabata, T., Saeki, K., Shikamura, M., et al. (2011). Efficient generation of transgene-free human induced pluripotent stem cells (iPSCs) by temperature-sensitive Sendai virus vectors. *Proc. Natl. Acad. Sci. U S A.* 108, 14234–14239. doi: 10.1073/pnas.1103509108

Barker, R. A., Studer, L., Cattaneo, E., Takahashi, J., and G-Force PD consortium (2015). G-Force PD: a global initiative in coordinating stem cell-based dopamine treatments for Parkinson's disease. *NPJ Parkinsons Dis.* 1:15017. doi: 10.1038/npjparkd.2015.17

Bassett, A. R. (2017). Editing the genome of hiPSC with CRISPR/Cas9: disease models. *Mamm. Genome.* 28, 348–364. doi: 10.1007/s00335-017-9684-9

Blesa, J., and Przedborski, S. (2014). Parkinson's disease: animal models and dopaminergic cell vulnerability. *Front. Neuroanatomy* 8:155. doi: 10.3389/fnana.2014.00155

Borghi, R., Marchese, R., Negro, A., Marinelli, L., Forloni, G., Zaccheo, D., et al. (2000). Full length alpha-synuclein is present in cerebrospinal fluid from Parkinson's disease and normal subjects. *Neurosci. Lett.* 287, 65–67. doi: 10.1016/S0304-3940(00)01153-8

Braak, H., Del Tredici, K., Rüb, U., de Vos, R. A., Jansen Steur, E. N., and Braak, E. (2003). Staging of brain pathology related to sporadic Parkinson's disease. *Neurobiol. Aging.* 24, 197–211. doi: 10.1016/S0197-4580(02)00065-9

Braak, H., Sastre, M., and Del Tredici, K. (2007). Development of α-synuclein immunoreactive astrocytes in the forebrain parallels stages of intraneuronal pathology in sporadic Parkinson's disease. *Acta Neuropathologica* 114, 231–241. doi: 10.1007/s00401-007-0244-3

Byers, B., Cord, B., Nguyen, H. N., Schüle, B., Fenno, L., Lee, P. C., et al. (2011). SNCA triplication Parkinson's patient's iPSC-derived DA neurons accumulate alpha-synuclein and are susceptible to oxidative stress. *PLoS ONE* 6:e26159. doi: 10.1371/journal.pone.0026159

Caiazzo, M., Dell'Anno, M. T., Dvoretskova, E., Lazarevic, D., Taverna, S., Leo, D., et al. (2011). Direct generation of functional dopaminergic neurons from mouse and human fibroblasts. *Nature* 476, 224–227. doi: 10.1038/nature10284

Carey, B. W., Markoulaki, S., Hanna, J., Saha, K., Gao, Q., Mitalipova, M., et al. (2009). Reprogramming of murine and human somatic cells using a single polycistronic vector. *Proc. Natl. Acad. Sci. U S A.* 106, 157–162. doi: 10.1073/pnas.0811426106

Chen, G., Gulbranson, D. R., Hou, Z., Bolin, J. M., Ruotti, V., Probasco, M. D., et al. (2011). Chemically defined conditions for human iPSC derivation and culture. *Nat. Methods* 8, 424–429. doi: 10.1038/nmeth.1593

Choi, S. H., Kim, Y. H., Hebisch, M., Sliwinski, C., Lee, S., D'Avanzo, C., et al. (2014). A three-dimensional human neural cell culture model of Alzheimer's disease. *Nature* 515, 274–278. doi: 10.1038/nature13800

Chung, S. Y., Kishinevsky, S., Mazzulli, J. R., Graziotto, J., Mrejeru, A., Mosharov, E. V., et al. (2016). Parkin and PINK1 patient iPSC-derived midbrain dopamine neurons exhibit mitochondrial dysfunction and alpha-synuclein accumulation. *Stem Cell Rep.* 7, 664–677. doi: 10.1016/j.stemcr.2016.08.012

Cooper, O., Hargus, G., Deleidi, M., Blak, A., Osborn, T., Marlow, E., et al. (2010). Differentiation of human ES and Parkinson's disease iPS cells into ventral midbrain dopaminergic neurons requires a high activity form of SHH, FGF8a and specific regionalization by retinoic acid. *Mol. Cell. Neurosci.* 45, 258–266. doi: 10.1016/j.mcn.2010.06.017

Cooper, O., Seo, H., Andrabi, S., Guardia-Laguarta, C., Graziotto, J., Sundberg, M., et al. (2012). Pharmacological rescue of mitochondrial deficits in iPSC-derived neural cells from patients with familial Parkinson's disease. *Sci. Transl. Med.* 4:141ra90. doi: 10.1126/scitranslmed.3003985

Cuervo, A. M., Stefanis, L., Fredenburg, R., Lansbury, P. T., and Sulzer, D. (2004). Impaired degradation of mutant alpha-synuclein by chaperone-mediated autophagy. *Science* 305, 1292–1295. doi: 10.1126/science.1101738

Danzer, K. M., Kranich, L. R., Ruf, W. P., Cagsal-Getkin, O., Winslow, A. R., Zhu, L., et al. (2012). Exosomal cell-to-cell transmission of alpha synuclein oligomers. *Mol. Neurodegener.* 7:42. doi: 10.1186/1750-1326-7-42

Desplats, P., Lee, H. J., Bae, E. J., Patrick, C., Rockenstein, E., Crews, L., et al. (2009). Inclusion formation and neuronal cell death through neuron-to-neuron transmission of alpha-synuclein. *Proc. Natl. Acad. Sci. U S A.* 106, 13010–13015. doi: 10.1073/pnas.0903691106

Devi, L., Raghavendran, V., Prabhu, B. M., Avadhani, N. G., and Anandatheerthavarada, H. K. (2008). Mitochondrial import and accumulation of alpha-synuclein impair complex I in human dopaminergic neuronal cultures and Parkinson disease brain. *J. Biol. Chem.* 283, 9089–9100. doi: 10.1074/jbc.M710012200

Devine, M. J., Ryten, M., Vodicka, P., Thomson, A. J., Burdon, T., Houlden, H., et al. (2011). Parkinson's disease induced pluripotent stem cells with triplication of the alpha-synuclein locus. *Nat. Commun.* 2:440. doi: 10.1038/ncomms1453

Di Giovannantonio, L. G., Di Salvio, M., Acampora, D., Prakash, N., Wurst, W., and Simeone, A. (2013). Otx2 selectively controls the neurogenesis of specific neuronal subtypes of the ventral tegmental area and compensates En1-dependent neuronal loss and MPTP vulnerability. *Dev. Biol.* 373, 176–183. doi: 10.1016/j.ydbio.2012.10.022

Doi, D., Samata, B., Katsukawa, M., Kikuchi, T., Morizane, A., Ono, Y., et al. (2014). Isolation of human induced pluripotent stem cell-derived dopaminergic progenitors by cell sorting for successful transplantation. *Stem Cell Rep.* 2, 337–350. doi: 10.1016/j.stemcr.2014.01.013

El-Agnaf, O. M., Salem, S. A., Paleologou, K. E., Curran, M. D., Gibson, M. J., Court, J. A., et al. (2006). Detection of oligomeric forms of alpha-synuclein protein in human plasma as a potential biomarker for Parkinson's disease. *FASEB J.* 20, 419–425. doi: 10.1096/fj.03-1449com

Emmanouilidou, E., Melachroinou, K., Roumeliotis, T., Garbis, S. D., Ntzouni, M., Margaritis, L. H., et al. (2010). Cell-produced alpha-synuclein is secreted in a calcium-dependent manner by exosomes and impacts neuronal survival. *J. Neurosci.* 30, 6838–6851. doi: 10.1523/JNEUROSCI.5699-09.2010

Evans, M. (2011). Discovering pluripotency: 30 years of mouse embryonic stem cells. *Nat. Rev. Mol. Cell Biol.* 12, 680–686. doi: 10.1038/nrm3190

Fasano, C. A., Chambers, S. M., Lee, G., Tomishima, M. J., and Studer, L. (2010). Efficient derivation of functional floor plate tissue from human embryonic stem cells. *Cell Stem Cell* 6, 336–347. doi: 10.1016/j.stem.2010.03.001

Fellner, L., Irschick, R., Schanda, K., Reindl, M., Klimaschewski, L., Poewe, W., et al. (2013). Toll-like receptor 4 is required for α-synuclein dependent activation of microglia and astroglia. *Glia* 61, 349–360. doi: 10.1002/glia.22437

Fernandes, H. J., Hartfield, E. M., Christian, H. C., Emmanoulidou, E., Zheng, Y., Booth, H., et al. (2016). ER stress and autophagic perturbations lead to elevated extracellular alpha-synuclein in GBA-N370S parkinson's iPSC-derived dopamine neurons. *Stem Cell Rep.* 6, 342–356. doi: 10.1016/j.stemcr.2016.01.013

Flierl, A., Oliveira, L. M., Falomir-Lockhart, L. J., Mak, S. K., Hesley, J., Soldner, F., et al. (2014). Higher vulnerability and stress sensitivity of neuronal precursor cells carrying an alpha-synuclein gene triplication. *PLoS ONE* 9:e112413. doi: 10.1371/journal.pone.0112413

Fusaki, N., Ban, H., Nishiyama, A., Saeki, K., and Hasegawa, M. (2009). Efficient induction of transgene-free human pluripotent stem cells using a vector based on Sendai virus, an RNA virus that does not integrate into the host genome. *Proc. Jpn Acad. Ser. B Phys. Biol. Sci.* 85, 348–362. doi: 10.2183/pjab.85.348

Hansen, C., Angot, E., Bergström, A. L., Steiner, J. A., Pieri, L., Paul, G., et al. (2011). alpha-Synuclein propagates from mouse brain to grafted dopaminergic neurons and seeds aggregation in cultured human cells. *J. Clin. Invest.* 121, 715–725. doi: 10.1172/JCI43366

Heinrich, C., Bergami, M., Gascón, S., Lepier, A., Viganò, F., Dimou, L., et al. (2014). Sox2-mediated conversion of NG2 glia into induced neurons in the injured adult cerebral cortex. *Stem Cell Rep.* 3, 1000–1014. doi: 10.1016/j.stemcr.2014.10.007

Hockemeyer, D., and Jaenisch, R. (2016). Induced pluripotent stem cells meet genome editing. *Cell Stem Cell* 18, 573–586. doi: 10.1016/j.stem.2016.04.013

Holmes, B. B., DeVos, S. L., Kfoury, N., Li, M., Jacks, R., Yanamandra, K., et al. (2013). Heparan sulfate proteoglycans mediate internalization and propagation of specific proteopathic seeds. *Proc. Natl. Acad. Sci. U.S.A.* 110, E3138–E3147. doi: 10.1073/pnas.1301440110

Hou, P., Li, Y., Zhang, X., Liu, C., Guan, J., Li, H., et al. (2013). Pluripotent stem cells induced from mouse somatic cells by small-molecule compounds. *Science* 341, 651–654. doi: 10.1126/science.1239278

Huh, C. J., Zhang, B., Victor, M. B., Dahiya, S., Batista, L. F., Horvath, S., et al. (2016). Maintenance of age in human neurons generated by microRNA-based neuronal conversion of fibroblasts. *Elife* 5:e18648. doi: 10.7554/eLife.18648

Imaizumi, Y., Okada, Y., Akamatsu, W., Koike, M., Kuzumaki, N., Hayakawa, H., et al. (2012). Mitochondrial dysfunction associated with increased oxidative stress and alpha-synuclein accumulation in PARK2 iPSC-derived neurons and postmortem brain tissue. *Mol. Brain.* 5:35. doi: 10.1186/1756-6606-5-35

Jang, Y., and Jung, J. H. (2017). Direct conversion from skin fibroblasts to functional dopaminergic neurons for biomedical application. *Biomed. Dermatol.* 1:4. doi: 10.1186/s41702-017-0004-5

Jiang, H., Xu, Z., Zhong, P., Ren, Y., Liang, G., Schilling, H. A., et al. (2015). Cell cycle and p53 gate the direct conversion of human fibroblasts to dopaminergic neurons. *Nat. Commun.* 6:10100. doi: 10.1038/ncomms10100

Jo, J., Xiao, Y., Sun, A. X., Cukuroglu, E., Tran, H. D., Göke, J., et al. (2016). Midbrain-like organoids from human pluripotent stem cells contain functional dopaminergic and neuromelanin-producing neurons. *Cell Stem Cell* 19, 248–257. doi: 10.1016/j.stem.2016.07.005

Kaji, K., Norrby, K., Paca, A., Mileikovsky, M., Mohseni, P., and Woltjen, K. (2009). Virus-free induction of pluripotency and subsequent excision of reprogramming factors. *Nature* 458, 771–775. doi: 10.1038/nature07864

Kamp, F., Exner, N., Lutz, A. K., Wender, N., Hegermann, J., Brunner, B., et al. (2010). Inhibition of mitochondrial fusion by alpha-synuclein is rescued by PINK1, Parkin and DJ-1. *EMBO J.* 29, 3571–3589. doi: 10.1038/emboj.2010.223

Kanaan, N. M., and Manfredsson, F. P. (2012). Loss of functional alpha-synuclein: a toxic event in Parkinson's disease? *J. Parkinsons. Dis.* 2, 249–267. doi: 10.3233/JPD-012138

Karpinar, D. P., Balija, M. B., Kugler, S., Opazo, F., Rezaei-Ghaleh, N., Wender, N., et al. (2009). Pre-fibrillar alpha-synuclein variants with impaired beta-structure increase neurotoxicity in Parkinson's disease models. *EMBO J.* 28, 3256–3268. doi: 10.1038/emboj.2009.257

Kawasaki, H., Mizuseki, K., Nishikawa, S., Kaneko, S., Kuwana, Y., Nakanishi, S., et al. (2000). Induction of midbrain dopaminergic neurons from ES cells by stromal cell-derived inducing activity. *Neuron* 28, 31–40. doi: 10.1016/S0896-6273(00)00083-0

Kim, D., Kim, C. H., Moon, J. I., Chung, Y. G., Chang, M. Y., Han, B. S., et al. (2009). Generation of human induced pluripotent stem cells by direct delivery of reprogramming proteins. *Cell Stem Cell* 4, 472–476. doi: 10.1016/j.stem.2009.05.005

Kim, J., Su, S. C., Wang, H., Cheng, A. W., Cassady, J. P., Lodato, M. A., et al. (2011). Functional integration of dopaminergic neurons directly converted from mouse fibroblasts. *Cell Stem Cell* 9, 413–419. doi: 10.1016/j.stem.2011.09.011

Kirkeby, A., Grealish, S., Wolf, D. A., Nelander, J., Wood, J., Lundblad, M., et al. (2012). Generation of regionally specified neural progenitors and functional neurons from human embryonic stem cells under defined conditions. *Cell Rep.* 1, 703–714. doi: 10.1016/j.celrep.2012.04.009

Kirkeby, A., and Parmar, M. (2012). Building authentic midbrain dopaminergic neurons from stem cells - lessons from development. *Transl. Neurosci.* 3, 314–319. doi: 10.2478/s13380-012-0041-x

Kisos, H., Pukaß, K., Ben-Hur, T., Richter-Landsberg, C., and Sharon, R. (2012). Increased neuronal α-synuclein pathology associates with its accumulation in oligodendrocytes in mice modeling α-synucleinopathies. *PLoS ONE* 7:e46817. doi: 10.1371/journal.pone.0046817

Klein, C., and Westenberger, A. (2012). Genetics of Parkinson's disease. *Cold Spring Harb. Perspect. Med.* 2:a008888. doi: 10.1101/cshperspect.a008888

Konno, M., Hasegawa, T., Baba, T., Miura, E., Sugeno, N., Kikuchi, A., et al. (2012). Suppression of dynamin GTPase decreases α-synuclein uptake by neuronal and oligodendroglial cells: a potent therapeutic target for synucleinopathy. *Mol. Neurodegener.* 7:38. doi: 10.1186/1750-1326-7-38

Kordower, J. H., Chu, Y., Hauser, R. A., Freeman, T. B., and Olanow, C. W. (2008). Lewy body-like pathology in long-term embryonic nigral transplants in Parkinson's disease. *Nat. Med.* 14, 504–506. doi: 10.1038/nm1747

Kordower, J. H., Dodiya, H. B., Kordower, A. M., Terpstra, B., Paumier, K., Madhavan, L., et al. (2011). Transfer of host-derived alpha synuclein to grafted dopaminergic neurons in rat. *Neurobiol. Dis.* 43, 552–557. doi: 10.1016/j.nbd.2011.05.001

Kouroupi, G., Taoufik, E., Vlachos, I. S., Tsioras, K., Antoniou, N., Papastefanaki, F., et al. (2017). Defective synaptic connectivity and axonal neuropathology in a human iPSC-based model of familial Parkinson's disease. *Proc. Natl. Acad. Sci. USA.* 114, E3679–E88. doi: 10.1073/pnas.1617259114

Kriks, S., Shim, J. W., Piao, J., Ganat, Y. M., Wakeman, D. R., Xie, Z., et al. (2011). Dopamine neurons derived from human ES cells efficiently engraft in animal models of Parkinson's disease. *Nature* 480, 547–551. doi: 10.1038/nature10648

Lancaster, M. A., and Knoblich, J. A. (2014). Generation of cerebral organoids from human pluripotent stem cells. *Nat. Protoc.* 9, 2329–2340. doi: 10.1038/nprot.2014.158

Lancaster, M. A., Renner, M., Martin, C. A., Wenzel, D., Bicknell, L. S., Hurles, M. E., et al. (2013). Cerebral organoids model human brain development and microcephaly. *Nature* 501, 373–379. doi: 10.1038/nature12517

Lashuel, H. A., Overk, C. R., Oueslati, A., and Masliah, E. (2012). The many faces of α-synuclein: from structure and toxicity to therapeutic target. *Nat. Rev. Neurosci.* 14:38–48. doi: 10.1038/nrn3406

Lee, H. J., Cho, E. D., Lee, K. W., Kim, J. H., Cho, S. G., and Lee, S. J. (2013). Autophagic failure promotes the exocytosis and intercellular transfer of alpha-synuclein. *Exp. Mol. Med.* 45:e22. doi: 10.1038/emm.2013.45

Lee, H. J., Suk, J. E., Patrick, C., Bae, E. J., Cho, J. H., Rho, S., et al. (2010). Direct transfer of alpha-synuclein from neuron to astroglia causes inflammatory responses in synucleinopathies. *J. Biol. Chem.* 285, 9262–9272. doi: 10.1074/jbc.M109.081125

Lee, P. H., Lee, G., Park, H. J., Bang, O. Y., Joo, I. S., and Huh, K. (2006). The plasma alpha-synuclein levels in patients with Parkinson's disease and multiple system atrophy. *J. Neural. Transm.* 113, 1435–1439. doi: 10.1007/s00702-005-0427-9

Li, J. Y., Englund, E., Holton, J. L., Soulet, D., Hagell, P., Lees, A. J., et al. (2008). Lewy bodies in grafted neurons in subjects with Parkinson's disease suggest host-to-graft disease propagation. *Nat. Med.* 14, 501–503. doi: 10.1038/nm1746

Lindström, V., Gustafsson, G., Sanders, L. H., Howlett, E. H., Sigvardson, J., Kasrayan, A., et al. (2017). Extensive uptake of α-synuclein oligomers in astrocytes results in sustained intracellular deposits and mitochondrial damage. *Mol. Cell. Neurosci.* 82, 143–156. doi: 10.1016/j.mcn.2017.04.009

Liu, X., Li, F., Stubblefield, E. A., Blanchard, B., Richards, T. L., Larson, G. A., et al. (2012). Direct reprogramming of human fibroblasts into dopaminergic neuron-like cells. *Cell Res.* 22, 321–332. doi: 10.1038/cr.2011.181

Luk, K. C., Kehm, V., Carroll, J., Zhang, B., O'Brien, P., Trojanowski, J. Q., et al. (2012a). Pathological alpha-synuclein transmission initiates Parkinson-like neurodegeneration in nontransgenic mice. *Science* 338, 949–953. doi: 10.1126/science.1227157

Luk, K. C., Kehm, V. M., Zhang, B., O'Brien, P., Trojanowski, J. Q., and Lee, V. M. (2012b). Intracerebral inoculation of pathological alpha-synuclein initiates a rapidly progressive neurodegenerative alpha-synucleinopathy in mice. *J. Exp. Med.* 209, 975–986. doi: 10.1084/jem.20112457

Malik, N., and Rao, M. S. (2013). A review of the methods for human iPSC derivation. *Methods Mol. Biol.* 997:23–33. doi: 10.1007/978-1-62703-348-0_3

Mao, X., Ou, M. T., Karuppagounder, S. S., Kam, T. I., Yin, X., Xiong, Y., et al. (2016). Pathological alpha-synuclein transmission initiated by binding lymphocyte-activation gene 3. *Science* 353:aah3374. doi: 10.1126/science.aah3374

Marton, R. M., and Paşca, S. P. (2016). Neural differentiation in the third dimension: generating a human midbrain. *Cell Stem Cell* 19, 145–146. doi: 10.1016/j.stem.2016.07.017

Masuda-Suzukake, M., Nonaka, T., Hosokawa, M., Kubo, M., Shimozawa, A., Akiyama, H., et al. (2014). Pathological alpha-synuclein propagates through neural networks. *Acta Neuropathologica Commun*. 2:88. doi: 10.1186/s40478-014-0088-8

Mertens, J., Paquola, A. C., Ku, M., Hatch, E., Böhnke, L., Ladjevardi, S., et al. (2015). Directly reprogrammed human neurons retain aging-associated transcriptomic signatures and reveal age-related nucleocytoplasmic defects. *Cell Stem Cell* 17, 705–718. doi: 10.1016/j.stem.2015.09.001

Miller, D., Johnson, J., Solano, S., Hollingsworth, Z., Standaert, D., and Young, A. (2005). Absence of α-synuclein mRNA expression in normal and multiple system atrophy oligodendroglia. *J. Neural Transm.* 112, 1613–1624. doi: 10.1007/s00702-005-0378-1

Miyoshi, N., Ishii, H., Nagano, H., Haraguchi, N., Dewi D., L., Kano, Y., et al. (2011). Reprogramming of mouse and human cells to pluripotency using mature microRNAs. *Cell Stem Cell* 8, 633–638. doi: 10.1016/j.stem.2011.05.001

Monzel, A. S., Smits, L. M., Hemmer, K., Hachi, S., Moreno, E. L., van Wuellen, T., et al. (2017). Derivation of human midbrain-specific organoids from neuroepithelial stem cells. *Stem Cell Rep.* 8, 1144–1154. doi: 10.1016/j.stemcr.2017.03.010

Mougenot, A. L., Nicot, S., Bencsik, A., Morignat, E., Verchère, J., Lakhdar, L., et al. (2012). Prion-like acceleration of a synucleinopathy in a transgenic mouse model. *Neurobiol. Aging* 33, 2225–2228. doi: 10.1016/j.neurobiolaging.2011.06.022

Muguruma, K., Nishiyama, A., Kawakami, H., Hashimoto, K., and Sasai, Y. (2015). Self-organization of polarized cerebellar tissue in 3D culture of human pluripotent stem cells. *Cell Rep.* 10, 537–550. doi: 10.1016/j.celrep.2014.12.051

Nakamura, K., Nemani, V. M., Azarbal, F., Skibinski, G., Levy, J. M., Egami, K., et al. (2011). Direct membrane association drives mitochondrial fission by the Parkinson disease-associated protein alpha-synuclein. *J. Biol. Chem.* 286, 20710–20726. doi: 10.1074/jbc.M110.213538

Paik, E. J., O'Neil, A. L., Ng, S. Y., Sun, C., and Rubin, L. L. (2018). Using intracellular markers to identify a novel set of surface markers for live cell purification from a heterogeneous hIPSC culture. *Sci. Rep.* 8, 804. doi: 10.1038/s41598-018-19291-4

Pang, Z. P., Yang, N., Vierbuchen, T., Ostermeier, A., Fuentes, D. R., Yang, T. Q., et al. (2011). Induction of human neuronal cells by defined transcription factors. *Nature* 476:220–223. doi: 10.1038/nature10202

Panman, L., Papathanou, M., Laguna, A., Oosterveen, T., Volakakis, N., Acampora, D., et al. (2014). Sox6 and Otx2 control the specification of substantia nigra and ventral tegmental area dopamine neurons. *Cell Rep.* 8, 1018–1025. doi: 10.1016/j.celrep.2014.07.016

Pan-Montojo, F., Anichtchik, O., Dening, Y., Knels, L., Pursche, S., Jung, R., et al. (2010). Progression of Parkinson's disease pathology is reproduced by intragastric administration of rotenone in mice. *PLoS ONE* 5:e8762. doi: 10.1371/journal.pone.0008762

Pan-Montojo, F., Schwarz, M., Winkler, C., Arnhold, M., O'Sullivan, G. A., Pal, A., et al. (2012). Environmental toxins trigger PD-like progression via increased alpha-synuclein release from enteric neurons in mice. *Sci. Rep.* 2:898. doi: 10.1038/srep00898

Peelaerts, W., Bousset, L., Van der Perren, A., Moskalyuk, A., Pulizzi, R., Giugliano, M., et al. (2015). alpha-Synuclein strains cause distinct synucleinopathies after local and systemic administration. *Nature* 522, 340–344. doi: 10.1038/nature14547

Perrier, A. L., Tabar, V., Barberi, T., Rubio, M. E., Bruses, J., Topf, N., et al. (2004). Derivation of midbrain dopamine neurons from human embryonic stem cells. *Proc. Natl. Acad. Sci. U.S.A.* 101, 12543–12548. doi: 10.1073/pnas.0404700101

Pfisterer, U., Kirkeby, A., Torper, O., Wood, J., Nelander, J., Dufour, A., et al. (2011). Direct conversion of human fibroblasts to dopaminergic neurons. *Proc. Natl. Acad. Sci. USA.* 108, 10343–10348. doi: 10.1073/pnas.1105135108

Plamont, M. A., Billon-Denis, E., Maurin, S., Gauron, C., Pimenta, F. M., Specht, C. G., et al. (2016). Small fluorescence-activating and absorption-shifting tag for tunable protein imaging *in vivo*. *Proc. Natl. Acad. Sci. USA.* 113, 497–502. doi: 10.1073/pnas.1513094113

Poulin, J. F., Zou, J., Drouin-Ouellet, J., Kim K-Y, A., Cicchetti, F., and Awatramani, R. B. (2014). Defining midbrain dopaminergic neuron diversity by single-cell gene expression profiling. *Cell Rep.* 9, 930–943. doi: 10.1016/j.celrep.2014.10.008

Qian, X., Nguyen, H. N., Song, M. M., Hadiono, C., Ogden, S. C., Hammack, C., et al. (2016). Brain region-specific organoids using mini-bioreactors for modeling ZIKV exposure. *Cell* 165, 1238–1254. doi: 10.1016/j.cell.2016.04.032

Rannikko, E. H., Weber, S. S., and Kahle, P. J. (2015). Exogenous α-synuclein induces toll-like receptor 4 dependent inflammatory responses in astrocytes. *BMC Neurosci.* 16:57. doi: 10.1186/s12868-015-0192-0

Recasens, A., Dehay, B., Bové, J., Carballo-Carbajal, I., Dovero, S., Pérez-Villalba, A., et al. (2014). Lewy body extracts from Parkinson disease brains trigger alpha-synuclein pathology and neurodegeneration in mice and monkeys. *Ann. Neurol.* 75, 351–362. doi: 10.1002/ana.24066

Rey, N. L., Petit, G. H., Bousset, L., Melki, R., and Brundin, P. (2013). Transfer of human alpha-synuclein from the olfactory bulb to interconnected brain regions in mice. *Acta Neuropathol.* 126, 555–573. doi: 10.1007/s00401-013-1160-3

Reyes, J. F., Rey, N. L., Bousset, L., Melki, R., Brundin, P., and Angot, E. (2014). Alpha-synuclein transfers from neurons to oligodendrocytes. *Glia* 62, 387–398. doi: 10.1002/glia.22611

Rostami, J., Holmqvist, S., Lindström, V., Sigvardson, J., Westermark, G. T., Ingelsson, M., et al. (2017). Human astrocytes transfer aggregated alpha-synuclein via tunneling nanotubes. *J. Neurosci.* 37, 11835–11853. doi: 10.1523/JNEUROSCI.0983-17.2017

Ryan, S. D., Dolatabadi, N., Chan, S. F., Zhang, X., Akhtar, M. W., Parker, J., et al. (2013). Isogenic human iPSC Parkinson's model shows nitrosative stress-induced dysfunction in MEF2-PGC1alpha transcription. *Cell* 155, 1351–1364. doi: 10.1016/j.cell.2013.11.009

Sacino, A. N., Brooks, M., McGarvey, N. H., McKinney, A. B., Thomas, M. A., Levites, Y., et al. (2013). Induction of CNS alpha-synuclein pathology by fibrillar and non-amyloidogenic recombinant alpha-synuclein. *Acta Neuropathol. Commun.* 1:38. doi: 10.1186/2051-5960-1-38

Seki, T., and Fukuda, K. (2015). Methods of induced pluripotent stem cells for clinical application. *World J. Stem Cells* 7, 116–125. doi: 10.4252/wjsc.v7.i1.116

Shaltouki, A., Sivapatham, R., Pei, Y., Gerencser, A. A., Momcilović, O., Rao, M. S., et al. (2015). Mitochondrial alterations by PARKIN in dopaminergic neurons using PARK2 patient-specific and PARK2 knockout isogenic iPSC lines. *Stem Cell Rep.* 4, 847–859. doi: 10.1016/j.stemcr.2015.02.019

Sharon, R., Goldberg, M. S., Bar-Josef, I., Betensky, R. A., Shen, J., and Selkoe, D. J. (2001). alpha-Synuclein occurs in lipid-rich high molecular weight complexes, binds fatty acids, and shows homology to the fatty acid-binding proteins. *Proc. Natl. Acad. Sci. USA.* 98, 9110–9115. doi: 10.1073/pnas.171300598

Shimozawa, A., Ono, M., Takahara, D., Tarutani, A., Imura, S., Masuda-Suzukake, M., et al. (2017). Propagation of pathological alpha-synuclein in marmoset brain. *Acta Neuropathol. Commun.* 5:12. doi: 10.1186/s40478-017-0413-0

Snyder, H., Mensah, K., Theisler, C., Lee, J., Matouschek, A., and Wolozin, B. (2003). Aggregated and monomeric alpha-synuclein bind to the S6' proteasomal protein and inhibit proteasomal function. *J. Biol. Chem.* 278, 11753–11759. doi: 10.1074/jbc.M208641200

Soldner, F., Laganière, J., Cheng, A. W., Hockemeyer, D., Gao, Q., Alagappan, R., et al. (2011). Generation of isogenic pluripotent stem cells differing exclusively at two early onset Parkinson point mutations. *Cell* 146, 318–331. doi: 10.1016/j.cell.2011.06.019

Somers, A., Jean, J. C., Sommer, C. A., Omari, A., Ford, C. C., Mills, J. A., et al. (2010). Generation of transgene-free lung disease-specific human iPS cells using a single excisable lentiviral stem cell cassette. *Stem Cells* 28, 1728–1740. doi: 10.1002/stem.495

Sommer, C. A., Stadtfeld, M., Murphy, G. J., Hochedlinger, K., Kotton, D. N., and Mostoslavsky, G. (2009). iPS cell generation using a single lentiviral stem cell cassette. *Stem Cells* 27, 543–549. doi: 10.1634/stemcells.2008-1075

Stefanis, L. (2012). alpha-synuclein in Parkinson's disease. *Cold Spring Harb. Perspect. Med.* 2:a009399. doi: 10.1101/cshperspect.a009399

Stefanis, L., Larsen, K. E., Rideout, H. J., Sulzer, D., and Greene, L. A. (2001). Expression of A53T mutant but not wild-type alpha-synuclein in PC12 cells induces alterations of the ubiquitin-dependent degradation system, loss of dopamine release, and autophagic cell death. *J. Neurosci.* 21, 9549–9560. doi: 10.1523/JNEUROSCI.21-24-09549.2001

Stefanova, N., Fellner, L., Reindl, M., Masliah, E., Poewe, W., and Wenning, G. K. (2011). Toll-like receptor 4 promotes α-synuclein clearance and survival of nigral dopaminergic neurons. *Am. J. Pathol.* 179, 954–963. doi: 10.1016/j.ajpath.2011.04.013

Stuendl, A., Kunadt, M., Kruse, N., Bartels, C., Moebius, W., Danzer, K. M., et al. (2016). Induction of alpha-synuclein aggregate formation by CSF exosomes from patients with Parkinson's disease and dementia with Lewy bodies. *Brain* 139(Pt 2), 481–494. doi: 10.1093/brain/awv346

Subramanyam, D., Lamouille, S., Judson, R. L., Liu, J. Y., Bucay, N., Derynck, R., et al. (2011). Multiple targets of miR-302 and miR-372 promote reprogramming of human fibroblasts to induced pluripotent stem cells. *Nat. Biotechnol.* 29, 443–448. doi: 10.1038/nbt.1862

Takahashi, K., and Yamanaka, S. (2006). Induction of pluripotent stem cells from mouse embryonic and adult fibroblast cultures by defined factors. *Cell* 126, 663–676. doi: 10.1016/j.cell.2006.07.024

Tanaka, Y., Engelender, S., Igarashi, S., Rao, R. K., Wanner, T., Tanzi, R. E., et al. (2001). Inducible expression of mutant alpha-synuclein decreases proteasome activity and increases sensitivity to mitochondria-dependent apoptosis. *Hum. Mol. Genet.* 10, 919–926. doi: 10.1093/hmg/10.9.919

Thakur, P., Breger, L. S., Lundblad, M., Wan, O. W., Mattsson, B., Luk, K. C., et al. (2017). Modeling Parkinson's disease pathology by combination of fibril seeds and alpha-synuclein overexpression in the rat brain. *Proc. Natl. Acad. Sci. USA.* 114, E8284–E93. doi: 10.1073/pnas.1710442114

Tian, C., Li, Y., Huang, Y., Wang, Y., Chen, D., Liu, J., et al. (2015). Selective generation of dopaminergic precursors from mouse fibroblasts by direct lineage conversion. *Sci. Rep.* 5:12622. doi: 10.1038/srep12622

Tokuda, T., Salem, S. A., Allsop, D., Mizuno, T., Nakagawa, M., Qureshi, M. M., et al. (2006). Decreased alpha-synuclein in cerebrospinal fluid of aged individuals and subjects with Parkinson's disease. *Biochem. Biophys. Res. Commun.* 349, 162–166. doi: 10.1016/j.bbrc.2006.08.024

Torrent, R., De Angelis Rigotti, F., Dell'Era, P., Memo, M., Raya, A., and Consiglio, A. (2015). Using iPS cells toward the understanding of Parkinson's disease. *J. Clin. Med.* 4, 548–566. doi: 10.3390/jcm4040548

Ubhi, K., Low, P., and Masliah, E. (2011). Multiple system atrophy: a clinical and neuropathological perspective. *Trends Neurosci.* 34, 581–590. doi: 10.1016/j.tins.2011.08.003

Vierbuchen, T., Ostermeier, A., Pang, Z. P., Kokubu, Y., Südhof, T. C., and Wernig, M. (2010). Direct conversion of fibroblasts to functional neurons by defined factors. *Nature* 463, 1035–1041. doi: 10.1038/nature08797

Warren, L., Manos, P. D., Ahfeldt, T., Loh, Y.-H., Li, H., Lau, F., et al. (2010). Highly efficient reprogramming to pluripotency and directed differentiation of human cells using synthetic modified mRNA. *Cell Stem Cell* 7, 618–630. doi: 10.1016/j.stem.2010.08.012

Winner, B., Jappelli, R., Maji, S. K., Desplats, P. A., Boyer, L., Aigner, S., et al. (2011). *In vivo* demonstration that alpha-synuclein oligomers are toxic. *Proc. Natl. Acad. Sci. U.S.A.* 108, 4194–4199. doi: 10.1073/pnas.1100976108

Woltjen, K., Michael, I. P., Mohseni, P., Desai, R., Mileikovsky, M., Hämäläinen, R., et al. (2009). piggyBac transposition reprograms fibroblasts to induced pluripotent stem cells. *Nature* 458, 766–770. doi: 10.1038/nature07863

Xilouri, M., Vogiatzi, T., Vekrellis, K., Park, D., and Stefanis, L. (2009). Abberant alpha-synuclein confers toxicity to neurons in part through inhibition of chaperone-mediated autophagy. *PLoS ONE* 4:e5515. doi: 10.1371/journal.pone.0005515

Xu, Z., Chu, X., Jiang, H., Schilling, H., Chen, S., and Feng, J. (2017). Induced dopaminergic neurons: a new promise for Parkinson's disease. *Redox Biol.* 11:606–612. doi: 10.1016/j.redox.2017.01.009

Yu, J., Hu, K., Smuga-Otto, K., Tian, S., Stewart, R., Slukvin, I. I., et al. (2009). Human induced pluripotent stem cells free of vector and transgene sequences. *Science* 324, 797–801. doi: 10.1126/science.1172482

Yu, W.-W., Cao, S.-N., Zang, C.-X., Wang, L., Yang, H.-Y., Bao, X.-Q., et al. (2018). Heat shock protein 70 suppresses neuroinflammation induced by α-synuclein in astrocytes. *Mol. Cell. Neurosci.* 86:58–64. doi: 10.1016/j.mcn.2017.11.013

Yusa, K., Rad, R., Takeda, J., and Bradley, A. (2009). Generation of transgene-free induced pluripotent mouse stem cells by the piggyBac transposon. *Nat. Methods* 6, 363–369. doi: 10.1038/nmeth.1323

Zhang, S. C., Wernig, M., Duncan, I. D., Brüstle, O., and Thomson, J. A. (2001). *In vitro* differentiation of transplantable neural precursors from human embryonic stem cells. *Nat. Biotechnol.* 19, 1129–1133. doi: 10.1038/nbt1201-1129

Zhang, W., Wang, T., Pei, Z., Miller, D. S., Wu, X., Block, M. L., et al. (2005). Aggregated α-synuclein activates microglia: a process leading to disease progression in Parkinson's disease. *FASEB J.* 19, 533–542. doi: 10.1096/fj.04-2751com

Zhou, H., Wu, S., Joo, J. Y., Zhu, S., Han, D. W., Lin, T., et al. (2009). Generation of induced pluripotent stem cells using recombinant proteins. *Cell Stem Cell* 4, 381–384. doi: 10.1016/j.stem.2009.04.005

Zhou, W., and Freed, C. R. (2009). Adenoviral gene delivery can reprogram human fibroblasts to induced pluripotent stem cells. *Stem Cells* 27, 2667–2674. doi: 10.1002/stem.201

Conflict of Interest Statement: The authors declare that the research was conducted in the absence of any commercial or financial relationships that could be construed as a potential conflict of interest.

frontiers in Cellular Neuroscience

ORIGINAL RESEARCH
published: 03 July 2020
doi: 10.3389/fncel.2020.00171

Convolutional Neural Networks Can Predict Retinal Differentiation in Retinal Organoids

Evgenii Kegeles[1,2†], *Anton Naumov*[3†], *Evgeny A. Karpulevich*[2,3,4], *Pavel Volchkov*[2,5] *and Petr Baranov*[1*]

[1]*Department of Ophthalmology, The Schepens Eye Research Institute of Massachusetts Eye and Ear, Harvard Medical School, Boston, MA, United States,* [2]*Genome Technologies and Bioinformatics Research Centre, Moscow Institute of Physics and Technology, Dolgoprudniy, Russia,* [3]*Department of Information Systems, Ivannikov Institute for System Programming of the Russian Academy of Sciences, Moscow, Russia,* [4]*National Research Center "Kurchatov Institute", Moscow, Russia,* [5]*Endocrinology Research Centre, Institute for Personalized Medicine, Moscow, Russia*

OPEN ACCESS

Edited by:
Lin Cheng,
University of Iowa, United States

Reviewed by:
Ming Zu Zhang,
Sun Yat-sen University, China
Stephanie C. Joachim,
Ruhr University Bochum, Germany
Ling Zhang,
Pall Inc., United States

***Correspondence:**
Petr Baranov
petr_baranov@meei.harvard.edu

†These authors have contributed equally to this work

Specialty section:
This article was submitted to Cellular Neuropathology, a section of the journal Frontiers in Cellular Neuroscience

Received: *25 February 2020*
Accepted: *20 May 2020*
Published: *03 July 2020*

Citation:
Kegeles E, Naumov A, Karpulevich EA, Volchkov P and Baranov P (2020) Convolutional Neural Networks Can Predict Retinal Differentiation in Retinal Organoids. Front. Cell. Neurosci. 14:171. doi: 10.3389/fncel.2020.00171

We have developed a deep learning-based computer algorithm to recognize and predict retinal differentiation in stem cell-derived organoids based on bright-field imaging. The three-dimensional "organoid" approach for the differentiation of pluripotent stem cells (PSC) into retinal and other neural tissues has become a major *in vitro* strategy to recapitulate development. We decided to develop a universal, robust, and non-invasive method to assess retinal differentiation that would not require chemical probes or reporter gene expression. We hypothesized that basic-contrast bright-field (BF) images contain sufficient information on tissue specification, and it is possible to extract this data using convolutional neural networks (CNNs). Retina-specific Rx-green fluorescent protein mouse embryonic reporter stem cells have been used for all of the differentiation experiments in this work. The BF images of organoids have been taken on day 5 and fluorescent on day 9. To train the CNN, we utilized a transfer learning approach: ImageNet pre-trained ResNet50v2, VGG19, Xception, and DenseNet121 CNNs had been trained on labeled BF images of the organoids, divided into two categories (retina and non-retina), based on the fluorescent reporter gene expression. The best-performing classifier with ResNet50v2 architecture showed a receiver operating characteristic-area under the curve score of 0.91 on a test dataset. A comparison of the best-performing CNN with the human-based classifier showed that the CNN algorithm performs better than the expert in predicting organoid fate (84% vs. 67 ± 6% of correct predictions, respectively), confirming our original hypothesis. Overall, we have demonstrated that the computer algorithm can successfully recognize and predict retinal differentiation in organoids before the onset of reporter gene expression. This is the first demonstration of CNN's ability to classify stem cell-derived tissue *in vitro*.

Keywords: deep learning, convolutional neural networks, stem cells, retinal organoids, mouse embryonic stem cells

INTRODUCTION

The differentiation of pluripotent stem cells (PSC) using a three-dimensional "organoid" approach has become the strategy of choice to recapitulate the development of the retina, brain, inner ear, intestine, pancreas, and many other tissues *in vitro* (McCauley and Wells, 2017). This technique allows to reproduce the process of normal development and does not require any exogenous stimulation of developmental pathways and genetic modification of the cells used (Eiraku et al., 2011; Meyer et al., 2011). Indeed hundreds of studies confirm that retinal organoids, differentiated from mouse or human pluripotent cells, show a unique resemblance to native tissue architecture, cell specification and sub-specification, function, and transcriptional profile (Hallam et al., 2018; Cowan et al., 2019). This demonstrates the robustness of the technology and makes it highly attractive for potential translation to the clinic as a source of high-quality retinal neurons for transplantation (Decembrini et al., 2014) or as a platform for the screening of new therapeutics (Baranov et al., 2017).

The process of the differentiation itself is stochastic, which causes the quantity of retinal differentiation to vary a lot even among organoids within one batch—not to say when different cell lines are used (Hiler et al., 2015; Hallam et al., 2018; Cowan et al., 2019). The current approach to select retinal tissue for further growth and maturation is based on subjective morphological observation and features visible with bright-field imaging: lamination of the neuroepithelium, adjacent pigment epithelium areas, *etc*., and/or on the expression of fluorescent reporter constructs driven by retina-specific promoters. These reporters allow to assess the differentiation on different stages of retinal development: from early eye field-specific genes [Pax6-GFP mESCs (Völkner et al., 2016) and Rx-GFP mESCs (Eiraku et al., 2011)] to terminal retinal cell types as rods Nrl-GFP miPSCs (Ueda et al., 2018), Six6 (Sluch et al., 2018), or Rx (Nakano et al., 2012) for early optic vesicles, Brn3a (Sluch et al., 2015) for retinal ganglion cells, Crx (Nakano et al., 2012) for photoreceptors, or Nrl (Phillips et al., 2018) for human rods.

The use of fluorescent reporters is a "gold standard"—it is a sensitive, specific, and easily quantifiable method to assess retinal differentiation (Vergara et al., 2017), although it cannot be used in cell manufacture for transplantation or to model inherited diseases due to genome modification. The manual selection under the microscope with bright-field imaging is limited in throughput and the classification criteria can be subjective, resulting in high variability between observers. This puts its limitations on the further transition of this technology "from the bench to bedside." Here we tried to address this issue by developing an automated non-invasive method which can predict retinal differentiation based on bright-field images of retinal organoids on the early stage of their development using artificial intelligence.

Machine learning has been evolving rapidly during the last decades. This is mostly due to the increase in accessible computational power and the ability to generate and store massive amounts of data. Nowadays, one of the most actively developing branches of artificial intelligence is deep learning, which was able to outperform the best conventional machine learning algorithms in multiple fields including speech and image recognition (LeCun et al., 2015). This technology was inspired by the principles which lay in cognition and data processing by the brain. In simple understanding, the biological neuron is receiving information from other neurons, combines it, and transmits a modified signal to the next pool of neurons. In general, the artificial neuron works in a similar way: it receives inputs from the group of neurons, combines them with some weights for each input, and transmits the result to the next set of neurons using some non-linear function. So, each artificial neuron itself can be interpreted as a function, which gets a vector of inputs from neurons from the previous layer and returns some value (activation) which is being transmitted to the next layer. The neural network usually contains several layers of these neurons connected together, starting from the input layer and finishing with the output layer which returns the result. The general task for supervised learning is to find optimal weights for each neuron in the network to minimize an error between the value predicted by the program and the value which was assigned before the training (e.g., ground truth label for classification or some score for regression task).

This approach showed itself to be extremely effective in solving multiple tasks such as speech recognition, computer vision (LeCun et al., 2015), processing of medical and biological data (Ching et al., 2018), etc. For the analysis of images (or any data which has local adjacency structure), the special type of neural networks was developed—convolutional neural networks (CNN). This type of neural network has a few so-called convolutional layers in the beginning of the learning process, which allows to find relationships between spatially adjacent parts of the image for the dimensionality reduction and extraction of features. This approach has found a lot of applications in multiple fields of biology and medicine. For example, for diagnosis of diabetic retinopathy based on fundus imaging (Gulshan et al., 2016) and for skin cancer classification (Esteva et al., 2017), and recently it was proven effective to predict the very early onset of PSC differentiation (Waisman et al., 2019) and the quality of retinal pigment epithelium (RPE) differentiation in a two-dimensional setting (Schaub et al., 2020). Being inspired by the success that this approach showed on the prediction of spontaneous differentiation of PSCs with basic bright-field imaging used as a source of information, we hypothesized that basic-contrast bright-field images contain sufficient information on tissue specification, and it is possible to extract it using convolutional neural networks. In this study, we decided to test the ability of CNN to: (1) recognize early retinal differentiation in organoids; and (2) predict retinal differentiation in individual organoids before the onset of the expression of the eye field-specific reporters—for instance, Rx.

To predict early retinal differentiation, we utilized a transfer learning approach: CNN is being pretrained on the ImageNet classification dataset (Deng et al., 2009) containing more than 10 million images which are split into more than 20,000 classes. This approach allows to transfer the ability of a pretrained network to extract low-level features from natural images and focus more on high-level features from the target dataset during

the training. Such a trick helps to achieve desirable results using lower amounts of training data and have been proven useful for the analysis of biological images (Ching et al., 2018).

MATERIALS AND METHODS

mES Cell Culture

mES reporter cell line RxGFP has been used in this study (RIKEN; Eiraku et al., 2011). The cells were cultured in the mES medium (**Supplementary Table S1**), fed every other day, and passaged at 70–80% confluence on a cell culture-treated T-75 flask coated with 1% Matrigel (Corning) solution for 1 h. For replating or seeding for retinal organoid formation, the cells were dissociated using 0.25 Trypsin solution (Gibco) for 7 min on 37°C in a CO_2 incubator.

Retinal Differentiation

Retinal differentiation was performed as was shown before, with minor modifications (Perepelkina et al., 2019). The protocol is outlined in **Figure 1A**. The RxGFP mES cells were dissociated from the flask with 0.25 trypsin and seeded in a differentiation medium (OV; **Supplementary Table S1**) on a 96-well U-bottom polystyrene plate (Greiner) at a cell density of 3,000 cells per well in 50 μl of the media. The cells were fed with 50 μl of OV supplemented with 1% Matrigel (Corning) on day 1 of differentiation. Additional feeding with 50 μl of OV with 0.5% Matrigel was performed on day 5 of differentiation. Further medium change was performed with OC media starting from day 9.

Automated Imaging

Both bright-field and fluorescent images of the organoids have been taken using the EVOS fl Auto microscope. For bright-field imaging, the plates were scanned with a 4× phase-contrast objective on day 5 of differentiation, with fine autofocus function. As each organoid is seeded separately in a separate well of a 96-well plate, each image contained no more than one organoid.

Immunohistochemistry and Confocal Imaging

Ten organoids from each batch were collected and fixed with 4% PFA for 20 min at room temperature (RT). Prior to staining, they were blocked with a blocking buffer for 1 h at RT. Staining with primary antibodies (Santa-Cruz anti-Rx antibody #SC-79031 and Hybridoma Bank anti-PAX6 antibody #AB528427) was performed overnight at +4°C in staining buffer. On the next day, after washing with a wash buffer (**Supplementary Table S2**), secondaries were applied overnight at +4°C. After staining with antibodies and washing, the organoids were stained with 4′,6-diamidino-2-phenylindole for 10 min at RT and mounted on concavity slides (Lab Scientific). Confocal images were taken using a Leica SP5 confocal microscope.

Classification Criteria for Fluorescent Images

The discrimination between retinal and non-retinal organoids for the purpose of assigning ground truth labels was based primarily on the expression of the Rx-GFP reporter, which is a very specific marker for early retinal progenitor cells (Medina-Martinez et al., 2009; Zagozewski et al., 2014). The criteria took into account the brightness of the reporter, localization, and pattern of the retinal area.

We have sorted organoids based on the fluorescent images on day 9 into three groups: "retina," "non-retina," and "satisfactory." The following criteria were utilized (**Figure 2**):

- The retinal organoids should have bright fluorescence or localized fluorescent retina-like structures.
- A satisfactory organoid should have sparse or scattered fluorescence pattern without clearly separable retinal areas.
- A non-retinal organoid should not be fluorescent or have uniformly distributed green background fluorescence.

Classification Criteria for Bright-Field Images

For sorting organoids on day 6 using bright-field images, the following criteria were defined:

- Retina—distinct layer-like (neuroepithelium) transparent areas on the periphery of the organoids
- Non-retina—uniform cellular aggregate without distinct transparent areas

Dataset Preparation and Images Preprocessing for Training the Network

The initial dataset (1,209 images in total) was split into three parts: the training one (64% of total), the validation (16% of total), and the test one (20% of total). The training and validation datasets were used for architecture and parameter selection. The test dataset was used only for the final validation of the best neural network after the whole process of parameter tuning and architecture selection is completed.

Before feeding the images to neural networks, we implemented a few preprocessing steps. First, we find the position of the organoid on an image and crop it out using Python OpenCV script based on blob detection. This is a very simple and straightforward approach for object detection. It works best if the target object is significantly darker or brighter than the background as it is based on automated thresholding (Otsu method). This is exactly the case for retinal organoids—they are significantly darker than the background and have pretty contrast borders. Thus, we found the algorithm to work very efficiently. Furthermore, it does not require any manual parameter adjustments, except for the average organoid size which stays stable, if the same quantity of cells is used for seeding in the beginning of differentiation.

We also applied Gaussian normalization to the images and augmented them with random horizontal and vertical flips, rotations, width and height shifts, and zoom transformations. Proportionally more transformations were applied to the non-retina class images in order to balance the number of images used for CNN training. Additional information on augmentation parameters can be found in the "**Supplementary Extended Methods**" section.

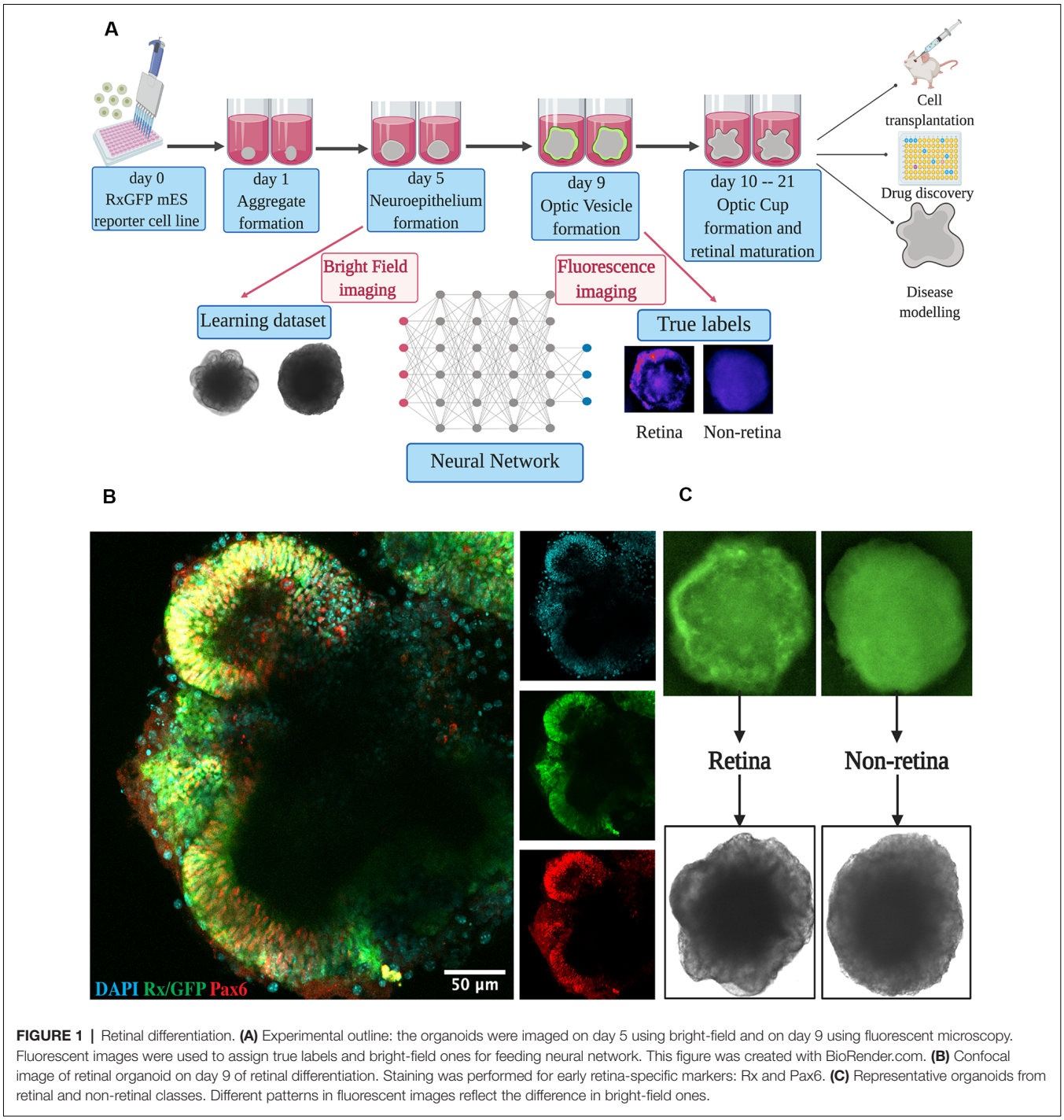

FIGURE 1 | Retinal differentiation. **(A)** Experimental outline: the organoids were imaged on day 5 using bright-field and on day 9 using fluorescent microscopy. Fluorescent images were used to assign true labels and bright-field ones for feeding neural network. This figure was created with BioRender.com. **(B)** Confocal image of retinal organoid on day 9 of retinal differentiation. Staining was performed for early retina-specific markers: Rx and Pax6. **(C)** Representative organoids from retinal and non-retinal classes. Different patterns in fluorescent images reflect the difference in bright-field ones.

Interpretation of CNN Output and Threshold Selection

The neural network takes some piece of data as an input, i.e., image, and is designed to predict the probability for it to be retinal—value between 0 and 1. This is done in the following way.

The network consists of small abstract units called neurons; each of those has several inputs (like axons/dendrites in real neurons). Each dendrite of each neuron has its own value called weight, and each neuron itself has its own value called bias. When a neuron gets some numerical values to its inputs, it multiplies them with the corresponding weights, sums them up, adds bias, and applies to the result some non-linear function (usually called activation function). The resulting value is sent to the output.

The neurons are aggregated into groups called layers. The inputs of the neurons of the first layer are attached to the pixels

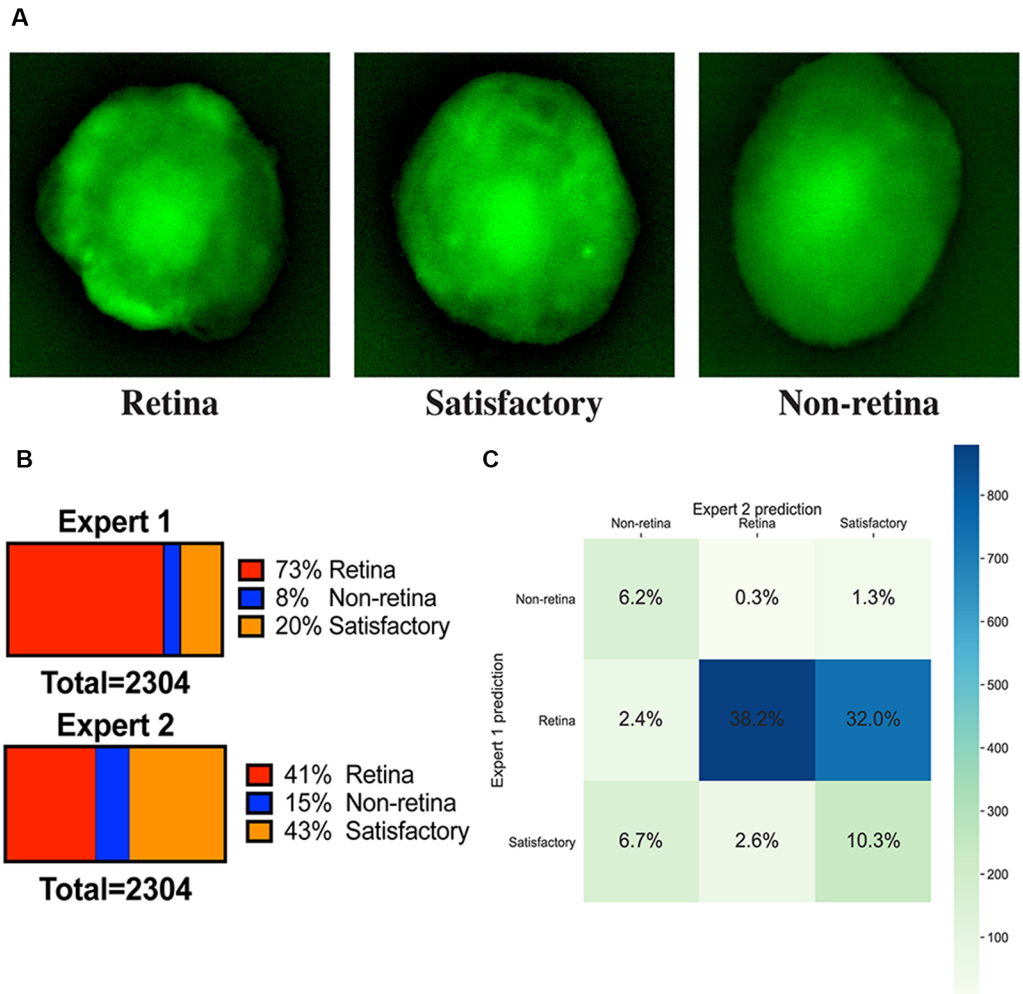

FIGURE 2 | Image annotations. **(A)** Fluorescent images of representative organoids from each class which experts have classified to "retina," "non-retina," and "satisfactory." **(B)** Ratios of labels assigned by two experts for the training dataset. **(C)** Summary of ratios for different classes which can be assigned after combining the votes from two experts.

of the input image. The inputs of the neurons from any internal layer are attached only to the outputs from the neurons in the preceding layers. The last layer consists only of one neuron—its output value is interpreted as the probability of the organoid to be a retinal one. The way to organize the neurons and the layers is called the architecture of the network.

Initially, the weights and the biases of the neurons are taken randomly. While the network gets training images, it tries to predict their classes, evaluates the results using true classes of the images, and adjusts the weights and the biases of its neurons using a backpropagation algorithm.

Therefore, after processing the image, CNN returns a value from 0 to 1, which can be interpreted as a probability for this organoid to belong to the "retina" class. Thus, the threshold should be selected to make the final prediction: organoids with scores higher than the threshold would be considered "retinal," and with lower—"non-retinal."

We determined a threshold by maximizing the value of sensitivity * specificity [true positive rate * (1- false positive rate)] on the training dataset. This approach helps to improve both the sensitivity and the specificity of the classifier, which can be affected by the imbalance between classes.

Selection of the Best CNN Architecture and Cross-Validation

For our task, we selected four convolutional neural networks with different architectures, which showed themselves effective on ImageNet competitions and in multiple biological applications (Esteva et al., 2017; Waisman et al., 2019): VGG19 (Simonyan and Zisserman, 2014), ResNet50v2 (He et al., 2016), DenseNet121 (Huang et al., 2017), and Xception (Chollet, 2017). All of these CNNs were initially pretrained on the ImageNet dataset (Deng et al., 2009).

For the selection of the best network, 10-folds cross-validation was used: the training dataset was split into 10

non-overlapping subsets. On each step of the process, the network is training on nine out of these 10 subsets and then uses the last subset for validation. Each subset is used for validation once. So, this allows to perform statistical tests for CNN performance comparison.

Hyperparameters Tuning and Training of the Networks

The training was performed on the training dataset, and multiple hyperparameters have been optimized using the validation dataset (learning rate, set of frozen layers, dropout rate of the last layer, etc.). Additional information on the actual values of the hyperparameters used for each CNN can be found in the "**Supplementary Extended Methods**" section and **Supplementary Table S3**. Also, as we are using transfer learning approach, only the few last layers of the CNN are trained. The number of these layers depends on the architecture chosen and should be also considered as a hyperparameter.

Assessment of CNN Performance

There are multiple approaches available to measure the performance of classifiers, including accuracy, F1 score, receiver operating characteristic-area under the curve (ROC-AUC), Mathews correlation coefficient (MCC), and many others.

The simplest and the most intuitive score is "accuracy"—the number of correct guesses divided by the total number of samples in the dataset. Additional metrics are "precision"—number of objects which were correctly predicted as positive divided by the total number of objects selected as positive, and "recall" or "true positive rate"—number of objects which were correctly predicted as positive divided by the total number of positive objects in the initial dataset. The accuracy shows how many selected objects are really the correct ones, and the recall shows how many of the relevant objects the algorithm was able to pick up. As precision and recall cannot be optimized separately, metrics which take into account both these values are usually used. The F1 score is a harmonic mean of precision and recall. However, all of these scores have some drawbacks, especially for imbalanced data, as both classes are treated equally and changes in a wrongly predicted minor class do not have a high impact on the score.

Alternatively, MCC can be calculated—the value which shows how well the predictions of the classifier and the true labels are correlated. One of the advantages of this metric is that it can be very sensitive even when classes are imbalanced.

Another option is using ROC-AUC score—the area under the ROC curve (true positive rate vs. false positive rate at different threshold values). It is the "gold standard" for binary classification with neural networks. It has a very meaningful interpretation: this value shows the probability of a randomly selected object from the "retina" class to have a higher score than a random object from the "non-retina" class. So, for a classifier that assigns labels randomly, the score would be 0.5, and for the perfect algorithm, it would be equal to 1. Therefore, this score can be considered as the measure of order which the classifier provides. Thus, we chose the ROC-AUC score as the main measure of performance for our CNN.

RESULTS

Retinal Differentiation and Initial Annotation of the Collected Images by Experts

For dataset collection, approximately 3,000 retinal organoids were differentiated and analyzed. For the training of our neural network and annotating the dataset, we collected bright-field and fluorescent images for each organoid on day 5 and day 9 of differentiation, respectively (**Figures 1A,C**). On day 9, in most organoids, distinct optic vesicle areas could be observed. In **Figure 1B**, a confocal image of retinal organoids on day 9 of differentiation is presented. Retina-like planar structures are formed on the periphery of the organoid; these areas are also positive for retina-specific markers Pax6 and Rx. As Rx is known to be an essential transcription factor for retinal development (Zagozewski et al., 2014), we chose its expression at day 9 to be a ground truth indication for early retinal differentiation.

All fluorescent images were collected on day 9 and pooled together, filtered to get rid of pictures with poor quality, anonymized, and offered to two independent experts for sorting in three groups: (1) good retina (**Figure 1C**, left; **Figure 2A**, left); (2) satisfactory retina (**Figure 2A**, center); and (3) not retina (**Figure 1C**, right; **Figure 2A**, right). The classification criteria are stated in the "Materials and Methods" section. The proportions of each class for each expert are provided in **Figure 2B**, and the cumulative distribution of organoids after classification is summarized in **Figure 2C**.

For our network, we stated the two-class classification problem: we asked the program to extract features which would distinguish high-quality organoids from bad ones based only on bright-field images. To do that, we generated the training dataset by assigning to organoids with label "retina" only if both experts put this organoid in class "retina" and "non-retina" if at least one suggested it to be non-retinal. Classes "retina/non-retina," "retina/satisfactory," and "satisfactory/satisfactory" were not used for training the network. The resulting dataset consisted a total of 1,209 bright-field images, with the proportion of classes at 73 vs. 27% for retina and non-retina, respectively. As each organoid is seeded in a separate well and they are developing independently, we consider each of them to be an independent biological replicate.

Selection of the Best CNN Architecture

Four networks based on different architectures (VGG19, ResNet50v2, Xception, and DenseNet121) have been trained and validated on the dataset. The learning curves are shown in **Figure 3A**. All networks were successfully trained, but the VGG19-based classifier shows signs of overfitting: loss score on validation dataset is significantly higher than on training dataset; so, for further comparison, we decided to keep only ResNet50v2-, Xception-, and DenseNet121-based CNNs.

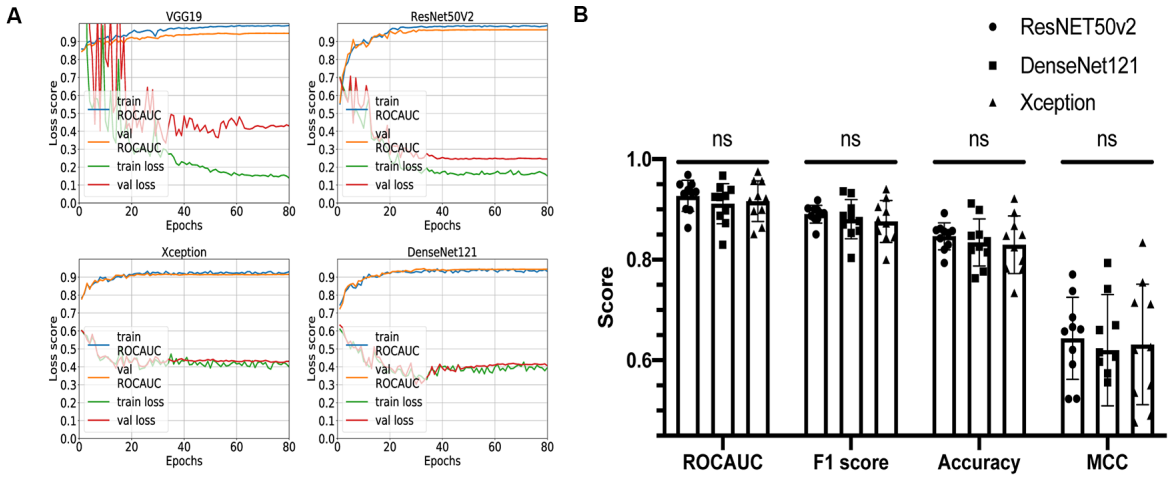

FIGURE 3 | Comparison of different convolutional neural network (CNN) architectures. **(A)** Loss curves and receiver operating characteristic-area under the curve (AUC) training curves for VGG19, ResNET50v2, DenseNet121, and Xception. **(B)** Comparison summary of three different CNNs using 10-fold cross-validation. The mean AUC scores were 0.93 ± 0.03 vs. 0.91 ± 0.04 vs. 0.92 ± 0.04 (P = 0.3) for ResNET50v2, DenseNet121, and Xception, respectively; the mean F1 scores were 0.89 ± 0.02 vs. 0.88 ± 0.04 vs. 0.88 ± 0.04 for ResNET50v2, DenseNet121, and Xception, respectively; the mean accuracy scores were 0.85 ± 0.03 vs. 0.83 ± 0.05 vs. 0.83 ± 0.06 for ResNET50v2, DenseNet121, and Xception, respectively; the mean Matthews correlation coefficients were 0.64 ± 0.08 vs. 0.62 ± 0.11 vs. 0.63 ± 0.12 for ResNET50v2, DenseNet121, and Xception, respectively. Each dot on the graph corresponds to one cross-validation step. ns, not significant (P-value > 0.05 on Friedman statistical test).

The remaining three networks were run through 10-fold cross-validation, and for each step, ROC-AUC score, optimal thresholds, F1, MCC, and accuracy scores were calculated (**Figure 3B**). The mean AUC scores were 0.93 ± 0.03 vs. 0.91 ± 0.04 vs. 0.92 ± 0.04 (P = 0.3) for ResNet50v2, DenseNet121, and Xception, respectively; the mean F1 scores were 0.89 ± 0.02 vs. 0.88 ± 0.04 vs. 0.88 ± 0.04 (P = 0.6) for ResNet50v2, DenseNet121, and Xception, respectively; the mean accuracy scores were 0.85 ± 0.03 vs. 0.83 ± 0.05 vs. 0.83 ± 0.06 (P = 0.6) for ResNet50v2, DenseNet121, and Xception, respectively; and the mean Matthews correlation coefficients were 0.64 ± 0.08 vs. 0.62 ± 0.11 vs. 0.63 ± 0.12 for ResNet50v2, DenseNet121, and Xception, respectively. All of the networks show similar results, and no significant difference has been found using the Friedman test (analog of Wilcoxon test when three or more samples are compared). So, we can conclude that all of these CNNs can potentially be utilized for solving our task. However, the Xception- and DenseNet121-based CNNs had a noticeable variation of the loss score for the different validation steps of cross-validation (**Supplementary Figure S1**). Also, we noticed that ResNet50v2 had the smallest standard deviation among other classifiers for each metric (**Figure 3B**); therefore, at this step, we selected this CNN.

Convolutional Neural Network Can Predict Early Retinal Differentiation

To evaluate the performance of the selected CNN, we utilized the test dataset which was not used during the training and parameter tuning process. The ROC curve is shown in **Figure 4A** and the confusion matrix in **Figure 4B**. For this dataset, the predictor showed the ROC-AUC score to be 0.91 (**Figure 4A**), accuracy—0.84, F1 score—0.89, and Matthews correlation coefficient—0.63. Despite a significant imbalance between the retinal and the non-retinal classes, the classifier was able to reach 0.85 sensitivity and 0.82 specificity scores on the test dataset. This indicates that augmentation and threshold selection allowed to efficiently tackle the imbalance problem.

The prediction scores for every single image and the threshold are shown in **Figure 4C**. As expected, the retinal and the non-retinal organoids are "condensed" at the corresponding values: 0 for non-retina and 1 for the retina; so, the model clearly can separate these two types of organoids.

Then, we decided to have a look at the performance of the model on different classes, which were obtained after combining the experts' annotations. The true prediction rates for each class are presented in **Figure 4D**. Expectedly, the best performance the model shows on organoids which came from "sure" classes: retina/retina and non-retina/non-retina, meaning that the CNN is more likely to be mistaken where experts are also less sure about the labels. Moreover, in **Figure 4E**, the distributions of the prediction scores are shown for each class. Again, retina/retina and non-retina/non-retina classes are clearly separated. Moreover, organoids from retina/satisfactory class, which were not used for training and validation, also were in most cases correctly attributed by the network to the retina class, although the median of the distribution is shifted from 1, showing that the program gets confused more often than on "retina/retina" class, which is also consistent with the result shown in **Figure 4D**.

Interestingly, the predictor could not separate organoids from the retina/non-retina group, which can be concluded from the fact that the median of the scores is located close to the threshold: it can be interpreted as CNN is working almost as a random predictor for organoids from this group. Organoids from

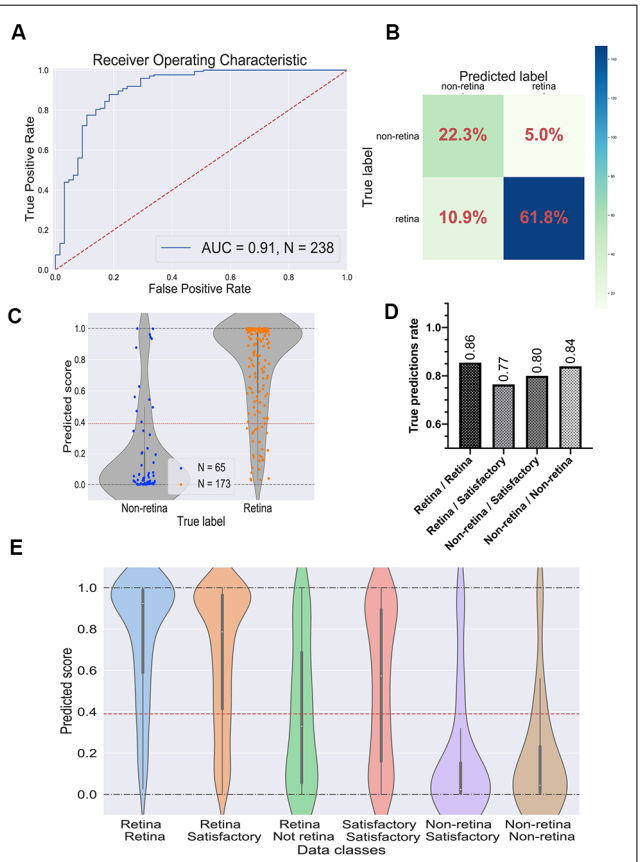

FIGURE 4 | Performance of the best convolutional neural network (CNN) on the test dataset. **(A)** Receiver operating characteristic (ROC) curve for the selected CNN on the test dataset. ROC-area under the curve value equals 0.91. **(B)** Confusion matrix for selected CNN. Values in the squares represent percentages of true negative, false positive, false negative, and true positive predictions. Color LUT shows the absolute number of images in each group. **(C)** Prediction scores for the test dataset; each dot represents a single organoid; the red line represents the threshold value for the classifier. **(D)** True prediction rates for each class of organoids with the CNN classifier. **(E)** Violin plots on all possible classes of organoids which can be assigned by combining the votes from two experts. The white dot in the center of each plot represents the median of the distribution; the boxes and the bars represent the first quartile and the upper/lower adjacent value, respectively; the red line is a classifier's threshold.

satisfactory/satisfactory class also can be poorly distinguished, but the median is shifted toward the retinal class, which is being in accordance with the criteria that we used for this class.

To identify the image areas and features that are used by the CNN, we utilized SHapley Additive exPlanations (SHAP) value approach (Lundberg and Lee, 2017). We noticed that the border of the organoids and, more specifically, the retina-like neuroepithelium loops on the periphery are zones of interest for the CNN (**Supplementary Figure S2**).

CNN Outperforms Human Classifier on Prediction of Retinal Differentiation

To compare the CNN performance with the human-based classifier, we asked four independent experts to assign the labels "retina" and "non-retina" for organoids from the test dataset. The criteria for this classification can be found in the "Materials and Methods" section.

True positive rates and false positive rates for each expert are plotted on the classifier's ROC curve (**Figure 5A**). The CNN is clearly outperforming a human in distinguishing retinal differentiation on the early stage of differentiation. Different metrics for the comparison are provided in **Figure 5B**. On average, a human expert has an accuracy of 0.67 $\pm$ 0.06, while CNN has an accuracy of 0.84.

The more striking difference gives the comparison of a Matthews correlation coefficient which takes into account class disbalance: 0.63 vs. 0.27 $\pm$ 0.06 for Matthews correlation coefficient for CNN and human, respectively.

DISCUSSION

Retinal organoid cultures have a great potential to model human disease and development and as source of retinal neurons for transplantation or platform for therapeutics testing. The remaining challenges, highlighted in RPE transplantation studies, include high variability between different cell lines (Leach et al., 2016), scaled production with automation or other approaches (Regent et al., 2019), and lack of cGMP-compatible non-invasive readouts for the assessment of differentiation during the development process (Schaub et al., 2020). The translational success of regenerative therapies based on iPSCs-derived RPE (Mandai et al., 2017; da Cruz et al., 2018) is largely due to the development of strategies to overcome these issues. In this study, we attempted to address the latter for retinal 3D organoids.

There are two distinct, non-mutually exclusive approaches to characterize and identify the differentiating cell with non-invasive imaging techniques. The classic strategy is to define the exact features and the thresholds that are characteristics of a particular cell type. This approach is based on our understanding on how the cell looks *in vivo*: this was demonstrated in decades of RPE differentiation studies *in vitro* (Thumann et al., 2013), where pigmentation, cell shape, and autofluorescence can be quantified and compared to the pre-set quality criteria thresholds (da Cruz et al., 2018; Schaub et al., 2020). The evolution of this approach involves better understanding of the thresholds as well as introduction of new imaging techniques that can detect new features—multispectral fluorescent and non-fluorescent imaging, optical coherence tomography (Browne et al., 2017; Capowski et al., 2019), and others. An alternative strategy is machine learning that is also highly dependent on the modality by which the information is collected. However, the information is processed in a different way: it does not require any predefined criteria for assessment—the CNN learns how to find and extract the most relevant features from the data by itself, provided that the program "has seen" enough samples to learn it from. Machine learning becomes particularly valuable when there are multiple criteria and definitions or when they are not very well established. In this case, the training of computer algorithm occurs with the help of experts, who would

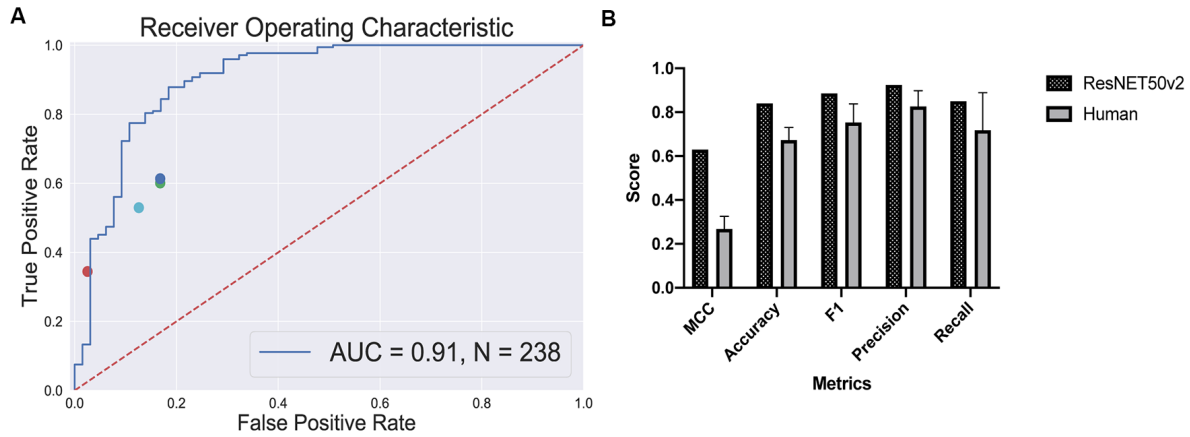

FIGURE 5 | Human-based classifier vs. CNN-based classifier. **(A)** The receiver operating characteristic curve for the convolutional neural networks (CNN); the area under the curve score for this classifier is 0.91. Each dot represents a single human expert predicting organoids to be from "retina" or "non-retina" class based on bright-field images. **(B)** Metrics comparison for human-based classifier and CNN-based. CNN showed better results on all the metrics that we measured: 0.63 vs. 0.27 ± 0.06 Matthews correlation coefficient for CNN and human, respectively; 0.84 vs. 0.67 ± 0.06 accuracy for CNN and human, respectively; 0.89 vs. 0.75 ± 0.09 F1 score for CNN and human, respectively; 0.92 vs. 0.83 ± 0.07 precision for CNN and human, respectively; 0.85 vs. 0.72 ± 0.17 recall for CNN and human, respectively.

classify or rank the training set of images, i.e., cats vs. dogs (Krizhevsky et al., 2012), early vs. late diabetic retinopathy (Pratt et al., 2016), etc. This technology becomes extremely powerful when it is possible to use an orthogonal approach, "other modality," to make a decision on what class the object belongs to: molecular profile (Waisman et al., 2019) or functional response (Schaub et al., 2020). This is the exact case of retinal differentiation using 3D organoid strategy: there are limited accurate criteria distinguishing good retinal organoids and bad ones with BF imaging, especially on the early stage of their development, although the availability of reporter cell lines allows to determine retinal differentiation with high accuracy. Here we showed that such discrimination is possible with a convolutional neural network which could predict early retinal differentiation based only on universal bright-field imaging.

One of the major questions in the area of deep learning is the role of individual features in image recognition. It is not clear which parts of the image are most important for the algorithm to classify an object. This issue of potential unpredictability becomes more important when the action is solely based on artificial intelligence decision. Also, by extracting individual features that are most important in predicting cell behavior, it may be possible to identify novel biological processes and identify the actual determinants of retinal formation in the embryoid bodies. By using SHAP value approach, we were able to show the importance of translucent neuroepithelium-like structures in decision-making (**Supplementary Figure S2**), although we were not able to show the actual causality of these structures in the decision-making process.

The program clearly outperformed the experts in a classification task (**Figure 5**) and was able to predict eye field induction better than a human performing a morphological observation of organoid with bright-field microscopy: 0.84 vs. 0.67 ± 0.06 accuracy for CNN vs. human, respectively. This additionally illustrates that the criteria for the selection of retinal organoids at this stage are subjective. Furthermore, the good performance of the CNN-based classifier shows that the morphology of the organoids, even on a very early stage, contains sufficient information to predict retinal differentiation, and the program can extract this information.

Moreover, the approach does not require any complicated imaging, fluorescent reporters, or dyes for analysis; so, it can be easily implemented in almost any laboratory or manufacturing setting. Therefore, our method offers a robust and universal non-invasive approach for the assessment of retinal differentiation.

As we have stated the problem as a classification task, we assume from the beginning that there should be some threshold which would distinguish retinal and non-retinal organoids. However, there are many organoids which are "on the border"—these organoids we called "satisfactory" organoids; these are hard to separate in two distinct classes with the single fluorescent reporter. Moreover, for different applications, different thresholds may be needed: for example, for disease or development modeling, the quality of the organoid should be prioritized to get the proper physiology and morphology of the retina, but for cell production, the yield may be a priority and a lower threshold can be applied for enrichment. Moreover, for drug discovery, using retinal organoids can be problematic as the amount of retinal differentiation varies between different organoids, and having a method to grade organoids can be helpful to interpret the assay results. Therefore, having an ability to select a threshold according to the task can be rather important for different applications. Thus, one of the further directions to

be considered is a statement of the regression problem for grading retinal organoids. This would significantly expand the possible applications of the approach. However, this task would require a reliable quantification method to assign "ground truth" values for the network training. One of the possible metrics which can be utilized is not only the simple quantification of total fluorescence in the organoid (Vergara et al., 2017) if using fluorescent reporters but also the localization and the shape of retina-like structures might be important parameters which should be taken into account, as well as the physiological and the metabolic state of the retinal neurons (Browne et al., 2017).

We have used mouse embryonic stem cells with Rx reporter in this work. Using this gene expression as a specific indicator of eye field induction, we were able to predict differentiation using CNN. We consider that the approach that we established can be easily translatable not only to other mouse reporter cell lines but also for human organoids. This is due to the fact that the method relies only on the morphology of the organoids during development, and Sasai's differentiation protocol has been shown to be effective on human embryonic stem cells (Nakano et al., 2012). Moreover, here are multiple retina-related human PSC reporter cell lines available, which target different cell types and differentiation stages: Six6 (Sluch et al., 2018) and Rx (Nakano et al., 2012) for early optic vesicles, Brn3a (Sluch et al., 2015) for retinal ganglion cells, Crx (Nakano et al., 2012) for photoreceptors, or Nrl (Phillips et al., 2018) for rods specifically. Therefore, our approach with training the CNN to predict the differentiation can also be utilized for human cells and possibly for later differentiation stages. However, to achieve the best results on human cells, additional training for mouse-pretrained neural network may be required to adjust to possible morphological differences between mouse and human organoids.

Moreover, as we have shown that CNN can accurately predict retinal differentiation based only on simple bright-field images of the organoids, we suppose that not only microscope images can be utilized for the CNN training. For example, probably this approach can be incorporated in the large-particle flow cytometer machines as an alternative to fluorescence.

DATA AVAILABILITY STATEMENT

The datasets generated for this study are available on request to the corresponding author.

AUTHOR CONTRIBUTIONS

EK, AN, and PB conceived the experiments. EK designed and performed the differentiation experiments, interpreted the results, and wrote the manuscript with the help of AN. AN and EAK trained the neural networks and performed the comparison of different CNN architectures. EK and PB developed an idea and annotated fluorescent and bright-field images. All the authors discussed the experiments and the manuscript. EAK, PV, and PB provided funding for this study. PB revised and corrected the manuscript. All the authors read and approved the final version of the manuscript.

FUNDING

This work was supported by NIH/NEI U24 grant EY029893, BrightFocus Foundation (PB), Gilbert Family Foundation, Research to Prevent Blindness Grant (PB), NIH National Eye Institute core grant P30EY003790, and Russian Academic Excellence project 5-100.

ACKNOWLEDGMENTS

We would like to thank Dr. Julia Oswald and Dr. Monichan Phay for their help with the classification of organoids based on the bright-field images. Also, we would like to thank Gennady Fedonin and Andrei Sonin for their advice. We want to thank RIKEN Cell Bank and Dr. Yoshiki Sasai for providing us with RxGFP mES cell line.

SUPPLEMENTARY MATERIAL

The Supplementary Material for this article can be found online at: https://www.frontiersin.org/articles/10.3389/fncel.2020.00171/full#supplementary-material.

REFERENCES

Baranov, P., Lin, H., McCabe, K., Gale, D., Cai, S., Lieppman, B., et al. (2017). A novel neuroprotective small molecule for glial cell derived neurotrophic factor induction and photoreceptor rescue. *J. Ocul. Pharmacol. Ther.* 33, 412–422. doi: 10.1089/jop.2016.0121

Browne, A. W., Arnesano, C., Harutyunyan, N., Khuu, T., Martinez, J. C., Pollack, H. A., et al. (2017). Structural and functional characterization of human stem-cell-derived retinal organoids by live imaging. *Invest. Ophthalmol. Vis. Sci.* 58, 3311–3318. doi: 10.1167/iovs.16-20796

Capowski, E. E., Samimi, K., Mayerl, S. J., Phillips, M. J., Pinilla, I., Howden, S. E., et al. (2019). Reproducibility and staging of 3D human retinal organoids across multiple pluripotent stem cell lines. *Development* 146:dev171686. doi: 10.1242/dev.171686

Ching, T., Himmelstein, D. S., Beaulieu-Jones, B. K., Kalinin, A. A., Do, B. T., Way, G. P., et al. (2018). Opportunities and obstacles for deep learning in biology and medicine. *J. R. Soc. Interface* 15:20170387. doi: 10.1098/rsif.2017.0387

Chollet, F. (2017). "Xception: deep learning with depthwise separable convolutions," in *Proceedings of the 2017 IEEE Conference on Computer Vision and Pattern Recognition (CVPR)*, 1800–1807.

Cowan, C. S., Renner, M., Gross-Scherf, B., Goldblum, D., Munz, M., Krol, J., et al. (2019). Cell types of the human retina and its organoids at single-cell resolution: developmental convergence, transcriptomic identity and disease map. *SSRN Electr. J.* doi: 10.2139/ssrn.3438371 [Epub ahead of print].

da Cruz, L., Fynes, K., Georgiadis, O., Kerby, J., Luo, Y. H., Ahmado, A., et al. (2018). Phase 1 clinical study of an embryonic stem cell-derived retinal pigment epithelium patch in age-related macular degeneration. *Nat. Biotechnol.* 36, 328–337. doi: 10.1038/nbt.4114

Decembrini, S., Koch, U., Radtke, F., Moulin, A., and Arsenijevic, Y. (2014). Derivation of traceable and transplantable photoreceptors from mouse embryonic stem cells. *Stem Cell Reports* 2, 853–865. doi: 10.1016/j.stemcr.2014.04.010

Deng, J., Dong, W., Socher, R., Li, L.-J., Li, K., and Fei-Fei, L. (2009). "ImageNet: a large-scale hierarchical image database," in *2009 IEEE Conference on Computer Vision and Pattern Recognition*, 248–255.

Eiraku, M., Takata, N., Ishibashi, H., Kawada, M., Sakakura, E., Okuda, S., et al. (2011). Self-organizing optic-cup morphogenesis in three-dimensional culture. *Nature* 472, 51–58. doi: 10.1038/nature09941

Esteva, A., Kuprel, B., Novoa, R. A., Ko, J., Swetter, S. M., Blau, H. M., et al. (2017). Dermatologist-level classification of skin cancer with deep neural networks. *Nature* 542, 115–118. doi: 10.1038/nature21056

Gulshan, V., Peng, L., Coram, M., Stumpe, M. C., Wu, D., Narayanaswamy, A., et al. (2016). Development and validation of a deep learning algorithm for detection of diabetic retinopathy in retinal fundus photographs. 316, 2402–2410. doi: 10.1001/jama.2016.17216

Hallam, D., Hilgen, G., Dorgau, B., Zhu, L., Yu, M., Bojic, S., et al. (2018). Human-induced pluripotent stem cells generate light responsive retinal organoids with variable and nutrient-dependent efficiency. *Stem Cells* 36, 1535–1551. doi: 10.1002/stem.2883

He, K., Zhang, X., Ren, S., and Sun, J. (2016). "Identity mappings in deep residual networks," in *Computer Vision—ECCV 2016*, eds B. Leibe, J. Matas, N. Sebe and M. Welling (Cham: Springer International Publishing), 630–645.

Hiler, D., Chen, X., Hazen, J., Kupriyanov, S., Carroll, P. A., Qu, C., et al. (2015). Quantification of retinogenesis in 3D cultures reveals epigenetic memory and higher efficiency in IPSCs derived from rod photoreceptors. *Cell Stem Cell* 17, 101–115. doi: 10.1016/j.stem.2015.05.015

Huang, G., Liu, Z., van der Maaten, L., and Weinberger, K. Q. (2017). "Densely connected convolutional networks," in *Proceedings of the 2017 IEEE Conference on Computer Vision and Pattern Recognition (CVPR)*, 2261–2269.

Krizhevsky, A., Sutskever, I., and Hinton, G. E. (2012). "ImageNet classification with deep convolutional neural networks," in *Proceedings of the Advances in Neural Information Processing Systems*, 1097–1105.

Leach, L. L., Croze, R. H., Hu, Q., Nadar, V. P., Clevenger, T. N., Pennington, B. O., et al. (2016). Induced pluripotent stem cell-derived retinal pigmented epithelium: a comparative study between cell lines and differentiation methods. *J. Ocul. Pharmacol. Ther.* 32, 317–330. doi: 10.1089/jop.2016.0022

LeCun, Y., Bengio, Y., and Hinton, G. (2015). Deep learning. *Nature* 521, 436–444. doi: 10.1038/nature14539

Lundberg, S. M., and Lee, S. I. (2017). "A unified approach to interpreting model predictions," in *Proceedings of the Advances in Neural Information Processing Systems*, 4766–4775.

Mandai, M., Watanabe, A., Kurimoto, Y., Hirami, Y., Morinaga, C., Daimon, T., et al. (2017). Autologous induced stem-cell-derived retinal cells for macular degeneration. *N. Engl. J. Med.* 376, 1038–1046. doi: 10.1056/NEJMoa1608368

McCauley, H. A., and Wells, J. M. (2017). Pluripotent stem cell-derived organoids: using principles of developmental biology to grow human tissues in a dish. *Development* 144, 958–962. doi: 10.1242/dev.140731

Medina-Martinez, O., Amaya-Manzanares, F., Liu, C., Mendoza, M., Shah, R., Zhang, L., et al. (2009). Cell-autonomous requirement for Rx function in the mammalian retina and posterior pituitary. *PLoS One* 4, 1–7. doi: 10.1371/journal.pone.0004513

Meyer, J. S., Howden, S. E., Wallace, K. A., Verhoeven, A. D., Wright, L. S., Capowski, E. E., et al. (2011). Optic vesicle-like structures derived from human pluripotent stem cells facilitate a customized approach to retinal disease treatment. *Stem Cells* 29, 1206–1218. doi: 10.1002/stem.674

Nakano, T., Ando, S., Takata, N., Kawada, M., Muguruma, K., Sekiguchi, K., et al. (2012). Self-formation of optic cups and storable stratified neural retina from human ESCs. *Cell Stem Cell* 10, 771–785. doi: 10.1016/j.stem.2012.05.009

Perepelkina, T., Kegeles, E., and Baranov, P. (2019). Optimizing the conditions and use of synthetic matrix for three-dimensional *in vitro* retinal differentiation from mouse pluripotent cells. *Tissue Eng. Part C Methods* 25, 433–445. doi: 10.1089/ten.tec.2019.0053

Phillips, M. J., Capowski, E. E., Petersen, A., Jansen, A. D., Barlow, K., Edwards, K. L., et al. (2018). Generation of a rod-specific NRL reporter line in human pluripotent stem cells. *Sci. Rep.* 8:2370. doi: 10.1038/s41598-018-20813-3

Pratt, H., Coenen, F., Broadbent, D. M., Harding, S. P., and Zheng, Y. (2016). Convolutional neural networks for diabetic retinopathy. *Proc. Comput. Sci.* 90, 200–205. doi: 10.1016/j.procs.2016.07.014

Regent, F., Morizur, L., Lesueur, L., Habeler, W., Plancheron, A., Ben M'Barek, K., et al. (2019). Automation of human pluripotent stem cell differentiation toward retinal pigment epithelial cells for large-scale productions. *Sci. Rep.* 9:10646. doi: 10.1038/s41598-019-47123-6

Schaub, N. J., Hotaling, N. A., Manescu, P., Padi, S., Wan, Q., Sharma, R., et al. (2020). Deep learning predicts function of live retinal pigment epithelium from quantitative microscopy. *J. Clin. Invest.* 130, 1010–1023. doi: 10.1172/JCI131187

Simonyan, K., and Zisserman, A. (2014). "Very deep convolutional networks for large-scale image recognition," in *Proceedings of the 3rd International Conference on Learning Representations, ICLR 2015—Conference Track*, 1–14. http://arxiv.org/abs/1409.1556.

Sluch, V. M., Davis, C. H. O., Ranganathan, V., Kerr, J. M., Krick, K., Martin, R., et al. (2015). Differentiation of human ESCs to retinal ganglion cells using a CRISPR engineered reporter cell line. *Sci. Rep.* 5:16595. doi: 10.1038/srep16595

Sluch, V. M., Chamling, X., Wenger, C., Duan, Y., Rice, D. S., and Zack, D. J. (2018). Highly efficient scarless knock-in of reporter genes into human and mouse pluripotent stem cells *via* transient antibiotic selection. *PLoS One* 13:e0201683. doi: 10.1371/journal.pone.0201683

Thumann, G., Dou, G., Wang, Y., and Hinton, D. R. (2013). "Chapter 16—Cell biology of the retinal pigment epithelium," in *Retina, Fifth Edition*, ed Stephen J. Ryan (Elsevier), 401–414.

Ueda, K., Onishi, A., Ito, S., Nakamura, M., and Takahashi, M. (2018). Generation of three-dimensional retinal organoids expressing rhodopsin and S- and M-cone opsins from mouse stem cells. *Biochem. Biophys. Res. Commun.* 495, 2595–2601. doi: 10.1016/j.bbrc.2017.12.092

Vergara, M. N., Flores-Bellver, M., Aparicio-Domingo, S., McNally, M., Wahlin, K. J., Saxena, M. T., et al. (2017). Three-dimensional automated reporter quantification (3D-ARQ) technology enables quantitative screening in retinal organoids. *Development* 144, 3698–3705. doi: 10.1242/dev.146290

Völkner, M., Zschätzsch, M., Rostovskaya, M., Overall, R. W., Busskamp, V., Anastassiadis, K., et al. (2016). Retinal organoids from pluripotent stem cells efficiently recapitulate retinogenesis. *Stem Cell Reports* 6, 525–538. doi: 10.1016/j.stemcr.2016.03.001

Waisman, A., La Greca, A., Möbbs, A. M., Scarafía, M. A., Velazque, N. L. S., Neiman, G., et al. (2019). Deep learning neural networks highly predict very early onset of pluripotent stem cell differentiation. *Stem Cell Reports* 12, 845–859. doi: 10.1016/j.stemcr.2019.02.004

Zagozewski, J. L., Zhang, Q., Pinto, V. I., Wigle, J. T., and Eisenstat, D. D. (2014). The role of homeobox genes in retinal development and disease. *Dev. Biol.* 393, 195–208. doi: 10.1016/j.ydbio.2014.07.004

Conflict of Interest: The authors declare that the research was conducted in the absence of any commercial or financial relationships that could be construed as a potential conflict of interest.

frontiers in Cellular Neuroscience

REVIEW
published: 20 August 2020
doi: 10.3389/fncel.2020.00265

The Use of Induced Pluripotent Stem Cells as a Model for Developmental Eye Disorders

Jonathan Eintracht[1], *Maria Toms*[1,2] *and Mariya Moosajee*[1,2,3,4]*

[1]UCL Institute of Ophthalmology, London, United Kingdom, [2]The Francis Crick Institute, London, United Kingdom, [3]Moorfields Eye Hospital NHS Foundation Trust, London, United Kingdom, [4]Great Ormond Street Hospital for Children NHS Foundation Trust, London, United Kingdom

Approximately one-third of childhood blindness is attributed to developmental eye disorders, of which 80% have a genetic cause. Eye morphogenesis is tightly regulated by a highly conserved network of transcription factors when disrupted by genetic mutations can result in severe ocular malformation. Human-induced pluripotent stem cells (hiPSCs) are an attractive tool to study early eye development as they are more physiologically relevant than animal models, can be patient-specific and their use does not elicit the ethical concerns associated with human embryonic stem cells. The generation of self-organizing hiPSC-derived optic cups is a major advancement to understanding mechanisms of ocular development and disease. Their development *in vitro* has been found to mirror that of the human eye and these early organoids have been used to effectively model microphthalmia caused by a *VSX2* variant. hiPSC-derived optic cups, retina, and cornea organoids are powerful tools for future modeling of disease phenotypes and will enable a greater understanding of the pathophysiology of many other developmental eye disorders. These models will also provide an effective platform for identifying molecular therapeutic targets and for future clinical applications.

Keywords: eye development, human induced pluripotent stem cells, developmental eye disorders, disease modeling, ocular maldevelopment, VSX2, microphthalmia, corneal hereditary endothelial dystrophy

OPEN ACCESS

Edited by:
Carla Mellough,
Lions Eye Institute, Australia

Reviewed by:
In-Hyun Park,
Yale University, United States
Roly Megaw,
University of Edinburgh,
United Kingdom

***Correspondence:**
Mariya Moosajee
m.moosajee@ucl.ac.uk

Specialty section:
This article was submitted to Cellular Neuropathology, a section of the journal Frontiers in Cellular Neuroscience

Received: *18 February 2020*
Accepted: *28 July 2020*
Published: *20 August 2020*

Citation:
Eintracht J, Toms M and Moosajee M (2020) The Use of Induced Pluripotent Stem Cells as a Model for Developmental Eye Disorders. Front. Cell. Neurosci. 14:265. doi: 10.3389/fncel.2020.00265

INTRODUCTION

Developmental eye disorders are amongst the most common cause of severe visual impairment in children, with a combined incidence of 1–2 per 10,000 births (Nedelec et al., 2019). They comprise a wide range of congenital abnormalities ranging from anophthalmia, aniridia, Leber congenital amaurosis, and congenital cataracts, and are frequently associated with extraocular features (Bardakjian et al., 2015). Childhood blindness can have extensive ramifications for the child and their family, particularly as the global cost is higher than adult-onset vision loss (Rahi et al., 1999; Dharmasena et al., 2017). Quality of life, educational opportunities, mental health, and independence are all affected by sight loss (Tseng and Coleman, 2018). Currently, there are no preventative strategies, and management is only supportive to maximize any residual vision and minimize amblyopia. Ocular malformations can result from several environmental factors, including exposure to teratogenic drugs or maternal infections; however, it has been estimated that genetic variants are responsible for approximately 80% of cases (Gregory-Evans et al., 2019). Approximately 70% of patients with a bilateral or severe phenotype will receive a molecular

diagnosis but 90% with a unilateral phenotype remain unresolved (Harding and Moosajee, 2019). The early *in utero* onset of these diseases poses a challenge for investigating underlying genetic mechanisms and developing suitable treatments.

There is a diverse range of developmental eye disorders, which can vary depending on the stage of development, genetic pathways and tissue(s) affected (Gregory-Evans et al., 2019). Additionally, there is large phenotypic and genetic heterogeneity within the same group of diseases (Williamson and FitzPatrick, 2014). One of the major early-onset disease groups arising between weeks 4–7 of gestation is the microphthalmia/anophthalmia/coloboma (MAC) spectrum, which varies in severity and includes the complete absence of an eye (anophthalmia), a small underdeveloped eye (microphthalmia) and incomplete fusion of the optic fissure leading to a persistent cleft in the inferior aspect of the eye spanning one or more of the following tissues: iris, ciliary body, retina, RPE, choroid and optic nerve (coloboma; Harding and Moosajee, 2019). All these disorders are caused by disruption to key regulatory genes, including numerous transcription factors, that are essential for normal eye development (Moosajee et al., 2018). By understanding the roles of these genes in development, the pathological mechanisms and phenotypic variation can be better understood, improving diagnosis and management.

A NEW TOOL TO STUDY OCULAR DEVELOPMENT

Animal models, including the mouse, rat, zebrafish, *drosophila, Xenopus*, chick and dog have all contributed to our understanding of ocular development and disease (Kaukonen et al., 2018; Kolosova et al., 2018; Moore et al., 2018; Sghari and Gunhaga, 2018; Zhu et al., 2018; Kha et al., 2019; Richardson et al., 2019). Despite their invaluable contribution, animal models are suboptimal for critical reasons: (i) Differences in gene expression between animal models do not inform our understanding of human disease mechanisms; for example, *MAB21L2*, which is required for eye morphogenesis and cell survival in the developing optic cup and lens, and is associated with microphthalmia and coloboma in humans (Gath and Gross, 2019; Eintracht et al., 2020). However, the closest expression pattern to humans is still unknown due to differing *mab21l2* expression patterns and localization in the chick, mouse, and zebrafish (Sghari and Gunhaga, 2018; Gath and Gross, 2019). (ii) Disease phenotypes observed in humans do not always mimic those seen in animals; for instance, heterozygous *PITX3* mutations in humans primarily result in dominant anterior segment dysgenesis and cataracts but homozygous loss-of-function mutations result in microphthalmia in mice (Rosemann et al., 2010; Ma et al., 2018a). (iii) The embryonic lethality described in many animal models e.g., *Sox2, Otx2*, and *Mab21l2* mouse and zebrafish models is incomparable (Reis and Semina, 2015). (iv) Ocular structures and developmental events differ between humans and animal models as highlighted in zebrafish, where the optic vesicles are solid neuroepithelial protrusions from the cell-dense neural tube (neural keel) that then cavitate, whereas human optic vesicles are hollow (Richardson et al., 2017). (v) The macula is not present in rodent eyes, thus disease pathophysiology differs greatly to human disorders affecting the central retina (Huber et al., 2010).

As a result, studying ocular development and disease using human tissue is more physiologically relevant. However, understanding mechanisms of early ocular malformations using human samples is near-impossible due to the inaccessibility to fetal tissue from 4 to 7 weeks of gestation (Lindsay et al., 2016). Consequently, the use of human-induced pluripotent stem cells is an attractive option to overcome these difficulties.

HUMAN INDUCED PLURIPOTENT STEM CELLS

Human-induced pluripotent stem cells (hiPSCs) are generated from somatic cells by delivery of the "Yamanaka" factors, *OCT4, SOX2, KLF-4*, and *C/L-MYC* (Takahashi et al., 2007; Okita et al., 2011). Overexpression of these transcription factors will activate endogenous gene expression regulating pluripotent gene expression (Black and Gersbach, 2018). Consequently, cells will revert to a pluripotent state in terms of morphology, proliferation, gene expression, epigenetics, and differentiation capacity (Takahashi et al., 2007). Morphological and molecular similarities between hiPSCs and human embryonic stem cells (hESCs) have been extensively demonstrated and recent data suggest they cannot be distinguished by a unique and consistent gene expression signature (Choi et al., 2015). Further comparisons of hESC- and hiPSC-derived neurons revealed that epigenetic and gene expression profiles are remarkably similar (de Boni et al., 2018).

While it is still unknown as to what extent hiPSCs can entirely replace hESCs due to the unique genetic signature contained in each line, it is important to note the distinct advantages over hESCs. hiPSC use circumvents the ethical concerns associated with the creation of hESC lines from embryos as they are generated from somatic cells such as blood, urine, and skin (Green, 2019). In terms of personalized medicine, lines can be created from the patient themselves with a wide range of applications including disease modeling *in vitro* to better understand the pathophysiology and provide targets for novel therapeutic development and testing (Doss and Sachinidis, 2019; Ortiz-Vitali and Darabi, 2019). For example, histone deacetylase 4 (HDAC4) was shown to be mislocalized in patient hiPSC-derived dopaminergic neurons modeling Parkinson's disease, causing downregulation of critical genes (Lang et al., 2019). Treatment of these neurons with compounds that specifically inhibited MAP4K4 action corrected HDAC4 mislocalization and rescued the Parkinson's disease phenotype (Lang et al., 2019). In patients with a confirmed genetic diagnosis, gene editing could be used correct the mutation in their specific hiPSC line (Yanai et al., 2019); for instance, CRISPR/Cas9 editing of a deep intronic mutation in *CEP290* removed the cryptic splice site and restored CEP290 expression (Burnight et al., 2018). Gene editing can also be used to introduce a known mutation into wild type hiPSCs where patient cells are not available as demonstrated by the generation of an hiPSC line with a single base insertion in the *COL1A1* gene (c.3969_3970insT) found in

patients with osteogenesis imperfecta (Hosseini Far et al., 2019). Introducing a known mutation into wild type hiPSCs can also be used as a control in disease models to ascertain its causative nature e.g., assessing the pathogenicity of induced *MYL3* variants associated with hypertrophic cardiomyopathy (Ma et al., 2018b). hESCs can also be engineered to contain a disease-causing mutation for the same *in vitro* disease-modeling as hiPSCs, as demonstrated by the introduction of *CHCHD2* mutations such as c.376C >T, p.(Gln126*) for modeling of Parkinson's disease and mitochondrial dysfunction (Zhou et al., 2019).

SOURCES OF INDUCED PLURIPOTENT STEM CELLS AND REPROGRAMMING METHODS

In principle, hiPSCs can be derived from any somatic cell (Raab et al., 2014). hiPSCs have been most commonly derived from cell sources such as skin, blood, urine, and hair (Takahashi et al., 2007; Wang et al., 2013; Agu et al., 2015; Cheng et al., 2017; **Figure 1**). Less invasive procedures such as urine collection or blood sampling will encourage more patient donors, particularly children, as this avoids a general anesthetic (Chen et al., 2013). Due to its safety and accessibility, blood is currently the most widely-used source of cells for reprogramming to hiPSCs (Sharma et al., 2018). Reprogramming efficiencies and kinetics vary greatly between each somatic cell type used (Raab et al., 2014; see **Supplementary Tables S1, S2** for a comprehensive overview of reprogramming techniques and somatic cell sources).

hiPSC MODELING OF HUMAN EYE DEVELOPMENT

From hiPSCs to Optic Cups

Nakano et al. (2012) developed a protocol for the creation of self-organizing optic cups complete with photoreceptors, retinal neurons and Muller glial cells using hESCs, building on extensive knowledge of retinal differentiation pathways *in vitro* gained through previous experimentation (Meyer et al., 2009, 2011; Nakano et al., 2012). Additionally, *in vivo* studies suggested the coordinated inhibition of critical signaling pathways such as Wnt/BMP and activation of others such as IGF were critical for ocular development (Llonch et al., 2018). It was hypothesized that the modulation of these specific pathways in tightly-controlled culture conditions could generate three-dimensional *in vitro* optic vesicles and mature retinal tissue.

Initially, embryoid bodies (9,000 cells/well) were formed in the presence of Y-27632, a selective inhibitor of Rho-associated coiled-coil containing protein kinase (ROCK) that reduces dissociation-induced apoptosis in hiPSCs and maintained in suspension culture. Embryoid bodies were initially cultured in retinal differentiation media from day 0 to 18. Basal media was supplemented with 20% knock-out serum residue (KOSR) alongside extracellular matrix Matrigel (1%) until day 18. Smoothened agonist (SAG) was added until day 12 to activate the hedgehog signaling pathway and replaced with Wnt agonist CHIR99021 from day 15 to 18. At day 18, differentiating optic cups were transitioned to an NR culture media comprised of DMEM/F12 and N2, a supplement promoting neural differentiation. From day 24, optic vesicle-like structures were excised from larger cell aggregates and retinoic acid, an essential signaling molecule involved in human eye development, was added to culture media to enhance optic cup differentiation. Through temporal control of culture conditions by extrinsic modulation of Wnt, fibroblast growth factor (FGF) and SHH signaling pathways that initially promote eye-field formation in the anterior plate and subsequent eye development, the group successfully generated a protocol modeling the patterning and evagination of the optic vesicle and the invagination of the bilateral optic cup. Both bright-field and confocal microscopy showed striking morphological changes in the first 30 days of differentiation and specification of cellular layers corresponding to early human ocular development.

Although initial experiments were performed with hESCs rather than hiPSCs, the work of Nakano and colleagues provided huge promise in the modeling of human ocular development and further understanding disease pathophysiology using hiPSCs. Many adaptations of the original protocol have differentiated hiPSCs to a retinal lineage and maintained a completely three-dimensional differentiation system (**Figure 2**; Kuwahara et al., 2015; Arno et al., 2016; Parfitt et al., 2016; Völkner et al., 2016; Wahlin et al., 2017). Novel three-dimensional protocols have also been developed where cells were differentiated in a descending concentration gradient of KOSR (20% from day 2, 15% from day 7 and 10% from day 11 and onwards) and in the presence of IGF-1 and B27, a supplement promoting growth and viability of central nervous system-associated neurons (Mellough et al., 2015). Remarkably, these protocols recapitulate ocular development despite the absence of *in vivo* cues such as the interaction between the optic vesicle and the surface ectoderm that induces optic cup invagination (Oltean et al., 2016).

Zhong et al. (2014) attempted to induce an anterior neuroepithelial fate in attached cells before directing them to a neuroretina (NR) fate (Zhong et al., 2014). Embryoid bodies were formed in the presence of Blebbistatin rather than ROCK inhibitor Y-27632 and transitioned to a neural induction media containing N2, to promote anterior neuroepithelium formation. Aggregates adhered to culture dishes on day 7 and were cultured in neural induction media containing B27 from day 16, until horseshoe-shaped neuroretinal domains were excised and cultured to form optic cups. Despite the physical constraints of a two-dimensional culture system, optic vesicle, and cup formation were observed (Zhong et al., 2014). This protocol differed by relying on autonomous retinal differentiation guided through *in vitro* intrinsic cues (Zhong et al., 2014; Achberger et al., 2018). Similar results were described by Reichman et al. (2017) who excised optic cups out of culture at day 28 (Reichman et al., 2017), and Gonzalez-Cordero et al. (2017) who excised NR vesicles between weeks 4–7.

Interestingly, the majority of recent protocols have combined two-dimensional and three-dimensional culture, opting to create optic vesicles and cups at an adherent stage before committing cells to long-term three-dimensional differentiation (**Figure 2**;

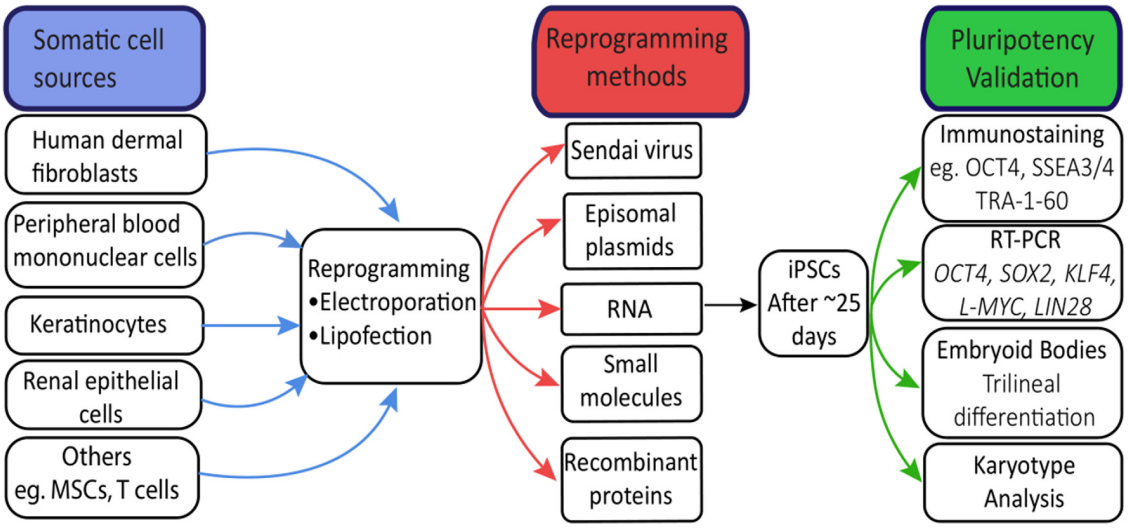

FIGURE 1 | Human-induced pluripotent stem cells (hiPSC) reprogramming. Common sources of somatic cells are reprogrammed by electroporation or lipofection. Induced overexpression of the Yamanaka factors by reprogramming methods drives hiPSC generation, visible after approximately 25 days as tightly packed colonies. Validation of hiPSCs through immunostaining and RT-PCR confirms expression patterns and levels of key pluripotency genes. Trilinear differentiation of embryoid bodies confirms the differentiation capacity of hiPSCs to all three germ layers, while karyotype analysis confirms no chromosomal abnormalities resulting from the reprogramming process.

Zhong et al., 2014; Lowe et al., 2016; Wahlin et al., 2017; Achberger et al., 2018). These protocols are advantageous due to the high level of scrutiny when excising retinal tissue from a monolayer of cells and the reduction of intra- and inter-culture variability (Capowski et al., 2019). Exclusively three-dimensional protocols are advantageous as they closely recapitulate retinal microarchitecture, generate a high percentage of retinal cells, and facilitate self-organization to mature ocular tissue with high fidelity to the human eye development (Capowski et al., 2019; Mellough et al., 2019b). However, these protocols are disadvantageous due to the emergence of ectopic retinal cells, and abnormal structures in culture, loss of inner cell types due to lengthy culture periods and increased variability amongst vesicles.

In most protocols, extrinsic modulation of differentiation cues decreases with time, based on the assumption that long-term differentiation gradually becomes guided by the intrinsic cues found in the differentiating tissue itself (Achberger et al., 2018). Morphological changes form the basis of a recently described rigorous stage-specific selection of optic vesicle-like structures for further differentiation to optic cups (Capowski et al., 2019).

A particular difficulty in optic cup formation lies in the variable efficiency of optic cup invagination *in vitro*, although stratified neuroretina formation is still efficiently induced even in the absence of invaginated optic cups (Nakano et al., 2012; Llonch et al., 2018). Optic cup formation has been reported at efficiencies ranging from 7 to 70% dependent on hiPSC line, reflecting an inherent difficulty in hiPSC modeling (Capowski et al., 2019; Mellough et al., 2019b). Efficiencies can also vary between subsequent differentiation of the same hiPSC line, posing a further difficulty for the generation of hiPSC-derived optic cups (Capowski et al., 2019).

A Faithful Model of Eye Development

The fidelity of previously published methods of hiPSC optic cup differentiation was established based on the expression of EFTFs and NR/RPE cell markers at appropriate stages of differentiation. However, comparative analysis with human fetal tissue (HFT) has been limited. Wang et al. (2015) differentiated hiPSCs to optic cups and detected the expression of key EFTFs during early ocular development for comparison with human fetal optic cups (Wang et al., 2015). Similar expression patterns were detected between the two tissue types; for instance, immunostaining revealed PAX6 and OTX2 expression was ubiquitous through both fetal and *in vitro* hiPSC-derived optic vesicles (Wang et al., 2015). Furthermore, MITF and OTX2 co-expression was detected in the RPE layer of both the human fetal and hiPSC-derived optic cups while SOX2 and VSX2 co-expression was observed ubiquitously in the NR layer (Wang et al., 2015). Overall, this study demonstrated consistency between the development of both *in vitro* and fetal bi-layered optic cups using several known stage-specific transcription factor markers (**Figure 3**).

Transcriptomic profiling of the human fetal ocular tissue has provided a more in-depth molecular insight into the developmental processes underlying ocular development. RNA-seq is an accurate and advanced high-throughput sequencing tool to evaluate temporal and differential gene expression between cell types and/or developmental stages, or delineate genetic networks underlying cell morphology (Mellough and Lako, 2016; Hoshino et al., 2017). The molecular mechanisms of the developing retina have been dissected in several studies yet only one has generated a transcriptomic profile of the early stages of eye development (Young et al., 2013; Aldiri et al., 2017; Hoshino et al., 2017; Welby et al., 2017;

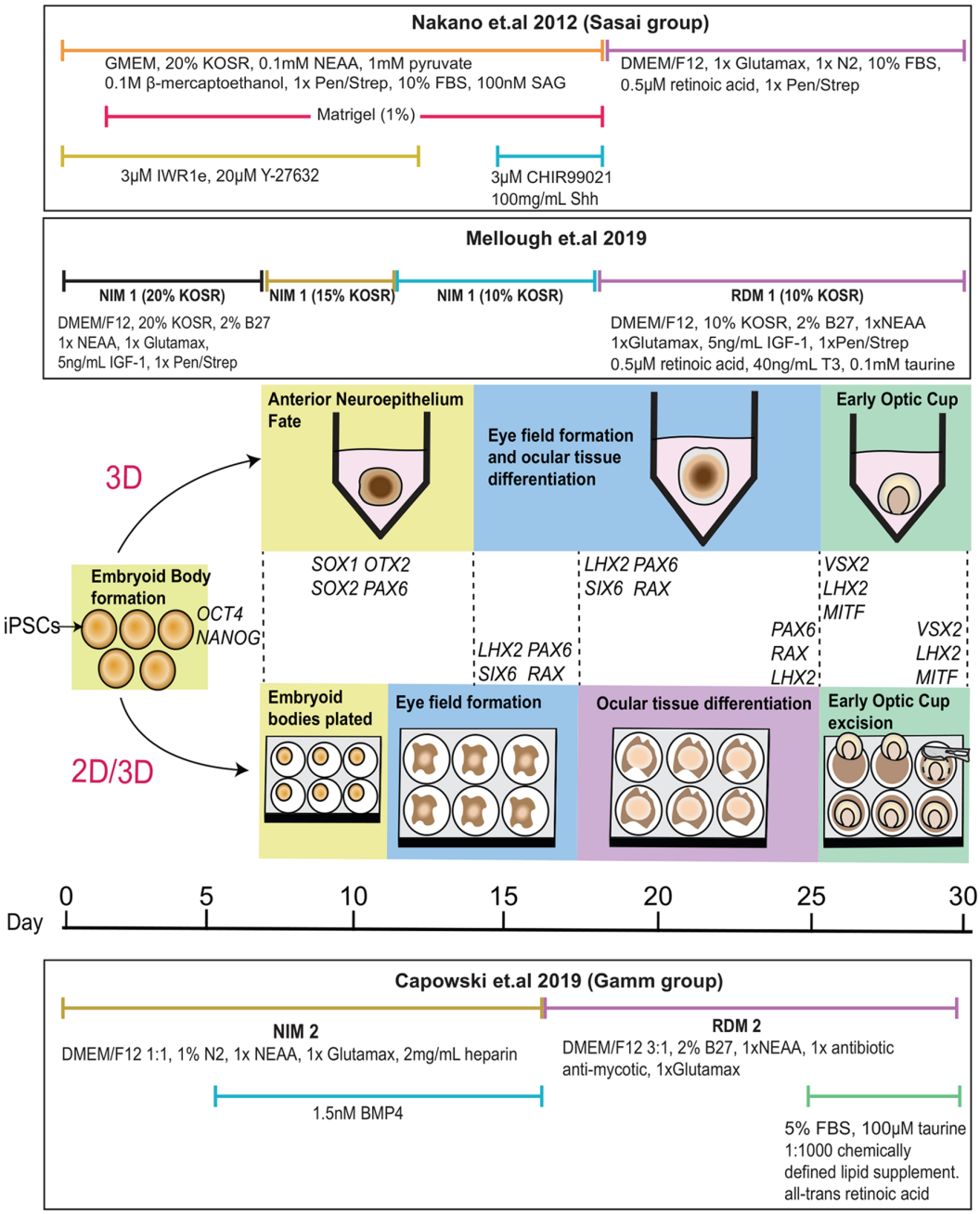

Key: NIM - Neural Induction Media, **RDM** - Retinal Differentiation Media, **KOSR** - Knockout serum residue,**NEAA**- non-essential amino acids, **FBS** - fetal bovine serum, **Pen/Strep** - penicilin/streptomycin, **SAG** - smoothend agonist, **IGF-1** - insulin growth factor

FIGURE 2 | *In vitro* optic cup differentiation with relevant genes expressed at each stage. Following the Sasai protocol, embryoid bodies are formed in the presence of ROCK inhibitor Y-27632 and cultured in a neural induction media supplemented with Wnt inhibitor IWR1e from day 0 to 12, and Wnt and SHH agonists CHIR99021 and Shh from day 15 to 18. Matrigel is added from day 2 to 18. Cells are transitioned to a retinal differentiation media supplemented with N2 and retinoic acid from day 18. According to the Mellough protocol, embryoid bodies are formed in the presence of ROCK inhibitor Y-27632 and cultured in a neural induction media supplemented with IGF-1 and B27 with decreasing knock-out serum residue (KOSR) concentrations adjusted from 20% to 15% at day 7 and from 15% to 10% at day 11. At day 18, cells are transitioned to a retinal differentiation media supplemented with retinoic acid, taurine, and triiodothyronine (T3). Following the 2D/3D differentiation technique most recently described by Capowski et al. (2019), embryoid bodies are formed from iPSCs after 2 days of culture with ROCK inhibitor Y-27632. Cells are weaned into a neural induction media containing N2 and supplemented with BMP4 from day 6 to day 16. At day 7, embryoid bodies are plated to differentiate as a 2D monolayer of cells. The eye field forms around day 10, as cells are guided towards optic cup-like structures. At day 16, cells were transitioned to retinal differentiation media supplemented with 2% B27. By ∼25 days, optic cup-like structures are visible and are excised from the adherent culture for further maintenance in suspension and cultured in retinal differentiation media supplemented with FBS, taurine, retinoic acid, and a chemically defined lipid supplement.

Mellough et al., 2019a). Mellough et al. (2019a) reported low expression levels of *PAX6* and *VSX2* despite upregulated *MITF* expression during optic cup formation (Mellough et al., 2019a). *SIX6* and *RAX* were also expressed at low levels although higher than *PAX6* and *VSX2*. *LHX2*, *SOX2*, and *VIM* were highly expressed at the optic cup stage, along with WNT, FGF, and BMP4 pathway genes including *WNT11, FGF19, BMP7*, and *BMP4*. In a later study, comparable *VSX2, OTX2*, and *ASCL1* expression levels were found in optic cups at week 5 compared to the fetal retina at a similar time point, although *FGF5* expression was elevated in the *in vitro* optic cups (Mellough et al., 2019b; **Figure 3**).

In modeling human ocular development *in vitro*, Kim and colleagues reported molecular congruency between day 15 and day 30 hiPSC-derived ocular tissue and HFT (Kim et al., 2019). Time-course analysis created four clusters of differentially expressed genes associated with different developmental stages of the eye. Differentiating hiPSCs at day 15 yielded highly expressed genes involved in the Wnt and BMP pathways and the developing forebrain including *BMP4, BMP7, WNT1*, and *VAX1* (Slavotinek et al., 2012; Kim et al., 2019). *LHX2* is highly expressed both at day 15 and 30 but significantly downregulated at future time points. By day 30, genes expressed during the optic cup and lens formation such as *VSX2*, or *CRYAA, CRYB4A*, and *CRYBB2* were significantly upregulated compared to day 15; expression levels closely mirrored those detected in HFT (Kim et al., 2019). Also, RNA splicing events and immunostaining expression patterns in differentiating optic cups mirrored those observed in HFT (Kim et al., 2019; **Figure 3**).

This initial RNA-seq data indicates a high-fidelity hiPSC-derived model of ocular development with extensive cellular and molecular similarities. Further improvement of these models, such as reduction of batch variability, will create more consistent data sets between studies. Additionally, a complete characterization of ocular development requires accessible HFT from earlier developmental stages than optic cup formation (Lindsay et al., 2016). Currently, transcriptomic profiles of the developing human retina do not include data from the early embryological stages of ocular development and cannot be compared with hiPSC models recapitulating those early processes (Aldiri et al., 2017; Hoshino et al., 2017). Future omics studies will provide further insight into early eye development and could be utilized for further understanding of ocular maldevelopment in an hiPSC-derived model at the single-cell level. For a summary of the major accomplishments of omics studies in establishing the molecular fidelity of *in vitro* hiPSC-derived optic vesicles to early human eye development, see **Figure 3**.

DEVELOPMENTAL EYE DISORDERS AND ASSOCIATED GENETIC VARIANTS MODELLED USING hiPSCs

Early Eye Development

Morphogenesis and Gene Regulatory Networks

Vertebrate eye development is tightly controlled by spatiotemporal gene expression patterns and interactions between the embryonic germ layers (**Figure 4**; Harding and

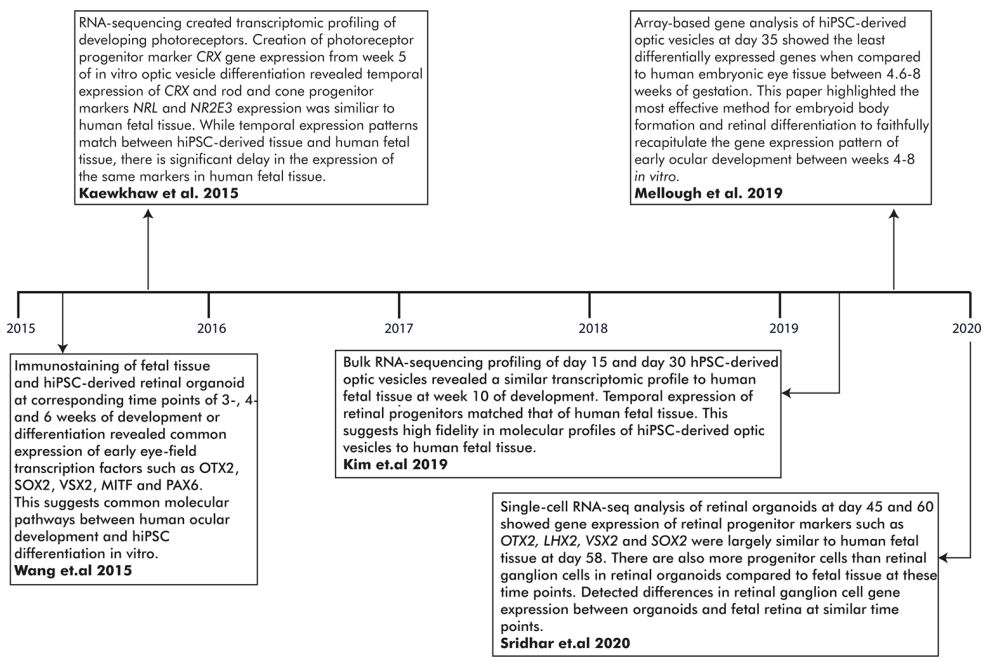

FIGURE 3 | Important milestones in establishing the fidelity of *in vitro*-generated optic vesicles to human fetal tissue (HFT) at early developmental time points. RNA-sequencing has generated transcriptomic profiles of hiPSC-derived optic vesicles and HFT. A comparison of these profiles has revealed novel genes involved in ocular development and highlighted the high molecular fidelity of *in vitro* optic vesicle development to human embryological development.

Moosajee, 2019). The eye is derived from: (i) neuroectoderm, which gives rise to the neural retina (NR), retinal pigment epithelium (RPE), optic nerve, iris dilator and sphincter muscles, and ciliary body; (ii) surface ectoderm, which contributes to the lens, conjunctival and corneal epithelia; and (iii) mesenchyme, which originates from the mesoderm and neural crest cells, forming the corneal endothelium and stroma, iris stroma, ciliary muscles, vasculature, and sclera. Human eye development is first evident at around day 22 of gestation and is not completed until several months after birth.

Following gastrulation and specification of the three germ layers, the formation of the eye field from the anterior neural plate takes place, this is characterized by expression domains of early eye-field transcription factors (EFTFs) *PAX6, OTX2, RAX, SIX6, SIX3* and *LHX2* (**Figure 4A**; Chen et al., 2017). The complex interactions between various signaling cascades and EFTFs are crucial to produce the appropriate cell types at the correct developmental time and ensure their correct optimal cell proliferation, migration, and polarity (Gregory-Evans et al., 2013). EFTFs regulate signaling pathways intrinsic to ocular tissue that drives the morphogenetic events of ocular development, such as optic vesicle and cup formation. Mutations in the genes encoding EFTFs lead to ocular maldevelopment.

OTX2 is initially expressed in the anterior neuroepithelium and is the earliest molecular marker in the eye field, together with *SOX2*, it activates *PAX6, RAX*, and *SIX3* expression and is subsequently downregulated (**Figure 5A**; Danno et al., 2008; FitzPatrick, 2016; Giger and Houart, 2018). *SIX3* regulates *SHH* expression in the sonic hedgehog (SHH) signaling pathway, required for dorso-ventral patterning of the forebrain and later modeling of the optic vesicle and cup, through canonical Wnt pathway antagonization (Jeong et al., 2008; Diacou et al., 2018). *RAX*, an early marker of ocular development, is critical for retinal progenitor proliferation and optic vesicle evagination but later restricts *OTX2* expression in the eye field (**Figure 5A**; Gregory-Evans et al., 2013; Zagozewski et al., 2014; Rodgers et al., 2018). *RAX* variants are associated with anophthalmia and microphthalmia (Reis and Semina, 2015). *SOX2* and *OTX2* expression in the early eye field regulate *RAX* by binding to a conserved enhancer element containing binding sequences for both factors (Danno et al., 2008; Slavotinek, 2019). *TBX3* is also expressed in the eye-field and induces neural induction and normal eye formation by repressing *BMP4* expression, and maintaining these eye-field neural progenitors in a multipotent state before retinal induction (Motahari et al., 2016).

The first morphological milestone in eye development is the bilateral evagination of the eye field region, which occurs during neurulation. The splitting of the eye field first appears as small indentations known as optic sulci at day 22 post-conception (**Figure 4B**; Harding and Moosajee, 2019). SHH and FGF signaling pathways, regulated by transforming growth factor (TGF) signaling, initiate the splitting of the eye field and the subsequent posterior to anterior migration of cells to drive optic vesicle evagination (Cardozo et al., 2020). SHH signaling originating from the midline tissue in the ventral forebrain by regulating the inverse expression of *PAX2*, expressed in the presumptive optic stalk, and *PAX6*, expressed in the presumptive neural retina and pigment epithelium, to mediate the partitioning of the optic primordia to optic stalk and presumptive optic cup (Macdonald et al., 1995).

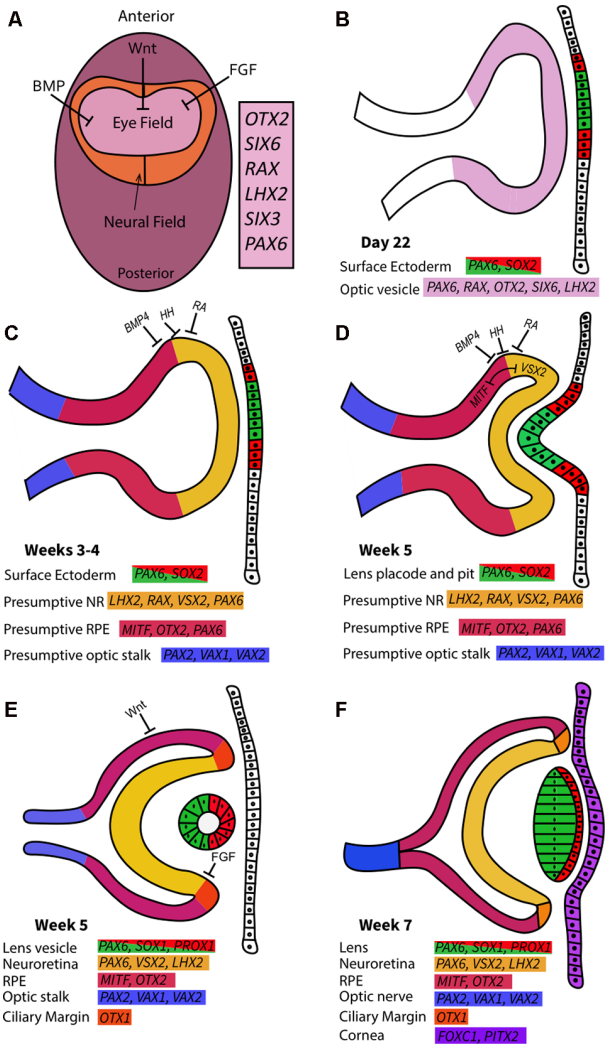

FIGURE 4 | Early ocular morphogenesis. **(A)** Developmental pathways such as Wnt, BMP, and fibroblast growth factor (FGF) drive upregulation of eye-field transcription factors in the anterior neural plate, creating the specified region known as the "eye-field." **(B)** Deepening of optic sulci and evagination of optic vesicle around 22 days post-conception. The newly formed optic vesicle ubiquitously expresses all eye-field transcription factors. **(C)** The action of signaling pathways determines presumptive regions in the optic vesicle characterized by unique gene expression patterns in the third and 4th weeks of gestation. **(D)** Interactions between the optic vesicle, surface ectoderm, and extraocular mesenchyme cause the invagination of the optic cup at approximately 5 weeks post-conception. MITF and VSX2 interactions create boundaries between retinal pigment epithelium (RPE) and neuroretina (NR) in the developing optic cups. The lens pit begins to form from the surface ectoderm. **(E)** In the 5th week of gestation following optic cup formation, Wnt and FGF pathways drive RPE/NR differentiation and clear definition of these regions through ciliary margin formation. The lens vesicle forms as the lens pit detach from the surface ectoderm. **(F)** By the 7th week of gestation, lens fibers extend to form the lens from the hollow lens vesicle. The cornea forms from the overlying surface ectoderm. NR and RPE are clearly defined and separated by the ciliary margins, while the optic nerve forms from the convergence of the optic stalk.

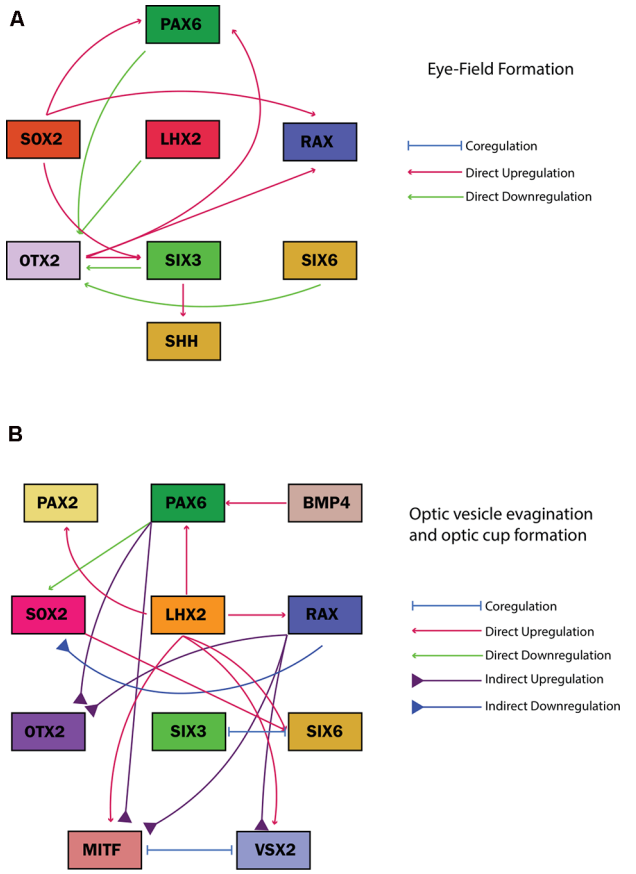

FIGURE 5 | Gene regulatory networks of common eye field transcription factors associated with ocular malformation guiding cell fates during **(A)** eye field formation and **(B)** optic vesicle evagination and optic cup formation. The regulatory effect of each transcription factor on the other is illustrated in the key adjacent to each figure along with the specific developmental stage.

Eph/Ephrin signaling likely plays a role mediating Wnt, SHH, and FGF signaling to control optic vesicle evagination as it branches off from the anterior forebrain (Cardozo et al., 2020). Failure of the eye field to split results in a single central eye known as cyclopia, often caused by defects in dorso-ventral patterning associated with *SHH* mutations (FitzPatrick, 2016; Placzek and Briscoe, 2018). LHX2 is required for correct optic sulci localization and loss of expression after optic vesicle formation may arrest optic cup formation (Roy et al., 2013). However, *LHX2* variants associated with anophthalmia have only been described in a mouse model and have not been linked to any ocular malformations in humans (Desmaison et al., 2010; Plaisancié et al., 2019).

The optic vesicles form as the optic sulci deepen in the 4th week of embryonic development. They are connected to the developing forebrain by the optic stalk which later develops into the optic nerve. Early EFTFs such as *PAX6* and *OTX2* are expressed in the optic vesicle and are required for cell fate-determining signaling pathways (Fuhrmann, 2010). Co-expression of *SOX2* and *PAX6* is ubiquitous throughout the optic vesicles (Hever et al., 2006; Matsushima et al., 2011; Kondoh et al., 2016). *RAX* expression is upregulated by LHX2 in the eye field and the evaginating optic vesicle (**Figure 5B**; Gregory-Evans et al., 2013).

Intrinsic and extrinsic factors provide patterning cues to establish molecular boundaries in the optic vesicles, while a distinct set of transcription factors are expressed in presumptive regions of the optic vesicle for the development of each cell type (**Figure 4C**; Heavner and Pevny, 2012; Giger and Houart, 2018). SHH, retinoic acid, and BMP4 signaling pathways create unique molecular regions, such as the *PAX6*-expression domain specified by BMP4 modulation in the distal optic vesicle (**Figure 4C**; FitzPatrick, 2016). Disruptions to this process can arrest eye development; for example, mutations in BMP4 antagonist *SMOC1* result in anophthalmia (Rainger et al., 2011).

Towards the end of the 4th week of gestation, the distal optic vesicle contacts the overlying surface ectoderm allowing BMP and retinoic acid released from the lens placode to bind to the optic vesicle and displace the intervening mesenchyme (Snell and Lemp, 2013; Harding and Moosajee, 2019). Within this region of contact, each optic vesicle and surface ectoderm thickens to form placodes and invaginate to form the optic cup and lens pit respectively (**Figure 4D**). The invagination of the optic vesicle to form the bi-layered optic cup is stimulated by BMP4 and retinoic acid (Harding and Moosajee, 2019). The inner layer develops into the NR, while the RPE is formed from the external layer. *TBX3* activates Noggin induction of *PAX6* expression and co-expression with *TBX3* drives retinal differentiation in the eye field (Motahari et al., 2016). *SOX2* expression is downregulated in the presumptive RPE region, upregulating *MITF* and *OTX2* expression to drive RPE formation (**Figure 5B**; Kondoh et al., 2016; Chen et al., 2017). *SOX2* and *PAX6* are expressed at an inverse gradient in the invaginating optic cup where *SOX2* has a critical role in maintaining the potential for neuronal differentiation as its expression is gradually confined to the outer layer of the NR (Chen et al., 2017). Loss of SOX2 reduces the capacity for NR formation during optic cup invagination and causes preferential differentiation to the non-neurogenic ciliary epithelium (Matsushima et al., 2011). Optic cup malformation caused by loss of SOX2 function is possibly due to the failed antagonism of the Wnt/β-catenin pathway that results in impaired NR/RPE differentiation and optic cup formation (Kelberman et al., 2008; Capowski et al., 2016). Accordingly, a large proportion of *SOX2* loss-of-function mutations cause anophthalmia (Slavotinek, 2019).

The reciprocal relationship between *MITF* and *VSX2*, coupled with FGF signaling, drives the establishment of pronounced NR and RPE domains (**Figure 4E**; Capowski et al., 2014). *LHX2* also acts upstream of *MITF, VSX2*, and *PAX2* for temporal control of their expression (**Figure 5B**; Chou and Tole, 2019). β-catenin/Wnt signaling specifies the RPE fate in the dorsal optic cup by directly upregulating *MITF* and *OTX2* expression while FGF signaling acts primarily through FGF9 through promoting the development of the ciliary margin at the NR/RPE junction (**Figure 4E**; Westenskow et al., 2009; Balasubramanian et al., 2018).

The proximal portion of the newly-formed optic vesicle expresses *PAX2, VAX1* and *VAX2* genes that are responsible for optic stalk formation (**Figure 4D**; Stanke et al., 2010; Patel and Sowden, 2019). In the evaginating optic vesicle, LHX2-regulated BMP4 expression induces the formation of the lens placode in the overlying surface ectoderm while PAX6 and SOX2 simultaneously bind to enhancers in the lens placode to drive early lens crystallin production, targeting critical genes such as *FOXE3* (Harding and Moosajee, 2019). The deceleration of cell division at the center of the lens placode causes its invagination, producing lens pits that detach from the overlying surface ectoderm to form the lens vesicle (Plaisancié et al., 2019). After detachment, PROX1 regulates lens differentiation and fiber elongation as *PAX6* expression is maintained in the lens vesicle (Cvekl and Zhang, 2017).

During the 5th week of ocular development, the optic fissure develops as a furrow along the ventral surface of the optic cup extending to the optic stalk (Plaisancié et al., 2019). This transient structure enables the vasculature to enter and supply the developing eye and completely fuses around week 7 (FitzPatrick, 2016; Richardson et al., 2017). Ocular coloboma will result from incomplete optic fissure fusion and has been associated with various genetic variants, including *PAX6* and *PAX2* that cause disrupted optic nerve/RPE boundaries (ALSomiry et al., 2019). Following optic fissure fusion, the formation of the major eye structures is mostly complete and maturation of the ocular tissues occurs subsequently.

By approximately the 6th week of gestation, interactions between the lens and optic cup induce the formation of the cornea from the surface ectoderm (Davies et al., 2009; Snell and Lemp, 2013). During the 7th week of embryonic development, periocular mesenchymal and neural crest cells migrate into the space between the surface ectoderm and the lens vesicle in three distinct waves to gradually form the corneal stroma, epithelium and endothelium (**Figure 4F**; Lwigale, 2015). The third wave of mesenchymal cell migration also contributes to iris formation (Eghrari et al., 2015). *PITX2* and *FOXC1* are key transcription factors expressed in the periocular mesenchyme regulating corneal development; mutations in these genes are associated with anterior segment dysgenesis (Hara et al., 2019). *PAX6* expression is still critical at this point for the development of the anterior segment structures originating from the mesenchyme (Cvekl and Tamm, 2004; see **Supplementary Table S3** for a comprehensive overview of the genes associated with development eye disorders)

Microphthalmia

Microphthalmia is defined by the presence of an eye with an axial length of more than two standard deviations (SD) below the age-adjusted population mean (21 mm in adults and <14 mm in newborns; Harding and Moosajee, 2019). Severe microphthalmia is characterized by a corneal diameter of <4 mm associated with a total axial length <10 mm at birth or <12 mm after 1 year (Harding and Moosajee, 2019). In complex cases, microphthalmia can be associated with other anterior or posterior segment abnormalities (Plaisancié et al., 2019). The common causative genes encode EFTFs such as *SOX2, PAX6, VSX2*, and *OTX2*, or those that encode components of the retinoic acid signaling pathway such as *STRA6* or *ALDH1A3* (Williamson and FitzPatrick, 2014). Chromosomal abnormalities are responsible for approximately 7–15% of syndromic cases (Eintracht et al., 2020).

To investigate ocular maldevelopment, hiPSCs containing a homozygous *VSX2* mutation (p.Arg200Gln) associated with microphthalmia were differentiated to early optic cups (Joseph Phillips et al., 2014). The early stages of ocular development were not impaired by the *VSX2* mutation, demonstrated by consistent eye field marker expression and the appearance of morphologically indistinguishable VSX2+ proliferative optic vesicle-like structures in both the wild type and mutant cultures. However, a disease-like phenotype was apparent after optic vesicle formation as mutant vesicles did not proliferate at the same rate as the healthy control. Mutant optic vesicles also showed a greater preference towards an RPE than NR fate, disrupting optic cup formation. This observation was verified using comparative RNA-seq analysis, where genes involved in Wnt and TGF signaling that drive RPE differentiation, such as *WNT11* and *BMP8A* respectively, were upregulated in mutant vesicles during optic cup formation. Simultaneously, genes involved in FGF signaling driving NR formation, such as *FGF19*, were downregulated in mutant vesicles.

Further investigation into the molecular etiology of microphthalmia, using the same patient hiPSC line, highlighted the transcriptional regulatory role of VSX2 (Capowski et al., 2016). In wild type vesicles, VSX2 and MITF were expressed exclusively in NR and RPE progenitor cells respectively by day 18 yet VSX2 and MITF co-expression was detected in *VSX2*-mutant vesicles. β-catenin, a marker of canonical Wnt pathway activation, was also co-expressed with VSX2+ cells in mutant but not wild type vesicles, indicative of dysregulated Wnt signaling. Altogether, the results suggested that defective VSX2 binding activity fails to repress Wnt signaling and MITF expression that is required to induce correct NR/RPE differentiation and optic cup formation. Tightly-controlled pharmacological inhibition of the Wnt pathway during specific windows of optic vesicle development in *VSX2* mutant vesicles restored functional NR differentiation and disrupted VSX2/MITF colocalization in the developing optic cup. VSX2+ cells were detected in a similar abundance and pattern as wild type vesicles, although MITF expression was not detected in treated vesicles. This partially rescued the disease phenotype as the NR layer of the bi-layered optic cup was restored, but not the RPE layer. Pharmacological activation of the Wnt pathway in wild type vesicles also effectively recapitulated the phenotype observed in *VSX2* mutant vesicles.

A recent study revealed that *FGF9* and *FGF19* were expressed at different times in the optic vesicles to direct early NR development and their expression was found to be reduced in the *VSX2* mutant (Gamm et al., 2019). NR differentiation was enhanced by FGF9 supplementation, as ERK1/2 expression was transiently upregulated and partially rescued the mutant phenotype observed in the *VSX2*-mutant vesicles. ERK1/2 is part of the ERK/MAP pathway that promotes cell proliferation (Mebratu and Tesfaigzi, 2009). The reverse action of withholding

FGF9 did not promote a non-NR fate. This possibly indicates a role for VSX2 in concert with FGF9 to promote NR development (Gamm et al., 2019). Despite limited work, the use of patient hiPSC-derived optic vesicles has already provided some insight into the pathophysiology of *VSX2*-related microphthalmia and highlighted potential therapeutic targets.

Modeling of microphthalmia-associated with the *VSX2* mutation (p. Arg200Gln) was only performed with one patient-specific hiPSC line and one unaffected sibling control (Joseph Phillips et al., 2014; Capowski et al., 2016; Gamm et al., 2019). Consequently, the reliability or reproducibility of published results can be questioned and larger sample size is required. These studies may skew our understanding of disease phenotype, etiology, and pathophysiology. The choice of age-, sex- and ethnicity-matched controls is an important consideration to minimize variability between cell lines (Ortmann and Vallier, 2017; Takasaki et al., 2018; Victor et al., 2018; Deneault et al., 2019).

Introducing specific mutations in wild type iPSC lines through CRISPR/Cas9 gene editing can create isogenic disease models. A comparison of isogenic and patient-derived disease models can ascertain the causative nature of disease-associated variants, such as the *VSX2* mutation (p. Arg200Gln) associated with microphthalmia. As an isogenic iPSC-derived disease model of *VSX2*-associated microphthalmia has not been produced alongside these patient models, it is harder to predict the causative nature of the *VSX2* mutation.

Corneal Hereditary Endothelial Dystrophy

Corneal hereditary endothelial dystrophy (CHED; OMIM:217700) is a rare autosomal recessive disorder leading to severe visual impairment caused by bilateral corneal edema characteristic of primary endothelial cell dysfunction (Brejchova et al., 2019). A subset of patients also suffers from progressive sensorineural hearing loss, in a condition known as Harboyan syndrome (Desir and Abramowicz, 2008; Brejchova et al., 2019). CHED is associated with biallelic pathogenic *SLC4A11* variants, where loss-of-function mutations cause cell adhesion and ion transport defects that reduce corneal endothelial cell viability (Brejchova et al., 2019; Malhotra et al., 2020). This developmental defect occurs around the 7th week of gestation as migrating periocular mesenchymal and neural crest cells begin to differentiate into specialized corneal cell types (Lwigale, 2015; Brejchova et al., 2019).

To characterize the effects of *SLC4A11* variants on corneal endothelial (CE) cells, Brejchova et al. (2019) differentiated both healthy and six patient-hiPSC lines with an *SLC4A11* mutation (c.2240 + 5G >A) to CE cells (Brejchova et al., 2019). Detection of corneal markers ZO-1, N-Cadherin, and CD166 confirmed the identity of differentiated cells. Eleven pathogenic variants were identified, including an alternatively spliced transcript detected in one patient line, revealing a cryptic donor site introduced by the c.2240 + 5G >A mutation. This led to the insertion of six bases, resulting in a premature stop codon (p.[Thr747*]).

One patient, compound heterozygous for c.2240 + 5G >A, p.(Thr747*) and c.625C >T, p.(Arg209Trp), in this study had late-onset CHED compared to the congenital form observed in all other patients. This variant was not located within the canonical splice site and its pathogenicity could not be determined without an experimental model. As *SLC4A11* is only expressed in CE cells, these needed to be generated from hiPSCs due to the inaccessibility of appropriate HFT.

Changes to *SLC4A11* splicing detected in hiPSC-derived models may inform our understanding of variable disease phenotypes caused by changing quantities of mutant *SLC4A11* transcript due to both alternative splicing and overriding mechanisms. The hiPSC-derived CHED model can be further utilized to investigate changes to SLC4A11 transport function, protein stability, and localization associated with *SLC4A11* variants.

LIMITATIONS OF hiPSC USE

Genetic variation imparts a donor-specific genomic and epigenetic signature on hiPSCs that can influence their differentiation capacity and downstream functionality (Kim et al., 2010; Vaskova et al., 2013; Noguchi et al., 2018). Each hiPSC line will have variable differentiation capacities and many cell lines may need to be initially differentiated in pilot experiments to select optimal lines for further experiments (Kyttälä et al., 2016; Cowan et al., 2019). Isogenic hiPSC lines created by gene editing can avoid the genetic variability of multiple hiPSC lines yet effectively model diseased or healthy phenotype (Chakrabarty et al., 2018). Reprogramming efficiency can also be impacted by specific epigenetic enzymes such as the SWI/SNF complex, the age and ancestral origins of the donor (Mackey et al., 2018). The practicalities of hiPSC production also need to be considered. The process to generate hiPSCs is time-consuming and costly, and reprogramming requires specialized equipment and expertise (Giacalone et al., 2016). Additionally, uniquely formulated costly media and reagents handled with a meticulous aseptic technique are required for reprogramming and culture (Giacalone et al., 2016). As there is no consensus on the optimal somatic cell source for reprogramming, it is important to consider the specific advantages and disadvantages of each cell type during experimental design (**Supplementary Tables S1, S2**, Foltz and Clegg, 2019).

An important disadvantage to consider is the loss of X-chromosome inactivation, the transcriptional silencing of one of the two X-chromosomes in female cells (Geens and Chuva De Sousa Lopes, 2017). This epigenetic regulation of X-chromosomal gene expression is critical to correctly modulating X-chromosome dosage to ensure healthy development. Aberrant X-chromosome states associated with the disease have been detected in hiPSCs and may impact their capability to model development and disease *in vitro* (Geens and Chuva De Sousa Lopes, 2017).

Following iPSC generation, it is critical to ensure any reprogramming vectors or plasmids are completely absent from cells, as common methods such as Sendai or episomal reprogramming can leave a transient footprint on the host genome. To ensure differentiation is not impaired by

these vectors or plasmids, low passage (<10) iPSCs should not be used.

hiPSC modeling is inherently limited as it does not replicate the entire biological system with intrinsic and extrinsic cues that control tissue development *in vivo* (Bartfeld and Clevers, 2017). Normal oxygen conditions do not mimic the hypoxic embryological microenvironment of optic vesicle and cup development (DiStefano et al., 2018). Additionally, secondary structures of the developing eye such as vascularization are lacking (Achberger et al., 2018).

It is also important to note that hiPSCs are not hESCs, for whom most of these limitations are not relevant. Yet hESCs have their specific shortcomings such as unclear genotype-phenotype correlations in hESC-based disease models and the need to genetically manipulate hESCs for disease modeling (Halevy and Urbach, 2014). The differences and similarities of hiPSCs and hESCs have been extensively discussed in the literature (Cherry and Daley, 2013; Halevy and Urbach, 2014; Marei et al., 2017; Zhao et al., 2017).

FUTURE WORK

Retina-on-a-chip and retinal differentiation using bioreactors are attempting to enhance *in vitro* differentiation to more closely recapitulate the human embryological environment, such as the outer blood-retina barrier (DiStefano et al., 2018; Achberger et al., 2019). A recently reported retina-on-a-chip system incorporated a vascularized retinal organoid-RPE unit with demonstrated capabilities for drug testing and greater recapitulation of native retina physiology (Achberger et al., 2019). Researchers at the National Eye Institute, USA are developing a three-dimensional *in vitro* RPE/choroid to improve understanding of the photoreceptor/RPE/choroid complex using patient-derived endothelial cells, choroidal fibroblasts and pericytes encapsulated in a collagen-based gel and bio-printed on one side of a biodegradable scaffold with an RPE monolayer derived from the same hiPSCs grown on the other side.

Of the numerous developmental eye diseases that can affect patients, only hiPSC-based modeling of microphthalmia and CHED has been described so far (Joseph Phillips et al., 2014; Brejchova et al., 2019; Gamm et al., 2019). The utility of hiPSC modeling for genetically heterogenous early-onset developmental eye disorders will enhance our understanding of their molecular and epigenetic mechanisms (Gregory-Evans et al., 2019). Future modeling of developmental eye disorders can assess the long-term effects of a mutation in, for example, an EFTF gene through retinal organoids. *VSX2* is involved with bipolar cell differentiation (Clark et al., 2008; Zou and Levine, 2012), and modeling of retinal development in *VSX2*-mutant hiPSCs revealed a complete absence of this cell type, indicating impaired retinal differentiation (Joseph Phillips et al., 2014). These models can provide information on cell patterning to be used for patient phenotyping with advanced ocular imaging techniques and help to predict the response to potential therapies (Ma et al., 2017).

hiPSC-derived models of ocular disease are powerful tools for the development of new therapies and are more physiologically relevant than animal models for pre-clinical testing. Gene editing and antisense oligonucleotide therapy have restored a healthy phenotype from patient-derived retinal organoids with *CEP290* and *RPGR* mutations (Parfitt et al., 2016; Deng et al., 2018). Nonsense suppression using read-through drugs such as PTC124 (ataluren) is a further promising approach which has been reported to restore full-length protein and functionality in $RP2^{R120X}$, *MERTK*-deficient and $KCNJ13^{W53X}$ hiPSC-derived RPE (Schwarz et al., 2015; Ramsden et al., 2017; Shahi et al., 2019). Once hiPSC-derived organoids that effectively recapitulate the hallmarks of each disease have been established, these models will provide ideal pre-clinical platforms for the discovery, testing and development of translational therapeutics.

CONCLUSION

Ocular maldevelopment accounts for a third of congenital blindness worldwide, and a genetic component is responsible for the majority of cases. hiPSC modeling of early eye development has advanced greatly in recent years and omics studies reveal a close cellular and molecular similarity with HFT of similar development stage. Improvement of hiPSC modeling protocols will enhance the fidelity of these models to early ocular morphogenesis. The use of hiPSCs to model developmental eye diseases has been effectively demonstrated in a patient-derived model of microphthalmia and CHED. These findings are encouraging for further investigation of many other developmental eye disorders, which will be essential to understand the mechanisms of ocular malformation due to their genetic heterogeneity. This will advance therapeutics testing and inform genetic counseling, to improve the quality of life of both patients and their families affected.

AUTHOR CONTRIBUTIONS

JE: writing and original draft. JE, MT, and MM: writing, review and editing. MM: funding.

FUNDING

This research was funded by the Wellcome Trust (205174/Z/16/Z), National Council for the Reduction, Replacement and Refinement of Animals in Research (NC3Rs), and Retina UK.

ACKNOWLEDGMENTS

MM gratefully acknowledges the support of the Wellcome Trust and National Institute for Health Research (NIHR) Biomedical Research Centre based at Moorfields Eye Hospital NHS Foundation Trust and UCL Institute of Ophthalmology.

SUPPLEMENTARY MATERIAL

The Supplementary Material for this article can be found online at: https://www.frontiersin.org/articles/10.3389/fncel.2020.00265/full#supplementary-material.

REFERENCES

Achberger, K., Haderspeck, J. C., Kleger, A., and Liebau, S. (2018). Stem cell-based retina models. *Adv. Drug Deliv. Rev.* 140, 33–50. doi: 10.1016/j.addr.2018.05.005

Achberger, K., Probst, C., Haderspeck, J., Bolz, S., Rogal, J., Chuchuy, J., et al. (2019). Merging organoid and organ-on-a-chip technology to generate complex multi-layer tissue models in a human retina-on-a-chip platform. *eLife* 8:e46188. doi: 10.7554/elife.46188

Agu, C. A., Soares, F. A. C., Alderton, A., Patel, M., Ansari, R., Patel, S., et al. (2015). Successful generation of human induced pluripotent stem cell lines from blood samples held at room temperature for up to 48 hr. *Stem Cell Reports* 5, 660–671. doi: 10.1016/j.stemcr.2015.08.012

Aldiri, I., Xu, B., Wang, L., Chen, X., Hiler, D., Griffiths, L., et al. (2017). The dynamic epigenetic landscape of the retina during development, reprogramming and tumorigenesis. *Neuron* 94, 550.e10–568.e10. doi: 10.1016/j.neuron.2017.04.022

ALSomiry, A. S., Gregory-Evans, C. Y., and Gregory-Evans, K. (2019). An update on the genetics of ocular coloboma. *Hum. Genet.* 138, 865–880. doi: 10.1007/s00439-019-02019-3

Arno, G., Agrawal, S. A., Eblimit, A., Bellingham, J., Xu, M., Wang, F., et al. (2016). Mutations in REEP6 cause autosomal-recessive retinitis pigmentosa. *Am. J. Hum. Genet.* 99, 1305–1315. doi: 10.1016/j.ajhg.2016.10.008

Balasubramanian, R., Tao, C., Polanco, K., Zhong, J., Wang, F., Ma, L., et al. (2018). Deficient FGF signaling in the developing peripheral retina disrupts ciliary margin development and causes aniridia. *bioRxiv* [Preprint]. doi: 10.1101/443416

Bardakjian, T., Weiss, A., and Schneider, A. (2015). "Microphthalmia/anophthalmia/coloboma spectrum," in *GeneReviews® [Internet]*, eds M. P. Adam, H. H. Ardinger, R. A. Pagon, S. E. Wallace, L. J. H. Bean, K. Stephens, et al. (Seattle, WA: University of Washington).

Bartfeld, S., and Clevers, H. (2017). Stem cell-derived organoids and their application for medical research and patient treatment. *J. Mol. Med.* 95, 729–738. doi: 10.1007/s00109-017-1531-7

Black, J. B., and Gersbach, C. A. (2018). Synthetic transcription factors for cell fate reprogramming. *Curr. Opin. Genet. Dev.* 52, 13–21. doi: 10.1016/j.gde.2018.05.001

Brejchova, K., Dudakova, L., Skalicka, P., Dobrovolny, R., Masek, P., Putzova, M., et al. (2019). IPSC-derived corneal endothelial-like cells act as an appropriate model system to assess the impact of SLC4A11 variants on Pre-mRNA splicing. *Invest. Ophthalmol. Vis. Sci.* 60, 3084–3090. doi: 10.1167/iovs.19-26930

Burnight, E. R., Giacalone, J. C., Cooke, J. A., Thompson, J. R., Bohrer, L. R., Chirco, K. R., et al. (2018). CRISPR-Cas9 genome engineering: treating inherited retinal degeneration. *Prog. Retin. Eye Res.* 65, 28–49. doi: 10.1016/j.preteyeres.2018.03.003

Capowski, E. E., Samimi, K., Mayerl, S. J., Phillips, M. J., Pinilla, I., Howden, S. E., et al. (2019). Reproducibility and staging of 3D human retinal organoids across multiple pluripotent stem cell lines. *Development* 146:dev171686. doi: 10.1242/dev.171686

Capowski, E. E., Simonett, J. M., Clark, E. M., Wright, L. S., Howden, S. E., Wallace, K. A., et al. (2014). Loss of MITF expression during human embryonic stem cell differentiation disrupts retinal pigment epithelium development and optic vesicle cell proliferation. *Hum. Mol. Genet.* 23, 6332–6344. doi: 10.1093/hmg/ddu351

Capowski, E. E., Wright, L. S., Liang, K., Phillips, M. J., Wallace, K., Petelinsek, A., et al. (2016). Regulation of Wnt signaling by VSX2 during optic vesicle patterning in human induced pluripotent stem cells. *Stem Cells* 34, 2625–2634. doi: 10.1002/stem.2414

Cardozo, M. J., Almuedo-Castillo, M., and Bovolenta, P. (2020). Patterning the vertebrate retina with morphogenetic signaling pathways. *Neuroscientist* 26, 185–196. doi: 10.1177/1073858419874016

Chakrabarty, K., Shetty, R., and Ghosh, A. (2018). Corneal cell therapy: with iPSCs, it is no more a far-sight. *Stem Cell Res. Ther.* 9:287. doi: 10.1186/s13287-018-1036-5

Chen, J., Lin, M., Foxe, J. J., Pedrosa, E., Hrabovsky, A., Carroll, R., et al. (2013). Transcriptome comparison of human neurons generated using induced pluripotent stem cells derived from dental pulp and skin fibroblasts. *PLoS One* 8:e75682. doi: 10.1371/journal.pone.0075682

Chen, J., Ma, L., Wang, S., Wang, X., Sun, Y., Gao, L., et al. (2017). Analysis of expression of transcription factors in early human retina. *Int. J. Dev. Neurosci.* 60, 94–102. doi: 10.1016/j.ijdevneu.2017.01.015

Cheng, L., Lei, Q., Yin, C., Wang, H.-Y., Jin, K., and Xiang, M. (2017). Generation of urine cell-derived non-integrative human iPSCs and iNSCs: a step-by-step optimized protocol. *Front. Mol. Neurosci.* 10:348. doi: 10.3389/fnmol.2017.00348

Cherry, A. B., and Daley, G. Q. (2013). Reprogrammed cells for disease modeling and regenerative medicine. *Annu. Rev. Med.* 64, 277–290. doi: 10.1146/annurev-med-050311-163324

Choi, J., Lee, S., Mallard, W., Clement, K., Tagliazucchi, G. M., Lim, H., et al. (2015). A comparison of genetically matched cell lines reveals the equivalence of human iPSCs and ESCs. *Nat. Biotechnol.* 33, 1173–1181. doi: 10.1038/nbt.3388

Chou, S.-J., and Tole, S. (2019). Lhx2, an evolutionarily conserved, multifunctional regulator of forebrain development. *Brain Res.* 1705, 1–14. doi: 10.1016/j.brainres.2018.02.046

Clark, A. M., Yun, S., Veien, E. S., Wu, Y. Y., Chow, R. L., Dorsky, R. I., et al. (2008). Negative regulation of Vsx1 by its paralog Chx10/Vsx2 is conserved in the vertebrate retina. *Brain Res.* 1192, 99–113. doi: 10.1016/j.brainres.2007.06.007

Cowan, C. S., Renner, M., Gross-Scherf, B., Goldblum, D., Munz, M., Krol, J., et al. (2019). Cell types of the human retina and its organoids at single-cell resolution: developmental convergence, transcriptomic identity and disease map. *bioRxiv* [Preprint]. doi: 10.1101/703348

Cvekl, A., and Tamm, E. R. (2004). Anterior eye development and ocular mesenchyme: new insights from mouse models and human diseases. *Bioessays* 26, 374–386. doi: 10.1002/bies.20009

Cvekl, A., and Zhang, X. (2017). Signaling and gene regulatory networks in mammalian lens development. *Trends Genet.* 33, 677–702. doi: 10.1016/j.tig.2017.08.001

Danno, H., Michiue, T., Hitachi, K., Yukita, A., Ishiura, S., and Asashima, M. (2008). Molecular links among the causative genes for ocular malformation: Otx2 and Sox2 coregulate Rax expression. *Proc. Natl. Acad. Sci. U S A* 105, 5408–5413. doi: 10.1073/pnas.0710954105

Davies, S. B., Chui, J., Madigan, M. C., Provis, J. M., Wakefield, D., and Di Girolamo, N. (2009). Stem cell activity in the developing human cornea. *Stem Cells* 27, 2781–2792. doi: 10.1002/stem.209

de Boni, L., Gasparoni, G., Haubenreich, C., Tierling, S., Schmitt, I., Peitz, M., et al. (2018). DNA methylation alterations in iPSC- and hESC-derived neurons: potential implications for neurological disease modeling. *Clin. Epigenetics* 10:13. doi: 10.1186/s13148-018-0440-0

Deneault, E., Faheem, M., White, S. H., Rodrigues, D. C., Sun, S., Wei, W., et al. (2019). *CNTN5*$^{-/+}$ or *EHMT2*$^{-/+}$ human iPSC-derived neurons from individuals with autism develop hyperactive neuronal networks. *Elife* 8:e40092. doi: 10.7554/elife.40092

Deng, W.-L., Gao, M.-L., Lei, X.-L., Lv, J.-N., Zhao, H., He, K.-W., et al. (2018). Gene correction reverses ciliopathy and photoreceptor loss in iPSC-derived retinal organoids from retinitis pigmentosa patients. *Stem Cell Reports* 10, 1267–1281. doi: 10.1016/j.stemcr.2018.05.012

Desir, J., and Abramowicz, M. (2008). Congenital hereditary endothelial dystrophy with progressive sensorineural deafness (Harboyan syndrome). *Orphanet J. Rare Dis.* 3:28. doi: 10.1186/1750-1172-3-28

Desmaison, A., Vigouroux, A., Rieubland, C., Peres, C., Calvas, P., and Chassaing, N. (2010). Mutations in the LHX2 gene are not a frequent cause of micro/anophthalmia. *Mol. Vis.* 16, 2847–2849.

Dharmasena, A., Keenan, T., Goldacre, R., Hall, N., and Goldacre, M. J. (2017). Trends over time in the incidence of congenital anophthalmia, microphthalmia and orbital malformation in England: database study. *Br. J. Ophthalmol.* 101, 735–739. doi: 10.1136/bjophthalmol-2016-308952

Diacou, R., Zhao, Y., Zheng, D., Cvekl, A., and Liu, W. (2018). Six3 and Six6 are jointly required for the maintenance of multipotent retinal progenitors through both positive and negative regulation. *Cell Rep.* 25, 2510.e4–2523.e4. doi: 10.1016/j.celrep.2018.10.106

DiStefano, T., Chen, H. Y., Panebianco, C., Kaya, K. D., Brooks, M. J., Gieser, L., et al. (2018). Accelerated and improved differentiation of retinal organoids

from pluripotent stem cells in rotating-wall vessel bioreactors. *Stem Cell Reports* 10, 300–313. doi: 10.1016/j.stemcr.2017.11.001

Doss, M. X., and Sachinidis, A. (2019). Current challenges of iPSC-based disease modeling and therapeutic implications. *Cells* 8:403. doi: 10.3390/cells8050403

Eghrari, A. O., Riazuddin, S. A., and Gottsch, J. D. (2015). "Chapter Two–overview of the cornea: structure, function and development," in *Progress in Molecular Biology and Translational Science*, eds J. F. Hejtmancik and J. M. Nickerson (Cambridge, MA: Academic Press), 7–23.

Eintracht, J., Corton, M., FitzPatrick, D., and Moosajee, M. (2020). CUGC for syndromic microphthalmia including next-generation sequencing-based approaches. *Eur. J. Hum. Genet.* 28, 679–690. doi: 10.1038/s41431-019-0565-4

FitzPatrick, D. R. (2016). "Developmental biology of the eye," in *Taylor and Hoyt's Pediatric Ophthalmology and Strabismus*, eds S. R. Lambert and C. J. Lyons (Amsterdam, Netherlands: Elsevier), 25.

Foltz, L. P., and Clegg, D. O. (2019). Patient-derived induced pluripotent stem cells for modelling genetic retinal dystrophies. *Prog. Retin. Eye Res.* 68, 54–66. doi: 10.1016/j.preteyeres.2018.09.002

Fuhrmann, S. (2010). "Eye morphogenesis and patterning of the optic vesicle," in *Current Topics in Developmental Biology* eds R. Cagen and T. Reh (Cambridge, MA: Academic Press, Elsevier), 61–84.

Gamm, D. M., Clark, E., Capowski, E. E., and Singh, R. (2019). The role of FGF9 in the production of neural retina and RPE in a pluripotent stem cell model of early human retinal development. *Am. J. Ophthalmol.* 206, 113–131. doi: 10.1016/j.ajo.2019.04.033

Gath, N., and Gross, J. M. (2019). Zebrafish mab21l2 mutants possess severe defects in optic cup morphogenesis, lens and cornea development. *Dev. Dyn.* 248, 514–529. doi: 10.1002/dvdy.44

Geens, M., and Chuva De Sousa Lopes, S. M. (2017). X chromosome inactivation in human pluripotent stem cells as a model for human development: back to the drawing board? *Hum. Reprod. Update* 23, 520–532. doi: 10.1093/humupd/dmx015

Giacalone, J. C., Wiley, L. A., Burnight, E. R., Songstad, A. E., Mullins, R. F., Stone, E. M., et al. (2016). Concise review: patient-specific stem cells to interrogate inherited eye disease. *Stem Cells Transl. Med.* 5, 132–140. doi: 10.5966/sctm.2015-0206

Giger, F. A., and Houart, C. (2018). The birth of the eye vesicle: when fate decision equals morphogenesis. *Front. Neurosci.* 12:87. doi: 10.3389/fnins.2018.00087

Gonzalez-Cordero, A., Kruczek, K., Naeem, A., Fernando, M., Kloc, M., Ribeiro, J., et al. (2017). Recapitulation of human retinal development from human pluripotent stem cells generates transplantable populations of cone photoreceptors. *Stem Cell Reports* 9, 820–837. doi: 10.1016/j.stemcr.2017.07.022

Green, R. M. (2019). "Chapter 76–ethical considerations⁎," in *Principles of Regenerative Medicine*, 3rd Edn. eds A. Atala, R. Lanza, A. G. Mikos and R. Nerem (Boston, MA: Academic Press), 1331–1343.

Gregory-Evans, C. Y., Wallace, V. A., and Gregory-Evans, K. (2013). Gene networks: dissecting pathways in retinal development and disease. *Prog. Retin. Eye Res.* 33, 40–66. doi: 10.1016/j.preteyeres.2012.10.003

Gregory-Evans, C. Y., Wang, X., and Gregory-Evans, K. (2019). Prospects and modalities for the treatment of genetic ocular anomalies. *Hum. Genet.* 138, 1019–1026. doi: 10.1007/s00439-018-01968-5

Halevy, T., and Urbach, A. (2014). Comparing ESC and iPSC-based models for human genetic disorders. *J. Clin. Med.* 3, 1146–1162. doi: 10.3390/jcm3041146

Hara, S., Kawasaki, S., Yoshihara, M., Winegarner, A., Busch, C., Tsujikawa, M., et al. (2019). Transcription factor TFAP2B up-regulates human corneal endothelial cell-specific genes during corneal development and maintenance. *J. Biol. Chem.* 294, 2460–2469. doi: 10.1074/jbc.ra118.005527

Harding, P., and Moosajee, M. (2019). The molecular basis of human anophthalmia and microphthalmia. *J. Dev. Biol.* 7:16. doi: 10.3390/jdb7030016

Heavner, W., and Pevny, L. (2012). Eye development and retinogenesis. *Cold Spring Harb. Perspect. Biol.* 4:a008391. doi: 10.1101/cshperspect.a008391

Hever, A., Williamson, K., and Van Heyningen, V. (2006). Developmental malformations of the eye: the role of PAX6, SOX2 and OTX2. *Clin. Genet.* 69, 459–470. doi: 10.1111/j.1399-0004.2006.00619.x

Hoshino, A., Ratnapriya, R., Brooks, M. J., Chaitankar, V., Wilken, M. S., Zhang, C., et al. (2017). Molecular anatomy of the developing human retina. *Dev. Cell* 43, 763.e4–779.e4. doi: 10.1016/j.devcel.2017.10.029

Hosseini Far, H., Patria, Y. N., Motazedian, A., Elefanty, A. G., Stanley, E. G., Lamandé, S. R., et al. (2019). Generation of a heterozygous COL1A1 (c.3969_3970insT) osteogenesis imperfecta mutation human iPSC line, MCRIi001-A-1, using CRISPR/Cas9 editing. *Stem Cell Res.* 37:101449. doi: 10.1016/j.scr.2019.101449

Huber, G., Heynen, S., Imsand, C., vom Hagen, F., Muehlfriedel, R., Tanimoto, N., et al. (2010). Novel rodent models for macular research. *PLoS One* 5:e13403. doi: 10.1371/journal.pone.0013403

Jeong, Y., Leskow, F. C., El-Jaick, K., Roessler, E., Muenke, M., Yocum, A., et al. (2008). Regulation of a remote Shh forebrain enhancer by the Six3 homeoprotein. *Nat. Genet.* 40, 1348–1353. doi: 10.1038/ng.230

Joseph Phillips, M., Perez, E. T., Martin, J. M., Reshel, S. T., Wallace, K. A., Capowski, E. E., et al. (2014). Modeling human retinal development with patient-specific induced pluripotent stem cells reveals multiple roles for visual system homeobox 2. *Stem Cells* 32, 1480–1492. doi: 10.1002/stem.1667

Kaukonen, M., Woods, S., Ahonen, S., Lemberg, S., Hellman, M., Hytönen, M. K., et al. (2018). Maternal inheritance of a recessive RBP4 defect in canine congenital eye disease. *Cell Rep.* 23, 2643–2652. doi: 10.1016/j.celrep.2018.04.118

Kelberman, D., de Castro, S. C. P., Huang, S., Crolla, J. A., Palmer, R., Gregory, J. W., et al. (2008). SOX2 plays a critical role in the pituitary, forebrain and eye during human embryonic development. *J. Clin. Endocrinol. Metab.* 93, 1865–1873. doi: 10.1210/jc.2007-2337

Kha, C. X., Guerin, D. J., and Tseng, K.A.-S. (2019). Using the *Xenopus* developmental eye regrowth system to distinguish the role of developmental versus regenerative mechanisms. *Front. Physiol.* 10:502. doi: 10.3389/fphys.2019.00502

Kim, K., Doi, A., Wen, B., Ng, K., Zhao, R., Cahan, P., et al. (2010). Epigenetic memory in induced pluripotent stem cells. *Nature* 467, 285–290. doi: 10.1038/nature09342

Kim, S., Lowe, A., Dharmat, R., Lee, S., Owen, L. A., Wang, J., et al. (2019). Generation, transcriptome profiling and functional validation of cone-rich human retinal organoids. *Proc. Natl. Acad. Sci. U S A* 116, 10824–10833. doi: 10.1073/pnas.1901572116

Kolosova, N. G., Kozhevnikova, O. S., Telegina, D. V., Fursova, A. Z., Stefanova, N. A., Muraleva, N. A., et al. (2018). p62/SQSTM1 coding plasmid prevents age related macular degeneration in a rat model. *Aging* 10, 2136–2147. doi: 10.18632/aging.101537

Kondoh, H., Uchikawa, M., and Ishii, Y. (2016). "Chapter 12–multiple roles for SOX2 in eye development," in *Sox2*, eds H. Kondoh and R. Lovell-Badge (Boston, MA: Academic Press), 217–233.

Kuwahara, A., Ozone, C., Nakano, T., Saito, K., Eiraku, M., and Sasai, Y. (2015). Generation of a ciliary margin-like stem cell niche from self-organizing human retinal tissue. *Nat. Commun.* 6:6286. doi: 10.1038/ncomms7286

Kyttälä, A., Moraghebi, R., Valensisi, C., Kettunen, J., Andrus, C., Pasumarthy, K. K., et al. (2016). Genetic variability overrides the impact of parental cell type and determines ipsc differentiation potential. *Stem Cell Reports* 6, 200–212. doi: 10.1016/j.stemcr.2015.12.009

Lang, C., Campbell, K. R., Ryan, B. J., Carling, P., Attar, M., Vowles, J., et al. (2019). Single-cell sequencing of ipsc-dopamine neurons reconstructs disease progression and identifies HDAC4 as a regulator of parkinson cell phenotypes. *Cell Stem Cell* 24, 93.e6–106.e6. doi: 10.1016/j.stem.2018.10.023

Lindsay, S. J., Xu, Y., Lisgo, S. N., Harkin, L. F., Copp, A. J., Gerrelli, D., et al. (2016). HDBR expression: a unique resource for global and individual gene expression studies during early human brain development. *Front. Neuroanat.* 10:86. doi: 10.3389/fnana.2016.00086

Llonch, S., Carido, M., and Ader, M. (2018). Organoid technology for retinal repair. *Dev. Biol.* 433, 132–143. doi: 10.1016/j.ydbio.2017.09.028

Lowe, A., Harris, R., Bhansali, P., Cvekl, A., and Liu, W. (2016). Intercellular adhesion-dependent cell survival and ROCK-regulated actomyosin-driven forces mediate self-formation of a retinal organoid. *Stem Cell Reports* 6, 743–756. doi: 10.1016/j.stemcr.2016.03.011

Lwigale, P. Y. (2015). "Chapter Four–corneal development: different cells from a common progenitor," in *Progress in Molecular Biology and Translational Science*, eds J. F. Hejtmancik and J. M. Nickerson (Cambridge, MA: Academic Press), 43–59.

Ma, A. S., Grigg, J. R., and Jamieson, R. V. (2018a). Phenotype-genotype correlations and emerging pathways in ocular anterior segment dysgenesis. *Hum. Genet.* 138, 899–915. doi: 10.1007/s00439-018-1935-7

Ma, N., Zhang, J. Z., Itzhaki, I., Zhang, S. L., Chen, H., Haddad, F., et al. (2018b). Determining the pathogenicity of a genomic variant of uncertain significance using CRISPR/Cas9 and human-induced pluripotent stem cells. *Circulation* 138, 2666–2681. doi: 10.1161/CIRCULATIONAHA.117.032273

Ma, K. K., Lin, J., Boudreault, K., Chen, R. W., and Tsang, S. H. (2017). Phenotyping choroideremia and its carrier state with multimodal imaging techniques. *Retin. Cases Brief Rep.* 11, S178–S181. doi: 10.1097/icb.0000000000000419

Macdonald, R., Barth, K. A., Xu, Q., Holder, N., Mikkola, I., and Wilson, S. W. (1995). Midline signalling is required for Pax gene regulation and patterning of the eyes. *Development* 121, 3267–3278.

Mackey, L. C., Annab, L. A., Yang, J., Rao, B., Kissling, G. E., Schurman, S. H., et al. (2018). Epigenetic enzymes, age and ancestry regulate the efficiency of human iPSC reprogramming. *Stem Cells* 36, 1697–1708. doi: 10.1002/stem.2899

Malhotra, D., Jung, M., Fecher-Trost, C., Lovatt, M., Peh, G. S. L., Noskov, S., et al. (2020). Defective cell adhesion function of solute transporter, SLC4A11, in endothelial corneal dystrophies. *Hum. Mol. Genet.* 29, 97–116. doi: 10.1093/hmg/ddz259

Marei, H. E., Althani, A., Lashen, S., Cenciarelli, C., and Hasan, A. (2017). Genetically unmatched human iPSC and ESC exhibit equivalent gene expression and neuronal differentiation potential. *Sci. Rep.* 7:17504. doi: 10.1038/s41598-017-17882-1

Matsushima, D., Heavner, W., and Pevny, L. H. (2011). Combinatorial regulation of optic cup progenitor cell fate by SOX2 and PAX6. *Development* 138, 443–454. doi: 10.1242/dev.055178

Mebratu, Y., and Tesfaigzi, Y. (2009). How ERK1/2 activation controls cell proliferation and cell death: is subcellular localization the answer? *Cell Cycle* 8, 1168–1175. doi: 10.4161/cc.8.8.8147

Mellough, C. B., Bauer, R., Collin, J., Dorgau, B., Zerti, D., Dolan, D. W. P., et al. (2019a). An integrated transcriptional analysis of the developing human retina. *Development* 146:dev169474. doi: 10.1242/dev.169474

Mellough, C. B., Collin, J., Queen, R., Hilgen, G., Dorgau, B., Zerti, D., et al. (2019b). Systematic comparison of retinal organoid differentiation from human pluripotent stem cells reveals stage specific, cell line and methodological differences. *Stem Cells Transl. Med.* 8, 694–706. doi: 10.1002/sctm.18-0267

Mellough, C. B., Collin, J., Khazim, M., White, K., Sernagor, E., Steel, D. H., et al. (2015). IGF-1 signaling plays an important role in the formation of three-dimensional laminated neural retina and other ocular structures from human embryonic stem cells. *Stem Cells* 33, 2416–2430. doi: 10.1002/stem.2023

Mellough, C. B., and Lako, M. (2016). Transcriptomics: how to build a human. *eLife* 5:e19826. doi: 10.7554/eLife.19826

Meyer, J. S., Howden, S. E., Wallace, K. A., Verhoeven, A. D., Wright, L. S., Capowski, E. E., et al. (2011). Optic vesicle-like structures derived from human pluripotent stem cells facilitate a customized approach to retinal disease treatment. *Stem cells* 29, 1206–1218. doi: 10.1002/stem.674

Meyer, J. S., Shearer, R. L., Capowski, E. E., Wright, L. S., Wallace, K. A., McMillan, E. L., et al. (2009). Modeling early retinal development with human embryonic and induced pluripotent stem cells. *Proc. Natl. Acad. Sci. U S A* 106, 16698–16703. doi: 10.1073/pnas.0905245106

Moore, B. A., Leonard, B. C., Sebbag, L., Edwards, S. G., Cooper, A., Imai, D. M., et al. (2018). Identification of genes required for eye development by high-throughput screening of mouse knockouts. *Commun. Biol.* 1:236. doi: 10.1038/s42003-018-0226-0

Moosajee, M., Hingorani, M., and Moore, A. T. (2018). "PAX6-related aniridia," in *GeneReviews®[Internet]*. eds M. P. Adam, H. H. Ardinger, R. A. Pagon, S. E. Wallace, L. J. H. Bean, K. Stephens, et al (Seattle, WA: University of Washington).

Motahari, Z., Martinez-De Luna, R. I., Viczian, A. S., and Zuber, M. E. (2016). Tbx3 represses bmp4 expression and, with Pax6, is required and sufficient for retina formation. *Development* 143, 3560–3572. doi: 10.1242/dev.130955

Nakano, T., Ando, S., Takata, N., Kawada, M., Muguruma, K., Sekiguchi, K., et al. (2012). Self-formation of optic cups and storable stratified neural retina from human ESCs. *Cell Stem Cell* 10, 771–785. doi: 10.1016/j.stem.2012.05.009

Nedelec, B., Rozet, J. M., and Fares Taie, L. (2019). Genetic architecture of retinoic-acid signaling-associated ocular developmental defects. *Hum. Genet.* 138, 937–955. doi: 10.1007/s00439-019-02052-2

Noguchi, H., Miyagi-Shiohira, C., and Nakashima, Y. (2018). Induced tissue-specific stem cells and epigenetic memory in induced pluripotent stem cells. *Int. J. Mol. Sci.* 19:930. doi: 10.3390/ijms19040930

Okita, K., Matsumura, Y., Sato, Y., Okada, A., Morizane, A., Okamoto, S., et al. (2011). A more efficient method to generate integration-free human iPS cells. *Nat. Methods* 8, 409–412. doi: 10.1038/nmeth.1591

Oltean, A., Huang, J., Beebe, D. C., and Taber, L. A. (2016). Tissue growth constrained by extracellular matrix drives invagination during optic cup morphogenesis. *Biomech. Model. Mechanobiol.* 15, 1405–1421. doi: 10.1007/s10237-016-0771-8

Ortiz-Vitali, J., and Darabi, R. (2019). iPSCs as a platform for disease modeling, drug screening and personalized therapy in muscular dystrophies. *Cells* 8:20. doi: 10.3390/cells8010020

Ortmann, D., and Vallier, L. (2017). Variability of human pluripotent stem cell lines. *Curr. Opin. Genet. Dev.* 46, 179–185. doi: 10.1016/j.gde.2017.07.004

Parfitt, D. A., Lane, A., Ramsden, C. M., Carr, A. J., Munro, P. M., Jovanovic, K., et al. (2016). Identification and correction of mechanisms underlying inherited blindness in human iPSC-derived optic cups. *Cell Stem Cell* 18, 769–781. doi: 10.1016/j.stem.2016.03.021

Patel, A., and Sowden, J. C. (2019). Genes and pathways in optic fissure closure. *Seminars Cell Dev. Biol.* 91, 55–65. doi: 10.1016/j.semcdb.2017.10.010

Placzek, M., and Briscoe, J. (2018). Sonic hedgehog in vertebrate neural tube development. *Int. J. Dev. Biol.* 62, 225–234. doi: 10.1387/ijdb.170293jb

Plaisancié, J., Ceroni, F., Holt, R., Zazo Seco, C., Calvas, P., Chassaing, N., et al. (2019). Genetics of anophthalmia and microphthalmia. Part 1: non-syndromic anophthalmia/microphthalmia. *Hum. Genet.* 138, 799–830. doi: 10.1007/s00439-019-01977-y

Raab, S., Klingenstein, M., Liebau, S., and Linta, L. (2014). A comparative view on human somatic cell sources for iPSC generation. *Stem Cells Int.* 2014, 768391–768391. doi: 10.1155/2014/768391

Rahi, J. S., Gilbert, C. E., Foster, A., and Minassian, D. (1999). Measuring the burden of childhood blindness. *Br. J. Ophthalmol.* 83, 387–388. doi: 10.1136/bjo.83.4.387

Rainger, J., van Beusekom, E., Ramsay, J. K., McKie, L., Al-Gazali, L., Pallotta, R., et al. (2011). Loss of the BMP antagonist, SMOC-1, causes ophthalmo-acromelic (waardenburg anophthalmia) syndrome in humans and mice. *PLOS Genet.* 7:e1002114. doi: 10.1371/journal.pgen.1002114

Ramsden, C. M., Nommiste, B., R. Lane, A., Carr, A.-J.F., Powner, M. B., J. K. Smart, M., et al. (2017). Rescue of the MERTK phagocytic defect in a human iPSC disease model using translational read-through inducing drugs. *Sci. Rep.* 7:51. doi: 10.1038/s41598-017-00142-7

Reichman, S., Slembrouck, A., Gagliardi, G., Chaffiol, A., Terray, A., Nanteau, C., et al. (2017). Generation of storable retinal organoids and retinal pigmented epithelium from adherent human iPS cells in xeno-free and feeder-free conditions. *Stem Cells* 35, 1176–1188. doi: 10.1002/stem.2586

Reis, L. M., and Semina, E. V. (2015). Conserved genetic pathways associated with microphthalmia, anophthalmia and coloboma. *Birth Defects Res. C Embryo Today* 105, 96–113. doi: 10.1002/bdrc.21097

Richardson, R., Owen, N., Toms, M., Young, R. M., Tracey-White, D., and Moosajee, M. (2019). Transcriptome profiling of zebrafish optic fissure fusion. *Sci. Rep.* 9:1541. doi: 10.1038/s41598-018-38379-5

Richardson, R., Tracey-White, D., Webster, A., and Moosajee, M. (2017). The zebrafish eye-a paradigm for investigating human ocular genetics. *Eye* 31, 68–86. doi: 10.1038/eye.2016.198

Rodgers, H. M., Huffman, V. J., Voronina, V. A., Lewandoski, M., and Mathers, P. H. (2018). The role of the Rx homeobox gene in retinal progenitor proliferation and cell fate specification. *Mech. Dev.* 151, 18–29. doi: 10.1016/j.mod.2018.04.003

Rosemann, M., Ivashkevich, A., Favor, J., Dalke, C., Hölter, S. M., Becker, L., et al. (2010). Microphthalmia, parkinsonism and enhanced nociception in Pitx3416insGmice. *Mamm. Genome* 21, 13–27. doi: 10.1007/s00335-009-9235-0

Roy, A., de Melo, J., Chaturvedi, D., Thein, T., Cabrera-Socorro, A., Houart, C., et al. (2013). LHX2 is necessary for the maintenance of optic identity and for the progression of optic morphogenesis. *J. Neurosci.* 33, 6877–6884. doi: 10.1523/JNEUROSCI.4216-12.2013

Schwarz, N., Carr, A.-J., Lane, A., Moeller, F., Chen, L. L., Aguilà, M., et al. (2015). Translational read-through of the RP2 Arg120stop mutation in patient iPSC-derived retinal pigment epithelium cells. *Hum. Mol. Genet.* 24, 972–986. doi: 10.1093/hmg/ddu509

Sghari, S., and Gunhaga, L. (2018). Temporal requirement of Mab21l2 during eye development in chick reveals stage-dependent functions for retinogenesis. *Invest. Ophthalmol. Vis. Sci.* 59, 3869–3878. doi: 10.1167/iovs.18-24236

Shahi, P. K., Hermans, D., Sinha, D., Brar, S., Moulton, H., Stulo, S., et al. (2019). Gene augmentation and readthrough rescue channelopathy in an ipsc-rpe model of congenital blindness. *Am. J. Hum. Genet.* 104, 310–318. doi: 10.1016/j.ajhg.2018.12.019

Sharma, A., Mücke, M., and Seidman, C. E. (2018). Human induced pluripotent stem cell production and expansion from blood using a non-integrating viral reprogramming vector. *Curr. Protoc. Mol. Biol.* 122:e58. doi: 10.1002/cpmb.58

Slavotinek, A. (2019). Genetics of anophthalmia and microphthalmia. Part 2: syndromes associated with anophthalmia-microphthalmia. *Hum. Genet.* 138, 831–846. doi: 10.1007/s00439-018-1949-1

Slavotinek, A. M., Chao, R., Vacik, T., Yahyavi, M., Abouzeid, H., Bardakjian, T., et al. (2012). VAX1 mutation associated with microphthalmia, corpus callosum agenesis and orofacial clefting: the first description of a VAX1 phenotype in humans. *Hum. Mutat.* 33, 364–368. doi: 10.1002/humu.21658

Snell, R. S., and Lemp, M. A. (2013). *Clinical Anatomy of the Eye.* Hoboken, NJ: John Wiley and Sons.

Stanke, J., Moose, H. E., El-Hodiri, H. M., and Fischer, A. J. (2010). Comparative study of Pax2 expression in glial cells in the retina and optic nerve of birds and mammals. *J. Comp. Neurol.* 518, 2316–2333. doi: 10.1002/cne.22335

Takahashi, K., Tanabe, K., Ohnuki, M., Narita, M., Ichisaka, T., Tomoda, K., et al. (2007). Induction of pluripotent stem cells from adult human fibroblasts by defined factors. *Cell* 131, 861–872. doi: 10.1016/j.cell.2007.11.019

Takasaki, A., Hirono, K., Hata, Y., Wang, C., Takeda, M., Yamashita, J. K., et al. (2018). Sarcomere gene variants act as a genetic trigger underlying the development of left ventricular noncompaction. *Pediatr. Res.* 84, 733–742. doi: 10.1038/s41390-018-0162-1

Tseng, V. L., and Coleman, A. L. (2018). Reducing the burden of unilateral vision impairment and blindness in australia. *JAMA Ophthalmol.* 136, 248–249. doi: 10.1001/jamaophthalmol.2017.6464

Vaskova, E., Stekleneva, A., Medvedev, S., and Zakian, S. (2013). "Epigenetic memory" phenomenon in induced pluripotent stem cells. *Acta Naturae* 5, 15–21. doi: 10.32607/20758251-2013-5-4-15-21

Victor, M. B., Richner, M., Olsen, H. E., Lee, S. W., Monteys, A. M., Ma, C., et al. (2018). Striatal neurons directly converted from Huntington's disease patient fibroblasts recapitulate age-associated disease phenotypes. *Nat. Neurosci.* 21, 341–352. doi: 10.1038/s41593-018-0075-7

Völkner, M., Zschätzsch, M., Rostovskaya, M., Overall, R. W., Busskamp, V., Anastassiadis, K., et al. (2016). Retinal organoids from pluripotent stem cells efficiently recapitulate retinogenesis. *Stem Cell Reports* 6, 525–538. doi: 10.1016/j.stemcr.2016.03.001

Wahlin, K. J., Maruotti, J. A., Sripathi, S. R., Ball, J., Angueyra, J. M., Kim, C., et al. (2017). Photoreceptor outer segment-like structures in long-term 3d retinas from human pluripotent stem cells. *Sci. Rep.* 7:766. doi: 10.1038/s41598-017-00774-9

Wang, Y., Liu, J., Tan, X., Li, G., Gao, Y., Liu, X., et al. (2013). Induced pluripotent stem cells from human hair follicle mesenchymal stem cells. *Stem Cell Rev. Rep.* 9, 451–460. doi: 10.1007/s12015-012-9420-5

Wang, X., Xiong, K., Lin, C., Lv, L., Chen, J., Xu, C., et al. (2015). New medium used in the differentiation of human pluripotent stem cells to retinal cells is comparable to fetal human eye tissue. *Biomaterials* 53, 40–49. doi: 10.1016/j.biomaterials.2015.02.065

Welby, E., Lakowski, J., Di Foggia, V., Budinger, D., Gonzalez-Cordero, A., Lun, A. T. L., et al. (2017). Isolation and comparative transcriptome analysis of human fetal and iPSC-derived cone photoreceptor cells. *Stem Cell Reports* 9, 1898–1915. doi: 10.1016/j.stemcr.2017.10.018

Westenskow, P., Piccolo, S., and Fuhrmann, S. (2009). β-catenin controls differentiation of the retinal pigment epithelium in the mouse optic cup by regulating Mitf and Otx2 expression. *Development* 136, 2505–2510. doi: 10.1242/dev.032136

Williamson, K. A., and FitzPatrick, D. R. (2014). The genetic architecture of microphthalmia, anophthalmia and coloboma. *Eur. J. Med. Genet.* 57, 369–380. doi: 10.1016/j.ejmg.2014.05.002

Yanai, A., McNab, P., and Gregory-Evans, K. (2019). Retinal therapy with induced pluripotent stem cells; leading the way to human clinical trials. *Expert Rev. Ophthalmol.* 14, 53–59. doi: 10.1080/17469899.2019.1568872

Young, T. L., Hawthorne, F., Feng, S., Luo, X., Germain, E. S., Wang, M., et al. (2013). Whole genome expression profiling of normal human fetal and adult ocular tissues. *Exp. Eye Res.* 116, 265–278. doi: 10.1016/j.exer.2013.08.009

Zagozewski, J. L., Zhang, Q., Pinto, V. I., Wigle, J. T., and Eisenstat, D. D. (2014). The role of homeobox genes in retinal development and disease. *Dev. Biol.* 393, 195–208. doi: 10.1016/j.ydbio.2014.07.004

Zhao, M.-T., Chen, H., Liu, Q., Shao, N.-Y., Sayed, N., Wo, H.-T., et al. (2017). Molecular and functional resemblance of differentiated cells derived from isogenic human iPSCs and SCNT-derived ESCs. *Proc. Natl. Acad. Sci. U S A* 114, E11111–E11120. doi: 10.1073/pnas.1708991114

Zhong, X., Gutierrez, C., Xue, T., Hampton, C., Vergara, M. N., Cao, L.-H., et al. (2014). Generation of three-dimensional retinal tissue with functional photoreceptors from human iPSCs. *Nat. Commun.* 5:4047. doi: 10.1038/ncomms5047

Zhou, W., Ma, D., Sun, A. X., Tran, H. D., Ma, D. L., Singh, B. K., et al. (2019). PD-linked CHCHD2 mutations impair CHCHD10 and MICOS complex leading to mitochondria dysfunction. *Hum. Mol. Genet.* 28, 1100–1116. doi: 10.1093/hmg/ddy413

Zhu, J., Ordway, A. J., Weber, L., Buddika, K., and Kumar, J. P. (2018). Polycomb group (PcG) proteins and Pax6 cooperate to inhibit in vivo reprogramming of the developing *Drosophila* eye. *Development* 145:dev160754. doi: 10.1242/dev.160754

Zou, C., and Levine, E. M. (2012). Vsx2 controls eye organogenesis and retinal progenitor identity via homeodomain and non-homeodomain residues required for high affinity DNA binding. *PLoS Genet.* 8:e1002924. doi: 10.1371/journal.pgen.1002924

Conflict of Interest: The authors declare that the research was conducted in the absence of any commercial or financial relationships that could be construed as a potential conflict of interest.

frontiers in Cellular Neuroscience

REVIEW
published: 10 September 2020
doi: 10.3389/fncel.2020.00179

Limitations and Promise of Retinal Tissue From Human Pluripotent Stem Cells for Developing Therapies of Blindness

Ratnesh K. Singh and Igor O. Nasonkin**

Lineage Cell Therapeutics, Alameda, CA, United States

The self-formation of retinal tissue from pluripotent stem cells generated a tremendous promise for developing new therapies of retinal degenerative diseases, which previously seemed unattainable. Together with use of induced pluripotent stem cells or/and CRISPR-based recombineering the retinal organoid technology provided an avenue for developing models of human retinal degenerative diseases "in a dish" for studying the pathology, delineating the mechanisms and also establishing a platform for large-scale drug screening. At the same time, retinal organoids, highly resembling developing human fetal retinal tissue, are viewed as source of multipotential retinal progenitors, young photoreceptors and just the whole retinal tissue, which may be transplanted into the subretinal space with a goal of replacing patient's degenerated retina with a new retinal "patch." Both approaches (transplantation and modeling/drug screening) were projected when Yoshiki Sasai demonstrated the feasibility of deriving mammalian retinal tissue from pluripotent stem cells, and generated a lot of excitement. With further work and testing of both approaches *in vitro* and *in vivo*, a major implicit limitation has become apparent pretty quickly: the absence of the uniform layer of Retinal Pigment Epithelium (RPE) cells, which is normally present in mammalian retina, surrounds photoreceptor layer and develops and matures first. The RPE layer polarize into apical and basal sides during development and establish microvilli on the apical side, interacting with photoreceptors, nurturing photoreceptor outer segments and participating in the visual cycle by recycling 11-trans retinal (bleached pigment) back to 11-cis retinal. Retinal organoids, however, either do not have RPE layer or carry patches of RPE mostly on one side, thus directly exposing most photoreceptors in the developing organoids to neural medium. Recreation of the critical retinal niche between the apical RPE and photoreceptors, where many retinal disease mechanisms originate, is so far unattainable, imposes clear limitations on both modeling/drug screening and transplantation approaches and is a focus of investigation in many labs. Here we dissect different retinal degenerative diseases and analyze how and where retinal organoid technology can contribute the most to developing therapies even with a current limitation and absence of long and functional outer segments, supported by RPE.

Keywords: retinal organoids, disease modeling, pluripotent stem cells, retinal degeneration, photoreceptors, assembloids, drug screening, retinal pigment epithelium

OPEN ACCESS

Edited by:
Carla Mellough,
Lions Eye Institute, Australia

Reviewed by:
Bela Volgyi,
University of Pécs, Hungary
Elisabetta Catalani,
University of Tuscia, Italy

****Correspondence:***
Ratnesh K. Singh
ratnein@gmail.com
Igor O. Nasonkin
igor.nasonkin@outlook.com

Specialty section:
This article was submitted to Cellular Neuropathology, a section of the journal Frontiers in Cellular Neuroscience

Received: *26 February 2020*
Accepted: *25 May 2020*
Published: *10 September 2020*

Citation:
Singh RK and Nasonkin IO (2020) Limitations and Promise of Retinal Tissue From Human Pluripotent Stem Cells for Developing Therapies of Blindness. Front. Cell. Neurosci. 14:179. doi: 10.3389/fncel.2020.00179

INTRODUCTION

Retina is a great model for developmental neuroscience and a very attractive therapeutic target for biotech companies working in the field of regenerative medicine. There are only several types of retinal neurons (rod and cone photoreceptors, amacrine, horizontal, rod & cone bipolar and retinal ganglion cells), one type of glial cells (Muller glia) and a pigmented layer of supportive cells (Retinal pigment epithelium), which form the retina and help to carry out visual function (Wallace, 2011). On the contrary, the cortical organization in the brain is much more complex and has six layers of cortical neurons, each carrying different cell types with different function (Molyneaux et al., 2007; Lodato and Arlotta, 2015). This relative simplicity creates a promise for ease of recapitulation of this process in a dish (compared to brain), as well as (expected) relative ease of cell replacement therapies (again, compared to the brain). This, in turn, is very attractive to regenerative medicine and biotechnology, which aim to convert the already "understood" and "worked out" knowledge and concepts into robust technologies and therapies to transition science from the bench to patients. Age related macular degeneration (AMD), glaucoma and retinitis pigmentosa (RP) are the major retinal degenerative diseases affecting people worldwide. Understanding the causes and mechanisms of these diseases (outlined below) is a key for developing organoid-based *in vitro* models of these diseases for drug screening and disease modeling.

According to eye health data and statistics, summarized on NEI's web site[1] and in a recent study published by Varma et al. (2016), the number of people with most common eye diseases is going to double by 2050. *AMD* is a leading cause of vision loss in United States and mainly affects the central vision. According to statistics presented by Brightfocus foundation[2] about 11 million of Americans have visual problem associated with AMD symptoms, and this number is projected only to increase and reach 22 million by 2050. The total number of people with macular degeneration worldwide is projected to be 196 million by now (2020) and 288 million by year 2040. About 30% of people age 75 and above have vision problems associated with AMD symptoms. Macular degeneration triggers loss of central vision and death of photoreceptors in the macula (*maculae*) (Molday, 1998; Molday and Moritz, 2015). *The dry form of AMD* accounts for 85 to 90 percent of all AMD cases (Klein et al., 1992; Bird et al., 1995; Vingerling et al., 1995). In dry AMD disruption and death of RPE causes accrual of yellow deposit (drusen) in the macula that contributes to accumulation of complement component and acute phase proteins leading to proinflammatory macrophage response (Ding et al., 2009) and eventually photoreceptor cell death. Geographic atrophy (GA) is devastating complication of dry AMD and is considered the late stage of this disease affecting more than 5 million people worldwide including nearly 1 million in the United States[4] (Bird et al., 1995; Wong et al., 2014) (Friedman et al., 2004; Rudnicka et al., 2015.Geographic atrophy is a frequent cause of legal blindness (42% of patients with GA) (Klein et al., 1995) and severe ($\geq$ 6 lines) vision loss (Sunness et al., 1999). Transplantation of human pluripotent stem cell (hPSC) derived-RPE into the subretinal space is one experimental therapy (in clinical trials now), which may address this condition (Schwartz et al., 2012, 2015, 2016; McGill et al., 2017; Cuzzani, 2018) and is aimed to support photoreceptors and prevent their cell death. In *wet (also neovascular or exudative) AMD* the abnormal growth of blood vessels (also known as choroidal neovascularization, CNV) beneath the macula causes separation between photoreceptors and RPE (Yeo et al., 2019). This is the only blinding disease, which has a robust treatment via suppressing neovasculogenesis with anti-Vascular Endothelial Growth Factor (VEGF) therapies (Meadows and Hurwitz, 2012) such as antibodies (or antibody fragments) to (bevacizumab, ranibizumab) (Rosenfeld et al., 2006; Raftery et al., 2007), VEGF-A soluble decoy (aflibercept) (Sarwar et al., 2016) or/and small molecules suppressing the tyrosine kinases induced by VEGF binding (lapatinib, sunitinib, pazopanib and a few other compounds). *Glaucoma* is another leading cause of irreversible vision loss. From 2011 to 2050, the number of people in the U.S. with glaucoma is expected to increase from 2.71 million in year 2011 to 3.72 million in year 2020 to 7.32 million by year 2050 (Vajaranant et al., 2012). Glaucoma affects retinal ganglion cells, carrying the visual signals from retina to brain, It is caused (mostly) by elevated intraocular pressure followed by loss of retinal ganglion cells and their axons (Weinreb et al., 2014) and impacts long-distance connectivity between the retina and the visual centers in the brain (discussed earlier). In retinitis pigmentosa, or rod-cone dystrophy (a group of inherited, mostly recessive diseases characterized by the onset of night blindness and gradual loss of peripheral vision, prevalence ~1:3500 to 1:4,000) loss of rod photoreceptor cells triggers the late stage degeneration of cone photoreceptors even though specific mutation affects only rods but no cones (Kaplan et al., 2017). Once the photoreceptors die it causes remodeling of inner retinal neurons and followed by cell death of inner retinal cells (Singh et al., 2014). In addition, cone-rod dystrophies (inherited retinal dystrophies/maculopathies, prevalence 1:40,000) (Hamel, 2007) and Leber Congenital Amaurosis (very early-onset child blindness, usually autosomal-recessive, prevalence 1-2:100,000, source[3,4]) add to the number of devastating blinding diseases affecting people and causing loss of life quality and partial loss of independence.

At present, there is no effective treatment available for most of these retinal disorders (except for wet AMD) despite most of the studies done on animal (mostly rodent) models to find new therapeutic options for retinal diseases. Rodent models can mimic only certain aspect of human retinal pathophysiology. They fail to reproduce the etiologic complexity of human RD diseases, including and especially some critically important characteristics of the primate retina like macula (Zeiss, 2010) [rodents don't have macula (Volland et al., 2015a); cats and

[1]https://www.nei.nih.gov/learn-about-eye-health/resources-for-health-educators/eye-health-data-and-statistics

[2]https://www.brightfocus.org/macular/article/age-related-macular-facts-figures

[3]https://rarediseases.org/rare-diseases/leber-congenital-amaurosis/

[4]https://ghr.nlm.nih.gov/condition/leber-congenital-amaurosis

dogs have *area centralis* (Petersen-Jones, 1998; Mowat et al., 2008)] or trichromacy important for visual acuity in patients (Kostic and Arsenijevic, 2016), and do not always mimic the retinal disease phenotype (Slijkerman et al., 2015). Nevertheless, the neuroanatomical structure and connectivity of young retinal organoids growing in a dish is very similar to the *developing* human fetal retina, which is being explored as new way to study early stages of human retinal development (Meyer et al., 2009). However, all studies, where retinal organoids were cultured for prolonged period of time (6 months or longer), note the gradual changes in retinal organoids (specifically, gradual loss of RGCs and thinning of INL) (Wahlin et al., 2017; DiStefano et al., 2018; Brooks et al., 2019; Capowski et al., 2019; Nasonkin et al., 2019), thus substantially reducing the ability to model diseases and derive therapeutically meaningful results from drug screening efforts. Human retinal tissue in a dish has a real potential to be a great tool for drug screening, as well as disease modeling and source of transplantable 3D retina for RP and AMD after these critical shortcomings of retinal organoid technology are addressed. Scientific retinal community is keenly aware of the immense potential of human retinal organoid technology and the urgency of addressing these critical deficiencies in organoid technologies, preventing us to use it to the fullest extent for basic and translational research and regenerative medicine treatments. However, even now some remarkable success has been achieved with modeling treatments of some types of blindness (e.g., some ciliopathies) in retinal organoids, highlighting precise disease mechanisms and new potential therapies, which could be challenging to decipher and discover in cultured cells and time-consuming in animals (Schwarz et al., 2017).

In this review, we discuss the biology of retinal organoids and similarities with human retinal development, translational applications of retinal organoids in disease modeling (based on today's technology state), cell or tissue replacement and discuss current major limitations of retinal organoid technology and how to overcome it. We provide a brief summary for each blinding disease (RP, AMD, glaucoma) to be aware of the current limitations as well as opportunities of retinal organoids as a tool for designing such models in a dish. We also use this summary throughout the text to discuss the key basic and translational research directions needed now to improve the retinal organoid models and technologies to enable faithful recapitulation of retinal biology, homeostasis and diseases in a dish for developing new drugs, delineating disease mechanisms and designing 3-Dimensional transplantable retina for replacement therapies.

We pay special attention to highlighting similarities and differences between human retinal organoids and human fetal and mature retinal tissue, and the impact of these similarities and differences on our ability to interrogate disease mechanisms, screen for drugs and use organoids for cell and tissue replacement therapies. Last, we present our opinion on how the technology will be developing in the next 3–7 years to focus on addressing the current limitations and urgent needs of biotech sector for developing therapies (drugs, biologics) using retinal organoids as a tool.

RETINAL ORGANOIDS FOR BASIC BIOLOGY AND TRANSLATIONAL STUDIES

Modeling Early Retinal Development

Early Cell Fate Decisions and Studying the Role of Morphogens

Ongoing retinogenesis in 3D retinal tissue derived from hPSCs (ES and iPS) recapitulate early stages of human retinal development (Meyer et al., 2009; Volkner et al., 2016) (**Figure 1**). A number of very informative and well-designed retinal cell fate studies in young organoids were done by Gamm lab, which uncovered the instructive signaling of WNT and FGFs and decisions between NR and RPE fate (Capowski et al., 2016; Gamm et al., 2019). Developing retinal organoids (even without RPE) seem to be a good model for dissecting such major cell fate decisions, cell cycle, number of progenitors of each cell type and their initial organization in developing mammalian retina. Nevertheless, one should be mindful of some differences such as lack of RPE and lens and changes in the extrinsic factors and morphogen gradients caused by these differences (Dakubo et al., 2008; Smith et al., 2018). Though these signaling cues have some major consequences for translational research (e.g., BMP/TGFb signaling from ocular surface ectoderm through Smad4, also modulated HH signaling (Li et al., 2016), these are very early developmental processes (NR vs RPE), typically related to microphthalmia (Bharti et al., 2006; Manuel et al., 2008; Bharti et al., 2012) and marginally related to RD diseases.

Retinal Ganglion Cell Development

Retinal ganglion cell development takes place early in retinogenesis (Marquardt and Gruss, 2002), and young retinal organoids (∼6–15 weeks) derived by various methods carry RGCs (Singh et al., 2015), which are typically detected with antibodies to BRN3A, BRN3B, ISL-1, sometimes SNCG, HuC/D, neuronal-specific class III ß-Tubulin (TUJ-1 antibody) and/or Thy-1 (Barnstable and Drager, 1984; Huang et al., 2006). A number of labs pursuing RGC development successfully study RGC development, early stages of axonogenesis and axon guidance in retinal organoids (Fligor et al., 2018). In the absence of their natural target (visual centers in the brain (Cruz-Martin et al., 2014; Dhande and Huberman, 2014; Ray and Kay, 2015) RGC axons may even traverse through the retinal tissue (Singh et al., 2015) but eventually degenerate, together with RGC cell bodies (Wahlin et al., 2017; Capowski et al., 2019; Nasonkin et al., 2019). This is because RGCs need connectivity with the brain to receive flow of neurotrophins; RGC axotomy models and cases of anencephalic brain (both severing this vital to RGC connection) indicate rapid degeneration of RGCs in human fetal retina (Mo et al., 2002; Nakazawa et al., 2002; van Adel et al., 2005; Hendrickson et al., 2006). With the conceptualization and development of assembloid technologies co-culturing of retinal and brain organoids became feasible (Gopalakrishnan, 2019; Pacitti et al., 2019). This extends the developmental window for RGC studies in retinal organoid model which can now include studies interrogating mechanisms guiding RGC projections to

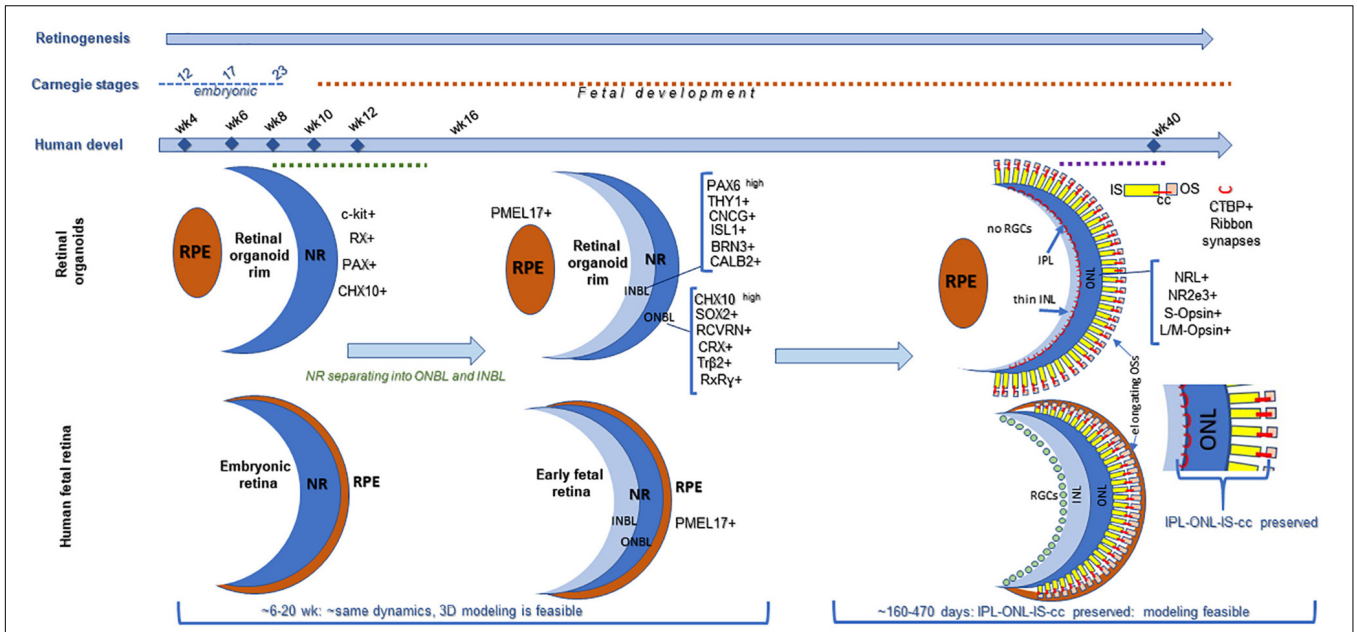

FIGURE 1 | Comparing retinogenesis between human pluripotent stem cell derived retinal organoid growing in a dish and in human fetal retina. Both retinal organoids and fetal retina develop neural retina (NR), but only fetal retina (not organoids) develop continuous layer of RPE surrounding NR (Stage1). Both fetal retina and retinal organoids undergo lamination (Stage 2), and develop outer and inner neuroblast layers (ONBL, where progenitors, including photoreceptor progenitor and young photoreceptors localize, and INBL, where RGCs and 2nd order neurons migrate). However, as tissue maturation proceeds in retinal organoids, the RGCs gradually die (no connectivity) and then a layer of 2nd order neurons becomes progressively thinner. And, while cilia and inner segments in photoreceptors develop, outer segments never elongate full-length, compared to that in mature mammalian retina (Stage 3). In fetal retina (2nd –>3rd trimester) photoreceptor layer undergoes maturation, cilia and inner segments are formed and elongation of outer segments takes place (which continues after birth). Organoids at stage3 preserve the features of immature human retina (IPL-ONL-IS-cc region, shown). This diagram is designed based on the following data: https://embryology.med.unsw.edu.au/embryology/index.php/Vision_-_Retina_Development, https://embryology.med.unsw.edu.au/embryology/index.php/Carnegie_Stage_Comparison, https://embryology.med.unsw.edu.au/embryology/index.php/Carnegie_stage_table (O'Brien et al., 2004; Hendrickson et al., 2008; Jukic et al., 2013; Hendrickson, 2016; Hoshino et al., 2017).

brain (Kurimoto et al., 2010; de Lima et al., 2012; Erskine and Herrera, 2014; Crair and Mason, 2016; Benowitz et al., 2017; Laha et al., 2017).

INL & Outer Plexiform Synaptic Layer

Several long-term *in vitro* and *in vivo* studies investigated connectivity of second order neurons (rod bipolar neurons, typically stained with anti-PKCα antibody) and photoreceptors in human and mouse retinal organoids (Wahlin et al., 2017; Capowski et al., 2019) and *in vivo*, between graft or host-specific bipolar neurons and graft-specific photoreceptors (Assawachananont et al., 2014; Gonzalez-Cordero et al., 2017; Tu et al., 2018). The formation of CTBP2[+] horseshoe-like ribbon synapses (Singh et al., 2014; Singh et al., 2017) was documented by both IHC and electron microscopy in organoids cultured for 5–6 months or longer by several teams. In the *in vivo* studies, where the INL-specific organoid cells (including the bipolar neurons) continue to be lost, graft-specific photoreceptors were found in contact with (in some cases) graft-specific and (in some other cases) host-specific bipolar neurons (Assawachananont et al., 2014; Shirai et al., 2016; Tu et al., 2018). Collectively, these studies demonstrate that connectivity at the OPL level in organoids and in grafts is feasible, which lays foundation for tissue replacement work using hESC-3D retinal tissue from organoids as source of transplantable tissue. In anticipation of improved 3D human retinal models with functional RPE-photoreceptor niche and photoreceptor-second order neuron connectivity, it becomes important to focus on defining cone bipolar-photoreceptor connectivity and cone bipolar cell markers. The classical cone bipolar marker Recoverin (RCVRN) (Milam et al., 1993; Euler and Wassle, 1995) is also strongly expressed in CRX[+] photoreceptor progenitors (Singh et al., 2015) and α-RCVRN staining is the method of choice for defining photoreceptor layer in retinal organoids. Because of the major emphasis of translational retinal work on AMD (in addition to glaucoma) for building models of human macula and designing transplantable retina for patients with advanced AMD, delineating new reliable markers of cone bipolar cells for demonstrating cone bipolar-cone photoreceptor connectivity in organoids and in subretinal grafts may be critical for moving such modeling and transplantation work forward. Some excellent new markers were recently described (Shekhar et al., 2016).

Photoreceptors (Rod and Cone)

Photoreceptors (rod and cone) in retinal organoids are the key cell types in retinal organoids, which seem to remain organized in a uniform layer in long-term organoid cultures (Wahlin et al., 2017; Capowski et al., 2019; Nasonkin et al.,

2019), and (in addition to RGCs) represent the primary drug-screening target for Big Pharma companies. Pioneering work has been done in human fetal retina by researchers like Drs. Anita Hendrickson, Tom Reh, Anand Swaroop and others to elucidated human retinal development with emphasis on photoreceptors (Abramov et al., 1982; O'Brien et al., 2004; Hendrickson et al., 2008; Hendrickson, 2016; Chao et al., 2017). A layer of photoreceptors with NRL[+] rods (Swaroop et al., 1992), OPN1SW[+] (S-cones) and TRß2[+] (Ng et al., 2001) M-cones robustly forms in organoids derived by multiple techniques, which highlights retinal organoids as a good model of human photoreceptor genesis and maturation in a 3D tissue in a dish. This enables to dissect the important of multiple small molecules, morphogens and canonical signaling pathways such as basic fibroblast growth factor (bFGF), docosahexaenoic acid, bone morphogenic protein (BMP), taurine, Retinoic Acid (RA), WNT (Wingless) (Murali et al., 2005; Pandit et al., 2015; Zhong et al., 2014; Capowski et al., 2016, 2019; Brooks et al., 2019; Gamm et al., 2019) important for photoreceptor development. Methods outlining mostly cone photoreceptor development from CRX[+] photoreceptor progenitors will be instrumental for modeling human macula in a dish as well as for designing transplantable 3D retinal grafts for treating patients with advanced AMD (Zhou et al., 2015).

SIGNALING PATHWAYS INVOLVED IN HUMAN RETINAL DEVELOPMENT, DERIVATION OF RETINAL ORGANOIDS AND POSTMITOTIC MAINTENANCE OF BOTH TISSUES

Human retinal organoids recapitulate stages of human embryonic and early fetal retinal development (Meyer et al., 2009; Volkner et al., 2016; Gonzalez-Cordero et al., 2017) (**Figure 1**) and use the same pathways, active in developing human embryonic and early fetal retina for retinogenesis (Hoshino et al., 2017). The embryonic patterning and cell fate decisions in embryogenesis in general are regulated by very conserved developmental cues throughout the animal phyla (Perrimon et al., 2012). Human retinal development is not an exception and is shaped by the same cues and pathways (Heavner and Pevny, 2012). Some of these pathways also participate in maintaining retinal homeostasis. The importance of the *complex interplay* of these pathways in formation and further maturation of 3D human retinal tissue in a dish (organoids) only recently became a subject of thorough investigation (Hoshino et al., 2017). Understanding of this complexity will help with developing better retinal tissue-in-a-dish models with all retinal layers and functional RPE/photoreceptor niche for biopharmaceutical companies for drug screening (; Aasen and Vergara, 2020), and better retinal transplants for curing advanced retinal degenerative diseases (Assawachananont et al., 2014; Mandai et al., 2017a; McLelland et al., 2018; Shirai et al., 2016; Singh et al., 2019). Retina develops from the anterior portion of the neural tube through evagination of the optic vesicles from diencephalon, followed by invagination of those vesicles to form the optic cups carrying RPE and neural retina (NR) layers (consisting of the multipotential retinal progenitors) (collectively, "retina") (Adler and Canto-Soler, 2007; Bharti et al., 2006; Fuhrmann et al., 2014). Invagination of each optic cup also leads to the formation of the optic stalk (the precursor of the optic nerve), which then becomes the optic nerve after the invagination of the stalk and closure of the choroid fissure (Remington, 2012; Forrester et al., 2016). MITF[+] RPE layer and CHX10 (same as VSX2[+]) NR layer carrying multipotential retinal progenitorsgive rise to the retinaand are collectively called "retina" (though some call NR "retina", in contrast to RPE). Following their formation, RPE consistently remains as a single, layer, accumulates pigmentation and undergoes gradual maturation (Bharti et al., 2006, 2012), while NR undergoes a fascinating process of retinogenesis, where multipotential retinal progenitors sequentially acquire cell fate and form different types of retinal neurons and Muller glia (Livesey and Cepko, 2001; Marquardt and Gruss, 2002; Cayouette et al., 2006; Matsushima et al., 2011; Bassett and Wallace, 2012). Rod and cone photoreceptor cell fate acquisition and development is part of this retinogenesis process, and leads to the formation of the therapeutically valuable light-sensing outer nuclear layer (ONL) consisting of rods and cones (Swaroop et al., 2010; Ng et al., 2011). The default pathway in rod versus cone photoreceptor cell fate acquisition is cone PRs (specifically short-wave cones, S-cones) (Swaroop et al., 2010; Hunt and Peichl, 2014; Zhou et al., 2015). This pathway is promoted by blocking Bone Morphogenic Protein signaling (BMP), also WNT and TGFß signaling in culture (Zhou et al., 2015), and mutations of *NRL* or *NR2E3* genes *in vivo* (enhanced S-cone syndrome) (Mears et al., 2001; Sharon et al., 2003; Cheng et al., 2006; Littink et al., 2018). The expression of transcription factor Neural Leucine Zipper (*NRL*) at about week 10.5 of human fetal development defines rod photoreceptor cell fate (Swaroop et al., 1992; Mears et al., 2001; Hendrickson et al., 2008) and *NR2E3* (activated by *NRL,* at about week 11.7 in human fetal retinal development) (O'Brien et al., 2004; Cheng et al., 2006) further strengthens rod PR identity. Both of these transcription factors are expressed prominently in rod PRs in retinal organoids. *Waves of signaling mediated by WNT, FGF, Hedgehog, BMP/TGFb NOTCH, Retinoic acid (RA) and IGF-1 pathways through retina* shape retinal development from earlier stages toward the completion of retinogenesis (Yaron et al., 2006; Liu et al., 2006; Das et al., 2008; Fuhrmann, 2008; Fuhrmann, 2010; Fujimura, 2016; Mills and Goldman, 2017). Signaling via diffusible ligands is also present in postmitotic retina (Chen et al., 2015). These principles of development neurobiology combined with pluripotent stem cell technology are used for derivation of retinal organoids (good summary was provided in Dr. Sally Temple's review Zhao et al., 2017). While some of these morphogen gradients seem to be present in retinal organoids (e.g., WNT pathway, judged by the presence of LGR5 and SFRP1 on the apical and basal side (**Figures 2**, **3**) some other key gradients may be completely or partially absent due to lack of choroid, retinal vasculature and a continuous layer of RPE around the organoids. Exploring these signaling pathways in retinal organoids and comparing them to

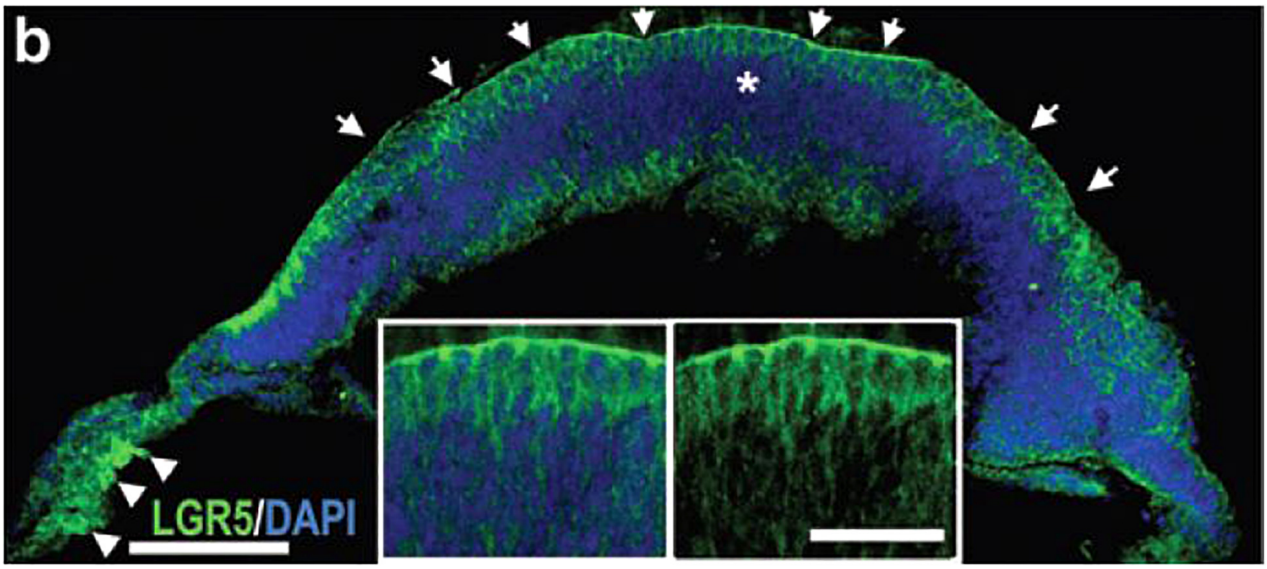

FIGURE 2 | Presence of LGR5 in retinal organoids. Immunostaining of human pluripotent stem cell derived retinal organoid with anti-LGR5 antibody.

signaling in developing and postmitotic mammalian retina will improve the development of better 3D *in vitro* models of human retina, which may be particularly critical for drug development.

WNT in Retina and Organoids

WNT is one of the most studied pathways in developing mammalian retina (Liu et al., 2006; Fuhrmann, 2008; Liu et al., 2010; Fujimura, 2016). Leucine rich repeat containing G protein-coupled receptor 5 (LGR5), a member of the G protein-coupled, 7-transmembrane receptor (GPCR) superfamily, is a receptor for R-spondins, and potentiates the canonical WNT signaling (de Lau et al., 2014). LGR5 is highly expressed in developing retinal organoids (300 fold) (Singh et al., 2015) and also present in developing human fetal retina (Chen et al., 2015). Formation of retinal organoids can be promoted by modulation of WNT pathway (Takata et al., 2017; Luo et al., 2018). WNT signaling remains important in postmitotic retina (Yao et al., 2016). WNT and Notch pathways acting together are known to regulate stem cell niches (birth, renewal and maintenance of multipotential stem cells, in short, stemness (Androutsellis-Theotokis et al., 2006; Clevers et al., 2014; Kessler et al., 2015) in tissues, including in the organoids (Kessler et al., 2015). Modulating these pathways in retinal organoids may be an interesting approach to study retinal regeneration and stemness (Jiang et al., 2020) to replenish cells lost in ageing, trauma or due to degenerative conditions.

Sonic Hedgehog (SHH)

Sonic Hedgehog (SHH) and members of the Hedgehog (HH) family (Indian- and Desert Hedgehog, IHH and DHH) are well studied in developing vertebrate retina (Levine et al., 1997; Neumann and Nuesslein-Volhard, 2000; Nguyen and Arnheiter, 2000; Vogel-Hopker et al., 2000; Zhang and Yang, 2001a,b; Wang et al., 2002; Dakubo et al., 2003, 2008; Spence et al., 2004; Locker et al., 2006; Yu et al., 2006), including mammalian retina, more relevant to the biology of human retinal organoids, and provide very important paracrine signaling cues. There seem to be two major sources of HH signaling, one coming from RGCs (Wang et al., 2002), and another from choroid/RPE (from endothelial cells Dakubo et al., 2008, also from RPE Nakayama et al., 1998; Perron et al., 2003) impacting RPE (Zhang and Yang, 2001b; Burnett et al., 2017; May-Simera et al., 2018) and likely photoreceptors (Levine et al., 1997). HH signaling impacts retinal progenitor proliferation and cell fate determination (Wang et al., 2002; Sakagami et al., 2009). Cilia is needed for SHH signaling and is very important part of both types of cells forming the subretinal niche (photoreceptors Gilliam et al., 2012; Rachel et al., 2012a,b; Yildiz and Khanna, 2012; Wheway et al., 2014 and RPE May-Simera et al., 2018). Problems with cilia development, structure and functions result in ciliopathies, and many of them involve RD conditions because of importance of primary cilia for visual transduction, RPE-photoreceptor connectivity and outer segment function (Chen H.Y. et al., 2019). RPE cilia length had a noticeable change in Dnmt1 conditional mutants with short outer segment, hypoplastic apical RPE and retinal degeneration (Nasonkin et al., 2013). Pharmacological drugs were found, which promote apical RPE maturation in hiPSC-RPE and promote cilia formation. In relation to SHH, the integrity and shape of cilia impact SHH signaling efficacy, dependent on cholesterol (derived from OS membranes) (Myers et al., 2013; Bangs and Anderson, 2017; Garcia et al., 2018; Kinnebrew et al., 2019; Kong et al., 2019). Cilia is present in maturing hPSC-retinal organoids ∼5-6 month and older (demonstrated by our lab (Nasonkin et al., 2019) and others (Wahlin et al., 2017; Hallam et al., 2018; Capowski et al., 2019). With cholesterol provided via FBS (Yang et al., 2014) (critically needed for further growth of organoids) (Zhong et al., 2014) and photoreceptor cilia present in organoids ∼5–6 month old and older, SHH signaling is probably reconstituted in tissue culture.

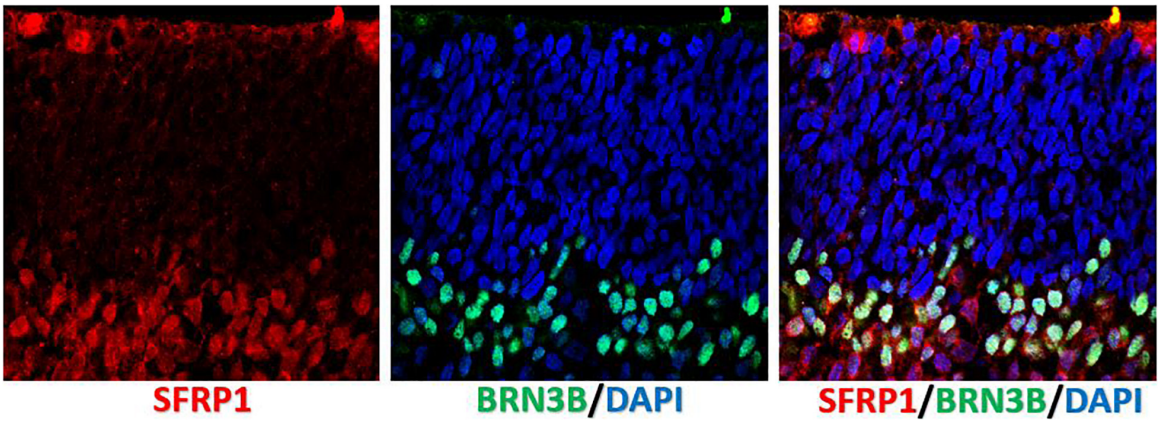

FIGURE 3 | Localization of SFRP1 in human fetal retina. Immunostaining of human fetal retina (wk10) with anti-SFRP1 and anti-BRN3B antibody shows SFRP1 presence in the apical side of ONBL and distal side of INBL. Anti BRN3B colocalized with SFRP1 in the INBL.

However, once the co-culture system between photoreceptor sheet in retinal organoids and the RPE (or RPE/choroid) sheet is created, this signaling will become closer to the one present in mammalian subretinal niche.

FGF1 and 9

FGF1 and 9 are important for neural retina formation (less for cell fate specification Cai et al., 2010 except for RGCs Chen et al., 2013) and then for photoreceptor survival and maintenance (Fontaine et al., 1998; Qin et al., 2011; Hochmann et al., 2012), and were used to enhance NR cell fate in mouse models and *in vitro* in hPSC- > retinal differentiation systems (2D and 3D) at the expense of RPE (Pittack et al., 1997; Zhao et al., 2001; Horsford et al., 2005; Cai et al., 2010; Hambright et al., 2012; Gamm et al., 2019). Separately, some lower (reduced) level of basic fibroblast growth factor (bFGF) signaling (Moore et al., 2004) but not the complete abrogation of FGF signaling (Meyer et al., 2009) is needed for initial eye field specification. FGF morphogens are potentially a great tool to enrich for neural retina cell fate in organoids and 2D monolayer cultures. However, in view of the importance for developing better *in vitro* retinal models with RPE and NR growing together for studying and treating RD diseases, it seems that keeping the developmentally relevant balance of these factors, rather than completely abrogating RPE cell fate in developing retinal organoids, may be the right approach for developing better 3D retinal models. Nevertheless, investigating neuroprotective abilities of FGFs for promoting photoreceptor survival (Fontaine et al., 1998; Qin et al., 2011; Hochmann et al., 2012) seems a doable and therapeutically relevant approach in 6-12 - month old organoids, where the predominant surviving cell type is rod and cone photoreceptors.

BMP and TGFβ Signaling

Contribution of BMP signaling is important in retinal development for determination of NR identity (Murali et al., 2005; Pandit et al., 2015) and originates from developing lens (Pandit et al., 2015), ocular surface ectoderm (Li et al., 2016) as well as retinal neurons (Close et al., 2005), RPE and vasculature (summarized in Ma et al., 2019). Activin A signaling through SMAD2/3 was found to increase number of photoreceptor precursors during retinal differentiation in 2D adherent monolayer (Lu et al., 2017). BMP/TGFb (and SHH) pathways modulation were used for derivation of organoids from human embryonic stem cells (hESCs) (Hallam et al., 2018; Kuwahara et al., 2019). Constitutive TGFβ signaling is needed in postmitotic retina (Ma et al., 2019). TGFβ (b1, b2, b3) are expressed by multiple developing and postmitotic retinal cell types including neurons, vasculature, RPE and microglia (Lutty et al., 1991; Lutty et al., 1993; Siegert et al., 2012; Close et al., 2005; Ma et al., 2019). Excessive TGFβ signaling causes epithelial to mesenchymal transition (EMT) in RPE and proliferative vitreoretinopathy (PVR) and fibrosis, while Cre-mediated deletion of *TGF*β in the whole eye and in vascular endothelium (but not RPE) caused choroidal neovascularization (CNV) (Schlecht et al., 2017). Both EMT- > PVR and CNV cause secondary changes in retina causing photoreceptor degeneration. These signaling are very relevant and important for developing vision restoration therapies (Kobayashi et al., 2019). However, in the absence of vasculature and subretinal niche in organoids we are so far limited in the ability to study them in the 3D retinal organoid model. A major source of BMPs and TGFs in retinal organoid culture is clearly delivered exogenously, with addition of 5–10% fetal bovine serum (FBS), and adding FBS is critical for maturation and growth (but not formation) of retinal organoids (Zhong et al., 2014). Modulating BMP-4 level in developing retinal organoids may help generate NR with RPE at the margin (ciliary margin-like zone, CMZ) (Kuwahara et al., 2015), which is a step in the right direction toward generating physiologically and therapeutically relevant 3D NR-RPE models (the subretinal niche).

NOTCH pathway is frequently mentioned when discussing retinal progenitor cell (RPC) proliferation/maintenance and specification, asymmetric cell division via Numb (where one RPC daughter acquires cell fate while another proceeds with symmetric cell division) (Shen et al., 2002; Ha et al., 2017)

as well as regenerative cues in retina supporting retinal tissue regeneration (Mills and Goldman, 2017). Notch signaling in retina (which involves 4 receptors) works via paracrine ligands (Ha et al., 2017), with downstream signaling cascade involving RBP-J transcription factor (Riesenberg et al., 2009; Zheng et al., 2009) and Hes1/Hes5 (Yaron et al., 2006). Inactivation of RBP-J and modulation of Notch pathway with inhibitors (DAPT being the most well-known ɣ-secretase/Notch pathway inhibitor) impacts the formation of NR, retinal lamination and may impact PR yield (Tomita et al., 1996; Yaron et al., 2006; Zheng et al., 2009), as well as determination of other cell types (Furukawa et al., 2000) depending on timing of Notch pathway inactivation during retinogenesis. Retinal cell types are born sequentially during retinogenesis (Livesey and Cepko, 2001; Marquardt and Gruss, 2002). Notch pathway promotes cell cycle progression in multipotential retinal progenitors (Yaron et al., 2006), while Notch suppression causes premature exit from a cell cycle, causing premature birth of later-developing cell types (Tomita et al., 1996). Therefore, it is clear that when Notch pathway is blocked earlier in retinal development (when e.g., cone PRs are developing), such modulation may increase cone PR yield (Yaron et al., 2006). This knowledge has been used productively for modulating the number of different cell types in human and mouse retinal organoids (Volkner et al., 2016). Because of the involvement of Notch1 in regeneration and major differences in species in the ability to regenerate retinal tissue we focused this paragraph mostly on reports outlining the role of Notch pathway in mammalian retina. Critically to retinal organoids (which usually do not have a sheet of RPE cells around PRs (Zhong et al., 2014). Notch signaling is active in RPE as well (providing signaling cues to nearby RPCs (Ha et al., 2017; Liu et al., 2013). Ablation of RPE in mouse development severely impacts retinal layer organization (lamination) (Raymond and Jackson, 1995). Likewise, lamination defects occur in two RBP-J -knockout mouse models (Riesenberg et al., 2009; Zheng et al., 2009) (summarized in Zheng et al., 2010), potentially pointing to the need of active Notch signaling (via RPE or diffusible Notch ligands) for organoid growth and contributing to retinal lamination in organoids. It is likely that serum provides some level of Notch ligands as it is needed for organoid growth (Zhong et al., 2014) and RPE-free lamination in retinal organoids has been reported (Capowski et al., 2019).

Insulin-Like Growth Factor 1 (IGF-1)

Insulin-like growth factor 1 (IGF-1)is one of the pathways, which was instrumental for derivation of retinal progenitors from hESCs in 2D adherent monolayers (Lamba et al., 2006; Lamba et al., 2010; Hambright et al., 2012) and 3D retinal organoids (Mellough et al., 2015; Singh et al., 2015). IGF-1 is a very important extrinsic factor (morphogen) in developing retina and was shown to promote proliferation multipotential retinal progenitors (RPCs) via PI3K/Akt and MAPK/Erk pathways (Wang et al., 2018) and rod photoreceptor precursors in the fish (teleost) retina (Mack and Fernald, 1993). IGF-1 signaling in general regulates tissue growth and development in embryogenesis by supporting cell survival and cell cycle progression (Schlueter et al., 2007). The transition of rod photoreceptor precursors to mature post-mitotic rod photoreceptors is also promoted by IGF-1 (Yi et al., 2005; Pinzon-Guzman et al., 2011) and is regulated (at least partially) by phosphatidylinositide concentration and 3-phosphoinositide-dependent protein kinase-1 (PDPK-1) (Xing et al., 2018). IGF-1 receptor immunoreactivity is present in the ONBL (where photoreceptor progenitors reside in developing retina and retinal organoids) and in ONL of postmitotic mammalian retina (Greenlee et al., 2006). Another report mapped IGF-1 receptor (IGF-1R) as well as insulin receptor, IR, predominantly to photoreceptors and blood vessels, with very low level in other retinal cell types (Lofqvist et al., 2009). IGF-1 is also a component of FBS (Singh and Armstrong, 1997), and, given the importance of IGF-1 for photoreceptor maintenance [above and (Arroba et al., 2009)] as well as RPE maintenance (Zheng et al., 2018) and the need of growing organoids for serum (Zhong et al., 2014), IGF-1 will likely be included in serum-free ("defined media") culturing methods of long-term organoid/RPE culture in the next few years. In addition, data from Igf-1$^{-/-}$ mutant mice (a model of human neurosensory syndromic deafness/blindness) indicated the gradual loss of ERGs, retinal morphology and significant loss of connectivity between photoreceptors and their synaptic partners (loss of bassoon and synaptophysin) while only small changes in the INL (Rodriguez-de la Rosa et al., 2012), highlighting the importance of IHG-1 pathway for photoreceptors and the need for IGF-1 in long-term photoreceptor-RPE cultures.

Retinoic Acid (RA)

Retinoic Acid (RA) is one of the best studied signaling pathways, active and important in many tissues during embryonic patterning and organogenesis (Rhinn and Dolle, 2012). Retinoic acid signaling is important at several stages of mammalian eye development, including promoting retinogenesis (Osakada et al., 2008, 2009; Cvekl and Wang, 2009; Lamba et al., 2010). Vitamin A and RA are indispensable for eye development and participate in several stages of eye and retina development (Matt et al., 2005; Cvekl and Wang, 2009). Early in development, *Raldh2* expression in the optic vesicle enables generation of RA signal needed for invagination of retina to form an optic cup (Mic et al., 2004). Retinoic Acid, a biologically active Vitamin A (retinol) derivative, serves as a ligand for nuclear receptors regulating gene expression (Duester, 2000; Duester, 2009) and regulates the expression of the key rod photoreceptor cell fate gene NRL (Khanna et al., 2006). However, the continuing presence of RA negatively impacts photoreceptor maturation (Nakano et al., 2012). Exposure to exogenous RA increased the number of rod and green cone photoreceptors and decreased the number of blue and UV cone opsin cells in zebrafish (Prabhudesai et al., 2005), suggesting RA as an instrumental factor in retinal organoid culture contributing to rod-cone photoreceptor development. The enzyme involved in RA synthesis (RALDH2) has been localized to RPE. Mimicking RA signaling in young retinal organoids for promoting photoreceptor development is now part of many protocols and can be done with addition of RA to differentiation medium (Zhong et al., 2014; Wahlin et al., 2017; Capowski et al., 2019). Retinol/RA was localized to photoreceptor

outer segments in long-term retinal organoid cultures (Capowski et al., 2019) and light-responsive (mature) retinal organoids have been generated (Hallam et al., 2018). However, restoring the chemistry of the retinoid (visual) cycle (Kiser et al., 2014) and recycling of all-trans-retinol back to 11-cis retinal by RPE (canonical pathway for chromophore recycling) (Saari, 2000; Wang et al., 2009) for natural reintroduction into photoreceptor outer segments seems unattainable until the establishment of long-term co-culture between sheets of photoreceptors in retinal organoids and RPE and rebuilding of functional photoreceptor-RPE subretinal niche.

Pigment Epithelium Derived Factor (PEDF, or SERPINF1)

Pigment epithelium derived factor (PEDF, or SERPINF1) signaling is an important paracrine and autocrine pathway in retina (Tombran-Tink et al., 1991; Malchiodi-Albedi et al., 1998; Tombran-Tink and Barnstable, 2003) for maintaining PR-RPE niche (Volpert et al., 2009; Akiyama et al., 2012), photoreceptor maturation (Jablonski et al., 2000; Akhtar et al., 2019) and survival (Comitato et al., 2018; Chen Y. et al., 2019). PEDF expression is a hallmark of RPE maturation and polarization (Strunnikova et al., 2010; Maruotti et al., 2015; McGill et al., 2017). High level of PEDF expression is produced by RPE differentiated from human pluripotent stem cells (Kanemura et al., 2013; Maruotti et al., 2015; Geng et al., 2017; McGill et al., 2017).

Pigment epithelium derived factor has a pleiotropic impact on many pathways, is considered a neuroprotective factor in retina and among other functions, may potentially have immunomodulatory function (Dawson et al., 1999; Gregerson et al., 2006; Ho et al., 2011; Chuderland et al., 2013; Nelius et al., 2013; Idelson et al., 2018). In view of increasing interest in co-culturing systems between photoreceptor sheets in retinal organoids and RPE sheets for recreating the subretinal niche, better 3D *in vitro* long-term retinal disease modeling as well as designing transplantable retinal patches, PEDF may become one of the important factors for establishing such cultures and maintaining homeostasis *in vitro* between the photoreceptors and RPE.

3D RETINAL TISSUE MODELS FOR ELUCIDATING DISEASE MECHANISMS & DRUG DISCOVERY

Though developmental biology questions were driving the discovery of retinal organoids, most work quickly shifted toward translational applications because of the unique ability to use organoids as a tool to design human retinal diseases in a dish (**Figure 4**). 3D-retinal organoids grown in a dish are developmentally, anatomically and physiologically similar to retinal tissue *in vivo*. Such ability has huge implication in disease modeling with organoids (Lancaster and Huch, 2019) although further improvements, particularly in formation of RPE and photoreceptor interaction and scalability, are definitely needed (Jin et al., 2011). Generation of human induced pluripotent stem cells (hiPSCs) from patients with retinal disease and further differentiating them to retinal organoid provide deep insight in understanding retinal diseases.

A number of studies have recently used retinal organoid for understanding retinal diseases (Jin et al., 2011), caused by *photoreceptor degeneration* (RP, AMD). Because most RP diseases are single-gene autosomal recessive, many RPs represent a very attractive target for organoid technologies for modeling and drug development.

Screening for small molecules ameliorating RD critically depends on the quality of model (retina-in a dish). For example, most RD diseases originate in the RPE-PR niche (either in PRs or/and RPE) and not having RPE-PR interaction in human retina-in-a-dish significantly impacts our ability to model these diseases (and screening for drugs preventing these RDs). Likewise, screening for drugs to ameliorate glaucoma (number one blinding disease) is so far challenging because RGCs degenerate in maturing retinal organoids (by ∼6 month in culture) (Capowski et al., 2019) due to the absence of the projection targets for RGCs (superior colliculus, lateral geniculate nucleus). However, a number of diseases focused on diseases originating at the level of photoreceptors can be studied and modeled. As one example, retinitis pigmentosa-39 (RP39) is caused by homozygous or compound mutations in *USH2A* gene, which encodes protein Usherin, required for photoreceptor (also hair cells in the cochlea) maintenance because of its role in cilia formation and function (Liu et al., 2007). In a study by Guo et al. the team reprogrammed cells from RP39 patient carrying (c.8559-2A > G/c.9127_9129delTCC) to iPSCs, generated mature retinal organoids from iPSC line with USH2A mutation and found significant defects in photoreceptor morphology with defective retinal progenitor cell development and retinal layer formation compared to control (Guo et al., 2019). Transcription profiling done on mutant retinal organoid revealed increase in apoptotic genes and abnormal gene expression compared to control. In another study iPSCs lines generated from three RPGR mutant patients [RP3 (Rozet et al., 2002), also RP15, cone-rod degeneration, X-linked (Mears et al., 2000)] were used for differentiation to retinal organoids (Deng et al., 2018). The team observed defects in photoreceptor morphology and localization, changes in transcriptional profiling and electrophysiological activity, in line with knowledge about the disease mechanisms. Interestingly, shortened cilium was found in patient iPSCs and RPE and photoreceptors in retinal organoids, derived from those iPSCs. Similarly, Megaw et al. (2017) showed that iPSCs-derived photoreceptors from *RPGR* mutation patients exhibited increased actin polymerization compared to the control, which was due to a disruption of cell signaling pathways regulating actin turnover via disruption of RPGR-Gelsolin interaction, which impacts Gelsolin activation (Megaw et al., 2017). Therefore, this study uncovered a disease mechanisms (loss of RPGR-mediated Gelsolin activation) using patient's iPSC- derived retinal organoids as a tool, cheaper and faster than an animal model, and therefore identified a ***druggable pathway***, amenable for regulation with small molecules.

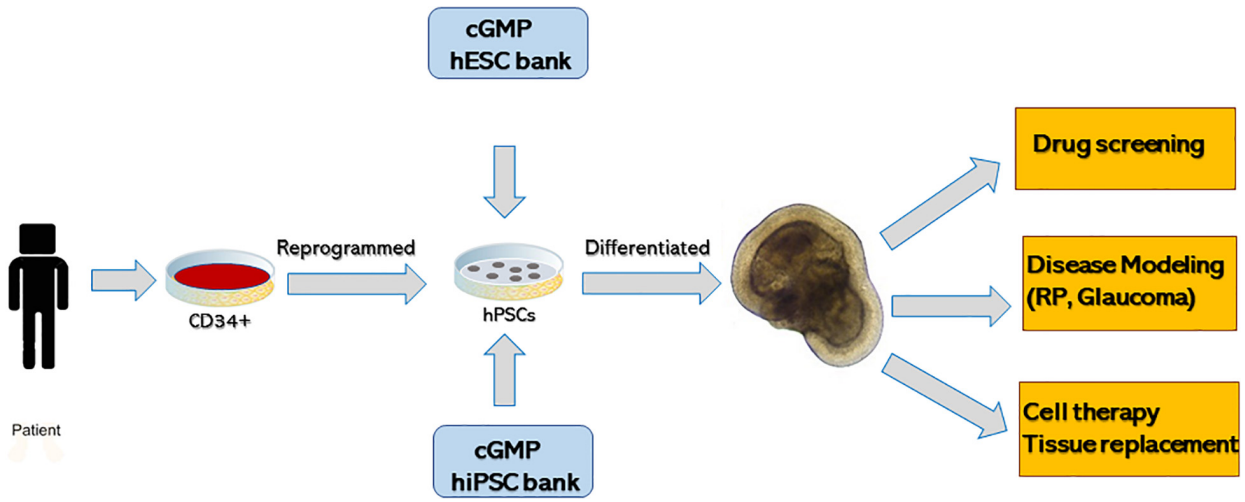

FIGURE 4 | Summary of generating three-dimensional retinal tissue from human pluripotent stem cells and its application in disease modeling, drug screening and cell therapy or tissue replacement.

Study by Schwarz et al. (2017) identified interacting partners (Kif7 and Kif17) of the RP2 protein [GTP-ase activating protein (Veltel et al., 2008)] and observed reduced kinesin Kif7 (a conserved regulator of HH signaling) and Kif17 staining at photoreceptor cilia tips in iPSC-derived 3D optic cups from a patient with the X-linked *RP2* nonsense mutation c.519C > T (p. R120X) compared to control mutation-free organoids (Schwarz et al., 2017). The team was able to correct the PR2 defect by using ***translational read-through drugs***, collectively elucidating the disease mechanism/etiology and highlighting the potential therapeutic approach to treat the disease. Kif7 (together with another ciliary protein Kif17) is reported to play a role in stabilizing cilia tips yet prior to this study multiple other studies done in various models including zebrafish, *C. elegans* and mice failed to elucidate the precise mechanism of this blinding ciliopathy disorder [reviewed in Schwarz et al. (2017)]. Interestingly, the study from another group done in mice indicated that loss of RP2 protein is associated with cone but not rod photoreceptor defects and leads to abnormal extension of cone outer segments (Li et al., 2015).

In yet another study focused on iPSCs disease modeling of RP Masayo Takahashi's team derived iPSCs from a patient with a RHO mutation, derived retinal organoids and demonstrated that photoreceptors in organoids recapitulate the disease phenotype and display signs of endoplasmic reticulum stress (Jin et al., 2012), typical feature in RHO models of RD (Kroeger et al., 2014).

What RD Diseases Caused by PR Degeneration Can and Cannot Be Modeled so Far

From these examples it is evident that modeling of diseases originating within PR cell bodies (e.g., ER) and cilia may be modeled successfully and are not dependent/less dependent on the presence of RPE. The connecting cilium of photoreceptors is a very specialized structure providing stability for fragile and very compartmentalized photoreceptor OSs as well as enabling protein trafficking across the ISs between photoreceptor cell body and OSs (Pearring et al., 2013). Perturbing such protein traffic triggers photoreceptor cell death in many neurosensory ciliopathies, which involve not only vision but also hearing (Rachel et al., 2012a,b; Chen H.Y. et al., 2019). Photoreceptor disk formation is initiated at the level of cilia via specialized recently described mechanism of peripherin-dependent suppression of ciliary ectosome release (Salinas et al., 2017). The capture of photons and initiation of phototransduction takes place in the outer segments, which critically dependent on well-developed microvilli of apical RPE around them (Finnemann and Chang, 2008). RPE microvilli wrap around the tips of outer segments though do not reach the base of photoreceptor cilium (Marmor, 2013).

Interaction of photoreceptor OSs with microvilli of apical RPE is critical for phototransduction, retina-RPE adhesion, stability/homeostasis of photoreceptors and their OSs, and long-term sustaining of vision (Bazan, 2007; Goldberg et al., 2016; Kevany and Palczewski, 2010; Molday and Moritz, 2015; Palczewski, 2014; Wang and Kefalov, 2011). RPE supports photoreceptor function directly (via receptor-ligand mechanism) and indirectly (by secreting interphotoreceptor matrix, recycling 11-cis retinal for phototransduction etc.) (Bonilha et al., 2006; Finnemann and Chang, 2008; Sparrow et al., 2010). And, while models of photoransduction defects and perturbed OS renewal (all causing RD) (Lolley et al., 1994; Molday, 1998; Molday and Moritz, 2015; Petersen-Jones et al., 2018) clearly cannot be built *in vitro* until such 3D long-term co-culture is recreated in a dish, cilia formation and function seems to be recapitulated well enough in retinal organoids likely because it is not dependent directly on microvilli (Figure. . ..) (Marmor, 2013). Therefore, when considering which RD diseases (discussed below) can be studied and modeled with retinal organoids, (some) ciliopathies

may be an interesting and very important class of RD diseases (Chen H.Y. et al., 2019), which may be modeled even in the absence of RPE microvilli.

Retinal Ganglion Cells

Retinal ganglion cells are primarily affected in Glaucoma and other optic neuropathies and glaucoma, a leading cause of irreversible blindness in the United States and the world[5]. The main technological limitation of modeling glaucoma with retinal organoids is clearly the lack of the connecting partners of RGC neurons (visual centers in the brain). Yet, with the development of assembloids (retina-brain organoid co-cultures) technologies, this limitation seems to be only temporary.

The optic nerve originates in the retina and is formed by the axons of retinal ganglion cells (RGCs), the only type of retinal neurons, which requires long-distance connectivity (compared to other cell types, which use short distance connectivity: photoreceptor: bipolar neurons and INL neurons: RGCs). Modeling of RGC biology and disease in retinal organoids is challenged the need of RGCs to establish long-distance connectivity with visual centers in the brain to survive. **RGC viability** critically depends on their connectivity to visual cortex neurons, and such nerve fibers carry supportive (trophic) factors between RGCs and visual cortex neurons (Johnson et al., 2009). Damage to the optic nerve (e.g., the axotomy) can cause interruption or destruction of nerve cell connections and therefore, disrupt the flow of trophic factors leading to the gradual but steady loss of vision caused and RGC death. Restoration of trophic support (even partial) leads to preservation of RGCs (Mo et al., 2002; Nakazawa et al., 2002; van Adel et al., 2005). RGC layer will survive for months to years post injury as long as there is preservation of axonal connectivity between the RGC nerve fibers (forming the optic nerve) and the neurons of the visual cortex (Chang et al., 2006; Chang, 2013). One may find the retina in advanced degeneration stage (no photoreceptors and thin/degenerated INL) but with almost a normal RGC layer and optic nerve (Chang et al., 2002). However, it is feasible to study RGC development, organization and initial steps of axonal outgrowth to uncover factors promoting neurite elongation, guidance and target selection (Fligor et al., 2018). In the absence of their natural targets (visual centers in the brain) the RGC axons may grow randomly and even traverse the retina (Singh et al., 2015). With newly developed concept of retina-brain ("assembloids") co-culturing methods (Gopalakrishnan, 2019; Pacitti et al., 2019) retinal organoids are becoming a very promising model of optic nerve regeneration, reconnection of retina to brain (Kurimoto et al., 2010; de Lima et al., 2012; Erskine and Herrera, 2014; Crair and Mason, 2016; Benowitz et al., 2017; Laha et al., 2017) and potentially glaucoma [when the chambers for ocular pressure mimicking may be designed for recreating intraocular pressure homeostasis (Acott et al., 2014; Wu et al., 2019)] .

Collectively, these studies demonstrate that retinal organoids can be successfully differentiated from hiPSCs lines derived from retinal disease patients and used for delineating and modeling complex disease mechanisms, closely recapitulating the featured of RD diseases in patients. This in turn makes them reliable models for drug discovery.

Cell and Tissue Replacement Therapies for Retinal Degenerative Diseases

Before the arrival of retinal organoid technology, the aborted human fetal tissue (Radtke et al., 2008; Seiler and Aramant, 2012) and retinal progenitors derived from hPSCs (Banin et al., 2006; Lamba et al., 2006; Hambright et al., 2012) (embryonic and induced) were the two cell sources for transplantation. Human fetal tissue is a gift, with strong ethical restrictions and limited supply (NCSL, 2008; NIH, 2009; Finklea et al., 2015; Gerrelli et al., 2015; Wadman, 2015). A very promising and pioneering work on fetal retinal tissue transplantation has been done by Drs. Seiler, Aramant and Radtke (Radtke et al., 2002, 2004, 2008; Seiler et al., 2010; Lin et al., 2018). As discussed above, retinal organoids provide unprecedented way of approaching basic and translational aspects of human retinal biology for disease modeling, drug screening and also as source of retinal cells and retinal tissue for subretinal transplantation aimed at treating blindness.

Age related macular degeneration and RP/LCA are very good and tempting diseases for evaluating retinal sheet replacement strategies with retinal organoids (Assawachananont et al., 2014; Shirai et al., 2016; Mandai et al., 2017a; McLelland et al., 2018; Tu et al., 2018). Though both types of diseases are good targets for such therapy, AMD is not a purely genetic disease and etiology is not completely elucidated, while most RPs are recessive and can be avoided in the near future with advanced genetic testing and genetic counseling. There are at least 15 million people in the US affected by AMD, with at least 2 million having an advanced AMD stage. Macular patch approach, depending on organoid-derived photoreceptor sheet-RPE sheet coculture, is an attractive approach to bring vision to central retina. The size of human maculae is about 5mm in diameter (Kolb, 2005), and biological retinal patch $\sim 4 \times 4$ or 5×5 millimeters (mm) on a flat sheet of biomaterial carrier seems like a doable strategy (Ramsden et al., 2013; Mandai et al., 2017b; Kashani et al., 2018). It can be grafted to the back of patient's eye to bring a layer of healthy and functional retinal tissue to replace patient's own retina (too damaged/degenerated after the injury). This tissue is expected to reconnect (based on studies in mice) (Seiler et al., 2010, 2017) to patient's RGCs and function as a bioprosthetic device similar to completely electronic chips currently approved for clinic (e.g., Argus II Stronks and Dagnelie, 2014). However, due to biological nature and much higher pixel density (which is expected to bring better vision Mathieson et al., 2012), where each individual light-capturing neuron [photoreceptor] of the patch is equal to a pixel, the biological retinal patch approach is expected to eventually supersede the electronic (neuroprosthetic) chip approach and to generate bioprosthetic retina capable of permanent integration into patient's globe. A large piece of tissue from a hESC-derived retinal organoid carrying a layer of PRs and second order neurons provides the light sensors that can synaptically transmit visual information to patient's RGCs, which persist even after all PRs are degenerated (Lin and Peng, 2013). Unlike electroprosthetic

[5]www.glaucoma.org

chips, a "bioprosthetic" implant based on hESC-derived retinal organoids enables long-lasting synaptic integration, and can be adjusted to carry more cones than rods (Mears et al., 2001) if the goal is to repair the macula. These technologies will be subject of intense studies in the next few years and will likely result in symbiosis of 2 approaches (biological and electronic) and neurobioprosthetic retinal implants, utilizing biomaterials and of course retinal organoids. Surgical technologies are already here to deliver such 3D constructs into the eye (Kashani et al., 2018).

CRISPR-Cas-9 gene correction in retinal organoids has been tested successfully in several human RD models (Deng et al., 2018; Huang et al., 2019; Lane et al., 2020) as well as *in vivo* in mice (with up to 45% efficiency of repair of dominant-negative Rho mutation to wild type allele in photoreceptors) (Li et al., 2018). CRISPR-Cas-9-based repair may be especially productive and needed for RP diseases, which are caused by dominant-negative mutations, and may potentially work together with retinal tissue replacement (discussed above).

CURRENT LIMITATIONS OF RETINAL ORGANOID TECHNOLOGY

The current key limitations of retinal organoids for modeling and treating RD diseases are the lack of vasculature, the lack of continuous layer of RPE around the organoids, gradual degeneration of RGC and then INL in mature organoid cultures, lack of the connecting partners for RGC axonal elongation (critical for glaucoma) and critically, lack of RPE-photoreceptor interaction (critical for dry AMD, RP and LCA). Here we discuss ongoing and future work needed to address these limitations.

Absence of Vasculogenesis in Retinal Organoids

The retina is one of the most energy-demanding tissues, with high need for oxygen and nutrients (Warburg, 1928; Ng et al., 2015; Sun and Smith, 2018). Adult retina generates energy via aerobic glycolysis, in addition to oxidative phosphorylation, to compensate for such high demand (Ng et al., 2015) similar to cancer cells (Warburg et al., 1927; Vander Heiden et al., 2009). The oxygen and nutrient supply are delivered either from the choroid side (thus, RPE and photoreceptor layers are avascular and depend on choriocapillaris), or central retinal artery (which brings oxygen to RGC and INL; these 2 layers carry vascular capillaries). These energy demands are caused by energy-demanding phototransduction and related neurotransmitter demand caused by constant depolarization/repolarization (collectively: hyperactive neuronal activity) (Wong-Riley, 2010). However, the initial steps in retinal development lack vasculature (Hughes et al., 2000; McLeod et al., 2006; Hasegawa et al., 2008) (about week14), while the nutrition and oxygenation are delivered from choroid (beneath the RPE) and hyaloid (above the developing retina) (Ye et al., 2010) (**Figure 5**). This can be easily recreated in tissue culture incubator in smaller-size organoids, where penetration of oxygen and metabolites are not yet impacted much by organoid size. This indicates that initial stages of retinogenesis in a dish may be not impacted by lack of vasculature in organoids (i.e., neurovascular niche is not relevant at this stage, additionally confirming young organoids as a good model of early retinal development (Meyer et al., 2009)). Indeed, human fetal retina (∼Carnegie stage 23, day 56–60 and slightly older retina week 11–13) highly resemble human retinal organoids (∼week 10–12), as CHX10[+] NR with multipotential retinal progenitors is gradually separating into outer and inner neuroblast layers (ONBL and INBL). There are differences in the dynamics of retinal vasculature development in humans versus mice, though it is not clear if this is relevant to retinal organoid culture. However, in humans vascular development is complete before birth, while in mice and rats vascular development takes place postnatally [discussed in Sun and Smith (2018)]. There is ongoing productive work to recreate choroid-RPE border in a dish, which is a step in the right direction toward building a complete "retina in a dish" model (Jha and Bharti, 2015; Song and Bharti, 2016) from retinal organoids, RPE sheets and biomaterials. In general, organoid vascularization is a very active research niche at the moment (Grebenyuk and Ranga, 2019) since the initial stages (organoid formation) has been worked out. However, because of the clear differences between the laminated and heavily vascularized structure of human inner retina and spheroid "closed" and avascular structure of retinal organoids, where the oxygen and nutrition supply have difficulty penetrating into the INL/RGC layers (closer to the organoid core (Capowski et al., 2019)), it seems so far impossible to maintain the long-term dynamics of development in retinal organoids, shaped as a sphere. As a result, a number of labs, including ours, noted the almost exclusive survival of photoreceptors in the ONL and gradual demise of INL and RGCs in the organoid core (Wahlin et al., 2017; Capowski et al., 2019), highlighting older retinal organoids (maintained with current level of technology) as a questionable models for a number of RD conditions. Hypoxia inducible factor 1 (HIF-1) plays an important role in response of retina to oxygen level (hypoxic conditions), specifically alpha (HIF-1α) subunit, which becomes stable and translocates to the nucleus only in hypoxic conditions (Hughes et al., 2010). There is constitutive HIF-1a signaling reported in the normal rat and human retina suggesting an important physiological role (Hughes et al., 2010). The level of HIF-1a is high in both developing human fetal retina and young and mature (6-month-old) retinal organoids (based on RNA-Seq data sets from various publications). Because hypoxic conditions and active HIF-1a were reportedly noted as important for tissue regeneration (Nauta et al., 2014; Zhang et al., 2015; Heber-Katz, 2017; Lee et al., 2019), retinal organoids may be an interesting model for exploring retinal tissue (specifically photoreceptor) regeneration by modulating HIF-1a pathway, active in organoids.

LACK OF RPE PHOTORECEPTOR INTERACTION IN RETINAL ORGANOIDS

Retinal organoids do not have the continuous layer of RPE around the organoids (**Figure 6**). Achieving photoreceptor-RPE interaction and designing a functional subretinal niche in retinal

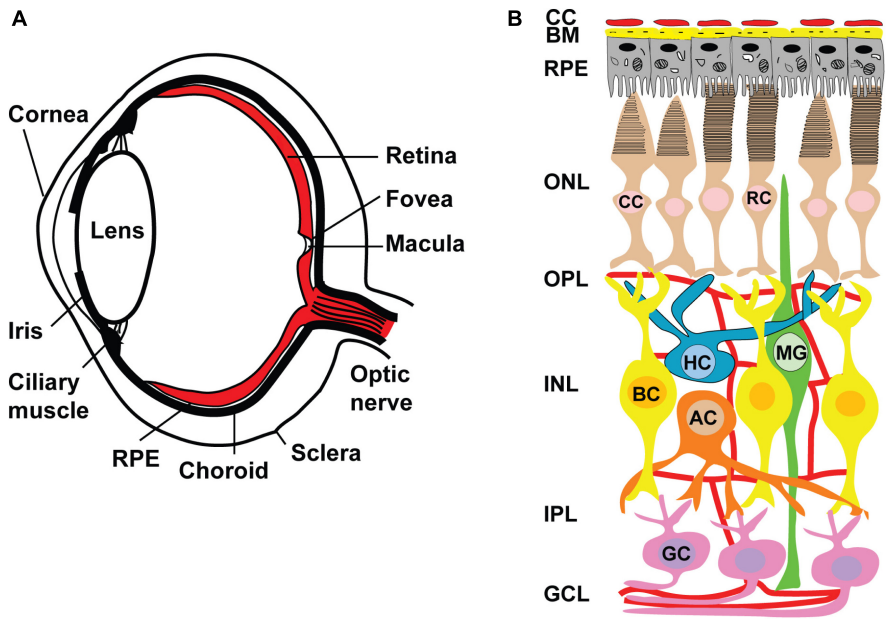

FIGURE 5 | Anatomy of human eye and retinal circuits. **(A)** Schematic drawing of a cross-section through human eye. Light enters the eye through the cornea, passes through the pupil, lens and strikes the retina. Retina is the light-sensitive tissue lining the inner surface of the eye. Visual information from retina transmits to the brain through optic nerve fiber. In the middle of the retina small depression is called the fovea and is responsible for high resolution vision. Region surrounding the fovea is called as macula and are rich in only cones. Retinal pigment epithelium (RPE) is a pigmented layer and separates the choroidal blood supply from the photoreceptors. Choroid is a vascular layer of the eye. The sclera is a tough white sheath around the outside of the eyeball. **(B)** Schematic diagram of normal retina circuits. Mammalian retina consists of six major types of neuronal cells – rod (RC) and cone (CC) photoreceptors also horizontal (HC), bipolar (BC), amacrine (AC) and retinal ganglion cell (RGC). The Muller cell are the glial cells that span across the retina and their somata. RPE provides metabolic and transport functions essential for homeostasis of the neural retina. Bruch's membrane (BM) is a highly specialized and multi-laminar structure in our retinas that forms the basis for mediating interactions between the retinal pigment epithelium and blood flow from the choroid. Choroidal capillaries (CC) are the blood capillaries present in choroid that supply oxygen and nourishment to the outer layer of the retina. Retinal blood vessels are present in OPL, IPL and RGC layers.

organoids is an urgent goal critically needed for designing better models of human retina for drug development and for tissue replacement. As photoreceptors develop their specialized structure adapted for phototransduction, they elongate the inner and outer segments (ISs and OSs) into microvilli, elongating in sync on the apical RPE side (**Figure 7**). This elongation process takes place rapidly in developing mouse eye between approximately postnatal day 9.5 and 14.5 (Nasonkin et al., 2013), while in human developing retina the process starts in the 3rd trimester and continues into infancy (Hendrickson et al., 2008). This indicates that to achieve outer segment elongation in human retinal organoid cultures one needs to wait approximately 24 weeks after the formation of retinal organoid, and 32 weeks or more to have OSs reach the maximum length, assuming that the organoid culture faithfully recapitulates human retinal development, and RPE-organoid co-culture system is established. Genetic ablation of RPE leads to complete loss of photoreceptor OSs (Longbottom et al., 2009), while hypoplastic changes in the apical RPE prevent OS elongation (Nasonkin et al., 2013), collectively pointing to the instructive and important role of RPE in outer segment elongation and maintenance. The interdigitation of OSs of photoreceptors and microvilli of apical RPE creates a stable NR-RPE border and a very specialized subretinal niche (absent or mostly absent in retinal organoids), where critical first steps of phototransduction take place in photoreceptor outer segments (Molday, 1998; Kefalov, 2012; Wang et al., 2009).

Photoreceptors have very compartmentalized structure adapted for phototransduction, which is supported by RPE microvilli (Molday and Moritz, 2015) (**Figure 7**). A number of extracellular ("interphotoreceptor") cell matrix (ECM) proteins important and some critical for phototransduction and photoreceptor OS maintenance reside in the ECM matrix surrounding photoreceptor OSs and apical RPE microvilli (Bonilha et al., 2006; Ebrahimi et al., 2014; Ishikawa et al., 2015; Kelley et al., 2015; Salido and Ramamurthy, 2019). One of them is Interphotoreceptor Retinol-Binding Protein (IRBP), which plays a very important role of shuttling 11-cis retinal from RPE cells and bleached pigment (all-trans retinol) from photoreceptors to RPE (**Figure 7**) (Jin et al., 2009). IRBP message is abundant in human retinal organoids (based on published RNA-Seq data from various labs). A number of other interphotoreceptor proteins were highlighted in recent publications, some focused on studying these proteins specifically in retinal organoids (Felemban et al., 2018; Salido and Ramamurthy, 2019). There is a lot of interest now in these proteins among the teams, trying to use retinal organoids for modeling of retinal diseases and for cell replacement therapies (Dorgau et al., 2019; Guo et al., 2019). This interest is guided by the expectations that

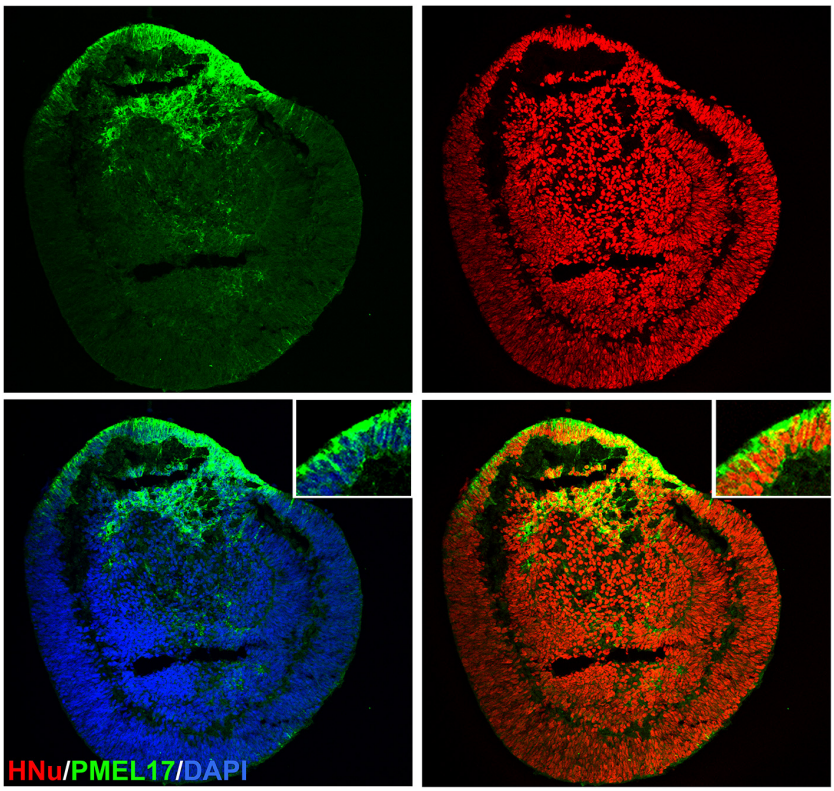

FIGURE 6 | Localization of PMEL17 in the retinal organoid. Immunostaining the retinal organoid (day 70) with pigmented RPE marker PMEL17 show patches of retinal organoids were pigmented. HNu stains the human nuclei. The insets in panel a are high magnification of area marked with asterisk (*). DAPI counter stains nuclei.

these "missing factors" (interphotoreceptor matrix proteins being some of them (Salido and Ramamurthy, 2019)) may help to build connectivity between RPE and photoreceptors in the organoids co-cultured with RPE *in vitro* to improve long-term culture of organoids and recapitulate the biology and structure of RPE-photoreceptor OS niche for disease modeling, drug screening and cell/tissue replacement therapies (Felemban et al., 2018; Achberger et al., 2019).

Lack of Photoreceptor Disk Morphogenesis, Outer Segment Shedding, Phagocytosis in Retinal Organoids

These processes are fundamental to photoreceptor biology and phototransduction, and are critically missing in organoids (so far), thus reducing our ability to model many retinal degenerative diseases in a dish. Disk shedding occurs on the distal side of OSs facing the RPE, and these disks are phagocytosed by RPE, while disk morphogenesis takes place at the base of the OSs (next to the cilium) (Kolb, 1995; Molday and Moritz, 2015; Volland et al., 2015b). Up to 10% of OS discs are renewed daily (Young, 1967). The stack of rod photoreceptor OSs consists of over 1000 compact disk structures in adult retina (Molday and Moritz, 2015). However, the maximum number of disks we and others observed in the retinal organoids cultured for 6–8 months is limited to several disks, and these are not typically organized tightly in a stack (Wahlin et al., 2017; Nasonkin et al., 2019). However, some *in vivo* results reveal better organization of OSs and longer OSs in the long-term subretinal grafts (Shirai et al., 2016), all pointing toward the lumen of rosette-like photoreceptor aggregates in subretinal space (Shirai et al., 2016; Nasonkin et al., 2019). Naturally, there is no ongoing renewal and phagocytosis processes in long term retinal cell and retinal organoid cultures, but it has been expected for a long while that with developing photoreceptor-RPE co-culture systems faithfully recapitulating structure and function of the subretinal niche, OS elongation and photoreceptor-RPE biology can be reestablished (German et al., 2008; Di Lauro et al., 2016; DiStefano et al., 2018; Akhtar et al., 2019; Brooks et al., 2019; Capowski et al., 2019). As work on retinal repair rapidly progresses (Holmes, 2018a,b; Makin, 2019), these technologies will likely be developed in the next 3–5 years as a cheaper and robust model for drug screening and discovery, as well as platform for biomanufacturing 3D retinal tissue transplants to repair vision in advanced RD patients.

The Visual Cycle

The visual cycle in mammalian retina (and lack of visual cycle in retinal organoids) Photoreceptors convert lights into an electrical signal that pass through the second and third

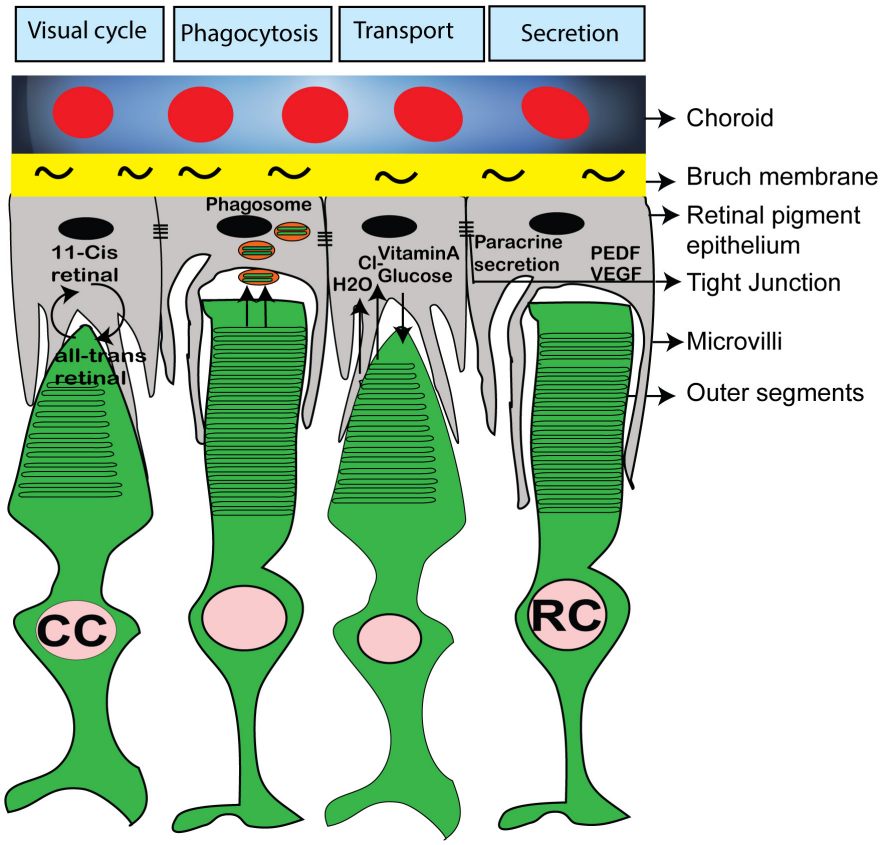

FIGURE 7 | Schematic diagram showing important functions of RPE and its interaction with rod and cone photoreceptor outer segments. The RPE microvili interacts with photoreceptor OS and RPE cells are involved in visual cycle, phagocytosis of outer segments disc, nutrient uptake and paracrine secretion of PEDF, VEGF.

layer of retinal neurons and conveys the information to the brain. Defect in RPE cell or photoreceptor cell impairs the visual function and causes retinal blinding diseases (Age related macular degeneration, Retinitis pigmentosa, Leber congenital amaurosis). The biochemistry of visual cycle has been worked out in seminal work of many laboratories (Hsu and Molday, 1993; Pugh and Lamb, 1993; Baehr and Palczewski, 2007; Luo et al., 2008; Arshavsky and Burns, 2012; Palczewski, 2014). Clearly, no similar Ca(2 +) or cGMP gradients (which are present in the subretinal niche) are present in developing retinal organoids though increased level of Na^+, K^+ and Ca^{2+} electric current are present in developing organoids (Singh et al., 2015). This could be one of many factors causing gradual degeneration of photoreceptors in long-term organoid cultures. It is expected that recreation of photoreceptor-RPE niche in a dish would make it possible to substantially increase the viability of photoreceptors in long-term *in vitro* cultures (Di Lauro et al., 2016; Achberger et al., 2019; Akhtar et al., 2019; Chen Y. et al., 2019), thus enabling disease modeling and drug screening of diseases, where the integrity of subretinal niche and photoreceptor-RPE structural and functional connectivity is of paramount importance for maintaining visual function.

11-cis Retinal

11-cis retinal is critical for visual process in the OSs and OSs do not have it if we don't have RPE. In the RPE65 mutant dogs a lack of 11-*cis* retinal supply to the photoreceptors leads to very reduced function of both rods and cones (Gearhart et al., 2008) similar to that observed in RPE65-mutant mice (Redmond et al., 1998). RPE is critically important for maintaining visual function (Strauss, 2005; Bharti et al., 2006, 2011) and recycles retinal between photoreceptors and RPE (11-cis -all-trans retinal). Though 11-cis retinal (or, more stable for of it, 9-cis form of retinal (Fan et al., 2003)) can be provided in trans to enhance visual responses (Gearhart et al., 2010), this will not substitute for OS homeostasis, turnover and recycling in photoreceptor sheets from organoids and RPE sheets (as discussed above) unless the subretinal niche with close OS-microvilli interaction will be recreated in a dish. After all, though hESC- and hiPSC-derived RPE sheets can indeed phagocytose photoreceptor OSs (Carr et al., 2009; Idelson et al., 2009; Bharti et al., 2011) (one of many functions of RPE in subretinal niche (Mazzoni et al., 2014)), OSs start degenerate pretty quickly after retinal detachment unless physical reattachment takes place quickly, within a day or less (Fisher and Lewis, 2010). Retinal detachment negatively impacts the biological process of disk production and disk shedding. Though

OS-specific proteins are synthesized, they start to localize to locations other than OSs: Opsin accumulates in the plasma membrane, Peripherin/rds appears in cytoplasmic vesicles. It was reported that proteins specific to cone OSs are more sensitive to OS damage, and after only one week of cone opsin mislocatization the expression of cone opsins is downregulated. It was noted that within 24 to 72 h after retinal detachment almost all rod and cone OSs display signs of OS degeneration: they are shorter, acquire abnormal morphology with disks not positioned as stacks (Fisher and Lewis, 2006; Wickham et al., 2013). These features of OS morphology are very similar to those observed by our lab and others in long-term cultures of human pluripotent stem cells (hPSC)-retinal organoids (Wahlin et al., 2017; Capowski et al., 2019; Nasonkin et al., 2019). severely shortened but yet visible OSs can persist for up to several weeks after retinal detachment (Fisher and Lewis, 2006; Wickham et al., 2013).

Variability in Size, Shape, Photoreceptor Density, Lamination

Variability in size, shape, photoreceptor density, lamination determined by cell line-specific and protocol-specific differences (both derivation and maintenance) were described and documented (Capowski et al., 2019; Cowan et al., 2019; Mellough et al., 2019). However, it is feasible even with current technologies to culture and maintain organoids for longer than one year, as a proof-of-principle (Capowski et al., 2019). It quickly became evident that once the self-formation of retinal organoids is done (which can be achieved with a number of protocols maintaining and promoting the propensity of retina (the outpocketing of anterior neuroectoderm) to form, further maturation and long-term maintenance of retina-in-a-dish requires more sophisticated media providing more salts, anti-oxidants, a milieu of supporting paracrine factors (provided by serum or serum plus RPE conditioned medium), etc. (Zhong et al., 2014; Bardy et al., 2015; Singh et al., 2015; Di Lauro et al., 2016; Achberger et al., 2019; Akhtar et al., 2019; Capowski et al., 2019). These issues are mostly technical, and current biomanufacturing technologies allow generating large number of aggregates of a defined size (e.g., for large-scale drug discovery) if needed.

SUMMARY

Modeling early retinal development with hESC and hiPSC approaches (from eye field determination and before photoreceptor develop outer segments) seems the most straightforward and very productive way of using retinal organoids for basic and translational research (Meyer et al., 2009). With arrival of methods of co-culturing between brain and retinal organoids (assembloids (Gopalakrishnan, 2019)), engineering vascularization of organoids (Grebenyuk and Ranga, 2019) and developing pressurized chambers (for glaucoma studies, all discussed above) it will become feasible, and very soon, to use human retinal organoids for studying wet AMD and glaucoma and developing better drugs tested in models faithfully representing pathophysiology of these diseases.

Conceptual Efforts

Conceptual efforts should be centered on better understanding of rebuilding PR-RPE niche with cells and layers of tissue

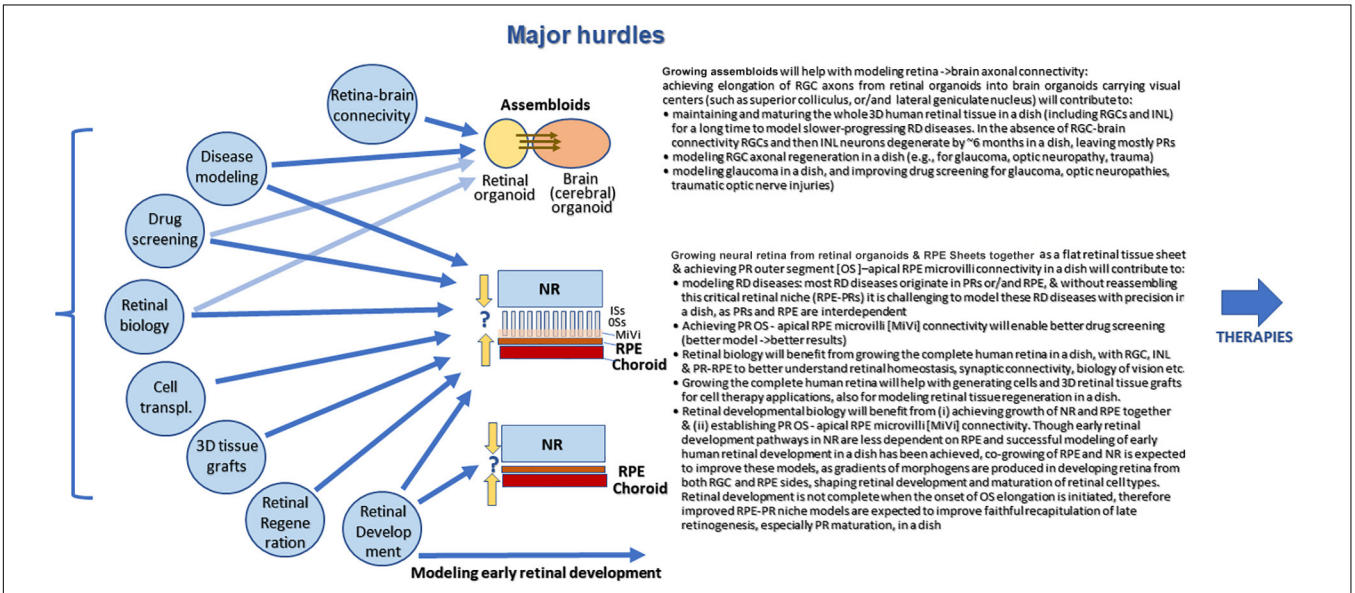

FIGURE 8 | Major challenges of human pluripotent stem cell derived retinal organoid approach growing in dish. In retinal organoid there islack of RPE interaction with neural retina and lack of RPE interaction with choroid. Also, there is lack of retina brain connectivity. However, early retinal development can be studied using retinal organoid (cell fate acquisition). Once the advanced systems of co-culturing will be established (retinal-brain organoids =assembloids, photoreceptor sheets in organoids -RPE sheets, and vascularized organoids) one will be able to design better models of human retina for both drug screening and therapeutic applications.

(e.g., PR layer and RPE sheet), building models of AMD and glaucoma with functional PR-RPE niche, developing techniques for designing cone photoreceptor-only sheets with RPE for modeling of human macula, generating retina-brain organoids co-culture methods for studying and treating glaucoma, and (potentially) investigating vascularization of hESC-retina in a dish. This will open the door for multiple therapeutic/translational approaches (drug testing, photoreceptor transplantation, 3D retinal tissue transplantation). 3D human retinal tissue model on a chip is still unattainable but technologies are being developed to make this a reality in the next 5–7 years (McUsic et al., 2012; Gu et al., 2018; Achberger et al., 2019; Haderspeck et al., 2019; Masaeli et al., 2020). Big Pharma companies need this tool to do large-scale screening of drugs to suppress/ameliorate RD. This screening is not possible with mouse models (not human, expensive, cannot be scaled up) and not productive in cultured retinal cells.Most cells in primary retinal culture are represented by Muller glia after 2–3 several passages; immortalized cell lines have multiple changes in signaling pathways, lack of cell-cell connectivity and loss of many feature of retinal biology, critically needed to faithfully recapitulate pathology.

Among Current Limitations

Among current limitations one can list lack of functional maturation of PRs caused by lack of PR-RPE niche, premature degeneration, gradual loss of RGCs and second order neurons (**Figure 8**) and lack of connecting targets for RGCs to elongate and project. Difficulty for large-scale isolation of "good" retinal organoids and standardization of retinal organoid size and shape are also limitations yet it is expected that progress in biomanufacturing and biologic product development will soon be able to solve these hurdles.

RPE-PR Interaction

RPE-PR interaction: (and lack of -in organoids) This hurdle is clearly biology-driven but the general expectation is that it could be circumvented with progress in technology, as organoid-biomaterial work progresses. Interestingly, even without RPE small stubby outer segments with rudimentary stacks of disks still grow, and in some cases even elongate, yet fail to develop organized stacks of outer segments, likely due to the absence of RPE-photoreceptor interaction. This interaction may be an inducing factor of elongation and most likely a stabilizing factor for disk formation. Equally interesting is the fact that there is hardly any data demonstrating the interaction between RPE and photoreceptors and elongation of outer segments in a dish, even in long-term organoid cultures.

The RPE layer is normally expected to polarize into apical and basal sides, and establish a network of microvilli on the apical side, interacting with photoreceptors and nurturing photoreceptor outer segments. Retinal organoids, however, normally carry patches of RPE on one side, thus directly exposing photoreceptors in the developing organoids to neural medium. Recreation of the critical retinal niche on the border between the apical RPE and photoreceptors, where many retinal disease mechanisms originate, is so far unattainable and is a focus of investigation in many labs. Interestingly, even without RPE small stubby outer segments with rudimentary stacks of disks still grow, and in some cases even elongate, yet fail to develop organized stacks of outer segments, likely due to the absence of RPE-photoreceptor interaction. This interaction may be an inducing factor of elongation and most likely a stabilizing factor for disk formation. Equally interesting is the fact that there is hardly any data demonstrating the interaction between RPE and photoreceptors and elongation of outer segments in a dish, even in long-term organoid cultures. Though the expectations are that the translational research in the near future may solve this hurdle (which is clearly biology-driven but could be clearly improved as organoid-biomaterial work progresses), so far the absence of this RPE-photoreceptor niche imposes clear limitations on both modeling/drug screening and transplantation approaches, especially for AMD/human macula work. Here we dissected the different retinal degenerative diseases and organoid technologies and present our thinking how and where retinal organoid technology can contribute the most to developing therapies even with a current limitation and absence of outer segments, elongating into the microvilli of RPE. Understanding how PR and RPE come together to rebuild functional subretinal niche is important not only for tissue transplantation and modeling of long-term RD disease in a dish, but also for promising cell therapy approaches, based on sorted photoreceptor transplantation (Singh et al., 2013; Gagliardi et al., 2018; Lakowski et al., 2018) (which is more feasible technically that grafting tissue (Seiler and Aramant, 2012) yet needs better understanding of biology to rebuild PR-RPE border with inner and outer segments). Photoreceptor (sorted CD73[+] cell suspension) transplantation so far has to depend on approaches circumventing this biological question like optogenetically engineered photoreceptors (Garita-Hernandez et al., 2019), where functional OSs, where light it converted to electricity are replaced by optogenetic constructs, mimicking OS function.

Now it is very interesting time in translational biology combining pluripotent stem cell technologies, biomaterials, 3D organoid and co-culture approaches in effort to model, rebuild in a dish and transplant the complex 3-dimensional tissue - the retina. This exciting time can be compared to the time when scientists were searching for elusive ways to dedifferentiate adult human cells back to pluripotent state. Developing 3D co-culture technology faithfully recapitulating the biology and physiology of the subretinal niche, together with organoid vascularization strategies, will open the new opportunities for designing better disease modeling in a dish to study the "late-onset" retinal diseases, which impact visual function at the lever of OS:RPE. In additional to biological breakthrough, this will be an ethical breakthrough, enabling us to avoid using animals excessively for studying development and treating diseases.

AUTHOR CONTRIBUTIONS

RS conceptualized the review, generated the data, and wrote the manuscript. IN conceptualized the review, processed the data, and wrote the manuscript.

FUNDING

The work was supported by National Eye Institute (NIH) Grants 5R44EY027654-01, 5R44EY027654-02, and 3 R44 EY 027654-02 S1.

REFERENCES

Aasen, D. M., and Vergara, M. N. (2020). New drug discovery paradigms for retinal diseases: a focus on retinal organoids. *J. Ocul. Pharmacol. Ther.* 36, 18–24. doi: 10.1089/jop.2018.0140

Abramov, I., Gordon, J., Hendrickson, A., Hainline, L., Dobson, V., and LaBossiere, E. (1982). The retina of the newborn human infant. *Science* 217, 265–267. doi: 10.1126/science.6178160

Achberger, K., Probst, C., Haderspeck, J., Bolz, S., Rogal, J., Chuchuy, J., et al. (2019). Merging organoid and organ-on-a-chip technology to generate complex multi-layer tissue models in a human retina-on-a-chip platform. *Elife* 8:e46188.

Acott, T. S., Kelley, M. J., Keller, K. E., Vranka, J. A., Abu-Hassan, D. W., Li, X., et al. (2014). Intraocular pressure homeostasis: maintaining balance in a high-pressure environment. *J. Ocul. Pharmacol. Ther.* 30, 94–101. doi: 10.1089/jop.2013.0185

Adler, R., and Canto-Soler, M. V. (2007). Molecular mechanisms of optic vesicle development: complexities, ambiguities and controversies. *Dev. Biol.* 305, 1–13. doi: 10.1016/j.ydbio.2007.01.045

Akhtar, T., Xie, H., Khan, M. I., Zhao, H., Bao, J., Zhang, M., et al. (2019). Accelerated photoreceptor differentiation of hiPSC-derived retinal organoids by contact co-culture with retinal pigment epithelium. *Stem Cell Res.* 39:101491. doi: 10.1016/j.scr.2019.101491

Akiyama, G., Sakai, T., Kuno, N., Kimura, E., Okano, K., Kohno, H., et al. (2012). Photoreceptor rescue of pigment epithelium-derived factor-impregnated nanoparticles in Royal College of Surgeons rats. *Mol. Vis.* 18, 3079–3086.

Androutsellis-Theotokis, A., Leker, R. R., Soldner, F., Hoeppner, D. J., Ravin, R., Poser, S. W., et al. (2006). Notch signalling regulates stem cell numbers in vitro and in vivo. *Nature* 442, 823–826. doi: 10.1038/nature04940

Arroba, A. I., Wallace, D., Mackey, A., de la Rosa, E. J., and Cotter, T. G. (2009). IGF-I maintains calpastatin expression and attenuates apoptosis in several models of photoreceptor cell death. *Eur. J. Neurosci.* 30, 975–986. doi: 10.1111/j.1460-9568.2009.06902.x

Arshavsky, V. Y., and Burns, M. E. (2012). Photoreceptor signaling: supporting vision across a wide range of light intensities. *J. Biol. Chem.* 287, 1620–1626. doi: 10.1074/jbc.r111.305243

Assawachananont, J., Mandai, M., Okamoto, S., Yamada, C., Eiraku, M., Yonemura, S., et al. (2014). Transplantation of embryonic and induced pluripotent stem cell-derived 3D retinal sheets into retinal degenerative mice. *Stem Cell Rep.* 2, 662–674. doi: 10.1016/j.stemcr.2014.03.011

Baehr, W., and Palczewski, K. (2007). Guanylate cyclase-activating proteins and retina disease. *Subcell. Biochem.* 45, 71–91. doi: 10.1007/978-1-4020-6191-2_4

Bangs, F., and Anderson, K. V. (2017). primary cilia and mammalian Hedgehog signaling. *Cold Spring Harb. Perspect. Biol.* 9:a028175. doi: 10.1101/cshperspect.a028175

Banin, E., Obolensky, A., Idelson, M., Hemo, I., Reinhardtz, E., Pikarsky, E., et al. (2006). Retinal incorporation and differentiation of neural precursors derived from human embryonic stem cells. *Stem Cells* 24, 246–257. doi: 10.1634/stemcells.2005-0009

Bardy, C., van den Hurk, M., Eames, T., Marchand, C., Hernandez, R. V., Kellogg, M., et al. (2015). Neuronal medium that supports basic synaptic functions and activity of human neurons in vitro. *Proc. Natl. Acad. Sci. U.S.A.* 112, E2725–E2734.

Barnstable, C. J., and Drager, U. C. (1984). Thy-1 antigen: a ganglion cell specific marker in rodent retina. *Neuroscience* 11, 847–855. doi: 10.1016/0306-4522(84)90195-7

Bassett, E. A., and Wallace, V. A. (2012). Cell fate determination in the vertebrate retina. *Trends Neurosci.* 35, 565–573. doi: 10.1016/j.tins.2012.05.004

Bazan, N. G. (2007). Homeostatic regulation of photoreceptor cell integrity: significance of the potent mediator neuroprotectin D1 biosynthesized from docosahexaenoic acid: the Proctor Lecture. *Invest. Ophthalmol. Vis. Sci.* 48, 4866–4881; biography 4864–4865.

Benowitz, L. I., He, Z., and Goldberg, J. L. (2017). Reaching the brain: advances in optic nerve regeneration. *Exp. Neurol.* 287, 365–373. doi: 10.1016/j.expneurol.2015.12.015

Bharti, K., Gasper, M., Ou, J., Brucato, M., Clore-Gronenborn, K., Pickel, J., et al. (2012). A regulatory loop involving PAX6, MITF, and WNT signaling controls retinal pigment epithelium development. *PLoS Genet.* 8:e1002757. doi: 10.1371/journal.pgen.1002757

Bharti, K., Miller, S. S., and Arnheiter, H. (2011). The new paradigm: retinal pigment epithelium cells generated from embryonic or induced pluripotent stem cells. *Pigment Cell Melanoma Res.* 24, 21–34. doi: 10.1111/j.1755-148x.2010.00772.x

Bharti, K., Nguyen, M. T., Skuntz, S., Bertuzzi, S., and Arnheiter, H. (2006). The other pigment cell: specification and development of the pigmented epithelium of the vertebrate eye. *Pigment Cell Res.* 19, 380–394. doi: 10.1111/j.1600-0749.2006.00318.x

Bird, A. C., Bressler, N. M., Bressler, S. B., Chisholm, I. H., Coscas, G., Davis, M. D., et al. (1995). An international classification and grading system for age-related maculopathy and age-related macular degeneration. The International ARM Epidemiological Study Group. *Surv. Ophthalmol.* 39, 367–374. doi: 10.1016/s0039-6257(05)80092-x

Bonilha, V. L., Rayborn, M. E., Bhattacharya, S. K., Gu, X., Crabb, J. S., Crabb, J. W., et al. (2006). The retinal pigment epithelium apical microvilli and retinal function. *Adv. Exp. Med. Biol.* 572, 519–524. doi: 10.1007/0-387-32442-9_72

Brooks, M. J., Chen, H. Y., Kelley, R. A., Mondal, A. K., Nagashima, K., De Val, N., et al. (2019). Improved retinal organoid differentiation by modulating signaling pathways revealed by comparative transcriptome analyses with development in vivo. *Stem Cell Rep.* 13, 891–905. doi: 10.1016/j.stemcr.2019.09.009

Burnett, J. B., Lupu, F. I., and Eggenschwiler, J. T. (2017). Proper ciliary assembly is critical for restricting Hedgehog signaling during early eye development in mice. *Dev. Biol.* 430, 32–40. doi: 10.1016/j.ydbio.2017.07.012

Cai, Z., Feng, G. S., and Zhang, X. (2010). Temporal requirement of the protein tyrosine phosphatase Shp2 in establishing the neuronal fate in early retinal development. *J. Neurosci.* 30, 4110–4119. doi: 10.1523/jneurosci.4364-09.2010

Capowski, E. E., Samimi, K., Mayerl, S. J., Phillips, M. J., Pinilla, I., Howden, S. E., et al. (2019). Reproducibility and staging of 3D human retinal organoids across multiple pluripotent stem cell lines. *Development* 146:dev171686. doi: 10.1242/dev.171686

Capowski, E. E., Wright, L. S., Liang, K., Phillips, M. J., Wallace, K., Petelinsek, A., et al. (2016). Regulation of WNT signaling by VSX2 during optic vesicle patterning in human induced pluripotent stem cells. *Stem Cells* 34, 2625–2634. doi: 10.1002/stem.2414

Carr, A. J., Vugler, A., Lawrence, J., Chen, L. L., Ahmado, A., Chen, F. K., et al. (2009). Molecular characterization and functional analysis of phagocytosis by human embryonic stem cell-derived RPE cells using a novel human retinal assay. *Mol. Vis.* 15, 283–295.

Cayouette, M., Poggi, L., and Harris, W. A. (2006). Lineage in the vertebrate retina. *Trends Neurosci.* 29, 563–570. doi: 10.1016/j.tins.2006.08.003

Chang, B. (2013). Mouse models for studies of retinal degeneration and diseases. *Methods Mol. Biol.* 935, 27–39. doi: 10.1007/978-1-62703-080-9_2

Chang, B., Hawes, N. L., Hurd, R. E., Davisson, M. T., Nusinowitz, S., and Heckenlively, J. R. (2002). Retinal degeneration mutants in the mouse. *Vis. Res* 42, 517–525. doi: 10.1016/s0042-6989(01)00146-8

Chang, B., Khanna, H., Hawes, N., Jimeno, D., He, S., Lillo, C., et al. (2006). In-frame deletion in a novel centrosomal/ciliary protein CEP290/NPHP6 perturbs its interaction with RPGR and results in early-onset retinal degeneration in the rd16 mouse. *Hum. Mol. Genet.* 15, 1847–1857. doi: 10.1093/hmg/ddl107

Chao, J. R., Lamba, D. A., Klesert, T. R., Torre, A., Hoshino, A., Taylor, R. J., et al. (2017). Transplantation of human embryonic stem cell-derived retinal cells into the subretinal space of a non-human primate. *Transl. Vis. Sci. Technol.* 6:4. doi: 10.1167/tvst.6.3.4

Chen, H. Y., Welby, E., Li, T., and Swaroop, A. (2019). Retinal disease in ciliopathies: recent advances with a focus on stem cell-based therapies. *Transl. Sci. Rare Dis.* 4, 97–115. doi: 10.3233/trd-190038

Chen, M., Tian, S., Glasgow, N. G., Gibson, G., Yang, X., Shiber, C. E., et al. (2015). Lgr5(+) amacrine cells possess regenerative potential in the retina of adult mice. *Aging Cell* 14, 635–643. doi: 10.1111/acel.12346

Chen, S., Li, H., Gaudenz, K., Paulson, A., Guo, F., Trimble, R., et al. (2013). Defective FGF signaling causes coloboma formation and disrupts retinal neurogenesis. *Cell Res.* 23, 254–273. doi: 10.1038/cr.2012.150

Chen, Y., Yang, J., Geng, H., Li, L., Li, J., Cheng, B., et al. (2019). Photoreceptor degeneration in microphthalmia (Mitf) mice: partial rescue by pigment epithelium-derived factor. *Dis. Model. Mech.* 12:dmm035642. doi: 10.1242/dmm.035642

Cheng, H., Aleman, T. S., Cideciyan, A. V., Khanna, R., Jacobson, S. G., and Swaroop, A. (2006). In vivo function of the orphan nuclear receptor NR2E3 in establishing photoreceptor identity during mammalian retinal development. *Hum. Mol. Genet.* 15, 2588–2602. doi: 10.1093/hmg/ddl185

Chuderland, D., Ben-Ami, I., Kaplan-Kraicer, R., Grossman, H., Komsky, A., Satchi-Fainaro, R., et al. (2013). Hormonal regulation of pigment epithelium-derived factor (PEDF) in granulosa cells. *Mol. Hum. Reprod.* 19, 72–81. doi: 10.1093/molehr/gas046

Clevers, H., Loh, K. M., and Nusse, R. (2014). Stem cell signaling. An integral program for tissue renewal and regeneration: Wnt signaling and stem cell control. *Science* 346:1248012. doi: 10.1126/science.1248012

Close, J. L., Gumuscu, B., and Reh, T. A. (2005). Retinal neurons regulate proliferation of postnatal progenitors and Muller glia in the rat retina via TGF beta signaling. *Development* 132, 3015–3026. doi: 10.1242/dev.01882

Comitato, A., Subramanian, P., Turchiano, G., Montanari, M., Becerra, S. P., and Marigo, V. (2018). Pigment epithelium-derived factor hinders photoreceptor cell death by reducing intracellular calcium in the degenerating retina. *Cell Death Dis.* 9:560.

Cowan, C. S., Renner, M., Gross-Scherf, B., Goldblum, D., Munz, M., Krol, J., et al. (2019). Cell types of the human retina and its organoids at single-cell resolution: developmental convergence, transcriptomic identity, and disease map. *bioRxiv* [Preprint]. doi: 10.1101/703348 bioRxiv: 703348,

Crair, M. C., and Mason, C. A. (2016). Reconnecting Eye to brain. *J. Neurosci.* 36, 10707–10722. doi: 10.1523/jneurosci.1711-16.2016

Cruz-Martin, A., El-Danaf, R. N., Osakada, F., Sriram, B., Dhande, O. S., Nguyen, P. L., et al. (2014). A dedicated circuit links direction-selective retinal ganglion cells to the primary visual cortex. *Nature* 507, 358–361. doi: 10.1038/nature12989

Cuzzani, O. (2018). Cell therapy-based approaches to treatment of AMD. An update on current research. *Retin. Phys.* 15, 44–48.

Cvekl, A., and Wang, W. L. (2009). Retinoic acid signaling in mammalian eye development. *Exp. Eye Res.* 89, 280–291. doi: 10.1016/j.exer.2009.04.012

Dakubo, G. D., Mazerolle, C., Furimsky, M., Yu, C., St-Jacques, B., McMahon, A. P., et al. (2008). Indian hedgehog signaling from endothelial cells is required for sclera and retinal pigment epithelium development in the mouse eye. *Dev. Biol.* 320, 242–255. doi: 10.1016/j.ydbio.2008.05.528

Dakubo, G. D., Wang, Y. P., Mazerolle, C., Campsall, K., McMahon, A. P., and Wallace, V. A. (2003). Retinal ganglion cell-derived sonic hedgehog signaling is required for optic disc and stalk neuroepithelial cell development. *Development* 130, 2967–2980. doi: 10.1242/dev.00515

Das, A. V., Bhattacharya, S., Zhao, X., Hegde, G., Mallya, K., Eudy, J. D., et al. (2008). The canonical Wnt pathway regulates retinal stem cells/progenitors in concert with Notch signaling. *Dev. Neurosci.* 30, 389–409. doi: 10.1159/000178017

Dawson, D. W., Volpert, O. V., Gillis, P., Crawford, S. E., Xu, H., Benedict, W., et al. (1999). Pigment epithelium-derived factor: a potent inhibitor of angiogenesis. *Science* 285, 245–248. doi: 10.1126/science.285.5425.245

de Lau, W., Peng, W. C., Gros, P., and Clevers, H. (2014). The R-spondin/Lgr5/Rnf43 module: regulator of Wnt signal strength. *Genes Dev.* 28, 305–316. doi: 10.1101/gad.235473.113

de Lima, S., Koriyama, Y., Kurimoto, T., Oliveira, J. T., Yin, Y., Li, Y., et al. (2012). Full-length axon regeneration in the adult mouse optic nerve and partial recovery of simple visual behaviors. *Proc. Natl. Acad. Sci. U.S.A.* 109, 9149–9154. doi: 10.1073/pnas.1119449109

Deng, W. L., Gao, M. L., Lei, X. L., Lv, J. N., Zhao, H., He, K. W., et al. (2018). Gene correction reverses ciliopathy and photoreceptor loss in iPSC-derived retinal organoids from retinitis pigmentosa patients. *Stem Cell Rep.* 10, 1267–1281. doi: 10.1016/j.stemcr.2018.02.003

Dhande, O. S., and Huberman, A. D. (2014). Retinal ganglion cell maps in the brain: implications for visual processing. *Curr. Opin. Neurobiol.* 24, 133–142. doi: 10.1016/j.conb.2013.08.006

Di Lauro, S., Rodriguez-Crespo, D., Gayoso, M. J., Garcia-Gutierrez, M. T., Pastor, J. C., Srivastava, G. K., et al. (2016). A novel coculture model of porcine central neuroretina explants and retinal pigment epithelium cells. *Mol. Vis.* 22, 243–253.

Ding, X., Patel, M., and Chan, C. C. (2009). Molecular pathology of age-related macular degeneration. *Prog. Retin. Eye Res.* 28, 1–18.

DiStefano, T., Chen, H. Y., Panebianco, C., Kaya, K. D., Brooks, M. J., Gieser, L., et al. (2018). Accelerated and improved differentiation of retinal organoids from pluripotent stem cells in rotating-wall vessel bioreactors. *Stem Cell Rep.* 10, 300–313. doi: 10.1016/j.stemcr.2017.11.001

Dorgau, B., Felemban, M., Hilgen, G., Kiening, M., Zerti, D., Hunt, N. C., et al. (2019). Decellularised extracellular matrix-derived peptides from neural retina and retinal pigment epithelium enhance the expression of synaptic markers and light responsiveness of human pluripotent stem cell derived retinal organoids. *Biomaterials* 199, 63–75. doi: 10.1016/j.biomaterials.2019.01.028

Duester, G. (2000). Families of retinoid dehydrogenases regulating vitamin A function: production of visual pigment and retinoic acid. *Eur. J. Biochem.* 267, 4315–4324. doi: 10.1046/j.1432-1327.2000.01497.x

Duester, G. (2009). Keeping an eye on retinoic acid signaling during eye development. *Chem. Biol. Interact.* 178, 178–181. doi: 10.1016/j.cbi.2008.09.004

Ebrahimi, V., Vojoudi, E., Fazel, A., and Ebrahimzadeh-Bideskan, A. (2014). Histochemical study of retinal photoreceptors development during pre- and postnatal period and their association with retinal pigment epithelium. *Iran J. Basic Med. Sci.* 17, 483–489.

Erskine, L., and Herrera, E. (2014). Connecting the retina to the brain. *ASN Neuro* 6:1759091414562107.

Euler, T., and Wassle, H. (1995). Immunocytochemical identification of cone bipolar cells in the rat retina. *J. Comp. Neurol.* 361, 461–478. doi: 10.1002/cne.903610310

Fan, J., Rohrer, B., Moiseyev, G., Ma, J.-X., and Crouch, R. K. (2003). Isorhodopsin rather than rhodopsin mediates rod function in RPE65 knock-out mice. *Proc. Natl. Acad. Sci. U.S.A.* 100, 13662–13667. doi: 10.1073/pnas.2234461100

Felemban, M., Dorgau, B., Hunt, N. C., Hallam, D., Zerti, D., Bauer, R., et al. (2018). Extracellular matrix component expression in human pluripotent stem cell-derived retinal organoids recapitulates retinogenesis in vivo and reveals an important role for IMPG1 and CD44 in the development of photoreceptors and interphotoreceptor matrix. *Acta Biomater.* 74, 207–221. doi: 10.1016/j.actbio.2018.05.023

Finklea, K., Jansen, D. J., Johnson, J. A., Panangala, S. V., Redhead, C. S., Reyes-Akinbileje, B., et al. (2015). *Fetal Tissue Research: Frequently Asked Questions*. Washington, DC: Congressional Research Service.

Finnemann, S. C., and Chang, Y. (2008). "Photoreceptor—RPE interactions," in *Visual Transduction and Non-Visual Light Perception*, eds J. Tombran-Tink and C. J. Barnstable (Totowa, NJ: Humana Press), 67–86. doi: 10.1007/978-1-59745-374-5_4

Fisher, S. K., and Lewis, G. P. (2006). "Chapter 115 – Cellular effects of detachment and reattachment on the neural retina and the retinal pigment epithelium," in *Retina*, 4th Edn, eds S. J. Ryan, D. R. Hinton, A. P. Schachat, and C. P. Wilkinson (Edinburgh: Mosby), 1991–2012. doi: 10.1016/b978-0-323-02598-0.50121-x

Fisher, S. K., and Lewis, G. P. (2010). "Chapter 71 – Retinal detachment," in *Ocular Disease*, eds L. A. Levin and D. M. Albert (Edinburgh: W.B. Saunders), 554–561.

Fligor, C. M., Langer, K. B., Sridhar, A., Ren, Y., Shields, P. K., Edler, M. C., et al. (2018). Three-dimensional retinal organoids facilitate the investigation of retinal ganglion cell development, organization and neurite outgrowth from human pluripotent stem cells. *Sci. Rep.* 8:14520.

Fontaine, V., Kinkl, N., Sahel, J., Dreyfus, H., and Hicks, D. (1998). Survival of purified rat photoreceptors in vitro is stimulated directly by fibroblast growth factor-2. *J. Neurosci.* 18, 9662–9672. doi: 10.1523/jneurosci.18-23-09662.1998

Forrester, J. V., Dick, A. D., McMenamin, P. G., Roberts, F., and Pearlman, E. (2016). "Chapter 2 – Embryology and early development of the eye and adnexa," in *The Eye*, 4th Edn, eds J. V. Forrester, A. D. Dick, P. G. McMenamin, F. Roberts, and E. Pearlman (Philadelphia, PA: W.B. Saunders), 103–129.e8. doi: 10.1016/b978-0-7020-5554-6.00002-2

Friedman, D. S., O'Colmain, B. J., Munoz, B., Tomany, S. C., McCarty, C., de Jong, P. T., et al. (2004). Prevalence of age-related macular degeneration in the United States. *Arch. Ophthalmol.* 122, 564–572.

Fuhrmann, S. (2008). Wnt signaling in eye organogenesis. *Organogenesis* 4, 60–67. doi: 10.4161/org.4.2.5850

Fuhrmann, S. (2010). Eye morphogenesis and patterning of the optic vesicle. *Curr. Top. Dev. Biol.* 93, 61–84. doi: 10.1016/b978-0-12-385044-7.00003-5

Fuhrmann, S., Zou, C., and Levine, E. M. (2014). Retinal pigment epithelium development, plasticity, and tissue homeostasis. *Exp. Eye Res.* 123, 141–150. doi: 10.1016/j.exer.2013.09.003

Fujimura, N. (2016). WNT/β-catenin signaling in vertebrate eye development. *Front. Cell Dev. Biol.* 4:138. doi: 10.3389/fcell.2016.00138

Furukawa, T., Mukherjee, S., Bao, Z. Z., Morrow, E. M., and Cepko, C. L. (2000). rax, Hes1, and notch1 promote the formation of Muller glia by postnatal retinal progenitor cells. *Neuron* 26, 383–394. doi: 10.1016/s0896-6273(00)81171-x

Gagliardi, G., Ben M'Barek, K., Chaffiol, A., Slembrouck-Brec, A., Conart, J. B., Nanteau, C., et al. (2018). Characterization and transplantation of CD73-positive photoreceptors isolated from human iPSC-derived retinal organoids. *Stem Cell Rep.* 11, 665–680. doi: 10.1016/j.stemcr.2018.07.005

Gamm, D. M., Clark, E., Capowski, E. E., and Singh, R. (2019). The role of FGF9 in the production of neural retina and RPE in a pluripotent stem cell model of early human retinal development. *Am. J. Ophthalmol.* 206, 113–131. doi: 10.1016/j.ajo.2019.04.033

Garcia, G. III, Raleigh, D. R., and Reiter, J. F. (2018). How the ciliary membrane is organized inside-out to communicate outside-in. *Curr. Biol.* 28, R421–R434.

Garita-Hernandez, M., Lampic, M., Chaffiol, A., Guibbal, L., Routet, F., Santos-Ferreira, T., et al. (2019). Restoration of visual function by transplantation of optogenetically engineered photoreceptors. *Nat. Commun.* 10:4524.

Gearhart, P. M., Gearhart, C., Thompson, D. A., and Petersen-Jones, S. M. (2010). Improvement of visual performance with intravitreal administration of 9-cis-retinal in Rpe65-mutant dogs. *Arch. Ophthalmol.* 128, 1442–1448.

Gearhart, P. M., Gearhart, C. C., and Petersen-Jones, S. M. (2008). A novel method for objective vision testing in canine models of inherited retinal disease. *Invest. Ophthalmol. Vis. Sci.* 49, 3568–3576.

Geng, Z., Walsh, P. J., Truong, V., Hill, C., Ebeling, M., Kapphahn, R. J., et al. (2017). Generation of retinal pigmented epithelium from iPSCs derived from the conjunctiva of donors with and without age related macular degeneration. *PLoS One* 12:e0173575. doi: 10.1371/journal.pone.0173575

German, O. L., Buzzi, E., Rotstein, N. P., Rodriguez-Boulan, E., and Politi, L. E. (2008). Retinal pigment epithelial cells promote spatial reorganization and differentiation of retina photoreceptors. *J. Neurosci. Res.* 86, 3503–3514. doi: 10.1002/jnr.21813

Gerrelli, D., Lisgo, S., Copp, A. J., and Lindsay, S. (2015). Enabling research with human embryonic and fetal tissue resources. *Development* 142, 3073–3076. doi: 10.1242/dev.122820

Gilliam, J. C., Chang, J. T., Sandoval, I. M., Zhang, Y., Li, T., Pittler, S. J., et al. (2012). Three-dimensional architecture of the rod sensory cilium and its disruption in retinal neurodegeneration. *Cell* 151, 1029–1041. doi: 10.1016/j.cell.2012.10.038

Goldberg, A. F., Moritz, O. L., and Williams, D. S. (2016). Molecular basis for photoreceptor outer segment architecture. *Prog. Retin. Eye Res.* 55, 52–81. doi: 10.1016/j.preteyeres.2016.05.003

Gonzalez-Cordero, A., Kruczek, K., Naeem, A., Fernando, M., Kloc, M., Ribeiro, J., et al. (2017). Recapitulation of human retinal development from human pluripotent stem cells generates transplantable populations of cone photoreceptors. *Stem Cell Rep.* 9, 820–837. doi: 10.1016/j.stemcr.2017.07.022

Gopalakrishnan, J. (2019). The emergence of stem cell-based brain organoids: trends and challenges. *Bioessays* 41:e1900011.

Grebenyuk, S., and Ranga, A. (2019). Engineering organoid vascularization. *Front. Bioeng. Biotechnol.* 7:39. doi: 10.3389/fbioe.2019.00039

Greenlee, H., Hecker, l, Akimoto, M., and Swaroop, A. (2006). Expression of the Igf–1 receptor in developing photoreceptors of the mouse retina and the importance of Igf–1 signaling during photoreceptor differentiation. *Invest. Ophthalmol. Vis. Sci.* 47:4190.

Gregerson, D. S., Lew, K. L., McPherson, S. W., Heuss, N. D., and Ferrington, D. A. (2006). RPE cells resist bystander killing by CTLs, but are highly susceptible to antigen-dependent CTL killing. *Invest. Ophthalmol. Vis. Sci.* 47, 5385–5394.

Gu, Q., Tomaskovic-Crook, E., Wallace, G. G., and Crook, J. M. (2018). Engineering human neural tissue by 3D bioprinting. *Methods Mol. Biol.* 1758, 129–138. doi: 10.1007/978-1-4939-7741-3_10

Guo, Y., Wang, P., Ma, J. H., Cui, Z., Yu, Q., Liu, S., et al. (2019). Modeling retinitis pigmentosa: retinal organoids generated from the iPSCs of a patient with the USH2A mutation show early developmental abnormalities. *Front. Cell. Neurosci.* 13:361. doi: 10.3389/fncel.2019.00361

Ha, T., Moon, K. H., Dai, L., Hatakeyama, J., Yoon, K., Park, H. S., et al. (2017). The retinal pigment epithelium is a notch signaling niche in the mouse retina. *Cell Rep.* 19, 351–363. doi: 10.1016/j.celrep.2017.03.040

Haderspeck, J. C., Chuchuy, J., Kustermann, S., Liebau, S., and Loskill, P. (2019). Organ-on-a-chip technologies that can transform ophthalmic drug discovery and disease modeling. *Expert Opin. Drug Discov.* 14, 47–57. doi: 10.1080/17460441.2019.1551873

Hallam, D., Hilgen, G., Dorgau, B., Zhu, L., Yu, M., Bojic, S., et al. (2018). Human-induced pluripotent stem cells generate light responsive retinal organoids with variable and nutrient-dependent efficiency. *Stem Cells* 36, 1535–1551. doi: 10.1002/stem.2883

Hambright, D., Park, K. Y., Brooks, M., McKay, R., Swaroop, A., and Nasonkin, I. O. (2012). Long-term survival and differentiation of retinal neurons derived from human embryonic stem cell lines in un-immunosuppressed mouse retina. *Mol. Vis.* 18, 920–936.

Hamel, C. P. (2007). Cone rod dystrophies. *Orphanet J. Rare Dis.* 2:7.

Hasegawa, T., McLeod, D. S., Prow, T., Merges, C., Grebe, R., and Lutty, G. A. (2008). Vascular precursors in developing human retina. *Invest. Ophthalmol. Vis. Sci.* 49, 2178–2192.

Heavner, W., and Pevny, L. (2012). Eye development and retinogenesis. *Cold Spring Harb. Perspect. Biol.* 4:a008391. doi: 10.1101/cshperspect.a008391

Heber-Katz, E. (2017). Oxygen, metabolism, and regeneration: lessons from mice. *Trends Mol. Med.* 23, 1024–1036. doi: 10.1016/j.molmed.2017.08.008

Hendrickson, A. (2016). Development of retinal layers in prenatal human retina. *Am. J. Ophthalmol.* 161, 29–35.e1. doi: 10.1016/j.ajo.2015.09.023

Hendrickson, A., Bumsted-O'Brien, K., Natoli, R., Ramamurthy, V., Possin, D., and Provis, J. (2008). Rod photoreceptor differentiation in fetal and infant human retina. *Exp. Eye Res.* 87, 415–426. doi: 10.1016/j.exer.2008.07.016

Hendrickson, A., Djajadi, H., Erickson, A., and Possin, D. (2006). Development of the human retina in the absence of ganglion cells. *Exp. Eye Res.* 83, 920–931. doi: 10.1016/j.exer.2006.04.017

Ho, T. C., Chen, S. L., Shih, S. C., Chang, S. J., Yang, S. L., Hsieh, J. W., et al. (2011). Pigment epithelium-derived factor (PEDF) promotes tumor cell death by inducing macrophage membrane tumor necrosis factor-related apoptosis-inducing ligand (TRAIL). *J. Biol. Chem.* 286, 35943–35954. doi: 10.1074/jbc.m111.266064

Hochmann, S., Kaslin, J., Hans, S., Weber, A., Machate, A., Geffarth, M., et al. (2012). Fgf signaling is required for photoreceptor maintenance in the adult zebrafish retina. *PLoS One* 7:e30365. doi: 10.1371/journal.pone.0030365

Holmes, D. (2018a). Reconstructing the retina. *Nature* 561, S2–S3.

Holmes, D. (2018b). Retinal repair: visions of the future. *Nature* 561:S1.

Horsford, D. J., Nguyen, M. T., Sellar, G. C., Kothary, R., Arnheiter, H., and McInnes, R. R. (2005). Chx10 repression of Mitf is required for the maintenance of mammalian neuroretinal identity. *Development* 132, 177–187. doi: 10.1242/dev.01571

Hoshino, A., Ratnapriya, R., Brooks, M. J., Chaitankar, V., Wilken, M. S., Zhang, C., et al. (2017). Molecular anatomy of the developing human retina. *Dev. Cell* 43, 763–779.e4.

Hsu, Y. T., and Molday, R. S. (1993). Modulation of the cGMP-gated channel of rod photoreceptor cells by calmodulin. *Nature* 361, 76–79. doi: 10.1038/361076a0

Huang, K. C., Wang, M. L., Chen, S. J., Kuo, J. C., Wang, W. J., Nhi Nguyen, P. N., et al. (2019). Morphological and molecular defects in human three-dimensional retinal organoid model of X-linked juvenile retinoschisis. *Stem Cell Rep.* 13, 906–923. doi: 10.1016/j.stemcr.2019.09.010

Huang, W., Fileta, J., Guo, Y., and Grosskreutz, C. L. (2006). Downregulation of Thy1 in retinal ganglion cells in experimental glaucoma. *Curr. Eye Res.* 31, 265–271. doi: 10.1080/02713680500545671

Hughes, J. M., Groot, A. J., van der Groep, P., Sersansie, R., Vooijs, M., van Diest, P. J., et al. (2010). Active HIF-1 in the normal human retina. *J. Histochem. Cytochem.* 58, 247–254. doi: 10.1369/jhc.2009.953786

Hughes, S., Yang, H., and Chan-Ling, T. (2000). Vascularization of the human fetal retina: roles of vasculogenesis and angiogenesis. *Invest. Ophthalmol. Vis. Sci.* 41, 1217–1228.

Hunt, D. M., and Peichl, L. (2014). S cones: evolution, retinal distribution, development, and spectral sensitivity. *Vis. Neurosci.* 31, 115–138. doi: 10.1017/s0952523813000242

Idelson, M., Alper, R., Obolensky, A., Ben-Shushan, E., Hemo, I., Yachimovich-Cohen, N., et al. (2009). Directed differentiation of human embryonic stem cells into functional retinal pigment epithelium cells. *Cell Stem Cell* 5, 396–408.

Idelson, M., Alper, R., Obolensky, A., Yachimovich-Cohen, N., Rachmilewitz, J., Ejzenberg, A., et al. (2018). Immunological properties of human embryonic stem cell-derived retinal pigment epithelial cells. *Stem Cell Rep.* 11, 681–695. doi: 10.1016/j.stemcr.2018.07.009

Ishikawa, M., Sawada, Y., and Yoshitomi, T. (2015). Structure and function of the interphotoreceptor matrix surrounding retinal photoreceptor cells. *Exp. Eye Res.* 133, 3–18. doi: 10.1016/j.exer.2015.02.017

Jablonski, M. M., Tombran-Tink, J., Mrazek, D. A., and Iannaccone, A. (2000). Pigment epithelium-derived factor supports normal development of photoreceptor neurons and opsin expression after retinal pigment epithelium removal. *J. Neurosci.* 20, 7149–7157. doi: 10.1523/jneurosci.20-19-07149.2000

Jha, B. S., and Bharti, K. (2015). Regenerating retinal pigment epithelial cells to cure blindness: a road towards personalized artificial tissue. *Curr. Stem Cell Rep.* 1, 79–91. doi: 10.1007/s40778-015-0014-4

Jiang, N., Zou, C., Zhu, Y., Luo, Y., Chen, L., Lei, Y., et al. (2020). HIF-1&-regulated miR-1275 maintains stem cell-like phenotypes and promotes the progression of LUAD by simultaneously activating Wnt/β-catenin and Notch signaling. *Theranostics* 10, 2553–2570.

Jin, M., Li, S., Nusinowitz, S., Lloyd, M., Hu, J., Radu, R. A., et al. (2009). The role of interphotoreceptor retinoid-binding protein on the translocation of visual retinoids and function of cone photoreceptors. *J. Neurosci.* 29, 1486–1495. doi: 10.1523/jneurosci.3882-08.2009

Jin, Z. B., Okamoto, S., Osakada, F., Homma, K., Assawachananont, J., Hirami, Y., et al. (2011). Modeling retinal degeneration using patient-specific induced pluripotent stem cells. *PLoS One* 6:e17084. doi: 10.1371/journal.pone.0017084

Jin, Z. B., Okamoto, S., Xiang, P., and Takahashi, M. (2012). Integration-free induced pluripotent stem cells derived from retinitis pigmentosa patient for disease modeling. *Stem Cells Transl. Med.* 1, 503–509. doi: 10.5966/sctm.2012-0005

Johnson, E. C., Guo, Y., Cepurna, W. O., and Morrison, J. C. (2009). Neurotrophin roles in retinal ganglion cell survival: lessons from rat glaucoma models. *Exp. Eye Res.* 88, 808–815. doi: 10.1016/j.exer.2009.02.004

Jukic, A. M., Baird, D. D., Weinberg, C. R., McConnaughey, D. R., and Wilcox, A. J. (2013). Length of human pregnancy and contributors to its natural variation. *Hum. Reproduc.* 28, 2848–2855. doi: 10.1093/humrep/det297

Kanemura, H., Go, M. J., Nishishita, N., Sakai, N., Kamao, H., Sato, Y., et al. (2013). Pigment epithelium-derived factor secreted from retinal pigment epithelium facilitates apoptotic cell death of iPSC. *Sci. Rep.* 3:2334.

Kaplan, H. J., Wang, W., and Dean, D. C. (2017). Restoration of cone photoreceptor function in retinitis pigmentosa. *Transl. Vis. Sci. Technol.* 6:5. doi: 10.1167/tvst.6.5.5

Kashani, A. H., Lebkowski, J. S., Rahhal, F. M., Avery, R. L., Salehi-Had, H., Dang, W., et al. (2018). A bioengineered retinal pigment epithelial monolayer for advanced, dry age-related macular degeneration. *Sci. Transl. Med.* 10:eaao4097.

Kefalov, V. J. (2012). Rod and cone visual pigments and phototransduction through pharmacological, genetic, and physiological approaches. *J. Biol. Chem.* 287, 1635–1641. doi: 10.1074/jbc.r111.303008

Kelley, R. A., Al-Ubaidi, M. R., and Naash, M. I. (2015). Retbindin is an extracellular riboflavin-binding protein found at the photoreceptor/retinal pigment epithelium interface. *J. Biol. Chem.* 290, 5041–5052. doi: 10.1074/jbc.m114.624189

Kessler, M., Hoffmann, K., Brinkmann, V., Thieck, O., Jackisch, S., Toelle, B., et al. (2015). The Notch and Wnt pathways regulate stemness and differentiation in human fallopian tube organoids. *Nat. Commun.* 6:8989.

Kevany, B. M., and Palczewski, K. (2010). Phagocytosis of retinal rod and cone photoreceptors. *Physiology (Bethesda)* 25, 8–15. doi: 10.1152/physiol.00038.2009

Khanna, H., Akimoto, M., Siffroi-Fernandez, S., Friedman, J. S., Hicks, D., and Swaroop, A. (2006). Retinoic acid regulates the expression of photoreceptor transcription factor NRL. *J. Biol. Chem.* 281, 27327–27334. doi: 10.1074/jbc.m605500200

Kinnebrew, M., Iverson, E. J., Patel, B. B., Pusapati, G. V., Kong, J. H., Johnson, K. A., et al. (2019). Cholesterol accessibility at the ciliary membrane controls hedgehog signaling. *Elife* 8:50051.

Kiser, P. D., Golczak, M., and Palczewski, K. (2014). Chemistry of the retinoid (visual) cycle. *Chem. Rev.* 114, 194–232. doi: 10.1021/cr400107q

Klein, R., Klein, B. E., and Linton, K. L. (1992). Prevalence of age-related maculopathy. The Beaver Dam Eye Study. *Ophthalmology* 99, 933–943.

Klein, R., Wang, Q., Klein, B. E., Moss, S. E., and Meuer, S. M. (1995). The relationship of age-related maculopathy, cataract, and glaucoma to visual acuity. *Invest. Ophthalmol. Vis. Sci.* 36, 182–191.

Kobayashi, M., Tokuda, K., Kobayashi, Y., Yamashiro, C., Uchi, S. H., Hatano, M., et al. (2019). Suppression of epithelial-mesenchymal transition in retinal pigment epithelial cells by an MRTF-a inhibitor. *Invest. Ophthalmol. Vis. Sci.* 60, 528–537.

Kolb, H. (1995). "Photoreceptors," in *Webvision: The Organization of the Retina and Visual System*, eds H. Kolb, E. Fernandez, and R. Nelson (Salt Lake City, UT: University of Utah Health Sciences Center).

Kolb, H. (2005). "Facts and figures concerning the human retina," in *Webvision: The Organization of the Retina and Visual System*, eds H. Kolb, E. Fernandez, and R. Nelson (Salt Lake City, UT: University of Utah Health Sciences Center).

Kong, J. H., Siebold, C., and Rohatgi, R. (2019). Biochemical mechanisms of vertebrate hedgehog signaling. *Development* 146:dev166892. doi: 10.1242/dev.166892

Kostic, C., and Arsenijevic, Y. (2016). Animal modelling for inherited central vision loss. *J. Pathol.* 238, 300–310. doi: 10.1002/path.4641

Kroeger, H., LaVail, M. M., and Lin, J. H. (2014). "Endoplasmic reticulum stress in vertebrate mutant rhodopsin models of retinal degeneration," in *Retinal Degenerative Diseases*, eds J. D. Ash, C. Grimm, J. G. Hollyfield, R. E. Anderson, M. M. LaVail, and C. Bowes Rickman (New York, NY: Springer New York), 585–592. doi: 10.1007/978-1-4614-3209-8_74

Kurimoto, T., Yin, Y., Omura, K., Gilbert, H. Y., Kim, D., Cen, L. P., et al. (2010). Long-distance axon regeneration in the mature optic nerve: contributions of oncomodulin, cAMP, and pten gene deletion. *J. Neurosci.* 30, 15654–15663. doi: 10.1523/jneurosci.4340-10.2010

Kuwahara, A., Ozone, C., Nakano, T., Saito, K., Eiraku, M., and Sasai, Y. (2015). Generation of a ciliary margin-like stem cell niche from self-organizing human retinal tissue. *Nat. Commun.* 6:6286.

Kuwahara, A., Yamasaki, S., Mandai, M., Watari, K., Matsushita, K., Fujiwara, M., et al. (2019). Preconditioning the initial state of feeder-free human pluripotent stem cells promotes self-formation of three-dimensional retinal tissue. *Sci. Rep.* 9:18936.

Laha, B., Stafford, B. K., and Huberman, A. D. (2017). Regenerating optic pathways from the eye to the brain. *Science* 356, 1031–1034. doi: 10.1126/science.aal5060

Lakowski, J., Welby, E., Budinger, D., Di Marco, F., Di Foggia, V., Bainbridge, J. W. B., et al. (2018). Isolation of human photoreceptor precursors via a cell surface marker panel from stem cell-derived retinal organoids and fetal retinae. *Stem Cells* 36, 709–722. doi: 10.1002/stem.2775

Lamba, D. A., Karl, M. O., Ware, C. B., and Reh, T. A. (2006). Efficient generation of retinal progenitor cells from human embryonic stem cells. *Proc. Natl. Acad. Sci. U.S.A.* 103, 12769–12774.

Lamba, D. A., McUsic, A., Hirata, R. K., Wang, P. R., Russell, D., and Reh, T. A. (2010). Generation, purification and transplantation of photoreceptors derived from human induced pluripotent stem cells. *PLoS One* 5:e8763. doi: 10.1371/journal.pone.0008763

Lancaster, M. A., and Huch, M. (2019). Disease modelling in human organoids. *Dis. Model. Mech.* 12:dmm039347. doi: 10.1242/dmm.039347

Lane, A., Jovanovic, K., Shortall, C., Ottaviani, D., Panes, A. B., Palfi, A., et al. (2020). Modelling and rescue of RP2 retinitis pigmentosa using iPSC derived retinal organoids. *bioRxiv* [Preprint]. doi: 10.1101/2020.01.28.923227

Lee, J. W., Ko, J., Ju, C., and Eltzschig, H. K. (2019). Hypoxia signaling in human diseases and therapeutic targets. *Exp. Mol. Med.* 51:68.

Levine, E. M., Roelink, H., Turner, J., and Reh, T. A. (1997). Sonic hedgehog promotes rod photoreceptor differentiation in mammalian retinal cells in vitro. *J. Neurosci.* 17, 6277–6288. doi: 10.1523/jneurosci.17-16-06277.1997

Li, J., Wang, S., Anderson, C., Zhao, F., Qin, Y., Wu, D., et al. (2016). Requirement of Smad4 from ocular surface ectoderm for retinal development. *PLoS One* 11:e0159639. doi: 10.1371/journal.pone.0159639

Li, L., Rao, K. N., Zheng-Le, Y., Hurd, T. W., Lillo, C., and Khanna, H. (2015). Loss of retinitis pigmentosa 2 (RP2) protein affects cone photoreceptor sensory cilium elongation in mice. *Cytoskeleton (Hoboken)* 72, 447–454. doi: 10.1002/cm.21255

Li, P., Kleinstiver, B. P., Leon, M. Y., Prew, M. S., Navarro-Gomez, D., Greenwald, S. H., et al. (2018). Allele-specific CRISPR/Cas9 genome editing of the single-base P23H mutation for rhodopsin associated dominant retinitis pigmentosa. *bioRxiv* [Preprint]. doi: 10.1101/197962

Lin, B., McLelland, B. T., Mathur, A., Aramant, R. B., and Seiler, M. J. (2018). Sheets of human retinal progenitor transplants improve vision in rats with severe retinal degeneration. *Exp. Eye Res.* 174, 13–28. doi: 10.1016/j.exer.2018.05.017

Lin, B., and Peng, E. B. (2013). Retinal ganglion cells are resistant to photoreceptor loss in retinal degeneration. *PLoS One* 8:e68084. doi: 10.1371/journal.pone.0068084

Littink, K. W., Stappers, P. T. Y., Riemslag, F. C. C., Talsma, H. E., van Genderen, M. M., Cremers, F. P. M., et al. (2018). Autosomal recessive NRL mutations in patients with enhanced S-Cone syndrome. *Genes (Basel)* 9:68. doi: 10.3390/genes9020068

Liu, H., Thurig, S., Mohamed, O., Dufort, D., and Wallace, V. A. (2006). Mapping canonical Wnt signaling in the developing and adult retina. *Invest. Ophthalmol. Vis. Sci.* 47, 5088–5097.

Liu, W., Jin, G., Long, C., Zhou, X., Tang, Y., Huang, S., et al. (2013). Blockage of notch signaling inhibits the migration and proliferation of retinal pigment epithelial cells. *ScientificWorldJournal* 2013:178708.

Liu, W., Lagutin, O., Swindell, E., Jamrich, M., and Oliver, G. (2010). Neuroretina specification in mouse embryos requires Six3-mediated suppression of Wnt8b in the anterior neural plate. *J. Clin. Invest.* 120, 3568–3577. doi: 10.1172/jci43219

Liu, X., Bulgakov, O. V., Darrow, K. N., Pawlyk, B., Adamian, M., Liberman, M. C., et al. (2007). Usherin is required for maintenance of retinal photoreceptors and normal development of cochlear hair cells. *Proc. Natl. Acad. Sci. U.S.A.* 104, 4413–4418. doi: 10.1073/pnas.0610950104

Livesey, F. J., and Cepko, C. L. (2001). Vertebrate neural cell-fate determination: lessons from the retina. *Nat. Rev. Neurosci.* 2, 109–118. doi: 10.1038/35053522

Locker, M., Agathocleous, M., Amato, M. A., Parain, K., Harris, W. A., and Perron, M. (2006). Hedgehog signaling and the retina: insights into the mechanisms controlling the proliferative properties of neural precursors. *Genes Dev.* 20, 3036–3048. doi: 10.1101/gad.391106

Lodato, S., and Arlotta, P. (2015). Generating neuronal diversity in the mammalian cerebral cortex. *Annu. Rev. Cell Dev. Biol.* 31, 699–720. doi: 10.1146/annurev-cellbio-100814-125353

Lofqvist, C., Willett, K. L., Aspegren, O., Smith, A. C., Aderman, C. M., Connor, K. M., et al. (2009). Quantification and localization of the IGF/insulin system expression in retinal blood vessels and neurons during oxygen-induced retinopathy in mice. *Invest. Ophthalmol. Vis. Sci.* 50, 1831–1837.

Lolley, R. N., Rong, H., and Craft, C. M. (1994). Linkage of photoreceptor degeneration by apoptosis with inherited defect in phototransduction. *Invest. Ophthalmol. Vis. Sci.* 35, 358–362.

Longbottom, R., Fruttiger, M., Douglas, R. H., Martinez-Barbera, J. P., Greenwood, J., and Moss, S. E. (2009). Genetic ablation of retinal pigment epithelial cells reveals the adaptive response of the epithelium and impact on photoreceptors. *Proc. Natl. Acad. Sci. U.S.A.* 106, 18728–18733. doi: 10.1073/pnas.0902593106

Lu, A. Q., Popova, E. Y., and Barnstable, C. J. (2017). Activin signals through SMAD2/3 to increase photoreceptor precursor yield during embryonic stem cell differentiation. *Stem Cell Rep.* 9, 838–852. doi: 10.1016/j.stemcr.2017.06.021

Luo, D.-G., Xue, T., and Yau, K. W (2008). How vision begins: an odyssey. *Proc. Natl. Acad. Sci. U.S.A.* 105, 9855–9862. doi: 10.1073/pnas.0708405105

Luo, Z., Zhong, X., Li, K., Xie, B., Liu, Y., Ye, M., et al. (2018). An optimized system for effective derivation of three-dimensional retinal tissue via Wnt signaling regulation. *Stem Cells* 36, 1709–1722. doi: 10.1002/stem.2890

Lutty, G., Ikeda, K., Chandler, C., and McLeod, D. S. (1991). Immunohistochemical localization of transforming growth factor-beta in human photoreceptors. *Curr. Eye. Res.* 10, 61–74. doi: 10.3109/02713689109007611

Lutty, G. A., Merges, C., Threlkeld, A. B., Crone, S., and McLeod, D. S. (1993). Heterogeneity in localization of isoforms of TGF-beta in human retina, vitreous, and choroid. *Invest. Ophthalmol. Vis. Sci.* 34, 477–487.

Ma, W., Silverman, S. M., Zhao, L., Villasmil, R., Campos, M. M., Amaral, J., et al. (2019). Absence of TGFbeta signaling in retinal microglia induces retinal degeneration and exacerbates choroidal neovascularization. *Elife* 8:e42049.

Mack, A. F., and Fernald, R. D. (1993). Regulation of cell division and rod differentiation in the teleost retina. *Brain Res. Dev. Brain Res.* 76, 183–187. doi: 10.1016/0165-3806(93)90206-p

Makin, S. (2019). Four technologies that could transform the treatment of blindness. *Nature* 568:S1.

Malchiodi-Albedi, F., Feher, J., Caiazza, S., Formisano, G., Perilli, R., Falchi, M., et al. (1998). PEDF (pigment epithelium-derived factor) promotes increase and maturation of pigment granules in pigment epithelial cells in neonatal albino rat retinal cultures. *Int. J. Dev. Neurosci.* 16, 423–432. doi: 10.1016/s0736-5748(98)00014-8

Mandai, M., Fujii, M., Hashiguchi, T., Sunagawa, G. A., Ito, S. I., Sun, J., et al. (2017a). iPSC-derived retina transplants improve vision in rd1 End-stage retinal-degeneration mice. *Stem Cell Rep.* 8:489. doi: 10.1016/j.stemcr.2017.01.018

Mandai, M., Watanabe, A., Kurimoto, Y., Hirami, Y., Morinaga, C., Daimon, T., et al. (2017b). Autologous induced stem-cell-derived retinal cells for macular degeneration. *N. Engl. J. Med.* 376, 1038–1046.

Manuel, M., Pratt, T., Liu, M., Jeffery, G., and Price, D. J. (2008). Overexpression of Pax6 results in microphthalmia, retinal dysplasia and defective retinal ganglion cell axon guidance. *BMC Dev. Biol.* 8:59. doi: 10.1186/1471-213X-8-59

Marmor, M. F. (2013). "Chapter 19 – mechanisms of normal retinal adhesion," in *Retina*, 5th Edn, eds S. R. Sadda, D. R. Hinton, A. P. Schachat, S. R. Sadda, C. P. Wilkinson, P. Wiedemann, et al. (London: W.B. Saunders), 447–464. doi: 10.1016/b978-1-4557-0737-9.00019-9

Marquardt, T., and Gruss, P. (2002). Generating neuronal diversity in the retina: one for nearly all. *Trends Neurosci.* 25, 32–38. doi: 10.1016/s0166-2236(00)02028-2

Maruotti, J., Sripathi, S. R., Bharti, K., Fuller, J., Wahlin, K. J., Ranganathan, V., et al. (2015). Small-molecule–directed, efficient generation of retinal pigment epithelium from human pluripotent stem cells. *Proc. Natl. Acad. Sci. U.S.A.* 112, 10950–10955. doi: 10.1073/pnas.1422818112

Masaeli, E., Forster, V., Picaud, S., Karamali, F., Nasr-Esfahani, M. H., and Marquette, C. (2020). Tissue engineering of retina through high resolution 3-dimensional inkjet bioprinting. *Biofabrication* 12:025006. doi: 10.1088/1758-5090/ab4a20

Mathieson, K., Loudin, J., Goetz, G., Huie, P., Wang, L., Kamins, T. I., et al. (2012). Photovoltaic retinal prosthesis with high pixel density. *Nat. Photonics* 6, 391–397. doi: 10.1038/nphoton.2012.104

Matsushima, D., Heavner, W., and Pevny, L. H. (2011). Combinatorial regulation of optic cup progenitor cell fate by SOX2 and PAX6. *Development* 138, 443–454. doi: 10.1242/dev.055178

Matt, N., Dupe, V., Garnier, J. M., Dennefeld, C., Chambon, P., Mark, M., et al. (2005). Retinoic acid-dependent eye morphogenesis is orchestrated by neural crest cells. *Development* 132, 4789–4800. doi: 10.1242/dev.02031

May-Simera, H. L., Wan, Q., Jha, B. S., Hartford, J., Khristov, V., Dejene, R., et al. (2018). Primary cilium-mediated retinal pigment epithelium maturation is disrupted in ciliopathy patient cells. *Cell Rep.* 22, 189–205. doi: 10.1016/j.celrep.2017.12.038

Mazzoni, F., Safa, H., and Finnemann, S. C. (2014). Understanding photoreceptor outer segment phagocytosis: use and utility of RPE cells in culture. *Exp. Eye Res.* 126, 51–60. doi: 10.1016/j.exer.2014.01.010

McGill, T. J., Bohana-Kashtan, O., Stoddard, J. W., Andrews, M. D., Pandit, N., Rosenberg-Belmaker, L. R., et al. (2017). Long-term efficacy of GMP grade

Xeno-Free hESC-derived RPE cells following transplantation. *Transl. Vis. Sci. Technol.* 6:17. doi: 10.1167/tvst.6.3.17

McLelland, B. T., Lin, B., Mathur, A., Aramant, R. B., Thomas, B. B., Nistor, G., et al. (2018). Transplanted hESC-derived retina organoid sheets differentiate, integrate, and improve visual function in retinal degenerate rats. *Invest. Ophthalmol. Vis. Sci.* 59, 2586–2603.

McLeod, D. S., Hasegawa, T., Prow, T., Merges, C., and Lutty, G. (2006). The initial fetal human retinal vasculature develops by vasculogenesis. *Dev. Dyn.* 235, 3336–3347. doi: 10.1002/dvdy.20988

McUsic, A. C., Lamba, D. A., and Reh, T. A. (2012). Guiding the morphogenesis of dissociated newborn mouse retinal cells and hES cell-derived retinal cells by soft lithography-patterned microchannel PLGA scaffolds. *Biomaterials* 33, 1396–1405. doi: 10.1016/j.biomaterials.2011.10.083

Meadows, K. L., and Hurwitz, H. I. (2012). Anti-VEGF therapies in the clinic. *Cold Spring Harb. Perspect. Med.* 2:a006577. doi: 10.1101/cshperspect.a006577

Mears, A. J., Hiriyanna, S., Vervoort, R., Yashar, B., Gieser, L., Fahrner, S., et al. (2000). Remapping of the RP15 locus for X-linked cone-rod degeneration to Xp11.4-p21.1, and identification of a de novo insertion in the RPGR exon ORF15. *Am. J. Hum. Genet.* 67, 1000–1003. doi: 10.1086/303091

Mears, A. J., Kondo, M., Swain, P. K., Takada, Y., Bush, R. A., Saunders, T. L., et al. (2001). Nrl is required for rod photoreceptor development. *Nat. Genet.* 29, 447–452. doi: 10.1038/ng774

Megaw, R., Abu-Arafeh, H., Jungnickel, M., Mellough, C., Gurniak, C., Witke, W., et al. (2017). Gelsolin dysfunction causes photoreceptor loss in induced pluripotent cell and animal retinitis pigmentosa models. *Nat. Commun.* 8:271.

Mellough, C. B., Collin, J., Khazim, M., White, K., Sernagor, E., Steel, D. H., et al. (2015). IGF-1 signaling plays an important role in the formation of three-dimensional laminated neural retina and other ocular structures from human embryonic stem cells. *Stem Cells* 33, 2416–2430. doi: 10.1002/stem.2023

Mellough, C. B., Collin, J., Queen, R., Hilgen, G., Dorgau, B., Zerti, D., et al. (2019). Systematic comparison of retinal organoid differentiation from human pluripotent stem cells reveals stage specific, cell line, and methodological differences. *Stem Cells Transl. Med.* 8, 694–706.

Meyer, J. S., Shearer, R. L., Capowski, E. E., Wright, L. S., Wallace, K. A., McMillan, E. L., et al. (2009). Modeling early retinal development with human embryonic and induced pluripotent stem cells. *Proc. Natl. Acad. Sci. U.S.A.* 106, 16698–16703.

Mic, F. A., Molotkov, A., Molotkova, N., and Duester, G. (2004). Raldh2 expression in optic vesicle generates a retinoic acid signal needed for invagination of retina during optic cup formation. *Dev. Dyn.* 231, 270–277. doi: 10.1002/dvdy.20128

Milam, A. H., Dacey, D. M., and Dizhoor, A. M. (1993). Recoverin immunoreactivity in mammalian cone bipolar cells. *Vis. Neurosci.* 10, 1–12. doi: 10.1017/s0952523800003175

Mills, E. A., and Goldman, D. (2017). The regulation of notch signaling in retinal development and regeneration. *Curr. Pathobiol. Rep.* 5, 323–331. doi: 10.1007/s40139-017-0153-7

Mo, X., Yokoyama, A., Oshitari, T., Negishi, H., Dezawa, M., Mizota, A., et al. (2002). Rescue of axotomized retinal ganglion cells by BDNF gene electroporation in adult rats. *Invest. Ophthalmol. Vis. Sci.* 43, 2401–2405.

Molday, R. S. (1998). Photoreceptor membrane proteins, phototransduction, and retinal degenerative diseases. The Friedenwald Lecture. *Invest. Ophthalmol. Vis. Sci.* 39, 2491–2513.

Molday, R. S., and Moritz, O. L. (2015). Photoreceptors at a glance. *J. Cell Sci.* 128, 4039–4045. doi: 10.1242/jcs.175687

Molyneaux, B. J., Arlotta, P., Menezes, J. R. L., and Macklis, J. D. (2007). Neuronal subtype specification in the cerebral cortex. *Nat. Rev. Neurosci.* 8, 427–437. doi: 10.1038/nrn2151

Moore, K. B., Mood, K., Daar, I. O., and Moody, S. A. (2004). Morphogenetic movements underlying eye field formation require interactions between the FGF and ephrinB1 signaling pathways. *Dev. Cell* 6, 55–67. doi: 10.1016/s1534-5807(03)00395-2

Mowat, F. M., Petersen-Jones, S. M., Williamson, H., Williams, D. L., Luthert, P. J., Ali, R. R., et al. (2008). Topographical characterization of cone photoreceptors and the area centralis of the canine retina. *Mol. Vis.* 14, 2518–2527.

Murali, D., Yoshikawa, S., Corrigan, R. R., Plas, D. J., Crair, M. C., Oliver, G., et al. (2005). Distinct developmental programs require different levels of Bmp signaling during mouse retinal development. *Development* 132, 913–923. doi: 10.1242/dev.01673

Myers, B. R., Sever, N., Chong, Y. C., Kim, J., Belani, J. D., Rychnovsky, S., et al. (2013). Hedgehog pathway modulation by multiple lipid binding sites on the smoothened effector of signal response. *Dev. Cell* 26, 346–357. doi: 10.1016/j.devcel.2013.07.015

Nakano, T., Ando, S., Takata, N., Kawada, M., Muguruma, K., Sekiguchi, K., et al. (2012). Self-formation of optic cups and storable stratified neural retina from human ESCs. *Cell Stem Cell* 10, 771–785. doi: 10.1016/j.stem.2012.05.009

Nakayama, A., Nguyen, M. T., Chen, C. C., Opdecamp, K., Hodgkinson, C. A., and Arnheiter, H. (1998). Mutations in microphthalmia, the mouse homolog of the human deafness gene MITF, affect neuroepithelial and neural crest-derived melanocytes differently. *Mech. Dev.* 70, 155–166. doi: 10.1016/s0925-4773(97)00188-3

Nakazawa, T., Tamai, M., and Mori, N. (2002). Brain-derived neurotrophic factor prevents axotomized retinal ganglion cell death through MAPK and PI3K signaling pathways. *Invest. Ophthalmol. Vis. Sci.* 43, 3319–3326.

Nasonkin, I. O., Bin, L., Binette, F., Hogge, G., Aramant, R., Singh, R. K., et al. (2019). Transplantation of human embryonic stem cell derived retinal tissue in the subretinal space of immunodeficient rats with retinal degeneration (RD). ARVO meeting abstract. *Invest. Ophthalmol. Vis. Sci.* 60:3109.

Nasonkin, I. O., Merbs, S. L., Lazo, K., Oliver, V. F., Brooks, M., Patel, K., et al. (2013). Conditional knockdown of DNA methyltransferase 1 reveals a key role of retinal pigment epithelium integrity in photoreceptor outer segment morphogenesis. *Development* 140, 1330–1341. doi: 10.1242/dev.086603

Nauta, T. D., van Hinsbergh, V. W., and Koolwijk, P. (2014). Hypoxic signaling during tissue repair and regenerative medicine. *Int. J. Mol. Sci.* 15, 19791–19815. doi: 10.3390/ijms151119791

NCSL (2008). *Embryonic and Fetal Research Laws*. Washington, DC: National Conference of State Legislatures.

Nelius, T., Samathanam, C., Martinez-Marin, D., Gaines, N., Stevens, J., Hickson, J., et al. (2013). Positive correlation between PEDF expression levels and macrophage density in the human prostate. *Prostate* 73, 549–561. doi: 10.1002/pros.22595

Neumann, C. J., and Nuesslein-Volhard, C. (2000). Patterning of the zebrafish retina by a wave of sonic hedgehog activity. *Science* 289, 2137–2139. doi: 10.1126/science.289.5487.2137

Ng, L., Hurley, J. B., Dierks, B., Srinivas, M., Salto, C., Vennstrom, B., et al. (2001). A thyroid hormone receptor that is required for the development of green cone photoreceptors. *Nat. Genet.* 27, 94–98. doi: 10.1038/83829

Ng, L., Lu, A., Swaroop, A., Sharlin, D. S., Swaroop, A., and Forrest, D. (2011). Two transcription factors can direct three photoreceptor outcomes from rod precursor cells in mouse retinal development. *J. Neurosci.* 31, 11118–11125. doi: 10.1523/jneurosci.1709-11.2011

Ng, S. K., Wood, J. P., Chidlow, G., Han, G., Kittipassorn, T., Peet, D. J., et al. (2015). Cancer-like metabolism of the mammalian retina. *Clin. Exp. Ophthalmol.* 43, 367–376. doi: 10.1111/ceo.12462

Nguyen, M., and Arnheiter, H. (2000). Signaling and transcriptional regulation in early mammalian eye development: a link between FGF and MITF. *Development* 127, 3581–3591.

NIH (2009). *FAQs on the Policy and Procedures for Research Using Human Fetal Tissue in the IRP*. Bethesda, MD: National Institutes of Health.

O'Brien, K. M. B., Cheng, H., Jiang, Y., Schulte, D., Swaroop, A., and Hendrickson, A. E. (2004). Expression of photoreceptor-specific nuclear receptor NR2E3 in rod photoreceptors of fetal human retina. *Invest. Ophthalmol. Vis. Sci.* 45, 2807–2812.

Osakada, F., Ikeda, H., Mandai, M., Wataya, T., Watanabe, K., Yoshimura, N., et al. (2008). Toward the generation of rod and cone photoreceptors from mouse, monkey and human embryonic stem cells. *Nat. Biotechnol.* 26, 215–224. doi: 10.1038/nbt1384

Osakada, F., Jin, Z. B., Hirami, Y., Ikeda, H., Danjyo, T., Watanabe, K., et al. (2009). In vitro differentiation of retinal cells from human pluripotent stem cells by small-molecule induction. *J. Cell Sci.* 122, 3169–3179. doi: 10.1242/jcs.050393

Pacitti, D., Privolizzi, R., and Bax, B. E. (2019). Organs to cells and cells to organoids: the evolution of in vitro central nervous system modelling. *Front. Cell. Neurosci.* 13:129. doi: 10.3389/fncel.2019.00129

Palczewski, K. (2014). Chemistry and biology of the initial steps in vision: the Friedenwald lecture. *Invest. Ophthalmol. Vis. Sci.* 55, 6651–6672.

Pandit, T., Jidigam, V. K., Patthey, C., and Gunhaga, L. (2015). Neural retina identity is specified by lens-derived BMP signals. *Development* 142, 1850–1859. doi: 10.1242/dev.123653

Pearring, J. N., Salinas, R. Y., Baker, S. A., and Arshavsky, V. Y. (2013). Protein sorting, targeting and trafficking in photoreceptor cells. *Prog. Retin. Eye Res.* 36, 24–51. doi: 10.1016/j.preteyeres.2013.03.002

Perrimon, N., Pitsouli, C., and Shilo, B. Z. (2012). Signaling mechanisms controlling cell fate and embryonic patterning. *Cold Spring Harb. Perspect. Biol.* 4:a005975. doi: 10.1101/cshperspect.a005975

Perron, M., Boy, S., Amato, M. A., Viczian, A., Koebernick, K., Pieler, T., et al. (2003). A novel function for Hedgehog signalling in retinal pigment epithelium differentiation. *Development* 130, 1565–1577. doi: 10.1242/dev.00391

Petersen-Jones, S. M. (1998). Animal models of human retinal dystrophies. *Eye (Lond)* 12(Pt 3b), 566–570. doi: 10.1038/eye.1998.146

Petersen-Jones, S. M., Occelli, L. M., Winkler, P. A., Lee, W., Sparrow, J. R., Tsukikawa, M., et al. (2018). Patients and animal models of CNGbeta1-deficient retinitis pigmentosa support gene augmentation approach. *J. Clin. Invest.* 128, 190–206. doi: 10.1172/jci95161

Pinzon-Guzman, C., Zhang, S. S., and Barnstable, C. J. (2011). Specific protein kinase C isoforms are required for rod photoreceptor differentiation. *J. Neurosci.* 31, 18606–18617. doi: 10.1523/jneurosci.2578-11.2011

Pittack, C., Grunwald, G. B., and Reh, T. A. (1997). Fibroblast growth factors are necessary for neural retina but not pigmented epithelium differentiation in chick embryos. *Development* 124, 805–816.

Prabhudesai, S. N., Cameron, D. A., and Stenkamp, D. L. (2005). Targeted effects of retinoic acid signaling upon photoreceptor development in zebrafish. *Dev. Biol.* 287, 157–167. doi: 10.1016/j.ydbio.2005.08.045

Pugh, E. N. Jr., and Lamb, T. D. (1993). Amplification and kinetics of the activation steps in phototransduction. *Biochim. Biophys. Acta* 1141, 111–149. doi: 10.1016/0005-2728(93)90038-h

Qin, Z., Kidd, A. R. III, Thomas, J. L., Poss, K. D., Hyde, D. R., Raymond, P. A., et al. (2011). FGF signaling regulates rod photoreceptor cell maintenance and regeneration in zebrafish. *Exp. Eye Res.* 93, 726–734. doi: 10.1016/j.exer.2011.09.003

Rachel, R. A., Li, T., and Swaroop, A. (2012a). Photoreceptor sensory cilia and ciliopathies: focus on CEP290, RPGR and their interacting proteins. *Cilia* 1:22. doi: 10.1186/2046-2530-1-22

Rachel, R. A., May-Simera, H. L., Veleri, S., Gotoh, N., Choi, B. Y., Murga-Zamalloa, C., et al. (2012b). Combining Cep290 and Mkks ciliopathy alleles in mice rescues sensory defects and restores ciliogenesis. *J. Clin. Invest.* 122, 1233–1245. doi: 10.1172/jci60981

Radtke, N. D., Aramant, R. B., Petry, H. M., Green, P. T., Pidwell, D. J., and Seiler, M. J. (2008). Vision improvement in retinal degeneration patients by implantation of retina together with retinal pigment epithelium. *Am. J. Ophthalmol.* 146, 172–182.

Radtke, N. D., Aramant, R. B., Seiler, M. J., Petry, H. M., and Pidwell, D. (2004). Vision change after sheet transplant of fetal retina with retinal pigment epithelium to a patient with retinitis pigmentosa. *Arch. Ophthalmol.* 122, 1159–1165.

Radtke, N. D., Seiler, M. J., Aramant, R. B., Petry, H. M., and Pidwell, D. J. (2002). Transplantation of intact sheets of fetal neural retina with its retinal pigment epithelium in retinitis pigmentosa patients. *Am. J. Ophthalmol.* 133, 544–550. doi: 10.1016/s0002-9394(02)01322-3

Raftery, J., Clegg, A., Jones, J., Tan, S. C., and Lotery, A. (2007). Ranibizumab (Lucentis) versus bevacizumab (Avastin): modelling cost effectiveness. *Br. J. Ophthalmol.* 91, 1244–1246. doi: 10.1136/bjo.2007.116616

Ramsden, C. M., Powner, M. B., Carr, A. J., Smart, M. J., da Cruz, L., and Coffey, P. J. (2013). Stem cells in retinal regeneration: past, present and future. *Development* 140, 2576–2585.

Ray, T. A., and Kay, J. N. (2015). Following directions from the retina to the brain. *Neuron* 86, 855–857. doi: 10.1016/j.neuron.2015.05.017

Raymond, S. M., and Jackson, I. J. (1995). The retinal pigmented epithelium is required for development and maintenance of the mouse neural retina. *Curr. Biol.* 5, 1286–1295. doi: 10.1016/s0960-9822(95)00255-7

Redmond, T. M., Yu, S., Lee, E., Bok, D., Hamasaki, D., Chen, N., et al. (1998). Rpe65 is necessary for production of 11-cis-vitamin A in the retinal visual cycle. *Nat. Genet.* 20, 344–351. doi: 10.1038/3813

Remington, L. A. (2012). "Chapter 7 – Ocular embryology," in *Clinical Anatomy and Physiology of the Visual System*, 3rd Edn, ed. L. A. Remington (Saint Louis, MO: Butterworth-Heinemann), 123–143. doi: 10.1016/b978-1-4377-1926-0.10007-4

Rhinn, M., and Dolle, P. (2012). Retinoic acid signalling during development. *Development* 139, 843–858. doi: 10.1242/dev.065938

Riesenberg, A. N., Liu, Z., Kopan, R., and Brown, N. L. (2009). Rbpj cell autonomous regulation of retinal ganglion cell and cone photoreceptor fates in the mouse retina. *J. Neurosci.* 29, 12865–12877. doi: 10.1523/jneurosci.3382-09.2009

Rodriguez-de la Rosa, L., Fernandez-Sanchez, L., Germain, F., Murillo-Cuesta, S., Varela-Nieto, I., de la Villa, P., et al. (2012). Age-related functional and structural retinal modifications in the Igf1-/- null mouse. *Neurobiol. Dis.* 46, 476–485. doi: 10.1016/j.nbd.2012.02.013

Rosenfeld, P. J., Brown, D. M., Heier, J. S., Boyer, D. S., Kaiser, P. K., Chung, C. Y., et al. (2006). Ranibizumab for neovascular age-related macular degeneration. *N. Engl. J. Med.* 355, 1419–1431.

Rozet, J. M., Perrault, I., Gigarel, N., Souied, E., Ghazi, I., Gerber, S., et al. (2002). Dominant X linked retinitis pigmentosa is frequently accounted for by truncating mutations in exon ORF15 of the RPGR gene. *J. Med. Genet.* 39, 284–285. doi: 10.1136/jmg.39.4.284

Rudnicka, A. R., Kapetanakis, V. V., Jarrar, Z., Wathern, A. K., Wormald, R., Fletcher, A. E., et al. (2015). Incidence of late-stage age-related macular degeneration in American Whites: systematic review and meta-analysis. *Am. J. Ophthalmol.* 160, 85–93.e3. doi: 10.1016/j.ajo.2015.04.003

Saari, J. C. (2000). Biochemistry of visual pigment regeneration: the Friedenwald lecture. *Invest. Ophthalmol. Vis. Sci.* 41, 337–348.

Sakagami, K., Gan, L., and Yang, X. J. (2009). Distinct effects of Hedgehog signaling on neuronal fate specification and cell cycle progression in the embryonic mouse retina. *J. Neurosci.* 29, 6932–6944. doi: 10.1523/jneurosci.0289-09.2009

Salido, E. M., and Ramamurthy, V. (2019). Proteoglycan IMPG2 shapes the interphotoreceptor matrix and modulates vision. *bioRxiv* [Preprint]. doi: 10.1523/JNEUROSCI.2994-19.2020 bioRxiv: 859116,

Salinas, R. Y., Pearring, J. N., Ding, J. D., Spencer, W. J., Hao, Y., and Arshavsky, V. Y. (2017). Photoreceptor discs form through peripherin-dependent suppression of ciliary ectosome release. *J. Cell Biol.* 216, 1489–1499. doi: 10.1083/jcb.201608081

Sarwar, S., Clearfield, E., Soliman, M. K., Sadiq, M. A., Baldwin, A. J., Hanout, M., et al. (2016). Aflibercept for neovascular age-related macular degeneration. *Cochrane Database Syst. Rev.* 2:CD011346.

Schlecht, A., Leimbeck, S. V., Jägle, H., Feuchtinger, A., Tamm, E. R., and Braunger, B. M. (2017). Deletion of endothelial transforming growth factor–β signaling leads to choroidal neovascularization. *Am. J. Pathol.* 187, 2570–2589.

Schlueter, P. J., Peng, G., Westerfield, M., and Duan, C. (2007). Insulin-like growth factor signaling regulates zebrafish embryonic growth and development by promoting cell survival and cell cycle progression. *Cell Death Differ.* 14, 1095–1105. doi: 10.1038/sj.cdd.4402109

Schwartz, S. D., Hubschman, J. P., Heilwell, G., Franco-Cardenas, V., Pan, C. K., Ostrick, R. M., et al. (2012). Embryonic stem cell trials for macular degeneration: a preliminary report. *Lancet* 379, 713–720. doi: 10.1016/s0140-6736(12)60028-2

Schwartz, S. D., Regillo, C. D., Lam, B. L., Eliott, D., Rosenfeld, P. J., Gregori, N. Z., et al. (2015). Human embryonic stem cell-derived retinal pigment epithelium in patients with age-related macular degeneration and Stargardt's macular dystrophy: follow-up of two open-label phase 1/2 studies. *Lancet* 385, 509–516. doi: 10.1016/s0140-6736(14)61376-3

Schwartz, S. D., Tan, G., Hosseini, H., and Nagiel, A. (2016). Subretinal transplantation of embryonic stem cell-derived retinal pigment epithelium for the treatment of macular degeneration: an assessment at 4 years. *Invest. Ophthalmol. Vis. Sci.* 57, ORSFc1–ORSFc9.

Schwarz, N., Lane, A., Jovanovic, K., Parfitt, D. A., Aguila, M., Thompson, C. L., et al. (2017). Arl3 and RP2 regulate the trafficking of ciliary tip kinesins. *Hum. Mol. Genet.* 26, 2480–2492. doi: 10.1093/hmg/ddx143

Seiler, M. J., and Aramant, R. B. (2012). Cell replacement and visual restoration by retinal sheet transplants. *Prog. Retin. Eye Res.* 31, 661–687. doi: 10.1016/j.preteyeres.2012.06.003

Seiler, M. J., Aramant, R. B., Thomas, B. B., Peng, Q., Sadda, S. R., and Keirstead, H. S. (2010). Visual restoration and transplant connectivity in degenerate rats implanted with retinal progenitor sheets. *Eur J. Neurosci.* 31, 508–520. doi: 10.1111/j.1460-9568.2010.07085.x

Seiler, M. J., Lin, R. E., McLelland, B. T., Mathur, A., Lin, B., Sigman, J., et al. (2017). Vision recovery and connectivity by fetal retinal sheet transplantation in an immunodeficient retinal degenerate rat model. *Invest. Ophthalmol. Vis. Sci.* 58, 614–630.

Sharon, D., Sandberg, M. A., Caruso, R. C., Berson, E. L., and Dryja, T. P. (2003). Shared mutations in NR2E3 in enhanced S-cone syndrome, goldmann-Favre syndrome, and many cases of clumped pigmentary retinal degeneration. *Arch. Ophthalmol.* 121, 1316–1323.

Shekhar, K., Lapan, S. W., Whitney, I. E., Tran, N. M., Macosko, E. Z., Kowalczyk, M., et al. (2016). Comprehensive classification of retinal bipolar neurons by single-cell transcriptomics. *Cell* 166, 1308–1323.e30. doi: 10.1016/j.cell.2016.07.054

Shen, Q., Zhong, W., Jan, Y. N., and Temple, S. (2002). Asymmetric numb distribution is critical for asymmetric cell division of mouse cerebral cortical stem cells and neuroblasts. *Development* 129, 4843–4853.

Shirai, H., Mandai, M., Matsushita, K., Kuwahara, A., Yonemura, S., Nakano, T., et al. (2016). Transplantation of human embryonic stem cell-derived retinal tissue in two primate models of retinal degeneration. *Proc. Natl. Acad. Sci. U.S.A.* 113, E81–E90.

Siegert, S., Cabuy, E., Scherf, B. G., Kohler, H., Panda, S., Le, Y. Z., et al. (2012). Transcriptional code and disease map for adult retinal cell types. *Nat. Neurosci.* 15, 487–495. doi: 10.1038/nn.3032

Singh, B., and Armstrong, D. T. (1997). Insulin-like growth factor-1, a component of serum that enables porcine cumulus cells to expand in response to follicle-stimulating hormone in vitro. *Biol. Reprod.* 56, 1370–1375. doi: 10.1095/biolreprod56.6.1370

Singh, M. S., Charbel Issa, P., Butler, R., Martin, C., Lipinski, D. M., Sekaran, S., et al. (2013). Reversal of end-stage retinal degeneration and restoration of visual function by photoreceptor transplantation. *Proc. Natl. Acad. Sci. U.S.A.* 110, 1101–1106. doi: 10.1073/pnas.1119416110

Singh, R. K., Kolandaivelu, S., and Ramamurthy, V. (2014). Early alteration of retinal neurons in Aipl1-/- animals. *Invest. Ophthalmol. Vis. Sci.* 55, 3081–3092.

Singh, R. K., Mallela, R. K., Cornuet, P. K., Reifler, A. N., Chervenak, A. P., West, M. D., et al. (2015). Characterization of three-dimensional retinal tissue derived from human embryonic stem cells in adherent monolayer cultures. *Stem Cells Dev.* 24, 2778–2795. doi: 10.1089/scd.2015.0144

Singh, R. K., Mallela, R. K., Hayes, A., Dunham, N. R., Hedden, M. E., Enke, R. A., et al. (2017). Dnmt1, Dnmt3a and Dnmt3b cooperate in photoreceptor and outer plexiform layer development in the mammalian retina. *Exp. Eye Res.* 159, 132–146. doi: 10.1016/j.exer.2016.11.014

Singh, R. K., Occelli, L. M., Binette, F., Petersen-Jones, S. M., and Nasonkin, I. O. (2019). Transplantation of human embryonic stem cell-derived retinal tissue in the subretinal space of the cat eye. *Stem Cells Dev.* 28, 1151–1166. doi: 10.1089/scd.2019.0090

Slijkerman, R. W., Song, F., Astuti, G. D., Huynen, M. A., van Wijk, E., Stieger, K., et al. (2015). The pros and cons of vertebrate animal models for functional and therapeutic research on inherited retinal dystrophies. *Prog. Retin. Eye Res.* 48, 137–159. doi: 10.1016/j.preteyeres.2015.04.004

Smith, J. N., Walker, H. M., Thompson, H., Collinson, J. M., Vargesson, N., and Erskine, L. (2018). Lens-regulated retinoic acid signalling controls expansion of the developing eye. *Development* 145:dev167171. doi: 10.1242/dev.167171

Song, M. J., and Bharti, K. (2016). Looking into the future: using induced pluripotent stem cells to build two and three dimensional ocular tissue for cell therapy and disease modeling. *Brain Res.* 1638, 2–14. doi: 10.1016/j.brainres.2015.12.011

Sparrow, J. R., Hicks, D., and Hamel, C. P. (2010). The retinal pigment epithelium in health and disease. *Curr. Mol. Med.* 10, 802–823.

Spence, J. R., Madhavan, M., Ewing, J. D., Jones, D. K., Lehman, B. M., and Del Rio-Tsonis, K. (2004). The hedgehog pathway is a modulator of retina regeneration. *Development* 131, 4607–4621. doi: 10.1242/dev.01298

Strauss, O. (2005). The retinal pigment epithelium in visual function. *Physiol. Rev.* 85, 845–881. doi: 10.1152/physrev.00021.2004

Stronks, H. C., and Dagnelie, G. (2014). The functional performance of the Argus II retinal prosthesis. *Expert Rev. Med. Devices* 11, 23–30. doi: 10.1586/17434440.2014.862494

Strunnikova, N. V., Maminishkis, A., Barb, J. J., Wang, F., Zhi, C., Sergeev, Y., et al. (2010). Transcriptome analysis and molecular signature of human retinal pigment epithelium. *Hum. Mol. Genet.* 19, 2468–2486. doi: 10.1093/hmg/ddq129

Sun, Y., and Smith, L. E. H. (2018). Retinal vasculature in development and diseases. *Annu. Rev. Vis. Sci.* 4, 101–122. doi: 10.1146/annurev-vision-091517-034018

Sunness, J. S., Gonzalez-Baron, J., Applegate, C. A., Bressler, N. M., Tian, Y., Hawkins, B., et al. (1999). Enlargement of atrophy and visual acuity loss in the geographic atrophy form of age-related macular degeneration. *Ophthalmology* 106, 1768–1779. doi: 10.1016/s0161-6420(99)90340-8

Swaroop, A., Kim, D., and Forrest, D. (2010). Transcriptional regulation of photoreceptor development and homeostasis in the mammalian retina. *Nat. Rev. Neurosci.* 11, 563–576. doi: 10.1038/nrn2880

Swaroop, A., Xu, J. Z., Pawar, H., Jackson, A., Skolnick, C., and Agarwal, N. (1992). A conserved retina-specific gene encodes a basic motif/leucine zipper domain. *Proc. Natl. Acad. Sci. U.S.A.* 89, 266–270. doi: 10.1073/pnas.89.1.266

Takata, N., Abbey, D., Fiore, L., Acosta, S., Feng, R., Gil, H. J., et al. (2017). An eye organoid approach identifies Six3 suppression of R-spondin 2 as a critical step in mouse neuroretina differentiation. *Cell Rep.* 21, 1534–1549. doi: 10.1016/j.celrep.2017.10.041

Tombran-Tink, J., and Barnstable, C. J. (2003). Therapeutic prospects for PEDF: more than a promising angiogenesis inhibitor. *Trends Mol. Med.* 9, 244–250. doi: 10.1016/s1471-4914(03)00074-1

Tombran-Tink, J., Chader, G. G., and Johnson, L. V. (1991). PEDF: a pigment epithelium-derived factor with potent neuronal differentiative activity. *Exp. Eye Res.* 53, 411–414. doi: 10.1016/0014-4835(91)90248-d

Tomita, K., Ishibashi, M., Nakahara, K., Ang, S. L., Nakanishi, S., Guillemot, F., et al. (1996). Mammalian hairy and enhancer of split homolog 1 regulates differentiation of retinal neurons and is essential for eye morphogenesis. *Neuron* 16, 723–734. doi: 10.1016/s0896-6273(00)80093-8

Tu, H. Y., Watanabe, T., Shirai, H., Yamasaki, S., Kinoshita, M., Matsushita, K., et al. (2018). Medium- to long-term survival and functional examination of human iPSC-derived retinas in rat and primate models of retinal degeneration. *EBioMedicine* 39, 562–574. doi: 10.1016/j.ebiom.2018.11.028

Vajaranant, T. S., Wu, S., Torres, M., and Varma, R. (2012). The changing face of primary open-angle glaucoma in the United States: demographic and geographic changes from 2011 to 2050. *Am. J. Ophthalmol.* 154, 303–314.e3. doi: 10.1016/j.ajo.2012.02.024

van Adel, B. A., Arnold, J. M., Phipps, J., Doering, L. C., and Ball, A. K. (2005). Ciliary neurotrophic factor protects retinal ganglion cells from axotomy-induced apoptosis via modulation of retinal glia in vivo. *J. Neurobiol.* 63, 215–234. doi: 10.1002/neu.20117

Vander Heiden, M. G., Cantley, L. C., and Thompson, C. B. (2009). Understanding the Warburg effect: the metabolic requirements of cell proliferation. *Science* 324, 1029–1033. doi: 10.1126/science.1160809

Varma, R., Vajaranant, T. S., Burkemper, B., Wu, S., Torres, M., Hsu, C., et al. (2016). Visual impairment and blindness in adults in the United States: demographic and geographic variations from 2015 to 2050. *JAMA Ophthalmol.* 134, 802–809.

Veltel, S., Gasper, R., Eisenacher, E., and Wittinghofer, A. (2008). The retinitis pigmentosa 2 gene product is a GTPase-activating protein for Arf-like 3. *Nat. Struct. Mol. Biol.* 15, 373–380. doi: 10.1038/nsmb.1396

Vingerling, J. R., Dielemans, I., Hofman, A., Grobbee, D. E., Hijmering, M., Kramer, C. F., et al. (1995). The prevalence of age-related maculopathy in the Rotterdam Study. *Ophthalmology* 102, 205–210. doi: 10.1016/s0161-6420(95)31034-2

Vogel-Hopker, A., Momose, T., Rohrer, H., Yasuda, K., Ishihara, L., and Rapaport, D. H. (2000). Multiple functions of fibroblast growth factor-8 (FGF-8) in chick eye development. *Mech. Dev.* 94, 25–36. doi: 10.1016/s0925-4773(00)00320-8

Volkner, M., Zschatzsch, M., Rostovskaya, M., Overall, R. W., Busskamp, V., Anastassiadis, K., et al. (2016). Retinal organoids from pluripotent stem cells efficiently recapitulate retinogenesis. *Stem Cell Rep.* 6, 525–538. doi: 10.1016/j.stemcr.2016.03.001

Volland, S., Esteve-Rudd, J., Hoo, J., Yee, C., and Williams, D. S. (2015a). A comparison of some organizational characteristics of the mouse central retina and the human macula. *PLoS One* 10:e0125631. doi: 10.1371/journal.pone.0125631

Volland, S., Hughes, L. C., Kong, C., Burgess, B. L., Linberg, K. A., Luna, G., et al. (2015b). Three-dimensional organization of nascent rod outer segment disk membranes. *Proc. Natl. Acad. Sci. U.S.A.* 112, 14870–14875. doi: 10.1073/pnas.1516309112

Volpert, K. N., Tombran-Tink, J., Barnstable, C., and Layer, P. G. (2009). PEDF and GDNF are key regulators of photoreceptor development and retinal neurogenesis in reaggregates from chick embryonic retina. *J. Ocul. Biol. Dis. Infor.* 2, 1–11. doi: 10.1007/s12177-009-9014-x

Wadman, M. (2015). The truth about fetal tissue research. *Nature* 528, 179–181.

Wahlin, K. J., Maruotti, J. A., Sripathi, S. R., Ball, J., Angueyra, J. M., Kim, C., et al. (2017). Photoreceptor outer segment-like structures in long-term 3D retinas from human pluripotent stem cells. *Sci. Rep.* 7:766.

Wallace, V. A. (2011). Concise review: making a retina–from the building blocks to clinical applications. *Stem Cells* 29, 412–417. doi: 10.1002/stem.602

Wang, J. S., Estevez, M. E., Cornwall, M. C., and Kefalov, V. J. (2009). Intra-retinal visual cycle required for rapid and complete cone dark adaptation. *Nat. Neurosci.* 12, 295–302. doi: 10.1038/nn.2258

Wang, J. S., and Kefalov, V. J. (2011). The cone-specific visual cycle. *Prog. Retin. Eye Res.* 30, 115–128. doi: 10.1016/j.preteyeres.2010.11.001

Wang, Y., Zhang, D., Zhang, Y., Ni, N., Tang, Z., Bai, Z., et al. (2018). Insulin-like growth factor-1 regulation of retinal progenitor cell proliferation and differentiation. *Cell Cycle* 17, 515–526. doi: 10.1080/15384101.2018.1431594

Wang, Y. P., Dakubo, G., Howley, P., Campsall, K. D., Mazarolle, C. J., Shiga, S. A., et al. (2002). Development of normal retinal organization depends on Sonic hedgehog signaling from ganglion cells. *Nat. Neurosci.* 5, 831–832. doi: 10.1038/nn911

Warburg, O. (1928). "Über die klassifizierung tierischer gewebe nach ihrem stoffwechsel," in *Über die Katalytischen Wirkungen der Lebendigen Substanz: Arbeiten aus dem Kaiser Wilhelm-Institut für Biologie · Berlin-Dahlem*, ed. O. Warburg (Berlin: Springer), 510–514. doi: 10.1007/978-3-642-47774-4_35

Warburg, O., Wind, F., and Negelein, E. (1927). The metabolism of tumors in the body. *J. Gen. Physiol.* 8, 519–530. doi: 10.1085/jgp.8.6.519

Weinreb, R. N., Aung, T., and Medeiros, F. A. (2014). The pathophysiology and treatment of glaucoma: a review. *JAMA* 311, 1901–1911.

Wheway, G., Parry, D. A., and Johnson, C. A. (2014). The role of primary cilia in the development and disease of the retina. *Organogenesis* 10, 69–85. doi: 10.4161/org.26710

Wickham, L., Lewis, G. P., Charteris, D. G., and Fisher, S. K. (2013). "Chapter 29 – Cellular effects of detachment and reattachment on the neural retina and the retinal pigment epithelium," in *Retina*, 5th Edn, eds S. J. Ryan, S. R. Sadda, D. R. Hinton, A. P. Schachat, S. R. Sadda, C. P. Wilkinson, et al. (London: W.B. Saunders), 605–617. doi: 10.1016/b978-1-4557-0737-9.00029-1

Wong, W. L., Su, X., Li, X., Cheung, C. M., Klein, R., Cheng, C. Y., et al. (2014). Global prevalence of age-related macular degeneration and disease burden projection for 2020 and 2040: a systematic review and meta-analysis. *Lancet Glob. Health* 2, e106–e116. doi: 10.1016/s2214-109x(13)70145-1

Wong-Riley, M. T. (2010). Energy metabolism of the visual system. *Eye Brain* 2, 99–116.

Wu, J., Mak, H. K., Chan, Y. K., Lin, C., Kong, C., Leung, C. K. S., et al. (2019). An in vitro pressure model towards studying the response of primary retinal ganglion cells to elevated hydrostatic pressures. *Sci. Rep.* 9:9057.

Xing, T., Hass, D. T., Zhang, S. S., and Barnstable, C. J. (2018). The 3-phosphoinositide-dependent protein kinase 1 inhibits rod photoreceptor development. *Front. Cell Dev. Biol.* 6:134. doi: 10.3389/fcell.2018.00134

Yang, N., Caratti, G., Ince, L. M., Poolman, T. M., Trebble, P. J., Holt, C. M., et al. (2014). Serum cholesterol selectively regulates glucocorticoid sensitivity through activation of JNK. *J. Endocrinol.* 223, 155–166. doi: 10.1530/joe-14-0456

Yao, K., Qiu, S., Tian, L., Snider, W. D., Flannery, J. G., Schaffer, D. V., et al. (2016). Wnt regulates proliferation and neurogenic potential of muller glial cells via a Lin28/let-7 miRNA-dependent pathway in adult mammalian retinas. *Cell Rep.* 17, 165–178. doi: 10.1016/j.celrep.2016.08.078

Yaron, O., Farhy, C., Marquardt, T., Applebury, M., and Ashery-Padan, R. (2006). Notch1 functions to suppress cone-photoreceptor fate specification in the developing mouse retina. *Development* 133, 1367–1378. doi: 10.1242/dev.02311

Ye, X., Wang, Y., and Nathans, J. (2010). The Norrin/Frizzled4 signaling pathway in retinal vascular development and disease. *Trends Mol. Med.* 16, 417–425. doi: 10.1016/j.molmed.2010.07.003

Yeo, N. J. Y., Chan, E. J. J., and Cheung, C. (2019). Choroidal neovascularization: mechanisms of endothelial dysfunction. *Front. Pharmacol.* 10:1363. doi: 10.3389/fphar.2019.01363

Yi, X., Schubert, M., Peachey, N. S., Suzuma, K., Burks, D. J., Kushner, J. A., et al. (2005). Insulin receptor substrate 2 is essential for maturation and survival of photoreceptor cells. *J. Neurosci.* 25, 1240–1248. doi: 10.1523/jneurosci.3664-04.2005

Yildiz, O., and Khanna, H. (2012). Ciliary signaling cascades in photoreceptors. *Vis. Res* 75, 112–116. doi: 10.1016/j.visres.2012.08.007

Young, R. W. (1967). The renewal of photoreceptor cell outer segments. *J. Cell Biol.* 33, 61–72. doi: 10.1083/jcb.33.1.61

Yu, C., Mazerolle, C. J., Thurig, S., Wang, Y., Pacal, M., Bremner, R., et al. (2006). Direct and indirect effects of hedgehog pathway activation in the mammalian retina. *Mol. Cell. Neurosci.* 32, 274–282. doi: 10.1016/j.mcn.2006.05.002

Zeiss, C. J. (2010). Animals as models of age-related macular degeneration: an imperfect measure of the truth. *Vet. Pathol.* 47, 396–413. doi: 10.1177/0300985809359598

Zhang, X. M., and Yang, X. J. (2001a). Regulation of retinal ganglion cell production by Sonic hedgehog. *Development* 128, 943–957.

Zhang, X. M., and Yang, X. J. (2001b). Temporal and spatial effects of Sonic hedgehog signaling in chick eye morphogenesis. *Dev. Biol.* 233, 271–290. doi: 10.1006/dbio.2000.0195

Zhang, Y., Strehin, I., Bedelbaeva, K., Gourevitch, D., Clark, L., Leferovich, J., et al. (2015). Drug-induced regeneration in adult mice. *Sci. Transl. Med.* 7:290ra92. doi: 10.1126/scitranslmed.3010228

Zhao, C., Wang, Q., and Temple, S. (2017). Stem cell therapies for retinal diseases: recapitulating development to replace degenerated cells. *Development* 144, 1368–1381. doi: 10.1242/dev.133108

Zhao, S., Hung, F. C., Colvin, J. S., White, A., Dai, W., Lovicu, F. J., et al. (2001). Patterning the optic neuroepithelium by FGF signaling and Ras activation. *Development* 128, 5051–5060.

Zheng, M., Zhang, Z., Zhao, X., Ding, Y., and Han, H. (2010). The Notch signaling pathway in retinal dysplasia and retina vascular homeostasis. *J. Genet. Genomics* 37, 573–582. doi: 10.1016/s1673-8527(09)60077-1

Zheng, M. H., Shi, M., Pei, Z., Gao, F., Han, H., and Ding, Y. Q. (2009). The transcription factor RBP-J is essential for retinal cell differentiation and lamination. *Mol. Brain* 2:38. doi: 10.1186/1756-6606-2-38

Zheng, W., Meng, Q., Wang, H., Yan, F., Little, P. J., Deng, X., et al. (2018). IGF-1-mediated survival from induced death of human primary cultured retinal pigment epithelial cells is mediated by an akt-dependent signaling pathway. *Mol. Neurobiol.* 55, 1915–1927. doi: 10.1007/s12035-017-0447-0

Zhong, X., Gutierrez, C., Xue, T., Hampton, C., Vergara, M. N., Cao, L. H., et al. (2014). Generation of three-dimensional retinal tissue with functional photoreceptors from human iPSCs. *Nat. Commun.* 5:4047.

Zhou, S., Flamier, A., Abdouh, M., Tetreault, N., Barabino, A., Wadhwa, S., et al. (2015). Differentiation of human embryonic stem cells into cone photoreceptors through simultaneous inhibition of BMP, TGFbeta and Wnt signaling. *Development* 142, 3294–3306. doi: 10.1242/dev.125385

Conflict of Interest: Both authors were employed by the company Lineage Cell Therapeutics.

The authors declare that the research was conducted in the absence of any commercial or financial relationships that could be construed as a potential conflict of interest.

frontiers in Cellular Neuroscience

MINI REVIEW
published: 03 December 2020
doi: 10.3389/fncel.2020.607399

Challenges in Modeling Human Neural Circuit Formation via Brain Organoid Technology

*Takeshi K. Matsui, Yuichiro Tsuru and Ken-ichiro Kuwako**

Department of Neural and Muscular Physiology, Shimane University School of Medicine, Izumo, Japan

Human brain organoids are three-dimensional self-organizing tissues induced from pluripotent cells that recapitulate some aspects of early development and some of the early structure of the human brain *in vitro*. Brain organoids consist of neural lineage cells, such as neural stem/precursor cells, neurons, astrocytes and oligodendrocytes. Additionally, brain organoids contain fluid-filled ventricle-like structures surrounded by a ventricular/subventricular (VZ/SVZ) zone-like layer of neural stem cells (NSCs). These NSCs give rise to neurons, which form multiple outer layers. Since these structures resemble some aspects of structural arrangements in the developing human brain, organoid technology has attracted great interest in the research fields of human brain development and disease modeling. Developmental brain disorders have been intensely studied through the use of human brain organoids. Relatively early steps in human brain development, such as differentiation and migration, have also been studied. However, research on neural circuit formation with brain organoids has just recently began. In this review, we summarize the current challenges in studying neural circuit formation with organoids and discuss future perspectives.

Keywords: human brain organoid, circuit formation, neural differentiation, neuronal migration, axonal projection, synapse formation

OPEN ACCESS

Edited by:
Janice R. Naegele,
Wesleyan University, United States

Reviewed by:
Zoltan Molnar,
University of Oxford, United Kingdom
Artur Pałasz,
Medical University of Silesia, Poland

***Correspondence:**
Ken-ichiro Kuwako
kuwako@med.shimane-u.ac.jp

Specialty section:
This article was submitted to Cellular Neurophysiology, a section of the journal Frontiers in Cellular Neuroscience

Received: *17 September 2020*
Accepted: *12 November 2020*
Published: *03 December 2020*

Citation:
Matsui TK, Tsuru Y and Kuwako K (2020) Challenges in Modeling Human Neural Circuit Formation via Brain Organoid Technology. Front. Cell. Neurosci. 14:607399. doi: 10.3389/fncel.2020.607399

INTRODUCTION

Human brain tissue is considered the best resource for analyzing the mechanisms of human brain development and diseases. However, ethical issues have prevented us from easily accessing human brain tissue samples, especially samples from living patients. Thus, researchers are mainly dependent on human postmortem brains and the brains of aborted fetuses to study the human brain. Additionally, rodent model animals have been used for tissue cultivation and genetic manipulation studies. However, approximately one decade ago, human pluripotent stem cell-derived retinal organoids composed of multiple cell types that imitate the three-dimensional (3D) structure of the retina were reported for the first time (Eiraku et al., 2011). This organoid technology paved the way for analyses of various cell-cell interactions in 3D human tissues *in vitro*. Many protocols for the generation of human organoids that imitate various tissues, such as colon, kidney, lung and liver tissues, have since been published (Jung et al., 2011; Sato et al., 2011; Takebe et al., 2013; Taguchi et al., 2014; Takasato et al., 2014; Dye et al., 2015). In 2013, Lancaster et al. reported the first method for inducing human cerebral organoids that recapitulate the structure of the ventricles and the neuronal layers of the human cerebral cortex, even though these organoids harbor other various brain regions (Lancaster et al., 2013). Following this report, many protocols for generating organoids

that mimic other brain components, including the midbrain (Jo et al., 2016), brainstem (Eura et al., 2020), choroid plexus (Pellegrini et al., 2020), cerebellum (Muguruma et al., 2015), and spinal cord (Ogura et al., 2018; Duval et al., 2019), were established. Furthermore, fine-tuned protocols for producing cerebral cortex-specific organoids were later reported (Paşca et al., 2015; Qian et al., 2016, 2018). These brain organoids have been used to study many diseases, such as lissencephaly (Iefremova et al., 2017), Zika virus infection (Qian et al., 2016), and ischemia (Paşca et al., 2019). Additionally, human brain organoids have contributed to investigations of neural development, such as differentiation (Paşca et al., 2015; Qian et al., 2016; Trujillo et al., 2019) and migration (Birey et al., 2017). The formation of precise neural networks and interactions between specific neurons are indispensable for information processing, but limited research on neural circuits has been conducted with human brain organoids. Direct investigation of neural circuits through the use of human organoids will contribute to the elucidation of the mechanisms that underlie the properties of human circuits. This approach will also facilitate the understanding of the mechanisms behind neural circuit-associated developmental diseases.

The developing human brain possesses human-specific cells, structures, gene expression profiles and functions. There is a 1,000-fold difference in brain volume and the number of cells in the brain between humans and mice (Hodge et al., 2019). In humans, outer radial glial cells, which are rare in rodents, produce a large number of cortical layer neurons and enable marked expansion and high complexity of the human cerebral cortex (Hansen et al., 2010; Pollen et al., 2015). *ARHGAP11B*, a human-specific gene that specifically expressed in radial glial cells, may contribute to this expansion in humans (Florio et al., 2015). In addition, human neural circuits are apparently distinct from those of mice. For example, humans harbor unique neuronal circuits around the caudate nucleus and anterior putamen that are associated with executive function and social/language regions in the striatum; however, these circuits are absent in mice (Balsters et al., 2020). In the spinal cord, the pyramidal tract descends from the motor cortex through the lateral column in humans and through the dorsal column in rodents (Lemon, 2008). Some human pyramidal neuron axons make direct connections with spinal motor neurons that are responsible for fine motor skills; however, in mice, pyramidal neuron axons mainly contact motor neurons via interneurons (Lemon, 2008). In humans, approximately 40% of the axons of retinal ganglion cells (RGCs) do not cross the midline at the optic chiasm to innervate the ipsilateral side, whereas in mice, most RGC axons cross the midline, thereby establishing a structural basis for binocular or monocular vision (Petros et al., 2008). In addition, potent human-specific excitatory connections exist between pyramidal neurons and GABAergic inhibitory interneurons, through which a single action potential from a pyramidal cell can induce polysynaptic GABAergic firing of interneurons (Molnár et al., 2008; Szegedi et al., 2016). Finally, human pyramidal neurons are known to have 4 times more docked vesicles at 2 times larger active zones than rat pyramidal neurons (Molnár et al., 2016). Many of these previous studies on human samples were carried out with biopsy/abortion samples, which have many disadvantages, including multiple genetic backgrounds, inconsistencies in patient age, and damage from surgery and diseases.

Fortunately, we can now employ human brain organoids to acquire genetically homogenous samples and introduce genetic manipulations, such as knockout of specific genes by CRISPR/Cas9-mediated genome editing. Although brain organoids still have the issues of variability and artificial metabolic stress, organoid technology provides a novel approach for investigating human neural circuits. In this review, we discuss previous accomplishments and future research directions regarding the use of organoids for studying neural circuits. Additionally, we address the current limitations of organoid technology in studying neural circuits and means for overcoming these limitations.

USE OF HUMAN BRAIN ORGANOIDS FOR RESEARCH ON TOPICS OTHER THAN NEURAL CIRCUIT FORMATION

Currently, there are two major protocols for generating brain organoids from pluripotent stem cells. In the first protocol (Lancaster et al., 2013), pluripotent stem cells are differentiated into brain organoids mostly through intrinsic signals; therefore, almost no additional growth factors are required. This protocol yields a random variety of brain components, such as the retina, hippocampus, cerebral cortex and colloid plexus, in each organoid (Lancaster et al., 2013). Neurons in organoids induced by this protocol mature into glutamatergic excitatory neurons and GABAergic inhibitory neurons after 3 months of cultivation (Matsui et al., 2018). Additionally, oligodendrocytes emerge after 6 months of cultivation and form myelin sheath-like structures around axons in the organoids (Matsui et al., 2018). Furthermore, microglial cells, of mesodermal origin, are also present in the long-cultivated organoids (Ormel et al., 2018). While these cerebral organoids resemble the developing human brain, in which intrinsic signals autonomously orchestrate the stepwise differentiation of each component, the low reproducibility and high variability of the induced brain components in the organoids sometimes limit the use of this protocol. The other major protocol for generating brain organoids requires fine tuning of additional growth factors such as BDNF, GDNF and NT-3. This protocol gives rise to more specific components with less variability than the previously mentioned protocol and is able to selectively induce specific brain components, such as the cerebral cortex, brainstem, midbrain, retina, cerebellum, and basal ganglia, in organoids (Paşca et al., 2015; Qian et al., 2016). The brain organoids generated by these two distinct methods have much in common; both types of organoids contain multiple neural cell populations, such as neural stem cells (NSCs), neurons and astrocytes, and exhibit basic neural structures, with NSCs surrounding ventricle-like cavities and neurons on the surface of NSC region forming layered structures similar to those in the developing human brain.

Organoid technology has provided new insights into human brain development and diseases. For example, in the field of development, studies on organoids have revealed that the *retinoblastoma* gene regulates apoptosis of NSCs and neuronal migration in humans (Matsui et al., 2017). Analysis of developing human brain organoids have revealed that the wrinkled structure of the human brain can be explained by two different mechanical forces that act on different regions of organoids, namely, cytoskeletal contraction at the core and nuclear accumulation at the perimeter (Karzbrun et al., 2018). In addition, molecular analysis of human cerebral organoids has shown that suppression of PTEN signaling is a key mechanism underlying proliferation of neural progenitor cells and subsequent folding of the cerebral cortex specifically in the human brain (Li et al., 2017). Evolutionary analysis comparing gene expression profiles in human brain organoids and those of other primates identified the mTOR pathway, which is specifically activated in human radial glial cells, as a signaling pathway that is unique to humans (Pollen et al., 2019). Furthermore, in the field of disease modeling, this technology has been used to demonstrate that impairment of N-cadherin/β-catenin signaling is a crucial mechanism underlying lissencephaly caused by deficiency of the LIS1/NDEL1/14.3.3ϵ complex (Iefremova et al., 2017). Investigation of the mechanism of Zika virus infection platforming organoids identified neural progenitor cells as the cell population that is primarily affected by infection (Qian et al., 2016). Additionally, brain organoid-based modeling of fetal brain hypoxia has revealed that intermediate progenitors in the subventricular zone are mainly damaged under hypoxic conditions, which was confirmed in patient samples (Paşca et al., 2019).

Thus, the multicellular and layered human brain-like structure of brain organoids has greatly contributed to the understanding of the mechanisms underlying human brain development and diseases.

CURRENT ANALYSIS OF HUMAN NEURAL CIRCUITS IN BRAIN ORGANOIDS

Organoid technology has only been applied in a few studies on the process of human neural circuit formation. To establish functional neural circuits, neurons precisely follow stepwise processes, including cell migration, axonal projection, dendritic growth, synapse formation and synapse elimination. Among those steps, so far, several organoid-based researches on cell migration, axonal projection and synapse formation have been published (Birey et al., 2017; Xiang et al., 2019). In this section, we discuss the use of human brain organoids for the analysis of neural circuits.

In humans as well as rodents, newborn neurons migrate radially or tangentially to a preprogrammed destination in the cerebral cortex and form a specific neural network (Marín et al., 2010; Bartolini et al., 2013; Paredes et al., 2016). In humans, excitatory glutamatergic neurons differentiate from radial glial cells around the lateral ventricles at approximately gestational week 15 and undergo directional radial migration to establish a six-layered structure (Das and Takahashi, 2018; Larkum et al., 2018). Electrophysiological analysis conducted in the mouse brain revealed that pyramidal neurons in layers II, III, IV, and V form local excitatory microcircuits between cortical layers, with prominent excitatory pathways from layer II/III to layer V (Thomson and Bannister, 2003; Hooks et al., 2011). However, these local excitatory circuits have not been analyzed in detail in human samples. Human brain organoids are able to partially recapitulate radial migration, producing cerebral cortex-like neuronal layers. Mice and humans share the same basic layered cortical structure composed of distinct neurons expressing markers specific for each of the six cortical layers: REELIN for layer I, CUX1 for layer II, BRN2 for layer III, SATB2 for layer IV, CTIP2 for layer V and TBR1 for layer VI (Leone et al., 2008; Qian et al., 2016). Forebrain organoids, which can be generated by the fine tuning of growth factors, reportedly include neurons expressing marker genes for each of the six neuronal layers, although the boundaries of cortical neural layers in forebrain organoids are not as distinct as those in the human fetal brain (Qian et al., 2016). The expression of layer-specific marker genes indicates that neurons in forebrain organoids recapitulate the gene expression profile of the human brain. Satb2, Ctip2, and Tbr1 are known to be transcription factors that determine the identity of neurons and affect the pattern of axonal projection and connectivity in rodents (Leone et al., 2008). Thus, for example, Satb2-expressing neurons in forebrain organoids likely establish, perhaps only partially, intracortical circuits that mimic those in the human cerebral cortex.

In humans, at approximately gestational week 17, inhibitory GABAergic interneurons originating from the ganglionic eminence migrate tangentially into the cerebral cortex (**Figure 1A**), connect to glutamatergic excitatory neurons via synapses, and form microcircuits in the cerebral cortex (Rakic and Zecevic, 2003). Mimicking tangential migration in organoids is more difficult than mimicking radial migration because tangentially migrating neurons travel a long distance between distinct components. In the fetal brain, the ganglionic eminence and the cerebral cortex develop in a highly synchronized manner that cannot be completely recapitulated simultaneously by current organoid technology. Thus, fused organoids composed of the glutamatergic excitatory neuron-rich cerebral organoids and GABAergic interneuron-rich subpallium organoids induced by fine tuning of growth factors have been generated to model neuronal migration between distant components (Birey et al., 2017; Xiang et al., 2017; **Figure 1A**). GABAergic interneurons reportedly migrate from subpallium organoids to cerebral organoids and form synapses with local glutamatergic neurons (Birey et al., 2017; Xiang et al., 2017). This observation indicates the existence of a mechanism allowing orientation of neuronal migration followed by synapse formation in the fused organoid system. Moreover, in these fused organoids, stimulation of migrated GABAergic interneurons induced evoked inhibitory postsynaptic currents in glutamatergic neurons, while stimulation of glutamatergic neurons induced evoked excitatory postsynaptic currents in GABAergic interneurons

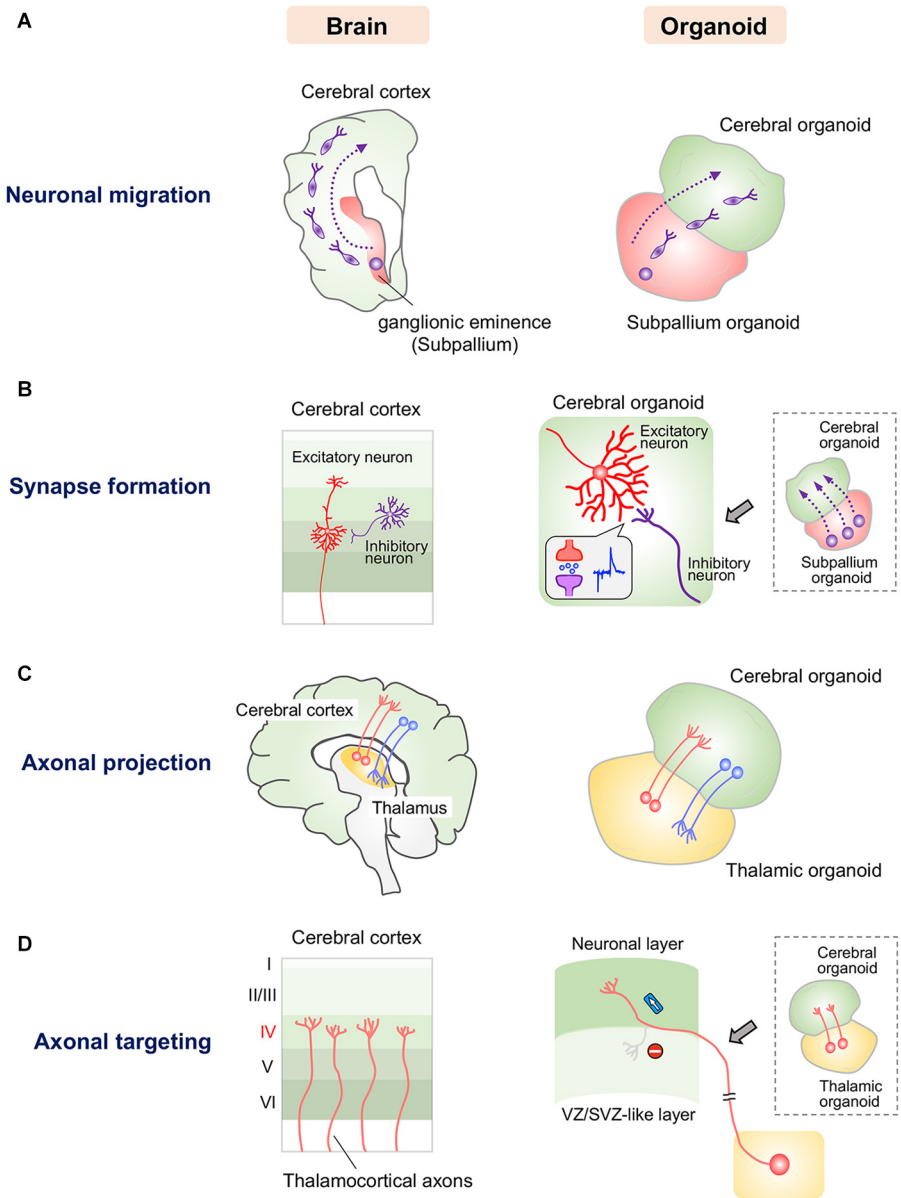

FIGURE 1 | Current approaches for modeling human neuronal circuit formation with fused brain organoids. **(A)** Left: Tangential migration of GABAergic interneurons from the ganglionic eminence to the cerebral cortex in the human brain. Right: GABAergic interneurons in subpallium organoids migrate into the cerebral organoid in fused organoids. **(B)** Left: Synapse formation between excitatory and inhibitory neurons in the human cerebral cortex. Right: GABAergic interneurons that migrate from subpallium organoids form functional synapses with excitatory neurons in cerebral organoids. **(C)** Left: Reciprocal axonal projection between the thalamus and cerebral cortex in the human brain. Right: Thalamic and cortical neurons reciprocally project axons into the other organoid in the fused system. **(D)** Left: Thalamocortical axons specifically innervate layer 4 of the somatosensory cortex. Right: Axons of thalamic organoids selectively innervate the neuronal layer but not the VZ/SVZ-like layer, in which neural stem/progenitor cells reside, in the fused cerebral organoid system.

(Birey et al., 2017; **Figure 1B**). These findings indicate that migrated GABAergic neurons are functionally integrated into local excitatory circuits in cerebral organoids (Birey et al., 2017). Additionally, human cerebral organoids and thalamic organoids have been combined to model the thalamocortical circuit (Xiang et al., 2019; **Figure 1C**). Cortical neurons and thalamic neurons extend axons and form synapses with each other, recapitulating the reciprocal thalamocortical axonal projections involved in the transmission of sensory and motor information in the human brain (López-Bendito and Molnár, 2003; Xiang et al., 2019). Interestingly, thalamic organoid-derived axons selectively innervate the upper neuronal layers of cortical organoids, avoiding the lower VZ/SVZ-like region in which NSCs reside (**Figure 1D**). This selectivity indicates that like the human brain, fused thalamocortical organoids possess orchestrated molecular machinery for proper axonal guidance and targeting.

The above mentioned six-layered forebrain organoids may be fused with other region-specific organoids in the future for analysis of the detailed patterns of neuronal migration, axonal innervation and synapse formation (Qian et al., 2016; Birey et al., 2017; Xiang et al., 2019). In addition, we may be able to utilize genome editing technology to analyze the fine structures of human neural circuits in brain organoids by labeling specific types of neurons with fluorescent reporter genes. We are also able to investigate the molecular mechanisms underlying human neural circuit formation through genome editing-mediated knockout of candidate genes. Moreover, the newly developed microelectrode array system will help us measure neural activity at the circuit level in organoids and facilitate functional mapping of neural networks formed in organoids.

CURRENT OBSTACLES AND PERSPECTIVES FOR ORGANOID-BASED ANALYSIS OF NEURAL CIRCUITS

As described above, there have been some reports on neuronal migration, axonal projection and synapse formation in fused human brain organoids, although the molecular mechanisms underlying these events have not been studied (Birey et al., 2017; Xiang et al., 2019). During neural development, spatiotemporally coordinated expression of various guidance molecules and cell adhesion molecules is essential for establishing precise neural circuits. These molecules are expressed by specific cells and sometimes form local gradients in restricted brain regions, enabling proper neuronal migration, axonal guidance, and synapse formation. However, the organoids generated by the currently available protocols possess multiple randomly positioned neural tube-like structures and therefore lack a fixed structural axis (**Figure 2A**). Morphogen gradients, such as sonic hedgehog (SHH) gradients and fibroblast growth factor gradients (Stevens et al., 2010; Oosterveen et al., 2012; Bökel and Brand, 2013), in organoids are indispensable for establishing appropriately positioned brain components that lead to precise circuit formation, especially in the early stage of neural differentiation. Nevertheless, the generation of morphogen gradients in current brain organoid protocols has rarely been successful.

To generate brain organoids bearing molecular gradients, we should first focus on relatively simple neural structures, such as the spinal cord. In the developing spinal cord, the gradients of morphogens, such as SHH and bone morphogenetic protein (BMP), play key roles in the determination of regional identity in the early developmental stage (Shirasaki and Pfaff, 2002; Ulloa and Briscoe, 2007; Osseward and Pfaff, 2019). The balance between roof plate-derived BMP and floor plate-derived SHH defines regional identity along the dorsoventral axis in the spinal cord. Subsequently, each neural progenitor cell along the dorsoventral axis acquires a region-specific expression profile of transcription factors that leads to differentiation of the cell into a specific neuronal subtype (Shirasaki and Pfaff, 2002; Ulloa and Briscoe, 2007; Osseward and Pfaff, 2019). Then, each neuron expresses a set of cell type-specific receptors for chemoattractants and cell adhesion molecules to form each circuit.

Although several groups have reported the generation of spinal cord organoids, these spinal cord organoids lack the proper molecular gradients (Ogura et al., 2018; Duval et al., 2019). Thus far, organoids mimicking the dorsal and ventral parts of the spinal cord cannot be induced simultaneously; therefore, these organoids fail to recapitulate the exact regionality and cell type specificity of the spinal cord. Because of these limitations, analysis of neural circuits seems impossible in these organoids (Ogura et al., 2018; Duval et al., 2019). The generation of spinal cord organoids with morphogen gradients may lead to region-specific expression of transcription factors and subsequent autonomous differentiation into specific neuronal subtypes. In addition, morphogen gradients may also produce surrounding cells such as floor plate cells, which secrete several axonal guidance molecules, including netrin and slit.

Newly developed devices, such as microfluidic devices and molds, are attracting interest for studying morphogen gradient axes in organoids (**Figure 2B**). A group reported successful modeling of the structure of the neural tube by the combined use of a mold, which enables the formation of a tube-like structure by pluripotent stem cells, and a microfluidic device, which produces a Wnt gradient that is critical for rostrocaudal axis formation in the neural tube (Rifes et al., 2020). In this study, a tube-like structure acquired region-specific gene expression profiles along the rostrocaudal axis under the action of a Wnt gradient. The rostral region exposed to low concentration of Wnt showed the marked expression of OTX2, a highly expressed gene in the developing forebrain and midbrain, while the caudal region exposed to high concentration of Wnt expressed GBX2, a highly expressed gene in the developing hindbrain. Additionally, transplantation of morphogen-secreting cells into the organoid may allow the formation of the dorsoventral axis. Indeed, embedding of SHH-secreting human pluripotent stem cells at one pole of a cerebral organoid was shown to successfully induce an SHH gradient and subsequent gene expression topography in one organoid, even though multiple neural structures randomly emerged in the organoid (Cederquist et al., 2019). Moreover, SHH-secreting floor plate-like tissue can be induced from pluripotent stem cells (Fasano et al., 2010).

Thus, by utilizing existing technologies, it may be feasible to generate spinal cord organoids with rostrocaudal and dorsoventral axes in the near future. If we obtain such organoids, we may recapitulate complicated spinal neural circuits, such as a circuit of commissural neurons that project axons that first extend ventrally, cross the midline, and subsequently turn orthogonally toward the anterior direction to form synapses with targets.

POTENTIAL MODELING OF THE SYNAPTIC PRUNING WITH BRAIN ORGANOIDS

In the course of neural circuit formation, neurons transiently form excess synapses. In rodents, some inactive synapses are

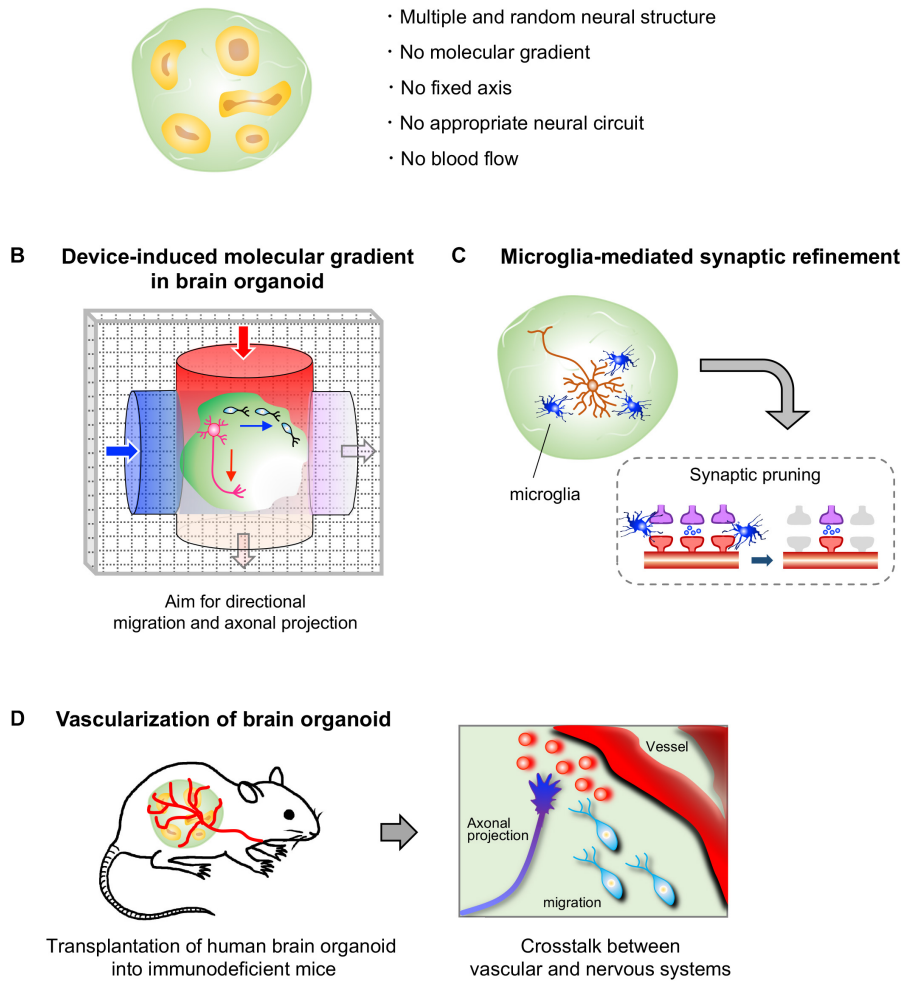

FIGURE 2 | Current limitations to brain organoids and prospective approaches. **(A)** Human brain organoids generated by current protocols lack a self-generating molecular gradient, as well as blood flow. These limitations hamper the formation of a structural axis assembled by orderly-positioned brain components; therefore the formation of appropriate neural circuits in brain organoids is impeded. **(B)** A device that generates molecular gradients would be effective in inducing directional migration and axonal projections, as well as a structural axis. Embedding of cells that secrete a certain molecule such as morphogens may also help to generate molecular gradients in brain organoids (not depicted). **(C)** Human brain organoids that contain microglial cells may allow us to analyze a process of synaptic refinement, such as microglia-mediated synapse pruning, in human neural circuits. **(D)** The transplantation of human brain organoids into highly vascularized organs of immunodeficient mice may allow us to analyze vascular system-mediated neural circuit formation in humans.

removed after birth, mainly by microglial cells, which selectively leave functional synapses (Paolicelli et al., 2011; Schafer et al., 2012). Brain organoids have not yet been utilized to investigate the pruning processes in humans. To model this phenomenon with brain organoids, both microglial cells and firing neurons with synapses must be included in a single organoid because microglial cells engulf the synapses of neurons with low neuronal activity (Schafer et al., 2012; **Figure 2C**). Neuronal firing has already been observed in some brain organoids (Giandomenico et al., 2019; Trujillo et al., 2019; Eura et al., 2020), and synapse formation between neurons has also been observed in long-cultivated organoids and fused organoids (Birey et al., 2017; Trujillo et al., 2019; Xiang et al., 2019). Microglial cells are not expected to be present in brain organoids because microglial cells are yolk sac-derived mesodermal cells (Gomez Perdiguero et al., 2015), whereas brain organoids are established by neuroectodermal induction. However, microglial cells expressing IBA-1, a microglial marker, have been detected in the brain organoids induced by the autonomous differentiation protocol without fine tuning of growth factors (Lancaster et al., 2013; Ormel et al., 2018). It is possible that, in this protocol, a few pluripotent cells differentiate into mesodermal linage cells as a result of weak neuroectodermal induction without fine tuning. Additionally, methods for inducing pure microglial populations from ES/iPSCs are already available (Muffat et al., 2016). Thus, theoretically, we are now able to model the human

brain with microglia through appropriate selection of a brain organoid protocol or by mixing human brain organoids with microglial cells induced from pluripotent stem cells. Accordingly, human brain organoids are expected to become a powerful tool for analyzing the molecular mechanism underlying microglia-mediated synaptic pruning. We can also manipulate neuronal firing in organoids through optogenetic tools and knockout specific genes by genome editing, which will further facilitate research on synaptic pruning. The establishment of a method for inducing organoids along with abundant microglial cells will also facilitate the development of more sophisticated brain organoids because microglial cells have been shown to support the proliferation of NSCs and neuronal survival in rodents (Ueno et al., 2013; Matsui and Mori, 2018).

POTENTIAL ANALYSIS OF VASCULAR SYSTEM-MEDIATED NEURAL CIRCUIT FORMATION WITH BRAIN ORGANOIDS

Blood vessels are another major non-neuronal component of the brain and are mainly composed of endothelial cells, smooth muscle cells and pericytes. In perinatal mice, neuroblasts around the corpus callosum require blood vessels as scaffolds for radial migration to cortical neuronal layers (Le Magueresse et al., 2012). Blood vessels also serve as scaffolds for elongating neurites in the cortical germinal zone (Stubbs et al., 2009). Several vascular-derived molecules have been identified to regulate neural circuit development. GABA and VEGF-A secreted by vascular vessels control tangential migration of interneurons from the medial ganglionic eminence to the cerebral cortex in mice (Inada et al., 2011; Won et al., 2013; Barber et al., 2018). Endothelin derived from endothelial cells directs the extension of sympathetic axons and their innervation of the external carotid artery (Makita et al., 2008). In addition to playing a regulatory role in migration, VEGF also facilitates synaptogenesis in the cerebral cortex (Wu et al., 2019). However, blood vessel-mediated neural circuit formation has yet to be confirmed in humans.

While several vascular cells, such as endothelial cells and smooth muscle cells, can be observed in brain organoids (Logan et al., 2020), a self-organizing vessel structure is absent in brain organoids generated with current protocols. On the other hand, several groups have achieved vascularization of human brain organoids by utilizing the mouse vascular system via transplantation of human brain organoids into the brains or limbs of immunodeficient mice (Daviaud et al., 2018; Mansour et al., 2018; Cakir et al., 2019; Shi et al., 2020). Thus, these vascularized organoids are expected to contribute to analyze the effect of vascularization on neural circuit formation in humans in the near future. Brain organoid-based modeling may provide an opportunity for studying the interaction between human vascular and neuronal systems, as no methods are currently available (**Figure 2D**).

CONCLUDING REMARKS

Research on human neural circuits in organoids has just begun. Fused organoids partially model some steps in the process of neural circuit formation. However, there are still many obstacles to mimicking human neural circuits in brain organoids. Thus, we need more sophisticated brain organoids containing a combination of functional neuronal types, brain residential non-neuronal cells, vascular structures, and perhaps most importantly, regionalizing mechanisms. Once we overcome these obstacles, we will be able to elucidate the human-specific molecular mechanisms that underlie neural circuits, leading to future modulation of human neural circuits.

AUTHOR CONTRIBUTIONS

TM and KK contributed to the writing and editing of the manuscript. YT contributed to the editing of the manuscript. All authors contributed to the article and approved the submitted version.

FUNDING

This work was supported by grants from the JSPS (KAKENHI #19K22476 and #20H03352), the Takeda Science Foundation and the Naito Science & Engineering Foundation to KK, as well as research grants from the JSPS (KAKENHI #19K16925), AMED The Program for Technological Innovation of Regenerative Medicine (JP19bm0704039h), and AMED Osaka University Seeds (A) to TM.

REFERENCES

Balsters, J. H., Zerbi, V., Sallet, J., Wenderoth, N., and Mars, R. B. (2020). Primate homologs of mouse cortico-striatal circuits. *Elife* 9:e53680. doi: 10.7554/eLife.53680

Barber, M., Andrews, W. D., Memi, F., Gardener, P., Ciantar, D., Tata, M., et al. (2018). Vascular-Derived Vegfa Promotes Cortical Interneuron Migration and Proximity to the Vasculature in the Developing Forebrain. *Cereb. Cortex* 28, 2577–2593. doi: 10.1093/cercor/bhy082

Bartolini, G., Ciceri, G., and Marín, O. (2013). Integration of GABAergic interneurons into cortical cell assemblies: lessons from embryos and adults. *Neuron* 79, 849–864. doi: 10.1016/j.neuron.2013.08.014

Birey, F., Andersen, J., Makinson, C. D., Islam, S., Wei, W., Huber, N., et al. (2017). Assembly of functionally integrated human forebrain spheroids. *Nature* 545, 54–59. doi: 10.1038/nature22330

Bökel, C., and Brand, M. (2013). Generation and interpretation of FGF morphogen gradients in vertebrates. *Curr. Opin. Genet. Dev.* 23, 415–422. doi: 10.1016/j.gde.2013.03.002

Cakir, B., Xiang, Y., Tanaka, Y., Kural, M. H., Parent, M., Kang, Y. J., et al. (2019). Engineering of human brain organoids with a functional vascular-like system. *Nat. Methods* 16, 1169–1175. doi: 10.1038/s41592-019-0586-5

Cederquist, G. Y., Asciolla, J. J., Tchieu, J., Walsh, R. M., Cornacchia, D., Resh, M. D., et al. (2019). Specification of positional identity in forebrain organoids. *Nat. Biotechnol.* 37, 436–444. doi: 10.1038/s41587-019-0085-3

Das, A., and Takahashi, E. (2018). Neuronal Migration and Axonal Pathways Linked to Human Fetal Insular Development Revealed by Diffusion MR Tractography. *Cereb. Cortex* 28, 3555–3563. doi: 10.1093/cercor/bhx224

Daviaud, N., Friedel, R. H., and Zou, H. (2018). Vascularization and Engraftment of Transplanted Human Cerebral Organoids in Mouse Cortex. *eNeuro* 5, 219–218. doi: 10.1523/ENEURO.0219-18.2018

Duval, N., Vaslin, C., Barata, T. C., Frarma, Y., Contremoulins, V., Baudin, X., et al. (2019). BMP4 patterns Smad activity and generates stereotyped cell fate organization in spinal organoids. *Development* 146:dev175430. doi: 10.1242/dev.175430

Dye, B. R., Hill, D. R., Ferguson, M. A., Tsai, Y. H., Nagy, M. S., Dyal, R., et al. (2015). In vitro generation of human pluripotent stem cell derived lung organoids. *Elife* 4:e05098. doi: 10.7554/eLife.05098

Eiraku, M., Takata, N., Ishibashi, H., Kawada, M., Sakakura, E., Okuda, S., et al. (2011). Self-organizing optic-cup morphogenesis in three-dimensional culture. *Nature* 472, 51–56. doi: 10.1038/nature09941

Eura, N., Matsui, T. K., Luginbühl, J., Matsubayashi, M., Nanaura, H., Shiota, T., et al. (2020). Brainstem Organoids From Human Pluripotent Stem Cells. *Front. Neurosci.* 14:538. doi: 10.3389/fnins.2020.00538

Fasano, C., Chambers, S., Lee, G., Tomishima, M., and Studer, L. (2010). Efficient Derivation of Functional Floor Plate Tissue from Human Embryonic Stem Cells. *Cell Stem Cell* 6, 336–347. doi: 10.1016/j.stem.2010.03.001

Florio, M., Albert, M., Taverna, E., Namba, T., Brandl, H., Lewitus, E., et al. (2015). Human-specific gene ARHGAP11B promotes basal progenitor amplification and neocortex expansion. *Science* 347, 1465–1470. doi: 10.1126/science.aaa1975

Giandomenico, S. L., Mierau, S. B., Gibbons, G. M., Wenger, L. M. D., Masullo, L., Sit, T., et al. (2019). Cerebral organoids at the air-liquid interface generate diverse nerve tracts with functional output. *Nat. Neurosci.* 22, 669–679. doi: 10.1038/s41593-019-0350-2

Gomez Perdiguero, E., Klapproth, K., Schulz, C., Busch, K., Azzoni, E., Crozet, L., et al. (2015). Tissue-resident macrophages originate from yolk-sac-derived erythro-myeloid progenitors. *Nature* 518, 547–551. doi: 10.1038/nature13989

Hansen, D. V., Lui, J. H., Parker, P. R., and Kriegstein, A. R. (2010). Neurogenic radial glia in the outer subventricular zone of human neocortex. *Nature* 464, 554–561. doi: 10.1038/nature08845

Hodge, R. D., Bakken, T. E., Miller, J. A., Smith, K. A., Barkan, E. R., Graybuck, L. T., et al. (2019). Conserved cell types with divergent features in human versus mouse cortex. *Nature* 573, 61–68. doi: 10.1038/s41586-019-1506-7

Hooks, B. M., Hires, S. A., Zhang, Y. X., Huber, D., Petreanu, L., Svoboda, K., et al. (2011). Laminar analysis of excitatory local circuits in vibrissal motor and sensory cortical areas. *PLoS Biol.* 9:e1000572. doi: 10.1371/journal.pbio.1000572

Iefremova, V., Manikakis, G., Krefft, O., Jabali, A., Weynans, K., Wilkens, R., et al. (2017). An Organoid-Based Model of Cortical Development Identifies Non-Cell-Autonomous Defects in Wnt Signaling Contributing to Miller-Dieker Syndrome. *Cell Rep.* 19, 50–59. doi: 10.1016/j.celrep.2017.03.047

Inada, H., Watanabe, M., Uchida, T., Ishibashi, H., Wake, H., Nemoto, T., et al. (2011). GABA regulates the multidirectional tangential migration of GABAergic interneurons in living neonatal mice. *PLoS One* 6:e27048. doi: 10.1371/journal.pone.0027048

Jo, J., Xiao, Y., Sun, A. X., Cukuroglu, E., Tran, H. D., Göke, J., et al. (2016). Midbrain-like Organoids from Human Pluripotent Stem Cells Contain Functional Dopaminergic and Neuromelanin-Producing Neurons. *Cell Stem Cell* 19, 248–257. doi: 10.1016/j.stem.2016.07.005

Jung, P., Sato, T., Merlos-Suárez, A., Barriga, F. M., Iglesias, M., Rossell, D., et al. (2011). Isolation and in vitro expansion of human colonic stem cells. *Nat. Med.* 17, 1225–1227. doi: 10.1038/nm.2470

Karzbrun, E., Kshirsagar, A., Cohen, S. R., Hanna, J. H., and Reiner, O. (2018). Human Brain Organoids on a Chip Reveal the Physics of Folding. *Nat. Phys.* 14, 515–522. doi: 10.1038/s41567-018-0046-7

Lancaster, M. A., Renner, M., Martin, C. A., Wenzel, D., Bicknell, L. S., Hurles, M. E., et al. (2013). Cerebral organoids model human brain development and microcephaly. *Nature* 501, 373–379. doi: 10.1038/nature12517

Larkum, M. E., Petro, L. S., Sachdev, R. N. S., and Muckli, L. (2018). A Perspective on Cortical Layering and Layer-Spanning Neuronal Elements. *Front. Neuroanat.* 12:56. doi: 10.3389/fnana.2018.00056

Le Magueresse, C., Alfonso, J., Bark, C., Eliava, M., Khrulev, S., and Monyer, H. (2012). Subventricular zone-derived neuroblasts use vasculature as a scaffold to migrate radially to the cortex in neonatal mice. *Cereb. Cortex* 22, 2285–2296. doi: 10.1093/cercor/bhr302

Lemon, R. N. (2008). Descending pathways in motor control. *Annu. Rev. Neurosci.* 31, 195–218. doi: 10.1146/annurev.neuro.31.060407.125547

Leone, D. P., Srinivasan, K., Chen, B., Alcamo, E., and McConnell, S. K. (2008). The determination of projection neuron identity in the developing cerebral cortex. *Curr. Opin. Neurobiol.* 18, 28–35. doi: 10.1016/j.conb.2008.05.006

Li, Y., Muffat, J., Omer, A., Bosch, I., Lancaster, M. A., Sur, M., et al. (2017). Induction of Expansion and Folding in Human Cerebral Organoids. *Cell Stem Cell* 20, 385.e–396.e. doi: 10.1016/j.stem.2016.11.017

Logan, S., Arzua, T., Yan, Y., Jiang, C., Liu, X., Yu, L. K., et al. (2020). Dynamic Characterization of Structural, Molecular, and Electrophysiological Phenotypes of Human-Induced Pluripotent Stem Cell-Derived Cerebral Organoids, and Comparison with Fetal and Adult Gene Profiles. *Cells* 9:1301. doi: 10.3390/cells9051301

López-Bendito, G., and Molnár, Z. (2003). Thalamocortical development: how are we going to get there? *Nat. Rev. Neurosci.* 4, 276–289. doi: 10.1038/nrn1075

Makita, T., Sucov, H. M., Gariepy, C. E., Yanagisawa, M., and Ginty, D. D. (2008). Endothelins are vascular-derived axonal guidance cues for developing sympathetic neurons. *Nature* 452, 759–763. doi: 10.1038/nature06859

Mansour, A. A., Gonçalves, J. T., Bloyd, C. W., Li, H., Fernandes, S., Quang, D., et al. (2018). An in vivo model of functional and vascularized human brain organoids. *Nat. Biotechnol.* 36, 432–441. doi: 10.1038/nbt.4127

Marín, O., Valiente, M., Ge, X., and Tsai, L. H. (2010). Guiding neuronal cell migrations. *Cold. Spring Harb. Perspect. Biol.* 2:a001834. doi: 10.1101/cshperspect.a001834

Matsui, T., Nieto-Estévez, V., Kyrychenko, S., Schneider, J. W., and Hsieh, J. (2017). Retinoblastoma protein controls growth, survival and neuronal migration in human cerebral organoids. *Development* 144, 1025–1034. doi: 10.1242/dev.143636

Matsui, T. K., Matsubayashi, M., Sakaguchi, Y. M., Hayashi, R. K., Zheng, C., Sugie, K., et al. (2018). Six-month cultured cerebral organoids from human ES cells contain matured neural cells. *Neurosci. Lett.* 670, 75–82. doi: 10.1016/j.neulet.2018.01.040

Matsui, T. K., and Mori, E. (2018). Microglia support neural stem cell maintenance and growth. *Biochem. Biophys. Res. Commun.* 503, 1880–1884. doi: 10.1016/j.bbrc.2018.07.130

Molnár, G., Oláh, S., Komlósi, G., Füle, M., Szabadics, J., Varga, C., et al. (2008). Complex events initiated by individual spikes in the human cerebral cortex. *PLoS Biol.* 6:e222. doi: 10.1371/journal.pbio.0060222

Molnár, G., Rózsa, M., Baka, J., Holderith, N., Barzó, P., Nusser, Z., et al. (2016). Human pyramidal to interneuron synapses are mediated by multi-vesicular release and multiple docked vesicles. *Elife* 5:e18167. doi: 10.7554/eLife.18167

Muffat, J., Li, Y., Yuan, B., Mitalipova, M., Omer, A., Corcoran, S., et al. (2016). Efficient derivation of microglia-like cells from human pluripotent stem cells. *Nat. Med.* 22, 1358–1367. doi: 10.1038/nm.4189

Muguruma, K., Nishiyama, A., Kawakami, H., Hashimoto, K., and Sasai, Y. (2015). Self-organization of polarized cerebellar tissue in 3D culture of human pluripotent stem cells. *Cell Rep.* 10, 537–550. doi: 10.1016/j.celrep.2014.12.051

Ogura, T., Sakaguchi, H., Miyamoto, S., and Takahashi, J. (2018). Three-dimensional induction of dorsal, intermediate and ventral spinal cord tissues from human pluripotent stem cells. *Development* 145:dev162214. doi: 10.1242/dev.162214

Oosterveen, T., Kurdija, S., Alekseenko, Z., Uhde, C. W., Bergsland, M., Sandberg, M., et al. (2012). Mechanistic differences in the transcriptional interpretation of local and long-range Shh morphogen signaling. *Dev. Cell* 23, 1006–1019. doi: 10.1016/j.devcel.2012.09.015

Ormel, P. R., Vieira, de Sá, R., van Bodegraven, E. J., Karst, H., Harschnitz, O., et al. (2018). Microglia innately develop within cerebral organoids. *Nat. Commun.* 9:4167. doi: 10.1038/s41467-018-06684-2

Osseward, P., and Pfaff, S. (2019). Cell type and circuit modules in the spinal cord. *Curr. Opin. Neurobiol.* 56, 175–184. doi: 10.1016/j.conb.2019.03.003

Paolicelli, R. C., Bolasco, G., Pagani, F., Maggi, L., Scianni, M., Panzanelli, P., et al. (2011). Synaptic pruning by microglia is necessary for normal brain development. *Science* 333, 1456–1458. doi: 10.1126/science.1202529

Paredes, M. F., James, D., Gil-Perotin, S., Kim, H., Cotter, J. A., Ng, C., et al. (2016). Extensive migration of young neurons into the infant human frontal lobe. *Science* 354:aaf7073. doi: 10.1126/science.aaf7073

Paşca, A. M., Sloan, S. A., Clarke, L. E., Tian, Y., Makinson, C. D., Huber, N., et al. (2015). Functional cortical neurons and astrocytes from human pluripotent stem cells in 3D culture. *Nat. Methods* 12, 671–678. doi: 10.1038/nmeth.3415

Paşca, A. M., Park, J. Y., Shin, H. W., Qi, Q., Revah, O., Krasnoff, R., et al. (2019). Human 3D cellular model of hypoxic brain injury of prematurity. *Nat. Med.* 25, 784–791. doi: 10.1038/s41591-019-0436-0

Pellegrini, L., Bonfio, C., Chadwick, J., Begum, F., Skehel, M., and Lancaster, M. A. (2020). Human CNS barrier-forming organoids with cerebrospinal fluid production. *Science* 369:eaaz5626. doi: 10.1126/science.aaz5626

Petros, T. J., Rebsam, A., and Mason, C. A. (2008). Retinal axon growth at the optic chiasm: to cross or not to cross. *Annu. Rev. Neurosci.* 31, 295–315. doi: 10.1146/annurev.neuro.31.060407.125609

Pollen, A. A., Bhaduri, A., Andrews, M. G., Nowakowski, T. J., Meyerson, O. S., Mostajo-Radji, M. A., et al. (2019). Establishing Cerebral Organoids as Models of Human-Specific Brain Evolution. *Cell* 176, 743.e–756.e. doi: 10.1016/j.cell.2019.01.017

Pollen, A. A., Nowakowski, T. J., Chen, J., Retallack, H., Sandoval-Espinosa, C., Nicholas, C. R., et al. (2015). Molecular identity of human outer radial glia during cortical development. *Cell* 163, 55–67. doi: 10.1016/j.cell.2015.09.004

Qian, X., Nguyen, H. N., Song, M. M., Hadiono, C., Ogden, S. C., Hammack, C., et al. (2016). Brain-Region-Specific Organoids Using Mini-bioreactors for Modeling ZIKV Exposure. *Cell* 165, 1238–1254. doi: 10.1016/j.cell.2016.04.032

Qian, X., Jacob, F., Song, M. M., Nguyen, H. N., Song, H., and Ming, G. L. (2018). Generation of human brain region-specific organoids using a miniaturized spinning bioreactor. *Nat. Protoc.* 13, 565–580. doi: 10.1038/nprot.2017.152

Rakic, S., and Zecevic, N. (2003). Emerging complexity of layer I in human cerebral cortex. *Cereb. Cortex* 13, 1072–1083. doi: 10.1093/cercor/13.10.1072

Rifes, P., Isaksson, M., Rathore, G. S., Aldrin-Kirk, P., Møller, O. K., Barzaghi, G., et al. (2020). Modeling neural tube development by differentiation of human embryonic stem cells in a microfluidic WNT gradient. *Nat. Biotechnol.* in press doi: 10.1038/s41587-020-0525-0

Sato, T., Stange, D. E., Ferrante, M., Vries, R. G., Van Es, J. H., Van den Brink, S., et al. (2011). Long-term expansion of epithelial organoids from human colon, adenoma, adenocarcinoma, and Barrett's epithelium. *Gastroenterology* 141, 1762–1772. doi: 10.1053/j.gastro.2011.07.050

Schafer, D. P., Lehrman, E. K., Kautzman, A. G., Koyama, R., Mardinly, A. R., Yamasaki, R., et al. (2012). Microglia sculpt postnatal neural circuits in an activity and complement-dependent manner. *Neuron* 74, 691–705. doi: 10.1016/j.neuron.2012.03.026

Shi, Y., Sun, L., Wang, M., Liu, J., Zhong, S., Li, R., et al. (2020). Vascularized human cortical organoids (vOrganoids) model cortical development in vivo. *PLoS Biol.* 18:e3000705. doi: 10.1371/journal.pbio.3000705

Shirasaki, R., and Pfaff, S. (2002). Transcriptional codes and the control of neuronal identity. *Annu. Rev. Neurosci.* 25, 251–281. doi: 10.1146/annurev.neuro.25.112701.142916

Stevens, H. E., Smith, K. M., Rash, B. G., and Vaccarino, F. M. (2010). Neural stem cell regulation, fibroblast growth factors, and the developmental origins of neuropsychiatric disorders. *Front. Neurosci.* 4:59. doi: 10.3389/fnins.2010.00059

Stubbs, D., DeProto, J., Nie, K., Englund, C., Mahmud, I., Hevner, R., et al. (2009). Neurovascular congruence during cerebral cortical development. *Cereb. Cortex* 19(Suppl. 1), i32–i41. doi: 10.1093/cercor/bhp040

Szegedi, V., Paizs, M., Csakvari, E., Molnar, G., Barzo, P., Tamas, G., et al. (2016). Plasticity in Single Axon Glutamatergic Connection to GABAergic Interneurons Regulates Complex Events in the Human Neocortex. *PLoS Biol.* 14:e2000237. doi: 10.1371/journal.pbio.2000237

Taguchi, A., Kaku, Y., Ohmori, T., Sharmin, S., Ogawa, M., Sasaki, H., et al. (2014). Redefining the in vivo origin of metanephric nephron progenitors enables generation of complex kidney structures from pluripotent stem cells. *Cell Stem Cell* 14, 53–67. doi: 10.1016/j.stem.2013.11.010

Takasato, M., Er, P. X., Becroft, M., Vanslambrouck, J. M., Stanley, E. G., Elefanty, A. G., et al. (2014). Directing human embryonic stem cell differentiation towards a renal lineage generates a self-organizing kidney. *Nat. Cell Biol.* 16, 118–126. doi: 10.1038/ncb2894

Takebe, T., Sekine, K., Enomura, M., Koike, H., Kimura, M., Ogaeri, T., et al. (2013). Vascularized and functional human liver from an iPSC-derived organ bud transplant. *Nature* 499, 481–484. doi: 10.1038/nature12271

Thomson, A. M., and Bannister, A. P. (2003). Interlaminar connections in the neocortex. *Cereb. Cortex* 13, 5–14. doi: 10.1093/cercor/13.1.5

Trujillo, C. A., Gao, R., Negraes, P. D., Gu, J., Buchanan, J., Preissl, S., et al. (2019). Complex Oscillatory Waves Emerging from Cortical Organoids Model Early Human Brain Network Development. *Cell Stem Cell* 25, 558.e–569.e. doi: 10.1016/j.stem.2019.08.002

Ueno, M., Fujita, Y., Tanaka, T., Nakamura, Y., Kikuta, J., Ishii, M., et al. (2013). Layer V cortical neurons require microglial support for survival during postnatal development. *Nat. Neurosci.* 16, 543–551. doi: 10.1038/nn.3358

Ulloa, F., and Briscoe, J. (2007). Morphogens and the control of cell proliferation and patterning in the spinal cord. *Cell Cycle* 6, 2640–2649. doi: 10.4161/cc.6.21.4822

Won, C., Lin, Z., Kumar, T. P., Li, S., Ding, L., Elkhal, A., et al. (2013). Autonomous vascular networks synchronize GABA neuron migration in the embryonic forebrain. *Nat. Commun.* 4, 2149. doi: 10.1038/ncomms3149

Wu, K. W., Lv, L. L., Lei, Y., Qian, C., and Sun, F. Y. (2019). Endothelial cells promote excitatory synaptogenesis and improve ischemia-induced motor deficits in neonatal mice. *Neurobiol. Dis.* 121, 230–239. doi: 10.1016/j.nbd.2018.10.006

Xiang, Y., Tanaka, Y., Patterson, B., Kang, Y. J., Gubbi, G., Roselaar, N., et al. (2017). Fusion of Regionally Specified hPSC-Derived Organoids Models Human Brain Development and Interneuron Migration. *Cell Stem Cell* 21, 383.e–398.e. doi: 10.1016/j.stem.2017.07.007

Xiang, Y., Tanaka, Y., Cakir, B., Patterson, B., Kim, K. Y., Sun, P., et al. (2019). hESC-Derived Thalamic Organoids Form Reciprocal Projections When Fused with Cortical Organoids. *Cell Stem Cell* 24, 487.e–497.e. doi: 10.1016/j.stem.2018.12.015

Conflict of Interest: The authors declare that the research was conducted in the absence of any commercial or financial relationships that could be construed as a potential conflict of interest.

frontiers in Cellular Neuroscience

ORIGINAL RESEARCH
published: 18 March 2021
doi: 10.3389/fncel.2021.648210

Control of Microbial Opsin Expression in Stem Cell Derived Cones for Improved Outcomes in Cell Therapy

Marcela Garita-Hernandez[1]†, Antoine Chaffiol[1], Laure Guibbal[1], Fiona Routet[1], Hanen Khabou[1], Luisa Riancho[1], Lyes Toualbi[1], Serge Picaud[1], José-Alain Sahel[1,2,3], Olivier Goureau[1], Jens Duebel[1,4] and Deniz Dalkara[1]*

[1]Institut de la Vision, Sorbonne Université, Paris, France, [2]CHNO des Quinze−Vingts, DHU Sight Restore, Paris, France, [3]Department of Ophthalmology, The University of Pittsburgh School of Medicine, Pittsburgh, PA, United States, [4]Department of Ophthalmology, University Medical Center Göttingen, Göttingen, Germany

OPEN ACCESS

Edited by:
Lin Cheng,
The University of Iowa, United States

Reviewed by:
Yani Liu,
Qingdao University, China
Gerrit Hilgen,
Northumbria University,
United Kingdom
Guilan Li,
Sun Yat-sen University, China

***Correspondence:**
Marcela Garita-Hernandez
marcela.garita@inserm.fr

†Present address:
Marcela Garita-Hernandez
Institut des Neurosciences de Montpellier, INSERM U1298, Université de Montpellier, Montpellier, France

Specialty section:
This article was submitted to Cellular Neuropathology, a section of the journal Frontiers in Cellular Neuroscience

Received: 31 December 2020
Accepted: 23 February 2021
Published: 18 March 2021

Citation:
Garita-Hernandez M, Chaffiol A, Guibbal L, Routet F, Khabou H, Riancho L, Toualbi L, Picaud S, Sahel J-A, Goureau O, Duebel J and Dalkara D (2021) Control of Microbial Opsin Expression in Stem Cell Derived Cones for Improved Outcomes in Cell Therapy. Front. Cell. Neurosci. 15:648210. doi: 10.3389/fncel.2021.648210

Human-induced pluripotent stem cell (hiPSC) derived organoids have become increasingly used systems allowing 3D-modeling of human organ development, and disease. They are also a reliable source of cells for transplantation in cell therapy and an excellent model to validate gene therapies. To make full use of these systems, a toolkit of genetic modification techniques is necessary to control their activity in line with the downstream application. We have previously described adeno-associated viruse (AAV) vectors for efficient targeting of cells within human retinal organoids. Here, we describe biological restriction and enhanced gene expression in cone cells of such organoids thanks to the use of a 1.7-kb L-opsin promoter. We illustrate the usefulness of implementing such a promoter to enhance the expression of the red-shifted opsin Jaws in fusion with a fluorescent reporter gene, enabling cell sorting to enrich the desired cell population. Increased Jaws expression after transplantation improved light responses promising better therapeutic outcomes in a cell therapy setting. Our results point to the importance of promoter activity in restricting, improving, and controlling the kinetics of transgene expression during the maturation of hiPSC retinal derivatives. Differentiation requires mechanisms to initiate specific transcriptional changes and to reinforce those changes when mature cell states are reached. By employing a cell-type-specific promoter we put transgene expression under the new transcriptional program of mature cells.

Keywords: human induced pluripotent stem cell, human retinal organoid, cones, optogenetics, vision restoration, cell therapy, promoter

INTRODUCTION

The generation of human retinal organoids has opened up new ways to study the brain and retinal development and evolution, as well as to model and treat neurodegenerative disorders (Ahmad et al., 2019; Gagliardi et al., 2019). Retinal organoids are multicellular 3D structures that mimic certain aspects of the cytoarchitecture and cell-type composition of the human retina. These structures are generated by the differentiation of Human-induced pluripotent stem cells (hiPSCs) or embryonic stem cells (ESCs; Llonch et al., 2018; Ahmad et al., 2019; Lidgerwood et al., 2019).

However, even the best accomplished 3D model of retinal development carries some limitations and can benefit from genetic modifications to control cellular functions. The ability to genetically modify retinal organoids is essential for their utility as disease models as well as their therapeutic use for regenerative medicine. Genetic modification is a powerful tool that allows for the introduction of alterations ranging from small changes in the genome to the removal or integration of entire genes to the expression of exogenous genes to control cellular function (Garita-Hernandez et al., 2016). This enables researchers to investigate individual genes relating to cellular functions, and interactions. Moreover, drugs (small molecule or gene-based) can be tested in a larger variety of disease states and in different genetic environments (Kalatzis et al., 2013; Cereso et al., 2014; Garita-Hernandez et al., 2018; Quinn et al., 2018). Any method of genetic modification of hiPSC derivatives needs to address three key issues: (i) the ultimate purpose of the modification (investigative study or therapy); (ii) the stage of differentiation and the bioavailability of receptors; and (iii) the proportion of cells target of the genetic transformation. For non-integrative genetic modifications to be stable, it should be made once the cell cycle arrest has been induced, circumventing cell divisions. The delivered genetic cargo is then maintained even in the absence of chromosomal integration and the transgene expression is dependent on the recruitment of transcription factors by the promoter sequence preceding the transgene.

Due to the cellular heterogeneity of retinal organoids, the third issue concerns the cell type(s) within the organoid that is/are subject to genetic modifications. Approaches can either target cells indiscriminately, regardless of their location and cell type (Garita-Hernandez et al., 2018, 2020; Gonzalez-Cordero et al., 2018) or, contrariwise, target a subset of cells. The latter can be achieved by biologically restricting the genetic modification to specific cell types by the use of cell type-specific promoters to drive transgene expression (Macé et al., 2015; El-Shamayleh et al., 2016; Chaffiol et al., 2017; Juettner et al., 2018; Khabou et al., 2018). In this work, we targeted to achieve high-level microbial opsin expression in cones derived from human retinal organoids to restore light responses in blind mice following transplantation of these cells. For this type of genetic modification, one of the most important aspects to consider is the mode of gene delivery and control of transgene expression. The two most widely used methods in the case of organoids are viral delivery *via* adeno-associated viruses (AAVs) and non-viral methods such as electroporation (Fischer et al., 2019). AAVs have been successfully used in transducing retinal organoids by simple addition to the cell culture medium, which results in gene expression throughout the entire organoid (Garita-Hernandez et al., 2018, 2019, 2020; Gonzalez-Cordero et al., 2018; Quinn et al., 2018). This is a reliable approach to broadly target the whole organoid, but it must be refined to meet the needs of the downstream application.

The spectrum of potential applications has so far ranged from the simple expression of fluorescent marker proteins (Gagliardi et al., 2018) to the modeling of disease conditions (Artegiani et al., 2020). Yet, significant untapped potential remains for the future use of gene delivery to retinal organoids in disease modeling and therapy (Dalkara et al., 2016). Over the last 5 years, efforts have been directed to the transplantation of photoreceptors derived from 3D retinal organoids (Gonzalez-Cordero et al., 2017; Gagliardi et al., 2018; Lakowski et al., 2018; Collin et al., 2019; Aboualizadeh et al., 2020) resulting in different levels of success but the formation of light-sensitive outer segments (Mandai et al., 2017; Iraha et al., 2018) and interaction with retinal pigment epithelium (RPE), which is necessary for the appropriate functioning of photoreceptor cells (Strauss, 2005) remain challenges for cell replacement with therapeutic outcomes. Microbial opsins can circumvent these issues as we have recently proposed (Garita-Hernandez et al., 2019). Using the hyperpolarizing microbial opsin Jaws, we have previously conferred light sensitivity to hiPSC-derived cones. After transplantation of optogenetically-transformed cones, we observed restoration of light responses in blind mice both at the retinal and behavioral levels under very bright light (Garita-Hernandez et al., 2019). Here, we demonstrate that the success of this approach can be increased by expressing the microbial opsin selectively and at a high level in the desired cell population within the organoid. The use of a strong and cell-type-specific promoter allows to isolate and enrich such population *via* fluorescence-activated cell sorting. We hypothesize that an increase in transgene expression occurs *via* increased availability of cone-specific transcription factors as cells mature in the subretinal space. Enhanced microbial opsin expression contributes to better light sensitivity and temporal resolution of light responses in the transplanted cones paving the way to better therapeutic efficacy in vision restoration. To our knowledge this is the first time a molecular strategy has been used to overcome issues related to the isolation of a target hiPSC-derived cell population and control of transgene expression within these cells, thereby improving the response amplitude and the kinetic profile of light responses *via* a microbial opsin.

MATERIALS AND METHODS

Maintenance of hiPSC Culture

All experiments were performed using hiPSC-2 and hiPSC-5f cell lines, previously established from human fibroblasts and Müller glial cells respectively (Reichman et al., 2014; Slembrouck-Brec et al., 2019). Cells were kept at 37°C, under 5% CO_2/95% air atmosphere, 20% oxygen tension, and 80%–85% humidity. Colonies were cultured in feeder-free conditions as previously described (Reichman et al., 2017) with Essential 8^{TM}medium (Thermo Fisher Scientific) in culture dishes coated with truncated recombinant human Vitronectin (Thermo Fisher Scientific). The medium was changed every day and the cells were passaged once a week when reaching 70% of confluency.

Differentiation of Human iPSCs Into Retinal Organoids

Optimization of previous protocols (Reichman et al., 2017) allowed the generation of retinal organoids from hiPSC. In brief, hiPSC cell lines were expanded until 80% confluence in Essential

TABLE 1 | Animal details used to generate figures.

Figure	Strain	Experimental group	Experiment	Transplant age (weeks)	Analysis age (weeks)	Number of mice *(N)*
2-C/D	rd1−/−	Enriched human Jaws-cones	Fundus	7	9	23
2-E	rd1−/−	Enriched human Jaws-cones	Fundus	7	10	23
2-F	rd1−/−	Enriched human Jaws-cones	2-photon	7	11	1
2-G	rd1−/−	Non transplanted	IHC	-	7	1
2-H/I	rd1−/−	Enriched human Jaws-cones	IHC	7	12	5
3	rd1−/−	Enriched human Jaws-cones	Patch clamp	7	12	5
4	rd1−/−	Enriched human Jaws-cones	Patch clamp	7	12	2
Supplementary Figure 1A	rd1−/−	Enriched human Jaws-cones	IHC	7	12	5
Supplementary Figure 1B	rd1−/−	Enriched human Jaws-cones	IHC	7	12	5
Supplementary Figure 1C	rd1−/−	Enriched human Jaws-cones	IHC	7	12	5

TABLE 2 | Media formulation for 100 ml total volume.

Medium	Formulation (100 ml)
Maintenance of hiPSCs	Essential 8^{TM} Basal medium (Thermo Fischer Scientific)– 98 ml. Essential 8^{TM} Supplement 50X (Thermo Fischer Scientific)–2 ml.
Proneural medium	Essential 6^{TM} medium (Thermo Fischer Scientific)–95ml. Penicillin/Streptomycin (Thermo Fischer Scientific)–100 μl. N2 supplement (Thermo Fischer Scientific)–5 ml.
Maturation medium	DMEM-F12 ^{TM} (Thermo Fischer Scientific)–97 ml. B27 Supplement (Thermo Fischer Scientific)–2 ml. MEM Non-Essential Amino Acids Solution 100X (Thermo Fischer Scientific)–1 ml. Penicillin/Streptomycin (Thermo Fischer Scientific)–100 μl.
Ringer Solution	NaCl 155 mM, KCl 5 mM, CaCl2 2 mM, NaCl2 1 mM, NaH2PO4 2 mM, HEPES 10 mM, glucose 10 mM.

8^{TM} medium before switched in Essential 6^{TM} medium (Thermo Fischer Scientific). After 3 days, cells were cultured in a *Proneural medium*. On day 28, NR-like structures grew out of the cultures and were mechanically isolated and further cultured in a 3D system in *Maturation medium* until day 70 of differentiation. **Table 2** summarizes media formulation. Floating organoids were passed to 6 well-plates (10 organoids per well) and supplemented with 10 ng/ml FGF2 (Preprotech) until day 35. Additionally, between day 42 and day 49, 10 μM DAPT (Selleckchem) was added to the *Maturation medium* to promote the photoreceptor commitment of retinal progenitors. The medium was changed every 2–3 days (**Figure 2**; Garita-Hernandez et al., 2018).

AAV Vector Production

Recombinant AAV2–7m8 were produced as previously described using the co-transfection method and purified by iodixanol gradient ultracentrifugation (Choi et al., 2007). Concentration and buffer exchange was performed against PBS containing 0.001% Pluronic. AAV vector stocks titers were then determined by the real-time quantitative PCR titration method (Aurnhammer et al., 2012) using SYBR Green (Thermo Fischer Scientific).

Infection of Retinal Organoids With AAV Encoding Jaws-GFP

Retinal organoids were transduced at day 44 using the recombinant AAV2–7m8 capsid variant (Dalkara et al., 2013) carrying the hyperpolarizing chloride pump Jaws (Chuong et al., 2014) fused to the fluorescent reporter GFP under the control of the cone-specific promoter PR1.7 (Ye et al., 2016). One single infection was performed by direct addition in *Proneural medium* (**Table 2**) of 5×10^{10} vg per organoid in 6-well plates containing 10–12 organoids. The medium was changed 72 h after infection.

Single-Cell Dissociation of Retinal Organoids

Retinal organoid dissociation was done with two units of pre-activated papain at 28.7 u/mg (Worthington) in Ringer solution. The samples were incubated 25 min at 37°C with several pipetting steps to obtain a homogenous suspension. The cell solution was filtered with a 40 μm filter (Miltenyi Biotec, Germany) and centrifuged for 5 min at 800 rpm. The pellet was resuspended at the desired concentration in a *Proneural medium* (**Table 2**) for cell transplantation.

Flow Cytometry Analysis

Dissociated retinal organoids were filtered with a 30 μm filter (Miltenyi, Bergisch Gladbach, Germany) and fixed for 10 min at 4°C with 4% paraformaldehyde. Cells were washed in PBS. The samples were analyzed by flow cytometry and at least 10,000 events were examined in each experiment using the FACSCalibur system (BD Biosciences, Allschwil, Switzerland). The number of GFP-positive cells within the gated population was measured using CellQuest^{TM} Pro (BD Biosciences) software. Non-infected organoids serve as controls.

Fluorescence-Activated Cell Sorting (FACS)

Sorting of GFP positive cells was performed from Papain single-cell dissociated retinal organoids. Dissociated cells were passed through a 30 μm filter (Miltenyi, Bergisch Gladbach, Germany) and resuspended in PBS/0.5% FBS/5 mM EDTA (2.10^6 cells/ml). The GFP positive cells were sorted with a MoFlo Astrios EQ FACS system (Beckman Coulter, Villepinte, France) in an enrichment mode.

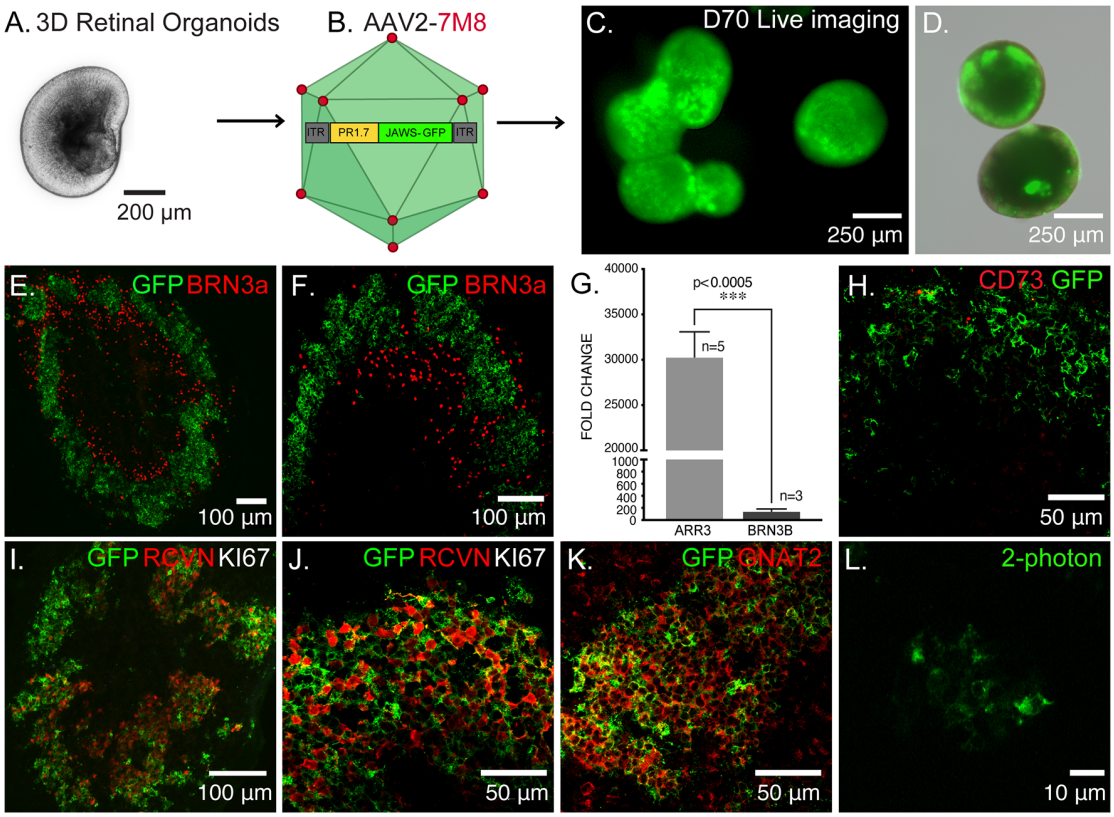

FIGURE 1 | Optogenetic engineering of retinal structures derived from human induced pluripotent stem cells (hiPSCs). **(A)** Bright-field/epifluorescence image of a hiPSC-derived retinal organoid after mechanical isolation on day 30 of differentiation. **(B)** Schematics of the adeno-associated viruses (AAV)-mediated strategy used to engineer 3D retinal organoids, AAV2–7m8-PR1.7-Jaws-GFP was used to transduce cone photoreceptors on day 44 of differentiation. **(C)** Live GFP fluorescence observed after prolong culture of retinal organoids showing strong and long-term expression of the transgene. **(D)** Merge of bright-field/epifluorescence and live GFP fluorescence images observed in 70-days old organoids. **(E)** Immunofluorescence (IF) analysis of a representative retinal organoid at day 70 of differentiation, depicting a thick layer of photoreceptors immunoreactive for GFP and some sparse ganglion precursors cells identified by BRN3a. **(F)** Magnification of the IF analysis in **(D)** in another organoid. **(G)** Real-time qRT-PCR analysis of cone specific marker, Cone arrestin (ARR3) and retinal ganglion cell specific marker BRN3B. *N* = number of biological replicates. Values are mean ± SEM. Error bars are SEM. Statistical significance assessed using Mann–Whitney Student's test (***$p < 0.0005$). **(H)** IF analysis of optogenetically engineered retinal organoids at day 70 showing Jaws+ cells do not express CD73 photoreceptor surface marker. **(I)** IF analysis confirming postmitotic photoreceptor identity of GFP positive cells, showing they are immunoreactive for the photoreceptor-specific marker Recoverin (RCVN) and complete absence of proliferation marker KI67. **(J)** Magnification of the IF analysis in **(I)** in another organoid. **(K)** IF analysis of confirming the cone identity of GFP positive cells, showing colocalization with cone-specific marker GNAT2. **(L)** 2-Photon laser image of GFP+ cells inside a retinal organoid at D70 of differentiation. Images correspond to representative retinal organoids from at least four different biological replicates, scale bar: **(C,D)** = 250 µm, **(E,F,I)** = 100 µm, **(H,J,K)** = 50 µm, **(L)** = 10 µm.

Animals

Retinal degeneration 1 (rd1) mice line (C3H *rd/rd*) was kindly provided by Dr. Thierry Leveillard and used as a cell recipient. Rd1 mice photoreceptor cells degenerate to a single row of cones by P20 (Farber and Lolley, 1974; Lavail and Sidman, 1974; Bowes et al., 1990). All mice were housed under a 12-h light-dark cycle with free access to food and water (certified animal facility of the "Institut de la Vision"; agreement number A751202). All experiments were carried out in strict accordance with the Association for Research in Vision and Ophthalmology statement for animal research in ophthalmology. Moreover, all procedures were approved by the local animal experimentation ethics committee (Charles Darwin Ethical Committee for Animal Experimentation C2EA-05) in strict accordance with French and European regulations for animal use in research (Directive 2010/63/EU).

Transplantation Procedures

Mice were anesthetized by intraperitoneal injection of ketamine (50 mg/kg) and xylazine (10 mg/kg) and placed on a heating pad to maintain body temperature at 37°C. Pupils were dilated with 0.5% mydriaticum (Thea) and a blunt 34-gauge needle was inserted tangentially through the conjunctiva and sclera. Using a Hamilton syringe, 1 µl total volume of cell suspension containing approximately 100,000 (97,667 ± 4,041) GFP+ cells were delivered into the subretinal space of each eye. A drop of antibiotic, Ophtalon (Tvm) was applied and mice were placed into a warm chamber after the surgery until their awakening. After transplantation, the mice were under oral treatment of

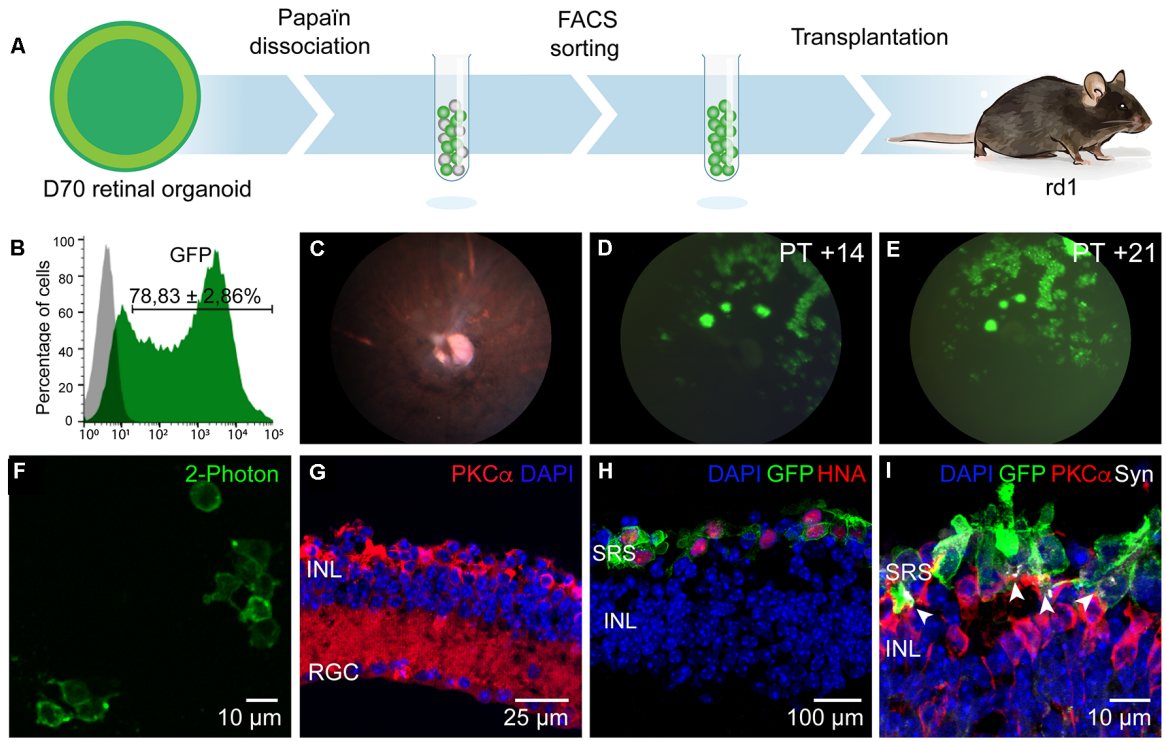

FIGURE 2 | Enrichment and transplantation of optogenetically-engineered cones. **(A)** Schematics of the general transplantation strategy. Human iPSC-derived retinal organoids were Papain-dissociated and Jaws-enriched expressing cells were transplanted subretinally into blind rd1 mice. **(B)** Representative histogram of flow cytometry analysis performed to determine Jaws-expressing cells within the retinal organoids (N = 8 biological replicates, n = 10,000 cells gated). **(C)** Fundus imaging analysis of representative rd1 mice retinae after 14 days of transplantation. **(D,E)** Representative fluorescent fundus images of rd1 mice in panel **(C)** showing Jaws-expressing cells 14 **(D)** and 21 **(E)** days after subretinal transplantation. **(F)** 2-Photon laser image of GFP+ cells in a rd1 transplanted retina. **(G)** Histological analysis of 7-week-old mice retina showing complete absence of photoreceptors layers, corresponding to the time of transplantation. Remaining cells are immunoreactive for bipolar specific marker PKCα. **(H,I)** IF analysis of vertical cryosections of rd1 mice retinae after transplantation of Jaws-enriched expressing cells (GFP). **(H)** Transplanted Jaws-cones depicted as GFP+ cells in rd1 mice were also immunoreactive for human marker HNA (red). **(I)** Transplanted cones overlie host PKCα bipolar cells and expressed synaptic marker Synaptophysin (Syn, white arrows) All images are representative of at least five different transplants. Animal details for each transplantation are provided in **Table 1**. Scale bars: **(F** and **I)** = 10 µm, **(G)** = 25 µm, **(H)** = 100 µm. INL, inner nuclear layer, RGC, retinal ganglion cells; SRS, subretinal space.

210 mg/L Cyclosporine A (Atopica™, Novartis) administrated in the drinking water. To improve stability Cyclosporine A was prepared in 5% glycosylated water and changed three times per week.

Fundus Analysis

Transplanted eyes were examined with a fluorescent fundus camera (MicronII, Phoenix Laboratories) weekly. Mice were sedated with 5% isofluorane and kept in 2% isofluorane during the experiment. The pupils were dilated with a drop of 0.5% mydriaticum (Thea) and 5% neosynephrine (Faure). The eyes were kept hydrated with a drop of Lubrithal (Dechra).

Cryosectionning and Immunohistochemistry

Ten micrometer-thick organoid sections were obtained with a Cryostat Microm and mounted on Super Frost Ultra Plu® slides (Menzel Gläser). Samples were washed in PBS to remove the rest of O.C.T. and then permeabilized in PBS containing 0.5% Triton® X-100 for 1 h at RT. Blocking was done with PBS containing 0.2% gelatin and 0.25% Triton X-100 for 30 min at RT. Incubation with primary antibodies (**Table 3**) was performed overnight at 4°C. Several washes with PBS containing 0.25% Tween20 were performed before incubation with Fluorochrome-conjugated secondary antibodies (**Table 4**) and DAPI (4'-6'-diamino-2-phenylindole, dilactate; Invitrogen-Molecular Probe; 1/1,000 dilution) to counterstain the nuclei for 1 h at RT. Samples were further washed in PBS and dehydrated with 100% ethanol before mounting using fluoromount Vectashield (Vector Laboratories).

Image Acquisition

Immunofluorescence was observed using a Leica DM6000 microscope (Leica microsystems, Wetzlar, Germany) equipped with a CCD CoolSNAP-HQ camera (Roper Scientific, Vianen, Netherlands) or using an Olympus FV1000 (inverted IX2 and upright BX2) laser scanning confocal microscopes equipped with a GaAsP PMT detector with 405, 488, 515, and 635 nm pulsing lasers. The images were acquired sequentially with the step size optimized based on the Nyquist–Shannon

TABLE 3 | Primary antibodies.

Antibody	Reference	Specie/Clonality	Dilution
BRN3a	Millipore MAB1585	Mouse Monoclonal	1/250
CD73	Biolegend 344002	Mouse Monoclonal	1/100
GFP	Abcam ab13970	Chicken Polyclonal	1/500
GNAT2	Santa Cruz sc-390	Rabbit Polyclonal	1/200
hCAR	Gift from Cheryl Craft	Rabbit Polyclonal	1/20,000
HNA	Millipore MAB4383	Mouse Monoclonal	1/200
KI67	BD Pharmagen BD4127608	Mouse Monoclonal	1/200
PKCα	Santa Cruz sc-208	Rabbit Polyclonal	1/100
Recoverin	Millipore AB5585	Rabbit Polyclonal	1/2,000
Ribeye (Anti-CtBP2)	BD Biosciences 612044	Mouse Monoclonal	1/500
Synaptophysin	Sigma S5768	Mouse Monoclonal	1/200
vGlut1	Abcam ab77822	Rabbit Polyclonal	1/500

TABLE 4 | Secondary antibodies.

Antibody	Reference	Dilution
Alexa Fluor-488 Donkey anti mouse	Thermo Fischer Scientific (A21202)	1/500
Alexa Fluor-488 Donkey anti rabbit	Thermo Fischer Scientific (A21206)	1/500
Alexa Fluor-488 Goat anti chicken	Thermo Fischer Scientific (A11039)	1/500
Alexa Fluor-546 Donkey anti mouse	Thermo Fischer Scientific (A10036)	1/500
Alexa Fluor-546 Donkey anti rabbit	Thermo Fischer Scientific (A10040)	1/500
Alexa Fluor-647 Donkey anti mouse	Thermo Fischer Scientific (A31571)	1/500
Alexa Fluor-647 Donkey anti rabbit	Thermo Fischer Scientific (A31573)	1/500

theorem. The analysis was conducted in FIJI (NIH). Images were put into a stack, Z-sections were projected on a 2D plane using the MAX intensity setting in the software's Z-project feature, and the individual channels were merged.

Two-Photon Imaging and Electrophysiological Recordings

A custom-made two-photon microscope equipped with a 25× water immersion objective (XLPlanN-25 × -W-MP/NA1.05, Olympus) and a pulsed femtosecond laser (InSight^{TM} DeepSee^{TM}—Newport Corporation) were used for imaging and targeting AAV-transduced fluorescent cells (Jaws-GFP+ or GFP+ cells) in retinal organoids or in C3H *rd/rd* (rd1) mice retinae. Two-photon images were acquired using the excitation laser at a wavelength of 930 nm. A CCD camera (Hamamatsu Corp.) was used to visualize cells under infrared light, and images were processed offline using ImageJ (NIH). Retinal organoids were placed in the recording chamber of the microscope at 36°C in oxygenated (95% O_2/5% CO_2) Ames medium (Sigma–Aldrich) during the whole experiment. Ames' Medium is a powder mixture of 42 different components, in which sodium bicarbonate is later added, its composition was initially formulated to support retinal tissue in short-term cultures (Ames and Nesbett, 1981). Transplanted mice were sacrificed by CO_2 inhalation followed by quick cervical dislocation, and eyeballs were removed. Retinae from rd1 mice were isolated in oxygenated (95% O_2/5% CO_2) Ames medium and whole-mount retinas with ganglion cell side down were placed in the recording chamber of the microscope at 36°C for the duration of the experiment for live two-photon imaging and electrophysiology.

For patch-clamp recordings, AAV-transduced fluorescent cells were targeted with a patch electrode under visual guidance using the reporter tag's fluorescence. Whole-cell recordings were obtained using the Axon Multiclamp 700B amplifier (Molecular Device Cellular Neurosciences). Patch electrodes were made from borosilicate glass (BF100-50-10, Sutter Instrument) pulled to 7–8 MΩ and filled with 115 mM K+ Gluconate, 10 mM KCl, 1 mM $MgCl_2$, 0.5 mM $CaCl_2$, 1.5 mM EGTA, 10 mM HEPES, and 4 mM ATP-Na2 (pH 7.2). Photocurrents were recorded while voltage-clamping cells at a potential of −40 mV. Cells were also recorded in the current-clamp configuration to monitor the membrane potential during light stimulations and measure the resting membrane potential.

Light Stimulation of Jaws-Positive and Control Cells

Light-triggered responses from Jaws-GFP+ cells were measured in donor cells in retinal organoids before transplantation and *ex-vivo* in transplanted mice retinae, control cells expressing only GFP were also recorded in both conditions (in organoids and after transplantation). To measure light responses (photocurrents or changes in cells membrane potential) a monochromatic light source was used (Polychrome V, TILL photonics). Photocurrent and voltage hyperpolarization of cells in organoids and rd1 transplanted retinae were recorded as a function of light intensities ranging between 10^{14} and 3.1×10^{17} photons.cm^{-2}.s^{-1} at 590 nm. To measure the activity spectrum of Jaws, 300 ms light flashes ranging from 400–650 nm (25 nm steps; interstimulus interval 1.5 s) were used at a constant light intensity of 8×10^{16} photons.cm^{-2}.s^{-1}. This light source was used at a constant wavelength of 590 nm to generate light pulses at different frequencies (ranging from 2 to 25 Hz) and durations (from 20 ms to 4 s) to determine the temporal response properties of transplanted cells expressing Jaws. Stimulation and analysis were performed using custom-written software in Matlab (Mathworks) and Labview (National Instruments) and output light intensities were calibrated using

a spectrophotometer (USB2000+, Ocean Optics). Both retinal organoids and retinae were dark-adapted for at least 45 min before electrophysiological recordings.

RESULTS

Generation of Optogenetically-Transformed Cone Photoreceptors

Using our previously published protocol of differentiation (Garita-Hernandez et al., 2018, 2019) we have generated cone-enriched retinal organoids in only 70 days. We have followed the 2D/3D protocol of Reichman et al. (2017) until mechanical isolation of retinal organoids (**Figure 1A**). 3D retinal organoids were allowed to grow in the presence of basic fibroblast growth factor-2 (FGF2) for a week and then cell cycle arrest was induced. This was performed by adding the gamma-secretase inhibitor DAPT, for a week from day 42 of differentiation. To favor differentiation towards cone lineage DAPT was added at the time point corresponding to the onset of cone arrestin (CAR) positive cells within the organoids (Garita-Hernandez et al., 2019). 3D retinal organoids were optogenetically-transformed with the recombinant AAV2-7m8 capsid variant selected for its improved performance in retinal organoids when compared to other capsids also known for their tropism towards cones (Garita-Hernandez et al., 2020). AAV2-7m8 vector carried the hyperpolarizing chloride pump Jaws (Chuong et al., 2014), under the control of the 1.7-kb cone-specific L-opsin promoter PR1.7 (Ye et al., 2016; **Figure 1B**). This vector-promoter combination has proven to be very efficient for gene delivery in non-human primate and human cone cells, including those in 3D retinal organoids (Khabou et al., 2018). Jaws was chosen over other hyperpolarizing microbial opsins, based on its enhanced expression levels and improved membrane trafficking in human cells (Chuong et al., 2014; Garita-Hernandez et al., 2018). The retinal organoids were transduced with AAV on day 44 of differentiation corresponding to the onset of cone-specific gene expression (Garita-Hernandez et al., 2019). We observed a strong and long-lasting expression of Jaws-GFP in retinal organoids, up to 30 days after infection (**Figures 1C,D**). GFP positive cells were organized in a layer in the outer part of the day 70 retinal organoids (**Figures 1E,F**) as a distinct major population identified as cones by the colocalization with the photoreceptor marker Recoverin (**Figures 1I,J**) and the cone-specific marker GNAT2 (**Figure 1K**). Additionally, no Jaws-GFP cells colocalize with the ganglion cell marker Brn3A (**Figures 1E,F**). Gene expression analysis by quantitative RT-PCR also confirmed a greater expression of cone-specific ARRESTIN in comparison with the ganglion cell marker BRN3b in our organoids (**Figure 1G**). Immunofluorescence analysis showed Jaws-GFP+ cells do not express the photoreceptor cell surface marker CD73 at day 70 of differentiation (**Figure 1H**) and no expression of the proliferation marker, Ki67 was found in day 70 organoids, excluding the presence of remaining retinal progenitor cells or tumorigenic pluripotent cells within the organoids (**Figures 1I,J**). These results show that using an efficient capsid promoter combination such as AAV2-7m8-PR1.7, is possible to drive a high-level specific expression of Jaws opsin in cones derived from retinal organoids.

Selection and Transplantation of Jaws-Expressing Cone Photoreceptors

Jaws-GFP engineered 3D organoids were dissociated with papain and Jaws expressing cells were selected by FACS using the endogenous GFP expression. Sorted cells were then transplanted *via* subretinal injections into blind rd1 mouse retinas lacking the outer nuclear layer (7 weeks old rd1 mice; **Figure 2A**). A fraction of 78.83 $\pm$ 2.86% of cells were GFP+ (n = 20 organoids, N = 3 differentiations; **Figure 2B**) and approximately 100,000 cells were injected in each eye of rd1 mice in a 1 μl volume. Using *in vivo* eye fundus imaging, we detected the widespread presence of Jaws-GFP+ cells as early as 7 days after injection (**Figure 2D**) and transgene expression levels increased in the transplanted cells until 21 days post-transplantation (**Figure 2E**). At the time of transplantation, there is no detectable outer nuclear layer in the rd1 retinae (**Figure 2G**). Three weeks after transplantation injected eyes were dissected and flat-mount retinas were observed live under our two-photon microscope. We found abundant Jaws-GFP positive cells within the organoids, before transplantation (**Figure 1L**) and in transplanted retinas (**Figure 2F**). We fixed and cryosectioned these retinas to perform histological analysis of the transplanted region. Cross-sections of host retinas showed that all GFP positive cells corresponded to human cone cells as evidenced by colocalization with the human nuclear marker HNA (**Figure 2H**) and the cone-specific marker cone ARRESTIN, hCAR (**Supplementary Figure 1**). Immunofluorescence against the bipolar cell marker, PKCα, demonstrated close contact between the transplanted Jaws-GFP+ cones and the underlying host inner retina as well as the capability to form Synaptophysin-mediated synapses (**Figure 2I**). Jaws-GFP+ cells also expressed vesicular glutamate transporter 1 (vGluT1), which packs glutamate into synaptic vesicles, at the synapses. Immunohistochemistry against RIBEYE confirmed the presence of ribbon synapses (**Supplementary Figure 1**). Morphological analysis of the transplanted cells revealed Jaws-expressing cells lack of outer segment as previously reported (Garita-Hernandez et al., 2019). Our strategy is an alternative approach to the CD73 MACS separation (Gagliardi et al., 2018), which cannot be performed in organoids younger than 100 days old due to lack of expression of the cell surface marker, CD73. This was confirmed at the time of FACS sorting when immunofluorescence analysis showed Jaws-GFP+ cells do not express CD73 (**Figure 1H**). Our results show that Jaws-GFP expression driven by PR1.7 promoter can be used to successfully isolate a transplantable population of cones from day 70 organoids, which integrate with the host retina forming synaptic connections with the host bipolar cells.

Transplanted Jaws-Expressing Cones Respond to Light Stimulus

Next, we tested if Jaws-GFP positive cells can elicit light responses in response to illumination. Two-photon guided patch-clamp

recordings revealed robust responses to orange light pulses (590 nm, 3.1×10^{17} photons.cm^{-2}.s^{-1}) in organoids (**Figure 3A**) and rd1 retinae after transplantation (**Figure 3B**). Jaws-elicited responses presented a typical photocurrent shape consisting of a fast onset (sometimes with a small transient) followed by a steady-state current. These light responses are based on the activity of the microbial opsin since organoids infected with control AAV-GFP did not elicit photocurrents upon stimulation. In the same way, age-matched transplanted mice with photoreceptors expressing GFP only showed no measurable light-evoked currents, which is consistent with the lack of outer segments in the transplanted cell population (gray traces in **Figures 3A,B**). Whole-cell patch-clamp recordings in GFP-Jaws cones exhibited robust light responses to orange light flashes, which increased continuously with increasing light intensity (**Figures 3C,D**). Of note, significant differences in photocurrents were found after transplantation compared to organoids starting at a stimulus intensity of 6×10^{15} photons.cm^{-2}.s^{-1} (**Figures 3A–F**). Accordingly, hyperpolarization expressed as transmembrane voltage, increased steadily when increasing the light intensity up to 3.1×10^{17} photons.cm^{-2}.s^{-1}, with all the light intensities, used remaining below the safety limit for optical radiation in the human eye (European Parliament and European Council, 2006; International Commission on Non-Ionizing Radiation Protection, 2013). Importantly, the mean values of the resting membrane potential (RMP) in the dark (at 0 current) were -42.76 ± 2.88 mV in organoids and were even more depolarized at -36.72 ± 1.52 mV after transplantation which is higher than with our previous approach for transplanted cells (**Figure 3E**, orange dots; Garita-Hernandez et al., 2019). Those significantly depolarized RMP values are consistent with the results reported by Busskamp et al. who showed dormant cone cell bodies completely lacking outer segments were found to be surprisingly depolarized (Busskamp et al., 2010). Indeed, a depolarized state in the dark is mandatory in photoreceptors to activate calcium channels necessary for glutamate release. Additionally, we comparatively analyzed the amplitude of the photocurrents generated by PR1.7-Jaws in organoids and transplanted retinas vs. those observed by mCAR-Jaws used in our past studies (Garita-Hernandez et al., 2019). We observed significantly higher response amplitudes in the transplanted retinas than in those measured in organoids transformed with PR1.7-Jaws, significant response differences started at the intensity of 6×10^{15} photons.cm^{-2}.s^{-1} as shown in **Figure 3** and at the highest light intensity of 3.1×10^{17} photons.cm^{-2}.s^{-1} we obtained 16.8 ± 2.91 pA in organoids ($n = 7$) and 74.57 ± 18.48 pA after transplantation ($n = 9$**, $p = 0.0012$, Mann–Whitney). More importantly, higher response amplitudes were recorded in retinae transplanted with PR1.7-Jaws when compared with mCAR-Jaws (**Figure 3F**) at the same intensity. By comparison, after transplantation with our precedent protocol, using mCAR promoter, we observed a mean response amplitude around 5 pA (Garita-Hernandez et al., 2019). Altogether, we show here that using a highly specific cone promoter we can increase Jaws expression levels in the cone membrane and observe an increase in light response amplitudes.

Temporal Properties of Jaws-Induced Responses in hiPSC-Derived Cones After Transplantation

To further characterize the properties of Jaws-induced light responses, we used two-photon guided patch-clamp techniques to record hyperpolarization in single cone cells under current-clamp whole-cell configuration. The spectral sensitivity of Jaws-expressing cells was measured by stimulating the cells at different wavelengths. The action spectrum of Jaws, with maximal responses between 575 nm and 600 nm was confirmed (**Figure 4A**). To examine temporal properties of Jaws-cones, we first recorded light-responses using illumination pulses at increasing frequencies and observed that cells could follow up to 25 Hz stimuli with an excellent signal-to-noise ratio (**Figure 4B**). This is in line with our previous observations that optogenetically-engineered photoreceptors respond to light at a faster pace than natural photoreceptors. Then we recorded light responses as a function of stimuli of increasing durations, from 20 ms to 4 s. Cells' responses were obtained at all durations, following the stimulus precisely, even at 4 s (**Figure 4C**). Because of the fast kinetics and the robustness of Jaws-cones responses, intermittent and complex stimuli can hence be applied and still elicit responses, thus also reducing drastically the total energy reaching the retina compared with a strategy that would use a single continuous light stimulation, which is important for clinical applications and light stimulation devices.

DISCUSSION

Genetic modification of cells within hiPSC-derived retinal organoids is essential to their utility as models of human organ development, as disease models, or for their therapeutic use as a source of cells for regenerative medicine. Genetic modifications to introduce small changes in the genome such as disease-causing mutations or the knock-out/integration of entire genes mostly use gene-editing tools at the single pluripotent stem cell stage, before selection and differentiation (Kruczek and Swaroop, 2020). However, the expression of exogenous genes to control cellular function after differentiation is needed for asking biological questions concerning disease mechanisms or using the cells for downstream therapeutic applications (Llonch et al., 2018). Moreover, the use of human retinal organoid models to test transgene expression has become a critical addition to the gene therapy pipeline bridging proof of concept work towards clinical applications by removing potential interspecies differences (Kalatzis et al., 2013; Cereso et al., 2014; Garita-Hernandez et al., 2018; Quinn et al., 2018). The specific features of transgene expression need to suit the ultimate purpose of the experiment both for gene therapy validation and transplantation. In our experiments, we sought to achieve a stable modification of the cone photoreceptor cell population within the human retinal organoids to render them light-sensitive using optogenetics. For our purpose, achieving detectable expression early in the cone cell population was necessary to isolate these cells before transplantation.

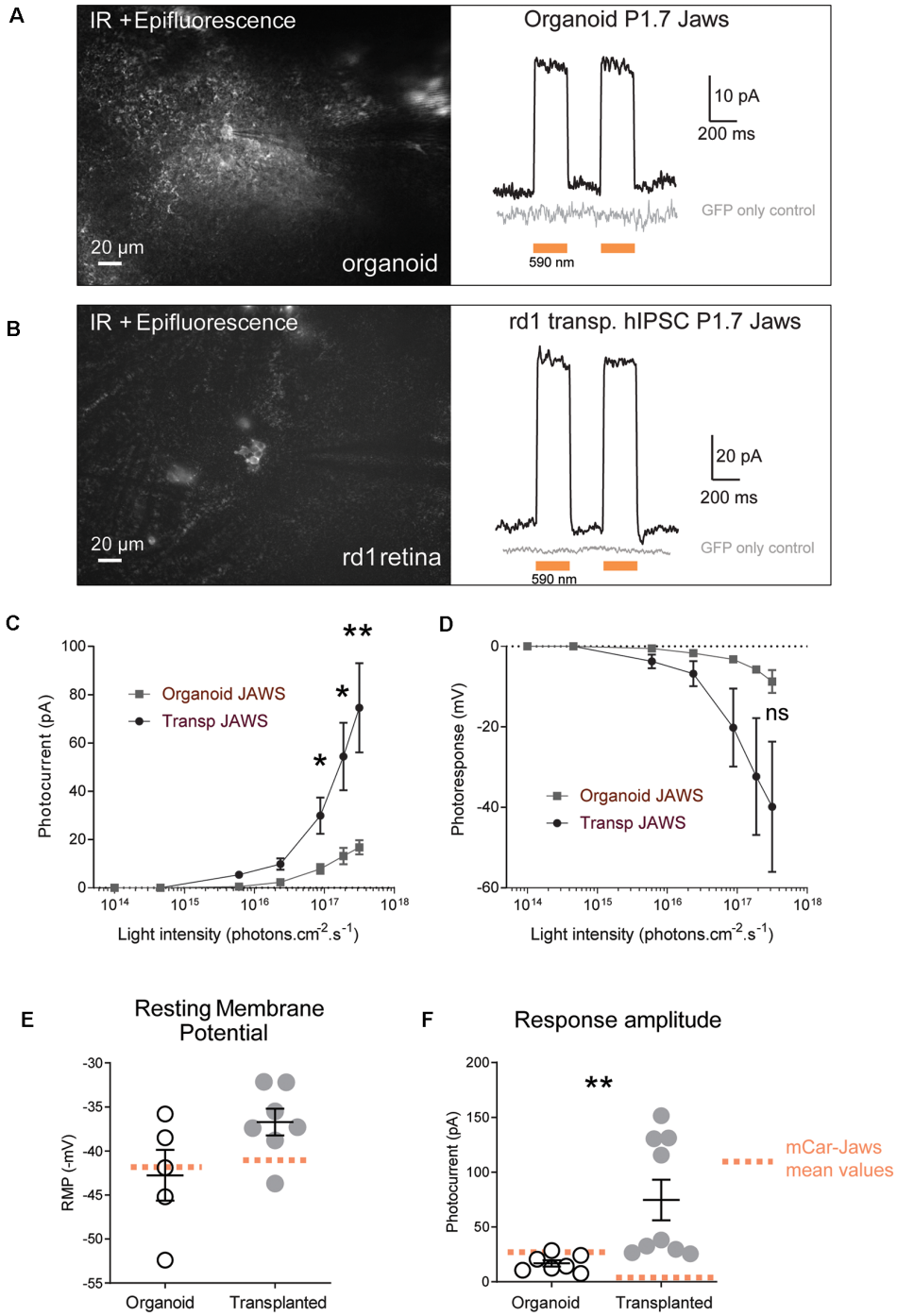

FIGURE 3 | Jaws-driven light responses in engineered retinal organoids before and after transplantation. **(A)** *Left*. Infrared (IR)/epifluorescence image showing a transfected organoid with an electrode contacting a GFP+ cell. *Right*, photocurrent responses after stimulation with two consecutive flashes at a light intensity of 3.1×10^{17} photons cm^{-2} s^{-1}, absence of response in GFP- cells is shown in gray. **(B)** *Left*. Infrared/epifluorescence-Infrared image of a rd1 transplanted retina depicting small clusters of fluorescent cells. *Right*, photocurrent responses after stimulation with two consecutive flashes at a light intensity of 3.1×10^{17} photons cm^{-2} s^{-1}, absence of response in GFP-cells is shown in gray. **(C,D)** Light-intensity dependency of photoresponse amplitude. Photocurrent **(C)** and voltage hyperpolarization **(D)** of GFP+ cells in organoids and rd1 transplanted retinae as a function of light intensities ranging between 10^{14} and 3.1×10^{17} photons cm^{-2} s^{-1}. **(E)** Resting membrane potential (RMP) of Jaws-expressing photoreceptors in the dark (at 0 current) for the recordings presented in panel **(D)**. Mean RMP values were −42, 76 ± 2, 88 mV in organoids and −36.72 ± 1.52 mV in transplanted cells. **(F)** Comparison of maximum photocurrent response amplitudes at the highest light stimulation intensity, for GFP+ cells in organoids (16.8 ± 2.92 pA) or after transplantation (74.57 ± 18.48 pA). Mean values obtained with our previous protocol (Garita-Hernandez et al., 2019) are depicted as doted orange lines. For all recordings the stimulation was performed at 590 nm if not stated otherwise. Values correspond to mean ± SEM. $*p < 0.05$, $**p < 0.001$, ns = not significant.

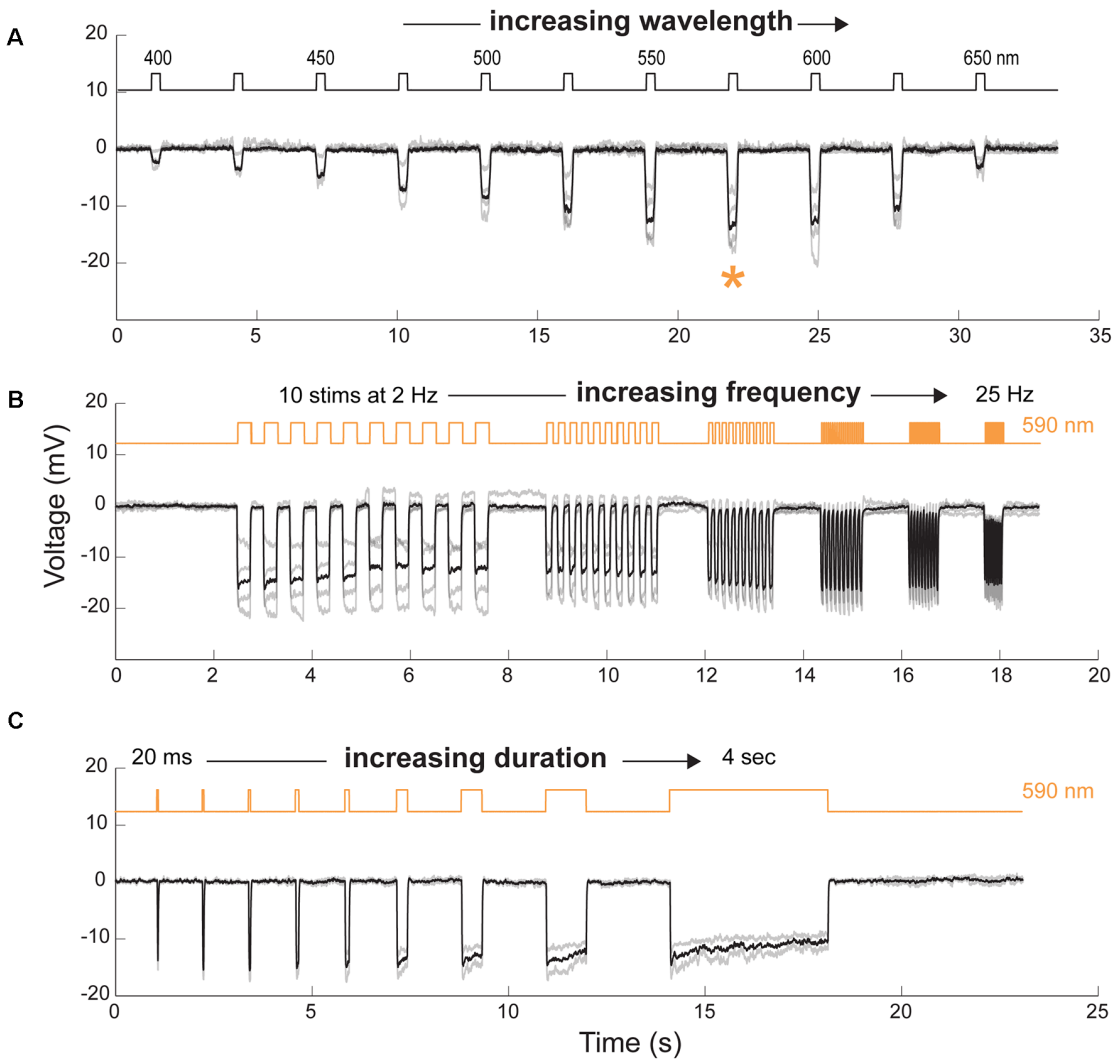

FIGURE 4 | Spectral and temporal properties of transplanted cells. **(A)** Cone hyperpolarization induced by Jaws as a function of increasing wavelengths stimuli ranging from 400 to 650 nm. Maximal responses, when recorded at an intensity of 8×10^{16} photons cm^{-2} s^{-1}, were obtained at a wavelength of 575 nm (orange asterisk). **(B)** Modulation of Jaws-induced voltage responses at increasing stimulation frequencies ranging from 2 to 25 Hz. **(C)** Modulation of Jaws-induced responses as a function of stimulus duration with stimuli ranging from 20 ms to 4 s in Jaws expressing cones at 8×10^{16} photons cm^2 s^{-1}. The timing and duration of stimulations are depicted with black lines in **(A)** or orange lines in **(B** and **C)** (590 nm stimuli). n = 4, 4 and 2 cells in **(A**, **B** and **C)**, respectively. Individual cell responses are represented in gray, mean response in black.

Increasing the light sensitivity within the sorted cell population post-transplantation was a second desirable feature fit for our downstream application.

In advanced stages of retinal degeneration where photoreceptor cells are lost, a promising therapeutic strategy would be to transplant healthy and functional photoreceptors. For this type of therapy to be successful, transplanted photoreceptor cells need to respond to light and transmit the information to second-order neurons of the host retina. Moreover, chromophore replenishment through the support cells should be ensured. Despite several advances in the field of retinal differentiation (Meyer et al., 2009; Reichman et al., 2014, 2017; Zhong et al., 2014; Mellough et al., 2015; Garita-Hernandez et al., 2018; Capowski et al., 2019), functional light responses remain sparsely reported at the cellular level (Zhong et al., 2014; Hallam et al., 2018; Cowan et al., 2020). Moreover, transplantation studies using a photoreceptor cell suspension, in end-stage retinal degeneration, have not reported a fully functional outer segment. Importantly in the field, direct proof of transplanted cell functionality by direct patch-clamp photoreceptor cell recordings is rarely provided. In the case of retinal sheet transplantation, seldom has a developing outer segment been described with some MEA responses (Mandai et al., 2017; Iraha et al., 2018; McLelland et al., 2018), but RPE contact with donor cells has not been studied extensively at this stage. In our recent work, we proposed a new approach and demonstrated that the combination of stem cell-derived photoreceptors and optogenetics can overcome the above-

mentioned issues. We have shown that optogenetically modified cone cells, expressing the microbial opsin Jaws under a mouse cone arrestin promoter can integrate into mouse retinas after the loss of endogenous photoreceptors and transmit the light signal to second and third-order neurons (Garita-Hernandez et al., 2019). This approach overcame the issues related to lack of outer segments and interaction with support cells, however, it required very high light levels for opsin activation and the expression levels were not compatible with cell sorting of the cone population before transplantation. In this work, we outweigh the limitations of our past work by a refined regulation of microbial opsin expression. Implementation of the strong PR1.7 cone promoter enhanced the expression of Jaws in 3D human retinal organoids and improved light responses especially after the cells matured in the subretinal space. Our work challenges the idea that photoreceptor precursors with integration capacity cannot be found at an earlier time point than other transplantation studies have shown, where the purification of a transplantable population has been based on cell surface markers that express later in differentiation using human pluripotent stem cells (**Figure 1H**; Gagliardi et al., 2018; Lakowski et al., 2018). It also highlights the importance of the promoter in driving transgene expression in retinal organoids both in terms of kinetics and expression levels.

DATA AVAILABILITY STATEMENT

Requests to access the datasets should be directed to marcela.garita@inserm.fr.

ETHICS STATEMENT

The animal study was reviewed and approved by local animal experimentation ethics committee (Le Comité d'Ethique pour l'Expérimentation Animale Charles Darwin) and National Institutes of Health guide for the care and use of laboratory animals as well as the Directive 2010/63/EU of the European Parliament.

AUTHOR CONTRIBUTIONS

MG-H optimized the generation and AAV mediated transduction of hiPSC-derived retinal organoids, performed culture, imaging, histology, designed experiments, and wrote the manuscript. AC performed patch-clamp recordings and 2-photon imaging and wrote the manuscript. LG generated hiPSC-derived retinal organoids, performed AAV infections, FACS, histology, imaging, subretinal injections, and fundus imaging. FR generated hiPSC derived retinal organoids, performed AAV infections, histology, and fundus imaging. HK performed subretinal injections. LR helped to optimize the FACS cell sorting. LT assisted in cell culture and AAV infections. LG, FR, and LT helped to draft the manuscript. SP and J-AS provided scientific input. OG provided hiPSCs, provided scientific input, and feedback on the manuscript. JD provided scientific input. DD designed the experiments, provided scientific input, and wrote the manuscript. All authors contributed to the article and approved the submitted version.

FUNDING

This work was supported by Fondation Voir et Entendre, ERC Starting Grants [OPTOGENRET, 309776/(JD), REGENETHER 639888/(DD)], the Centre National de la Recherche Scientifique (CNRS), the Institut National de la Santé et de la Recherche Médicale (INSERM), Sorbonne Université, the Agence Nationale pour la Recherche—Recherche Hospitalo-Universitaire en santé (RHU; Light4Deaf), PhD fellowship from the AFM-Téléthon (HK), and LCL Foundation (DD).

ACKNOWLEDGMENTS

We thank Camille Robert and Céline Winckler for their help in producing viral vectors and performing molecular cloning. Amelie Slembrouck for her assistance in the maintenance of the iPS cultures. We thank Karen Daoud and Marylin Harinquet for their assistance in cryosectioning organoids and retinae. We are grateful to Thierry Léveillard for providing the C3H *rd/rd* (rd1) mice and Cheryl Craft for providing the hCAR antibody. We thank Annie Munier and the CISA Cytometry Platform, INSERM, UMS 30, Sorbonne University, Paris.

SUPPLEMENTARY MATERIAL

The Supplementary Material for this article can be found online at: https://www.frontiersin.org/articles/10.3389/fncel.2021.648210/full#supplementary-material.

REFERENCES

Aboualizadeh, E., Phillips, M. J., McGregor, J. E., DiLoreto, D. A., Strazzeri, J. M., Dhakal, K. R., et al. (2020). Imaging transplanted photoreceptors in living nonhuman primates with single-cell resolution. *Stem Cell Reports* 15, 482–497. doi: 10.1016/j.stemcr.2020.06.019

Ahmad, I., Teotia, P., Erickson, H., and Xia, X. (2019). Recapitulating developmental mechanisms for retinal regeneration. *Prog. Retin. Eye Res.* 76:100824. doi: 10.1016/j.preteyeres.2019.100824

Artegiani, B., Hendriks, D., Beumer, J., Kok, R., Zheng, X., Joore, I., et al. (2020). Fast and efficient generation of knock-in human organoids using homology-independent CRISPR-Cas9 precision genome editing. *Nat. Cell Biol.* 22, 321–331. doi: 10.1038/s41556-020-0472-5

Aurnhammer, C., Haase, M., Muether, N., Hausl, M., Rauschhuber, C., Huber, I., et al. (2012). Universal real-time PCR for the detection and quantification of adeno-associated virus serotype 2-derived inverted terminal repeat sequences. *Hum. Gene Ther. Methods* 23, 18–28. doi: 10.1089/hgtb.2011.034

Bowes, C., Li, T., Danciger, M., Baxter, L. C., Applebury, M. L., and Farber, D. B. (1990). Retinal degeneration in the rd mouse is caused by a defect in the β subunit of rod cGMP-phosphodiesterase. *Nature* 347, 677–680. doi: 10.1038/347677a0

Busskamp, V., Duebel, J., Balya, D., Fradot, M., Viney, T. J., Siegert, S., et al. (2010). Genetic reactivation of cone photoreceptors restores visual responses in retinitis pigmentosa. *Science* 329, 413–417. doi: 10.1126/science.1190897

Capowski, E. E., Samimi, K., Mayerl, S. J., Phillips, M. J., Pinilla, I., Howden, S. E., et al. (2019). Reproducibility and staging of 3D human retinal organoids across

multiple pluripotent stem cell lines. *Development* 146, 1–13. doi: 10.1242/dev.171686

Cereso, N., Pequignot, M. O., Robert, L., Becker, F., De Luca, V., Nabholz, N., et al. (2014). Proof of concept for AAV2/5-mediated gene therapy in iPSC-derived retinal pigment epithelium of a choroideremia patient. *Mol. Ther. Methods Clin. Dev.* 1:14011. doi: 10.1038/mtm.2014.11

Chaffiol, A., Caplette, R., Jaillard, C., Brazhnikova, E., Desrosiers, M., Dubus, E., et al. (2017). A new promoter allows optogenetic vision restoration with enhanced sensitivity in macaque retina. *Mol. Ther.* 25, 2546–2560. doi: 10.1016/j.ymthe.2017.07.011

Choi, V. W., Asokan, A., Haberman, R. A., and Samulski, R. J. (2007). Production of recombinant adeno-associated viral vectors for *in vitro* and *in vivo* use. *Curr. Protoc. Mol. Biol.* 78, 1–16. doi: 10.1002/0471142727.mb1625s78

Chuong, A. S., Miri, M. L., Busskamp, V., Matthews, G. A. C. C., Acker, L. C., Sørensen, A. T., et al. (2014). Noninvasive optical inhibition with a red-shifted microbial rhodopsin. *Nat Neurosci* 17, 1123–1129. doi: 10.1038/nn.3752

Collin, J., Zerti, D., Queen, R., Santos-Ferreira, T., Bauer, R., Coxhead, J., et al. (2019). CRX expression in pluripotent stem cell-derived photoreceptors marks a transplantable subpopulation of early cones. *Stem Cells* 37, 609–622. doi: 10.1002/stem.2974

Cowan, C. S., Renner, M., De Gennaro, M., Gross-Scherf, B., Goldblum, D., Hou, Y., et al. (2020). Cell types of the human retina and its organoids at single-cell resolution. *Cell* 182, 1623–1640. e34. doi: 10.1016/j.cell.2020.08.013

Dalkara, D., Byrne, L. C. L. C., Klimczak, R. R. R. R., Visel, M., Yin, L. L., Merigan, W. H. W. H., et al. (2013). *In vivo*-directed evolution of a new adeno-associated virus for therapeutic outer retinal gene delivery from the vitreous. *Sci. Transl. Med.* 5:189ra76. doi: 10.1126/scitranslmed.3005708

Dalkara, D., Goureau, O., Marazova, K., and Sahel, J.-A. A. (2016). Let there be light: gene and cell therapy for blindness. *Hum. Gene Ther.* 27, 134–147. doi: 10.1089/hum.2015.147

El-Shamayleh, Y., Ni, A. M., and Horwitz, G. D. (2016). Strategies for targeting primate neural circuits with viral vectors. *J. Neurophysiol.* 116, 122–134. doi: 10.1152/jn.00087.2016

European Parliament and European Council (2006). Directive No. 2006/25/EC, of 5 April 2006, on the minimum health and safety requirements regarding the exposure of workers to risks arising from physical agents (artificial optical radiation). *Off. J. Eur. Union* 114, 38–59. Available online at: https://eur-lex.europa.eu/eli/dir/2006/25/oj.

Farber, D. B., and Lolley, R. N. (1974). Cyclic guanosine monophosphate: Elevation in degenerating photoreceptor cells of the C3H mouse retina. *Science* 186, 449–451. doi: 10.1126/science.186.4162.449

Fischer, J., Heide, M., Huttner, W. B., Renato Muotri, A., Guizzetti, M., MacGillavry, H., et al. (2019). Genetic modification of brain organoids. *Front. Cell. Neurosci.* 13, 433–437. doi: 10.3389/fncel.2019.00558

Gagliardi, G., Ben M'Barek, K., and Goureau, O. (2019). Photoreceptor cell replacement in macular degeneration and retinitis pigmentosa: a pluripotent stem cell-based approach. *Prog. Retin. Eye Res.* 71, 1–25. doi: 10.1016/j.preteyeres.2019.03.001

Gagliardi, G., Ben M'Barek, K., Chaffiol, A., Slembrouck-Brec, A., Conart, J.-B. B., Nanteau, C., et al. (2018). Characterization and transplantation of CD73-positive photoreceptors isolated from human iPSC-derived retinal organoids. *Stem Cell Reports* 11, 665–680. doi: 10.1016/j.stemcr.2018.07.005

Garita-Hernandez, M., Goureau, O., Dalkara, D., Garita-Hernandez, M., Goureau, O., and Dalkara, D. (2016). Gene and cell therapy for inherited retinal dystrophies. *eLS* 1:16. doi: 10.1002/9780470015902.a0026565

Garita-Hernandez, M., Guibbal, L., Toualbi, L., Routet, F., Chaffiol, A., Winckler, C., et al. (2018). Optogenetic light sensors in human retinal organoids. *Front. Neurosci.* 12:789. doi: 10.3389/fnins.2018.00789

Garita-Hernandez, M., Lampič, M., Chaffiol, A., Guibbal, L., Routet, F., Santos-Ferreira, T., et al. (2019). Restoration of visual function by transplantation of optogenetically engineered photoreceptors. *Nat. Commun.* 10:399725. doi: 10.1038/s41467-019-12330-2

Garita-Hernandez, M., Routet, F., Guibbal, L., Khabou, H., Toualbi, L., Riancho, L., et al. (2020). AAV-mediated gene delivery to 3d retinal organoids derived from human induced pluripotent stem cells. *Int. J. Mol. Sci.* 21:994. doi: 10.3390/ijms21030994

Gonzalez-Cordero, A., Goh, D., Kruczek, K., Naeem, A., Fernando, M., kleine Holthaus, S.-M., et al. (2018). Assessment of AAV vector tropisms for mouse and human pluripotent stem cell-derived RPE and photoreceptor cells. *Hum. Gene Ther.* 29, 1124–1139. doi: 10.1089/hum.2018.027

Gonzalez-Cordero, A., Kruczek, K., Naeem, A., Fernando, M., Kloc, M., Ribeiro, J., et al. (2017). Recapitulation of human retinal development from human pluripotent stem cells generates transplantable populations of cone photoreceptors. *Stem Cell Reports* 9, 1–18. doi: 10.1016/j.stemcr.2017.07.022

Hallam, D., Hilgen, G., Dorgau, B., Zhu, L., Yu, M., Bojic, S., et al. (2018). Human-induced pluripotent stem cells generate light responsive retinal organoids with variable and nutrient-dependent efficiency. *Stem Cells* 36, 1535–1551. doi: 10.1002/stem.2883

International Commission on Non-Ionizing Radiation Protection (2013). ICNIRP guidelines on limits of exposure to incoherent visibl...: health physics health physics. *Health Phys.* 105, 74–96. doi: 10.1097/HP.0b013e3182983fd4

Iraha, S., Tu, H. Y., Yamasaki, S., Kagawa, T., Goto, M., Takahashi, R., et al. (2018). Establishment of immunodeficient retinal degeneration model mice and functional maturation of human ESC-derived retinal sheets after transplantation. *Stem Cell Reports* 10, 1059–1074. doi: 10.1016/j.stemcr.2018.01.032

Juettner, J., Szabo, A., Gross-Scherf, B., Morikawa, R., Rompani, S., Teixeira, M., et al. (2018). Targeting neuronal and glial cell types with synthetic promoter AAVs in mice, non-human primates and humans. *bioRxiv* [Preprint]. doi: 10.1101/434720

Kalatzis, V., Hamel, C. P., and Macdonald, I. M. (2013). Choroideremia: towards a therapy. *Am. J. Ophthalmol.* 156, 433.e3–437.e3. doi: 10.1016/j.ajo.2013.05.009

Khabou, H., Garita-Hernandez, M., Chaffiol, A., Reichman, S., Jaillard, C., Brazhnikova, E., et al. (2018). Noninvasive gene delivery to foveal cones for vision restoration. *JCI Insight* 3:e96029. doi: 10.1172/jci.insight.96029

Kruczek, K., and Swaroop, A. (2020). Pluripotent stem cell-derived retinal organoids for disease modeling and development of therapies. *Stem Cells* 38, 1–10. doi: 10.1002/stem.3239

Lakowski, J., Welby, E., Budinger, D., Di Marco, F., Di Foggia, V., Bainbridge, J. W. B., et al. (2018). Isolation of Human photoreceptor precursors *via* a cell surface marker panel from stem cell-derived retinal organoids and fetal retinae. *Stem Cells* 36, 709–722. doi: 10.1002/stem.2775

Lavail, M. M., and Sidman, R. L. (1974). C57BL/6J Mice with inherited retinal degeneration. *Arch. Ophthalmol.* 91, 394–400. doi: 10.1001/archopht.1974.03900060406015

Lidgerwood, G. E., Hewitt, A. W., and Pébay, A. (2019). Human pluripotent stem cells for the modelling of diseases of the retina and optic nerve: toward a retina in a dish. *Curr. Opin. Pharmacol.* 48, 114–119. doi: 10.1016/j.coph.2019.09.003

Llonch, S., Carido, M., and Ader, M. (2018). Organoid technology for retinal repair. *Dev. Biol.* 433, 132–143. doi: 10.1016/j.ydbio.2017.09.028

Macé, E., Caplette, R., Marre, O., Sengupta, A., Chaffiol, A., Barbe, P., et al. (2015). Targeting channelrhodopsin-2 to ON-bipolar cells with vitreally administered AAV restores ON and OFF visual responses in blind mice. *Mol. Ther.* 23, 7–16. doi: 10.1016/j.jep.2021.113940

Mandai, M., Fujii, M., Hashiguchi, T., Sunagawa, G. A., Ito, S. S., Sun, J., et al. (2017). iPSC-derived retina transplants improve vision in rd1 end-stage retinal-degeneration mice. *Stem Cell Reports* 8, 69–83. doi: 10.1016/j.stemcr.2016.12.008

McLelland, B. T., Lin, B., Mathur, A., Aramant, R. B., Thomas, B. B., Nistor, G., et al. (2018). Transplanted hESC-derived retina organoid sheets differentiate, integrate and improve visual function in retinal degenerate rats. *Investig. Ophthalmol. Vis. Sci.* 59, 2586–2603. doi: 10.1167/iovs.17-23646

Mellough, C. B., Collin, J., Khazim, M., White, K., Sernagor, E., Steel, D. H. W. W., et al. (2015). IGF-1 signaling plays an important role in the formation of three-dimensional laminated neural retina and other ocular structures from human embryonic stem cells. *Stem Cells* 33, 2416–2430. doi: 10.1002/stem.2023

Meyer, J. S., Shearer, R. L., Capowski, E. E., Wright, L. S., Wallace, K. A., McMillan, E. L., et al. (2009). Modeling early retinal development with human embryonic and induced pluripotent stem cells. *Proc. Natl. Acad. Sci. U S A* 106, 16698–16703. doi: 10.1073/pnas.0905245106

Quinn, P. M., Buck, T. M., Ohonin, C., Mikkers, H. M. M., and Wijnholds, J. (2018). "Production of iPS-derived human retinal organoids for use in

transgene expression assays," in *Retinal Gene Therapy* (New York, NY: Humana Press), 261–273.

Reichman, S., Slembrouck, A., Gagliardi, G., Chaffiol, A., Terray, A., Nanteau, C., et al. (2017). Generation of storable retinal organoids and retinal pigmented epithelium from adherent human iPS cells in xeno-free and feeder-free conditions. *Stem Cells* 35, 1176–1188. doi: 10.1002/stem.2586

Reichman, S., Terray, A., Slembrouck, A., Nanteau, C., Orieux, G., Habeler, W., et al. (2014). From confluent human iPS cells to self-forming neural retina and retinal pigmented epithelium. *Proc. Natl. Acad. Sci. U S A* 111, 8518–8523. doi: 10.1073/pnas.1324212111

Slembrouck-Brec, A., Rodrigues, A., Rabesandratana, O., Gagliardi, G., Nanteau, C., Fouquet, S., et al. (2019). Reprogramming of adult retinal Müller glial cells into human-induced pluripotent stem cells as an efficient source of retinal cells. *Stem Cells Int.* 2019, 1–13. doi: 10.1155/2019/7858796

Strauss, O. (2005). The retinal pigment epithelium in visual function. *Physiol. Rev.* 85, 845–881. doi: 10.1152/physrev.00021.2004

Ye, G.-J. G. J., Budzynski, E., Sonnentag, P., Nork, T. M. M., Sheibani, N., Gurel, Z., et al. (2016). Cone-specific promoters for gene therapy of achromatopsia and other retinal diseases. *Hum. Gene Ther.* 27, 72–82. doi: 10.1089/hum.2015.130

Zhong, X., Gutierrez, C., Xue, T., Hampton, C., Natalia, M., Cao, L., et al. (2014). Generation of three dimensional retinal tissue with functional photoreceptors from human iPSCs. *Nat. Commun.* 5:4047. doi: 10.1038/ncomms5047

Conflict of Interest: MG-H, AC, OG, DD, JD, and J-AS are inventors on a patent on the use of hiPSC to treat retinal degeneration (WO2018055131). DD is an inventor on a patent of adeno-associated virus virions with variant capsid and methods of use thereof with royalties paid to Avalanche Biotech (WO2012145601 A2). DD and HK are inventors on pending patent applications on noninvasive methods to target cone photoreceptors (EP17306429.6 and EP17306430.4) licensed to Gamut Tx. DD, HK and OG are founders of Gamut Tx. OG and J-AS are inventors on a patent on hiPSC retinal differentiation (WO2014174492 A1). J-AS is a founder and consultant for Pixium Vision and GenSight Biologics and is a consultant for Sanofi-Fovea, Genesignal, and Vision Medicines.

The remaining authors declare that the research was conducted in the absence of any commercial or financial relationships that could be construed as a potential conflict of interest.

frontiers in Cellular Neuroscience

MINI REVIEW
published: 05 May 2021
doi: 10.3389/fncel.2021.667880

Organoids for the Study of Retinal Development and Developmental Abnormalities

Anne Vielle[1,2], *Yuna K. Park*[1], *Conner Secora*[1,2,3] *and M. Natalia Vergara*[1,2]*

[1]CellSight Ocular Stem Cell and Regeneration Program, Sue Anschutz-Rodgers Eye Center, University of Colorado School of Medicine, Aurora, CO, United States, [2]Linda Crnic Institute for Down Syndrome, Aurora, CO, United States, [3]Master of Science in Modern Human Anatomy Program, Aurora, CO, United States

The cumulative knowledge of retina development has been instrumental in the generation of retinal organoid systems from pluripotent stem cells; and these three-dimensional organoid models, in turn, have provided unprecedented opportunities for retinal research and translational applications, including the ability to model disease in a human setting and to apply these models to the development and validation of therapeutic drugs. In this review article, we examine how retinal organoids can also contribute to our understanding of retinal developmental mechanisms, how this knowledge can be applied to modeling developmental abnormalities, and highlight some of the avenues that remain to be explored.

Keywords: retina, development, stem cells, organoids, congenital abnormalities

OPEN ACCESS

Edited by:
Lin Cheng,
The University of Iowa, United States

Reviewed by:
Stephanie C. Joachim,
Ruhr University Bochum, Germany
Igor O. Nasonkin,
AIVITA Biomedical, Inc., United States
Gerrit Hilgen,
Northumbria University, United Kingdom

***Correspondence:**
M. Natalia Vergara
natalia.vergara@cuanschutz.edu

Specialty section:
This article was submitted to Cellular Neuropathology, a section of the journal Frontiers in Cellular Neuroscience

Received: *15 February 2021*
Accepted: *12 April 2021*
Published: *05 May 2021*

Citation:
Vielle A, Park YK, Secora C and Vergara MN (2021) Organoids for the Study of Retinal Development and Developmental Abnormalities. Front. Cell. Neurosci. 15:667880. doi: 10.3389/fncel.2021.667880

INTRODUCTION

The vertebrate retina is an extension of the central nervous system composed of seven main types of neurons and glia specialized for visual function. Its delicate and complex organization arises during embryonic development through tightly spatiotemporally regulated mechanisms that are highly conserved among vertebrates (**Figure 1**).

The retina originates from the ventral diencephalon, where a group of cells begins to co-express a set of transcription factors including Pax6, Rax, Six3, Six6, and Lhx2, and becomes specified as the eye field (Zuber et al., 2003; Byerly and Blackshaw, 2009). This eye field evaginates bilaterally to form the optic vesicles, which grow distally towards the surface ectoderm where inductive signals from the lens placode contribute to the specification of the retinal placode. Next is a concerted invagination of both tissues to form the lens vesicle and the bilayered optic cup (**Figure 1**). As the inner layer continues to proliferate and become established as the retinal neuroepithelium, interactions with the extraocular mesenchyme and surface ectoderm specify retinal pigmented epithelial (RPE) fate in the outer layer of the optic cup (Adler and Canto-Soler, 2007; Fuhrmann, 2010; Heavner and Pevny, 2012).

Retinogenesis begins at the posterior pole of the retinal neuroepithelium, spreading anteriorly as a wave, with cell cycle exit and fate specification following a sequential yet overlapping pattern that is highly conserved in vertebrates (Cepko et al., 1996). The first cells to differentiate are retinal ganglion cells (RGC), followed by cone photoreceptor precursors, amacrine and horizontal cells, and later by rod photoreceptor precursors, bipolar cells, and Müller glia (Brzezinski and Reh, 2015; Hoshino et al., 2017). Differentiation of cell subtypes and maturation follow, and synaptic formation then leads to the development of plexiform layers, completing the retinal circuitry.

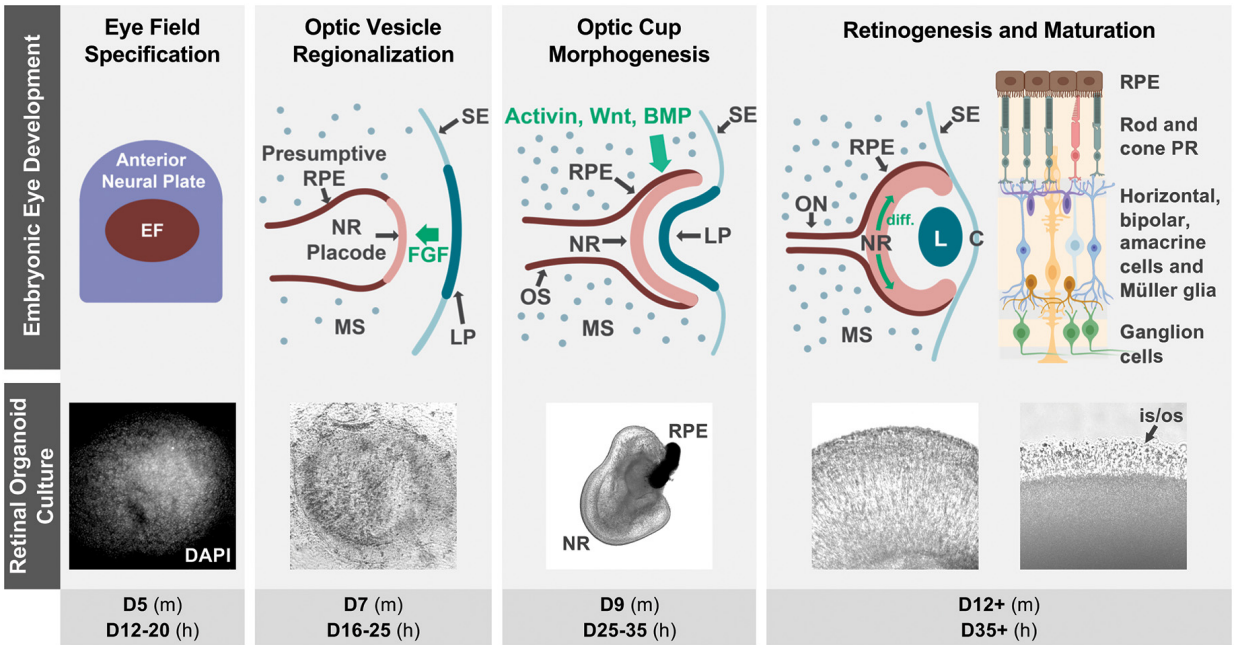

FIGURE 1 | Retinal organoid cultures recapitulate *in vivo* retinal development. The top row illustrates some of the hallmarks of retinal development *in vivo*, as well as some key signaling interactions that specify the neural retina and RPE territories in the optic vesicle (notice that interactions contributing to ventral optic vesicle/optic stalk specification are not described, as they are outside of the scope of this review). Fluorescence (DAPI) and bright field micrographs in the middle row show examples of retinal organoid morphology at each of the corresponding developmental stages (retinal organoids were derived from hiPSC using the Zhong et al., 2014 protocol). The bottom row indicates the approximate timing of each developmental step in mouse (m) and human (h) retinal organoid cultures. The retinal diagram was generated using BioRender. Abbreviations: BMP, bone morphogenetic protein; C, cornea; D, days of differentiation; diff., differentiation wave; EF, eye field; FGF, fibroblast growth factor; L, lens; LP, lens placode; MS, mesenchyme; NR, neural retina; ON, optic nerve; OS, optic stalk; is/os, photoreceptor inner and outer segments; PR, photoreceptors; RPE, retinal pigmented epithelium; SE, surface ectoderm.

Considering its complexity, it is extraordinary that this process could be reproduced *in vitro*, leading to the generation of three-dimensional (3D) retinas or retinal "organoids" from embryonic and induced pluripotent stem cells (ESC and iPSC) from different species. But how does this happen? What can we learn about retinal development by studying organoids? And can we harness the potential of organoids to gain a better understanding of congenital retinal abnormalities? Rather than compiling a comprehensive account of the literature on these topics, we highlight some key studies that illustrate the contributions of retinal organoids to answering these critical questions and propose avenues for further exploration.

CHARACTERISTICS OF RETINAL ORGANOID MODELS

Retinal organoids mimic the cellular composition and histoarchitecture of the native retina, including the differentiation of all major cell types organized in the characteristic trilaminar structure. Moreover, they are capable of achieving an advanced level of maturation, including the ability to respond to light stimulation and form functional synapses (Zhong et al., 2014; Wahlin et al., 2017; Hallam et al., 2018; Cowan et al., 2020). Remarkably, to date, the only way to achieve this high level of complexity is by harnessing the stem cells' ability to recapitulate development (**Figure 1**; Meyer et al., 2009; Eiraku et al., 2011; Nakano et al., 2012; Zhong et al., 2014; Volkner et al., 2016; O'hara-Wright and Gonzalez-Cordero, 2020).

During retinal organoid generation, stem cell aggregates are cultured in conditions favoring their differentiation into neuroectodermal lineages. At this point, structures expressing a complete component of eye field transcription factors begin to form spontaneously (Zhong et al., 2014). These eye fields later differentiate into a central region expressing VSX2, a marker of neural retinal fate, surrounded by microphthalmia transcription factor (MITF)-positive cells representative of RPE fates, which in turn are surrounded by neural rosettes that molecularly resemble neural progenitors from the anterior neural tube, a topological arrangement that mimics the optic vesicle in early development (**Figure 1**; Eiraku et al., 2011; Zhong et al., 2014; Takata et al., 2017).

When these optic vesicle analogs are dissected and cultured in suspension, they fold into structures that mimic the inner layer of the optic cup. These early retinal organoids consist of a pseudostratified neuroepithelium where cell division occurs in the external ("apical") surface, with interkinetic nuclear migration displacing nuclei radially to their final location (Eiraku et al., 2011; Zhong et al., 2014). The same pattern of apical cell division is observed even in protocols in which

retinal organoid-like tissues are grown in attachment conditions. Intriguingly, those adherent retinal cultures express LGR5, a Wnt signaling activating receptor in the apical side (Singh et al., 2015). Retinogenesis in organoids also follows the sequence observed *in vivo*, including the posterior to anterior differentiation wave (Zhong et al., 2014; Vergara et al., 2017; Fligor et al., 2018; Langer et al., 2018; Luo et al., 2019). Strikingly, each of the main developmental hallmarks in retinal organoid generation roughly matches the timing of their *in vivo* counterparts in a species-specific temporal sequence (**Figure 1**), as confirmed by molecular, immunohistochemical, and more recently transcriptomic and single cell RNA-sequencing studies (Brooks et al., 2019; Collin et al., 2019a,b; Kaya et al., 2019; Cowan et al., 2020). However, despite the substantial conservation in cellular composition at each developmental stage, significant variability has been noted in the efficiency of retina induction among different pluripotent stem cell lines (Mellough et al., 2019; Cowan et al., 2020).

LIMITATIONS OF THE MODEL

These characteristics make retinal organoids an attractive model to study development, especially in humans, where knowledge is sparse due to the obvious inability to perform experimental manipulations. However, there are important differences between these *in vitro* systems and the *in vivo* scenario (Aasen and Vergara, 2020). Most notably, even though RPE is formed in retinal organoid cultures, it is not juxtaposed to the apical side of the neural retina (Eiraku et al., 2011; Zhong et al., 2014; Takata et al., 2017; Singh et al., 2019). Instead, when the presumptive optic vesicle is excised during organoid generation, the RPE tissue, which remains continuous with the neural retina, lacks the attachment to the neural tube that would hold its position in the embryo *in vivo* and thus folds onto itself forming a clump at the "anterior" end of the organoid.

Retinal organoids also lack microglia, yolk-sac derivatives that invade the optic cup during the period of retinogenesis *in vivo*, and blood vessels, which are of mesodermal origin and enter the developing optic cup through the optic fissure. Organoid cultures instead favor neuroectodermal derivatives, and optic vesicle-like structures are mechanically isolated, thus preventing the formation of an optic stalk and folding of the optic fissure. Moreover, the optic nerve does not form, forcing RGC axons to remain within the organoid cavity. Eventually, as organoids continue to mature, RGCs are lost (Kaya et al., 2019; Cowan et al., 2020).

Finally, even though recent protocols have achieved an increased ratio of the cone to rod photoreceptors (Kim et al., 2019), no macula formation has yet been demonstrated in human retinal organoids, and the ability of these *in vitro* models to respond to light stimulation, albeit remarkable, is significantly smaller in magnitude than that of a mature retina (Zhong et al., 2014; Hallam et al., 2018; Cowan et al., 2020). This may be reflective of an embryonic scenario, even though studies comparing the organoid light response with the onset of function *in vivo* have not been performed.

Considering these and other deficiencies, what insights can stem cell-derived organoid systems contribute to our knowledge of the mechanisms of retinal development?

RETINAL ORGANOIDS OFFER NEW PERSPECTIVES ON DEVELOPMENTAL MECHANISMS

One of the most underappreciated lessons from organoid systems is the largely tissue-autonomous nature of their development. Decades of research have identified the mechanisms that drive retina development, yet organoid systems now bring to light new interpretations and nuances, contributing to a richer understanding of this process.

One example of this is the optic vesicle regionalization. It has been established in animal models that as the optic vesicle evaginates, fibroblast growth factor (FGF) signaling from the surface ectoderm is necessary to specify the presumptive neural retina territory by upregulating the transcription factor Vsx2, which is involved in a cross-repressive loop with MITF. In mouse and chick, removal of the surface ectoderm at the optic vesicle stage results in failure to specify a neural retina, leading to the development of microphthalmic pigmented vesicles, which can be rescued by exogenous FGF administration (Pittack et al., 1997; Hyer et al., 1998; Nguyen and Arnheiter, 2000; Horsford et al., 2005). Conversely, RPE specification and maintenance are driven by signaling molecules including Wnt, bone morphogenetic proteins, and the transforming growth factor-β (TGF-β) family member activin (Fuhrmann, 2008; Westenskow et al., 2009; Heavner and Pevny, 2012; Steinfeld et al., 2013). Studies in chicks indicate that these inductive signals originate from the extraocular mesenchyme (Fuhrmann et al., 2000; Kagiyama et al., 2005; Fuhrmann, 2010), whereas mouse studies implicate the surface ectoderm in this process (Carpenter et al., 2015).

In this context, the fact that retinal organoid development involves the consistent generation of optic vesicle-like structures composed of a central presumptive neural retina and surrounding RPE is remarkable, considering the lack of both surface ectoderm and extraocular mesenchyme. Additionally, even if these cells were produced elsewhere in the culture, the secreted factors that mediate signaling between these tissues *in vivo* would be available to the whole culture and thus would be unlikely to specify positional information. Moreover, the neural retina and RPE are known to remain plastic for some time after specification, and disruption of these external signals causes transdetermination between these two fates *in vivo*. Yet during organoid generation, once the neural retina and RPE are specified, these fates are maintained and the cells continue to differentiate and mature accordingly. This suggests that once the eye field is specified, the cells have the intrinsic ability to undergo differentiation in a manner that maintains the topological organization and subsequent maturation of the neural retina and RPE in the absence of inductive interactions with other tissues. Rather than refuting the importance of tissue interactions in optic vesicle regionalization, this seemingly contradictory finding may favor the hypothesis that interactions

between embryonic tissues *in vivo* orchestrate a dynamic balance of inductive and repressive forces that restrict the endogenous differentiation program of the optic vesicle to specific spatial territories, thus ensuring the correct location and size of the developing eye structures.

Another area where retinal organoids are contributing to our understanding of eye development is in optic cup morphogenesis. Organoid systems have strengthened a model in which the morphogenetic events that result in optic vesicle to optic cup transition can be driven by intrinsic forces in the absence of external structures. Eiraku et al. (2011) used atomic force microscopy on mouse retinal organoids and identified a difference in stiffness between the developing neural retina and RPE. They proposed that RPE stiffness, coupled with the apical constriction that occurs at the hinge region between the neural retina and RPE due to the action of contractile myosin, are sufficient to drive invagination of the neural retina and shape the optic cup (Eiraku et al., 2011). This hypothesis was later refined by Carpenter et al. (2015) who, taking these findings back to an *in vivo* mouse model, proposed that proliferation of RPE cells near the hinge region driven by Wnt signaling from the surface ectoderm lengthens the stiffer RPE tissue, thus ensuring the correct curvature and shape of the optic cup (Carpenter et al., 2015).

Furthermore, retinal organoids have been used to elucidate the mechanisms that generate the mosaic of cone photoreceptor subtypes in the human retina. Eldred et al. (2018) identified thyroid hormone signaling as a regulator of the temporal switch in cone subtype specification in human retinal organoids. Moreover, they discovered that retinal organoids express thyroid hormone modulators in a temporally dynamic manner that allows them to endogenously regulate the production and ratios of S and L/M cone photoreceptors.

These are only some examples of the power of organoids to contribute to our understanding of retinal development, an exploration that is only in its beginnings.

POTENTIAL OF ORGANOIDS FOR MODELING CONGENITAL RETINAL DEFECTS

Retinal organoids can also contribute to our understanding of how the disruption of developmental mechanisms leads to congenital retinal abnormalities, an approach that has already yielded promising results. Human retinal organoids generated from a patient with microphthalmia due to an R200Q mutation in VSX2 were used to investigate how this mutation leads to the pathological phenotype (Phillips et al., 2014). The study found a significant growth deficit in (R200Q)VSX2 retinal organoids compared to controls, resulting at least in part from reduced neural progenitor cell proliferation. This was accompanied by increased production of RPE at the expense of the neural retina, confirming the important pro-neural role of this gene in human retina development. Moreover, bipolar cell production and photoreceptor maturation were also compromised in mutant organoids, and RNASeq analysis identified some of the signaling pathways that seem to mediate the action of VSX2 in neural retina specification/maintenance. Numerous WNT receptors and downstream effectors, as well as TGF-β family members, were upregulated in VSX2 mutant organoids, while there was a downregulation in the pro-neurogenic FGF3, 9, and 19 genes, exemplifying how these organoids can provide insights into the mechanisms of congenital retinal abnormalities.

Additionally, retinal organoids are already contributing to our understanding of congenital glaucoma. Ohlemacher et al. (2016) compared retinal organoids derived from a patient with an E50K mutation in the Optineurin (*OPTN*) gene that causes familial forms of glaucoma, with organoids derived from control subjects, and found that RGCs in OPTN mutant organoids displayed a significant increase in caspase-3 activation. Further, treatment of OPTN RGCs with BDNF or PEDF caused a reduction in caspase-3 activation, highlighting the utility of this model as a tool for pharmacological development (Ohlemacher et al., 2016). In line with this, a later study using CRISPR/Cas9 gene editing to introduce the same OPTN(E50K) mutation in hiPSC, compared retinal organoids derived from these lines with isogenic controls. Organoids were then dissociated to further evaluate the physiological characteristics of RGCs. The results showed that RGCs differentiated from OPTN(E50K) hiPSC exhibited neurodegenerative deficits including neurite retraction, autophagy dysfunction, and increased excitability (VanderWall et al., 2020).

Retinal organoids have also been recently used to investigate how a human mutation in the *NRL* gene affects cone photoreceptor specification (Kallman et al., 2020). Mutations in this gene can cause enhanced S-cone syndrome, characterized by increased S-cone numbers at the expense of rod photoreceptors. The phenotypic manifestations range from night blindness to visual defects comparable to retinitis pigmentosa (Nishiguchi et al., 2004; Littink et al., 2018). Kallman et al. (2020) found that patient-derived retinal organoids lacking NRL are enriched in S-opsin expressing photoreceptors, and identified MEF2C as a candidate regulator of cone cell fate specification in the human retina, a function that differs from its proposed role in mouse (Kallman et al., 2020).

Furthermore, the fact that retinal organoids are capable of forming inner and outer segments, albeit immature, even in the absence of RPE juxtaposition is remarkable, and allows the possibility to study ciliopathies that affect photoreceptors leading to vision loss, such as Leber congenital amaurosis caused by mutations in the *CEP290* gene (Rachel et al., 2015; Shimada et al., 2017). For example, Parfitt et al. (2016) generated retinal organoids from patient-derived hiPSC harboring a mutation in *CEP290* and found that this mutation led to defective ciliogenesis in photoreceptors, which could be restored by antisense morpholino treatment (Parfitt et al., 2016). Additional examples of inherited retinal dystrophies that have been modeled using human retinal organoids include retinitis pigmentosa due to mutations in *RPGR* (Deng et al., 2018), *PRPF31* (Buskin et al., 2018), *USH2A* (Guo et al., 2019), and *RP2* (Lane et al., 2020).

Additionally, the combination of stem cell-derived RPE cultures with neural retinal organoids to recreate the native

juxtaposition is an active field of research. Achberger et al. (2019) used an organ-on-a-chip technology to show that retinal organoid-RPE contact enhanced photoreceptor outer segment formation and re-established physiological processes including outer segment phagocytosis and calcium dynamics (Achberger et al., 2019). This could have important implications for modeling developmental, physiological, and disease processes that depend on the interaction between these tissues (Singh and Nasonkin, 2020).

Finally, retinal organoids have also been used to model retinoblastoma, the most prevalent intraocular malignancy in children, which has a developmental origin (Liu et al., 2020). Retinal organoids generated from hESC harboring biallelic mutations in the *RB1* gene developed tumor-like structures, and single-cell RNASeq analysis implicated ARR3-positive developing cone precursors as the cell of origin of these tumors. Additionally, the study found that inhibitors of spleen tyrosine kinase (SYK), which was significantly upregulated in this model, led to apoptosis in cancerous organoids, which could be relevant as a potential therapeutic agent (Liu et al., 2020).

Despite these and other encouraging results, the potential of organoids to study congenital retinal defects remains largely untapped. For instance, these models could be used to elucidate the mechanisms that lead to the retinal phenotype observed in conditions like Down syndrome, where progress has been slow due in part to the limitations of animal models in recapitulating human pathophysiology; and they could also contribute to our understanding of how viruses, toxins and other environmental exposures affect the human retina during embryonic development, as it has been described for human brain organoids. For example, infection with Zika virus, which causes fetal microcephaly, has been modeled in forebrain organoids from hiPSCs (Garcez et al., 2016; Qian et al., 2016). These studies showed preferential infection of neural progenitors which led to increased cell death and decreased proliferation, resulting in reduced neuronal cell-layer volume resembling microcephaly. Similar strategies could be used to establish the effect of the Zika virus in retinal organoids. Additionally, in the case of environmental toxins, Wang et al. (2018) used a brain organoid-on-a-chip system to simulate nervous system exposure to prenatal nicotine, and found that it can cause premature differentiation and apoptosis of neurons, with inhibition of neurite outgrowth and structural development of the cortex (Wang et al., 2018). Similar studies exploring the effect of environmental toxins in the retina are currently lacking.

CONCLUSION

The cumulative knowledge of retina development has been instrumental in the generation of retinal organoid systems. The time is now ripe for retinal organoids to inform our understanding of retina development. This deeper understanding, combined with the advantages of retinal organoids as culture models that allow tight control of experimental manipulations and the possibility to model disease in a human setting, offer unique opportunities to gain insights into the pathophysiology of congenital retinal abnormalities for the development of potential therapeutic approaches.

AUTHOR CONTRIBUTIONS

MV and AV wrote the initial manuscript draft. YP and CS prepared the illustrations. All authors contributed to the article and approved the submitted version.

FUNDING

This work was supported in part by a Challenge Grant to the Department of Ophthalmology at the University of Colorado from Research to Prevent Blindness and by the Linda Crnic Institute for Down Syndrome.

REFERENCES

Aasen, D. M., and Vergara, M. N. (2020). New drug discovery paradigms for retinal diseases: a focus on retinal organoids. *J. Ocul. Pharmacol. Ther.* 36, 18–24. doi: 10.1089/jop.2018.0140

Achberger, K., Probst, C., Haderspeck, J., Bolz, S., Rogal, J., Chuchuy, J., et al. (2019). Merging organoid and organ-on-a-chip technology to generate complex multi-layer tissue models in a human retina-on-a-chip platform. *eLife* 8:e46188. doi: 10.7554/eLife.46188

Adler, R., and Canto-Soler, M. V. (2007). Molecular mechanisms of optic vesicle development: complexities, ambiguities and controversies. *Dev. Biol.* 305, 1–13. doi: 10.1016/j.ydbio.2007.01.045

Brooks, M. J., Chen, H. Y., Kelley, R. A., Mondal, A. K., Nagashima, K., De Val, N., et al. (2019). Improved retinal organoid differentiation by modulating signaling pathways revealed by comparative transcriptome analyses with development *in vivo*. *Stem Cell Rep.* 13, 891–905. doi: 10.1016/j.stemcr.2019.09.009

Brzezinski, J. A., and Reh, T. A. (2015). Photoreceptor cell fate specification in vertebrates. *Development* 142, 3263–3273. doi: 10.1242/dev.127043

Buskin, A., Zhu, L., Chichagova, V., Basu, B., Mozaffari-Jovin, S., Dolan, D., et al. (2018). Disrupted alternative splicing for genes implicated in splicing and ciliogenesis causes PRPF31 retinitis pigmentosa. *Nat. Commun.* 9:4234. doi: 10.1038/s41467-018-06448-y

Byerly, M. S., and Blackshaw, S. (2009). Vertebrate retina and hypothalamus development. *Wiley Interdiscip. Rev. Syst. Biol. Med.* 1, 380–389. doi: 10.1002/wsbm.22

Carpenter, A. C., Smith, A. N., Wagner, H., Cohen-Tayar, Y., Rao, S., Wallace, V., et al. (2015). Wnt ligands from the embryonic surface ectoderm regulate 'bimetallic strip' optic cup morphogenesis in mouse. *Development* 142, 972–982. doi: 10.1242/dev.120022

Cepko, C. L., Austin, C. P., Yang, X., Alexiades, M., and Ezzeddine, D. (1996). Cell fate determination in the vertebrate retina. *Proc. Natl. Acad. Sci. U S A* 93, 589–595. doi: 10.1073/pnas.93.2.589

Collin, J., Queen, R., Zerti, D., Dorgau, B., Hussain, R., Coxhead, J., et al. (2019a). Deconstructing retinal organoids: single cell RNA-Seq reveals the cellular components of human pluripotent stem cell-derived retina. *Stem Cells* 37, 593–598. doi: 10.1002/stem.2963

Collin, J., Zerti, D., Queen, R., Santos-Ferreira, T., Bauer, R., Coxhead, J., et al. (2019b). CRX expression in pluripotent stem cell-derived photoreceptors marks a transplantable subpopulation of early cones. *Stem Cells* 37, 609–622. doi: 10.1002/stem.2974

Cowan, C. S., Renner, M., De Gennaro, M., Gross-Scherf, B., Goldblum, D., Hou, Y., et al. (2020). Cell types of the human retina and its organoids at single-cell resolution. *Cell* 182, 1623–1640.e1634.doi: 10.1016/j.cell.2020.08.013

Deng, W. L., Gao, M. L., Lei, X. L., Lv, J. N., Zhao, H., He, K. W., et al. (2018). Gene correction reverses ciliopathy and photoreceptor loss in iPSC-derived retinal organoids from retinitis pigmentosa patients. *Stem Cell Rep.* 10, 1267–1281. doi: 10.1016/j.stemcr.2018.02.003

Eiraku, M., Takata, N., Ishibashi, H., Kawada, M., Sakakura, E., Okuda, S., et al. (2011). Self-organizing optic-cup morphogenesis in three-dimensional culture. *Nature* 472, 51–56. doi: 10.1038/nature09941

Eldred, K. C., Hadyniak, S. E., Hussey, K. A., Brenerman, B., Zhang, P. W., Chamling, X., et al. (2018). Thyroid hormone signaling specifies cone subtypes in human retinal organoids. *Science* 362:eaau6348. doi: 10.1126/science.aau6348

Fligor, C. M., Langer, K. B., Sridhar, A., Ren, Y., Shields, P. K., Michael, C. E., et al. (2018). Three-dimensional retinal organoids facilitate the investigation of retinal ganglion cell development, organization and neurite outgrowth from human pluripotent stem cells. *Sci. Rep.* 8:14520. doi: 10.1038/s41598-018-32871-8

Fuhrmann, S. (2008). Wnt signaling in eye organogenesis. *Organogenesis* 4, 60–67. doi: 10.4161/org.4.2.5850

Fuhrmann, S. (2010). Eye morphogenesis and patterning of the optic vesicle. *Curr. Top. Dev. Biol.* 93, 61–84. doi: 10.1016/B978-0-12-385044-7.00003-5

Fuhrmann, S., Levine, E. M., and Reh, T. A. (2000). Extraocular mesenchyme patterns the optic vesicle during early eye development in the embryonic chick. *Development* 127, 4599–4609. doi: 10.1242/dev.127.21.4599

Garcez, P. P., Loiola, E. C., Madeiro Da Costa, R., Higa, L. M., Trindade, P., Delvecchio, R., et al. (2016). Zika virus impairs growth in human neurospheres and brain organoids. *Science* 352, 816–818. doi: 10.1126/science.aaf6116

Guo, Y., Wang, P., Ma, J. H., Cui, Z., Yu, Q., Liu, S., et al. (2019). Modeling retinitis pigmentosa: retinal organoids generated from the iPSCs of a patient with the USH2A mutation show early developmental abnormalities. *Front. Cell. Neurosci.* 13:361. doi: 10.3389/fncel.2019.00361

Hallam, D., Hilgen, G., Dorgau, B., Zhu, L., Yu, M., Bojic, S., et al. (2018). Human-induced pluripotent stem cells generate light responsive retinal organoids with variable and nutrient-dependent efficiency. *Stem Cells* 36, 1535–1551. doi: 10.1002/stem.2883

Heavner, W., and Pevny, L. (2012). Eye development and retinogenesis. *Cold. Spring. Harb. Perspect. Biol.* 4:a008391. doi: 10.1101/cshperspect.a008391

Horsford, D. J., Nguyen, M. T., Sellar, G. C., Kothary, R., Arnheiter, H., Mcinnes, R. R., et al. (2005). Chx10 repression of Mitf is required for the maintenance of mammalian neuroretinal identity. *Development* 132, 177–187. doi: 10.1242/dev.01571

Hoshino, A., Ratnapriya, R., Brooks, M. J., Chaitankar, V., Wilken, M. S., Zhang, C., et al. (2017). Molecular anatomy of the developing human retina. *Dev. Cell* 43, 763–779.e764. doi: 10.1016/j.devcel.2017.10.029

Hyer, J., Mima, T., and Mikawa, T. (1998). FGF1 patterns the optic vesicle by directing the placement of the neural retina domain. *Development* 125, 869–877. doi: 10.1242/dev.125.5.869

Kagiyama, Y., Gotouda, N., Sakagami, K., Yasuda, K., Mochii, M., Araki, M., et al. (2005). Extraocular dorsal signal affects the developmental fate of the optic vesicle and patterns the optic neuroepithelium. *Dev. Growth Differ.* 47, 523–536. doi: 10.1111/j.1440-169X.2005.00828.x

Kallman, A., Capowski, E. E., Wang, J., Kaushik, A. M., Jansen, A. D., Edwards, K. L., et al. (2020). Investigating cone photoreceptor development using patient-derived NRL null retinal organoids. *Commun. Biol.* 3:82. doi: 10.1038/s42003-020-0808-5

Kaya, K. D., Chen, H. Y., Brooks, M. J., Kelley, R. A., Shimada, H., Nagashima, K., et al. (2019). Transcriptome-based molecular staging of human stem cell-derived retinal organoids uncovers accelerated photoreceptor differentiation by 9-cis retinal. *Mol. Vis.* 25, 663–678. Available online at: http://www.molvis.org/molvis/v25/663.

Kim, S., Lowe, A., Dharmat, R., Lee, S., Owen, L. A., Wang, J., et al. (2019). Generation, transcriptome profiling and functional validation of cone-rich human retinal organoids. *Proc. Natl. Acad. Sci. U S A* 116, 10824–10833. doi: 10.1073/pnas.1901572116

Lane, A., Jovanovic, K., Shortall, C., Ottaviani, D., Panes, A. B., Schwarz, N., et al. (2020). Modeling and rescue of RP2 retinitis pigmentosa using iPSC-derived retinal organoids. *Stem Cell Rep.* 15, 67–79. doi: 10.1016/j.stemcr.2020.05.007

Langer, K. B., Ohlemacher, S. K., Phillips, M. J., Fligor, C. M., Jiang, P., Gamm, D. M., et al. (2018). Retinal ganglion cell diversity and subtype specification from human pluripotent stem cells. *Stem Cell Rep.* 10, 1282–1293. doi: 10.1016/j.stemcr.2018.02.010

Littink, K. W., Stappers, P. T. Y., Riemslag, F. C. C., Talsma, H. E., Van Genderen, M. M., Cremers, F. P. M., et al. (2018). Autosomal recessive nrl mutations in patients with enhanced s-cone syndrome. *Genes* 9:68. doi: 10.3390/genes9020068

Liu, H., Zhang, Y., Zhang, Y. Y., Li, Y. P., Hua, Z. Q., Zhang, C. J., et al. (2020). Human embryonic stem cell-derived organoid retinoblastoma reveals a cancerous origin. *Proc. Natl. Acad. Sci. U S A* 117, 33628–33638. doi: 10.1073/pnas.2011780117

Luo, Z., Xu, C., Li, K., Xian, B., Liu, Y., Li, K., et al. (2019). Islet1 and Brn3 expression pattern study in human retina and hiPSC-derived retinal organoid. *Stem Cells Int.* 2019:8786396. doi: 10.1155/2019/8786396

Mellough, C. B., Collin, J., Queen, R., Hilgen, G., Dorgau, B., Zerti, D., et al. (2019). Systematic comparison of retinal organoid differentiation from human pluripotent stem cells reveals stage specific, cell line and methodological differences. *Stem Cells Transl. Med.* 8, 694–706. doi: 10.1002/sctm.18-0267

Meyer, J. S., Shearer, R. L., Capowski, E. E., Wright, L. S., Wallace, K. A., Mcmillan, E. L., et al. (2009). Modeling early retinal development with human embryonic and induced pluripotent stem cells. *Proc. Natl. Acad. Sci. U S A* 106, 16698–16703. doi: 10.1073/pnas.0905245106

Nakano, T., Ando, S., Takata, N., Kawada, M., Muguruma, K., Sekiguchi, K., et al. (2012). Self-formation of optic cups and storable stratified neural retina from human ESCs. *Cell Stem Cell* 10, 771–785. doi: 10.1016/j.stem.2012.05.009

Nguyen, M., and Arnheiter, H. (2000). Signaling and transcriptional regulation in early mammalian eye development: a link between FGF and MITF. *Development* 127, 3581–3591. doi: 10.1242/dev.127.16.3581

Nishiguchi, K. M., Friedman, J. S., Sandberg, M. A., Swaroop, A., Berson, E. L., Dryja, T. P., et al. (2004). Recessive NRL mutations in patients with clumped pigmentary retinal degeneration and relative preservation of blue cone function. *Proc. Natl. Acad. Sci. U S A* 101, 17819–17824. doi: 10.1073/pnas.0408183101

O'hara-Wright, M., and Gonzalez-Cordero, A. (2020). Retinal organoids: a window into human retinal development. *Development* 147:dev189746. doi: 10.1242/dev.189746

Ohlemacher, S. K., Sridhar, A., Xiao, Y., Hochstetler, A. E., Sarfarazi, M., Cummins, T. R., et al. (2016). Stepwise differentiation of retinal ganglion cells from human pluripotent stem cells enables analysis of glaucomatous neurodegeneration. *Stem Cells* 34, 1553–1562. doi: 10.1002/stem.2356

Parfitt, D. A., Lane, A., Ramsden, C. M., Carr, A. F., Munro, P. M., Jovanovic, K., et al. (2016). Identification and correction of mechanisms underlying inherited blindness in human iPSC-derived optic cups. *Cell Stem Cell* 18, 769–781. doi: 10.1016/j.stem.2016.03.021

Phillips, M. J., Perez, E. T., Martin, J. M., Reshel, S. T., Wallace, K. A., Capowski, E. E., et al. (2014). Modeling human retinal development with patient-specific induced pluripotent stem cells reveals multiple roles for visual system homeobox 2. *Stem Cells* 32, 1480–1492. doi: 10.1002/stem.1667

Pittack, C., Grunwald, G. B., and Reh, T. A. (1997). Fibroblast growth factors are necessary for neural retina but not pigmented epithelium differentiation in chick embryos. *Development* 124, 805–816. doi: 10.1242/dev.124.4.805

Qian, X., Nguyen, H. N., Song, M. M., Hadiono, C., Ogden, S. C., Hammack, C., et al. (2016). Brain-region-specific organoids using mini-bioreactors for modeling ZIKV exposure. *Cell* 165, 1238–1254. doi: 10.1016/j.cell.2016.04.032

Rachel, R. A., Yamamoto, E. A., Dewanjee, M. K., May-Simera, H. L., Sergeev, Y. V., Hackett, A. N., et al. (2015). CEP290 alleles in mice disrupt tissue-specific cilia biogenesis and recapitulate features of syndromic ciliopathies. *Hum. Mol. Genet.* 24, 3775–3791. doi: 10.1093/hmg/ddv123

Shimada, H., Lu, Q., Insinna-Kettenhofen, C., Nagashima, K., English, M. A., Semler, E. M., et al. (2017). *in vitro* modeling using ciliopathy-patient-derived cells reveals distinct cilia dysfunctions caused by CEP290 mutations. *Cell Rep.* 20, 384–396. doi: 10.1016/j.celrep.2017.06.045

Singh, R. K., Mallela, R. K., Cornuet, P. K., Reifler, A. N., Chervenak, A. P., West, M. D., et al. (2015). Characterization of three-dimensional retinal tissue

derived from human embryonic stem cells in adherent monolayer cultures. *Stem Cells Dev.* 24, 2778–2795. doi: 10.1089/scd.2015.0144

Singh, R. K., and Nasonkin, I. O. (2020). Limitations and promise of retinal tissue from human pluripotent stem cells for developing therapies of blindness. *Front. Cell. Neurosci.* 14:179. doi: 10.3389/fncel.2020.00179

Singh, R. K., Occelli, L. M., Binette, F., Petersen-Jones, S. M., and Nasonkin, I. O. (2019). Transplantation of human embryonic stem cell-derived retinal tissue in the subretinal space of the cat eye. *Stem Cells Dev.* 28, 1151–1166. doi: 10.1089/scd.2019.0090

Steinfeld, J., Steinfeld, I., Coronato, N., Hampel, M. L., Layer, P. G., Araki, M., et al. (2013). RPE specification in the chick is mediated by surface ectoderm-derived BMP and Wnt signalling. *Development* 140, 4959–4969. doi: 10.1242/dev.096990

Takata, N., Abbey, D., Fiore, L., Acosta, S., Feng, R., Gil, H. J., et al. (2017). An eye organoid approach identifies Six3 suppression of R-spondin 2 as a critical step in mouse neuroretina differentiation. *Cell Rep.* 21, 1534–1549. doi: 10.1016/j.celrep.2017.10.041

VanderWall, K. B., Huang, K. C., Pan, Y., Lavekar, S. S., Fligor, C. M., Allsop, A. R., et al. (2020). Retinal ganglion cells with a glaucoma OPTN(E50K) mutation exhibit neurodegenerative phenotypes when derived from three-dimensional retinal organoids. *Stem Cell Rep.* 15, 52–66. doi: 10.1016/j.stemcr.2020.05.009

Vergara, M. N., Flores-Bellver, M., Aparicio-Domingo, S., Mcnally, M., Wahlin, K. J., Saxena, M. T., et al. (2017). Three-dimensional automated reporter quantification (3D-ARQ) technology enables quantitative screening in retinal organoids. *Development* 144, 3698–3705. doi: 10.1242/dev.146290

Volkner, M., Zschatzsch, M., Rostovskaya, M., Overall, R. W., Busskamp, V., Anastassiadis, K., et al. (2016). Retinal organoids from pluripotent stem cells efficiently recapitulate retinogenesis. *Stem Cell Rep.* 6, 525–538. doi: 10.1016/j.stemcr.2016.03.001

Wahlin, K. J., Maruotti, J. A., Sripathi, S. R., Ball, J., Angueyra, J. M., Kim, C., et al. (2017). Photoreceptor outer segment-like structures in long-term 3D retinas from human pluripotent stem cells. *Sci. Rep.* 7:766. doi: 10.1038/s41598-017-00774-9

Wang, Y., Wang, L., Zhu, Y., and Qin, J. (2018). Human brain organoid-on-a-chip to model prenatal nicotine exposure. *Lab Chip* 18, 851–860. doi: 10.1039/c7lc01084b

Westenskow, P., Piccolo, S., and Fuhrmann, S. (2009). Beta-catenin controls differentiation of the retinal pigment epithelium in the mouse optic cup by regulating Mitf and Otx2 expression. *Development* 136, 2505–2510. doi: 10.1242/dev.032136

Zhong, X., Gutierrez, C., Xue, T., Hampton, C., Vergara, M. N., Cao, L. H., et al. (2014). Generation of three-dimensional retinal tissue with functional photoreceptors from human iPSCs. *Nat. Commun.* 5:4047. doi: 10.1038/ncomms5047

Zuber, M. E., Gestri, G., Viczian, A. S., Barsacchi, G., and Harris, W. A. (2003). Specification of the vertebrate eye by a network of eye field transcription factors. *Development* 130, 5155–5167. doi: 10.1242/dev.00723

Conflict of Interest: The authors declare that the research was conducted in the absence of any commercial or financial relationships that could be construed as a potential conflict of interest.

frontiers in Cellular Neuroscience

MINI REVIEW
published: 28 June 2021
doi: 10.3389/fncel.2021.638439

Retinal Organoids: Cultivation, Differentiation, and Transplantation

*Xuying Li[1], Li Zhang[1], Fei Tang[2] and Xin Wei[1,2]**

[1] Department of Ophthalmology, West China Hospital, Sichuan University, Chengdu, China, [2] Department of Ophthalmology, Shangjin Nanfu Hospital, Chengdu, China

Retinal organoids (ROs), which are derived from stem cells, can automatically form three-dimensional laminar structures that include all cell types and the ultrastructure of the retina. Therefore, they are highly similar to the retinal structure in the human body. The development of organoids has been a great technological breakthrough in the fields of transplantation therapy and disease modeling. However, the translation of RO applications into medical practice still has various deficiencies at the current stage, including the long culture process, insufficient yield, and great heterogeneity among ROs produced under different conditions. Nevertheless, many technological breakthroughs have been made in transplanting ROs for treatment of diseases such as retinal degeneration. This review discusses recent advances in the development of ROs, improvements of the culture protocol, and the latest developments in RO replacement therapy techniques.

Keywords: retinal organoid, stem cell, retinal ganglion cell, photoreceptor cell, replacement therapy

OPEN ACCESS

Edited by:
Maeve Ann Caldwell,
Trinity College Dublin, Ireland

Reviewed by:
Cecilia Laterza,
University of Padua, Italy
Wang Xuejian,
Weifang Medical University, China

***Correspondence:**
Xin Wei
weixin_1982@163.com

Specialty section:
This article was submitted to Cellular Neuropathology, a section of the journal Frontiers in Cellular Neuroscience

Received: *06 December 2020*
Accepted: *08 June 2021*
Published: *28 June 2021*

Citation:
Li X, Zhang L, Tang F and Wei X (2021) Retinal Organoids: Cultivation, Differentiation, and Transplantation. Front. Cell. Neurosci. 15:638439. doi: 10.3389/fncel.2021.638439

INTRODUCTION

An organoid is a type of tissue induced from stem cells that is able to automatically form three-dimensional structures with a variety of cell types. Organoid structures are highly similar to the organ structures in the human body (Khan et al., 2016). At present, the types of brain organoids that can be induced include the hippocampus, pituitary gland, forebrain, and retina (Brawner et al., 2017; Eastlake et al., 2019; Hua et al., 2020). Retinal organoids (ROs) are induced from stem cells and develop into the optic vesicle and optic cups, which are finally compressed, thinned, and matured. Mature ROs have all of the cell types and structures included in the retina (Miltner and La Torre, 2019). Currently, human embryonic stem cells, induced pluripotent stem cells (iPSCs), retinal progenitor cells (RPCs), mesenchymal stem cells, and other types of stem cells have been used to cultivate ROs with multi-cell retinal laminar structure and ultrastructure (Capowski et al., 2019).

The development of ROs is a major technological breakthrough in the field of transplantation therapy. Because ROs are highly similar to the retinal structure and include all of the cell types of the human retina, the corresponding tissue slices can be separated from the cultured organoids and transplanted into the diseased layers of the retina. This functional replacement also preserves the original structure of the retina, overcoming the disadvantage of previous single cell type transplantation techniques (Singh et al., 2018; Ahmad et al., 2020). Some studies have shown that ROs provide an opportunity to restore vision in patients with advanced retinal degeneration (McLelland et al., 2018; Ahmad et al., 2020).

Compared with two-dimensional stem cell techniques, three-dimensional ROs can more realistically simulate the interaction between the micro-environment in each layer *in vivo*, which allows investigation of the poor efficacy of some drugs in practical applications and may therefore result in the development of more efficient drugs. Additionally, the three-dimensional suspension medium is beneficial for generation of certain cell types, such as neurons, thus providing the possibility to improve the production efficiency of retinal ganglion cells (RGCs) and obtain longer axons. This is particularly beneficial for the study of the pathogenesis and repair of neuro-degenerative diseases such as glaucoma (Wright et al., 2015). Goureau et al. (2020) induced and cultured iPSCs from blind patients and obtained ROs with pathological characteristics, in which early loss of photoreceptor cells (PRCs) could be observed.

However, the use of ROs for disease modeling and even clinical applications still has various deficiencies at the current stage. These limitations mainly include the long culture process, insufficient yield, and great heterogeneity among ROs cultivated by different protocols. Meanwhile, research on various diseases requires differentiation of ROs to produce sufficient numbers of specific cells.

This review focuses on the development process of ROs, improvements in the culture protocol of ROs, and the induction of differentiation of PRCs and RGCs in ROs to provide useful information about disease modeling and clinical applications of ROs.

DEVELOPMENT OF RETINAL ORGANOIDS

The development of ROs occurs as follows. First, stem cells proliferate and aggregate and are then induced to form neuroepithelial cells. Then, the cells develop into neuro–spheres, including forebrain progenitor cells and optic vesicles. The latter will develop into optic cups and the neural retina, and the cells will differentiate into RGCs, amacrine cells and horizontal cells, followed by PRCs (including rods and cones), as well as bipolar cells and Muller glial cells (Reichman et al., 2014).

The differentiated cells spontaneously undergo nuclear migration, form a spire-like shape, and finally arrange into a laminated structure, where the RGCs are located in the inner layer and the PRCs are located in the outer layer of ROs (Nakano et al., 2012; Ohlemacher et al., 2015, 2019; Cui et al., 2020; Fligor et al., 2020). At the same time, the mature PRCs in the organoids have an outer segment and photosensitivity, which can be used in the study of retinal degeneration and other related diseases (Zhong et al., 2014).

Eiraku et al. (2011) showed that this migration is determined by intracellular processes, such as expression of high levels of myosin at the initial stage of organoid invagination, resulting in a certain degree of rigidity, and this process is related to the specific local regulation of the epithelium. Phillips et al. also found that the human–derived retina expresses intercellular communication genes such as *CX36* at this stage. Meanwhile, the genes expressed, such as *VGLUT1*, *SNAP-25*, *AMPA1*, *NMDA2A*, and *MGLUR6*, are also closely related to the formation of synaptic connections, and the platelet reactive protein gene *THBS2* is up-regulated (Phillips et al., 2012; Palomo et al., 2014).

Currently, the development and differentiation process of ROs can be continuously monitored and quantitatively evaluated. Some studies have developed an algorithm based on deep learning using bright-field images, allowing researchers to predict the direction of differentiation and identify differentiation even before gene expression in the mouse–derived organoid culture (Kegeles et al., 2020a). When human–derived organoids develop into a lamellar structure, real-time imaging modalities such as fluorescence lifetime imaging microscopy, hyperspectral imaging, and optical coherence tomography can be used to monitor the metabolic status of ROs and even PRCs, and these methods will not damage the culture structure (Browne et al., 2017). The above-mentioned technologies that can be used to evaluate and monitor the development and differentiation of ROs have been summarized in **Figure 1**. Immunocytochemistry methods have also been used to monitor typical genes such as *VSX2* (corresponding to RPCs), *HuC/D* (corresponding to RGCs), *CHAT* (corresponding to starburst amacrine cells), *Crx* (corresponding to PRCs), and *RXR* (corresponding to cone precursors), aiming to observe and map the progression of differentiation of each human–derived cell type (Chichagova et al., 2019). The improved protocols mentioned in this chapter are summarized in **Table 1**.

IMPROVEMENT OF RETINAL ORGANOID CULTURE

Promotion of Retinal Organoid Differentiation

The culture process of ROs is very time-consuming. According to reports, at least 100 days are required for human pluripotent stem cells to form ROs and differentiate into mature and functional PRCs (Gasparini et al., 2019). Therefore, promotion of the differentiation of organoids to shorten the culture time is an important issue. Cells expressing *PAX6* have been shown to be the major cell type comprising ROs. In one study, mouse embryonic stem cells were added to serum-free 96-well plates with approximately 3,000 floating cells in each well to induce clumped embryoids. Then, extracellular matrix was added to the culture medium to differentiate the culture into neuroepithelial cells with a degree of rigidity. After a week, transcription factors specific to the eye such as *PAX6* were expressed, and differentiation into optic vesicles began (Llonch et al., 2018). Zhu et al. attempted to induce iPSC NCL-1 produced by CD34(+) umbilical cord blood cells to produce rosette-like nerve aggregates by culturing cells for 2–4 weeks and then manually separating the cells and switching to ultra-low adhesion 6-well plates with neural stem cells medium. Changing the medium 2–3 times a week can induce the aggregates to self-organize and differentiate into organoids. The organoids also have a laminated cell structure and take the shape of the optic cup (Zhu et al., 2018). For the induction culture of human pluripotent stem cells, the stem cells need to be suspended in

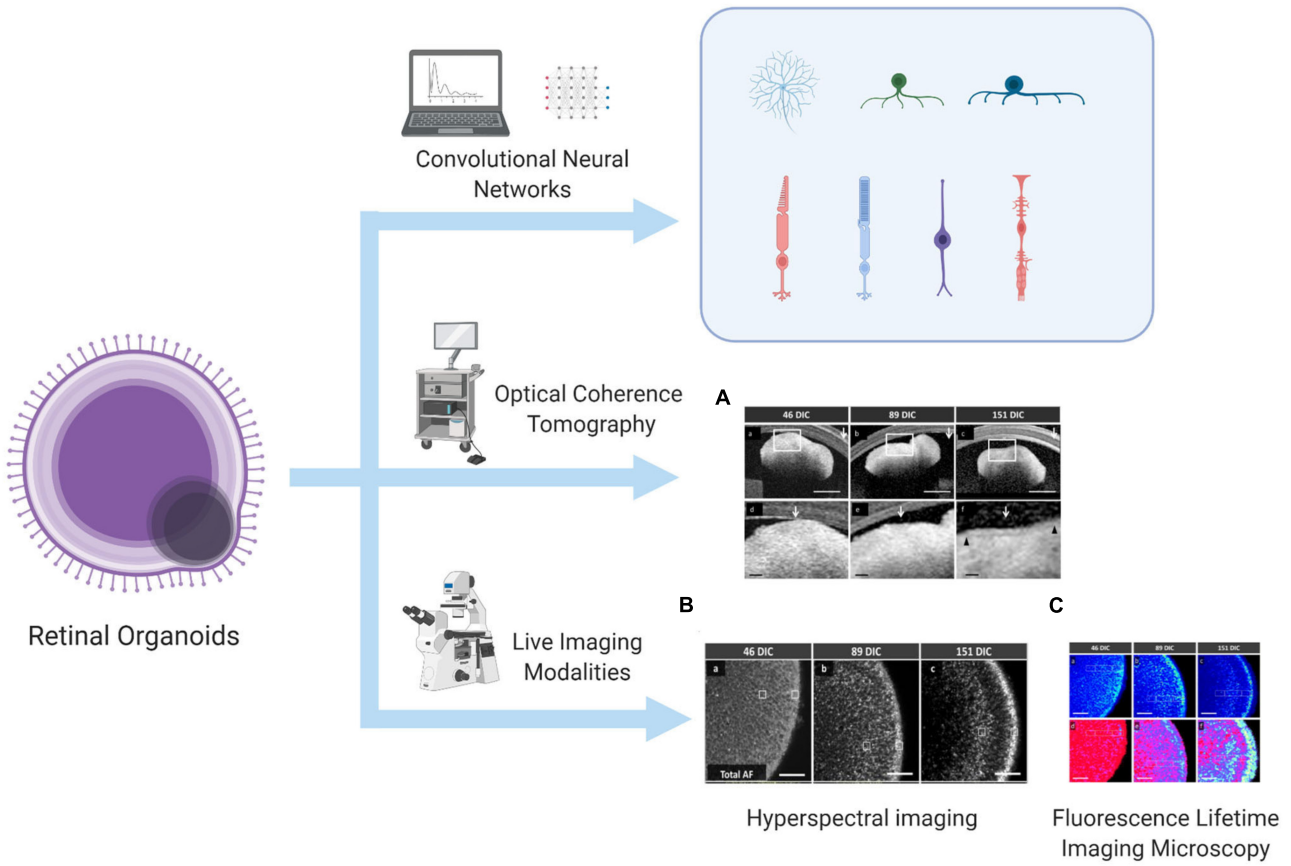

FIGURE 1 | Algorithm to predict and identify organoid differentiation, and real-time imaging modalities to monitor the metabolic status of the lamellar structure of ROs. This illustration is created by Biorender.com **(A)** OCT image, **(B)** HSpec image, and **(C)** FLIM image are reprinted with permission from ref (Browne et al., 2017). Copyright © 2017 Browne AW. et al.

neural induction medium to form aggregates and differentiate into neuroepithelium. After 2 weeks, the aggregates are cultured in retinal differentiation medium to induce their differentiation into three-dimensional optical vesicles (Ohlemacher et al., 2015). However, the xenogeneic/feeder-free culture protocol can greatly shorten the culture time. Reichman et al. used Essential 8 medium, which is a pure chemical medium, to induce human iPSCs to differentiate into RPCs and neuroretinal structures after five passages, bypassing the embryoid body stage and thus shortening the culture time from 6 months to 1 month. Additionally, this process can extend the lifespan of PRCs that are functional in organoids for up to 10 months (Reichman et al., 2017). There is another protocol achieving a xenogeneic-free cell culture. Perepelkina et al. suggested that a low concentration of Synthemax SC II (vitronectin mimic peptide) can be used to replace the Matrigel medium to induce the early differentiation of the mouse ESC–derived retina. Furthermore, Synthemax SC II concentrations in the range of 0.005–0.02 mg/ml have no dose-dependent effects on the cells (Perepelkina et al., 2019).

It is currently thought that insulin-like growth factor 1, retinoic acid, and triiodo thyroxine not only play an important role in the development of actual retinas, but are also essential for cell differentiation in ROs. Studies have also found that adding serum and high glucose concentrations to the medium promotes the differentiation and development of human iPSC–derived ROs (Chichagova et al., 2019; Slembrouck-Brec et al., 2019).

In addition, an electrospinning polybenzyl glutamate scaffold is also used. This material is composed of polypeptides containing glutamate. Because the glutamic acid pathway is related to the development of neurons, it promotes an increase in RGCs and axon growth in human iPSC–derived Ros. Moreover, compared with ordinary culture medium, hiPSC on PBG takes a shorter time to form organoids and differentiate into RGC (Chen et al., 2019). Previous studies have designed the electrospun scaffold, which can simulate the growth process of RGC axons *in vivo*, thereby promoting the survival of RGCs and guiding the axons to project along the radial direction of the scaffold (Kador et al., 2013). Kador et al. (2014) designed the concentration gradient of Netrin-1, a guidance factor, on the electrospun scaffold to promote the polarization of RGCs, and further promote the connection of RGC and visual pathway during stem cell

TABLE 1 | Summary of improved protocols of retinal organoids.

Study	Improved protocols	Effects
Development of retinal organoids		
Kegeles et al., 2020a	An algorithm based on deep learning using bright-field images	Predicting the direction of differentiation and identify differentiation
Browne et al., 2017	Real-time imaging modalities including fluorescence lifetime imaging microscopy, hyperspectral imaging, and optical coherence tomography	Non-invasive real-time monitoring of metabolic status of ROs and even PRCs
Chichagova et al., 2019	Immunocytochemistry methods	Observing and mapping the progression of differentiation
Promotion of retinal organoid differentiation		
Llonch et al., 2018	Adding mESC to a serum-free 96-well plate to keep the cell density at 3000/well, then adding extracellular matrix after induction of embryoid bodies	Differentiating the culture into rigid neuroepithelium, express PAX6 after 1 week, and differentiate into optic vesicles
Zhu et al., 2018	Stem cells were manually separated after 2–4 weeks to form rosette-like aggregates and were cultured in a low-adhesion 6-well culture plate and NSC medium which was changed every 2–3 times a week.	Promoting the differentiation of stem cells into organoids with an optic cup shape and multi-layered cell structure.
Ohlemacher et al., 2015	Human iPSCs are induced into RPCs by neural induction medium and retinal differentiation medium, and then remain suspended in the neural induction medium to form aggregates.	Inducing hPSC into RPCs and visual vesicles
Reichman et al., 2017	Passing human iPSC five times in Essential 8	Skipping the embryoid body stage and directly differentiating into RPCs and neuroretinal structures, shortening the time from 6 months to 1 month.
Perepelkina et al., 2019	Using Synthemax SC II (vitronectin mimic peptide) at a concentration of 0.005–0.02 mg/ml to induce early differentiation of the retina	Achieving xenogeneic-free cell culture without the dose-dependent effects
Chen et al., 2019	Polybenzyl glutamate scaffold	Promoting the increase in RGCs and axon growth in ROs.
Kador et al., 2013	Electrospun scaffold	Promoting the survival of RGC and guide axons to project radially along the scaffold
Kador et al., 2014	Creating the concentration gradient of Netrin-1 on the electrospun scaffold	Promoting the polarization of RGC cells
Yao et al., 2015	Subretinal space transplantation of mRPC with PCL stent	Guiding stem cells to differentiate, help cells move and express corresponding markers
Augmentation of retinal organoid production		
Zhu et al., 2018	Passing the aggregates in the ratio of 1:3, and use low-adhesion culture plates and NSC medium for the neuroepithelium	Increasing the yield of ROs
Völkner et al., 2016, 2019	Induceing mESC differentiation with Matrigel. The neuroepithelium is separated at the ratio of 1:3, and 40% oxygen is added before maturity.	Increasing the yield of ROs
Regent et al., 2020	Dispersing the adherent cell clusters and keep them in suspension	Increasing the yield of ROs by 5 times
Perepelkina et al., 2019	Adding 2% lipid concentrate or 0.06% methyl cellulose to the medium	Reducing the aggregation of culture.
Reduction of retinal organoid heterogeneity		
Llonch et al., 2018	Adding mESC to a serum-free 96-well plate to keep the cell density per well of 96-well plate at 10000/well	Reducing heterogeneity and increase production
Zhu et al., 2018	RO culture staging system, including light microscopy, electron microscopy, optical coherence tomography, metabolic imaging, immunohistochemistry, and other technologies.	Synchronizing the cultivation phase and reduce heterogeneity
Extraction and transplantation of ganglion cells		
Wang et al., 2019	Transplanting RPC in RO to the ganglion cell layer	Making up for the lack of RGC in the ganglion cell layer
Rabesandratana et al., 2020	Intravitreal injection of RGC screened by cell marker THY1	Contacting the remaining RGCs
Tanaka et al., 2015	BDNF transforms organoids into the two-dimensional development model after developing into the three-dimensional vesicle structure	Increasing the differentiation efficiency of ganglion cells and making them have higher-level functions
Extraction and transplantation of photoreceptor cells		
Chen et al., 2016	The High Efficiency Hypoxia Induced Generation of Photoreceptors in Retinal Organoids protocol	Restoring the development of photoreceptor cells *in vivo*
Pan et al., 2020	The reporter gene tdTomato	Non-invasive monitoring of photoreceptor cell differentiation

transplantation. Studies have also reported that the use of polycaprolactone scaffold for mouse RPC subretinal space transplantation is able to guide stem cell differentiation and help cells move to the outer nuclear layer of the retina, and express photoreceptor-related markers. These strategies may provide references for promoting the effective transplantation of ROs (Yao et al., 2015).

In summary, maintaining a certain cell density and keeping the cells in suspension can induce the formation of embryoid body, and the addition of extracellular matrix promotes the rigidity of the culture. When high-quality iPSCs are suspended, rosette-like nerve aggregates will appear first, and they can differentiate into ROs after being induced by neural stem cells medium. And hPSC can be cultured by neural induction

medium and retinal differentiation medium to produce optical vesicles. The xenogeneic-free cell culture protocols such as Essential 8 medium and low-concentration Synthemax SC II medium can bypass the embryoid body stage and greatly shorten the time required for differentiation. In addition, electrospun scaffolds can promote RGC axon projection, and glutamate-containing scaffold can shorten the differentiation time of RGCs, and the Netrin-1 protein gradient can increase the polarization ratio of RGCs. There are also scaffolds such as polycaprolactone scaffold, which can promote the movement of the culture to the corresponding level of the retina, thereby providing the possibility for precise replacement therapy. The improved protocols mentioned in this section are summarized in **Table 1**.

Augmentation of Retinal Organoid Production

One of the major problems within RO research is the insufficient yield of organoid culture. In suspension, stem cells tend to aggregate, resulting in low organoid yields. At present, most studies suggest separating organoids manually to improve production efficiency (Völkner et al., 2016). Zhu et al. (2018) attempted to improve the production efficiency of human–derived ROs by screening high-quality iPSC NCL-1, subculturing the cells at 1:3 when aggregation is observed, and isolating and cultivating the neuroretina part in neural stem cell medium in a low-adhesion culture plate. Some studies have explored protocols to produce large-scale laminated organoids. In contrast to the mainstream protocol, this method does not require separation of aggregates, but instead induces the aggregated mouse embryonic stem cells to form neurons using Matrigel. The resulting neuroepithelium is then separated into three equal-sized parts, and 40% oxygen is added when the neuroepithelium nears maturity. This solution can double the production of organoids and improve their quality (Völkner et al., 2016, 2019). In addition to separating aggregates, some studies have explored a different method to increase yield, that is, promoting the development and differentiation of cultures that have not yet formed the three-dimensional structure of organoids. Regent et al. extracted and dispersed human–derived cell clusters that were not suspended in medium with a cell scraper, and the small clumps were kept floating. 24 h later, a large number of ROs shaped like neuroepithelium could be observed. This method increased the yield by five times, and no significant difference was observed compared with ROs cultured by dissection and separation (Regent et al., 2020). This finding indicates that the yield of the cultures is related to the degree of culture suspension. Perepelkina et al. (2019) suggested that adding 2% lipid concentrate or 0.06% methyl cellulose to the medium can reduce aggregation of the culture, thus improving the mouse–derived culture efficiency.

In short, the organoid production is closely related to the degree of suspension of the culture. Manual separation of aggregates or neuroepithelium is the most direct solution to increase organoid production. Reducing the degree of cell aggregation or suspending adherent cells is another strategy to increase yield. The improved protocols mentioned in this section are summarized in **Table 1**.

Reduction of Retinal Organoid Heterogeneity

In addition to the low yield of organoid cultures, another obstacle to organoid research lies in the great heterogeneity among various organoid cultures. Therefore, it is urgent to explore a reproducible culture protocol to reduce heterogeneity. This is also a major problem that hinders the translation of RO research into clinical practice and leads to the risk of damaging the normal retinal structure of the recipient and causing teratoma when retinal organ transplantation is performed clinically (Ahmad et al., 2020). Although studies have shown that, for ROs derived from reprogrammed human iPSCs, the culture process itself may enable the ROs to acquire immunogenicity and cause the recipient to produce a T-cell immune response in the transplantation stage, thus avoiding the risk of teratomas caused by organoid heterogeneity (Phillips et al., 2012). Studies that have summarized the culture schemes that promote RO differentiation have shown that the shape of the well, cell number in each well, composition of each medium, and method of culturing aggregates are factors that lead to the great heterogeneity among ROs in different culture conditions. When the mouse ESC–derived cell number is 10,000/well in a 96-well plate, the size of the aggregates generated will be 380–550 μm, which will significantly reduce the degree of heterogeneity of organoids among different batches and greatly increase the number of organoids at the same time (Perepelkina et al., 2019).

Capowski et al. developed a human–derived RO culture staging system using light microscopy, optical coherence tomography, metabolic imaging, electron microscopy, immunohistochemistry, and other technologies to synchronize various culture stages and reduce organoid heterogeneity. First, the organoids were divided into the neuroepithelial stage, dark nucleus stage, and hairlike surface appendage stage using light microscopy. Optical coherence tomography scanning of these three culture stages revealed that no layered structures were present in stage 1 and 2, and alternating high and low reflectivity layers appeared in stage 3. Immunohistochemistry results showed that the main cells in stage 1 were neural RPCs, RGCs, and starburst amacrine cells. A large number of PRC precursors and gradually maturing cone and rod cells appeared in stage 2. Stage 3 included more mature outer nuclear layer and plexiform layer cells, as well as mature upper and inner core layer cells. At this time, PRCs already have light-sensing function, but the cells formed in stage 1 exhibit structural disorder and degeneration (Capowski et al., 2019).

In a nutshell, maintaining the consistency of cell density in each culture dish can reduce the heterogeneity of organoids. The use of light microscopy, electron microscopy, optical coherence tomography and other methods can synchronize the differentiation process of cultures, thereby reducing the

heterogeneity between products. The improved protocols mentioned in this section are summarized in **Table 1**.

EXTRACTION AND TRANSPLANTATION OF VARIOUS CELL TYPES IN THE RETINA

Extraction and Transplantation of Ganglion Cells

Ganglion cells are closely related to glaucoma. Diseases that can cause glaucoma may lead to the loss of ganglion cells through mechanical compression, abnormal blood supply, and immune mechanisms (Cohen and Pasquale, 2014). Wang et al. attempted to transplant RPCs in human–derived ROs into the ganglion cell layer of mice, but only a portion of RGCs remained in this layer. The implanted RPCs filled the original positions of RGCs in the ganglion cell layer and even expressed the RGC-specific marker BRN3A (Wang et al., 2019). Rabesandratana et al. also reported that the cell marker THY1 can be used to screen out effective human-derived RGCs. When these cells are injected into recipient mice vitreous, they will associate with the remaining RGCs and survive for 1 month (Rabesandratana et al., 2020).

Unfortunately, the number of ganglion cells in organoids is not substantial, and they will gradually degenerate over time (Pereiro et al., 2020). In ROs derived from PSCs of Thy1-EGFP transgenic mice, the ganglion cell markers BRN3B and SMI-312 can be maintained for 2–3 weeks, and the RO ganglion cells obtained from human iPSCs can be identified for 4 weeks (Kobayashi et al., 2018), but the expression time is still much shorter than that of PRCs. Miltner and La Torre (2019) suggested that ganglion cell apoptosis may be mediated by the Bax signaling pathway. Therefore, to study RGCs in ROs, it is necessary to explore a protocol that can efficiently produce RGCs in large numbers. Converting three-dimensional organoid cultures into two-dimensional cultures is an effective method to amplify ganglion cells. Tanaka et al. found that brain-derived neurotrophic factor can transform human–derived organoids into a two-dimensional development model after the formation of three-dimensional optic vesicle structures, thereby increasing the differentiation efficiency of ganglion cells. The differentiation rate was as high as 90%, and the cells expressed BRN3B, MATH5, and other specific markers. The cells also had characteristics of ganglion and nerve cells, such as axoplasmic transport and action potentials, suggesting that these cells have a higher level of function (Tanaka et al., 2015).

A study by Fligor et al. also suggested that another factor that influences the effect of RGC transplantation is the length of RGC axons. An insufficient RGC axon length will affect the synaptic connections between ganglion cells and the visual pathway, leading to failure of RGC transplantation. Thus, investigation of factors affecting the length of ganglion cell axons in organoids is conducive to the improvement of RGC replacement therapy (Fligor et al., 2018). Prolonging the survival time of ganglion cells is another strategy for RGC replacement. Kobayashi et al. (2018) found that ganglion cells extracted from more mature organoids have a greater ability to elongate axons, allowing easier establishment of connections with the brain. Aparicio et al. found that human–derived RPCs and ganglion cell precursors express high levels of CD184 markers, while mature ganglion cells mainly express CD171. Therefore, this differential expression of ganglion cell markers allows monitoring of ganglion cell development and collection of cells at specific times to obtain ganglion cells that can produce sufficiently long axons (Aparicio et al., 2017). Tanaka et al. (2015) found that addition of Muller cells to human–derived ganglion cell medium can significantly improve the survival rate of ganglion cells and significantly extend their functional axons.

Injection of Muller glial cells derived from ROs into rats with NMDA-depleted RGCs could partially restore vision, which suggested that transplantation of Muller cells might be helpful to repair retinal degeneration and vision loss caused by RGC degeneration (Eastlake et al., 2019). Pereiro et al. (2020) suggested that this process is related to up-regulation of the transcription factor *ATOH7*, which is required for mouse–derived ganglion cell development, in Muller cells. However, over-expression of *ATOH7* during mouse–derived RGC formation also correspondingly reduced the number of remaining progenitor cells, resulting in a decrease in the number of PRCs, which develop later than ganglion cells (Zhang et al., 2018).

In conclusion, the RGC of RO can be connected with the remaining ganglion cells in the diseased retina. However, the low yield of RGC and the inability to obtain axons of sufficient length are currently obstacles to clinical transformation. Two-dimensional expansion of RGC through brain-derived neurotrophic factor is a feasible strategy to solve the problem of low yield; screening and purifying mature RGC from RO for transplantation, adding Muller cells to the culture medium to promote the development of ganglion cells is a potential strategy to solve the problem of insufficient axon length. The improved protocols and research findings mentioned in this section are separately summarized in **Tables 1**, **2**.

Extraction and Transplantation of Photoreceptor Cells

For retinal degenerative diseases caused by the loss of photoreceptors, subretinal transplantation of RO sheets and PRCs or even RPCs can be performed to compensate for the function of degraded PRCs, which acts as a type of patch (Singh and Nasonkin, 2020). Pearson et al. (2012) found that an integrated graft can provide vision in mice with retinal degeneration under low-light conditions and can project signals to the V1 area of the brain, which is mainly responsible for visual processing.

Studies have found that the development of human–derived ROs after 30–70 days of culture *in vitro* is equivalent to that of embryos at 8–14 weeks. At the same time, the implanted organoids can continue to develop, differentiate, and constantly integrate information with the recipient's retina. McLelland et al. (2018) showed that connection of the donor lamina to the receptor's inner plexiform layer indicates the establishment of synaptic connections. Assawachananont et al.

TABLE 2 | Summary of findings related to retinal organoid culture process and transplantation.

Study	Findings
Retinal ganglion cells	
Kobayashi et al., 2018	Mature ganglion cells are more capable of extending axons.
Aparicio et al., 2017	Ganglion cell precursors express CD184. Mature ganglion cells express CD171.
Tanaka et al., 2015	Muller cells promote ganglion cells to survive and extend axons.
Eastlake et al., 2019	Transplanting Muller cells conduces to repair RGC degeneration-related diseases.
Photoreceptor cells	
Singh and Nasonkin, 2020	Organoid lamellar transplantation compensates for degraded photoreceptor cells. Transplanting PR and neurons together can increase the survival rate of neurons.
Pearson et al., 2012	Organoid grafts provides dark vision.
McLelland et al., 2018	The connection with the IPL of the receptor indicates the synaptic connection.
Assawachananont et al., 2014	Organoids cultured for 11–17 days are most likely to have synaptic connections. Transplanting the outer nuclear layer with a small amount of the inner core layer promotes the connection between the ONL of the donor and the INL of the recipient.
Goureau and Orieux, 2020	The purified PR precursor cells injected into the subretinal space and are more easily integrated with the recipient neurons.
Kegeles et al., 2020b	Adding Forskolin, an activator of adenylate cyclase, on the first day of organoid culture improves the efficiency of visual field induction.
Chen et al., 2016	70% of organoids are rod cells.
Pan et al., 2020	COCO promotes the generation of PR precursor cells.
Völkner et al., 2016	Inhibitors of the Notch pathway can promote cone cells when added in the early stage, and can promote rod cells when added in the later.
Gagliardi et al., 2018	Magnetically activated cell sorting (MACS) can separate CD73(+) CRX + photoreceptor cells.
Lakowski et al., 2015, 2018	CD73(+) marked mouse-derived PR precursors will differentiate into rod cells after implantation in the subretinal space, and will be marked by Recoverin. CD73(+) can screen mouse-derived rod cells, but it is not effective for human-derived cells. Cell marker CD29 (–)/SSEA-1 (–) can screen human-derived photoreceptor cells.

suggested the use of mouse–derived ROs cultured for 11 to 17 days for transplantation. These ROs have not matured, but they make the most efficient synaptic connections with the recipient (Assawachananont et al., 2014). Studies have found that transplantation of organoid sheets is not an effective therapy because of their unorganized structure and complex cell types. Goureau and Orieux (2020) suggested that direct injection of purified mouse–derived photoreceptor precursor cells into the subretinal space can promote the production of a single cell type in the graft and facilitate the exchange of information and substances with receptor neurons, resulting in more efficient and accurate replacement therapy. Therefore, PRCs should be extracted from organoids before transplantation into the subretinal space. Additionally, Singh et al. found that if PRCs and neurons in mouse–derived ROs were transplanted together, the neurons connected to RGCs could still survive even if the PRCs subsequently underwent apoptosis (Lin and Peng, 2013). Assawachananont et al. (2014) suggested that if the outer nuclear layer to be transplanted in the mouse–derived RO contains a small amount of the inner nuclear layer, connections between the donor outer nuclear layer and the recipient's inner nuclear layer will be promoted. Kegeles et al. (2020b) added forskolin, an adenylate cyclase activator, on the first day of mouse ESC–derived RO culture, and the induction efficiency of the visual field was significantly improved.

Some studies have also used embryonic stem cells and iPSCs from Nrl–green fluorescent protein mice to induce ROs and evaluate the development of rod cells *in vitro*. The results showed that up to 70% of the cells in ROs were rods (Chen et al., 2016). The addition of COCO as an auxiliary supplement to medium has also been shown to promote the production of human–derived photoreceptor precursor cells and, in the long term, leads to more cones than rods (Tanaka et al., 2015). Nakano et al. (2012) found that Notch signaling pathway inhibitors is able to accelerate the generation of human–derived photoreceptors. Völkner et al. found that it can also control the differentiation trend of mouse–derived precursors. If a Notch pathway inhibitor is added in the early stage of differentiation, the generation of cones will increase. If the inhibitor is added in the late stage, the growth of rod cells will be promoted (Völkner et al., 2016).

Labeling PRC–specific reporter genes such as *CRX* also plays an important role in separating PRCs of ROs for subsequent transplantation. Gagliardi et al. showed that the *mCherry* gene is specifically expressed in all *CRX*(+) PRCs, and surface antigen marker CD73 is specifically expressed in *mCherry*(+) cells, which provides a feasible method to efficiently collect *CRX*(+) PRCs. Magnetic activated cell sorting can thus be used for targeted separation of *CRX*(+) PRCs with the specific surface antigen marker CD73 (Gagliardi

et al., 2018). CD73(+) is a rod-specific marker for mouse-derived ROs that can be labeled with rhodopsin, but its specificity is low for human–derived ROs. Lakowski et al. (2015, 2018) suggested that a higher proportion of PRCs can be obtained from human–derived ROs by identifying CD29(−)/SSEA-1(−) cells. There is also research on targeted screening of mouse–derived CD73(+) CD24(+) CD133(+) CD47(+) CD15(−) photoreceptor precursors, which will then differentiate into functional rods that can be labeled by Recoverin (Lakowski et al., 2015).

The differentiation and maturation processes of PRCs of ROs from different sources obviously differ (Hallam et al., 2018). Therefore, to reduce the heterogeneity of culture, the currently used protocol, serum-free floating culture of embryoid body–like aggregates with quick reaggregation, has been improved, and the modified protocol called High Efficiency Hypoxia Induced Generation of Photoreceptors in ROs protocol was used so that the development of mouse–derived ROs and their PRCs could be highly representative of the retina *in vivo* (Chen et al., 2016). Labeling a specific gene of PRCs, *CRX*, with the reporter gene *tdTomato* can help to track the differentiation process of human–derived cones and rod cells. This alteration will not affect the differentiation of ROs. Additionally, the fluorescence intensity of the *tdTomato* gene is consistent with that of flow cytometry; therefore, the degree of differentiation of precursor cells can be quantified (Pan et al., 2020).

At present, the transplantation therapy of PRC is more mature than that of ganglion cells. It has been proven to be an alternative treatment for retinal degenerative diseases and provide scotopic vision. This is achieved through a successful synaptic connection with the inner plexiform layer of the receptor. However, the current difficulty lies in the complex and disordered structure of the organoid lamellar tissue itself, which affects the therapeutic effect. Therefore, the better solution is to separate and extract the PRCs to a certain extent. Using *CRX* reporter gene and cell markers such as CD73, PRCs can be separated more accurately. At the same time, COCO and Notch signal inhibitors can control the relative proportion of cone and rod cells in ROs, indirectly making the transplant more precise. On the other hand, the High Efficiency Hypoxia Induced Generation of Photoreceptors in ROs protocol and *tdTomato* reporter gene can reduce the heterogeneity between PRCs from different sources. The improved protocols and research findings mentioned in this section are separately summarized in **Tables 1**, **2**.

DISCUSSION

Because ROs have highly similar structures and cell types to retinas, the RO model will be an ideal choice for studying the mechanisms of diseases, developing efficient drugs, and examining organ transplantation. However, because of their low yield, long culture time, and high heterogeneity of products under different culture conditions, the application and translation of ROs are restricted at this stage.

Currently, methods such as computer deep learning algorithms, multimodal imaging, and immunohistochemistry can be used to predict the direction of differentiation, monitor development and even metabolic processes in real time, and perform quantitative evaluations without destroying the structure of organoids. This has allowed the development process of ROs to be categorized into three stages, which greatly reduces the heterogeneity among products under different conditions. Regarding the problem of low yield, existing research has improved the efficiency of organoid culture by dividing the original product in advance and improving the utilization of cells. Controlling cell density, the use of pure chemical culture media, and the addition of retinal developmental substances to the culture medium can promote organoid differentiation, and the development of related biological scaffold materials will undoubtedly shorten the maturation process of ROs.

Currently, studies have shown that ganglion cells can be transplanted into the corresponding ganglion cell layer, and the transplanted cells can compensate for the loss of function. However, the implanted ganglion cells have a relatively short lifespan, and there is also the problem that the number of ganglion cells and the length of axons available in the traditional RO protocol are not sufficient to connect to the visual pathway. Some studies have suggested that the combination of three-dimensional and two-dimensional protocols can promote the expansion of ganglion cells. Additionally, as the survival time of ganglion cells increases, the ability of ganglion cells to grow axons in organoids increases, and axon functions become more mature. The addition of Muller cells can increase the short lifespan of RGCs in culture and promote the functional recovery of RGCs that have degenerated because of disease after transplantation into the receptor. This effect may be related to the transcription factor ATOH7, which promotes RGC development, but it may decrease the number of progenitors in organoids, thus reducing the number of PRCs during subsequent development.

The current technology can also provide scotopic vision for mice with retinal degeneration via transplantation of RO sheets or subretinal cells. Synaptic connections can be verified when the inner plexiform layer of the receptor is connected to the donor, and these connections will not degenerate over time. In addition, the use of early-stage ROs is recommended to establish connections more effectively. A higher proportion of cone or rod cells can be obtained using photoreceptor precursor cells extracted from ROs, adding a Notch signaling inhibitor to RO culture at different stages, or targeted isolation based on cell markers, resulting in more accurate and efficient cell replacement therapy. The existing technology can be used to develop photoreceptors that are similar to those in retinas and assess the degree of cell differentiation. Optical coherence tomography, visual dynamics tests, immunohistochemistry, and other methods can be used to determine the effect of transplantation.

As mentioned above, the latest studies have made progress in solving the problems of insufficient yield, large heterogeneity,

and long process of ROs culture. However, when the ganglion cells or PRCs produced from organoids are transplanted into the body, it is still unknown whether they can create long-term clinical functional connections with visual pathways. Therefore, in order to apply the cultivated organoids to the clinical practice and benefit the patients, there is still a long way to go.

AUTHOR CONTRIBUTIONS

XL and XW contributed conception and design of the review. LZ and FT provided critcial revisions to the content. All authors contributed to the article and approved the submitted version.

FUNDING

This work was supported by grants from the Natural Science Foundation of China (No. 82070954), The Applied Basic Research Programs of Science and Technology Commission Foundation of Sichuan Province (No. 19YYJC0790), and The Innovative Spark Grant of Sichuan University (No. 2018SCUH0062).

REFERENCES

Ahmad, I., Teotia, P., Erickson, H., and Xia, X. (2020). Recapitulating developmental mechanisms for retinal regeneration. *Prog. Retin. Eye Res.* 76:100824. doi: 10.1016/j.preteyeres.2019.100824

Aparicio, J. G., Hopp, H., Choi, A., Mandayam Comar, J., Liao, V. C., Harutyunyan, N., et al. (2017). Temporal expression of CD184(CXCR4) and CD171(L1CAM) identifies distinct early developmental stages of human retinal ganglion cells in embryonic stem cell derived retina. *Exp. Eye Res.* 154, 177–189. doi: 10.1016/j.exer.2016.11.013

Assawachananont, J., Mandai, M., Okamoto, S., Yamada, C., Eiraku, M., Yonemura, S., et al. (2014). Transplantation of embryonic and induced pluripotent stem cell-derived 3D retinal sheets into retinal degenerative mice. *Stem Cell Rep.* 2, 662–674. doi: 10.1016/j.stemcr.2014.03.011

Brawner, A. T., Xu, R., Liu, D., and Jiang, P. (2017). Generating CNS organoids from human induced pluripotent stem cells for modeling neurological disorders. *Int. J. Physiol. Pathophysiol. Pharmacol.* 9, 101–111.

Browne, A. W., Arnesano, C., Harutyunyan, N., Khuu, T., Martinez, J. C., Pollack, H. A., et al. (2017). Structural and functional characterization of human stem-cell-derived retinal organoids by live imaging. *Invest. Ophthalmol. Vis. Sci.* 58, 3311–3318. doi: 10.1167/iovs.16-20796

Capowski, E. E., Samimi, K., Mayerl, S. J., Phillips, M. J., Pinilla, I., Howden, S. E., et al. (2019). Reproducibility and staging of 3D human retinal organoids across multiple pluripotent stem cell lines. *Development* 146:dev171686. doi: 10.1242/dev.171686

Chen, H. Y., Kaya, K. D., Dong, L., and Swaroop, A. (2016). Three-dimensional retinal organoids from mouse pluripotent stem cells mimic in vivo development with enhanced stratification and rod photoreceptor differentiation. *Mol. Vis.* 22, 1077–1094.

Chen, T.-C., She, P.-Y., Chen, D. F., Lu, J.-H., Yang, C.-H., Huang, D.-S., et al. (2019). Polybenzyl glutamate biocompatible scaffold promotes the efficiency of retinal differentiation toward retinal ganglion cell lineage from human-induced pluripotent stem cells. *Int. J. Mol. Sci.* 20:178. doi: 10.3390/ijms20010178

Chichagova, V., Dorgau, B., Felemban, M., Georgiou, M., Armstrong, L., and Lako, M. (2019). Differentiation of retinal organoids from human pluripotent stem cells. *Curr. Protoc. Stem Cell Biol.* 50:e95. doi: 10.1002/cpsc.95

Cohen, L. P., and Pasquale, L. R. (2014). Clinical characteristics and current treatment of glaucoma. *Cold Spring Harb. Perspect. Med.* 4:a017236. doi: 10.1101/cshperspect.a017236

Cui, Z., Guo, Y., Zhou, Y., Mao, S., Yan, X., Zeng, Y., et al. (2020). Transcriptomic analysis of the developmental similarities and differences between the native retina and retinal organoids. *Invest. Ophthalmol. Vis. Sci.* 61:6. doi: 10.1167/iovs.61.3.6

Eastlake, K., Wang, W., Jayaram, H., Murray-Dunning, C., Carr, A. J. F., Ramsden, C. M., et al. (2019). Phenotypic and functional characterization of müller glia isolated from induced pluripotent stem cell-derived retinal organoids: improvement of retinal ganglion cell function upon transplantation. *Stem Cells Transl. Med.* 8, 775–784. doi: 10.1002/sctm.18-0263

Eiraku, M., Takata, N., Ishibashi, H., Kawada, M., Sakakura, E., Okuda, S., et al. (2011). Self-organizing optic-cup morphogenesis in three-dimensional culture. *Nature* 472, 51–56. doi: 10.1038/nature09941

Fligor, C. M., Huang, K.-C., Lavekar, S. S., VanderWall, K. B., and Meyer, J. S. (2020). Differentiation of retinal organoids from human pluripotent stem cells. *Methods Cell Biol.* 159, 279–302. doi: 10.1016/bs.mcb.2020.02.005

Fligor, C. M., Langer, K. B., Sridhar, A., Ren, Y., Shields, P. K., Edler, M. C., et al. (2018). Three-dimensional retinal organoids facilitate the investigation of retinal ganglion cell development, organization and neurite outgrowth from human pluripotent stem cells. *Sci. Rep.* 8:14520. doi: 10.1038/s41598-018-32871-8

Gagliardi, G., Ben M'Barek, K., Chaffiol, A., Slembrouck-Brec, A., Conart, J.-B., Nanteau, C., et al. (2018). Characterization and transplantation of CD73-positive photoreceptors isolated from human iPSC-derived retinal organoids. *Stem Cell Rep.* 11, 665–680. doi: 10.1016/j.stemcr.2018.07.005

Gasparini, S. J., Llonch, S., Borsch, O., and Ader, M. (2019). Transplantation of photoreceptors into the degenerative retina: current state and future perspectives. *Prog. Retin. Eye Res.* 69, 1–37. doi: 10.1016/j.preteyeres.2018.11.001

Goureau, O., and Orieux, G. (2020). [Photoreceptor cell transplantation for future treatment of retinitis pigmentosa]. *Med. Sci.* 36, 600–606. doi: 10.1051/medsci/2020097

Goureau, O., Reichman, S., and Orieux, G. (2020). [Retinal organoids as a new tool for understanding and treating retinal diseases]. *Med. Sci.* 36, 626–632. doi: 10.1051/medsci/2020098

Hallam, D., Hilgen, G., Dorgau, B., Zhu, L., Yu, M., Bojic, S., et al. (2018). Human-induced pluripotent stem cells generate light responsive retinal organoids with variable and nutrient-dependent efficiency. *Stem Cells* 36, 1535–1551. doi: 10.1002/stem.2883

Hua, Z.-Q., Liu, H., Wang, N., and Jin, Z.-B. (2020). Towards stem cell-based neuronal regeneration for glaucoma. *Prog. Brain Res.* 257, 99–118. doi: 10.1016/bs.pbr.2020.05.026

Kador, K. E., Alsehli, H. S., Zindell, A. N., Lau, L. W., Andreopoulos, F. M., Watson, B. D., et al. (2014). Retinal ganglion cell polarization using immobilized guidance cues on a tissue-engineered scaffold. *Acta Biomater.* 10, 4939–4946. doi: 10.1016/j.actbio.2014.08.032

Kador, K. E., Montero, R. B., Venugopalan, P., Hertz, J., Zindell, A. N., Valenzuela, D. A., et al. (2013). Tissue engineering the retinal ganglion cell nerve fiber layer. *Biomaterials* 34, 4242–4250. doi: 10.1016/j.biomaterials.2013.02.027

Kegeles, E., Naumov, A., Karpulevich, E. A., Volchkov, P., and Baranov, P. (2020a). Convolutional neural networks can predict retinal differentiation in retinal organoids. *Front. Cell. Neurosci.* 14:171. doi: 10.3389/fncel.2020.00171

Kegeles, E., Perepelkina, T., and Baranov, P. (2020b). Semi-automated approach for retinal tissue differentiation. *Transl. Vis. Sci. Technol.* 9:24. doi: 10.1167/tvst.9.10.24

Khan, S., Hung, S. S.-C., and Wong, R. C.-B. (2016). The use of induced pluripotent stem cells for studying and treating optic neuropathies. *Curr. Opin. Organ Transplant.* 21, 484–489. doi: 10.1097/MOT.0000000000000348

Kobayashi, W., Onishi, A., Tu, H.-Y., Takihara, Y., Matsumura, M., Tsujimoto, K., et al. (2018). Culture systems of dissociated mouse and human pluripotent stem cell-derived retinal ganglion cells purified by two-step immunopanning. *Invest. Ophthalmol. Vis. Sci.* 59, 776–787. doi: 10.1167/iovs.17-22406

Lakowski, J., Gonzalez-Cordero, A., West, E. L., Han, Y.-T., Welby, E., Naeem, A., et al. (2015). Transplantation of photoreceptor precursors isolated via a cell

surface biomarker panel from embryonic stem cell-derived self-forming retina. *Stem Cells* 33, 2469–2482. doi: 10.1002/stem.2051

Lakowski, J., Welby, E., Budinger, D., Di Marco, F., Di Foggia, V., Bainbridge, J. W. B., et al. (2018). Isolation of human photoreceptor precursors via a cell surface marker panel from stem cell-derived retinal organoids and fetal retinae. *Stem Cells* 36, 709–722. doi: 10.1002/stem.2775

Lin, B., and Peng, E. B. (2013). Retinal ganglion cells are resistant to photoreceptor loss in retinal degeneration. *PLoS One* 8:e68084. doi: 10.1371/journal.pone.0068084

Llonch, S., Carido, M., and Ader, M. (2018). Organoid technology for retinal repair. *Dev. Biol.* 433, 132–143. doi: 10.1016/j.ydbio.2017.09.028

McLelland, B. T., Lin, B., Mathur, A., Aramant, R. B., Thomas, B. B., Nistor, G., et al. (2018). Transplanted hESC-derived retina organoid sheets differentiate, integrate, and improve visual function in retinal degenerate rats. *Invest. Ophthalmol. Vis. Sci.* 59, 2586–2603. doi: 10.1167/iovs.17-23646

Miltner, A. M., and La Torre, A. (2019). Retinal ganglion cell replacement: current status and challenges ahead. *Dev. Dyn.* 248, 118–128. doi: 10.1002/dvdy.24672

Nakano, T., Ando, S., Takata, N., Kawada, M., Muguruma, K., Sekiguchi, K., et al. (2012). Self-formation of optic cups and storable stratified neural retina from human ESCs. *Cell Stem Cell* 10, 771–785. doi: 10.1016/j.stem.2012.05.009

Ohlemacher, S. K., Iglesias, C. L., Sridhar, A., Gamm, D. M., and Meyer, J. S. (2015). Generation of highly enriched populations of optic vesicle-like retinal cells from human pluripotent stem cells. *Curr. Protoc. Stem Cell Biol.* 32, 1H.8.1–1H.8.20. doi: 10.1002/9780470151808.sc01h08s32 1H.8.1-1H.8.20,

Ohlemacher, S. K., Langer, K. B., Fligor, C. M., Feder, E. M., Edler, M. C., and Meyer, J. S. (2019). Advances in the differentiation of retinal ganglion cells from human pluripotent stem cells. *Adv. Exp. Med. Biol.* 1186, 121–140. doi: 10.1007/978-3-030-28471-8_5

Palomo, A. B. A., Lucas, M., Dilley, R. J., McLenachan, S., Chen, F. K., Requena, J., et al. (2014). The power and the promise of cell reprogramming: personalized autologous body organ and cell transplantation. *J. Clin. Med.* 3, 373–387. doi: 10.3390/jcm3020373

Pan, D., Xia, X.-X., Zhou, H., Jin, S.-Q., Lu, Y.-Y., Liu, H., et al. (2020). COCO enhances the efficiency of photoreceptor precursor differentiation in early human embryonic stem cell-derived retinal organoids. *Stem Cell Res. Ther.* 11:366. doi: 10.1186/s13287-020-01883-5

Pearson, R. A., Barber, A. C., Rizzi, M., Hippert, C., Xue, T., West, E. L., et al. (2012). Restoration of vision after transplantation of photoreceptors. *Nature* 485, 99–103. doi: 10.1038/nature10997

Pereiro, X., Miltner, A. M., La Torre, A., and Vecino, E. (2020). Effects of adult müller cells and their conditioned media on the survival of stem cell-derived retinal ganglion cells. *Cells* 9:1759. doi: 10.3390/cells9081759

Perepelkina, T., Kegeles, E., and Baranov, P. (2019). Optimizing the conditions and use of synthetic matrix for three-dimensional in vitro retinal differentiation from mouse Pluripotent cells. *Tissue Eng. Part C Methods* 25, 433–445. doi: 10.1089/ten.TEC.2019.0053

Phillips, M. J., Wallace, K. A., Dickerson, S. J., Miller, M. J., Verhoeven, A. D., Martin, J. M., et al. (2012). Blood-derived human iPS cells generate optic vesicle-like structures with the capacity to form retinal laminae and develop synapses. *Invest. Ophthalmol. Vis. Sci.* 53, 2007–2019. doi: 10.1167/iovs.11-9313

Rabesandratana, O., Chaffiol, A., Mialot, A., Slembrouck-Brec, A., Joffrois, C., Nanteau, C., et al. (2020). Generation of a transplantable population of human iPSC-derived retinal ganglion cells. *Front. Cell Dev. Biol.* 8:585675. doi: 10.3389/fcell.2020.585675

Regent, F., Chen, H. Y., Kelley, R. A., Qu, Z., Swaroop, A., and Li, T. (2020). A simple and efficient method for generating human retinal organoids. *Mol. Vis.* 26, 97–105.

Reichman, S., Slembrouck, A., Gagliardi, G., Chaffiol, A., Terray, A., Nanteau, C., et al. (2017). Generation of storable retinal organoids and retinal pigmented epithelium from adherent human iPS Cells in Xeno-free and feeder-free conditions. *Stem Cells* 35, 1176–1188. doi: 10.1002/stem.2586

Reichman, S., Terray, A., Slembrouck, A., Nanteau, C., Orieux, G., Habeler, W., et al. (2014). From confluent human iPS cells to self-forming neural retina and retinal pigmented epithelium. *Proc. Natl. Acad. Sci. U.S.A.* 111, 8518–8523. doi: 10.1073/pnas.1324212111

Singh, R., Cuzzani, O., Binette, F., Sternberg, H., West, M. D., and Nasonkin, I. O. (2018). Pluripotent stem cells for retinal tissue engineering: current status and future prospects. *Stem Cell Rev. Rep.* 14, 463–483. doi: 10.1007/s12015-018-9802-4

Singh, R. K., and Nasonkin, I. O. (2020). Limitations and promise of retinal tissue from human pluripotent stem cells for developing therapies of blindness. *Front. Cell. Neurosci.* 14:179. doi: 10.3389/fncel.2020.00179

Slembrouck-Brec, A., Rodrigues, A., Rabesandratana, O., Gagliardi, G., Nanteau, C., Fouquet, S., et al. (2019). Reprogramming of adult retinal müller glial cells into human-induced pluripotent stem cells as an efficient source of retinal cells. *Stem Cells Int.* 2019:7858796. doi: 10.1155/2019/7858796

Tanaka, T., Yokoi, T., Tamalu, F., Watanabe, S.-I., Nishina, S., and Azuma, N. (2015). Generation of retinal ganglion cells with functional axons from human induced pluripotent stem cells. *Sci. Rep.* 5:8344. doi: 10.1038/srep08344

Völkner, M., Kurth, T., and Karl, M. O. (2019). The mouse retinal organoid trisection recipe: efficient generation of 3D retinal tissue from mouse embryonic stem cells. *Methods Mol. Biol.* 1834, 119–141. doi: 10.1007/978-1-4939-8669-9_9

Völkner, M., Zschätzsch, M., Rostovskaya, M., Overall, R. W., Busskamp, V., Anastassiadis, K., et al. (2016). Retinal organoids from pluripotent stem cells efficiently recapitulate retinogenesis. *Stem Cell Rep.* 6, 525–538. doi: 10.1016/j.stemcr.2016.03.001

Wang, S.-T., Chen, L.-L., Zhang, P., Wang, X.-B., Sun, Y., Ma, L.-X., et al. (2019). Transplantation of retinal progenitor cells from optic cup-like structures differentiated from human embryonic stem cells *in vitro* and *in vivo* generation of retinal ganglion-like cells. *Stem Cells Dev.* 28, 258–267. doi: 10.1089/scd.2018.0076

Wright, L. S., Pinilla, I., Saha, J., Clermont, J. M., Lien, J. S., Borys, K. D., et al. (2015). VSX2 and ASCL1 are indicators of neurogenic competence in human retinal progenitor cultures. *PLoS One* 10:e0135830. doi: 10.1371/journal.pone.0135830

Yao, J., Ko, C. W., Baranov, P. Y., Regatieri, C. V., Redenti, S., Tucker, B. A., et al. (2015). Enhanced differentiation and delivery of mouse retinal progenitor cells using a micropatterned biodegradable thin-film polycaprolactone scaffold. *Tissue Eng. Part A* 21, 1247–1260. doi: 10.1089/ten.TEA.2013.0720

Zhang, X.-M., Hashimoto, T., Tang, R., and Yang, X.-J. (2018). Elevated expression of human bHLH factor ATOH7 accelerates cell cycle progression of progenitors and enhances production of avian retinal ganglion cells. *Sci. Rep.* 8:6823. doi: 10.1038/s41598-018-25188-z

Zhong, X., Gutierrez, C., Xue, T., Hampton, C., Vergara, M. N., Cao, L.-H., et al. (2014). Generation of three-dimensional retinal tissue with functional photoreceptors from human iPSCs. *Nat. Commun.* 5:4047. doi: 10.1038/ncomms5047

Zhu, J., Reynolds, J., Garcia, T., Cifuentes, H., Chew, S., Zeng, X., et al. (2018). Generation of transplantable retinal photoreceptors from a current good manufacturing practice-manufactured human induced pluripotent stem cell line. *Stem Cells Transl. Med.* 7, 210–219. doi: 10.1002/sctm.17-0205

Conflict of Interest: The authors declare that the research was conducted in the absence of any commercial or financial relationships that could be construed as a potential conflict of interest.

frontiers | Frontiers in Cellular Neuroscience

ORIGINAL RESEARCH
published: 19 May 2022
doi: 10.3389/fncel.2022.820396

Spatial and Temporal Development of Müller Glial Cells in hiPSC-Derived Retinal Organoids Facilitates the Cell Enrichment and Transcriptome Analysis

Rong Ning[1†], Dandan Zheng[1†], Bingbing Xie[1†], Guanjie Gao[1], Jinhai Xu[2], Ping Xu[1], Yuan Wang[1], Fuhua Peng[3], Bin Jiang[2], Jian Ge[1] and Xiufeng Zhong[1]*

[1] State Key Laboratory of Ophthalmology, Zhongshan Ophthalmic Center, Sun Yat-sen University, Guangdong Provincial Key Laboratory of Ophthalmology and Visual Science, Guangzhou, China, [2] Guangdong Provincial Key Laboratory of Brain Function and Disease, Faculty of Forensic Medicine, Zhongshan School of Medicine, Sun Yat-sen University, Guangzhou, China, [3] Department of Neurology, The Third Affiliated Hospital of Sun Yat-Sen University, Guangzhou, China

OPEN ACCESS

Edited by:
Lin Cheng,
The University of Iowa, United States

Reviewed by:
Igor O. Nasonkin,
Phythera Therapeutics, United States
Kin-Sang Cho,
Schepens Eye Research Institute and Harvard Medical School, United States

***Correspondence:**
Xiufeng Zhong
zhongxf7@mail.sysu.edu.cn

[†] These authors have contributed equally to this work and share first authorship

Specialty section:
This article was submitted to Cellular Neuropathology, a section of the journal Frontiers in Cellular Neuroscience

Received: 23 November 2021
Accepted: 19 April 2022
Published: 19 May 2022

Citation:
Ning R, Zheng D, Xie B, Gao G, Xu J, Xu P, Wang Y, Peng F, Jiang B, Ge J and Zhong X (2022) Spatial and Temporal Development of Müller Glial Cells in hiPSC-Derived Retinal Organoids Facilitates the Cell Enrichment and Transcriptome Analysis. Front. Cell. Neurosci. 16:820396. doi: 10.3389/fncel.2022.820396

Müller glial cells (MGCs) play important roles in human retina during physiological and pathological conditions. However, the development process of human MGCs *in vivo* remains unclear, and how to obtain large numbers of human MGCs with high quality faces technical challenges, which hinder the further study and application of MGCs. Human induced pluripotent stem cell (hiPSC)-derived retinal organoids (ROs) with all retinal cell subtypes provide an unlimited cell resource and a platform for the studies of retinal development and disorders. This study explored the development of human MGCs in hiPSC-derived ROs and developed an approach to select and expand the induced MGCs (iMGCs). In ROs, retinal progenitor cells progressively differentiated into SOX9+ Ki67− MGC precursors during differentiation day (D) 60 to D90, while mature MGCs expressing markers CRALBP and GS gradually appeared since D120, which spanned the entire thickness of the neural retina layer. Cells isolated from ROs aged older than 120 days was an optimal source for the enrichment of iMGCs with high purity and expansion ability. They had typical features of human MGCs in morphological, structural, molecular and functional aspects, and could be passaged serially at least 10 times, yielding large numbers of cells in a short period. The transcriptome pattern of the expanded iMGCs was also revealed. This study firstly clarified the timecourse of human MGC development in the RO model, where the iMGCs could be enriched and expanded, paving the way for downstream investigation and application in MGC-related retinal disorders.

Keywords: Müller glial cells, human induced pluripotent stem cells, retinal organoids, development, enrichment, transcriptome

INTRODUCTION

Müller glial cells (MGCs), which are the principal glial component of vertebrate retina, originate along with retinal neurons from retinal progenitor cells (RPCs). It is reported that they are the last-born cell type during mouse retinal development (Dvoriantchikova et al., 2019). They span radially across the entire width of neural retina and constitute a structural scaffold to contact nearly all

of retinal neurons (Bringmann et al., 2006; Eastlake et al., 2020). Due to this unique anatomical distribution, MGCs perform many vital physiological functions throughout the retina, including the formation of blood-retinal barrier, the control of extracellular space volume, ion and water homeostasis, and thus maintain the integrity of retina (Bringmann et al., 2006; Eastlake et al., 2020). They also provide neurotrophic, metabolic and anti-oxidative support for retinal neurons, and regulate the neuronal activity by neurotransmitters recycling, which are considered to be neuroprotective in nature (Reichenbach and Bringmann, 2013). These important characteristics of MGCs have generated scientific interests in their potential therapeutic applications, including as a vehicle to deliver benefit factors into the retina (Eastlake et al., 2020).

However, in pathological conditions, some studies indicate that MGCs can dedifferentiate into retinal progenitor-like cells to replenish injured neurons in zebrafish and chick (Raymond et al., 2006). This regenerative ability in the adult mammalian and human retina is still controversial. Many efforts have been made to identify the mechanism underlying regenerative potential of MGCs in order to establish new strategies for treatment of late-stage retinal diseases. In multiple types of human retinal diseases such as retinal detachment, proliferative vitreoretinopathy, diabetic retinopathy and retinal degenerative diseases, MGCs become activated by various pathogenic stimuli such as hypoxia and stress (Bringmann et al., 2006). The slight activation of MGCs may promote the survival of retinal neurons and so repair the retina, while the persistent activation may contribute to the formation of reactive gliosis and eventually lead to glial scar, accelerating the retinal neurodegeneration and greatly impeding the retinal repair (Bringmann et al., 2009; Bringmann and Wiedemann, 2012).

At present, most insights into MGCs are gained from experimental animal models and await confirmation on human cells. However, the pathophysiological mechanisms of human MGCs are still largely unknown due to the limited human cell source. To date, human MGCs are mostly obtained from cadaveric donors and samples after vitreoretinal surgery (Limb et al., 2002; Lawrence et al., 2007). In adult human retina, astrocytes, which share many features with MGCs, also present in retinal nerve fiber layer, and interfere the expansion and purification of MGCs *in vitro* (Lawrence et al., 2007). Moreover, immune rejection and risk of disease transmission are also obstacles of translational applications of these human MGCs (Eastlake et al., 2019). However, great progress in human induced pluripotent stem cells (hiPSCs) makes it possible to solve the above challenges. Retinal organoids (ROs), which can be generated by hiPSCs, are able to recapitulate the retinal development and form laminated retinal tissues (Zhong et al., 2014). Studies have demonstrated that the MGCs are the only glial cell type sharing a common progenitor with the retinal neurons, and they can emerge and survive in hiPSC-derived ROs (Zhong et al., 2014; Fligor et al., 2018; Capowski et al., 2019; Singh et al., 2021), providing many advantages in exploring the features of human MGCs.

Since there are many vital functions of MGCs in the human retina, the aim of our study is to clarify the developmental characteristics of human MGCs in hiPSC-derived ROs and establish protocols to enrich these cells, thus to facilitate the pathophysiological mechanism study of human MGCs and the treatment of MGC-related retinal diseases. Originating from RPCs, Ki67– SOX9+ CRALBP– GS– induced MGC (iMGC) precursors were identified in the early-stage ROs, while the Ki67– SOX9+ CRALBP+ GS+ mature iMGCs presented in the late-stage ROs. Importantly, the iMGCs were successfully enriched and expanded from the late-stage ROs, which exhibited similar morphological, structural, molecular and physiological features of primary human MGCs. The transcriptome pattern of the expanded iMGCs was also identified. Our findings provided new insights into the temporal and spatial development of human MGCs *in vivo* and established a simple approach to enrich these cells, laying the foundation for downstream investigation and application of human MGCs.

MATERIALS AND METHODS

hiPSC Culture and RO Induction

Two hiPSC lines, BC1 and BC1-GFP lines were used in this study, which were gifts from Professor Linzhao Cheng (University of Science and Technology of China) (Chou et al., 2011; Zou et al., 2012). hiPSCs were cultured on Matrigel-coated (Corning, USA) plates in mTeSR1 medium (Stem Cell Technologies, Canada) and passaged at ∼80% confluence every 5–7 days. RO induction was performed as previously described (Zhong et al., 2014; Li et al., 2018; Guan et al., 2021). Briefly, on differentiation day (D) 0, hiPSCs were dissociated and cultured in low adherent dishes to form embryoid bodies (EBs). EBs were plated on Matrigel-coated dishes during D5–D7 with neural induction medium (NIM), which was composed of DMEM/F12 (1:1), 1% N2 supplement (Invitrogen), 1% non-essential amino acids (NEAA) (Gibco) and 2 μg/ml heparin (Sigma-Aldrich). From D16, the culture medium was changed to retinal differentiation medium (RDM), containing DMEM/F12 (12:5), 2% B27 (without vitamin A, Invitrogen), 1% NEAA, and 1% antibiotic-antimycotic (Gibco). By week (W) 4–6, optic vesicles with neural retina (NR) domains turned up and were lifted up with tungsten needles, then cultured in suspension to spontaneously form ROs. Retinal culture medium (RCM), which comprised RDM, 10% fetal bovine serum (FBS) (Gibco), 100 μM Taurine (Sigma-Aldrich), and 2 mM GlutaMAX (Invitrogen) were used after 1 week of detachment. From D90, B27 supplemented in RCM was replaced by N2 for long-term RO culture. Medium was changed twice a week.

Expansion Culture of iMGCs

NR layers were isolated from ROs at different timepoints (D60, D90, D120, and D150) after differentiation, dissected into small pieces with a pair of tungsten needles, and then dissociated into single cells by incubation of accutase (Gibco) for 15–25 min at 37°C. Afterwards, cell suspension was plated at a density of 1×10^4 cells per cm^2 on Matrigel-coated plates with MGC culture medium consisting of DMEM, 10% FBS, 2 mM GlutaMAX, 1% NEAA and 1% antibiotic-antimycotic. These cells were noted as passage 0 (P0). After cells were expanded, they were passaged at approximately 90% confluence every 6–10 days. Medium

was changed every 3–4 days. MIO-M1, a commercial MGC line obtained from human retina (Limb et al., 2002; Lawrence et al., 2007), served as a control in designated experiments, was cultured and expanded at a density of 1×10^4 cells per cm^2 on Matrigel-coated plates in 1640 medium containing 10% FBS and 1% antibiotic-antimycotic. They were passaged at ∼90% confluence every 4–6 days. Medium was changed every 2–3 days. The cell doubling time (DT) of the passaged cells were measured according to the following equation (Zou et al., 2019):

$$DT = \mathrm{t} \times \left[\lg 2 / \left(\lg N\mathrm{t} - \lg N0\right)\right]$$

where N_t represents the cell number at time period t (days) and N_0 represents the initial cell number at the cell-plating day.

Immunofluorescence Staining

Collected ROs were fixed in 4% paraformaldehyde (PFA, Sigma) for 30 min at room temperature. Mouse eyeballs were fixed in 4% PFA overnight at 4°C. Fixed ROs and mouse eyeballs were dehydrated through ascending grades of sucrose solutions from 6.25, 12.5, to 25%. Then they were embedded in O.C.T compound for frozen sections. Cells cultured on coverslips were fixed with 4% PFA for 8 min. Coverslips or sections were incubated in blocking solution consisting of 10% donkey serum and 0.25% Triton X-100 for 1 h at room temperature. Primary antibodies were incubated in the proper dilution overnight at 4°C. After that, the cells or sections were incubated with the corresponding secondary antibodies with either Alexa Fluor 488, 555, or 647 (Life Technologies, USA) for 1 h at room temperature. DAPI (4',6-diamidino-2-phenylindole, Dojindo Molecular Technologies, China) was used for counterstaining nuclei. The used primary antibodies are listed in **Supplementary Table S1**. Fluorescence images were acquired with a fluorescence microscope (Zeiss, Germany), a microscope slide scanner (Zeiss, Germany) or an LSM 880 confocal microscope (Zeiss, Germany).

Scanning Electron Microscope

The passaged iMGCs were grown on coverslips and fixed in a mixture containing 2.5% glutaraldehyde and 2% PFA at 4°C overnight. Then these samples were sent to Electron Microscopy Core Facility at Fuda Testing Group (Guangzhou, China) for dehydration, drying, coating, and observed by scanning electron microscope (Apreo 2; FEI, Inc., Carlsbad, CA, USA).

Transmission Electron Microscopy

The passaged iMGCs were cultured on plates and dissociated into cell suspension with 0.25% trypsin-EDTA (Gibco). Then cells were centrifuged into cell aggregates and fixed in mixture containing 2.5% glutaraldehyde and 2% PFA at 4°C overnight. After that, these samples were sent to Electron Microscopy Core Facility at Fuda Testing Group (Guangzhou, China) for dehydration, bedding, sectioning, staining and observed by transmission electron microscope (Tecnai G2 Spirit; FEI, Inc, Carlsbad, CA, USA).

Electrophysiological Experiment

Whole-cell recordings at current-clamp mode were performed using an Integrated Patch-Clamp Amplifier (Sutter Instrument, USA) controlled by Igor 8 software (WaveMetrics, USA), filtered at 5 kHz and sampled at 20 kHz. Patch pipettes (4–6 MΩ) were filled with the internal solution containing the following (in mM): 130 K-gluconate, 10 HEPES, 10 KCl, biocytin 0.1–0.4%, 4 MgATP, 0.5 Na3GTP and 10 Na-phosphocreatine; pH 7.2–7.4. Osmolarity was adjusted to 290–300 mOsm. Recordings were performed at room temperature. Cultured iMGCs were perfused with ACSF (in mM): 124 NaCl, 3 KCl, 1.25 NaH_2PO_4, 1 $MgCl_2$, 2 $CaCl_2$, 26 $NaHCO_3$, and 10 dextrose, bubbled with 95% O_2/5% CO_2. iMGCs were selected for study if they had a resting membrane potential <-30 mV. L-glutamate was applied to iMGCs by Picospritzer III (General Valve Corporation, USA) with Puff perfusion. The tip diameter of puff micropipettes was about 2–5 μm and puff pressure was between 4 and 6 psi. Glutamate at 100 μM was locally delivered using local pressure-puff.

RNA-seq and Data Analysis

Samples from BC1-GFP hiPSCs and their derivatives were used to perform RNA-seq and data analysis. HiPSCs (∼2×10^6 cells per experiment, three independent experiments), NR layers isolated from D70-ROs and D150-ROs (five ROs per experiment, three independent experiments), P1 and P5 iMGCs from NR layers of D150-ROs (∼1×10^6 cells per experiment, three independent experiments) were collected in Trizol reagent (Invitrogen) and stored in a −80°C freezer. Then all of these samples were submitted to Gene Denovo Biotechnology Co. (Guangzhou, China) for RNA extraction, library construction, sequencing and data analyses. Total RNA was extracted using Trizol reagent kit (Invitrogen) according to the manufacturer's protocol. RNA quality was assessed on an Agilent 2100 Bioanalyzer (Agilent Technologies). Oligo (dT) beads were used to isolate the poly mRNA from the total RNA. The enriched mRNA was fragmented and reverse transcribed into cDNA using random primers. After synthesis of the second strand, the cDNA was purified, end-repaired and ligated to Illumina sequencing adapters. The ligation products were size selected, amplified, and sequenced. Raw reads were filtered and the clean reads were obtained. Afterwards, an index of the reference genome was built, and paired-end clean reads were mapped to the reference genome using HISAT2 (Kim et al., 2015). The mapped reads of each sample were assembled by using StringTie (Pertea et al., 2016). For each transcription region, a fragment per kilobase of transcript per million mapped reads (FPKM) value was calculated to quantify its expression abundance and variations, using RSEM software (Li and Dewey, 2011). Correlation analysis was performed by R. Correlation and principal component analysis (PCA) was performed with R package gmodels (http://www.r-project.org/). Differential expression analysis was performed by DESeq2 software (Love et al., 2014) between two different groups. The genes/transcripts with the parameter of false discovery rate (FDR) below 0.05 and absolute fold change ≥2 were considered differentially expressed genes/transcripts (DEGs). Then the upregulated DEGs were underwent Gene Ontology

(GO) and Kyoto Encyclopedia of Genes and Genomes (KEGG) pathway enrichment analysis, and the GO terms or pathways with an adjust p-value ≤ 0.05 (qvalue) were defined as significant enriched GO terms or pathways.

Animals and Subretinal Transplantation of iMGCs

NOD/SCID mice were used in this study. The animal study was reviewed and approved by the Animal Ethics Committee of the Zhongshan Ophthalmic Center, Sun Yat-Sen University. All experiments complied with national animal care guidelines. Four to six-week-old NOD/SCID mice were divided into two groups: a treatment group injected with the P2 or P5 iMGCs from BC1-GFP or BC1 ROs older than D120 (1×10^5 cells in 1.5 μl DMEM per eye), and a vehicle control group injected with DMEM (1.5 μl per eye). Subretinal injections were performed using a 2.5 μl Hamilton syringe and 33 G needle (Hamilton, Swizerland). Fundus photography (Topcon TCR-50DX) and optical coherence tomography (OCT, Envisu R-Class) examination were done to dynamically track the donor cells in subretinal space (SRS). These transplanted mice were monitored for about 4 weeks. The mice were sacrificed by cervical dislocation at days 3, 7, and 21 after surgery. The experimental eyeballs of mice were removed and fixed with 4% PFA overnight at 4°C.

Statistical Analysis

Statistical analyses were performed using GraphPad Prism Software 8.0.1 (GraphPad Software, USA). The results of electrophysiological experiment are presented as the mean ± SEM (standard error of mean), and other results are presented as the mean ± SD (Standard Deviation). $P < 0.05$ was considered statistically significant. For statistical analysis of RNA-seq, see RNA-seq and Data Analysis for more details.

RESULTS

Temporal and Spatial Development of MGCs in hiPSC-Derived ROs

To observe the development of human MGCs, dissociated hiPSCs were differentiated into ROs according to our published retinal differentiation protocol (Zhong et al., 2014; Li et al., 2018; Guan et al., 2021). During W4–W7, three-dimensional (3D) ROs with thick and transparent NRs spontaneously formed, resembling human eye-cups (**Figure 1A**; **Supplementary Figure S1**). Immunofluorescence staining of these ROs showed that at the early stage of differentiation (D60–D90), most cells in the NR layer firstly co-expressed RPC markers Ki67, SOX9, VSX2, vimentin and nestin, representing a population of RPCs (**Figures 1B,C**). Some early-born retinal neurons such as BRN3+ PAX6+ ganglion cells and CRX+ photoreceptor cells were also seen in the NR layer at this stage (**Supplementary Figures S2A–C**). As the differentiation progressed, RPCs exited the cell cycle and differentiated into Ki67– VSX2– SOX9+ CRALBP- GS- cells, which gradually migrated to the intermediate layer of NRs and were defined as MGC precursors to represent a transitional period of developing MGCs between RPCs and mature MGCs (**Figures 1B,C**). At the late stage of differentiation (D120 afterwards), the MGCs expressed markers CRALBP and GS specific for mature MGCs (Limb et al., 2002; Eastlake et al., 2019) and stretched the whole width of NRs with their cell processes (**Figures 1B,C**; **Supplementary Figures S3A,B**). RPC and MGC markers SOX9, nestin and vimentin were also expressed in the intermediate layer of NRs from D120 (**Figures 1B,C**), implying the mature MGCs emerged in the late-stage RO (Zhong et al., 2014; Fligor et al., 2018; Capowski et al., 2019). Surprisingly, GFAP, a marker for astrocyte and active MGC (Vecino et al., 2016; Reichenbach and Bringmann, 2020), was not expressed in the NR of ROs at both the early and late stages (**Supplementary Figures S2D, S4**). In addition, the NR layers were negative for optic stalk marker PAX2 and forebrain cell marker SOX1, further confirming MGCs in NR layers indeed originated from retina (**Supplementary Figure S2D**).

RNA-seq analysis further characterized the development of MGCs during retinal differentiation. PCA indicated developmental age as the first principal component explaining almost 74% of the variance (**Figure 2A**). Differential expression analysis showed that there were substantial differences among hiPSCs and ROs at different stages (**Figure 2B**; **Supplementary Figures S5A,B**). When compared with hiPSCs, the number of differential expression genes (DEGs) that showed more than or equal to 2-fold change in D70-ROs or D150-ROs was, respectively, up to 6860 and 9238. And when compared with D70-ROs, there were 5214 DEGs in D150-ROs (**Figure 2B**; **Supplementary Figures S5A,B**). GO analysis showed that the upregulated DEGs of D150-ROs comparing to hiPSCs were enriched in cellular components related to MGCs development, such as cytoskeleton, cilium, cell projection (**Figure 2C**). While KEGG analysis revealed that the upregulated DEGs of D150-ROs comparing to hiPSCs were enriched in signaling pathways related to the functions of MGCs, such as Glutamatergic synapse (**Figure 2D**). Pluripotency marker genes including *FOXD3*, *TERT*, *TDGF1,* and *NANOG* were high expressed in hiPSCs but low in hiPSC-derived ROs (**Figure 2E**). In addition, RPC-related genes such as *OLIG2 and DLL3* were enriched in the early-stage ROs (**Figure 2F**). While MGC-related genes, such as *CRYAB*, *RLBP1*, *CA2*, and *SLC1A3* were progressively upregulated over the differentiation process (**Figure 2G**; **Supplementary Figure S5C**), which were consistent with the previous studies (Hoshino et al., 2017; Kim et al., 2019; Yan et al., 2020; Couturier et al., 2021). The expression of RPC and MGC genes *SOX9* and *VIM* significantly increased in the early-stage ROs when compared to hiPSCs and kept high expression level in late-stage ROs (**Figure 2G**). Additionally, the expression of astrocyte marker *GFAP* and forebrain cell marker *SOX1* were not detectable, and the expression level of the optic stalk marker *PAX2* was very low in ROs at different stages (**Supplementary Figure S5C**). Part of these results were verified by the immunostaining analysis described above (**Figure 1B**; **Supplementary Figures S2D, S4**).

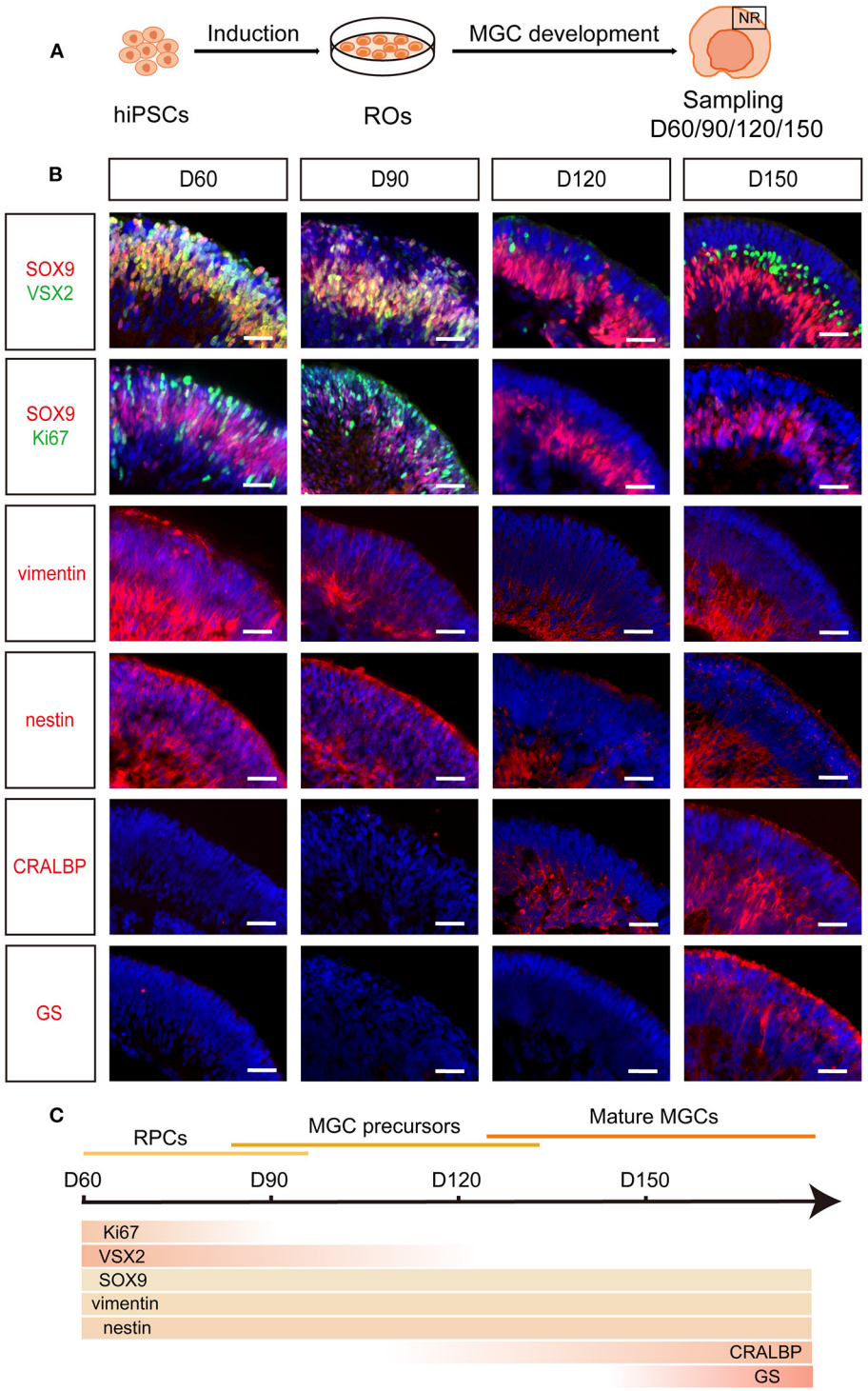

FIGURE 1 | Spatiotemporal development of MGCs in hiPSC-derived ROs. **(A)** Schematic overview of the development of MGCs in ROs. **(B)** Immunofluorescence staining showed the expression of markers VSX2, SOX9, Ki67, vimentin, nestin, CRALBP and GS in D60-, D90-, D120-, and D150-ROs. **(C)** Schematic diagram of MGCs development in hiPSC-derived ROs. hiPSC, human induced pluripotent stem cell; ROs, retinal organoids; MGC, Müller glial cell; NR, neural retina. Scale bars = 50 μm **(B)**.

Altogether, RPCs from both hiPSC lines sequentially differentiated into MGC precursors and mature MGCs in hiPSC-derived ROs and the mature MGCs were spatially located in the intermediate layer of NRs, which recapitulates the spatiotemporal pattern of MGC development in human fetal retina (**Figure 1C**) (Xiang, 2013; Quinn and Wijnholds, 2019).

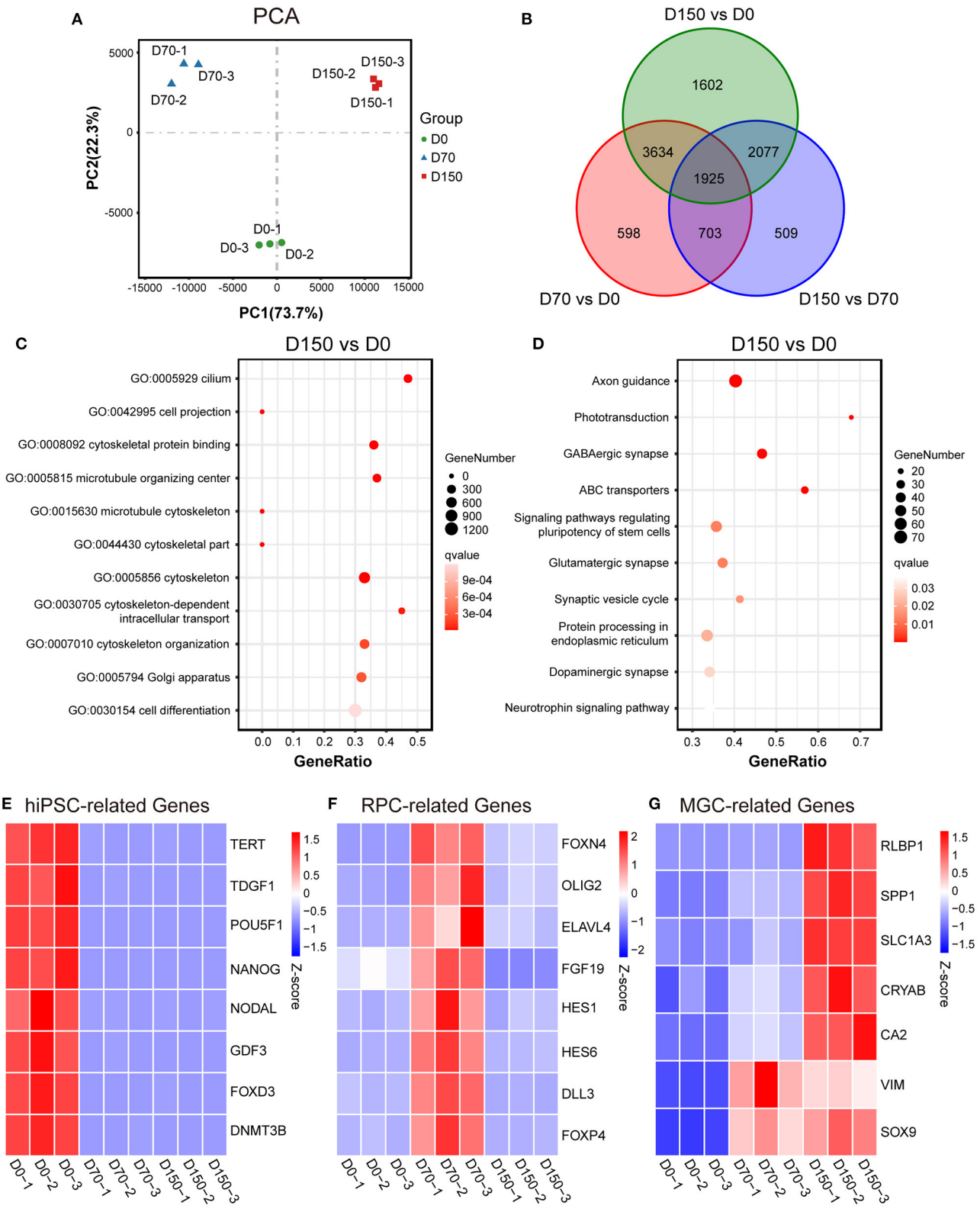

FIGURE 2 | RNA-seq analysis of MGC development in ROs at different stages. **(A)** Principal components analysis (PCA) showed a comparison of the transcriptome data in hiPSCs (D0) and ROs at different stages. **(B)** Venn diagram showed the number and overlapping relations of the differentially expressed genes (DEGs) among hiPSCs and ROs at different stages. **(C)** Dot plot showed Gene Ontology (GO) analysis of the upregulated DEGs of D150-ROs comparing to hiPSCs; GO terms with

(Continued)

FIGURE 2 | an adjust *p*-value (qvalue) ≤ 0.05 were defined as significant enriched GO terms. **(D)** Dot plot showed Kyoto Encyclopedia of Genes and Genomes (KEGG) analysis of the upregulated DEGs of D150-ROs comparing to hiPSCs; signaling pathways with qvalue ≤ 0.05 were defined as significant enriched pathways. **(E–G)** Heatmap showed the expression pattern of the hiPSC-related genes **(E)**, RPC-related genes **(F)** and MGC-related genes **(G)** in hiPSCs (D0), D70-ROs (D70), and D150-ROs (D150). Blue to red indicated a gradient from low to high gene expression. hiPSC, human induced pluripotent stem cell; NR, neural retina; ROs, retinal organoids; RPC, retinal progenitor cell; MGC, Müller glial cell; −1, −2, and −3, experimental replicates; VS, versus. *VIM*, gene name of vimentin; *RLBP1*, gene name of CRALBP.

The Enrichment of iMGCs From hiPSC-Derived ROs

To acquire MGCs with high purity and expansion ability, according to the timecourse of MGC development in ROs described above, we tried to expand the MGCs from ROs at early (D60, D90) and late (D120, D150) stages. NR layers isolated from ROs were dissociated into retinal cells, and these cells were seeded in culture plates, noted as P0 (**Figure 3A**). The primary cells from early- and late-stage ROs are both expandable, but exhibited different growth patterns (**Figure 3B**). As for cells from the early-stage ROs, majority of primary cells survived, proliferated quickly and reached confluency in about 1 week (**Figure 3B**). In contrast, only a few of primary cells from the late-stage ROs could survive, grew in a single clone, proliferated slowly and took more than 2 weeks to reach confluency (**Figure 3B**). In addition, the cell doubling time of the passaged cells peaked at P6 cells from the early stage ROs and P10 ones from the late-stage ROs, respectively (**Figure 3C**), indicating that cells from the latter could expand more times than from the former. After passage, the expanded cells from both the early- and late-stage ROs were progressively elongated and exhibited a spindle-like shape with rough membrane and abundant projections in a few days (**Figure 3D**), showing similar morphological features of primary MGCs isolated from human adult retina (Limb et al., 2002; Lawrence et al., 2007).

Immunofluorescence staining was performed to validate the molecular signature of the passaged cells from ROs at different stages. The majority of passaged cells from early-stage ROs strongly expressed RPC and MGC markers SOX9, vimentin and nestin, but did not express key mature MGC marker GS (**Figures 4A,B**). Some of these cells weakly expressed VSX2 and PAX6 and a few of them expressed photoreceptor cell marker CRX (**Figures 4A,B**). These results indicated that the passaged cells from early-stage ROs might be mixtures of RPCs, MGC precursors and the other retinal neurons. Whereas, nearly all passaged cells from late-stage ROs were positive for MGCs markers SOX9, vimentin, nestin and GS, but rarely expressed markers VSX2, PAX6, or CRX, indicating that these cells were MGCs with high purity (**Figures 4A–C**; **Supplementary Figure S6A**).

Collectively, above data indicated that the late-stage ROs were the optimal choice for the enrichment of iMGCs which could be serially expanded more than 10 passages, yielding large numbers of cells with high quality and purity. For example, 10 late-stage ROs could produce ∼100 million P2 cells within 15 days. These cells could be also cryopreserved for future applications. The P1 to P5 iMGCs were used for further characterization in this study unless otherwise noted. In addition, although the morphological and molecular features of the expanded iMGCs from the BC1 and BC1-GFP hiPSCs tested were quite similar, the variability of iMGCs from these two lines were also observed. The iMGCs from BC1-GFP ROs had a slightly stronger expansion ability than those from BC1 ROs at the same developmental stage.

Transcriptome Analysis and Phenotype Stability of the Passaged iMGCs

Next, we examined the transcriptomes of the passaged iMGCs from the late-stage ROs. RNA-seq analysis showed the global difference of transcriptomes between ROs and the iMGCs (**Figures 5A–C**). Photoreceptor-related genes such as *CRX* and *RCVRN*, amacrine and horizontal cell-related genes such as *PROX1* and *TFAP2A*, retinal ganglion cell-related genes such as *ATOH7* and *ISL1*, and bipolar cell-related genes such as *GRM6* and *CA10*, were downregulated in the iMGCs, but up-regulated in D150 ROs. While the expression of MGC-related genes such as *VIM*, *CRYAB*, *APOE,* and *CCL2* (Hoshino et al., 2017; Kim et al., 2019; Yan et al., 2020; Couturier et al., 2021) were enriched in the passaged iMGCs, but down-regulated in D150 ROs (**Figures 5D–H**). Moreover, all of these passaged iMGCs expressed neither GFAP protein (**Supplementary Figure S7**), nor *GFAP*, *SOD3*, *S100B*, *PAX2*, *CSF1R,* or *CX3CR1* mRNA (FPKM < 1, data not shown), indicating there were no contamination of non-retinal cells or tissue such as astrocyte, optic stalk and microglia in these passaged iMGCs (Westergard and Rothstein, 2020; Bosze et al., 2021). Therefore, RNA-seq data further confirmed that the iMGCs from the late-stage ROs were enriched with typical transcriptome signature, and not contaminated with other retinal subtypes or non-retinal cells.

We further analyzed the phenotype stability of the iMGCs after serial passages. Immunofluorescence staining showed that there were no significant differences in the expression of specific markers between P1 and P5 iMGCs (**Supplementary Figure S6A**). Both the P1 and P5 iMGCs abundantly expressed MGC markers SOX9 and GS, but rarely expressed markers VSX2, PAX6 or CRX for other retinal subtypes (**Supplementary Figure S6A**). Surprisingly, the MGC marker CRALBP became negative from passage 1 (**Supplementary Figure S6A**), which was consistent with a previous study on MGCs isolated from ROs (Couturier et al., 2021). RNA-seq analysis illustrated that the majority of genes including the classical MGC marker genes such as *SOX9*, *VIM*, *GLUL*, *APOE,* and *SPP1* presented similar transcript level between the P1 and P5 iMGCs, demonstrating the phenotype stability of the iMGCs after several passages (**Supplementary Figures S6B–D**).

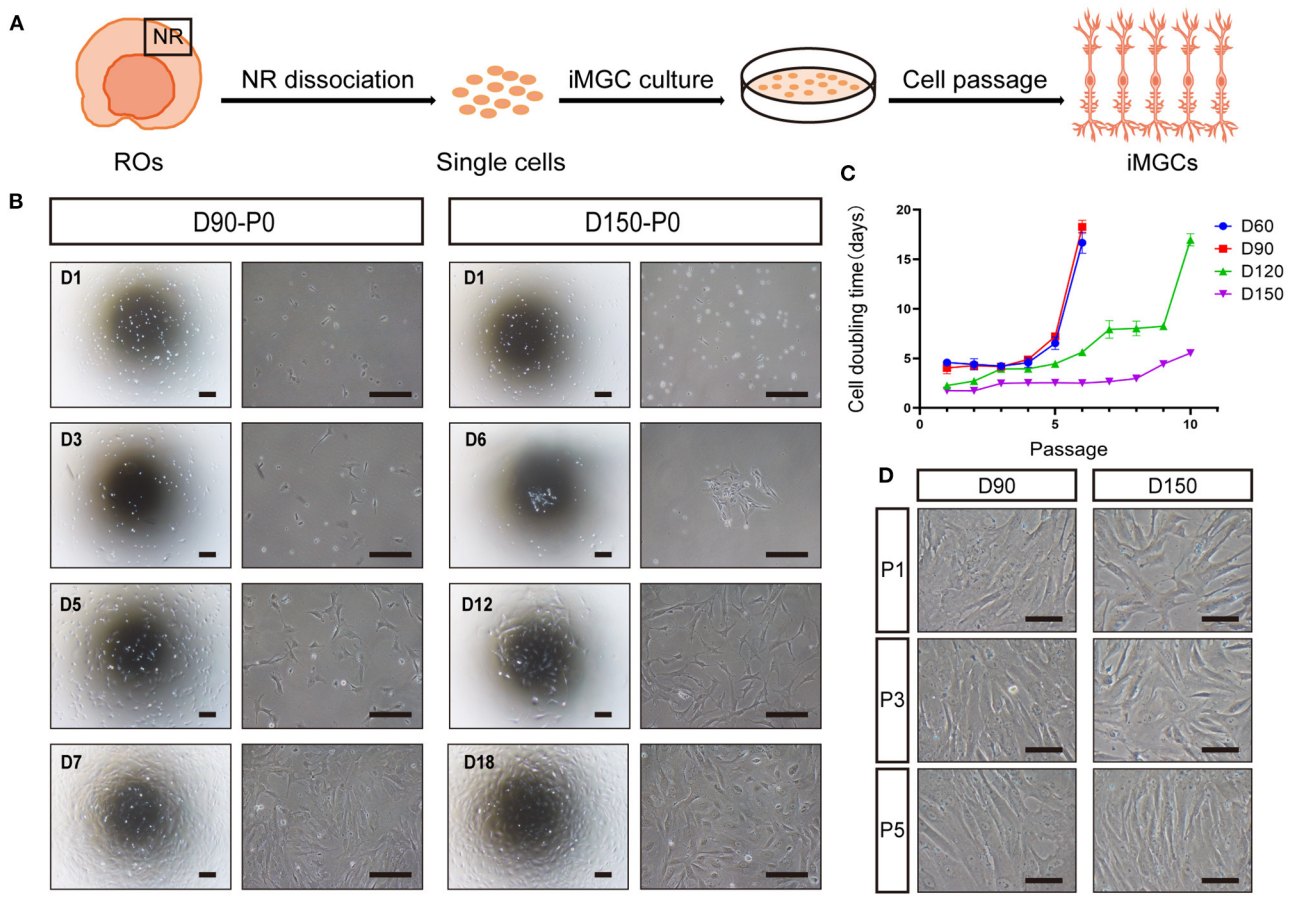

FIGURE 3 | Optimal expansion of induced MGCs (iMGCs) from hiPSC-derived ROs. **(A)** Schematic diagram of expansion of iMGCs from hiPSC-derived ROs. **(B)** Bright-field images showed the distinguished morphological features of the passage 0 (P0) cells isolated from D90-ROs (D90-P0) and D150-ROs (D150-P0). **(C)** The cell doubling time showed different expansion capability of cells isolated from D60-, D90-, D120-, and D150-ROs. **(D)** Bright-field images showed no obvious morphological difference in P1, P3, and P5 cells expanded from D90- and D150-ROs, all appearing a spindle-like shape. ROs, retinal organoids; NR, neural retina. Scale bars = 200 μm **(B)** and 100 μm **(D)**.

Remarkably, when compared to MIO-M1, a spontaneously immortalized MGC line obtained from human retina (Limb et al., 2002), iMGCs were much larger in size with a long, spindle-like shape and abundant cytoplasm, and expressed only the MGC markers SOX9, vimentin, nestin and GS. While some MIO-M1 cells expressed not only the MGC markers, but also markers such as VSX2, PAX6, and CRX for other retinal subtypes and GFAP for astrocytes (**Supplementary Figures S7A,B**). These findings implied that long-term expanded MIO-M1 over 65 passages might progressively lose the molecular and morphological signatures of human MGCs under 2D culture conditions. Altogether, iMGCs expanded from hiPSC-derived ROs did not contaminate astrocytes, and maintained the typical features of primary human MGCs within several passages.

The Ultrastructural and Functional Characteristics of iMGCs

To further characterize the structural signatures of the passaged iMGCs, SEM and TEM were used to observe the ultrastructure of the passaged iMGCs (**Figures 6A,B**). The cells displayed a spindle-like morphology with microvillus projections and contained large nucleus with obvious nucleoli. In these iMGCs, Golgi apparatus, mitochondria, endoplasmic reticulum surrounded the nucleus. Abundant glycogen particles and cytoskeletal elements including microtubules, intermediate filaments and actin filaments presented in cytoplasm (**Figures 6A,B**), which were consistent with the features of MGCs isolated from human retina (Limb et al., 2002; Lawrence et al., 2007).

Then membrane potential of iMGCs were recorded in response to L-glutamate puff. The electrophysiological properties of these iMGCs were similar to MGCs isolated from human retina (Limb et al., 2002; Lawrence et al., 2007) (**Figure 6C**). At current-clamp mode, the membrane potential depolarized from −34.97 to ∼ −28.38 mV (6.59 ± 1.64 mV change, resting membrane potential −34.97 ± 2.10 mV, $N = 13$ cells) in P1 iMGCs, and from −40.01 to −33.37 mV (6.64 ± 1.29 mV change, resting membrane potential −40.01 ± 1.74 mV, $N = 16$ cells) in P5 iMGCs (**Figure 6C**). There was no significant difference in resting membrane potential and the magnitude of depolarization

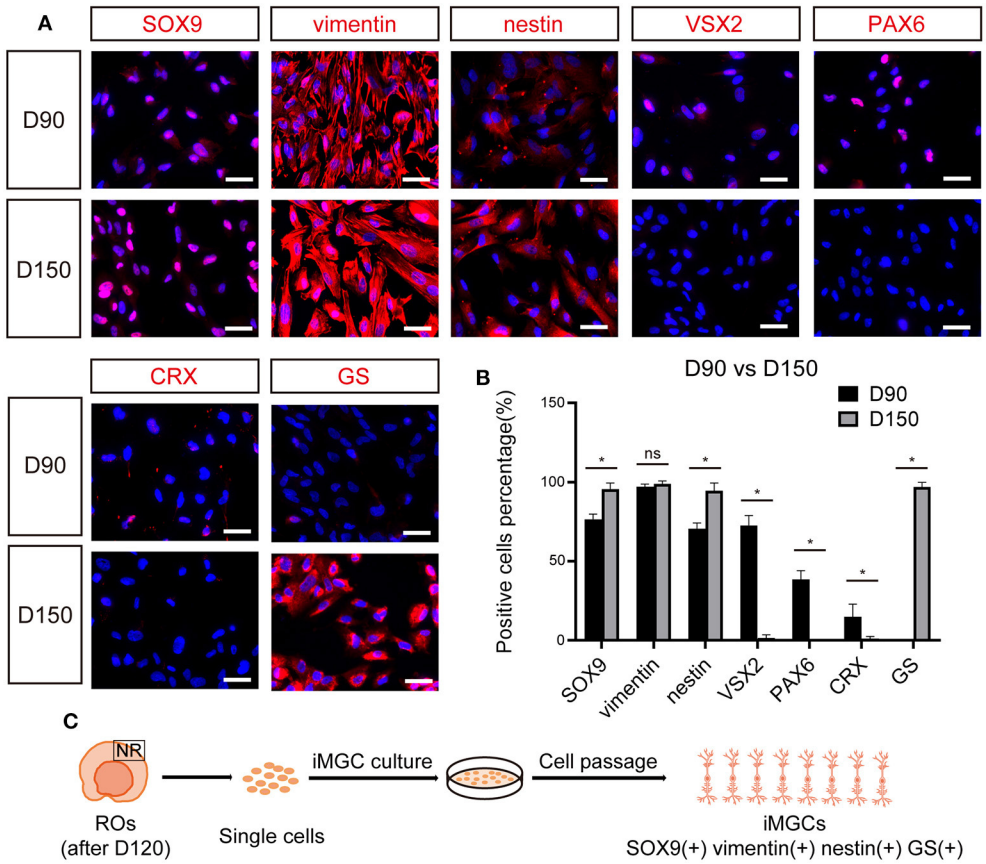

FIGURE 4 | The expression of cell-specific markers in passaged iMGCs from early- and late- stage ROs. **(A)** Immunofluorescence staining showed the expression of markers SOX9, vimentin, nestin, VSX2, PAX6, CRX, and GS in the passaged cells isolated from D90- and D150-ROs. **(B)** Percentage of positive cells in **(A)**. Cell number > 100, $^*p < 0.05$. **(C)** Schematic diagram of molecular characteristics of iMGCs isolated from the late-stage ROs. ROs, retinal organoids; ns, no significance; Scale bars = 50 μm **(A)**.

induced by L-glutamate between P1 and P5 iMGCs (**Figure 6D**, $p > 0.05$, unpaired t-test), suggesting the iMGCs still maintained the functional characteristics of human MGCs even after several passages.

Evaluation of Cell Survival of the iMGCs After Subretinal Transplantation Into Mice

Although studies have shown that MGCs can serve as endogenous stem cells to regenerate neural retina in zebrafish and chick (Fischer and Reh, 2001; Raymond et al., 2006), this regenerative capacity remain debatable in mammalian and human retina. Here, we performed a preliminary evaluation about the cell survival of the iMGCs in subretinal space of NOD/SCID mice (**Figure 7A**). A total of 19 eyes were injected with iMGCs, followed by 21-day observations. During the observation period, all mice kept healthy and no tumors were observed. Fundus photography and OCT examination showed the successful delivery of cells with high reflection located in the subretinal space (SRS) in 3 days after transplantation (DAT) (**Figures 7B,C**). Immunofluorescence staining confirmed that the substantial grafted cells survived in 3 DAT, and co-expressed MGC marker SOX9 and human nucleus antigen marker (HNA), but were negative for other retinal neuron markers VSX2, PAX6, or CRX (**Figures 7D,E**). However, the grafted cells gradually deteriorated since 7 DAT and almost disappeared in SRS at 21 DAT (**Figure 7E**). During the observation period, the donor cells rarely migrated into the host retina of mice. The above data indicated that the iMGCs could not survive well and transdifferentiate into other retinal neurons after transplantation.

DISCUSSION

In this study, we firstly clarified the spatiotemporal development of human MGCs in a hiPSC-derived RO model and developed a simple approach to enrich human MGCs from ROs. MGC precursors and mature MGCs emerged sequentially from the early to the late-stage ROs, where they spatially spanned the entire thickness of NR with their soma located in the intermediate layer of NR. These observations were consistent with the developmental timecourse and the spatial characteristics of

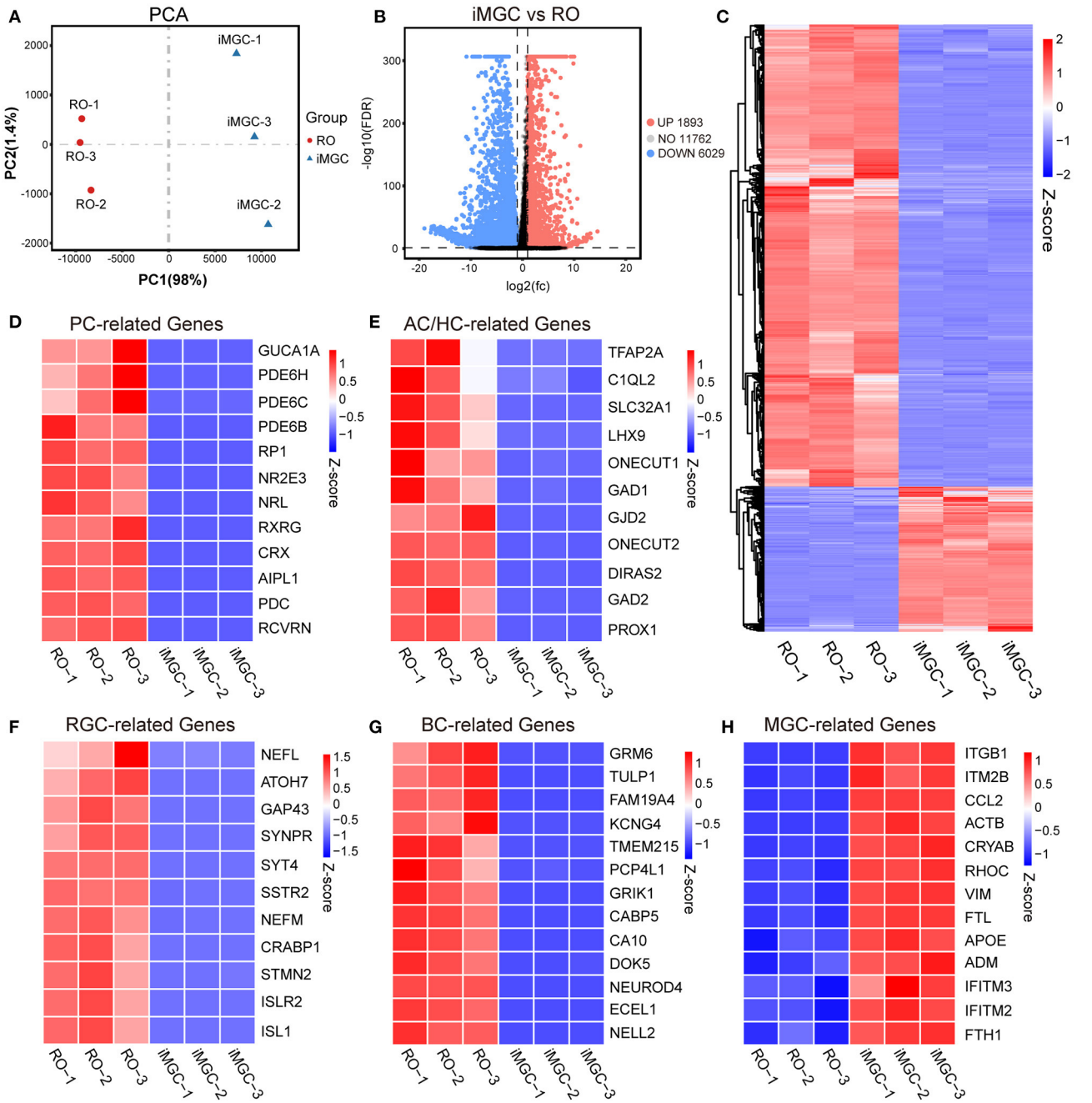

FIGURE 5 | The transcriptome signatures of the passaged iMGCs. **(A)** Principal components analysis (PCA) showed a comparison of the transcriptome data in the passaged iMGCs and D150-ROs. **(B)** Volcano plot showed the total number of the upregulated (UP) and downregulated (DOWN) differentially expressed genes (DEGs) between the NR layers and the passaged iMGCs. **(C)** Heatmap showed the total DEGs between the NR layers and the passaged iMGCs. **(D–H)** Heatmap exhibited the expression of the photoreceptor-related (PC-related) genes **(D)**, amacrine and horizontal cell-related (AC/HC-related) genes **(E)**, retinal ganglion cell-related (RGC-related) genes **(F)**, bipolar cell-related (BC-related) genes **(G)**, and Müller glial cell-related (MGC-related) genes **(H)** between the NR layers and the passaged iMGCs. Blue to red indicated a gradient from low to high gene expression. ROs, retinal organoids; NR, neural retina; FDR, false discovery rate; FC, fold change; iMGC, the passaged iMGCs isolated from D150-ROs; RO, NR layers isolated from D150-ROs; −1, −2, and −3: experimental replicates; NO, no significance; VS, versus.

MGCs in human retina (Ohsawa and Kageyama, 2008; Kohwi and Doe, 2013; Xiang, 2013; Quinn and Wijnholds, 2019; Singh et al., 2021). Importantly, the optimal timepoint of ROs to enrich MGCs were explored. Although cells isolated from both early- and late-stage ROs were expandable, the late-stage ROs were the most optimal option for enriching iMGCs with high purity

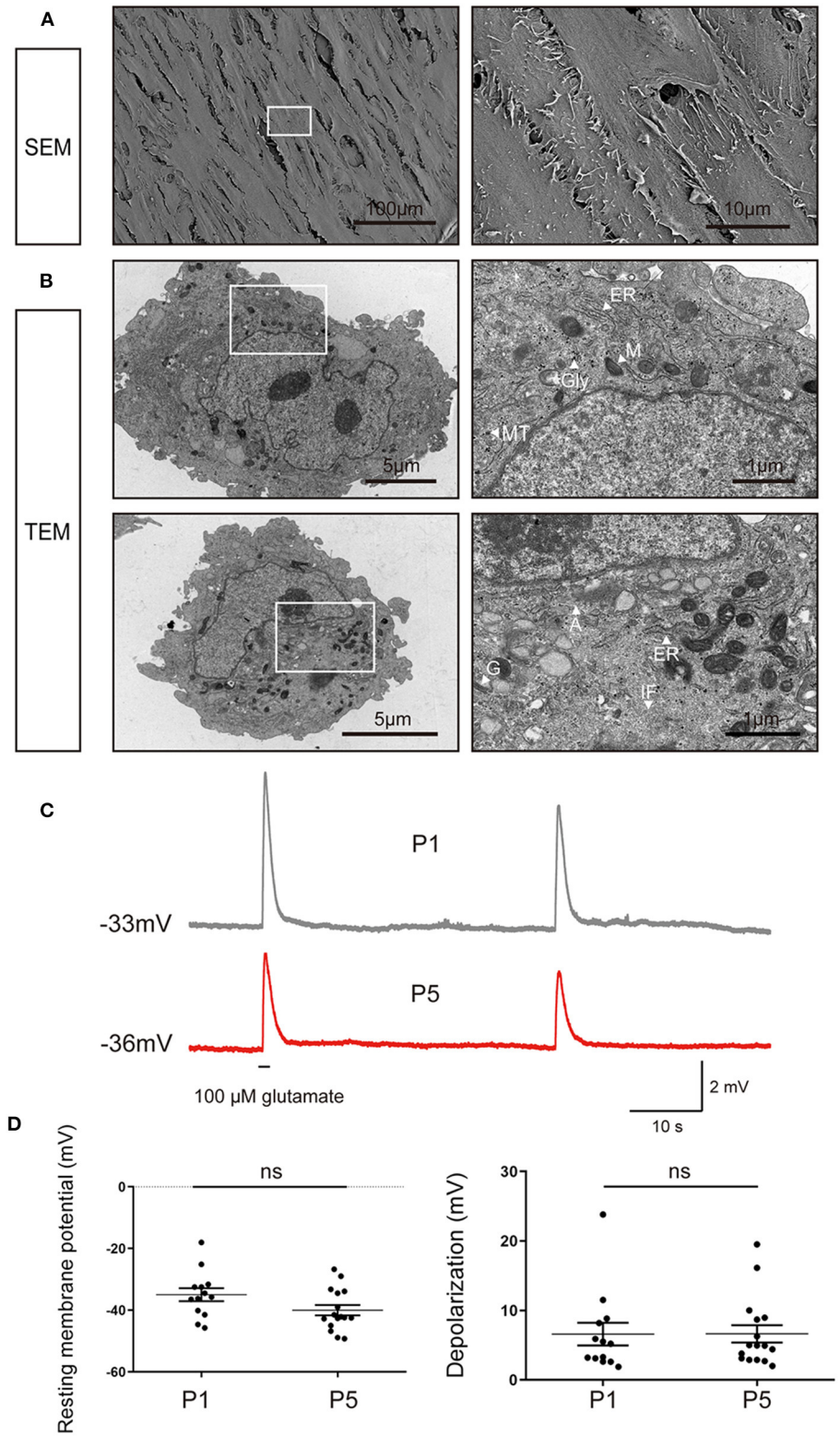

FIGURE 6 | Ultrastructural and electrophysiological characteristics of the passaged iMGCs. **(A)** SEM images showed the iMGCs possessed a typical spindle-like morphology with many microvillus. **(B)** TEM images showed the iMGCs with abundant mitochondria (M), endoplasmic reticulum (ER), Golgi apparatus (G), glycogen (Gly), microtubules (MT), intermediate filaments (IF) and actins (A) in the cytoplasm. **(C)** Both P1 and P5 iMGCs depolarized after application of L-glutamate in current-clamp recordings. **(D)** P1 and P5 iMGCs presented no significant difference in resting membrane potential and the magnitude of depolarization. SEM, scanning electron microscope; TEM, transmission electron microscope; P1 and P5, passage 1 and 5; ns, no significance.

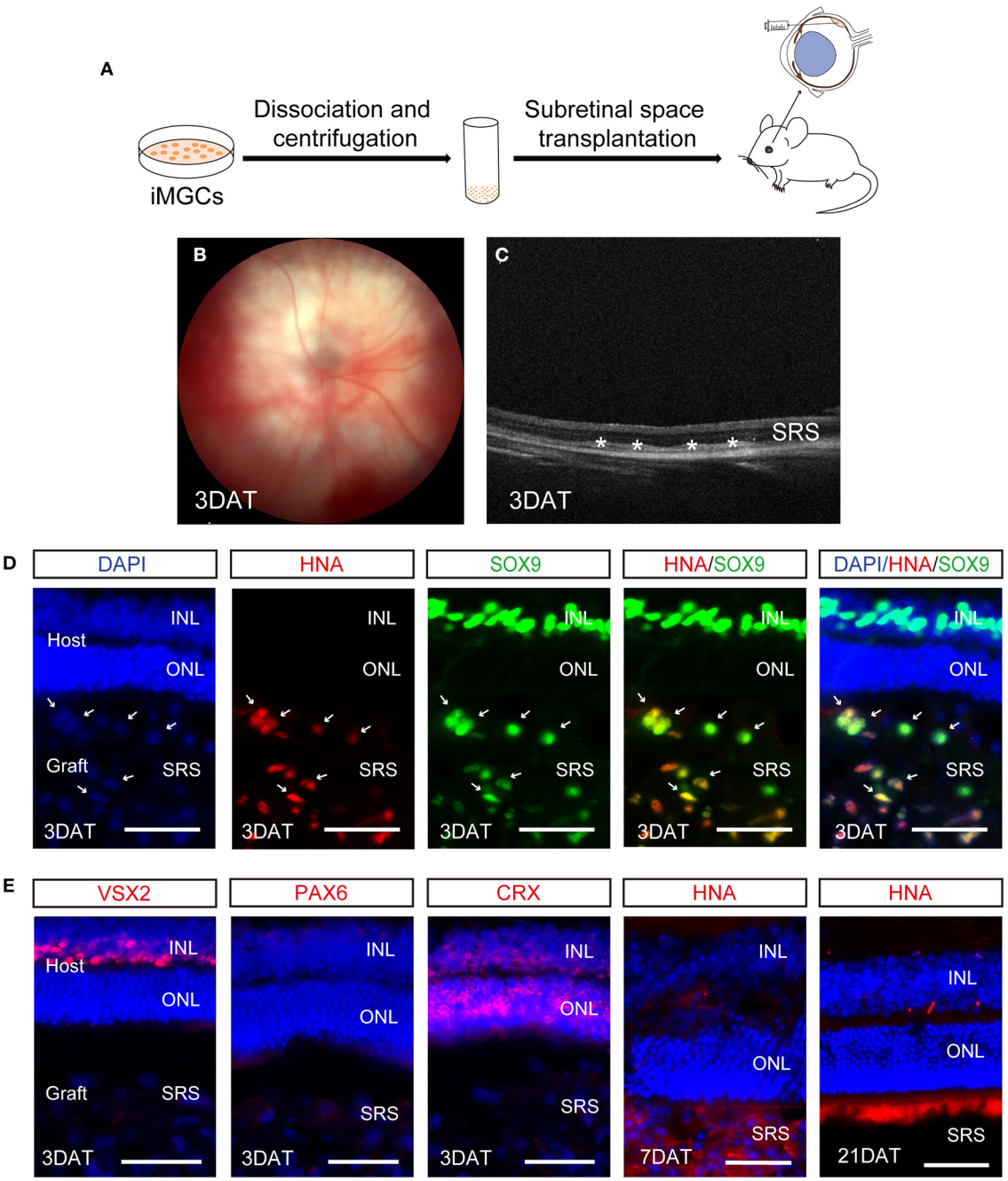

FIGURE 7 | Evaluation of cell survival of the passaged iMGCs after subretinal transplantation into NOD/SCID mice. **(A)** Schematic overview of the subretinal transplantation process of the iMGCs. **(B,C)** Fundus photography **(B)** and optical coherence tomography (OCT) **(C)** showed the successful delivery of the iMGCs into subreinal space (SRS) in NOD/SCID mice 3 days after transplantation (DAT). *The grafted cells. **(D,E)** Immunofluorescence staining showed the grafted iMGCs (D3, P2 iMGCs from D120 BC1-ROs) were positive for HNA and SOX9, but negative for VSX2, PAX6, and CRX at 3 DAT, and gradually disappeared from 7 to 21 DAT. INL, inner nuclear layer; ONL, outer nuclear layer. Scale bars = 50 μm **(D,E)**.

and long-term expansion ability. They possessed morphological, structural, molecular and functional characteristics of primary human MGCs, had the ability to serially expand for at least 10 passages, producing a large population of iMGCs in a short period. The transcriptome pattern of the expanded iMGCs was also revealed. Surprisingly, the passaged iMGCs survived only a short-term period and did not transdifferentiate into other types of retinal cells after transplantation into NOD/SCID mice. Altogether, this study has revealed the developmental and biological features of human MGCs and provided a valuable cell

source, which would significantly promote the investigation and application in MGC-related retinal disorders.

Studies in animal models and cell lines show that the retinal glia differentiates from a progenitor-like state, via a stage of immature glia, and finally to mature MGCs (Ohsawa and Kageyama, 2008; Kohwi and Doe, 2013; Xiang, 2013; Dvoriantchikova et al., 2019; Quinn and Wijnholds, 2019). These differentiation progresses involve morphological, biochemical and physiological changes (Ohsawa and Kageyama, 2008; Kohwi and Doe, 2013; Xiang, 2013; Dvoriantchikova et al., 2019; Quinn and Wijnholds, 2019). However, there are few reports referring to the marker sets which can be used to define immature MGCs or MGC precursors. In this study, RPCs appeared at the early stage of ROs, co-expressing markers Ki67, VSX2, and SOX9; while at D90 ROs, SOX9+ VSX2– or SOX9+ Ki67– cells began to appear in the NR layer, which lost the characteristics of RPCs but did not express mature MGC markers CRALBP or GS. Since D120, Ki67– SOX9+ VSX2– CRALBP+ GS + mature MGCs were clearly identified in the NR layer. Therefore, we defined the Ki67– SOX9+ CRALBP– GS– cells as MGC precursors to represent a transitional period of developing MGCs between RPCs and mature MGCs. These MGC precursors eventually differentiated into mature MGCs, sufficiently expressing CRALBP and GS, which is consistent with the fact that mature MGCs accumulate glia-specific protein and enzymes such as CRALBP and GS (Limb et al., 2002; Lawrence et al., 2007). RNA-seq analysis also revealed that from the early to the late stage ROs, RPC-related genes were downregulated, while MGC-related genes were continuously upregulated, indicating that RPCs progressively obtained the MGC fate as differentiation progressed. In addition, the unique morphology and special distribution of MGCs are associated with many vital physiological functions. For example, they provide an orientation scaffold and migration substrate for post-mitotic young neurons (Reichenbach and Bringmann, 2013, 2020). In hiPSC-derived ROs, the mature MGCs radially spanned the entire thickness of NR with their soma located in the intermediate layer of NR, which is consistent to the morphological features of MGCs in human retina (Reichenbach and Bringmann, 2020). The detailed elucidation of the temporal and spatial development of iMGCs in hiPSC-derived ROs greatly promotes the understanding of human MGC development *in vivo*.

MGCs possess plenty of significant functions in the retinal pathological conditions, but the functional mechanisms are still largely unknown. Enrichment of human MGCs *in vitro* is of great significance for further MGC mechanism studies, which may help to develop effective therapeutic targets for the treatment of various MGC-related human retinal disorders. However, at present, human MGCs are mostly obtained from cadaveric donors and samples after vitreoretinal surgery (Limb et al., 2002; Lawrence et al., 2007), which is limited by scarce donor, astrocyte contamination, immune rejection and risk of disease transmission (Eastlake et al., 2019). There are also some spontaneously immortalized MGC lines obtained from human retina, such as MIO-M1 (Limb et al., 2002; Lawrence et al., 2007). However, in this study, we found that after too many serial passages, their molecular and morphological signatures have altered progressively and there was still astrocyte contamination among these cells. hiPSC-derived ROs containing MGCs can serve as an unlimited source for the selection and enrichment of human MGCs without immune rejection and risk of disease transmission. Moreover, we noticed that the optic stalk marker PAX2, forebrain cell marker SOX1 and astrocyte marker GFAP were negative in the NRs of late-stage ROs in our differentiation system, which could exclude the contamination of non-retinal cells in the subsequent MGCs isolation. Therefore, ROs have advantages to provide purer MGCs than retinal tissues for downstream studies, solving an issue existing in the field for long-term.

A couple of groups have tried to expand iMGCs from ROs at different developmental stages ranged from D34 to D281 (Chung et al., 2019; Eastlake et al., 2019; Couturier et al., 2021). However, the optimal stage of ROs for enrichment of iMGCs has not been discussed. In this study, we compared the cells isolated from ROs at early- (D60-90) and late-stages (D120 and afterwards) in detail. Although both were expandable, cells isolated from the late-stage ROs were the most optimal choice for the selection and enrichment of human MGCs, as they expanded to daughter MGCs with higher purity and expansion capability, and expressed typical MGC markers GS, which is consistent with the reported iMGCs expanded from ROs older than D160 (Couturier et al., 2021). In addition, Eastlake and colleagues reported that all of MGCs isolated from ROs aged at D34–D281 could express mRNA coding for the MGC markers CRALBP, GS, nestin and vimentin in two different passages (Eastlake et al., 2019). However, based on our results, cells from the early-stage ROs (D60–D90) did not express key MGC marker GS in protein level, and lost proliferative ability after six passages. According to the timecourse of iMGC development in ROs described above, we presumed that cells isolated from the early-stage ROs, which mainly consisted of RPCs or MGC precursors other than mature MGCs, were not able to continue differentiating or growing into mature MGCs under 2D culture conditions. Therefore, the late-stage ROs older than D120 were recommended to enrich iMGCs which recapitulated the features of primary human MGCs and were suitable for downstream investigation.

In the adult human retina, much controversy has arisen on the regeneration of MGCs, although it has been reported that MGCs have regenerative potential after retinal injury in the zebrafish, chick and mouse (Fischer and Reh, 2001; Raymond et al., 2006; Karl et al., 2008). Our current study along with previous reports demonstrated that the expanded iMGCs possessed the morphological, molecular and functional characteristics of primary human MGCs (Couturier et al., 2021). However, it remains unknown whether these iMGCs are capable of survival, regeneration or transdifferentiation *in vivo* or not. In 2019, Eastlake and colleagues intravitreally transplanted iMGCs into a rat model with NMDA-induced RGC depletion, and found that these iMGC grafts integrated into the retinal ganglion cell layer, leading to a partial rescue of the retinal ganglion cell function (Eastlake et al., 2019). In this study, we preliminarily explored the cell behavior of the expanded iMGCs after subretinal transplantation into the healthy NOD/SCID mice. Our results showed that the iMGCs expanded from the late-stage ROs could survive only for a short time and could not transdifferentiate

into other types of retinal cells. HNA, a marker specific for human cells, was clearly expressed in the nucleus of the grated cells on 3 DAT, but in both nucleus and cytoplasm on 7 DAT, indicating the donor cells did not survive well, and started to deteriorate or apoptosis leading their nucleus to break down and spread out. Finally, these cells all disappeared on 21 DAT. Many factors contributing to the graft failure have been discussed in previous studies. For instance, the NOD/SCID mice without retinal defects in our current study could not provide specific microenvironments to promote the growth of donor cells, or the plasticity of the passaged iMGCs is limited. The passaged iMGCs growing in a 2D culture condition might have changed the characteristics of iMGCs in ROs which grow in a 3D culture environment mimicking human retina *in vivo*. Although immune rejection is believed to be one of the main causes of the graft failure (Singhal et al., 2008), it may not be the case since we used immunodeficiency NOD/SCID mice in our current study. However, we did not completely exclude this possibility since our immunostaining with anti-Iba1 antibody did show a certain degree activation of microglia following cell transplantation in NOD/SCID mice (data not shown). Therefore, substantial investigations will be needed to further evaluate the cell behavior of iMGCs *in vivo*, such as using a diseased mouse model, transplanting MGC precursors or MGCs directly isolated from hiPSC-derived ROs.

In conclusion, MGCs play important roles in physiological and pathological conditions in vertebrate retina, whose roles and related mechanisms still remain elusive in human retina due to the species differences, human tissue source limits and ethical concerns. Our results demonstrated that hiPSC-derived ROs could provide an accessible platform to directly study the developmental, morphological, molecular and functional characteristics of human MGCs. The simple approach and the optimal stage of ROs to enrich iMGCs have been established. Especially, iMGCs expanded from ROs lack of astrocyte contamination in comparison with those from human retinal tissue, which would serve as a better model and facilitate the follow-up investigation of MGC-related retinal disorders. This study also has limitations, such as only two hiPSC lines were evaluated and the expanded iMGCs did not survive well in the SRS of mouse retina. More studies are necessary to further explore the characteristics and applications of the enriched iMGCs.

DATA AVAILABILITY STATEMENT

The datasets presented in this study can be found in online repositories. The names of the repository/repositories and accession number(s) can be found below: https://www.ncbi.nlm.nih.gov/genbank/, GSE188698.

ETHICS STATEMENT

The animal study was reviewed and approved by the Animal Ethics Committee of the Zhongshan Ophthalmic Center, Sun Yat-sen University.

AUTHOR CONTRIBUTIONS

RN, DZ, BX, GG, JX, PX, and YW performed the experiments and analyzed the data. RN and XZ designed the experiments. FP, BJ, JG, and XZ interpreted data. RN, DZ, and XZ wrote the manuscript. XZ conceived the study, supervised the project, secured the funds, and approved the manuscript. All authors contributed to the article and approved the submitted version.

FUNDING

This work was supported by grants from the Science & Technology Project of Guangdong Province (2017B020230003), National Key Research and Development Program of the Ministry of Science and Technology (2017YFA0104101), National Natural Science Foundation of China (81970842, 82071265, and 82172957), and Science & Technology Project of Guangzhou (202102010288).

ACKNOWLEDGMENTS

The authors would like to thank Professor Linzhao Cheng (University of Science and Technology of China) for gifts of BC1 and BC1-GFP hiPSC lines.

SUPPLEMENTARY MATERIAL

The Supplementary Material for this article can be found online at: https://www.frontiersin.org/articles/10.3389/fncel.2022.820396/full#supplementary-material

REFERENCES

Bosze, B., Suarez-Navarro, J., Soofi, A., Lauderdale, J. D., Dressler, G. R., and Brown, N. L. (2021). Multiple roles for Pax2 in the embryonic mouse eye. *Dev. Biol.* 472, 18–29. doi: 10.1016/j.ydbio.2020.12.020

Bringmann, A., Iandiev, I., Pannicke, T., Wurm, A., Hollborn, M., Wiedemann, P., et al. (2009). Cellular signaling and factors involved in Muller cell gliosis: neuroprotective and detrimental effects. *Prog. Retin. Eye Res.* 28, 423–451. doi: 10.1016/j.preteyeres.2009.07.001

Bringmann, A., Pannicke, T., Grosche, J., Francke, M., Wiedemann, P., Skatchkov, S. N., et al. (2006). Muller cells in the healthy and diseased retina. *Prog. Retin. Eye Res.* 25, 397–424. doi: 10.1016/j.preteyeres.2006.05.003

Bringmann, A., and Wiedemann, P. (2012). Muller glial cells in retinal disease. *Ophthalmologica* 227, 1–19. doi: 10.1159/000328979

Capowski, E. E., Samimi, K., Mayerl, S. J., Phillips, M. J., Pinilla, I., Howden, S. E., et al. (2019). Reproducibility and staging of 3D human retinal organoids across multiple pluripotent stem cell lines. *Development* 146. doi: 10.1242/dev.171686

Chou, B. K., Mali, P., Huang, X., Ye, Z., Dowey, S. N., Resar, L. M., et al. (2011). Efficient human iPS cell derivation by a non-integrating plasmid from blood cells with unique epigenetic and gene expression signatures. *Cell Res.* 21, 518–529. doi: 10.1038/cr.2011.12

Chung, S. H., Shen, W., Davidson, K. C., Pebay, A., Wong, R. C. B., Yau, B., et al. (2019). Differentiation of retinal glial cells from human embryonic stem

cells by promoting the notch signaling pathway. *Front. Cell. Neurosci.* 13, 527. doi: 10.3389/fncel.2019.00527

Couturier, A., Blot, G., Vignaud, L., Nanteau, C., Slembrouck-Brec, A., Fradot, V., et al. (2021). Reproducing diabetic retinopathy features using newly developed human induced-pluripotent stem cell-derived retinal Muller glial cells. *Glia* 69, 1679–1693. doi: 10.1002/glia.23983

Dvoriantchikova, G., Seemungal, R. J., and Ivanov, D. (2019). Development and epigenetic plasticity of murine Muller glia. *Biochim. Biophys. Acta Mol. Cell. Res.* 1866, 1584–1594. doi: 10.1016/j.bbamcr.2019.06.019

Eastlake, K., Luis, J., and Limb, G. A. (2020). Potential of muller glia for retina neuroprotection. *Curr. Eye Res.* 45, 339–348. doi: 10.1080/02713683.2019.1648831

Eastlake, K., Wang, W., Jayaram, H., Murray-Dunning, C., Carr, A. J. F., Ramsden, C. M., et al. (2019). Phenotypic and functional characterization of muller glia isolated from induced pluripotent stem cell-derived retinal organoids: improvement of retinal ganglion cell function upon transplantation. *Stem Cells Transl. Med.* 8, 775–784. doi: 10.1002/sctm.18-0263

Fischer, A. J., and Reh, T. A. (2001). Müller glia are a potential source of neural regeneration in the postnatal chicken retina. *Nat. Neurosci.* 4, 247–252. doi: 10.1038/85090

Fligor, C. M., Langer, K. B., Sridhar, A., Ren, Y., Shields, P. K., Edler, M. C., et al. (2018). Three-dimensional retinal organoids facilitate the investigation of retinal ganglion cell development, organization and neurite outgrowth from human pluripotent stem cells. *Sci. Rep.* 8, 14520. doi: 10.1038/s41598-018-32871-8

Guan, Y., Xie, B., and Zhong, X. (2021). Retinal organoid induction system for derivation of 3D retinal tissues from human pluripotent stem cells. *J. Vis. Exp.* doi: 10.3791/62435

Hoshino, A., Ratnapriya, R., Brooks, M. J., Chaitankar, V., Wilken, M. S., Zhang, C., et al. (2017). Molecular anatomy of the developing human retina. *Dev. Cell* 43, 763–779 e764. doi: 10.1016/j.devcel.2017.10.029

Karl, M. O., Hayes, S., Nelson, B. R., Tan, K., Buckingham, B., and Reh, T. A. (2008). Stimulation of neural regeneration in the mouse retina. *Proc. Natl. Acad. Sci. U. S. A.* 105, 19508–19513. doi: 10.1073/pnas.0807453105

Kim, D., Langmead, B., and Salzberg, S. L. (2015). HISAT: a fast spliced aligner with low memory requirements. *Nat. Methods* 12, 357–360. doi: 10.1038/nmeth.3317

Kim, S., Lowe, A., Dharmat, R., Lee, S., Owen, L. A., Wang, J., et al. (2019). Generation, transcriptome profiling, and functional validation of cone-rich human retinal organoids. *Proc. Natl. Acad. Sci. U. S. A.* 116, 10824–10833. doi: 10.1073/pnas.1901572116

Kohwi, M., and Doe, C. Q. (2013). Temporal fate specification and neural progenitor competence during development. *Nat. Rev. Neurosci.* 14, 823–838. doi: 10.1038/nrn3618

Lawrence, J. M., Singhal, S., Bhatia, B., Keegan, D. J., Reh, T. A., Luthert, P. J., et al. (2007). MIO-M1 cells and similar muller glial cell lines derived from adult human retina exhibit neural stem cell characteristics. *Stem Cells* 25, 2033–2043. doi: 10.1634/stemcells.2006-0724

Li, B., and Dewey, C. N. (2011). RSEM: accurate transcript quantification from RNA-Seq data with or without a reference genome. *BMC Bioinformat.* 12, 323. doi: 10.1186/1471-2105-12-323

Li, G., Xie, B., He, L., Zhou, T., Gao, G., Liu, S., et al. (2018). Generation of retinal organoids with mature rods and cones from urine-derived human induced pluripotent stem cells. *Stem Cells Int.* 2018, 4968658. doi: 10.1155/2018/4968658

Limb, G. A., Salt, T. E., Munro, P. M., Moss, S. E., and Khaw, P. T. (2002). *In vitro* characterization of a spontaneously immortalized human Müller cell line (MIO-M1). *Invest. Ophthalmol. Vis. Sci.* 43, 864–869.

Love, M. I., Huber, W., and Anders, S. (2014). Moderated estimation of fold change and dispersion for RNA-seq data with DESeq2. *Genome Biol.* 15, 550. doi: 10.1186/s13059-014-0550-8

Ohsawa, R., and Kageyama, R. (2008). Regulation of retinal cell fate specification by multiple transcription factors. *Brain Res.* 1192, 90–98. doi: 10.1016/j.brainres.2007.04.014

Pertea, M., Kim, D., Pertea, G. M., Leek, J. T., and Salzberg, S. L. (2016). Transcript-level expression analysis of RNA-seq experiments with HISAT, StringTie and Ballgown. *Nat. Protoc.* 11, 1650–1667. doi: 10.1038/nprot.2016.095

Quinn, P. M. J., and Wijnholds, J. (2019). Retinogenesis of the human fetal retina: an apical polarity perspective. *Genes* 10. doi: 10.3390/genes10120987

Raymond, P. A., Barthel, L. K., Bernardos, R. L., and Perkowski, J. J. (2006). Molecular characterization of retinal stem cells and their niches in adult zebrafish. *BMC Dev. Biol.* 6, 36. doi: 10.1186/1471-213X-6-36

Reichenbach, A., and Bringmann, A. (2013). New functions of Muller cells. *Glia* 61, 651–678. doi: 10.1002/glia.22477

Reichenbach, A., and Bringmann, A. (2020). Glia of the human retina. *Glia* 68, 768–796. doi: 10.1002/glia.23727

Singh, R. K., Winkler, P. A., Binette, F., Petersen-Jones, S. M., and Nasonkin, I. O. (2021). Comparison of developmental dynamics in human fetal retina and human pluripotent stem cell-derived retinal tissue. *Stem Cells Dev.* 30, 399–417. doi: 10.1089/scd.2020.0085

Singhal, S., Lawrence, J. M., Bhatia, B., Ellis, J. S., Kwan, A. S., Macneil, A., et al. (2008). Chondroitin sulfate proteoglycans and microglia prevent migration and integration of grafted Muller stem cells into degenerating retina. *Stem Cells* 26, 1074–1082. doi: 10.1634/stemcells.2007-0898

Vecino, E., Rodriguez, F. D., Ruzafa, N., Pereiro, X., and Sharma, S. C. (2016). Glia-neuron interactions in the mammalian retina. *Progr. Retina Eye Res.* 51, 1–40. doi: 10.1016/j.preteyeres.2015.06.003

Westergard, T., and Rothstein, J. D. (2020). Astrocyte diversity: current insights and future directions. *Neurochem. Res.* 45, 1298–1305. doi: 10.1007/s11064-020-02959-7

Xiang, M. (2013). Intrinsic control of mammalian retinogenesis. *Cell. Mol. Life Sci.* 70, 2519–2532. doi: 10.1007/s00018-012-1183-2

Yan, W., Peng, Y. R., van Zyl, T., Regev, A., Shekhar, K., Juric, D., et al. (2020). Cell atlas of the human fovea and peripheral retina. *Sci. Rep.* 10, 9802. doi: 10.1038/s41598-020-66092-9

Zhong, X., Gutierrez, C., Xue, T., Hampton, C., Vergara, M. N., Cao, L. H., et al. (2014). Generation of three-dimensional retinal tissue with functional photoreceptors from human iPSCs. *Nat. Commun.* 5, 4047. doi: 10.1038/ncomms5047

Zou, C., Chou, B. K., Dowey, S. N., Tsang, K., Huang, X., Liu, C. F., et al. (2012). Efficient derivation and genetic modifications of human pluripotent stem cells on engineered human feeder cell lines. *Stem Cells Dev.* 21, 2298–2311. doi: 10.1089/scd.2011.0688

Zou, T., Gao, L., Zeng, Y., Li, Q., Li, Y., Chen, S., et al. (2019). Organoid-derived C-Kit(+)/SSEA4(-) human retinal progenitor cells promote a protective retinal microenvironment during transplantation in rodents. *Nat. Commun.* 10, 1205. doi: 10.1038/s41467-019-08961-0

Conflict of Interest: The authors declare that the research was conducted in the absence of any commercial or financial relationships that could be construed as a potential conflict of interest.

Publisher's Note: All claims expressed in this article are solely those of the authors and do not necessarily represent those of their affiliated organizations, or those of the publisher, the editors and the reviewers. Any product that may be evaluated in this article, or claim that may be made by its manufacturer, is not guaranteed or endorsed by the publisher.

frontiers | Frontiers in Cellular Neuroscience

TYPE Original Research
PUBLISHED 08 December 2022
DOI 10.3389/fncel.2022.1050432

OPEN ACCESS

EDITED BY
Lin Cheng,
The University of Iowa, United States

REVIEWED BY
Karen Litwa,
East Carolina University, United States
Andrea Laurato Sertie,
Hospital Israelita Albert Einstein, Brazil

*CORRESPONDENCE
Gabriel G. Haddad
ghaddad@ucsd.edu

SPECIALTY SECTION
This article was submitted to Cellular Neuropathology, a section of the journal Frontiers in Cellular Neuroscience

RECEIVED 21 September 2022
ACCEPTED 14 November 2022
PUBLISHED 08 December 2022

CITATION
Zhao HH and Haddad GG (2022) Alzheimer's disease like neuropathology in Down syndrome cortical organoids.
Front. Cell. Neurosci. 16:1050432.
doi: 10.3389/fncel.2022.1050432

Alzheimer's disease like neuropathology in Down syndrome cortical organoids

Helen H. Zhao[1] and Gabriel G. Haddad[1,2,3]*

[1]Department of Pediatrics, University of California San Diego, La Jolla, CA, United States, [2]Department of Neurosciences, University of California San Diego, La Jolla, CA, United States, [3]The Rady Children's Hospital, San Diego, CA, United States

Introduction: Down syndrome (DS) is a genetic disorder with an extra copy of chromosome 21 and DS remains one of the most common causes of intellectual disabilities in humans. All DS patients have Alzheimer's disease (AD)-like neuropathological changes including accumulation of plaques and tangles by their 40s, much earlier than the onset of such neuropathological changes in AD patients. Due to the lack of human samples and appropriate techniques, our understanding of DS neuropathology during brain development or before the clinical onset of the disease remains largely unexplored at the cellular and molecular levels.

Methods: We used induced pluripotent stem cell (iPSC) and iPSC-derived 3D cortical organoids to model Alzheimer's disease in Down syndrome and explore the earliest cellular and molecular changes during DS fetal brain development.

Results: We report that DS iPSCs have a decreased growth rate than control iPSCs due to a decreased cell proliferation. DS iPSC-derived cortical organoids have a much higher immunoreactivity of amyloid beta (Aß) antibodies and a significantly higher amount of amyloid plaques than control organoids. Although Elisa results did not detect a difference of Aß40 and Aß42 level between the two groups, the ratio of Aß42/Aß40 in the detergent-insoluble fraction of DS organoids was significantly higher than control organoids. Furthermore, an increased Tau phosphorylation (pTau S396) in DS organoids was confirmed by immunostaining and Western blot. Elisa data demonstrated that the ratio of insoluble Tau/total Tau in DS organoids was significantly higher than control organoids.

Conclusion: DS iPSC-derived cortical organoids mimic AD-like pathophysiologyical phenotype *in vitro*, including abnormal Aß and insoluble Tau accumulation. The molecular neuropathologic signature of AD is present in DS much earlier than predicted, even in early fetal brain development, illustrating the notion that brain organoids maybe a good model to study early neurodegenerative conditions.

KEYWORDS

Down syndrome, Alzheimer's disease (AD), iPSC, proliferation, amyloid-beta, tau pathology, cortical organoid

Introduction

Down syndrome (DS) is a genetic disorder with an extra copy of chromosome 21, characterized by physical growth delay, mild to moderate intellectual disability, and characteristic facial features. DS is one of the most common causes of intellectual disabilities in humans, with an incidence of one in 700 newborns. Moreover, DS patients often have an increased risk to develop many other health problems including Alzheimer's disease (AD), obstructive sleep apnea, congenital heart defect, and leukemia (Asim et al., 2015). Almost all DS patients have AD-like neuropathological changes (AD-DS) such as accumulation of plaques and tangles at about 40 years of age. Approximately 40%–80% of DS patients develop AD-like dementia by 50–60 years, much earlier than the majority of AD patients (Oliver and Holland, 1986; Holland et al., 1998; Zigman et al., 2004). DS and AD patients share many neuropathological changes such as amyloid beta accumulation, tau pathology, endosomal dysfunction, synaptic dysfunction, and neurogenesis defects. The earliest neuropathological changes such as enlarged endosomes, impaired synaptogenesis, and neurogenesis can be traced back to early life even at the fetal brain in DS patients (Marin-Padilla, 1972; Wisniewski et al., 1984; Cataldo et al., 2000; Baburamani et al., 2019; Patkee et al., 2020; Tang et al., 2021). However, due to the lack of human samples and appropriate techniques, our understanding of DS neuropathology during brain development or before the clinical onset of the disease remains largely unexplored at the cellular and molecular levels.

Induced pluripotent stem cell (iPSC) technology, first introduced by Yamanaka in 2007 (Takahashi et al., 2007) has been widely used by many laboratories to study a variety of human diseases, including Alzheimer's disease (Kondo et al., 2013), Parkinson's disease (Hargus et al., 2010), and Autism spectrum disorder (Russo et al., 2019). iPSC-derived 3D cortical organoids have been shown to closely simulate the key endogenous neurodevelopmental events with a cytoarchitecture resembling regions of the developing human brain (Paşca, 2018) and recapitulate the trajectory of human brain development and maturation (Lancaster and Knoblich, 2014; Paşca et al., 2015). Moreover, brain organoids have a transcriptome profile that is close to that in the early human brain (Camp et al., 2015; Paşca et al., 2015; Nascimento et al., 2019; Trujillo et al., 2019). Therefore, iPSC-derived brain organoids represent an optimized approach for modeling neurodevelopmental disorders such as Down syndrome and allow us to explore the earliest cellular and molecular changes during DS fetal brain development.

To our knowledge, currently only one published study used iPSC-derived organoids to investigate the AD-like pathology to compare a DS patient and a healthy control (Gonzalez et al., 2018). Here, by comparing DS-specific iPSC lines and their isogenic control iPSC lines, we demonstrate that abnormalities in Down syndrome start as early as the iPSC stage and AD-like neuropathological phenotype including abnormal Aß accumulation and Tau pathology progressively manifest themselves in organoids during early development.

Materials and methods

Karyotype of iPSC lines

All iPSC lines were obtained from Dr. Stuart Orkin at Boston Children's Hospital through a material transfer agreement. The use of cells was approved by IRB at the University of California San Diego. Two DS iPSC subclones and two isogenic control subclones were isolated from DS1-iPS4 cells as previously described (Maclean et al., 2012). The iPSCs were fed daily with mTeSR medium. DNA was extracted from iPSCs using a DNase Blood and Tissue kit (Qiagen, CA), the presence of an extra copy of chromosome 21 in DS iPSCs was confirmed by a high-resolution karyotyping performed by the Cell Line Genetics (Madison, WI).

Real time PCR

RNA from iPSCs was extracted using the RNase Mini kit (Qiagen, CA). One microgram of total RNA was converted to complementary DNA using SuperScript First-Strand Synthesis System for RT-PCR (Life Technologies, CA). Real time PCR was performed using a GeneAmp 7900 sequence detection system with POWER SYBR Green (Applied Biosystems, CA). Gene expression of *GAPDH* levels was used as a loading control. Real time PCR data were presented after normalization with *GAPDH* expression. Primers used in the current study are listed in **Table 1**.

TABLE 1 List of primers.

Genes	Primer sequence
APP	FW: TTTGGCACTGCTCCTGCT RV: CCACAGAACATGGCAATCTG
DYRK1A	FW: CTGGACTCTTCCCTCCCTTC RV: GCCGAACAGATGAAGGTTTG
BACE2	FW: TGCCTGGGATTAAATGGAATGG RV: CAGGGAGTCGAAGAAGGTCTC
RCAN1	FW: GCGTGGTGGTCCATGTATGT RV: TGAGGTGGATCGGCGTGTA
CSTB	FW: ATTCAAGAGCCAGGTGGTCG RV: CACTCGCAGGTGTACGAAGT
DSCAM	FW: CCTACGAACACGCCAAGATG RV: TACTCATTTGTCCCTGCCGT
GAPDH	FW: GCACCGTCAAGGCTGAGAAC RV: CGCCCCACTTGATTTTGG

Cell growth analysis

Both DS and isogenic control iPSCs were seeded in a 6-well plate with a density of 10^5 live cells/well and total cells are collected and counted after 3, 5, and 7 days in culture using Bio-Rad TC20 cell counter. The cell numbers were compared between the two groups.

Cell proliferation experiments

DS and isogenic control iPSCs were seeded in a 4-well chamber slide with a density of 10^4 live cells/well and cultured for 5 days. Immunostaining of Ki67 in iPSCs was followed the standard immunofluorescence staining protocol. Double labeling of EdU and BrdU was performed as previously described (Deshpande et al., 2017) with minor modifications. In brief, iPSCs were treated with EdU (20 μM) for 1 h and then with BrdU (10 μM) for an additional 1 h of incubation. Cells were fixed with 4% paraformaldehyde for 15 min and then permeabilized with 0.5% triton in PBS for 20 min. DNA was denatured with 4 M HCl for 20 min and followed by phosphate citric acid buffer for 10 min. EdU detection was performed using Click-iT^{TM} Plus EdU Cell Proliferation Kit following the manufacturer's protocol. BrdU detection was performed following the standard immunofluorescence protocol with BrdU antibody (clone MoBU-1). Nuclei were stained with Hoechst 33342. EdU$^+$ and BrdU$^+$ cells were compared between the two groups.

Generation of cortical organoids

Cortical organoids were generated from iPSCs and organoid spheres were kept in suspension under rotation (95 rpm) as previously described (Camp et al., 2015; Trujillo et al., 2019; Yao et al., 2020). In brief, on day 0, iPSCs colonies were dissociated into single cells using accutase with PBS at a ratio of 1:1, approximately 4 × 10^6 cells were transferred to one well of a 6-well plate in mTeSR1 supplemented with 5 μM Y-27632, 10 μM SB431542 (SB), and 1 μM Dorsomorphin (Dorso) for 3 days. Y-27632 was removed after 24 h; on day 3, mTeSR1 was substituted by base medium containing neurobasal, glutamax, 1% MEM nonessential amino acids (NEAA), 2% Gem21, and 1% penicillin/streptomycin (PS) supplemented with 1% N_2, 10 μM SB, and 1 μM Dorso. The medium was changed every other day. On day 9, organoids were fed with a base medium supplemented with 20 ng/ml FGF2 for a week and the medium was changed every day. On day 16, the medium was switched to base medium supplemented with 20 ng/ml of FGF2 and 20 ng/ml EGF. On day 22, organoids were fed with the base medium supplemented with 10 ng/ml of BDNF, 10 ng/ml of GDNF, 10 ng/ml of NT-3, 200 μM L-ascorbic acid, and 1 mM dibutyryl-cAMP. Four weeks later, cortical organoids were maintained in the base medium with media changes twice a week. All reagents and chemicals used in the current study are listed in **Table 2**.

Elisa of amyloid beta and tau

Detergent soluble and insoluble fractions of amyloid beta (Aβ40, Aβ42) and total Tau were quantified using Elisa kits following the manufacturer's instructions. Soluble and insoluble fractions were prepared based on the previously published study (Wang et al., 2021). In brief, organoids were homogenized in RIPA buffer with protease inhibitors, the homogenate was centrifuged at 15,000× *g* for 10 min, and the supernatant was collected to yield a detergent soluble fraction. The remaining organoid pellet was then resuspended in 5 M guanidine-HCl diluted in 50 mM Tris, pH 8.0 with protease inhibitor and mechanically agitated at room temperature for 4 h to extract the detergent-insoluble fraction. Guanidine treated samples were diluted 1:2 in sterile PBS and centrifuged at 16,000× *g* for 20 min. The supernatant was collected to yield an insoluble fraction. The protein concentration of both soluble and insoluble supernatants was determined using a BCA assay and an equal amount of total protein was used for the Elisa assay.

Immunofluorescence staining

Organoids were fixed with 4% paraformaldehyde for 30 min and then were transferred to 30% sucrose solution at 4°C overnight. Cryopreserved organoids were embedded in OCT and sectioned into 14 μm-thick slices for immunofluorescence staining. The sections were treated with 0.5% triton in PBS for 20 min and followed by blocking with 5% BSA in PBS for 1 h at room temperature. The sections were then incubated with the primary antibody (see **Table 2**) diluted in PBS with 5% BSA overnight and Alexa 488 and Alexa 555 conjugated secondary antibodies to specific IgG types for 1 h. Prolong Diamond anti-fade mountant with DAPI was used as a counterstain (Sigma, St. Louis, MO).

Amylo-Glo staining

Amyloid plaque staining on organoid sections was performed using the Amylo-Glo RTD amyloid plaque stain reagent (Biosensis, Australia) following the manufacturer's instructions.

Western blot

Twenty micrograms of soluble protein from 12 weeks DS and control organoids were separated on NuPAGE 4%–12% Bis-Tris gels and then transferred to polyvinylidene difluoride membranes (Millipore, CA). The membranes were probed with a primary antibody in PBST with 5% BSA overnight at 4°C and followed by an appropriate horseradish peroxidase-conjugated secondary antibody (Invitrogen, CA). Immunoreactive bands were visualized using Bio-Rad ChemiDoc XRS with enhanced chemiluminescence (Perkin Elmer, MA). Equal loading was assessed using GAPDH and data were analyzed using ImageLab software (version 3.0, Bio-Rad).

Imaging analysis

All immunofluorescence images were captured using a 20× objective on a Nikon A1 confocal microscopy with NIS elements AR 5.20.02 software (Nikon Instruments Inc, Melville, NY). All

TABLE 2 List of reagents and chemicals.

Reagents and kits	Catalog number	Company
mTeSR1	85850	Stemcell technologies
Accutase	A6964	Sigma-Aldrich
Y-27632	125410	Fisher
SB431542	04-0010-10	Stemgent
Dorsomorphin	3093	Fisher
Neurobasal	21103049	Life Technologies
Glutamax	35050061	Life Technologies
MEM nonessential amino acids	11140050	Life Technologies
Gem21	400160	Gemini Bio-Products
penicillin/streptomycin	15140122	Life Technologies
N2 NeuroPlex	400163	Gemini Bio-Products
FGF2	PHG0263	Stemcell technologies
EGF	AF-100-15	PeproTech
BDNF	450-02	PeproTech
GDNF	450-10	PeproTech
NT3	450-03	PeproTech
L-ascorbic acid	A4403	Sigma-Aldrich
dibutyryl-cAMP	D0627	Sigma-Aldrich
BrdU (5-bromodeoxyuridin)	B23151	Themo fisher
Goat Anti-Rabbit IgG H&L (Alexa Fluor® 555)	ab150078	Abcam
Goat Anti-Mouse IgG H&L (Alexa Fluor® 488)	ab150113	Abcam
TRA-1-60 Antibody	SC-21705	Santa Cruz
Nanog (1E6C4) Mouse mAb	4893	Cell signaling
Nestin (E4O9E) XP® Rabbit mAb	73349	Cell signaling
Anti-Sox-2 Antibody, clone 1A2	ZRB5603	Sigma
Anti-MAP2 antibody	Ab5392	Abcam
S100 Beta Polyclonal antibody rabbit	15146-1-AP	Proteintech
anti-cleaved-caspase-3 (rabbit)	9661S	Cell signalling
anti-Ki67 (rabbit)	ab15580	Abcam
BrdU Monoclonal Antibody (MoBU-1)	B35141	Thermofisher
β-Amyloid (D54D2) XP® Rabbit	8243S	Cell signaling
Amyloid beta (N) (82E1) anti-human mouse IGG	10323	IBL-America
Amylo-Glo RTD Amyloid Plaque Stain Reagent	TR-300-AG	Biosensis
Phospho-Tau (Ser396) Polyclonal Antibody	44-752G	Thermofisher
Tau Antibody (A-10)	SC-390476	Santa Cruz
GAPDH antibody	2118s	Cell signaling
guanidine-HCl	G3272	Sigma
RIPA buffer	9806S	Cell signaling
protease inhibitor	1860932	Thermoscientific
PMSF	8553S	Cell signaling
Click-iT™ Plus EdU Cell Proliferation Kit for Imaging, Alexa Fluor™ 594 dye	C10639	Themofisher
Tau (Total) Human ELISA Kit	KHB0041	Themofisher
Amyloid beta 40 Human ELISA Kit	KHB3481	Life Technologies
Amyloid beta 42 Human ELISA Kit	KHB3441	Life Technologies

images that were compared were obtained with identical settings and quantified using FIJI/ImageJ (version 2.5.0).

Statistical analyses

All data analysis and plots were done by OriginPro 2018b software (Northampton, MA, USA). All data were subjected to Shapiro-Wilk normality testing, normally distributed data were analyzed by one way ANOVA and non-normal distributed data were analyzed by non-parametric Mann-Whitney test. Results are expressed as mean ± SEM and the threshold for statistical significance (p-value) was set at 0.05. All the experiments were repeated at least three times.

Results

Characterization of DS and isogenic control iPSCs

To confirm the presence of an extra copy of chromosome 21 in DS lines, stem array, a higher resolution of karyotyping, was performed and confirmed that DS iPSC lines indeed have a third copy of chromosome 21 while the isogenic control iPSC lines have a normal karyotype (**Figure 1A**).

To examine whether an extra copy of chromosome 21 results in overexpression of chromosome 21-encoded genes, we compared the expression profile of six genes between DS iPSCs and isogenic control iPSCs using real time PCR. Five of them were known to be overexpressed in both DS and AD patients (Gomez et al., 2020) and DSCAM was known to play an important role in synaptic plasticity and maturation (Stachowicz, 2018; Chen et al., 2022). As shown in **Figure 1B**, all six chromosome 21-encoded genes tested have a significantly increased expression in DS iPSCs as compared to isogenic controls (**Figure 1B** and **Supplementary Figure 1**, $p < 0.05$ or $p < 0.001$), indicating a gene dose effect of trisomy 21 in DS lines.

Decreased cell growth in DS iPSCs

Previous studies have shown that DS fibroblasts and neural progenitor cells exhibited decreased cell proliferation or increased apoptosis (Kimura et al., 2005; Gimeno et al., 2014; Hibaoui et al., 2014), while DS astrocyte precursor cells exhibited an accelerated proliferation (Kawatani et al., 2021). Since we made the preliminary observation in our experiments that the expansion of DS iPSC lines is slower than control iPSC lines, we wanted to know whether the rate of proliferation or cell death is different in DS from control. We first cultured both DS and control iPSC lines with the same number of live cells (10^5 cells) at day 0, and total cell numbers were counted at day 3, day 5, and day 7. As shown in **Figure 2A**, there was a significantly reduced number of DS iPSCs as compared to control lines at 5 and 7 days in culture (**Figure 2A** and **Supplementary Figure 2A**, $p < 0.05$ and $p < 0.001$). We next used Ki67, BrdU, and EdU as cell proliferation markers to compare the number of proliferating cells between DS iPSCs and control iPSCs. Ki67 labels cells in the G1, S, G2 and M phase. BrdU and EdU label cells in the S phase only. Interestingly, since most of the DS and control iPS cells were immunoreactive for $Ki67^+$ (**Figure 2B**), we compared and quantified the $BrdU^+$ and EdU^+ cells between the two groups. As shown in **Figures 2C,D**, DS iPSCs have a significantly decreased number of $BrdU^+$ and EdU^+ cells than control cells (**Figures 2C,D** and **Supplementary Figure 2B**, $p < 0.01$), suggesting a decreased proliferation in DS iPSCs. To exclude a potential effect of loss of pluripotency on a decreased proliferation in DS iPSCs, we confirmed that both DS and control iPSCs remain in a stem cell state at day 5, positive for pluripotency markers TRA-1-60, Nanog, and SOX2 and negative for neural progenitor marker nestin (**Supplementary Figure 2C**). Last, we used cleaved caspase 3 as a cell death marker to compare the number of cell death between DS and control iPSCs. There were no significant differences in cleaved caspase 3^+ cells between the two groups (**Figures 2E,F** and **Supplementary Figure 2D**, $p = 0.21$), suggesting that a slower growth of DS iPSCs is not due to an increased cell death but due to a decreased proliferation.

Abnormal accumulation of Aß in DS organoids

Accumulation of Aß is a major AD-like neuropathology feature in DS patients. Aβ is a cleavage product of APP through sequential proteolytic processing by β- and γ-secretases, a process that generates a number of Aβ isoforms with 36–43 amino acid residues in length. Aβ40 and Aβ42 are two major isoforms and the longer isoform, e.g., Aβ42, is more prone to form aggregates and be more toxic. Most amyloid plaques contain beta amyloid with 40 and 42 isoforms (Antzutkin et al., 2000; Balbach et al., 2002; Gu and Guo, 2013). In the current study, we used three different methods to examine the presence of Aß accumulation in DS organoids. First, immunostaining was performed on 8-week-old and 12-week-old organoids using two different Aß antibodies, D54D2 and 82E1 (Horikoshi et al., 2004; Ruiz-Riquelme et al., 2021), that recognize Aß 37–42 and Aß 40–42, respectively. In general, there are much more immunoreactivity of D54D2 than 82E1 in both 8-week and 12- week organoid sections. Immunoreactivity of D54D2 was significantly increased in both 8-week (data not shown) and 12-week-old DS organoids (**Figures 3A,B**, $p < 0.01$) as compared to control organoids. In contrast, immunoreactivity of 82E1 was hardly detected in 8-week organoid sections but can

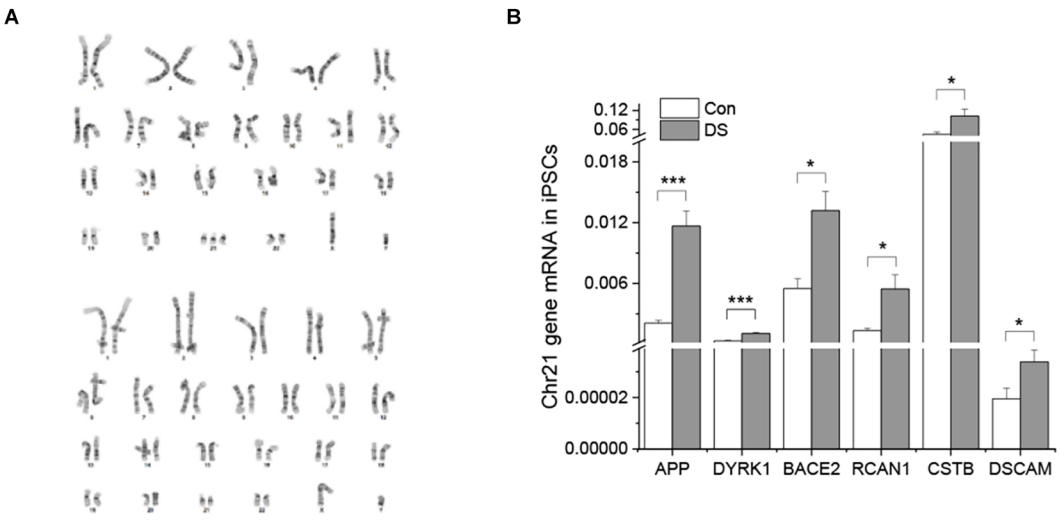

FIGURE 1
Characterizations of DS iPSC and isogenic control cell lines. **(A)** DS iPSC (top) and isogenic control (bottom) lines have correct karyotypes. **(B)** Overexpression of chromosome 21 genes in DS iPSCs was confirmed by real time PCR ($n = 4$). *$p < 0.05$ and ***$p < 0.001$ vs. control.

be detected in the 12-week organoid sections. The difference in 82E1 immunoreactivity between DS and control organoids was significant at 12 weeks (**Figures 3A,B** and **Supplementary Figures 3A,B**, $p < 0.01$). Next, we used Amylo-Glo plaque stain reagent to stain the amyloid plaque in the organoid sections and observed a significantly increased Amylo-Glo$^+$ staining in DS organoids than control organoids (**Figures 3C,D** and **Supplementary Figure 3C**, $p < 0.05$). Lastly, we used Elisa to quantify amyloid beta including Aß40 and Aß42 in the detergent soluble and insoluble fractions of DS and control organoids. No significant difference of Aß42, Aß40, or Aß42/Aß40 was observed in the soluble fraction between the two groups in either 8 weeks or 12 weeks. Instead, we found a significantly increased Aß42/Aß40 in the insoluble fraction of 12 weeks DS organoids than that in control organoids at the same age (**Figure 3E** and **Supplementary Figure 3D**, $p < 0.05$).

Abnormal accumulation of tau pathology in DS organoids

Hyperphosphorylation of Tau is another AD-like pathological hallmark in DS patients and occurs following Aß accumulation. We, therefore, compared the immunoreactivity of phospho-tau S396 (pTau S396, PHF-1), a widely used antibody to study Tau pathology in AD, in DS and control organoids at 12 weeks (Citron et al., 1994; Foidl and Humpel, 2018; Aragao Gomes et al., 2021). Immunoreactivity of phosphorylated Tau S396 was significantly increased in DS organoids as compared with control organoids (**Figures 4A,B** and **Supplementary Figures 4A,B**, $p < 0.001$). This increased phosphorylation of Tau was also confirmed by Western blot when using pTau S396 and total Tau (A-10) antibody: the ratio of pTau S396/Tau was significantly increased in DS organoids than control organoids (**Figures 4C,D** and **Supplementary Figure 4C**, $p < 0.001$).

The pathologic hyperphosphorylation of tau proteins induces the formation of insoluble aggregates and neurofibrillary tangles (NFTs) that abnormally accumulate inside neurons in AD or AD-like DS brains (Mondragon-Rodriguez et al., 2014). Levels of soluble and insoluble tau reflect the overall status of tau phosphorylation *in vivo* (Hirata-Fukae et al., 2009) and the insoluble tau correlates with the pathological features of tauopathy (Ren and Sahara, 2013). Therefore, we measured the amount of Tau in the soluble and insoluble fractions of organoids using Elisa. The ratio of insoluble Tau/total Tau was significantly increased in DS organoids at 12 weeks as compared to control organoids (**Figure 4E** and **Supplementary Figure 4D**, $p < 0.05$), further confirming a relatively increased insoluble tau aggregates in DS organoids.

Discussion

Virtually all DS patients over 40 years of age have AD-like neuropathology including abnormal Aß accumulation and neurofibrillary tangles (Wisniewski et al., 1985; Mann and Esiri, 1989). According to the National Down Syndrome Society, about 30% of DS patients are diagnosed with dementia in their 50s, and 50% of DS patients are diagnosed with dementia by their 60s. However, how the disease progresses or how early does it start in DS or AD-DS brain before the clinical

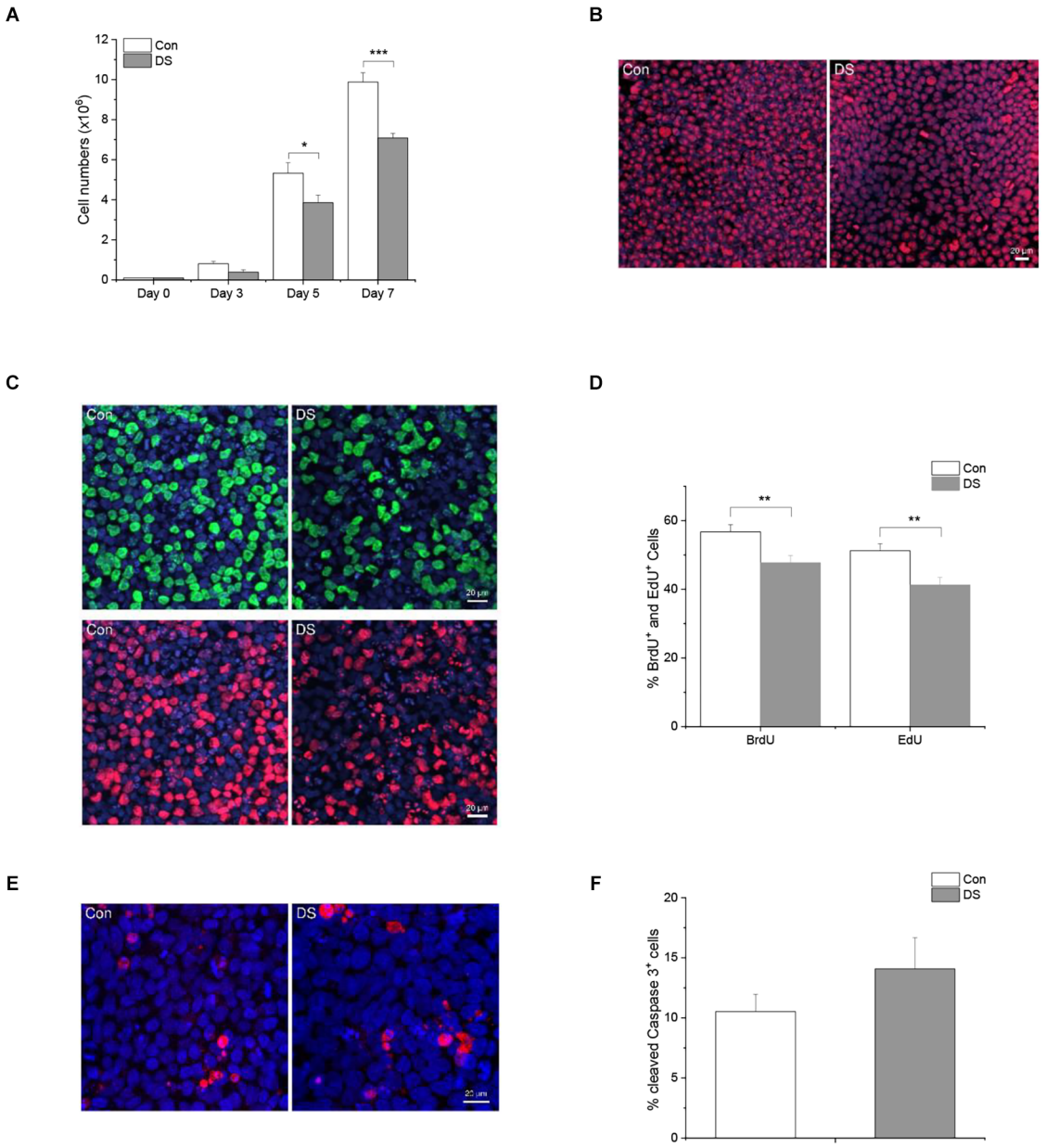

FIGURE 2
Decreased cell growth in DS iPS cells. **(A)** iPSCs were seeded in a 6-well plate with a density of 10^5 live cells/well and total cell numbers were counted after 3, 5, and 7 days in culture. DS iPSCs have a significantly reduced cell number as compared to control iPSCs at day 5 (n = 12, $p < 0.05$) and day 7 (n = 12, $p < 0.001$). **(B)** A representative immunostaining of Ki67 in DS and control iPSCs. **(C)** A representative double labeling of BrdU (green) and EdU (red) in DS and control iPSCs. **(D)** Immunohistochemical analysis of $BrdU^+$ and EdU^+ cells revealed that DS iPSCs have a significantly decreased number of $BrdU^+$ and EdU^+ cells than control iPSCs (n = 1,690–1,897 cells, $p < 0.01$). **(E)** A representative immunostaining of cleaved caspase 3 in DS and control iPSCs. **(F)** Immunohistochemical analysis of cleaved caspase 3 revealed a similar percentage of cell death in DS and control iPSCs (n = 1,045–1,570 cells, $p > 0.05$). *$p < 0.05$, **$p < 0.01$, and ***$p < 0.001$ vs. Control.

onset of the disease is still obscure and much less explored. IPSC-derived 3D organoids closely simulate key endogenous neurodevelopmental events with a cytoarchitecture resembling the developing human brain (Helen Zhao et al., 2021) with the trajectory of human brain development and maturation (Trujillo et al., 2019). Therefore, we used DS-specific iPSC-derived brain organoids as a model system to study the AD-like disease pathology in DS.

Clinically, individuals with DS have an overall reduced brain volume. Hypocellularity has been associated with impaired neurogenesis and lower proliferative rate potency that can be observed as early as 24 weeks during gestation

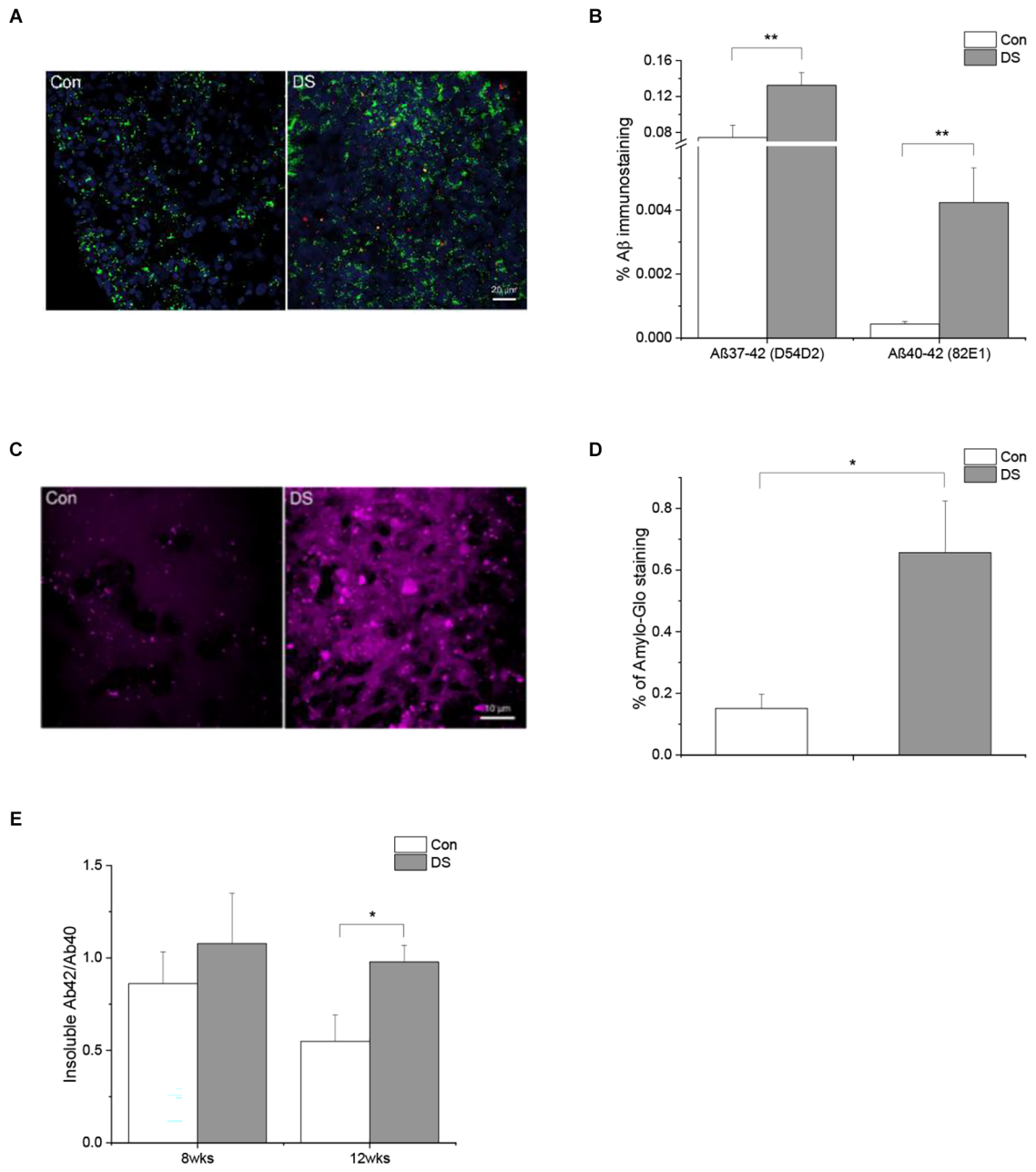

FIGURE 3
Abnormal Aß accumulation in DS iPSCs-derived cortical organoids. **(A)** A representative Aß immunostaining in 12 weeks DS and isogenic control organoids with two different antibodies D54D2 (Aß37-42, green) and 82E1 (Aß40-42, red). **(B)** Immunohistochemical analysis of Aß antibodies D54D2 and 82E1 revealed a significantly increased Aß immunoreactivity in DS organoids (n = 10–11, $p < 0.01$). **(C)** A representative Aß plaque staining in DS and control organoids using Amylo-Glo. **(D)** Immunohistochemical analysis of Amylo-Glo revealed a significantly increased amyloid plaque load in DS organoids (n = 8, $p < 0.05$). **(E)** Aß40 and Aß42 in the soluble and insoluble fractions of 8 weeks and 12 weeks DS and control organoids were quantified using Elisa and the ratio of Aß42/Aß40 was significantly increased in the insoluble fractions of 12 weeks DS organoids (n = 10–11, $p < 0.05$). *$p < 0.05$, and **$p < 0.01$ vs. Control.

in the DS brain (Stagni et al., 2018; Utagawa et al., 2022). This phenomenon was not only observed in neurons but also in other cell types *in vitro*. For instance, DS fibroblasts have a decreased proliferation (Gimeno et al., 2014); DS iPSC-derived neural progenitor cells show a decreased proliferation and increased apoptosis (Hibaoui et al., 2014); DS iPSC-derived astrocytes have however an increased proliferation rate than control cells (Kawatani et al., 2021). In the current study, we report that DS iPSCs have a slower growth rate and a decreased proliferation than control

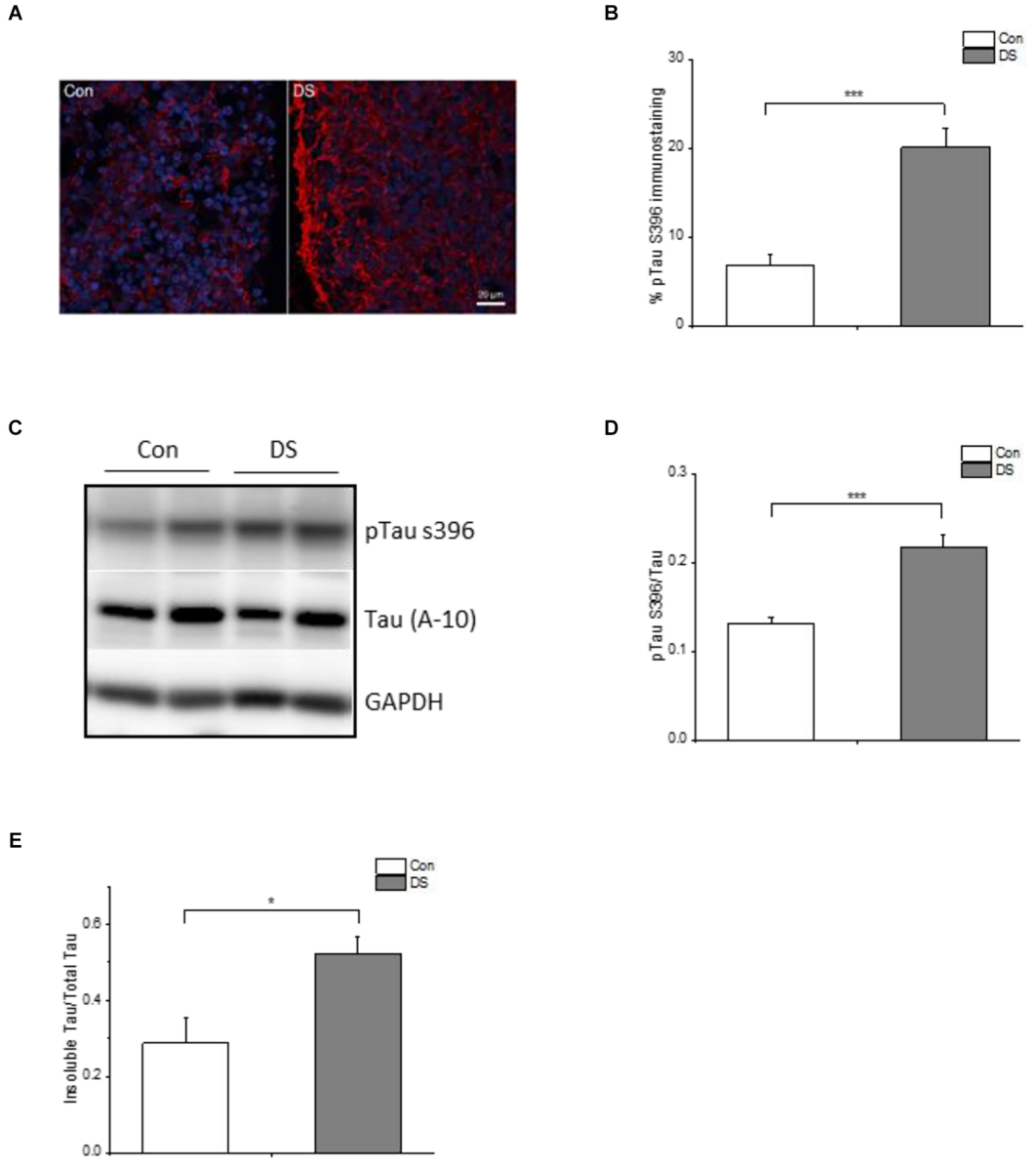

FIGURE 4
Tau pathology in DS iPSCs-derived cortical organoids. **(A)** A representative pTau S396 (red) and DAPI (blue) immunostaining in 12 weeks DS and isogenic control organoids. **(B)** Immunohistochemical analysis of pTau S396 revealed a significantly increased pTau S396 immunoreactivity in DS organoids (n = 24–28, $p < 0.001$). **(C)** A representative Western blot of pTau S396 and Tau expression in 12 weeks DS and isogenic control organoids. **(D)** Immunoblotting analysis of pTau S396 and Tau revealed a significantly increased pTau S396/Tau ratio in DS organoids (n = 6, $p < 0.001$). **(E)** Both soluble and insoluble Tau in 12 weeks of DS and control organoids are measured and Elisa data revealed that DS organoids have an increased insoluble Tau/total Tau (soluble Tau + insoluble Tau; n = 6, $p < 0.05$). *$p < 0.05$, and ***$p < 0.001$ vs. Control.

cells, without any difference in cell death between the two groups.

Abnormal accumulation of extracellular amyloid beta (Aß) and intracellular Tau hyperphosphorylation are two major pathological features in the AD brain and the AD-like DS brain. Aß are by-products of the normal cellular metabolism of amyloid precursor protein (APP; Sinha and Lieberburg, 1999). APP is an integral membrane protein encoded by the APP gene located on chromosome 21. APP has two primary endogenous processing pathways including the non-amyloidogenic pathway and the amyloidogenic pathway. Under physiological conditions, the majority of APP is processed through the non-amyloidogenic pathway; a small portion of APP is processed through the amyloidogenic pathway and yields Aβ 37, Aβ38, Aβ40, and Aβ42. Aβ40 is the most abundant form of Aβ, but Aβ42 is more prone to form insoluble aggregate. Under pathological

conditions such as in Alzheimer's disease and Down syndrome, altered amyloidogenic pathway and increased APP dose promote Aβ accumulation, Aβ aggregation, as well as the formation of insoluble fibrils into amyloid plaques. In DS patients, abnormal Aß accumulation starts as early as 8 years of age (Leverenz and Raskind, 1998). Here *in the organoids*, we were actually able to see increased Aß immunostaining and increased accumulation of amyloid plaque in DS cortical organoids at a very early age in 8 and 12 weeks old organoids in culture. In this regard, it is noteworthy to mention that the difference between both Aß 82E1 immunoreactivity and Aß42/Aß40 was not significant at 8 weeks but started at 12 weeks. Skovronsky previously described that the intracellular pool of insoluble Aß accumulates in a time-dependent manner in NT2N neuronal culture (Skovronsky et al., 1998). A time-dependent increasing difference of Aß between DS and control organoids confirmed that abnormal Aß accumulation is a progressive process and a disease-specific property in DS organoids as compared to controls. These data suggest that disease-specific iPSC-derived organoid culture shed important light on the pathophysiology of DS in that abnormal brain formation starts very early in life, probably in fetal life.

Elevated phosphorylation of Tau and abnormal aggregation are widely considered pathological hallmarks in AD. Here we show that both protein expression and immunoreactivity of pTau S396 are significantly increased in DS organoids, demonstrating hyperphosphorylation of Tau in DS organoids, which in general leads to Tau protein aggregation. Pathological aggregation of Tau protein forms insoluble twisted fibers, named neurofibrillary tangles, inside the cells and acts as a biomarker in AD-like pathology. Consistently, we found an increased composition of insoluble Tau in DS organoids that may therefore contribute to Tau pathology in DS patients. It is worth mentioning that, we have noticed that differences between individual clones (**Supplementary Figures**) did exist. For example, the differences between two DS lines occurred so that the *p*-value of cleaved caspase 3^+ cell death did not reach significance (**Supplementary Figure 2D**, $p = 0.21$). However, differences between DS and their isogenic control in insoluble tau/tau reached significance in spite of differences in DS clones (**Supplementary Figure 4D**, $p < 0.02$). We speculate that the differences between individual lines might be a consequence of differentiation efficiency among batches, but that the difference observed between DS and control is due to disease phenotype. In the current study, we used isogenic lines to avoid genetic variations and confounding factors.

Recent Tau studies, however, lead us to reconsider the role of Tau phosphorylation in Alzheimer's disease (Wegmann et al., 2021). Due to the fact that the phosphorylation patterns of physiological and pathological Tau are surprisingly similar and heterogenous, and the phosphorylation levels of Tau seem insufficient to differentiate between healthy and diseased Tau, high phosphorylation does not necessarily lead to Tau aggregation (Wegmann et al., 2021). In addition, the posttranslational modification of Tau other than phosphorylation such as ubiquitination, acetylation, and methylation may also regulate the formation of Tau aggregates (Wegmann et al., 2021). Indeed, abnormal posttranslational modifications have been reported in DS patients (Kerkel et al., 2010; Jones et al., 2013; Sailani et al., 2015; Tramutola et al., 2017) and may need additional examination in future studies.

In contrast to a previously published article on DS organoids (Gonzalez et al., 2018), we reported a difference between the DS iPSC lines and their isogenic controls at the iPSC stage. Furthermore, we systemically quantify the abnormalities of AD-like neuropathological phenotype at two time points and demonstrated that the AD-like neuropathology progressively manifests itself in organoids during early development. In summary, we have demonstrated that DS disease-specific iPS cells have a slower growth rate due to decreased proliferation. DS iPSC-derived brain organoids mimic AD-like pathophysiological phenotype including abnormal Aß accumulation and insoluble Tau accumulation. Our data strongly suggest that DS iPSC-derived cortical organoids illustrate well the notion that the molecular pathobiology in DS starts early in brain development and can be used as a model system to study the AD-like pathology and its progress before the clinical onset of the disease.

Data availability statement

The raw data supporting the conclusions of this article will be made available by the authors, without undue reservation.

Ethics statement

The studies involving human participants were reviewed and approved by IRB at the University of California San Diego. Written informed consent for participation was not required for this study in accordance with the national legislation and the institutional requirements.

Author contributions

HZ and GH designed the experiments and wrote the manuscript. HZ performed the experiments and data analysis. All authors contributed to the article and approved the submitted version.

Funding

This project was supported by National Institutes of Health (NIH) grant (1R01DA053372).

Acknowledgements

We acknowledge the Boston Children's Hospital Stem Cell program and Dr. Stuart H. Orkin for providing the Down syndrome iPS and isogenic cell lines. We thank the Nikon Imaging Center at the University of California San Diego for imaging assistance. We also thank Ms. Juan Wang and Ms. Ying Lu-Bo for assistance with organoid experiments.

Conflict of interest

The authors declare that the research was conducted in the absence of any commercial or financial relationships that could be construed as a potential conflict of interest.

Publisher's note

All claims expressed in this article are solely those of the authors and do not necessarily represent those of their affiliated organizations, or those of the publisher, the editors and the reviewers. Any product that may be evaluated in this article, or claim that may be made by its manufacturer, is not guaranteed or endorsed by the publisher.

Supplementary material

The Supplementary Material for this article can be found online at: https://www.frontiersin.org/articles/10.3389/fncel.2022.1050432/full#supplementary-material.

SUPPLEMENTARY FIGURE 1
Corresponding to **Figure 1B**: expression profile of chromosome 21 genes from individual DS iPSC and isogenic control iPSC lines.

SUPPLEMENTARY FIGURE 2
(A) Corresponding to **Figure 2A**: total cell numbers were counted after 3, 5, and 7 days in culture from individual DS iPSC and isogenic control iPSC lines. **(B)** Corresponding to **Figure 2D**: the number of $BrdU^+$ and EdU^+ cells was summarized from individual DS iPSC and isogenic control iPSC lines. **(C)** A representative double labeling of SOX2 (red) and Tra-1-60 (green) in DS and control iPSCs at day 5 (top panel); a representative double labeling of Nestin (red) and Nanog (green) in DS and control iPSCs at day 5 (bottom panel left) and in 4-week old control organoids (bottom panel right). Immunostaining of organoids was used as a positive control for Nestin (red) antibody under the same conditions of immunostaining and imaging processes. **(D)** Corresponding to **Figure 2F**: the number of cleaved caspase 3^+ cells was summarized from individual DS iPSC and isogenic control iPSC lines.

SUPPLEMENTARY FIGURE 3
(A) Corresponding to **Figure 3B**: immunoreactivity of Aß antibody D54D2 and 82E1 was summarized from individual DS and isogenic control iPSC line derived organoids respectively. **(B)** A representative double labeling of Aß antibody 82E1 (red) and MAP2 (green) in DS and control organoids (top panel). A representative double labeling of S100 (red) and MAP2 (green) in DS and control organoids (bottom panel). **(C)** Corresponding to **Figure 3D**: immunoreactivity of Amylo-Glo was summarized from individual DS and isogenic control iPSC line derived organoids. **(D)** Corresponding to **Figure 3E**: ratio of Aß42/Aß40 was summarized from individual DS and isogenic control iPSC line derived organoids.

SUPPLEMENTARY FIGURE 4
(A) Corresponding to **Figure 4B**: immunoreactivity of pTau S396 was summarized from individual DS and isogenic control iPSC line derived organoids. **(B)** A representative double labeling of pTau S396 (red) and MAP2 (green) in DS and control organoids. **(C)** Corresponding to **Figure 4E**: immunoblotting analysis of pTau S396/Tau was summarized from individual DS and isogenic control iPSC line derived organoids. **(D)** Corresponding to **Figure 4D**: the ratio of insoluble Tau/total Tau (soluble Tau + insoluble Tau) was summarized from individual DS and isogenic control iPSC line derived organoids.

References

Antzutkin, O. N., Balbach, J. J., Leapman, R. D., Rizzo, N. W., Reed, J., Tycko, R., et al. (2000). Multiple quantum solid-state NMR indicates a parallel, not antiparallel, organization of β-sheets in Alzheimer's β-amyloid fibrils. *Proc. Natl. Acad. Sci. U S A* 97, 13045–13050. doi: 10.1073/pnas.230315097

Aragao Gomes, L., Uytterhoeven, V., Lopez-Sanmartin, D., Tome, S. O., Tousseyn, T., Vandenberghe, R., et al. (2021). Maturation of neuronal AD-tau pathology involves site-specific phosphorylation of cytoplasmic and synaptic tau preceding conformational change and fibril formation. *Acta Neuropathol.* 141, 173–192. doi: 10.1007/s00401-020-02251-6

Asim, A., Kumar, A., Muthuswamy, S., Jain, S., and Agarwal, S. (2015). Down syndrome: an insight of the disease. *J. Biomed. Sci.* 22:41. doi: 10.1186/s12929-015-0138-y

Baburamani, A. A., Patkee, P. A., Arichi, T., and Rutherford, M. A. (2019). New approaches to studying early brain development in down syndrome. *Dev. Med. Child Neurol.* 61, 867–879. doi: 10.1111/dmcn.14260

Balbach, J. J., Petkova, A. T., Oyler, N. A., Antzutkin, O. N., Gordon, D. J., Meredith, S. C., et al. (2002). Supramolecular structure in full-length Alzheimer's β-amyloid fibrils: evidence for a parallel β-sheet organization from solid-state nuclear magnetic resonance. *Biophys. J.* 83, 1205–1216. doi: 10.1016/S0006-3495(02)75244-2

Camp, J. G., Badsha, F., Florio, M., Kanton, S., Gerber, T., Wilsch-Brauninger, M., et al. (2015). Human cerebral organoids recapitulate gene expression programs of fetal neocortex development. *Proc. Natl. Acad. Sci. U S A* 112, 15672–15677. doi: 10.1073/pnas.1520760112

Cataldo, A. M., Peterhoff, C. M., Troncoso, J. C., Gomez-Isla, T., Hyman, B. T., Nixon, R. A., et al. (2000). Endocytic pathway abnormalities precede amyloid β deposition in sporadic Alzheimer's disease and down syndrome: differential effects of APOE genotype and presenilin mutations. *Am. J. Pathol.* 157, 277–286. doi: 10.1016/s0002-9440(10)64538-5

Chen, P., Liu, Z., Zhang, Q., Lin, D., Song, L., Liu, J., et al. (2022). DSCAM deficiency leads to premature spine maturation and autism-like behaviors. *J. Neurosci.* 42, 532–551. doi: 10.1523/JNEUROSCI.1003-21.2021

Citron, B. A., Davis, M. D., and Kaufman, S. (1994). Electrostatic activation of rat phenylalanine hydroxylase. *Biochem. Biophys. Res. Commun.* 198, 174–180. doi: 10.1006/bbrc.1994.1025

Deshpande, A., Yadav, S., Dao, D. Q., Wu, Z. Y., Hokanson, K. C., Cahill, M. K., et al. (2017). Cellular phenotypes in human iPSC-derived neurons from a genetic model of autism spectrum disorder. *Cell Rep.* 21, 2678–2687. doi: 10.1016/j.celrep.2017.11.037

Foidl, B. M., and Humpel, C. (2018). Differential hyperphosphorylation of Tau-S199, -T231 and -S396 in organotypic brain slices of Alzheimer mice. A model to study early tau hyperphosphorylation using okadaic acid. *Front. Aging Neurosci.* 10:113. doi: 10.3389/fnagi.2018.00113

Gimeno, A., Garcia-Gimenez, J. L., Audi, L., Toran, N., Andaluz, P., Dasi, F., et al. (2014). Decreased cell proliferation and higher oxidative stress in fibroblasts from Down syndrome fetuses. Preliminary study. *Biochim. Biophys. Acta* 1842, 116–125. doi: 10.1016/j.bbadis.2013.10.014

Gomez, W., Morales, R., Maracaja-Coutinho, V., Parra, V., and Nassif, M. (2020). Down syndrome and Alzheimer's disease: common molecular traits beyond the amyloid precursor protein. *Aging (Albany NY)* 12, 1011–1033. doi: 10.18632/aging.102677

Gonzalez, C., Armijo, E., Bravo-Alegria, J., Becerra-Calixto, A., Mays, C. E., Soto, C., et al. (2018). Modeling amyloid β and tau pathology in human cerebral organoids. *Mol. Psychiatry* 23, 2363–2374. doi: 10.1038/s41380-018-0229-8

Gu, L., and Guo, Z. (2013). Alzheimer's Aβ42 and Aβ40 peptides form interlaced amyloid fibrils. *J. Neurochem.* 126, 305–311. doi: 10.1111/jnc.12202

Hargus, G., Cooper, O., Deleidi, M., Levy, A., Lee, K., Marlow, E., et al. (2010). Differentiated Parkinson patient-derived induced pluripotent stem cells grow in the adult rodent brain and reduce motor asymmetry in Parkinsonian rats. *Proc. Natl. Acad. Sci. U S A* 107, 15921–15926. doi: 10.1073/pnas.1010209107

Helen Zhao, P. A., Hang, Y., Wei, W., Ila, D., and Gabriel, G. H. (2021). "Chapter 3 - Induced pluripotent stem cell technology to model chronic mountain sickness," in *Current Progress in iPSC Disease Modeling* (Vol. 107), ed A. Birbrair (Amsterdam, Netherlands: Elsevier Inc.).

Hibaoui, Y., Grad, I., Letourneau, A., Sailani, M. R., Dahoun, S., Santoni, F. A., et al. (2014). Modelling and rescuing neurodevelopmental defect of Down syndrome using induced pluripotent stem cells from monozygotic twins discordant for trisomy 21. *EMBO Mol. Med.* 6, 259–277. doi: 10.1002/emmm.201302848

Hirata-Fukae, C., Li, H. F., Ma, L., Hoe, H. S., Rebeck, G. W., Aisen, P. S., et al. (2009). Levels of soluble and insoluble tau reflect overall status of tau phosphorylation *in vivo*. *Neurosci. Lett.* 450, 51–55. doi: 10.1016/j.neulet.2008.11.023

Holland, A. J., Hon, J., Huppert, F. A., Stevens, F., and Watson, P. (1998). Population-based study of the prevalence and presentation of dementia in adults with Down's syndrome. *Br. J. Psychiatry* 172, 493–498. doi: 10.1192/bjp.172.6.493

Horikoshi, Y., Mori, T., Maeda, M., Kinoshita, N., Sato, K., Yamaguchi, H., et al. (2004). Aβ N-terminal-end specific antibody reduced β-amyloid in Alzheimer-model mice. *Biochem. Biophys. Res. Commun.* 325, 384–387. doi: 10.1016/j.bbrc.2004.10.039

Jones, M. J., Farre, P., Mcewen, L. M., Macisaac, J. L., Watt, K., Neumann, S. M., et al. (2013). Distinct DNA methylation patterns of cognitive impairment and trisomy 21 in Down syndrome. *BMC Med. Genomics* 6:58. doi: 10.1186/1755-8794-6-58

Kawatani, K., Nambara, T., Nawa, N., Yoshimatsu, H., Kusakabe, H., Hirata, K., et al. (2021). A human isogenic iPSC-derived cell line panel identifies major regulators of aberrant astrocyte proliferation in Down syndrome. *Commun. Biol.* 4:730. doi: 10.1038/s42003-021-02242-7

Kerkel, K., Schupf, N., Hatta, K., Pang, D., Salas, M., Kratz, A., et al. (2010). Altered DNA methylation in leukocytes with trisomy 21. *PLoS Genet.* 6:e1001212. doi: 10.1371/journal.pgen.1001212

Kimura, M., Cao, X., Skurnick, J., Cody, M., Soteropoulos, P., Aviv, A., et al. (2005). Proliferation dynamics in cultured skin fibroblasts from Down syndrome subjects. *Free Radic. Biol. Med.* 39, 374–380. doi: 10.1016/j.freeradbiomed.2005.03.023

Kondo, T., Asai, M., Tsukita, K., Kutoku, Y., Ohsawa, Y., Sunada, Y., et al. (2013). Modeling Alzheimer's disease with iPSCs reveals stress phenotypes associated with intracellular Aβ and differential drug responsiveness. *Cell Stem Cell* 12, 487–496. doi: 10.1016/j.stem.2013.01.009

Lancaster, M. A., and Knoblich, J. A. (2014). Generation of cerebral organoids from human pluripotent stem cells. *Nat. Protoc.* 9, 2329–2340. doi: 10.1038/nprot.2014.158

Leverenz, J. B., and Raskind, M. A. (1998). Early amyloid deposition in the medial temporal lobe of young Down syndrome patients: a regional quantitative analysis. *Exp. Neurol.* 150, 296–304. doi: 10.1006/exnr.1997.6777

Maclean, G. A., Menne, T. F., Guo, G., Sanchez, D. J., Park, I. H., Daley, G. Q., et al. (2012). Altered hematopoiesis in trisomy 21 as revealed through *in vitro* differentiation of isogenic human pluripotent cells. *Proc. Natl. Acad. Sci. U S A* 109, 17567–17572. doi: 10.1073/pnas.1215468109

Mann, D. M., and Esiri, M. M. (1989). The pattern of acquisition of plaques and tangles in the brains of patients under 50 years of age with Down's syndrome. *J. Neurol. Sci.* 89, 169–179. doi: 10.1016/0022-510x(89)90019-1

Marin-Padilla, M. (1972). Structural abnormalities of the cerebral cortex in human chromosomal aberrations: a golgi study. *Brain Res.* 44, 625–629. doi: 10.1016/0006-8993(72)90324-1

Mondragon-Rodriguez, S., Perry, G., Luna-Munoz, J., Acevedo-Aquino, M. C., and Williams, S. (2014). Phosphorylation of tau protein at sites Ser (396–404) is one of the earliest events in Alzheimer's disease and Down syndrome. *Neuropathol. Appl. Neurobiol.* 40, 121–135. doi: 10.1111/nan.12084

Nascimento, J. M., Saia-Cereda, V. M., Sartore, R. C., Da Costa, R. M., Schitine, C. S., Freitas, H. R., et al. (2019). Human cerebral organoids and fetal brain tissue share proteomic similarities. *Front. Cell. Dev. Biol.* 7:303. doi: 10.3389/fcell.2019.00303

Oliver, C., and Holland, A. J. (1986). Down's syndrome and Alzheimer's disease: a review. *Psychol. Med.* 16, 307–322. doi: 10.1017/s0033291700009120

Paşca, A. M., Sloan, S. A., Clarke, L. E., Tian, Y., Makinson, C. D., Huber, N., et al. (2015). Functional cortical neurons and astrocytes from human pluripotent stem cells in 3D culture. *Nat. Methods* 12, 671–678. doi: 10.1038/nmeth.3415

Paşca, S. P. (2018). Building three-dimensional human brain organoids. *Nat. Neurosci.* doi: 10.1038/s41593-018-0107-3

Patkee, P. A., Baburamani, A. A., Kyriakopoulou, V., Davidson, A., Avini, E., Dimitrova, R., et al. (2020). Early alterations in cortical and cerebellar regional brain growth in Down syndrome: an *in vivo* fetal and neonatal MRI assessment. *Neuroimage Clin.* 25:102139. doi: 10.1016/j.nicl.2019.102139

Ren, Y., and Sahara, N. (2013). Characteristics of tau oligomers. *Front. Neurol.* 4:102. doi: 10.3389/fneur.2013.00102

Ruiz-Riquelme, A., Mao, A., Barghash, M. M., Lau, H. H. C., Stuart, E., Kovacs, G. G., et al. (2021). Aβ43 aggregates exhibit enhanced prion-like seeding activity in mice. *Acta Neuropathol. Commun.* 9:83. doi: 10.1186/s40478-021-01187-6

Russo, F. B., Brito, A., De Freitas, A. M., Castanha, A., De Freitas, B. C., Beltrao-Braga, P. C. B., et al. (2019). The use of iPSC technology for modeling autism spectrum disorders. *Neurobiol. Dis.* 130:104483. doi: 10.1016/j.nbd.2019.104483

Sailani, M. R., Santoni, F. A., Letourneau, A., Borel, C., Makrythanasis, P., Hibaoui, Y., et al. (2015). DNA-methylation patterns in trisomy 21 using cells from monozygotic twins. *PLoS One* 10:e0135555. doi: 10.1371/journal.pone.0135555

Sinha, S., and Lieberburg, I. (1999). Cellular mechanisms of β-amyloid production and secretion. *Proc. Natl. Acad. Sci. U S A* 96, 11049–11053. doi: 10.1073/pnas.96.20.11049

Skovronsky, D. M., Doms, R. W., and Lee, V. M. (1998). Detection of a novel intraneuronal pool of insoluble amyloid β protein that accumulates with time in culture. *J. Cell Biol.* 141, 1031–1039. doi: 10.1083/jcb.141.4.1031

Stachowicz, K. (2018). The role of DSCAM in the regulation of synaptic plasticity: possible involvement in neuropsychiatric disorders. *Acta Neurobiol. Exp. (Wars)* 78, 210–219. doi: 10.21307/ane-2018-019

Stagni, F., Giacomini, A., Emili, M., Guidi, S., and Bartesaghi, R. (2018). Neurogenesis impairment: an early developmental defect in Down syndrome. *Free Radic. Biol. Med.* 114, 15–32. doi: 10.1016/j.freeradbiomed.2017.07.026

Takahashi, K., Tanabe, K., Ohnuki, M., Narita, M., Ichisaka, T., Tomoda, K., et al. (2007). Induction of pluripotent stem cells from adult human fibroblasts by defined factors. *Cell* 131, 861–872. doi: 10.1016/j.cell.2007.11.019

Tang, X. Y., Xu, L., Wang, J., Hong, Y., Wang, Y., Zhu, Q., et al. (2021). DSCAM/PAK1 pathway suppression reverses neurogenesis deficits in iPSC-derived cerebral organoids from patients with Down syndrome. *J. Clin. Investig.* 131:e135763. doi: 10.1172/JCI135763

Tramutola, A., Di Domenico, F., Barone, E., Arena, A., Giorgi, A., Di Francesco, L., et al. (2017). Polyubiquitinylation profile in Down syndrome brain before and after the development of Alzheimer neuropathology. *Antioxid. Redox Signal* 26, 280–298. doi: 10.1089/ars.2016.6686

Trujillo, C. A., Gao, R., Negraes, P. D., Gu, J., Buchanan, J., Preissl, S., et al. (2019). Complex oscillatory waves emerging from cortical organoids model early human brain network development. *Cell Stem Cell* 25, 558–569. doi: 10.1016/j.stem.2019.08.002

Utagawa, E.C., Moreno, D.G., Schafernak, K.T., Arva, N.C., Malek-Ahmadi, M.H., Mufson, E.J., et al. (2022). Neurogenesis and neuronal differentiation in the postnatal frontal cortex in Down syndrome. *Acta Neuropathol. Commun.* 10:86. doi: 10.1186/s40478-022-01385-w

Wang, H., Kulas, J. A., Wang, C., Holtzman, D. M., Ferris, H. A., Hansen, S. B., et al. (2021). Regulation of beta-amyloid production in neurons by astrocyte-derived cholesterol. *Proc. Natl. Acad. Sci. U S A* 118:e2102191118. doi: 10.1073/pnas.2102191118

Wegmann, S., Biernat, J., and Mandelkow, E. (2021). A current view on Tau protein phosphorylation in Alzheimer's disease. *Curr. Opin. Neurobiol.* 69, 131–138. doi: 10.1016/j.conb.2021.03.003

Wisniewski, K. E., Laure-Kamionowska, M., and Wisniewski, H. M. (1984). Evidence of arrest of neurogenesis and synaptogenesis in brains of patients with Down's syndrome. *N. Engl. J. Med.* 311, 1187–1188. doi: 10.1056/NEJM198411013111818

Wisniewski, K. E., Wisniewski, H. M., and Wen, G. Y. (1985). Occurrence of neuropathological changes and dementia of Alzheimer's disease in Down's syndrome. *Ann. Neurol.* 17, 278–282. doi: 10.1002/ana.410170310

Yao, H., Wu, W., Cerf, I., Zhao, H. W., Wang, J., Negraes, P. D., et al. (2020). Methadone interrupts neural growth and function in human cortical organoids. *Stem Cell Res.* 49:102065. doi: 10.1016/j.scr.2020.102065

Zigman, W. B., Schupf, N., Devenny, D. A., Miezejeski, C., Ryan, R., Urv, T. K., et al. (2004). Incidence and prevalence of dementia in elderly adults with mental retardation without Down syndrome. *Am. J. Ment. Retard.* 109, 126–141. doi: 10.1352/0895-8017(2004)109<126:IAPODI>2.0.CO;2

frontiers | Frontiers in Cellular Neuroscience

TYPE Methods
PUBLISHED 04 April 2023
DOI 10.3389/fncel.2023.1114420

OPEN ACCESS

EDITED BY
Maeve Ann Caldwell,
Trinity College Dublin, Ireland

REVIEWED BY
Cecilia Laterza,
University of Padua, Italy
Xing Guo,
Nanjing Medical University, China

*CORRESPONDENCE
Debbie L. C. van den Berg
✉ d.vandenberg@erasmusmc.nl

SPECIALTY SECTION
This article was submitted to Cellular Neuropathology, a section of the journal Frontiers in Cellular Neuroscience

RECEIVED 02 December 2022
ACCEPTED 13 March 2023
PUBLISHED 04 April 2023

CITATION
Eigenhuis KN, Somsen HB, van der Kroeg M, Smeenk H, Korporaal AL, Kushner SA, de Vrij FMS and van den Berg DLC (2023) A simplified protocol for the generation of cortical brain organoids.
Front. Cell. Neurosci. 17:1114420.
doi: 10.3389/fncel.2023.1114420

A simplified protocol for the generation of cortical brain organoids

Kristel N. Eigenhuis[1], Hedda B. Somsen[1], Mark van der Kroeg[2], Hilde Smeenk[2], Anne L. Korporaal[1], Steven A. Kushner[2,3], Femke M. S. de Vrij[2] and Debbie L. C. van den Berg[1]*

[1]Department of Cell Biology, Erasmus MC, Rotterdam, Netherlands, [2]Department of Psychiatry, Erasmus MC, Rotterdam, Netherlands, [3]Department of Psychiatry, Columbia University Irving Medical Center, New York, NY, United States

Human brain organoid technology has the potential to generate unprecedented insight into normal and aberrant brain development. It opens up a developmental time window in which the effects of gene or environmental perturbations can be experimentally tested. However, detection sensitivity and correct interpretation of phenotypes are hampered by notable batch-to-batch variability and low reproducibility of cell and regional identities. Here, we describe a detailed, simplified protocol for the robust and reproducible generation of brain organoids with cortical identity from feeder-independent induced pluripotent stem cells (iPSCs). This self-patterning approach minimizes media supplements and handling steps, resulting in cortical brain organoids that can be maintained over prolonged periods and that contain radial glial and intermediate progenitors, deep and upper layer neurons, and astrocytes.

KEYWORDS

cortical brain organoids, human brain development, self-patterning, dorsal identity, feeder-independent, induced pluripotent stem cells

1. Introduction

The human developing brain is unique compared to any other organism due to its increased size, complexity, and expansion of neuronal output (Benito-Kwiecinski et al., 2021). Most of the current understanding of mammalian brain development is derived from studies in rodent models. However, these do not fully recapitulate the dynamic and complex architecture of the human brain nor model the genetic basis of prominent human neurodevelopmental disorders (Velasco et al., 2020). Therefore, in recent years, major advances have been made to generate protocols for *in vitro* differentiation of human pluripotent stem cells (PSCs) into 3D tissue cultures such as cortical organoids, that closely mimic key features of *in vivo* corticogenesis (Lancaster et al., 2013; Camp et al., 2015).

Cortical organoids grow from PSCs that self-aggregate into embryoid bodies and spontaneously acquire neuronal fate, resulting in the formation of polarized neuroepithelial structures (Kadoshima et al., 2013). As described in the initial hallmark protocols (Kadoshima et al., 2013; Lancaster et al., 2013; Lancaster and Knoblich, 2014), supplementing the growth medium of forming organoids with a 3D scaffold (Matrigel) in combination with agitation results in various brain region identities being formed within the organoids in several weeks to months. Defined progenitor zones, containing apical radial glial cells (aRGCs), intermediate progenitor cells (IPCs), and outer radial glial cells (oRGCs), surround ventricle-like lumens and generate deep and upper layer neurons that organize into

the cortical plate, the embryonic precursor of the cerebral cortex. In addition to the similar cytoarchitecture, cellular composition, and maturation, cortical organoids have been shown to resemble gene expression profiles of the developing human cortex beyond the second trimester, up to early postnatal stages (Camp et al., 2015; Velasco et al., 2019; Gordon et al., 2021).

Despite their great potential, generating cortical organoids is a delicate and lengthy process, challenged by low reproducibility and sensitivity to perturbations. Therefore, the field is constantly and rapidly developing improved protocols to overcome organoid-to-organoid variability and batch-to-batch variation and to ensure the reproducibility of cell types within single organoids being generated (Velasco et al., 2019). While "self-patterned" generation of cortical organoids as described in initial protocols will spontaneously generate forebrain, midbrain, and hindbrain identities, more recent protocols have focused on guiding or directing toward region-specific identities in organoids, using exogenous patterning factors. Several groups have shown that during embryoid body formation, the addition of WNT (Kadoshima et al., 2013; Mariani et al., 2015; Pasca et al., 2015; Qian et al., 2016; Pollen et al., 2019; Velasco et al., 2019), BMP (Mariani et al., 2015; Pasca et al., 2015; Qian et al., 2016; Xiang et al., 2017), and TGF-β (Kadoshima et al., 2013; Mariani et al., 2015; Xiang et al., 2017; Pollen et al., 2019; Velasco et al., 2019) inhibitors can act as rostralizing signal and promote the generation of (dorsal) forebrain organoids. During neural induction, WNT activators (Lancaster et al., 2017) and Matrigel (Kadoshima et al., 2013; Lancaster et al., 2013) stimulate lateral expansion and budding of the neuroepithelium, respectively. Single-cell RNA-seq on different batches of dorsally patterned forebrain organoids by WNT and TGF-β inhibition has shown that sample-to-sample reproducibility of cell types generated was similar to that between individual endogenous brains (Velasco et al., 2019). However, the addition of small molecules to media compositions can also be a source of variation due to low concentrations added, batch-to-batch variability, and storage conditions.

Here, we combine a robust embryoid body-based method for the generation of cortical NPC-derived neural networks (Gunhanlar et al., 2018) with 3D organoid culture to reproducibly generate and mature cortical brain organoids from induced pluripotent stem cells (iPSCs), without the addition of patterning factors (Velasco et al., 2019). In short, 9,000 single-iPSCs derived from feeder-independent cultures are seeded per V-bottom well of a 96-well plate to aggregate into embryoid bodies. Seeding consistent numbers of iPSCs in individual wells in their original culture medium will stimulate the rapid formation of uniform embryoid bodies within 2 days. Subsequently, robust neural induction for 6 days in a simple medium formulation will stimulate the generation of neuroectoderm and neuroepithelial tissues. These tissues acquire a spontaneous preference to develop into brain regions with dorsal forebrain identity. After 18 days of differentiation, formed organoids are transferred into non-adherent dishes and placed on an orbital shaker. Under agitating conditions, the cortical organoids will further grow until they reach a diameter of 2–3 mm after 35 days. At this time point, the organoids can be harvested for immunohistochemical and expression analysis. If preferred, organoids can be further matured by adding Matrigel to the medium to serve as a 3D scaffold (Figure 1). This protocol is optimized to maximize efficiency and minimize the complexity of handling steps, resulting in a practical and reproducible method to generate dorsal forebrain organoids.

2. Materials and equipment

2.1. Reagents

- WTC-11 human iPSC line (Coriell Repository, GM25256);
- StemFlex™ Medium (ThermoFisher Scientific, #A3349401);
- RevitaCell™ Supplement 100X (ThermoFisher Scientific, #A2644501);
- Geltrex, LDEV-Free, hESC-Qualified, Reduced Growth Factor Basement Membrane Matrix (ThermoFisher Scientific, #A1413301);
- Dulbecco's Phosphate Buffered Saline (Sigma-Aldrich, #D8537);
- UltraPure™ 0.5M EDTA, pH 8.0 (Invitrogen™, #15575-038);
- StemPro™ Accutase™ Cell Dissociation Reagent (ThermoFisher Scientific, #11599686);
- Advanced DMEM/F-12 (ThermoFisher Scientific, #12634028);
- Penicillin-Streptomycin (Sigma-Aldrich, #P0781);
- N-2 Supplement 100X (ThermoFisher Scientific, 17502048);
- Heparin (Sigma, #H3149);
- Glasgow-MEM, GMEM (ThermoFisher Scientific, #11710035);
- MEM Non-Essential Amin Acids Solution (ThermoFisher Scientific, #11140050);
- DMEM/F-12, HEPES (ThermoFisher Scientific, #11330032);
- GlutaMAX Supplement (ThermoFisher Scientific, #35050061);
- Chemically Defined Lipid Concentrate (ThermoFisher Scientific, #11905031);
- Amphotericin B (ThermoFisher Scientific, #15290018);
- Fetal Bovine Serum, qualified, Brazil (ThermoFisher Scientific, #10270106);
- Matrigel (Corning, #356234);
- Trypan Blue Solution, 0.4% (ThermoFisher Scientific, #15250061);
- Paraformaldehyde (Sigma-Aldrich, #P-6148);
- Sodium hydroxide solution (Sigma, #72068);
- Hydrochloric acid fuming 37% (Sigma, #30721-M);
- TWEEN® 20 (Sigma-Aldrich, #P1379);
- Sucrose (Merck Millipore, #84100);
- Gelatin from porcine skin (Merck Millipore, #04055);
- Trisodium citrate dihydrate (Merck Millipore, #106448);
- Triton™ X-100 (Sigma, #T8787);
- Aqua-Poly/Mount (Polysciences, #18606-20).

2.2. Equipment

- PrimeSurface® 3D culture: Ultra-low Attachment Plates: 96-well, V bottom, Clear plates (Sbio Japan, #MS9096VZ);

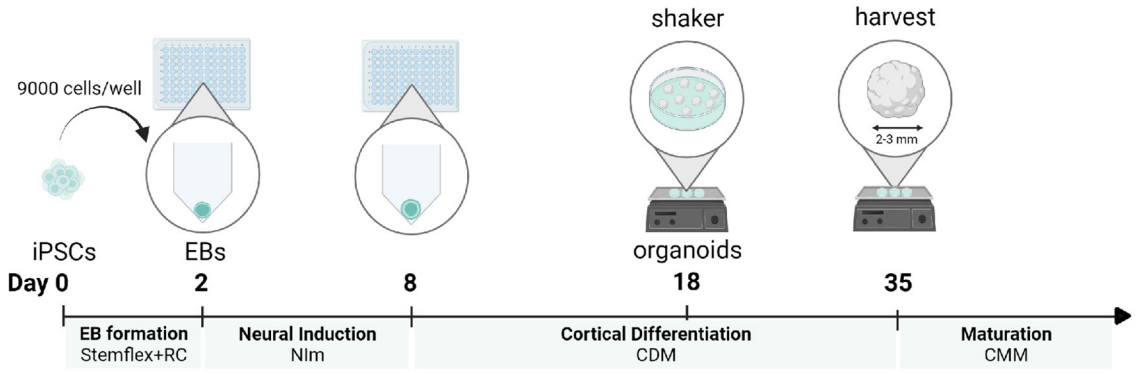

FIGURE 1
Protocol timeline for a cortical organoid generation. For each developmental stage, the corresponding medium is displayed. iPSCs, induced pluripotent stem cells; EB, embryoid body; NI, neural induction; CDM, cortical differentiation medium; CMM, cortical maturation medium. This figure was created with BioRender.com.

- Nunc 6-Well Plates, Round (ThermoFisher Scientific, # 140675);
- 5 mL Serological Pipette (VWR, #89130896);
- 10 mL Serological Pipette (VWR, #89130898);
- 15 mL Conical Tubes, Polystyrene (VWR, #352097);
- 50 mL Conical Tubes, Polystyrene (VWR, #352070);
- Hemocytometer (EMS, #68052-14, 68052-15);
- Eppendorf Tubes® 3810X 1.5 ml (Eppendorf, #0030125150);
- Heraeus Megafuge 40R Benchtop Centrifuge (ThermoScientific, #75004519);
- Inverted Phase Contrast Microscope (Olympus CKX31);
- Reagent reservoir, 50 ml (Greiner, #960305);
- 60 mm TC-Treated Cell Culture Dish (Corning, #353002);
- Digital CO_2-resistant orbital shaker (ThermoScientific, #88881101);
- CO_2 incubator;
- Multichannel pipet (20–200 μL) (VWR, # 613-2901);
- pH meter (Mettler Toledo, SevenExcellence pH meter S400);
- Glass beaker;
- Stir plate;
- Bijou sample containers (700EA, Sigma-Aldrich, #Z645338);
- Sterile Syringe filters, Pore size 0.2 μm (Cytiva Whatman, #10462200);
- Aluminum PCR heating block;
- Cryomold Bpsy 10 × 10 × 5 mm (Sakura Finetek, #1S-VW-4565-PK);
- SuperFrost Plus™ Adhesion Microscopic Slides (Epredia, #J1800AMNZ);
- ImmunoPen™ (Millipore, #402176);
- Heat-resistant plastic Coplin staining jar (VWR, #470174-652);
- Microscope cover glasses 24 × 60 mm (VWR, #4833 220).

2.3. Reagents set-up

2.3.1. Heparin solution

The potency (units/mg) of heparin varies per batch and is reported by the manufacturer on the certificate of analysis. The exact amount of mg present is calculated by dividing the number of units of the batch by the potency in units per mg. The batch is reconstituted in the volume of D-PBS needed to make a 1-mg/ml stock solution (500×). If sterile and filtered through a 0.22-μm filter, this stock solution can be stored at 2–8°C for up to 2 years.

2.3.2. FBS heat inactivation

Heat inactivate serum by placing the bottle in a 56°C water bath for 30 min. Store aliquots at −20°C.

2.3.3. Media preparation

The composition, preparation, and storage conditions of the different media are outlined in Table 1.

2.3.4. 20% Paraformaldehyde (PFA) stock solution

To prepare 100 ml of 20% PFA stock solution, heat 80 ml of D-PBS in a glass beaker on a stir plate to 55–60°C, in a ventilated hood, Add 20 g of PFA to the heated solution. A cloudy suspension will be the result. Slowly raise the pH by dropwise adding 1M NaOH, until the solution clears. Let the solution cool, filter, and finally, add D-PBS to a volume of 100 ml. Recheck the pH, and adjust with 1 M HCl to pH 6.9. Prepare aliquots and store at −20°C. Dilute 20% PFA in D-PBS to a 4% working solution. Only use 4% PFA on the day of preparation and do not re-freeze or store.

2.3.5. 0.1% PBS-T

To prepare 1 L of 0.1% PBS-T, add 1 ml of Tween® 20 to 1 L of D-PBS and mix thoroughly.

2.3.6. 30% sucrose solution

To prepare 1 L of 30% sucrose solution, weigh 300 g of sucrose and add D-PBS to a final volume of 1 L. Mix using a magnetic stirrer at room temperature until all sucrose has dissolved. Aliquot and store at −20°C.

TABLE 1 Media preparation.

Seeding medium (SM)	For 10 ml
StemFlex™ medium	10 ml
1% RevitaCell™ supplement [1X]	100 µl
Neural induction medium (NIM)	**For 100 ml**
Prepare a small aliquot of seeding medium freshly on the day of seeding. Do not store or re-use.	
Advanced DMEM/F12 (#12634028)	98 ml
1% Penicillin/streptomycin solution	1 ml
1% N-2 supplement [1X]	1 ml
Heparin [1 mg/ml stock, 2 µg/ml final concentration]	200 µl
Cortical differentiation medium (CDM)[a]	**For 100 ml**
This medium can be stored and used for 1 week after preparation, at 4°C.	
DMEM/F-12 (#11330-032)	96 ml
1% GlutaMAX supplement	1 ml
1% Chemically defined lipid concentrate	1 ml
1% N-2 supplement [1X]	1 ml
Amphotericin B [250 µg/ml stock, 0.25µg/ml final]	100 µl
1% Penicillin/streptomycin solution	1 ml
Cortical maturation medium (CMM)[a]	**For 200 ml**
This medium can be stored and used for 2 weeks after preparation at 4°C.	
DMEM/F-12 (#11330-032)	169 ml
1% GlutaMAX supplement	2 ml
1% chemically defined lipid concentrate	2 ml
1% N-2 supplement [1X]	2 ml
Amphotericin B [250 µg/ml stock, 0.25µg/ml final]	200 µl
1% penicillin/streptomycin solution	2 ml
10% fetal bovine serum	20 ml
Heparin [1 mg/ml stock, 5 µg/ml final concentration]	1 ml
1% matrigel*	2 ml

*Add Matrigel only to cold medium, and only after filtering the medium. If added when the medium is warm, Matrigel will solidify and not properly mix into the solution.
This medium should be filtered before use and can be stored and used for 2 weeks after preparation at 4°C.
[a]CDM and CMM formulations were originally described as cortical differentiation medium-II (CDM-II) and cortical differentiation medium-III (CDM-III) respectively by: Velasco S. et al., Individual brain organoids reproducibly form cell diversity of the human cerebral cortex, Nature, 2019. Jun; 570(7762): 523–527.

2.3.7. Gelatin Solution (10% gelatin–7.5% sucrose–PBS)

To prepare 100 ml of gelatin solution, add 10 g of sucrose to 100 ml of D-PBS. To this solution, add 7.5 g of gelatin and mix using a magnetic stirrer at room temperature until both components have completely dissolved. Aliquot and store at −20°C.

2.3.8. Antigen retrieval buffer (10 mM Sodium Citrate, pH 6.0)

To prepare 1 L of Sodium Citrate buffer (10 mM), add 2.94 g of Trisodium citrate dihydrate to 950 ml of dH_2O. Adjust pH to 6.0 with HCl/NaOH and autoclave. Store at room temperature.

2.3.9. Washing buffer (0.01% Triton X-100–PBS)

To prepare the washing buffer, add Triton X-100 to D-PBS to a final concentration of 0.01%. Store at room temperature.

2.3.10. Blocking buffer/antibody diluent (0.1% Triton X-100–10% FBS-PBS)

To prepare the blocking buffer, add Triton X-100 and FBS to D-PBS to a final concentration of 0.1% and 10%, respectively. Filter using a 0.2-µm syringe filter and store at 4°C for a maximum of 2 days. Prepare freshly on the day of use.

3. Methods

3.1. Step-by-step procedure: Generation of cortical organoids

3.1.1. iPSC culture

- This protocol describes how to generate cortical organoids from feeder-independent cultured pluripotent stem cells (PSCs). PSCs are cultured in wells of a six-well plate in StemFlex™ Medium, on Geltrex coating ([0.08 mg/ml] final concentration).
- PSCs are cultured in colonies and passaged in clumps every 3–4 days in a 1:4–1:6 ratio by 5′-8′ incubation of 0.5 mM EDTA.
- It is recommended to use PSCs of a passage below 50 and to perform a chromosome count for every 10 passages to confirm a stable karyotype.

3.1.2. Generation of cortical organoids

Day 0: seeding single iPSCs to generate embryoid bodies—TIMING 1–2 h

- It is recommended to seed a maximum of 32 embryoid bodies per batch, to allow for optimal handling conditions.
- 9,000 iPSCs per well are seeded in a 96-well plate to form an embryoid body, in a 200 µL seeding medium.
- To start a batch of 32 EBs, one 80–90% confluent six-well iPSC colony is sufficient. iPSC colonies should not show any sign of differentiation (Figure 2a).

To seed 32 EBs:

1. Prepare 10 ml seeding medium by supplementing 10 ml of StemFlex™ Medium with RevitaCell™ Supplement (1:100). Place in a water bath to warm at 37°C.
2. Wash cells 1× with 1 ml of PBS. To dissociate cells, first, add 1 ml of cold 0.5 mM EDTA per well and incubate for 5′.
3. Aspirate EDTA and add 1 ml of pre-warmed StemPro Accutase per well. Gently disturb the well after 4 min to promote cell dissociation, and incubate for another 4–6 min. All cells should have detached and be floating as single or very small groups of cells (Figure 2b).

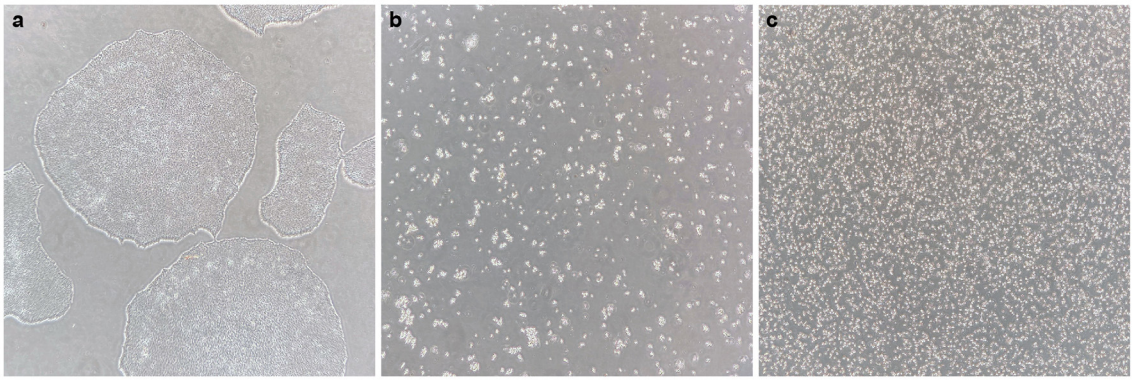

FIGURE 2
Generating a single-cell iPS suspension. **(a)** Healthy iPS colonies at 70–80% confluency, without signs of differentiation. **(b)** After 0.5 mM EDTA incubation and subsequent incubation with accutase, all cells have dissociated into single cells or small groups of cells, and all cells are floating. **(c)** After gentle trituration of the dissociated cell suspension, a pure single-cell suspension is created.

4. Collect the cells by pipetting up and down in the Accutase for a maximum of five times with a P1000 pipet. Transfer 1 ml of the cell suspension to a 15-ml falcon tube. Rinse the well with 1 ml seeding medium and add to the collection tube.
5. Quickly count the number of cells/ml by mixing 50 μL of cell suspension with 50 μL of trypan blue. Use a hemocytometer to count cells manually in multiple squares of a counting chamber, and the average will determine the correct cell concentration.

At this stage, it can be observed under the microscope whether a pure single-cell suspension is generated (as shown in Figure 2c). If not, the cell suspension should be gently triturated some more.

6. For 32 EBs, 288.000 (32 × 9,000) cells in 6,400 μL (32 × 200) seeding medium are needed. Taking into account an extra 10%, 316.800 cells in a 7,040-μL seeding medium are needed. Aliquot the required amount of cell suspension into a separate 15-ml falcon tube and centrifuge for 4′ at 200×*g*.
7. Remove the supernatant and resuspend the cell pellet first in 1 ml pre-warmed seeding medium using a P1000, pipetting up and down as little as possible. Add another 6,040 μL of seeding medium to create a cell suspension of the desired concentration.
8. Seed 200 μL cell suspension per well of a 96 v-bottom well plate, using a P1000 pipet. Gently swirl the tube to mix your cell suspension after every eight wells are filled.
9. Place in the incubator at 37°C and 5% CO_2, on a flat surface, and do not touch or disturb the plate for 48 h.

Day 2: Refresh embryoid bodies to start germ layer differentiation and neural induction—TIMING 30 min

Observe whether EBs have formed 48 h after seeding. Ensure to minimize the time of the plate being out of the incubator and minimize disturbance and movement of the plate to retain embryoid bodies in an optimal condition. Round EBs with a clear border and a diameter of 400–500 μm should have formed (Figure 3b). A small number of dead cells likely will surround the EB.

10. Refresh EBs by taking out 180 μL medium/well and adding a fresh pre-warmed 180 μL neural induction medium (NIM)/well. Use a multichannel pipet to remove and add medium, and be cautious not to aspirate EBs into the pipette tips.
11. Return the plate to the incubator and leave it to incubate for another 72 h.

Day 5: Refresh embryoid bodies with neural induction medium—TIMING 30 min

When observing at day 5, EBs should have grown to a diameter of 450–550 μm. A clear and defined border should still be visible, and an optically clear and radially organized neurectoderm should have appeared on the outer edge (Figure 3c). Buds of neurectoderm without obvious radial organization can also grow within the EBs, which is acceptable as they will possibly still grow into neuroepithelial structures.

12. Refresh EBs by taking out 180 μL medium/well and adding a fresh pre-warmed 180 μL NIM/well. Use a multichannel pipet to remove and add medium and be cautious not to aspirate EBs into the pipette tips.
13. Return the plate to the incubator and leave it to incubate for 72 h.

Day 8: Refresh early organoids with cortical differentiation medium—TIMING 30 min

At day 8, the early organoids should have grown to a diameter of 500–600 μm. The organoids have a denser appearance, and small folds of neuroepithelial structures might be visible on the outer edge. At this stage, the organoid may lose its round shape and adopt a more asymmetrical form. From this day, the medium is switched from NIM to cortical differentiation medium (CDM).

14. Refresh organoids by taking out 180 μL NIM/well and adding a fresh pre-warmed 180 μL CDM per well. Use a multichannel pipet to remove and add medium and be cautious not to aspirate organoids into the pipette tips.
15. Return the plate to the incubator and leave it to incubate for 48 h.

Day 11–day 18: Refresh organoids with cortical differentiation medium—TIMING 30 min

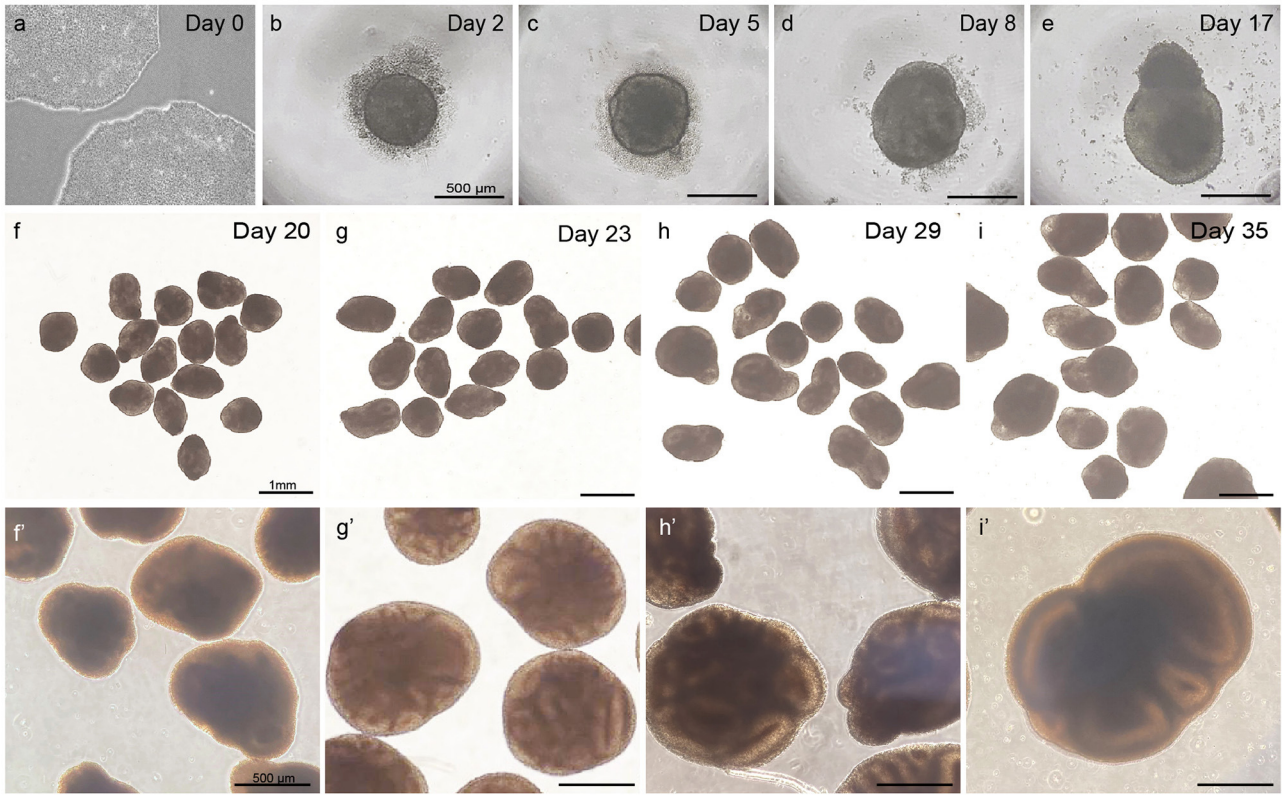

FIGURE 3
Overview of different steps in embryoid body and cortical organoid development from PSCs. Healthy PSCs **(a)**. The scalebar in panels **(b–e)** represents 500 µm; the scalebar in panels **(f–i)** represents 1 mm; the scalebar in panels **(f′–i′)** represents 500 µm.

16. Refresh organoids three times in 7 days with CDM as described in step 17, leaving a maximum of 48 h in between refreshing steps.

As shown in Figures 3d, e, the neuroepithelium should further grow and form buds that are visible in a translucent and thick edge on the outside of the organoid.

Day 18: Transfer organoids to 6-cm dishes in cortical differentiation medium and transfer to shaker—TIMING 60 min

On day 18, the organoids are transferred to non-adherent 6-cm dishes using cut P200 tips. The dishes are placed on an orbital shaker to continue culturing under agitating conditions.

17. First prepare cut P200 tips by cutting off the bottom part of the pipette tip using sterile scissors, creating a tip diameter of ∼2 mm. Prewarm the amount of CDM needed. A maximum of 10 organoids is transferred to one ϕ6 cm dish, normally resulting in three ϕ6 cm dishes per batch of organoids seeded. Per dish, 5 ml of CDM is needed.
18. Fill out 5 ml of pre-warmed CDM per ϕ6 cm dish and place it next to the 96-well plate with organoids to be transferred.
19. To pipette up an organoid from its 96-well, place the pipette with the cut P200 tip straight into the well and gently pipette up. It is important not to enter the V-bottom of the well, where the organoid is located. The organoid in the pipette tip will be visible. Let the organoid sink to the bottom of the pipette tip by holding the pipette up straight and finally let it be released in the CDM in the dish, taking along as little adherent medium as possible.
20. Repeat step 19 until 10 organoids are transferred into a dish. Place the dish on an orbital shaker that is placed in an incubator and set it at the right speed. For the CO_2-resistant orbital shaker used in this protocol (Thermo Scientific™, Cat. 88881102, orbit 1.9 cm), this is 65 rpm. Refer to Box 1 to calculate the correct shaker speed for other shaker types.
21. Leave organoids to incubate under continuous agitating conditions for 48 h.

Day 20–35: Refresh organoids with cortical differentiation medium—TIMING 30 min

Between days 20–35, the CDM medium needs to be refreshed three times per week, leaving a maximum of 48 h in between refreshing steps.

22. To refresh, pause the shaker and transfer dishes to the cell culture hood. Slightly tilt the dishes and pipet off 4.5 ml of medium using a P1000. Avoid disturbance of the organoids in the dish and always leave in 0.5 ml to prevent the organoids from drying out.
23. Slowly add 4.5 ml of fresh and pre-warmed CDM medium.
24. Place dishes back on the shaker and continue incubation under continuous agitation.

BOX 1 Calculating shaker speed.

Shaker speed (in revolutions per minute, RPM) is dependent on the orbit size of the orbital shaker used. For a shaker with an orbit of 1.9 cm, 65 RPM is the desired shaker speed. The correct shaker speed for shakers with a different orbit can be converted using the equation below:

$$r2=\sqrt{(r1)^2 \times \frac{d1}{d2}}$$

r1 = shaker speed of first shaker (rpm)
r2 = shaker speed of second shaker (rpm)
d1 = diameter(throw) of first shaker (cm)
d2 = diameter (throw) of second shaker (cm)

For the Thermo Scientific™ (#88881102) orbital shaker used in this protocol:
$r1 = 65$ rpm
$d_1 = 1.9$ cm

As displayed in Figures 3f–i, the organoids should steadily increase in size and density during this phase to a diameter of >800 μm.

Day 35 and on: Refresh organoids with cortical maturation medium

From day 35 onward, the medium is changed to cortical maturation medium (CMM). The addition of Matrigel will provide a degree of stiffness to the medium that supports healthy further growth of the organoids.

Be aware to prepare CMM first without Matrigel and filter it using a bottle top filter. After filtering, add Matrigel only if the medium is cold.

25. Refresh organoids three times per week with CMM as described in step 22, leaving a maximum of 48 h in between refreshing steps.

3.2. Fixation, embedding, and cryosectioning of cortical organoids

From day 25 onward, the generated organoids can be harvested and processed to observe the developed structures and to verify the presence of dorsal forebrain cell types *via* immunofluorescent staining.

3.2.1. Fixation and equilibration

1. Use a cut-P1000 pipette tip to transfer organoids to a bijou container. Cut a P1000 tip such that the diameter is 3 mm, and ensure that the cutting edge is smooth to prevent organoids from being damaged.
2. Slowly pipette up organoids and collect a maximum of five organoids per container.
3. Aspirate excess medium from the collected organoids and wash by adding 5 ml of D-PBS. Incubate for 5 min and remove D-PBS. Repeat this washing step once more.
4. Add 5 ml of fresh 4% PFA per container and incubate for 4–6 h at 4°C, standing still.
5. Remove PFA from the container and dispose. Wash organoids 2 × 5 min in PBS-T, by adding 5 ml of PBS-T per container.

At this point, organoids can be stored in PBS-T at 2–8°C for up to 1 week. Alternatively, directly continue with sucrose equilibration.

6. To equilibrate organoids, remove PBS-T and discard. Add 5 ml/container of 30% sucrose solution and allow to equilibrate overnight at 2–8°C.

Organoids will float right after the sucrose solution is added. Once the organoids no longer float, equilibration has been successful.

3.2.2. Embedding

Organoids are embedded in gelatin solution in small square embedding molds, and subsequently snap-frozen.

7. Thaw the gelatin solution in a 37°C water bath. Keep the gelatin solution at 37°C continuously to prevent it from polymerizing.
8. Prepare a dry ice/ethanol slurry by spraying 100% ethanol onto dry ice in a styrofoam box multiple times. Once the mixture has stopped boiling, place an aluminum PCR heating block on top of the dry ice and press it down firmly. Wait for 15 min to ensure that the block is ice cold. At this time, let the container with organoids in sucrose solution warm to room temperature.
9. Pipette sucrose solution out of the container containing the organoids and discard. Add 1–2 ml of warm gelatin solution to the organoids and place the container in a small layer of warm water to prevent polymerization.
10. Fill an embedding mold with gelatin solution such that the block is nearly filled. Right after, pipette up organoids with a cut P1000 tip and release them into the embedding mold. Work fast to prevent polymerization of the gelatin. Up to five organoids can be embedded per small embedding mold.
11. The organoids should be positioned at the bottom of the mold, and not be floating. Optionally, use a P200 pipette tip to gently move/reposition the organoids in the mold by hand.
12. If positioned correctly, place the mold on the aluminum block in one movement to snap-freeze. Let it freeze for a minimum of 10 min and do not move the mold during this process.
13. Store snap-frozen samples at −80°C until cryosectioning.

3.2.3. Cryosectioning

14. Remove embedded blocks from the −80°C freezer and allow them to warm up for 30 min in the cryostat chamber that is set at −20°C. Set up the specimen holder temperature at −26°C for gelatin solution-embedded samples.
15. Cut 14–16 μm thick sections and apply them to SuperFrost® Plus adhesion slides. Divide sections over slides in a consecutive sequence to allow for optimal comparison.
16. Let slides air-dry for 15 min before storage at −80°C.

TABLE 2 Primary antibodies for cortical organoid characterization.

Cell type/tissue	Antigen	Host	Supplier	Cat. No.	Dilution	Antigen retrieval
Radial glia/NSCs	PAX6	Rabbit	BioLegend	901301	1:300	10 mM sodium-citrate, 90°C, 20 min
Forebrain	FOXG1	Rabbit	Abcam	ab18259	1:400	10 mM sodium-citrate, 90°C, 20 min
Intermediate progenitors	TBR2	Rabbit	Abcam	ab23345	1:500	10 mM sodium-citrate, 90°C, 20 min
Neurons	TUJ1	Mouse	BioLegend	801201	1:800	10 mM sodium-citrate, 90°C, 20 min
Deep-layer neurons	CTIP2	Rat	Abcam	ab18465	1:500	10 mM sodium-citrate, 90°C, 20 min
Proliferating cells	Ki-67	Mouse	BD Pharmigen	550609	1:50	10 mM sodium-citrate, 90°C, 20 min
Upper layer neurons	SATB2	Mouse	Abcam	ab51502	1:200	10 mM sodium-citrate, 90°C, 20 min
Astrocytes	GFAP	Rat	Invitrogen	13-0300	1:500	10 mM sodium-citrate, 90°C, 20 min
Cortical neural progenitors and neurons	EMX-1	Rabbit	Atlas antibodies	HPA006421	1:50	10 mM sodium-citrate, 90°C, 20 min
Choroid plexus	TTR	Sheep	BioRad	AHP1837	1:100	10 mM sodium-citrate, 90°C, 20 min
Ventral forebrain progenitors	GSX2	Rabbit	Merck Millipore	ABN162	1:500	10 mM sodium-citrate, 90°C, 20 min
Neuroepithelium and radial glia cells	NESTIN	Mouse	R&D Systems	MAB1259	1:50	10 mM sodium-citrate, 90°C, 20 min

3.3. Immunofluorescent characterization of cortical organoid sections

A panel of 12 markers (Table 2) is used to confirm the identity of developed brain regions, as well as cell types that have been generated in cortical organoid sections.

1. Remove slides from the freezer and allow them to dry at room temperature for 15 min.
2. To perform antigen retrieval, place the slides in a plastic coplin staining jar in antigen retrieval buffer (10 mM sodium citrate) and place the jar in a 90°C water bath for 20 min.

Antigen retrieval is applied to the specific primary antibodies listed in Table 2, but the suitability for antigen retrieval might vary for other antibodies.

3. Let the jar cool to room temperature by opening the lid for 15 min.
4. Pour out the antigen retrieval buffer and replace it with washing buffer, and let it stand for 5 min. Repeat this washing step once more.
5. Place slides on a flat surface (e.g., in a microscope slide box) and pipette 300 µl blocking buffer/slide. Incubate at room temperature for 30 min. Keep the incubation space humidified by placing wet towels.
6. Prepare primary antibody mixes in antibody diluent. Refer to Table 2 for antibody concentrations.
7. Pour off the blocking buffer and optionally mark section areas with an ImmunoPen^{TM}. Pipette sufficient primary antibody mix onto slides to cover all slices and incubate overnight in a humidified chamber at 4°C.
8. Prepare secondary antibody mixes in antibody diluent and protect from light. Refer to Table 3 for antibody concentrations.
9. Wash slides 3 × 5 min in a plastic coplin jar in washing buffer.

TABLE 3 Secondary antibodies.

Antibody	Vendor	Cat. No.	Dilution
Alexa Fluor® D α Rt-594	Invitrogen	A-21209	1:1,000
Alexa Fluor® D α Rb-568	Invitrogen	A-11011	1:1,000
Alexa Fluor® Gt α Rb-488	Invitrogen	A-11034	1:1,000
Alexa Fluor® Gt α Ms-488	Invitrogen	A-11029	1:1,000
Alexa Fluor® D α Rb-647	Invitrogen	A-31573	1:1,000
Alexa Fluor® D α Sh-488	Invitrogen	A-11015	1:500
DAPI for nuclei stain	Sigma	D9542	[0.5µg/ml] final

10. Pipette sufficient secondary antibody mix onto slides to cover all slices and incubate for 1.5 h in a humidified and dark space at room temperature.
11. Pour the secondary antibody mix and wash slides 3 × 5 min in D-PBS in a coplin jar. Keep dark.
12. Quickly dip slides in dH_2O, add an aqua-poly mount, and cover with a coverslip. Allow to dry overnight in a dark environment at room temperature, and store at 2–8°C before imaging.

4. Anticipated results

This protocol outlines a simplified method to generate cortical organoids from human pluripotent stem cells in which embryoid bodies are formed in the absence of exogenous patterning factors. The resulting organoids will develop brain regions with predominantly dorsal forebrain identity, in a spontaneous matter. This protocol also describes how to examine and characterize generated organoids at various time points and developmental stages.

TABLE 4 Troubleshooting.

Days	Problem	Possible explanation	Suggested solution
0–2	No EB formation	Too low cell viability/unhealthy PSCs	Check PSC pluripotency by microscopic assessment and by staining for OCT3/4 and NANOG markers.
			Perform a karyotype analysis/chromosome count to assess chromosome stability.
	Too small/too big EBs	Inaccurate cell counting	Count cells manually using a hemocytometer
	Much cell death	Too harsh pipetting causing dead cells	Work as fast as possible in generating a single cell suspension, and limit pipetting of cells with a P1000.
2–8	No formation of neuroectoderm	Cells are not pluripotent or EBs are too immature for neural induction	Check PSC pluripotency by microscopic assessment and by staining for OCT3/4 and NANOG markers.
			Healthy and mature EBs should have a uniform round morphology and exhibit defined edges. Too many dead cells surrounding EBs indicate an unhealthy state.
8–18	No formation of neuroepithelial buds	Failed neuroepithelium development	Do not continue culturing these organoids
18–35	Growth arrest of organoids	Change of medium and transfer to agitating conditions	Wait for organoids to recover and grow again after 2–3 days
	Organoids aggregate and collapse	Shaker speed is too low or too many organoids per 6 cm dish	Calculate the correct shaker speed using Box 1 and try different speeds.
			Lower the number of organoids per 6-cm dish
	Organoids break apart/shatter	Shaker speed is too high	Calculate the correct shaker speed using Box 1 and try different speeds.

Per batch of 32 seeded embryoid bodies, typically at least 25 (∼80%) correctly developed cortical organoids will have formed after 20 days, which can be further matured for over 100 days. As depicted in Figure 3, at day 5, EBs should exhibit an optically clear and radially organized neurectoderm on the outer edge. In 60–80% of these EBs, the neuroectoderm will further develop and expand after 8 days of culture in a neural induction medium. Subsequent cortical differentiation (days 9–18) should start the generation of neuroepithelial structures inside the EBs, which results in observable growth and increased density of the inner parts. Transferring the EBs to small dishes and the associated change in the medium after 18 days, to further stimulate cortical differentiation, will cause a temporary stagnation of growth for about 2 days. During these 2 days, it is normal to observe slight shrinkage of the now-called organoids. After this critical phase, ∼50–80% of the organoids will grow multiple neuroepithelial buds and structures. Neuroepithelial buds can grow in long continuous sheets or round and compact structures, this may vary per organoid and per batch. Budding of neural structures will cause the organoids to steeply increase in size and density, and therefore, it will be difficult to examine the structures by microscope from this phase on. Common pitfalls that might occur during the differentiation of PSCs to organoids, possible explanations, and suggested solutions are described in the troubleshooting table below (Table 4).

After 35 days of differentiation, cortical organoids should have developed multiple PAX6$^+$ progenitor zones in the shape of rosettes or larger continuous folds (Figure 4A). Progenitor zones form around ventricle-like cavities and are characterized by the absence of neurons (TUJ1 negativity) and the presence of NESTIN-positive aRGCs (Figure 4B). Neuronal differentiation can be recognized by the early neuronal marker TUJ1 and by the presence of early-born deep-layer neurons (CTIP2$^+$) that reside outside of the progenitor zones (Figure 4A).

Since different types of brain regions may have formed, a combination of TBR2, FOXG1, and PAX6 staining is used to confirm dorsal forebrain identity (Figure 4C). Correctly formed organoids exhibit organized progenitor zones (TUJ1 negative) that contain FOXG1- and PAX6-expressing radial glial progenitor cells, surrounded by intermediate progenitor cells (TBR2$^+$). Deep-layer neurons will locate outside previously formed, radially organised progenitor zones. The efficiency of correctly formed organoids is ∼80% (Figure 4D). Incorrectly formed organoids lack the proper structure of progenitor zones, visible by increased TUJ1 signal and loss of radial organization (Figure 4C). These organoids typically do not express dorsal progenitor markers FOXG1, TBR2, or PAX6. CTIP2-positive neurons are often present in incorrectly formed organoids, but lack organized localization (Figure 4C). The efficiency of cortical- and neuronal marker expression within organoids over different batches is displayed in Figure 4E. An in-depth overview of the batch success rate and expression of these different markers across individual batches is provided in Supplementary Table 1.

Dorsal forebrain progenitor cells are marked by nuclear FOXG1 expression (Figure 5A). Forebrain progenitor zones are highly proliferative, as shown by positivity for proliferation marker Ki-67 (Figure 5A). Consistent with Ki-67 expression reaching a maximum in mitosis, its levels are highest near the apical surface where mitosis takes place following interkinetic nuclear migration (Bruno and Darzynkiewicz, 1992; Kulikova et al., 2011).

In addition to FOXG1 and PAX6 expression in aRGCs, the presence of TBR2-expressing IPCs confirms dorsal forebrain identity (Figure 5A). IPCs align at the outer edge of progenitor

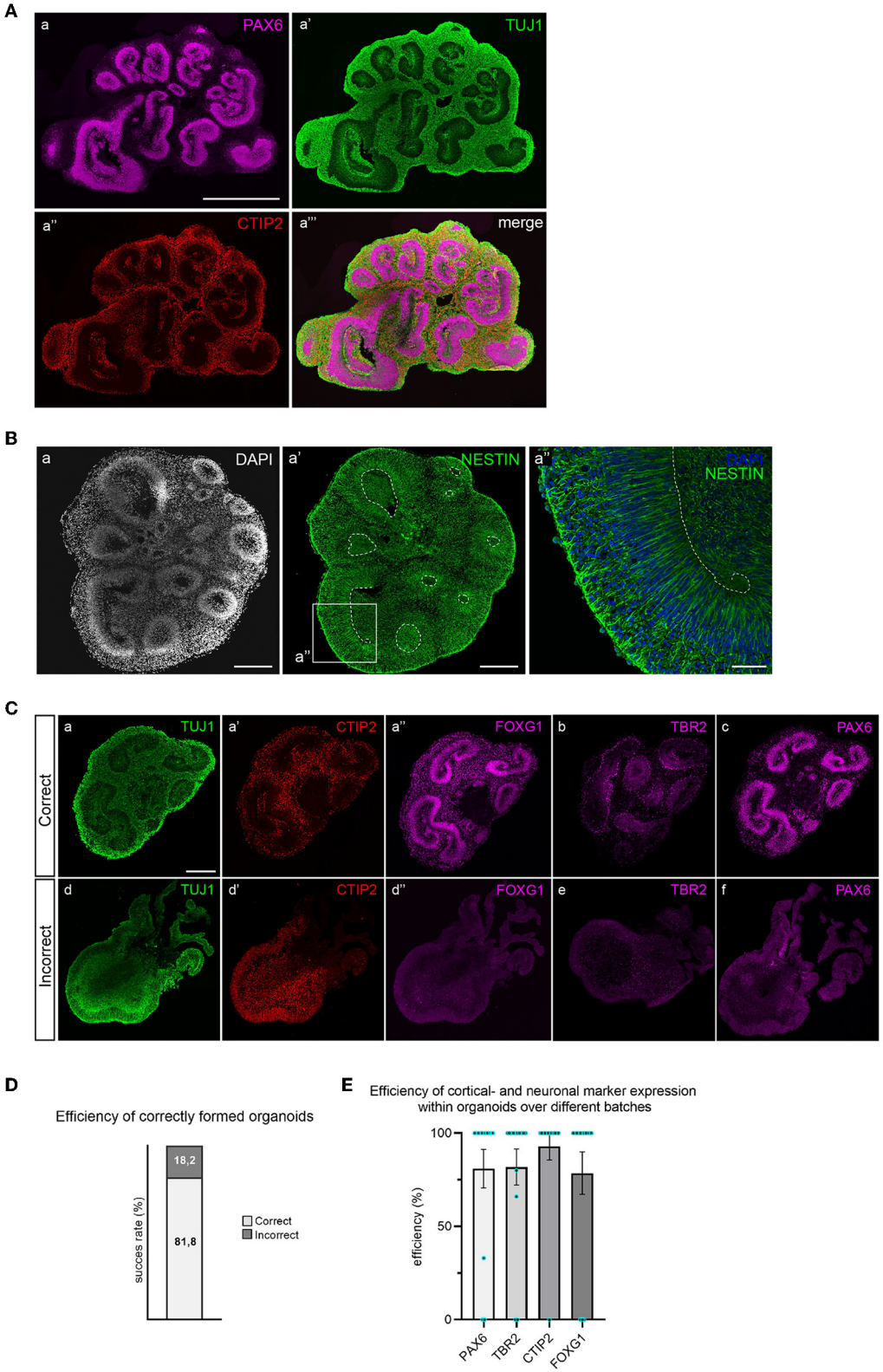

FIGURE 4
Immunofluorescent staining for brain regions and neuronal cell types in 35-day old cortical organoids. **(A)** Multiple PAX6^{+} progenitor zones are distributed throughout the organoid in the shape of large folds or small rosettes, and surrounding ventricle-like cavities. Whereas progenitor zones are negative for TUJ1 (class-III tubulin), early neuronal differentiation outside of progenitor zones is marked by abundant TUJ1 expression. Early-born deep-layer neurons (CTIP2) reside outside of progenitor zones. Scalebar: 1 mm for all panels. **(B)** Apical radial glial cells (NESTIN^{+}) occupy progenitor zones and extend from the apical to the basal surface (panel a″). Scalebar a, a′: 250 μm, a″: 50 μm. **(C)** Correctly formed organoids show structured progenitor zones (panel a), presence of deep-layer neurons (CTIP2, panel a′), and expression of dorsal forebrain markers FOXG1, TBR2, and PAX6 (panels a″, b, and c). Incorrect organoids lack organized progenitor zones (panel d), contain dispersed deep-layer neurons (panel d′), and show absence of dorsal forebrain progenitor markers (panels d″, e, and f). Scalebar: 250 μm for all panels. **(D)** Batch efficiency of brain organoid differentiation. **(E)** Efficiency of cortical identity acquisition.

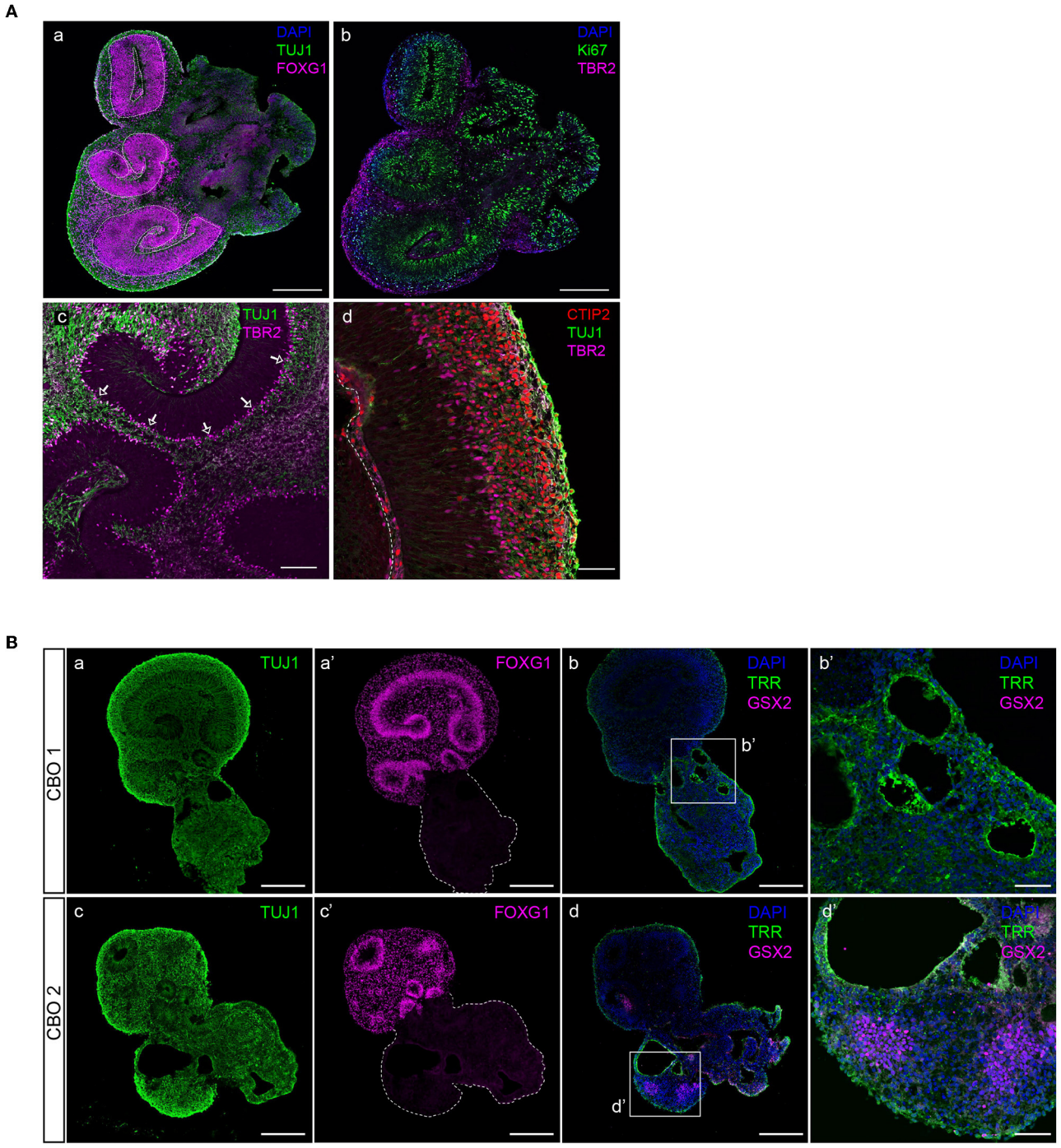

FIGURE 5
Characterization of dorsal forebrain identity in cortical organoid brain regions. **(A)** A 35-day-old organoid showing multiple radial glial progenitor regions (indicated by dashed lines) marked by FOXG1-positive neural progenitor cells, and early neuronal differentiation (TUJ1) (panel a), proliferative progenitors (Ki-67, panel b), and IPCs (TBR2, panel b). Intermediate progenitor cells (TBR2) are generated in the proliferative zone and migrate to align at the basal side (indicated by arrows), where they generate neurons (TUJ1) (panel c). Magnification of a typically organized proliferative zone (TUJ1 negative) located next to a ventricle-like cavity with intermediate progenitors (TBR2) that give rise to deep-layer neurons (CTIP2) that form a layer right above (panel d). Scalebar a, b: 300 μm, c: 100 μm, d: 50 μm. **(B)** Non-dorsal forebrain identity regions can be recognized by aberrant TUJ1 morphology, lacking progenitor zones (panels a, c), or FOXG1 expression (panels a′ and c′). The presence of ventral forebrain progenitors (GSX2) and choroid plexus epithelia (TRR) surrounding ventricle-like cavities can be identified (panels b, b′, d, and d′). CBO, cortical brain organoid. Scalebar a, a′, b, c, c′, and d: 250 μm, b′ and d′: 50 μm.

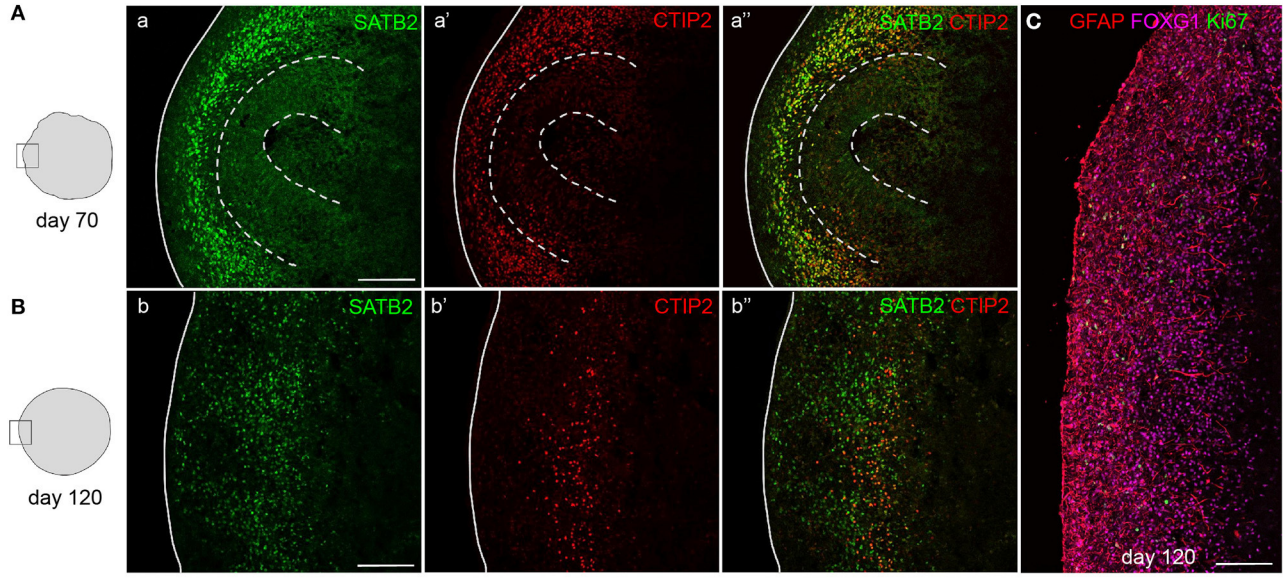

FIGURE 6
Mature cortical organoids. Staining for upper-layer neurons (SATB2) and deep-layer neurons (CTIP2) in 70- and 120-day-old mature cortical organoids. After 70 days, progenitor zones are still present (indicated by dashed lines) and both types of neurons reside outside of these zones in a disorganized manner **(A).** In 120-day-old organoids, progenitor zones are absent and deep-layer neurons have compacted into a more organized layer, positioned below a layer of abundantly present upper-layer neurons **(B)**. Staining for astrocytes (GFAP), neurons (FOXG1), and proliferating cells (Ki-67) in a 120-day-old cortical organoid cortex-like region **(C)**. Scalebar: 150 μm in all images.

zones and are the main source of the early deep-layer neurons (CTIP2) that will settle outside of the progenitor zones (Figure 5A). However, infrequent brain regions with non-dorsal identity might develop in organoids. These regions are morphologically different from dorsal forebrain regions, lack clear progenitor zones, and do not express dorsal forebrain marker FOXG1 (Figure 5B). Immunofluorescent characterization shows that such regions contain ventricle-like cavities surrounded by choroid plexus epithelia (TRR$^+$), as well as GSX2-expressing ventral forebrain progenitor cells (Figure 5B), which are both cell types that derive from the rostral neural tube during early embryonic development (Liddelow, 2015; Leung et al., 2022).

Whereas, newborn neurons at early stages can still be dispersed, and more compact and organized bands of neurons will be visible in mature organoids (Figure 6). After 70 days of differentiation, mature organoids have expanded their neuronal population with later-born superficial-layer identity neurons (SATB2$^+$) having been generated in addition to deep-layer neurons (CTIP2$^+$) (Figure 6A). At this stage, both types of neurons settle outside the still-present ventricular zone structures in an intermingled manner. If allowed to further mature up to 120 days *in vitro*, a more structured organization of neurons can be observed, with early-born neurons forming a compact deep layer and later-born neurons being localized outside of this layer (Figure 6B). Progenitor zones gradually thin and eventually disappear, as indicated by the near-absence of Ki-67$^+$ cells (Figure 6C). The maturity of 120-day-old organoids is confirmed by the presence of glial cell populations such as astrocytes. As shown in Figure 6C, GFAP$^+$ astrocytes are widely distributed throughout the cortex-like organoid tissue, while post-mitotic neurons still express FOXG1 to promote cell survival.

5. Discussion

We have described a simple protocol for the generation of cortical organoids from human pluripotent stem cells. The particular focus of this protocol has been to minimize the complexity of handling steps and media formulations while describing a robust and reproducible method. Organoids generated with this protocol were shown to contain brain regions with a cortical identity by the presence of intermediate progenitor cells and NPCs expressing forebrain marker FOXG1. During a differentiation period of 35 days, three different medium formulations are used, and only one switch in culture ware is required. Furthermore, no exogenous patterning factors are added to the culture medium, contributing to the straightforwardness of this protocol.

Various existing protocols have described the differentiation of pluripotent stem cells into embryoid bodies, and subsequent neural induction steps to generate neural stem cells, neural rosettes, or cortical organoids (Kadoshima et al., 2013; Lancaster and Knoblich, 2014; Renner et al., 2017; Sloan et al., 2018; Velasco et al., 2019). *In vitro* modeling of neurogenesis heavily relies on the intrinsic bias of embryonic stem cells toward the neural lineage and their spontaneous preference to differentiate into neuroectoderm and forebrain identity (Gaspard et al., 2008). Where initial brain organoid protocols described self-patterning methods, more recent protocols have focused on directing toward region-specific identities in organoids, using exogenous patterning factors. Mainly the addition of certain inhibitors (TFGβ, BMP, and WNT) is suggested to increase neural induction efficiency and block non-neural differentiation (Chiaradia and Lancaster,

2020). However, we show that robust neural induction of embryoid bodies is sufficient to stimulate the formation of neuroectoderm that will grow into neuroepithelial structures. We describe the formation and neural induction of embryoid bodies *via* a procedure that is very similar to that established by Gunhanlar et al. (2018), where neural induction of embryoid bodies in a simple medium without patterning factors results in NPCs with dorsal forebrain identity. These NPCs could be further differentiated into electrophysiologically mature cortical neuronal networks. A substantial improvement compared to this and other protocols is that we aggregate pluripotent stem cells in a PSC culture medium. This ensures the robust formation of embryoid bodies and minimizes extrinsic disturbance during the fragile process of neural induction. This protocol is in concept comparable to early hallmark protocols that have described the self-patterned generation of cortical organoids (Lancaster et al., 2013; Lancaster and Knoblich, 2014), but is simplified in several ways. In the initial protocols, embryoid body formation, neural induction, and cortical differentiation require four changes of culture ware and four different medium formulations within 15 days of differentiation. Furthermore, neuroepithelial bud expansion requires transferring of early organoids into Matrigel droplets, a vulnerable and time-consuming step. The protocol that we describe uses three different medium formulations and involves only one change in culture ware. In line with published brain organoid differentiation methods (Kadoshima et al., 2013; Velasco et al., 2019), the protocol that we describe incorporates a low concentration of Matrigel in the medium to provide a degree of stiffness that will support the 3D expansion of neuroepithelial structures, without having to incorporate an embedding step.

Since this protocol is focused on the practicality of differentiation conditions and handling, it creates certain limitations for specific downstream applications. To our opinion, generating relatively small amounts of organoids per batch contributes to accurate execution and thereby reproducibility of the protocol. By limiting the time that developing organoids are taken out of their incubator (e.g., to refresh media or take microscopic images), the efficiency at which well-developed organoids are being formed is increased. However, the small number of organoids being generated per batch can be limiting if certain effects need to be studied in larger groups of samples at the same time. Formation of non-dorsal forebrain identity brain regions may occur throughout organoid batches more variably compared to directed protocols, which could be a disadvantage for gene expression analysis such as (single-cell) RNA sequencing.

Data availability statement

The original contributions presented in the study are included in the article/Supplementary material, further inquiries can be directed to the corresponding author.

Author contributions

KE: conceptualization, methodology, investigation, formal analysis, and writing—original draft. HBS and AK: investigation. MK and HS: methodology. SK: supervision and funding acquisition. FV: writing—review and editing and supervision. DB: conceptualization, methodology, writing—review and editing, supervision, and funding acquisition. All authors contributed to the article and approved the submitted version.

Funding

DB is supported by a Horizon 2020 Marie Curie Individual Fellowship (#799214) and an Erasmus University Rotterdam Fellowship. FV is supported by the Erasmus MC Human Disease Model Award. FV and SK are supported by the Netherlands Organ-on-Chip Initiative, an NWO Gravitation project (024.003.001) funded by the Ministry of Education, Culture, and Science of the Government of the Netherlands.

Acknowledgments

We thank Mehrnaz Ghazvini and the iPS Core Facility for advice on PSC culture and the Optical Imaging Center for the provision of training and infrastructure.

Conflict of interest

The authors declare that the research was conducted in the absence of any commercial or financial relationships that could be construed as a potential conflict of interest.

Publisher's note

Supplementary material

The Supplementary Material for this article can be found online at: https://www.frontiersin.org/articles/10.3389/fncel.2023.1114420/full#supplementary-material

SUPPLEMENTARY FIGURE 1
Cortical brain identity is marked by EMX-1 expression in organoids. Immunofluorescent staining of a 35-day organoid for dorsal forebrain progenitor marker EMX-1. Top: entire organoid, bottom: magnification view of panel b.

SUPPLEMENTARY TABLE 1
Efficiency of correctly formed organoids and expression of cortical and neuronal markers within and between batches.

References

Benito-Kwiecinski, S., Giandomenico, S. L., Sutcliffe, M., Riis, E. S., Freire-Pritchett, P., Kelava, I., et al. (2021). An early cell shape transition drives evolutionary expansion of the human forebrain. *Cell* 184, 2084–2102.e2019. doi: 10.1016/j.cell.2021.02.050

Bruno, S., and Darzynkiewicz, Z. (1992). Cell cycle dependent expression and stability of the nuclear protein detected by Ki-67 antibody in HL-60 cells. *Cell Prolif.* 25, 31–40.

Camp, J. G., Badsha, F., Florio, M., Kanton, S., Gerber, T., Wilsch-Brauninger, M., et al. (2015). Human cerebral organoids recapitulate gene expression programs of fetal neocortex development. *Proc. Natl. Acad. Sci. U. S. A.* 112, 15672–15677. doi: 10.1073/pnas.1520760112

Chiaradia, I., and Lancaster, M. A. (2020). Brain organoids for the study of human neurobiology at the interface of *in vitro* and *in vivo*. *Nat. Neurosci.* 23, 1496–1508. doi: 10.1038/s41593-020-00730-3

Gaspard, N., Bouschet, T., Hourez, R., Dimidschstein, J., Naeije, G., Van Den Ameele, J., et al. (2008). An intrinsic mechanism of corticogenesis from embryonic stem cells. *Nature* 455, 351–357. doi: 10.1038/nature07287

Gordon, A., Yoon, S. J., Tran, S. S., Makinson, C. D., Park, J. Y., Andersen, J., et al. (2021). Long-term maturation of human cortical organoids matches key early postnatal transitions. *Nat. Neurosci.* 24, 331–342. doi: 10.1038/s41593-021-00802-y

Gunhanlar, N., Shpak, G., Van Der Kroeg, M., Gouty-Colomer, L. A., Munshi, S. T., Lendemeijer, B., et al. (2018). A simplified protocol for differentiation of electrophysiologically mature neuronal networks from human induced pluripotent stem cells. *Mol. Psychiatry* 23, 1336–1344. doi: 10.1038/mp.2017.56

Kadoshima, T., Sakaguchi, H., Nakano, T., Soen, M., Ando, S., Eiraku, M., et al. (2013). Self-organization of axial polarity, inside-out layer pattern, and species-specific progenitor dynamics in human ES cell-derived neocortex. *Proc. Natl. Acad. Sci. U. S. A.* 110, 20284–20289. doi: 10.1073/pnas.1315710110

Kulikova, S., Abatis, M., Heng, C., and Lelievre, V. (2011). Interkinetic nuclear migration: reciprocal activities of dynein and kinesin. *Cell Adh. Migr.* 5, 277–279. doi: 10.4161/cam.5.4.17432

Lancaster, M. A., Corsini, N. S., Wolfinger, S., Gustafson, E. H., Phillips, A. W., Burkard, T. R., et al. (2017). Guided self-organization and cortical plate formation in human brain organoids. *Nat. Biotechnol.* 35, 659–666. doi: 10.1038/nbt.3906

Lancaster, M. A., and Knoblich, J. A. (2014). Generation of cerebral organoids from human pluripotent stem cells. *Nat. Protoc.* 9, 2329–2340. doi: 10.1038/nprot.2014.158

Lancaster, M. A., Renner, M., Martin, C. A., Wenzel, D., Bicknell, L. S., Hurles, M. E., et al. (2013). Cerebral organoids model human brain development and microcephaly. *Nature* 501, 373–379. doi: 10.1038/nature12517

Leung, R. F., George, A. M., Roussel, E. M., Faux, M. C., Wigle, J. T., and Eisenstat, D. D. (2022). Genetic regulation of vertebrate forebrain development by homeobox genes. *Front. Neurosci.* 16, 1933. doi: 10.3389/fnins.2022.843794

Liddelow, S. A. (2015). Development of the choroid plexus and blood-CSF barrier. *Front. Neurosci.* 9, 32. doi: 10.3389/fnins.2015.00032

Mariani, J., Coppola, G., Zhang, P., Abyzov, A., Provini, L., Tomasini, L., et al. (2015). FOXG1-dependent dysregulation of GABA/glutamate neuron differentiation in autism spectrum disorders. *Cell* 162, 375–390. doi: 10.1016/j.cell.2015.06.034

Pasca, A. M., Sloan, S. A., Clarke, L. E., Tian, Y., Makinson, C. D., Huber, N., et al. (2015). Functional cortical neurons and astrocytes from human pluripotent stem cells in 3D culture. *Nat. Methods* 12, 671–678. doi: 10.1038/nmeth.3415

Pollen, A. A., Bhaduri, A., Andrews, M. G., Nowakowski, T. J., Meyerson, O. S., Mostajo-Radji, M. A., et al. (2019). Establishing cerebral organoids as models of human-specific brain evolution. *Cell* 176, 743–756.e717. doi: 10.1016/j.cell.2019.01.017

Qian, X., Nguyen, H. N., Song, M. M., Hadiono, C., Ogden, S. C., Hammack, C., et al. (2016). Brain-region-specific organoids using mini-bioreactors for modeling ZIKV exposure. *Cell* 165, 1238–1254. doi: 10.1016/j.cell.2016.04.032

Renner, M., Lancaster, M. A., Bian, S., Choi, H., Ku, T., Peer, A., et al. (2017). Self-organized developmental patterning and differentiation in cerebral organoids. *EMBO J.* 36, 1316–1329. doi: 10.15252/embj.201694700

Sloan, S. A., Andersen, J., Pasca, A. M., Birey, F., and Pasca, S. P. (2018). Generation and assembly of human brain region-specific three-dimensional cultures. *Nat. Protoc.* 13, 2062–2085. doi: 10.1038/s41596-018-0032-7

Velasco, S., Kedaigle, A. J., Simmons, S. K., Nash, A., Rocha, M., Quadrato, G., et al. (2019). Individual brain organoids reproducibly form cell diversity of the human cerebral cortex. *Nature* 570, 523–527. doi: 10.1038/s41586-019-1289-x

Velasco, S., Paulsen, B., and Arlotta, P. (2020). 3D brain organoids: studying brain development and disease outside the embryo. *Annu. Rev. Neurosci.* 43, 375–389. doi: 10.1146/annurev-neuro-070918-050154

Xiang, Y., Tanaka, Y., Patterson, B., Kang, Y. J., Govindaiah, G., Roselaar, N., et al. (2017). Fusion of regionally specified hPSC-derived organoids models human brain development and interneuron migration. *Cell Stem Cell* 21, 383–398.e387. doi: 10.1016/j.stem.2017.07.007

Frontiers in
Cellular Neuroscience

Leading research in cellular mechanisms underlying brain function and development

Part of the world's most cited neuroscience journal series that advances our understanding of the cellular mechanisms underlying cell function in the nervous system across all species.

Discover the latest Research Topics

See more →

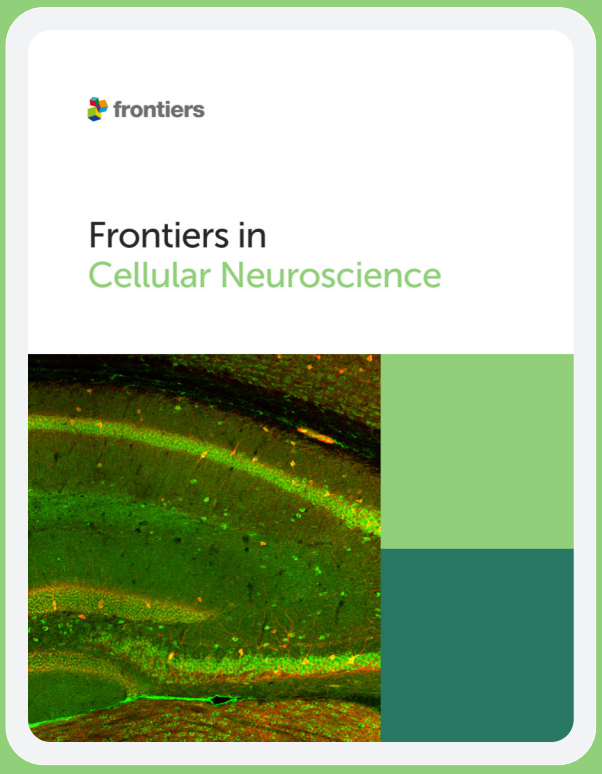

Frontiers

Avenue du Tribunal-Fédéral 34
1005 Lausanne, Switzerland
frontiersin.org

Contact us

+41 (0)21 510 17 00
frontiersin.org/about/contact